INTEGRATED MID-CONTINENT STACKED CARBON STORAGE HUB

Phase I Final Report

WORK PERFORMED UNDER AGREEMENT

DE-FE0029264

SUBMITTED BY

Battelle Memorial Institute
505 King Ave
Columbus, OH 43201
DUNS Number: 00 790 1598

October 12, 2018

PRINCIPAL INVESTIGATOR

Andrew Duguid, Ph.D., P.E.
614-424-3516
duguid@battelle.org

SUBMITTED TO

U.S. Department of Energy
National Energy Technology Laboratory
Project Manager: Venkat Venkataraman, Ph.D.
Venkat.Venkataraman@NETL.DOE

INTEGRATED MID-CONTINENT STACKED CARBON STORAGE HUB

Phase I Final Report

Authors

Diana H. Bacon[1], Dan Blankenau[2], Dana Divine[2], Andrew Duguid[4], Isis Fukai[4], Justin Glier[4], Jared Hawkins[4], Martin Jimenez[4], R.M. Joeckel[3], Scott McDonald[5], Richard Middleton[6], Rick Peterson[4], Mackenzie Scharenberg[4], Valerie Smith[4], Signe K. White[1], Sean Patrick Yaw[6]

1. Pacific Northwest National Laboratory
2. Great Plains Energy, Inc., Lincoln, Nebraska, USA
3. Conservation and Survey Division, University of Nebraska, Lincoln, Nebraska, USA
4. Battelle, Columbus, Ohio, USA
5. Archer Daniels Midland, Decatur, Illinois, USA
6. Los Alamos National Laboratory, Los Alamos, New Mexico, USA

DISCLAIMER

Contents

Figures vii
Tables xiv
Acronyms and Abbreviations 18
Executive Summary 19
1 Introduction 30
2 CO_2 Sources 33
2.1 Background 33
2.2 Methods 33
2.3 Results 34
2.3.1 General Results 34
2.3.2 Electric Power 38
2.3.3 Ethanol 40
2.3.4 Other Facilities 42
2.4 Discussion 43
2.5 Conclusions 48
3 Geology 48
3.1 Introduction 48
3.2 Methods 49
3.3 Pennsylvanian-Permian Storage Complex 50
3.4 Geologic Background and Selected Study Areas 52
3.4.1 Overview 52
3.4.2 Basin Framework of the Midcontinent Region 52
3.4.3 Regional Stratigraphy 53
3.4.4 Existing Hydrocarbon Resources 55
3.5 Sub-Basin Evaluation 58
3.5.1 Data Compilation and Management 58
3.5.2 Petrophysical Calculations 62
3.5.3 Three-Dimensional (3D) Static Earth Model (SEM) Development 67
3.5.4 Geologic Mapping 74
3.5.5 Prospective Storage Resource Calculations 78
DOE-NETL Static (Volumetric) Method 78

3.5.2 Site-Specific CO_2 Storage Efficiency 80
3.6 Results 84
3.6.1 Regional Geologic Structures, Crustal Stress, and Seismicity 84
3.6.2 SEM Results 87
3.6.3 Site-Specific Characterization and Geologic Maps 109
3.6.4 Prospective Storage Resource Estimates 146
3.7 Discussion 149
3.7.1 Structural and Stratigraphic Framework of the Selected Study Areas 149
3.7.2 Pennsylvanian-Permian Confining System 149
3.7.3 Site-Scale Reservoir Characterization and Comparison of Study Areas 150
3.7.4 Data Gaps and Future Work 151
3.8 Conclusions 152
4 Reservoir Simulation 154
4.1 Scope 154
4.2 Pennsylvanian-Permian Storage Complex 154
4.3 ECLIPSE Model and Model Settings 154
4.3.1 ECLIPSE 154
4.3.2 Simulation Grid and Properties 155
4.3.3 Fluid Properties 157
4.3.4 Relative Permeability 157
4.3.5 Reservoir Boundaries 158
4.3.6 Model Equilibration 158
4.3.7 Injection Well Locations 158
4.3.8 Injection Constraints 159
4.4 Dynamic Modeling 160
4.4.1 Single-Well Injection Cases 160
4.4.2 Simulated Injectivity 160
4.4.3 Multi-Well Injection Cases 161
4.4.4 Sensitivity Cases 170
4.5 Conclusions 175
5 Assessment of the Area of Review for the Sleepy Hollow Field using the NRAP-IAM-CS 177
5.1 Introduction 177
5.2 Organization 177

5.3 Risk-Based Approach for Determining the Area of Review (AoR) 178
5.3.1 Description of NRAP-IAM-CS and Assumptions 178
5.4 Critical Pressure Calculations 183
5.4.1 Application of NRAP-IAM-CS to Determine Risk of Brine Leakage at the Sleepy Hollow Site 185
5.5 Summary and Conclusions 188
5.6 Recommendations 188
6 CO_2 Capture and Transport 190
6.1 Introduction 190
6.2 Methods 190
6.3 Capture Requirements 191
6.3.1 Ethanol Surface Facility Description 192
6.3.2 Design Requirements 192
6.3.3 Conceptual Process Design: Ethanol Plant 193
6.3.4 CO_2 Capture from Coal-Fired Power Plants 193
6.4 Near-Field Transport Requirements 197
6.5 Far-Field Transport Requirements 197
6.5.1 Pipeline design and specifications 198
6.5.2 Pipeline Routing: SimCCS 209
6.5.3 Overview of existing CO_2 pipelines 219
6.5.4 Property ownership 222
6.5.5 Pipeline Safety 224
6.5.6 Protected and sensitive areas 225
6.5.7 Obstacles and barriers to operations 236
6.6 Discussion 238
6.7 Conclusions 241
7 Economics and Liability 243
7.1 Study Area Introduction and Background 243
7.1.1 Overview 243
7.1.2 CO_2 Sources: Ethanol Plants 243
7.1.3 CO_2 Sinks: Deep Saline Storage Zones and EOR Reservoirs 244
7.2 Economic and Liability Assessment Framework 244
7.2.1 Liability Assessment Considerations 244
7.2.2 Economic Assessment Methodology and Project Scenarios 245

CO_2 Capture and Pipeline Transport Cost Models 245
CO_2-EOR and Storage Cost Models 247
7.3 Liability Assessment Results 249
7.3.1 Potential Business Models and Contractual Liability 249
7.3.2 Potential Impact of State Incentives and Policies 250
7.3.3 Long-Term Liability of Stored CO_2 251
7.3.4 Surface Access and Environmental Considerations 252
7.4 Economic Analysis Results 255
7.4.1 CO_2 Capture and Pipeline Costs 255
7.4.2 CO_2-EOR and Saline Storage Costs 255
7.5 Discussion and Conclusions 259
7.6 Conclusions 261
8 Phase II Planning 262
8.1 Introduction 262
8.2 Challenges Being Addressed in Phase II 264
8.2.1 Mapping the Extent of the Confining System 264
8.2.2 Minimize the Areas of Review 265
8.2.3 Public Outreach 265
8.2.4 Regulatory, Contractual, and Permitting 265
8.2.5 Long-term Liability 265
8.2.6 Pipeline Rights of Way 266
8.3 Phase II Objectives 266
8.4 Phase II Project Tasks 268
9 Conclusions 275
References 281

Figures

Figure ES-1. Study area showing CO_2 sources and oil fields. 19
Figure ES-2. Phase I projects represented going forward in Phase II. 20
Figure ES-3. Ethanol sources in the study area. 22
Figure ES-4. Plot showing individual facility and total ethanol-related emissions 22
Figure ES-5. Simplified stratigraphic column showing the deep saline formations of interest and overlying caprocks evaluated in both study areas. 25
Figure ES-6. Simulated cumulative CO_2 injection (metric tons) vs. time for singe-well cases. 27

Figure ES-7. Edge of the simulated CO_2 plume after 10, 20, and 30-year injection and 10-year post-injection period. 27
Figure ES-8. (A) Map showing existing natural gas pipelines in Nebraska and Kansas along with locations of ethanol plants, power plants, and the potential Sleepy Hollow storage site;(B) Map showing the Sleepy Hollow site alongside oil/gas fields and existing and potential CO_2 pipelines in the United States (map data from EIA, 2016; NATCARB, 2017). 28
Figure 1-1. Study area showing CO_2 sources and oil fields. 30
Figure 1-2. Phase I projects represented going forward in Phase II. 31
Figure 2-1. Locations of Nebraska facilities reporting in the US EPA GHGRP (US EPA, 2016). 34
Figure 2-2. Map showing the location of all sources in the study area. 38
Figure 2-3. Electric power sources in the study area. 39
Figure 2-4. Plot showing individual facility and total power-related emissions. 39
Figure 2-5. Ethanol sources in the study area 41
Figure 2-6. Plot showing individual facility and total ethanol-related emissions 41
Figure 2-7. Plot showing individual and total other-facility-related emissions 43
Figure 2-8. Map showing the approximate location of Source Corridor 1. 45
Figure 2-9. Map showing the approximate location of Source Corridor 2. 46
Figure 2-10. Map showing the approximate location of Source Corridor 3. 47
Figure 3-1. Regional map showing the Sleepy Hollow Field (SHF) in Red Willow County, Nebraska and the Huffstutter Field (HF) in Phillips County, Kansas. Image modified from Steeples (1982). 50
Figure 3-2. Simplified stratigraphic column showing the deep saline formations of interest and overlying caprocks evaluated in both study areas. 51
Figure 3-3. Map of Nebraska showing the outline of the Sleepy Hollow study area in Red Willow County along with the location of 205 wells with logs used for petrophysical analysis, SEM development, and storage resource calculations. 56
Figure 3-4. Map of Kansas showing the outline of the Huffstutter study area in Phillips County along with the location of 96 wells with logs used for petrophysical analysis, SEM development, and storage resource calculations. 57
Figure 3-5. Flow chart illustrating data relationships and integration procedures used for generating total porosity, effective porosity, and permeability curves. 62
Figure 3-6. Porosity-permeability transform derived from core data from the Lansing-Kansas City groups in the Sleepy Hollow study area. 65
Figure 3-7. Porosity-permeability transform derived from core data from the Pennsylvanian Interval groups in the Sleepy Hollow study area. 66
Figure 3-8. Generalized static earth modeling workflow. 69
Figure 3-9. Gamma ray and effective porosity log from (A) Sleepy Hollow Field and (B) Huffstutter Field. 73
Figure 3-10. Comparison of CO_2 storage and petroleum industry classification systems as defined by the U.S. DOE-NETL (2017), and adapted from the SPE/WPC/AAPG/SPEE Resource Classification System (© Society of Petroleum Engineers, Petroleum Resources Management System). 79
Figure 3-11. Well locations (gray dots) with well tops in and around the Sleepy Hollow study area 88
Figure 3-12. Example formation tops from the center of Sleepy Hollow Field. Potential storage intervals are in areas of low GR response and are separated by zones that are considered tighter. 89

Figure 3-13. Example well logs from the SH Reagan 98 well. From left to right: GR, facies, resistivity, sonic, porosity, and permeability. 90
Figure 3-14. Example of the carbonate cyclicity observed in gamma ray well log correlated across the Sleepy Hollow Field. Log signatures indicate significant continuity of formations. Section appears on map in Figure 3-11. 91
Figure 3-15. Oblique view of SEM area with wells, well tops, and surfaces. A) Well tops appear as colored disks along the wells. B) Close-up of the lower 13 surfaces used to define the framework for the petrophysical modeling. 92
Figure 3-16. The structural framework of the Sleepy Hollow study area. Population of petrophysical properties was conducted for zones from the Wabaunsee Group down to Precambrian basement top. 92
Figure 3-17. Facies model for the Sleepy Hollow study area. A) Cross-section of facies model through Sleepy Hollow Field. B) Oblique view of the facies model showing the top of the Wabaunsee Group and underlying units. Wells correspond to cross-section above. C) Basal Sand facies model with basal sandstone being bounded by either weather basement rock or laterally by less porous rock. 94
Figure 3-18. Example porosity and permeability log adjustments. A) Original effective porosity and permeability logs in red, with adjusted (attenuated) log values in black. B) Same logs as on left, but showing upscaled values into SEM cells along well path. 95
Figure 3-19. Property distribution maps spanning the 10mi x 10mi SEM. A) Effective porosity on top of the LKC A Zone. (B) Permeability on top of the LKC A Zone. (C) Effective porosity on top of the basal sandstone. (D) Permeability on top of the basal sandstone. Red rectangle is approximate location of the Sleepy Hollow Field. Black Dots are well locations with petrophysical logs. 96
Figure 3-20. Cross-sections through the property models. A) Effective porosity model. B) Permeability model. Cross-section appears in map view in Figure 3-11. 97
Figure 3-21. Histograms depicting property distributions of the SEM for the Sleepy Hollow study area. A) Effective porosity (XPHIAE_Fin) and B) Permeability (XPERM_Fin). 98
Figure 3-22. Wells location (yellow) with well tops in and around the Huffstutter study area. 99
Figure 3-23. Formation tops in one well from the Huffstutter study area. The gamma ray log reveals the carbonate cycles. Potential storage intervals are in areas of low GR response and are separated. 100
Figure 3-24. Example well logs from the 1514720612 well. From left to right: GR, facies, resistivity, sonic, porosity, and permeability. 101
Figure 3-25. Log cross-section showing carbonate cyclicity observed in gamma ray well logs correlated across the Huffstutter study area. Log signatures indicate significant continuity of formations. Cross-section on map in Figure 3-22. 102
Figure 3-26. Oblique view of SEM area with wells, well tops, and surfaces. A) Well tops appear as beads along the wells. B) Close-up of the lower 19 surfaces used to define the framework for the petrophysical modeling. 103
Figure 3-27. The structural framework of the Huffstutter Field study area. SEM is 10 miles by 10 miles. Petrophysical modeling was conducted for zones from the Wabaunsee Group down to Precambrian basement top. 103
Figure 3-28 Facies Model for the Huffstutter study area. A) Well section of facies model through Huffstutter Field. Well section is mapped in Figure 3-22B) Oblique view of facies model showing the top of the Wabaunsee Group. Wells correspond to cross-section above. 105

Figure 3-29. Example porosity and permeability log adjustments for the Huffstutter SEM. A) Original effective porosity and permeability logs in red, with adjusted (attenuated) log values in black. B) Same logs as on left, but showing upscaled values into SEM cells along the well path. 106
Figure 3-30. Property distribution maps spanning the 10 mi x 10 mi SEM. A) Effective porosity on top of the LKC A Zone. B) Permeability on top of the LKC A Zone. Red polygon demarks the Huffstutter Field. Black dots are well locations with petrophysical logs. 107
Figure 3-31. Cross-sections through the property models. A) Effective porosity model (XPHIAE_Fin). B) Permeability model (XPERM_Fin). 108
Figure 3-32. Histograms depicting property distributions. A) Effective porosity (XPHIAE_Fin) and B) Permeability (XPERM_Fin). 109
Figure 3-33. (A) Structure and (B) isopach map for the lower Nippewalla shale in the Sleepy Hollow study area. 111
Figure 3-34. (A) Structure and (B) isopach map for the Sumner Group in the Sleepy Hollow study area. 111
Figure 3-35. (A) Structure and (B) isopach map for the Council Grove Group in the Sleepy Hollow study area. 112
Figure 3-36. (A) Structure and (B) isopach map for the Admire Group in the Sleepy Hollow study area. 112
Figure 3-37. Structural cross-section showing lateral extent and thickness of the primary caprock units along a general west-to-east transect in the Sleepy Hollow study area. 114
Figure 3-38. Structural cross-section showing lateral extent and thickness of the primary caprock units along a general south-to-north transect in the Sleepy Hollow study area. 115
Figure 3-39. (A) Structure and (B) isopach of the Wabaunsee Group in the Sleepy Hollow study area. 117
Figure 3-40. (A) Structure and (B) isopach of the Shawnee-Douglas groups in the Sleepy Hollow study area. 118
Figure 3-41. (A) Structure and (B) isopach map of the Lansing-Kansas City groups in the Sleepy Hollow study area. 119
Figure 3-42. (A) Structure and (B) isopach map of the Pleasanton-Marmaton groups in the Sleepy Hollow study area. 120
Figure 3-43. Structural cross-section showing lateral extent, gross thickness, and net reservoir intervals of the deep saline formations and oil-bearing zones along a west-to-east transect in the Sleepy Hollow study area. 122
Figure 3-44. Structural cross-section showing lateral extent, gross thickness, and net reservoir intervals of the deep saline formations and oil-bearing zones along a general south-to-north transect in the Sleepy Hollow study area. 123
Figure 3-45. Porosity footage map of the Wabaunsee Group in the Sleepy Hollow study area. 125
Figure 3-46. Porosity footage map of the Shawnee-Douglas groups in the Sleepy Hollow study area. 126
Figure 3-47. Porosity footage map of the Lansing-Kansas City groups in the Sleepy Hollow study area. 127
Figure 3-48. Porosity footage map of the Pleasanton-Marmaton groups in the Sleepy Hollow study area. 128
Figure 3-49. Porosity footage map of the four saline storage zones in the Sleepy Hollow study area. 129
Figure 3-50. (A) Structure and (B) isopach map for the lower Nippewalla Group in the Huffstutter study area. 131
Figure 3-51. (A) Structure and (B) isopach map for the Sumner Group in the Huffstutter study area. 132

Figure 3-52. (A) Structure and (B) isopach map for the Council Grove Group in the Huffstutter study area. 133
Figure 3-53. (A) Structure and (B) isopach map for the Admire Group in the Huffstutter study area. 134
Figure 3-54. Structural cross-section showing lateral extent and thickness of the primary caprock units along a general west-to-east transect in the Huffstutter study area. 135
Figure 3-55. (A) Structure and (B) isopach map of the Wabaunsee Group in the Huffstutter study area. 137
Figure 3-56. (A) Structure and (B) isopach map of the Shawnee-Douglas groups in the Huffstutter study area. 138
Figure 3-57. (A) Structure and (B) isopach map of the Lansing-Kansas City groups in the Huffstutter study area. 139
Figure 3-58. (A) Structure and (B) isopach map of the Pleasanton-Marmaton groups in the Huffstutter study area. 140
Figure 3-59. Structural cross-section showing lateral extent, gross thickness, and net reservoir intervals of the deep saline formations and oil-bearing zones along a west-to-east transect in the Huffstutter study area. 141
Figure 3-60. Porosity footage map of the Wabaunsee Group in the Huffstutter study area. 142
Figure 3-61. Porosity footage map of the Shawnee-Douglas groups in the Huffstutter study area. 143
Figure 3-62. Porosity footage map of the Lansing-Kansas City groups in the Huffstutter study area. 144
Figure 3-63. Porosity footage map of the Pleasanton-Marmaton groups in the Huffstutter study area. 145
Figure 3-64. Combined porosity footage map of the stacked saline storage zones in the Huffstutter study area. 146
Figure 4-1. Dynamic model domain and Sleepy Hollow oil field unit boundary. 156
Figure 4-2. 3D permeability distribution after upscaling. Vertical exaggeration is 10x. 156
Figure 4-3. 3D porosity distribution after upscaling. Vertical exaggeration is 10x. 157
Figure 4-4. Relative permeability (Kr) curves assumed for the numerical simulations. Note: Krw is the relative permeability of brine and Krg is the relative permeability of CO_2. 158
Figure 4-5. Cumulative KH map and location of 8 injection wells. 159
Figure 4-6. Perforation intervals and petrophysical properties (porosity and permeability) in the injector no. 1 (INJ #1). Unit of measured depth (MD) is in feet. 160
Figure 4-7. Simulated CO_2 injection rate (metric tons/d) vs. time for singe-well cases. 161
Figure 4-8. Simulated cumulative CO_2 injection (metric tons) vs. time for singe-well cases. 161
Figure 4-9. Simulated CO_2 injection rate (metric tons/d) and cumulative injection (metric tons) for INJ #1, #2, and #3. 162
Figure 4-10. 3D simulated CO_2 plume distribution after 10 years since injection started. Vertical exaggeration is 10x. 163
Figure 4-11. 3D simulated CO_2 plume distribution after 20 years since injection started. Vertical exaggeration is 10x. 163
Figure 4-12. 3D simulated CO_2 plume distribution after 30 years since injection started. Vertical exaggeration is 10x. 164
Figure 4-13. 3D simulated CO_2 plume distribution after 10 years since injection ended. Vertical exaggeration is 10x. 164
Figure 4-14. Satellite imagery showing the location of injectors (INJ #1 ~ #8). A-A' is the cross-section line including both injector INJ #1 and INJ #2. Cross-section line B-B' includes injector INJ #1 and INJ #5

which is almost perpendicular to A-A'. Third cross-section line C-C' includes injector INJ #2 and INJ #5. 165
Figure 4-15. Simulated CO_2 saturation profile along the cross-section A-A' after 10- (a), 20- (b), 30-year (c) injection, and 10-year post-injection (d). Vertical exaggeration is 10x. 166
Figure 4-16. Simulated CO_2 saturation profile along the cross-section B-B' after 10- (a), 20- (b), 30-year (c) injection, and 10-year post-injection (d). Vertical exaggeration is 10x. 167
Figure 4-17. Simulated CO_2 saturation profile along the cross-section C-C' after 10- (a), 20- (b), 30-year (c) injection, and 10-year post-injection (d). Vertical exaggeration is 10x. 168
Figure 4-18. Edge of the simulated CO_2 plume after 10, 20, and 30-year injection and 10-year post-injection period. 169
Figure 4-19. Cumulative CO_2 in each target formation. 170
Figure 4-20. Tornado chart for sensitivity analysis. ±10% variation for the upper and lower level in each parameter except for the perforation intervals. 173
Figure 4-21. Relative permeability curves for Lower, Base, and Upper Case created by Brooks and Corey (1966) equation. 174
Figure 5-1. Components of the risk-based AoR approach (grey components are part of the NRAP-IAM-CS system model). 179
Figure 5-2. Pressure distribution in MPa for Eclipse model layer 21 at time 30 years interpolated to a 100x100 grid. 181
Figure 5-3. Pressure distribution in MPa for Eclipse model layer 21 at time 40 years interpolated to a 100x100 grid. 182
Figure 5-4. CO_2 gas saturation distribution Eclipse model layer 21 at time 30 years interpolated to a 100x100 grid. 182
Figure 5-5. CO_2 gas saturation distribution for Eclipse model layer 21 at time 30 years interpolated to a 100x100 grid. 183
Figure 5-6. Locations of hypothetical wells superimposed on the gas saturation contour plot for year 30. The grid has units of meters. 186
Figure 5-7. Pressure vs. time at each hypothetical well location. The maximum pressure difference is shown in parenthesis for each well. 187
Figure 5-8 Brine leakage rates (kg/s) over time at hypothetical well. 187
Figure 5-9. Cumulative mass of brine leakage (MT) over time at hypothetical well locations. 188
Figure 6-1. Conceptual simplified schematic illustrating the expected equipment for the CO_2 compression facilities. 193
Figure 6-2. Simplified schematic of a coal-fired power plant with a generic post-combustion CO_2 capture system. Other major air pollutants (nitrogen oxides, particulate matter, and sulfur dioxide) are removed from the flue gas prior to CO_2 capture (Battelle, 2001). 194
Figure 6-3. Large-scale CCS projects proceeding to operate and execute since 2011 (Global CCS Institute, 2016). 196
Figure 6-4. The Petra Nova CO_2 capture facility located in Thompsons, Texas. Photo courtesy of NRG Energy, Inc. 196
Figure 6-5. Approximate route for the source corridor pipeline from Section 2. 199
Figure 6-6. PIPESIM pipeline model showing an approximate route and related ethanol CO_2 sources .. 200
Figure 6-7. Pressure versus distance between Blair, NE and Columbus, NE for 6, 8, 10, and 12 Inside diameter pipeline. 200

Figure 6-8. Nodal analysis showing operating points for 6- through 12-inch pipeline and 1500-2100 psi outlet pressure at ADM 201
Figure 6-9. Mass flowrate versus distance between Blair, NE and Sleepy Hollow Field. 202
Figure 6-10. Ten-inch ID pipeline running between Blair, NE and Sleepy Hollow Field with a compressor station at each source. 202
Figure 6-11. Ten-inch ID pipeline running between Blair, NE and Sleepy Hollow Field with a compressor station bringing the CO_2 keeping the pressure sufficient to keep the CO_2 in a dense phase. 202
Figure 6-12. 12-inch ID pipeline running between Blair, NE and Sleepy Hollow Field with the minimum number of compressor stations from the 10-inch pipeline simulation. 203
Figure 6-13. 12-inch ID pipeline running between Blair, NE and Sleepy Hollow Field with the minimum number of compressor stations. 203
Figure 6-14. System pressure versus distance for 8-, 10-, and 12-inch lines between Blair, NE and Sleepy Hollow Field (compressor station at AGP Soy Corn Processing and Chief Ethanol). 204
Figure 6-15. Outlet pressure versus mass flow rate for 8-, 10-, and 12-inch lines between Blair, NE and Sleepy Hollow Field (compressor station at AGP Soy Corn Processing and Chief Ethanol). 205
Figure 6-16. NIST REFPROP Modeling of CO_2 density versus pressure at 50 °F. 205
Figure 6-17. System pressure versus distance for 8-, 10-, and 12-inch lines between Blair, NE and Sleepy Hollow Field (compressor station at Pacific Ethanol). 206
Figure 6-18. Outlet pressure versus flowrate for 8-, 10-, and 12-inch lines between Blair, NE and Sleepy Hollow Field (compressor station at Pacific Ethanol). 206
Figure 6-19. System pressure versus distance for 8-inch line to the AGP Soy Corn Processing and Chief Ethanol node followed by a 10-inch line to Sleepy Hollow Field or a 10-inch line to the AGP Soy Corn Processing and Chief Ethanol node followed by a 12-inch line to Sleepy Hollow Field. 207
Figure 6-20. Outlet pressure versus flowrate for 8-inch line to the AGP Soy Corn Processing and Chief Ethanol node followed by a 10-inch line to Sleepy Hollow Field or a 10-inch line to the AGP Soy Corn Processing and Chief Ethanol node followed by a 12-inch line to Sleepy Hollow Field. 207
Figure 6-21. System pressure versus distance for 8-inch line to the Pacific Ethanol node followed by a 10-inch line to Sleepy Hollow Field or a 10-inch line to the Pacific Ethanol node followed by a 12-inch line to Sleepy Hollow Field. 208
Figure 6-22. Outlet pressure versus flowrate for 8-inch line to the Pacific Ethanol node followed by a 10-inch line to Sleepy Hollow Field or a 10-inch line to the Pacific Ethanol node followed by a 12-inch line to Sleepy Hollow Field 208
Figure 6-23. 10-inch ID pipeline running between Blair, NE and the first compressor station and 12-inch pipeline running from the first compressor station to Sleepy Hollow Field 209
Figure 6-24. Pipeline routes generated using SimCCS (summarized in Table 6-6) overlain with existing natural gas and hazard liquid pipelines (U.S. DOT, 2018). The numbers indicate the sources and correspond with the numbers on Table 6-1. 211
Figure 6-25. Six individual pipeline routes modeled using SimCCS. Numbers indicate segments of the pipeline that correspond with Table 6-6 and Table 6-7. 218
Figure 6-26. Map showing the potential storage sites and CO_2 pipeline for the IMSCS-HUB Project along with existing CO_2 pipelines and oil/gas fields in the United States (map data from NATCARB, 2017). 220
Figure 6-27. National Hydrological Database (NHD) surface waterbodies within study area. 226
Figure 6-28. Principal aquifers of the study area. 227
Figure 6-29. Wetlands map of study area. 228

Figure 6-30. Land cover map of study area. 228
Figure 6-31. Map of GAP Status Code (PAD-US) and critical habitats in the study area. 233
Figure 6-32. Publicly-owned lands in the study area. 233
Figure 6-33. Airports, Dams, and Schools in the proposed study area. 234
Figure 6-34. Mining operations in the proposed study area. 234
Figure 6-35. Population density in the study area. 235
Figure 6-36. 2015 Unemployment rate in the study area. 236
Figure 6-37. Median annual household income in the study area. 236
Figure 6-38. Map of simplified land use and project obstacles and barriers. 238
Figure 7-1. Map showing source-sinks pairs and pipeline routes for (A) Scenarios 1 and 3, (B) Scenario 2, and (C) Scenario 4 (Figure Credit: Great Plains Institute (GPI) and Improved Hydrocarbon Recovery, Inc.). Ethanol plant production capacity is represented by the relative size of each circle from 40 to 250 million gallons per year (DOE-EIA, 2017; State CO_2-EOR Deployment Workgroup, 2017; Dubois, 2018). 246
Figure 7-2. Map showing general land use and protected and sensitive areas within and near the modeled plumes at the potential Sleepy Hollow storage site in Nebraska. 253
Figure 7-3. (A) Map showing existing natural gas pipelines in Nebraska and Kansas along with locations of ethanol plants, power plants, and the potential Sleepy Hollow storage site;(B) Map showing the Sleepy Hollow site alongside oil/gas fields and existing and potential CO_2 pipelines in the United States (map data from EIA, 2016; NATCARB, 2017). 254
Figure 7-4. Incremental CO_2-EOR and storage performance results for one 40-acre 5-spot well pattern producing from the basal sandstone. *Incremental oil produced is reported in thousand stock tank barrels (MSTB); Incremental CO_2 storage is reported in kilotonnes (kt). 257
Figure 7-5. Incremental CO_2-EOR and storage performance results for one 40-acre 5-spot well pattern producing from the LKC "C" zone. *Incremental oil produced is reported in thousand stock tank barrels (MSTB); Incremental CO_2 storage is reported in kilotonnes (kt). 257
Figure 7-6. Cumulative CO_2-EOR and storage performance results for one 40-acre 5-spot well pattern producing from both the basal sandstone and LKC "C" zone. *Incremental oil produced is reported in thousand stock tank barrels (MSTB); Incremental CO_2 storage is reported in kilotonnes (kt). 258
Figure 8-1 Phase I CarbonSAFE projects combining to form the Phase II team. 262
Figure 8-2. The IMSCS-HUB Study area showing the ethanol source and stacked storage corridors. 263
Figure 8-3 Figure 2. Potential pipeline route that could include ethanol plants in Iowa and Illinois (data source: DOE-EIA, 2017; State CO_2-EOR Deployment Workgroup, 2017). 268

Tables

Table ES-1. Reported emissions (in Mt CO_2e), 2011-2015, for ethanol facilities in study area (US EPA, 2016). 21
Table ES-2. Stakeholders expressing support for Phase II. 24
Table 2-1. Reported emissions (Mt CO_2e), 2011-2015, for facilities in study area (US EPA, 2016). Facilities are organized by descending average annual emissions (2011-2015). 35
Table 2-2. Reported emissions (Mt CO_2e), 2011-2015, for counties in study area (US EPA, 2016). 37
Table 2-3. Annual, total, and average emissions by facility type, 2011-2015 (US EPA, 2016). 37
Table 2-4. Reported emissions (Mt CO_2e), 2011-2015, for power plant facilities in study area (US EPA, 2016). 38

Table 2-5. Reported emissions (in Mt CO_2e), 2011-2015, for ethanol facilities in study area (US EPA, 2016). 40
Table 2-6. Reported emissions (Mt CO_2e), 2011-2015, for facilities in study area (US EPA, 2016). Facilities are organized from most to least average annual emissions (2011-2015). 42
Table 2-7. Sources included in Source Corridor 1. 44
Table 2-8. Sources included in Source Corridor 2. 45
Table 2-9. Sources included in Source Corridor 3. 46
Table 2-10. Likely ethanol plants for project outreach. 48
Table 3-1. Inventory of log data available in the Sleepy Hollow and Huffstutter study areas. 58
Table 3-2. Inventory of core data available for Pennsylvanian-age formations in the Sleepy Hollow study area. 59
Table 3-3. Minimum, maximum, and mean core grain density values for Pennsylvanian-age formations in the Sleepy Hollow study area. 59
Table 3-4. Minimum, maximum, and mean core porosity values for Pennsylvanian-age formations in the Sleepy Hollow study area. 60
Table 3-5. Minimum, maximum, and mean core permeability values for Pennsylvanian-age formations in the Sleepy Hollow study area. 60
Table 3-6. Definitions of total and net reservoir and associated data used in this study to quantify each. 66
Table 3-7. Names of formations, members, and informal zones associated with each of the four major lithostratigraphic groups evaluated in this study (in stratigraphic order). 68
Table 3-8. Gamma ray intervals used to delineate facies from the well logs. 71
Table 3-9. Gamma ray intervals used to delineate facies from the well logs. 73
Table 3-10. Number of well data points used to generate structure and isopach maps for caprocks in the Sleepy Hollow study area (in stratigraphic order). 75
Table 3-11. Number of well data points used to generate structure and isopach maps for caprocks in the Huffstutter study area 75
Table 3-12. Names of formations, members, and informal zones associated with each of the four major lithostratigraphic groups evaluated in this study (in stratigraphic order). 76
Table 3-13. Number of well data points used to generate structure and isopach maps for deep saline formations in the Sleepy Hollow study area. 76
Table 3-14. Number of well data points used to generate structure and isopach maps for deep saline formations in the Huffstutter study area 77
Table 3-15. Number of well data points used to generate porosity-footage maps for deep saline formations in the Sleepy Hollow study area. 77
Table 3-16. Number of well data points used to generate porosity-footage maps for deep saline formations in the Huffstutter study area 78
Table 3-17. Definitions and data input used in this study to quantify parameters in the DOE-NETL Prospective storage resource equation for deep saline formations.[a] 80
Table 3-18. Definitions and data input used in this study to quantify storage efficiency parameters[a] for deep saline formations in the Sleepy Hollow study area. 81
Table 3-19. Total number of cells and cell area (At), used in heterogenous CO_2-SCREEN calculations for the Sleepy Hollow study area. Also shown are averages for total reservoir thickness (hg) and total reservoir porosity (□t) calculated from cell data. 83

Table 3-20. Default p-values used as input in CO_2-SCREEN for Ev and Ed in both study areas. 83
Table 3-21. Mean values for total reservoir area (At), total reservoir thickness (hg), and total reservoir porosity (⍰t) used in single-cell CO_2-SCREEN calculations for the Huffstutter study area. 84
Table 3-22. Average depth and total thickness values derived from gridded SEM surfaces for the Pennsylvanian intervals of interest in the Sleepy Hollow study area. 87
Table 3-23. SEM zone layering types and divisions for the Sleepy Hollow study area. 93
Table 3-24 Average depth and total thickness values derived from gridded SEM surfaces for the Pennsylvanian intervals of interest in the Huffstutter study area. 99
Table 3-25 SEM zone layering types and divisions For the Huffstutter study area. 104
Table 3-26. Mean and standard deviation (σ) of caprock depth and gross thickness of caprocks along with the associated well count (n) for the Sleepy Hollow study area. 110
Table 3-27. Average total reservoir thickness, total reservoir porosity and permeability, and total reservoir pore volume along with net-to-total reservoir pore volume ratio for the Sleepy Hollow study area. 124
Table 3-28. Mean and standard deviation (σ) of caprock depth and gross thickness along with the associated well count (n) for the Huffstutter study area. 130
Table 3-29. Average total reservoir thickness, total reservoir porosity and permeability, and total reservoir pore volume for the Huffstutter study area. 142
Table 3-30. Site-specific EPVn/PVt values calculated from well data in the Sleepy Hollow study area and default EV and Ed values used in CO_2-SCREEN calculations. 147
Table 3-31. Prospective storage resource and storage efficiency estimates for the deep saline formations of interest in the Sleepy Hollow study area. 147
Table 3-32. EPVn/PVt values calculated from well data in the Sleepy Hollow study area and default EV and Ed values used in CO_2-SCREEN calculations for the Huffstutter Study area. 148
Table 3-33. Prospective storage resource and storage efficiency estimates for the deep saline formations of interest in the Huffstutter study area 148
Table 4-1. Summary of sensitivity cases. 171
Table 5-1. Carbonate Aquifer ROM wellbore leakage parameter maximum values. 180
Table 5-2. NRAP-IAM-CS Input Parameters for Sleepy Hollow Field. 180
Table 5-3. Inputs for Critical Pressure and Threshold Pressure Calculations (Equations 5-1 and 5-2) 185
Table 5-4. Locations of hypothetical open wells. 186
Table 6-1. Ethanol sources and average annual emissions between 2011 and 2015 based on the analysis in Section. 191
Table 6-2. Ethanol sources included in the source corridor pipeline model. 199
Table 6-3. Inside diameter and system outlet pressure at ADM for 6- through 12-inch ID pipe. 201
Table 6-4. Flowrate at operating points for 6- through 12-inch ID pipeline segment between 1500 and 2100 psig. 201
Table 6-5. Flowrates for investigation of line capacity between Blair, NE and Sleepy Hollow Field. Please note that the standard English unit of lbs/s shows up in the legends for the plots below and could not be changed within PIPESIM to show up as kg/day or tones/day. 204
Table 6-6. Summary of pipeline routes generated using SimCCS with overlapping existing pipeline. 212
Table 6-7. Pipeline segments lengths and flow rates. 219
Table 6-8. Existing CO_2 pipelines throughout the United States. 220

Table 6-9. Summary of property ownership (in Nebraska only) for pipeline routes simulated by SimCCS (see Section 6.5.2)..... 223
Table 6-10. Property ownership of parcels intersected by the simulated 40-year plume in the Sleepy Hollow Field. 224
Table 6-11. Current attainment status for criteria pollutants for Nebraska and Kansas (U.S. EPA, 2016). 226
Table 6-12. Federally listed protected species in Nebraska and Kansas (U.S. FWS, 2015a, b; Nebraska Environmental Trust, nd; Kansas Department of Wildlife, Parks, and Tourism, nd). 230
Table 6-13. State listed protected species in the selected areas Note: 1. State Status: E - Endangered, T – Threatened (KDWPT, nd; Nebraska Environmental Trust, nd). 231
Table 7-1. CO_2 source-sink pairs and pipeline routing scenarios evaluated for the IMSCS-HUB Project. 245
Table 7-2. Value of the 45Q tax credit, in dollars per tonne, for CO_2 storage in saline formations and EOR reservoirs calculated for 12 years of project operation*. 247
Table 7-3. Input and definitions of select reservoir parameters used for CO_2-Prophet simulations in the LKC C zone and basal sandstone. 248
Table 7-4. Summary of estimated capture and transport costs and economics with and without 45Q tax credits for six source-sink scenarios. 255
Table 7-5. Summary of estimated saline storage parameters, costs, and project economics with and without 45Q storage credits for the three source-sink scenarios of interest. 256
Table 7-6 . Per pattern CO_2-EOR reservoir performance results for the basal sandstone and LKC “C” zone in the Sleepy Hollow study area. 258
Table 7-7. Summary of estimated per pattern CO_2-EOR costs and project economics with and without 45Q storage credits for the three source-sink scenarios of interest. 259
Table 8-1. List of source providing letters of support (in bold) or considering joining in the IMSCS-HUB along with their average annual emissions (2016 US EPA Reported Data or Personal Communication 2017). 264
Table 9-1. Stakeholders expressing support for Phase II. 276

Acronyms and Abbreviations

2D	Two-Dimensional
3D	Three-Dimensional
CCS	CO_2 Capture and Storage
CO_2	Carbon Dioxide
CO_2-SCREEN	CO_2 Storage prospeCtive Resource Estimation Excel aNalysis
DPHI	Density Porosity
DOE	United States Department of Energy
DT	Sonic Porosity
EDX	Energy Data Exchange
EOR	Enhanced Oil Recovery
ft	Foot
gAPI	American Petroleum Institute Gamma Ray Unit
GR	Gamma Ray Log
GRFS	Gaussian Random Function Simulation
IEAGHG	International Energy Agency Greenhouse Gas
KB	Kelly Bushing
km	Kilometer
LKC	Lansing-Kansas City
Ma	Million Years
md	Measured Depth
mD	Millidarcy
mi	Mile
MPa	Megapascals
msl	Mean Sea Level
Mt	Megatonne; million metric tonnes
NPHI	Neutron Porosity Log
NETL	National Energy Technology Laboratory
OOIP	Original Oil-in-Place
P-value	Probability Value
P_{10}	Probability Value at the 10th Percentile
P_{50}	Probability Value at the 50th Percentile
P_{90}	Probability Value at the 90th Percentile
PHI_e	Effective Porosity
PHI_t	Total Porosity
psi/ft	Pounds per Square Inch per Foot
PV	Pore Volume
RHOB	Bulk Density Log
RT	Resistivity
SEM	Static Earth Model
SPHI	Sonic Porosity
USDWs	Underground Sources of Drinking Water
V_{shale}	Shale Fraction

Executive Summary

Battelle, Archer Daniels Midland (ADM), Schlumberger, the Geological Survey of the Nebraska Conservation and Survey Division (CSD), and Great Plains Energy are developing the Integrated Midcontinent Stacked Carbon Storage Hub (IMSCS HUB) in Nebraska and Kansas. The hub will gather CO_2 along a corridor running between eastern Nebraska (approximately Washington County) and transport it southwest to, approximately, Red Willow County, NE. ADM's corn-ethanol production plant at Columbus, Nebraska will anchor the source corridor pipeline. At the end of the source corridor, the CO_2 will be utilized in local stacked-storage and piped southeast into central Kansas along a stacked-storage corridor accessing additional storage sites. Stacked-storage will be employed using CO_2 enhanced oil recovery (EOR) as a bridge to monetize the CO_2 and offset project costs. The project area (Figure ES-1) includes central and southwest Nebraska and central Kansas. This report describes the work conducted in the first phase, Phase I, of the project.

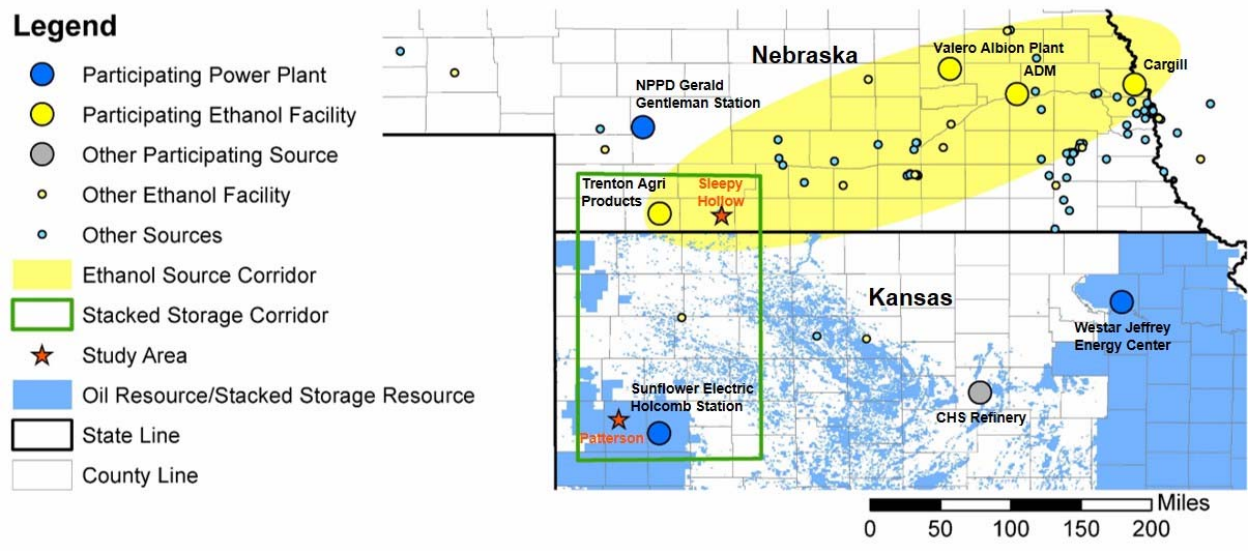

Figure ES-1. Study area showing CO_2 sources and oil fields.

The objectives of Phase I of this project were:

- to establish that a site or sites within the study area will likely be feasible for commercial-scale storage by 2025, and

- To create a coordination team capable of completing future phases of the project.

Team building activities during the project led to the development of a larger team moving into Phase II. Accordingly, the IMSCS-HUB project combined with the Nebraska Integrated Carbon Capture and Storage Pre-Feasibility Study led by Energy and Environment Research Center (EERC), and the Integrated Carbon Capture and Storage for Kansas (ICKan) led by Kansas Geological Survey (KGS).

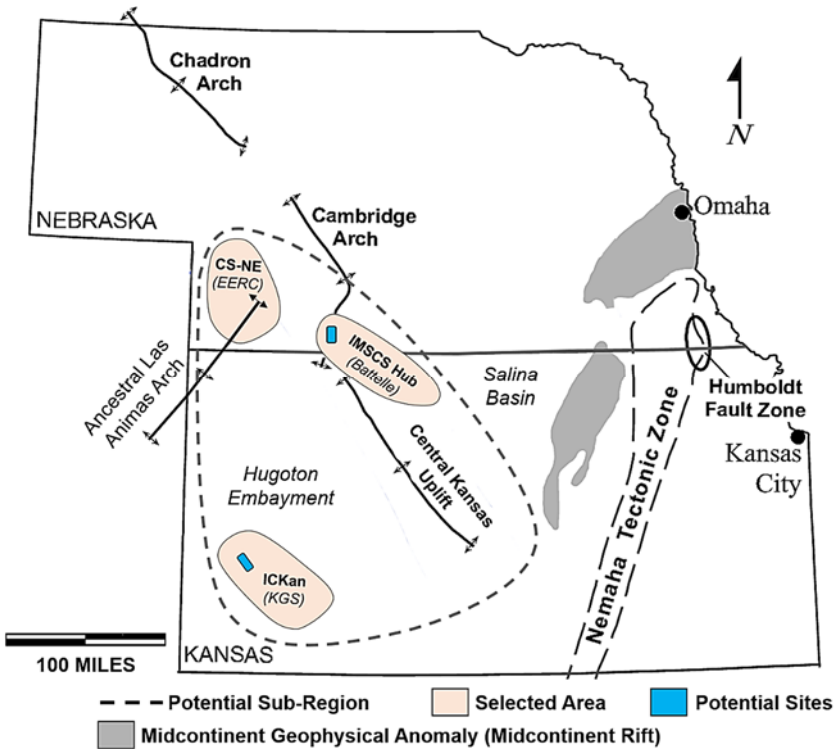

Figure ES-2. Phase I projects represented going forward in Phase II.

The Nebraska-Kansas area offers a unique opportunity for early development of a stacked storage hub due to a high density of ethanol plants which have relatively low capture costs in comparison to other CO_2 sources. This project examined the pre-feasibility of an integrated, geologic CO_2 storage hub in the Mid-Continent Region of the United States (U.S.). The project consisted of six main technical tasks:

- Task 2 – CO_2 Source Identification
- Task 3 – Sub-Basinal Geologic Assessment
- Task 4 – CO_2 Injection/Storage Assessment
- Task 5 – CO_2 Capture and Transportation Assessment
- Task 6 – Economic and Liability Assessment
- Task 7 – Policy, Outreach, and Permitting
- Task 8 – Phase II Planning

This report describes the results of these tasks and the task-specific objectives, methodologies, and results and how they relate to the next phase, Phase II, of the project. The combined results from Phase I indicate that a commercial scale project in the study area is likely feasible. The Paleozoic deep saline storage zones in southwest-central Nebraska and southwest Kansas have prospective storage resource ranging from 30 Mt to 50 Mt at the P10 percentile, suggesting a high probability of storing commercial-scale quantities of CO_2 at individual sites in these selected areas. Dynamic simulations at potential sites in the Sleepy Hollow oilfield in Nebraska, and the Patterson oilfield in Kansas indicate permanent and safe injection of 50-60 Mt of CO_2 is feasible over 30 years at injection pressures below 90% of the fracture pressure.

The source identification assessment examined a 44-county study area running from eastern to southwestern Nebraska comprising 46 point sources. The results of the CO_2 source assessment indicate that the commercialization of the hub can employ CO_2 derived from ethanol sources. Within the ethanol source corridor, there are 18 ethanol plants with average annual emissions of 5.7 Mt of CO_2 and a standard deviation over the last 5 years of 0.1 Mt per year, indicating that the ethanol production in the area is reliable.

Average annual emissions for the 18 ethanol production facilities in the study area are presented by facility in Table 2-5, Figure 2-5, and Figure 2-6. Several large ethanol plants exist in the study area, including the ADM facility, which is the fourth largest emitting facility in the state. Overall, ethanol emissions rose between 2011 and 2015 from 3.1 MMt CO_2e to 3.3 MMt CO_2e, respectively (Figure 2-6).

Table ES-1. Reported emissions (in Mt CO_2e), 2011-2015, for ethanol facilities in study area (US EPA, 2016).

Facility	County	Rank Based on Annual Emissions	Ethanol Category Rank	2011-2015 Total Emissions (Mt CO_2e)	Average Emissions 2011-2015 (Mt CO_2e)	Standard Deviation of Emissions 2011-2015 (Mt CO_2e)
Archer Daniel Midland	Platte	4	1	5,863,690	1,172,738	38,824
Cargill Corn Milling North America	Washington	7	2	2,237,276	447,455	71,799
AGP Soy/Corn Processing	Adams	8	3	1,021,652	204,330	53,361
Green Plains Wood River, LLC.	Hall	10	4	826,192	165,238	49,478
Chief Ethanol Fuels, Inc.	Adams	11	5	817,142	163,428	8,100
Flint Hills Resources, Fairmont, LLC	York	12	6	798,112	159,622	6,872
Valero Albion Plant	Boone	13	7	778,630	155,726	32,397
Green Plains Central City	Merrick	15	8	624,058	124,812	2,477
Abengoa Bioenergy of Nebraska, LLC	Buffalo	16	9	573,838	114,768	13,523
Abengoa Bioenergy Co., LLC[1]	Fillmore	18	10	508,180	101,636	6,488
Green Plains ORD	Valley	19	11	403,842	80,768	2,265
Pacific Ethanol Aurora West LLC	Hamilton	22	12	212,985	70,995	69,297
Elkhorn Valley Ethanol, LLC	Madison	24	13	316,339	63,268	5,773
Kaapa Ethanol, LLC	Kearney	26	14	304,608	60,922	4,099
AltEn, LLC	Saunders	29	15	51,140	51,140	-
Nebraska Corn Processing	Furnas	30	16	254,590	50,918	2,474
Trenton Agri Products	Hitchcock	32	17	224,025	44,805	2,806
Pacific Ethanol Aurora East, LLC	Hamilton	35	18	178,059	35,612	24,449
All Facilities				**15,994,358**	**3,268,182**	**-**

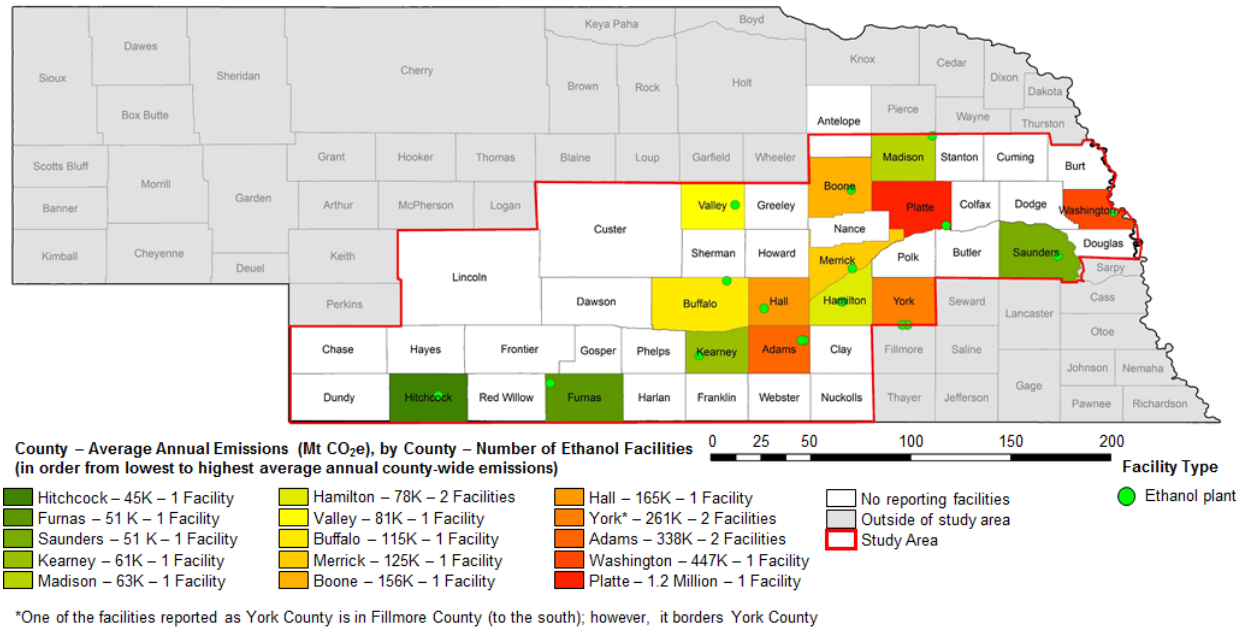

Figure ES-3. Ethanol sources in the study area.

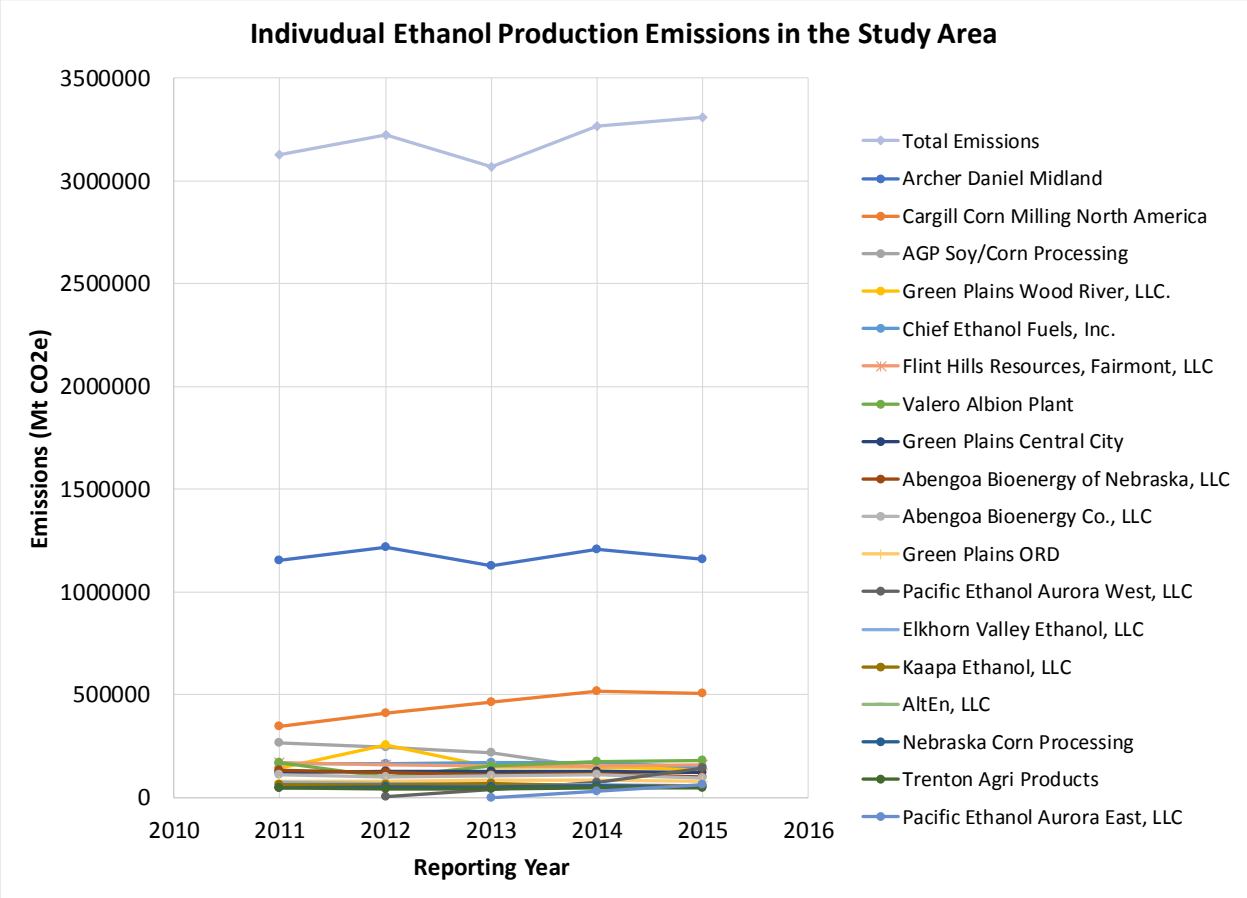

Figure ES-4. Plot showing individual facility and total ethanol-related emissions

In addition to ethanol plants, two large coal-fired electric generation plants that could act as CO_2 emission sources that can deliver CO_2 to the pipeline were also identified. The Westar Energy Company's Jeffery Energy Center (JEC) is a large coal-fired power plant located in St. Mary's, Kansas, and contains three separate 800 MWe (megawatt electricity) units. JEC has 10.8 Mt of annual CO_2 emissions. Nebraska Public Power District's (NPPD) Gerald Gentleman Station (GGS) is Nebraska's largest coal-fired electricity-generating station. GGS is located near Sutherland, Nebraska. GGS consists of 665 MWe and 700 MWe generating units with annual emissions of 7.5 Mt of CO_2.

The simpler and cheaper capture process associated with ethanol-derived CO_2 led the Phase I project to focus on ethanol plants as an initial CO_2 Source. This will remain the focus in Phase II. Three hypothetical source corridor routes connecting ethanol plants were discussed. Each possible corridor had commercial-scale CO_2 emissions, between 2.1 and 2.4 MMt CO_2e/year. This helps to validate the results of the transportation assessment demonstrating that multiple viable pipeline routes capable of delivering 1.7 MMt per year or more can connect the ethanol and coal fired power plant sources in Nebraska and northeastern Kansas with the storage corridor in southwestern Nebraska and western Kansas. The presence of many existing pipelines in the study area demonstrates the viability of pipeline projects in terms of public perception and government regulations. The pipeline sizing results show that a pipeline can be developed to handle the CO_2 from current ethanol source and still have some extra capacity for growth with a minimal number of booster stations.

An analysis of property owners along the pipeline route shows that the pipeline can be routed through an area with large parcels and relatively few landowners. The routes can be optimized to deal with as few land owners as possible and to take advantage of the most existing rights-of-way as possible in future phases. The assessment of sensitive populations and sensitive area did not find any significant problems that could affect the overall success of the project. Sensitive areas and populations can be avoided by pulling the maps created into SimCCS for further modeling to develop routes around them without significant impact on pipeline length.

Stakeholders, in addition to ethanol plants, for the IMSCS-HUB project include state agencies, businesses, trade associations, non-governmental organizations (NGOs), and the public. During Phase I, the IMSCS-HUB team engaged in outreach with state agencies, businesses, trade associations, and NGOs and secured letters of support from the organizations outlined in Table 9-1.

Table ES-2. Stakeholders expressing support for Phase II.

Agency	NGO/Association	Ethanol Prodicer	Electric Utility	Oil Producer	Other
KS Gov. Colyer	Clean Air Task Force	ADM	NPPD	Berexco	ION Engineering
NE Ethanol Board	Great Plains Institute	Cargill	Westar Energy	Merit Energy	MV Purchasing
NE Dept. of Agriculture	Kansas Independent Oil and Gas Association	Trenton Agri Products	Sunflower Electric Power	Great Plains Energy	The Linde Group
NE Dept. of Environmental Quality	NE Petroleum Producers Association	Valero Renewables	Kansas City Board of Public Utilities	Casillas Petroleum	
NE Corn Board	Renew Kansas	Pacific Eth.		Central Operating	
NE Energy Office					

Analysis of stakeholders and communities potentially affected by the proposed project indicates there is a low population density near each potential site, with a majority of the land being used for agricultural and industrial purposes. Nearby residents will be familiar with negotiating oil and gas leases and seeing oil and gas equipment operating; and as such they could be more amenable to leasing pore space beneath their property.

The pre-feasibility assessment of commercial-scale geologic CO_2 storage hub in the Midcontinent evaluated the suitability of the Pennsylvanian-Permian interval to serve as a geologic CO_2 storage complex at two selected areas, the Sleepy Hollow Field and the Patterson Heinitz Hartland Field. Porous and permeable Paleozoic deep saline formations have been identified as potential geologic storage complexes in southwest-central Nebraska and western Kansas. Paleozoic sedimentary rocks in the sub-region are characterized by thick stratigraphic successions of alternating marine and non-marine sedimentary rocks comprised of deep saline formations, oil-bearing reservoirs, shales, and evaporites. The proportion of shales and evaporites increases upward through the Paleozoic interval, forming regionally extensive caprock units for the underlying storage zones.

At Sleepy Hollow Field, four main lithostratigraphic groups in the Pennsylvanian System were evaluated for deep saline CO_2 storage. In ascending order, they include: the Pleasanton-Marmaton, the Lansing-Kansas City, the Shawnee-Douglas, and the Wabaunsee groups (Figure 3-2). Potential storage targets within each group include sandstone intervals (5-20 feet [ft]) in the Wabaunsee and Pleasanton-Marmaton groups, and porous limestones (5-25 ft) in the Shawnee-Douglas and Lansing-Kansas City groups. The deep saline zones of interest in the Lansing-Kansas City occur at the top and the base of the unit; and are separated by productive oil-bearing zones.

Directly overlying the Wabaunsee Group, shales, carbonates, and evaporites deposited during the Late Pennsylvanian and Permian have potential to act as caprocks for the underlying storage reservoirs. These potential caprocks include, in ascending order: Admire, Council Grove, Sumner, and lower Nippewalla groups (Figure 3-2).

Secondary confining units are present at shallower depths in each study area (200-400 ft), and include the Dakota Formation (Dakota Group in Nebraska), Graneros Shale, Greenhorn Limestone, and Carlile Shale.

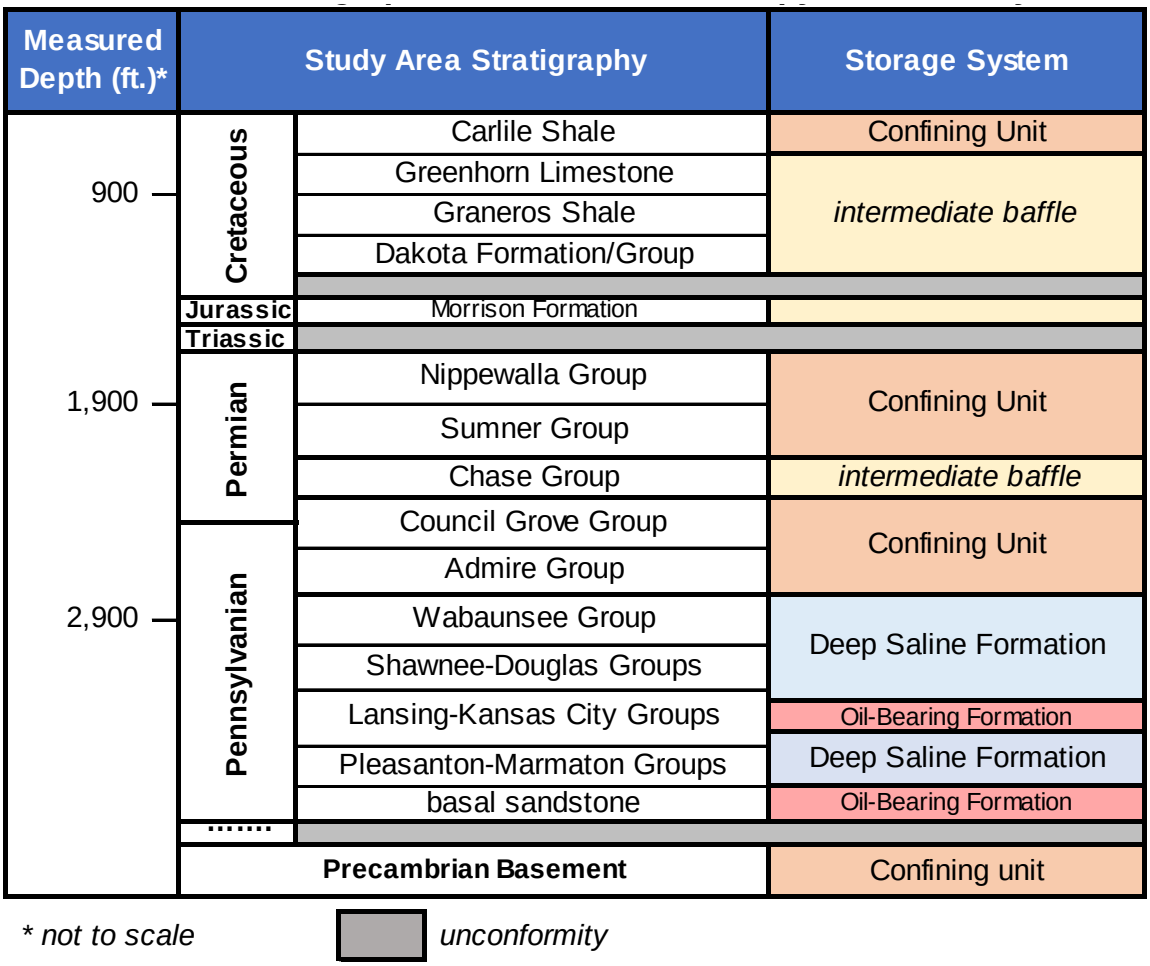

Figure ES-5. Simplified stratigraphic column showing the deep saline formations of interest and overlying caprocks evaluated in both study areas.

Alternating stratigraphic successions of marine and non-marine sediments are a distinguishing feature of the Pennsylvanian-Permian sequence in the Midcontinent. These stratigraphic successions are unique to the study region and have critical importance in the development of geologic conditions conducive to commercial-scale CO_2 injection and storage.

The structural and stratigraphic framework of Nebraska and Kansas was defined to guide data analysis and inform geologic modeling efforts. Site-specific geologic characterization was conducted via petrophysical analysis, construction of heterogenous site models and geologic maps, and calculation of prospective storage resources for the deep saline interval of the Pennsylvanian system.

Analysis of data from more than 300 digital well logs and more than 200 core analyses in the selected areas indicates the Paleozoic intervals of interest have suitable reservoir properties for storing large

quantities of CO_2. Porosities as high as 16–32% and maximum permeabilities ranging from approximately 100 to 1,000 millidarcies (mD) have been measured at each potential site.

Results were used to identify potential qualified sites for further characterization and help establish the groundwork for commercial-scale development of geologic CO_2 storage resources in the Midcontinent Region.

The assessment included:

- Construction of 3D SEMs representing the geologic storage framework of the Pennsylvanian-Permian interval at each of the selected study areas
- Development of workflows to establish a consistent, repeatable methodology for site-scale geologic resource characterization that can be easily applied to other potential sites in the region
- Characterization of key confining system components including hydrocarbon trapping mechanisms, and caprock structural and stratigraphic continuity
- Quantification of site-specific storage efficiencies and prospective storage resource of the deep saline Pennsylvanian interval in both study areas

Site-scale analysis and mapping of potential storage zones generally show small variation in formation properties within the Sleepy Hollow Field, with regional structures such as the Cambridge Arch likely responsible for local map variations and the development of reservoir properties. Other key outcomes and takeaways for Sleepy Hollow Field are summarized below:

- Distinct, laterally continuous net reservoir intervals observed in the Wabaunsee and Pleasanton-Marmaton groups at both study areas suggest net reservoir zones may be traceable and continuous over distances of 50 miles or greater.
- Prospective storage resource results calculated at the P_{10} probability value (49.7 - 80.8 Mt) indicate a high level of confidence in the likelihood that the deep saline CO_2 storage resource is 50 Mt or greater at each site; sufficient for commercial-scale CO_2 storage.

Numerical reservoir modeling of the Sleepy Hollow Field was conducted based on the static earth model of the site. The simulations included different well location configurations, and a sensitivity analysis.

The ECLIPSE E300 compositional reservoir simulator was used to model saline storage at Sleepy Hollow Field. Continuous injection was modeled for eight individual hypothetical wells subject to the maximum allowable BHP constraint. After the continuous 30-year injection, the greatest cumulative CO_2 storage was obtained from INJ #2 and #6 then followed by INJ #5, #1, #4, and #8. INJ #3 and #7 showed the lowest injectivity. The greatest cumulative CO_2 injection at INJ #2 was approximately 34.8 million metric tons after 30 years resulting in a 30-year average injection rate of 3,177 metric tons per day (Figure 4-8). The lowest average injection rate was found at INJ #7 with a rate of 2,662 metric tons per day. The single well simulation results show very good injectivity performance. No single well injection case could achieve the storage target (50 million metric tons for 30 years), which led to a three-well CO_2 storage system to meet the injection goal.

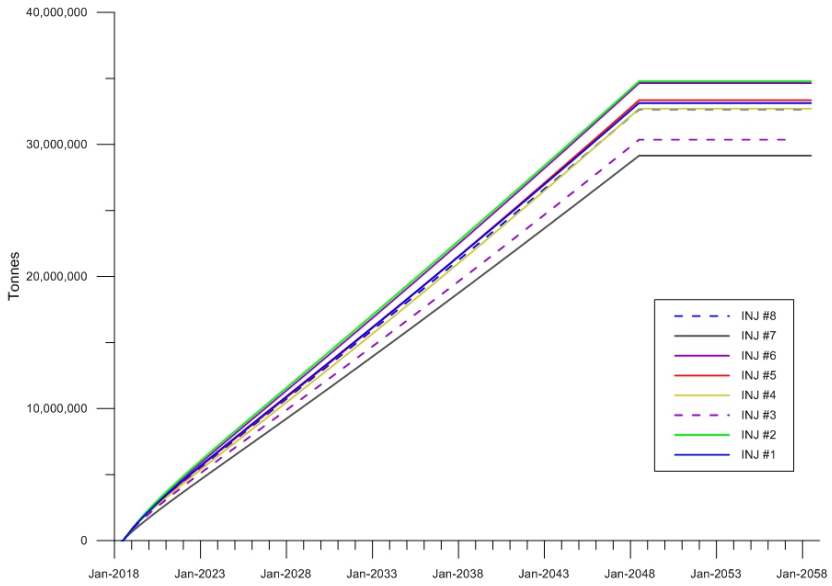

Figure ES-6. Simulated cumulative CO_2 injection (metric tons) vs. time for singe-well cases.

Figure 4-18 illustrates the temporal evolution of the CO_2 plume during and post CO_2 injection by plotting the edge of the CO_2 plume defined as CO_2 gas saturation of 0.01 (or 1%). The CO_2 plume edge centered from each injector tends to grow radially. The entire CO_2 plume from three injectors extends approximately 9 km in the East-West direction and 11 km in the North-South direction after the 30-year injection.

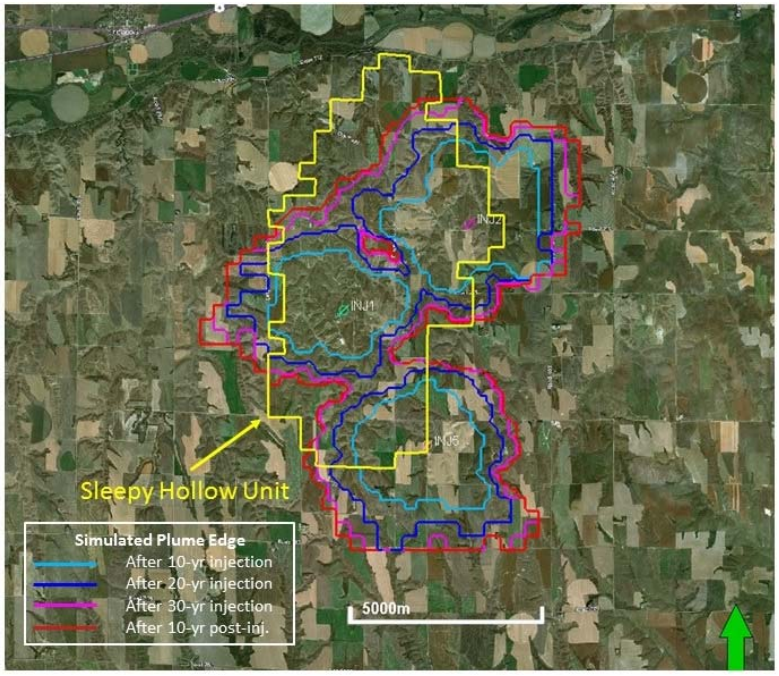

Figure ES-7. Edge of the simulated CO_2 plume after 10, 20, and 30-year injection and 10-year post-injection period.

The following conclusions are drawn based on the results of the modelling efforts:

- The simulation results with a single injector show very good injectivity performance. INJ #2 could inject approximately 34.8 million metric tons after 30 years resulting in an average injection rate of 3,177 metric tons per day.
- No single-well injection case could achieve the storage target (50 million metric tons for 30 years); a multi-injector system is required.
- At least three injection wells are required to satisfy the injection target in the study area. Best results were obtained when using INJ #1, #2, and #5.
- Major CO_2 storage occurs at Wabaunsee (26%), Kansas City Base (19%), Topeka (18%), Oread (15%), LKC A (8%), and Deer Creek (6%).

Potential challenges identified as part of the economic and liability assessment for the IMSCS-HUB Project included development of pipeline infrastructure and Underground Injection Control Program (UIC) Class VI corrective actions from existing wellbores in the study area. Existing natural gas pipelines routed directly to ethanol plants occur within 3 miles of each potential storage site, and the IMSCS-HUB study area is roughly located between existing CO_2 pipeline networks in the U.S. These pipeline rights of way can be leveraged for CO_2 pipeline development for the project.

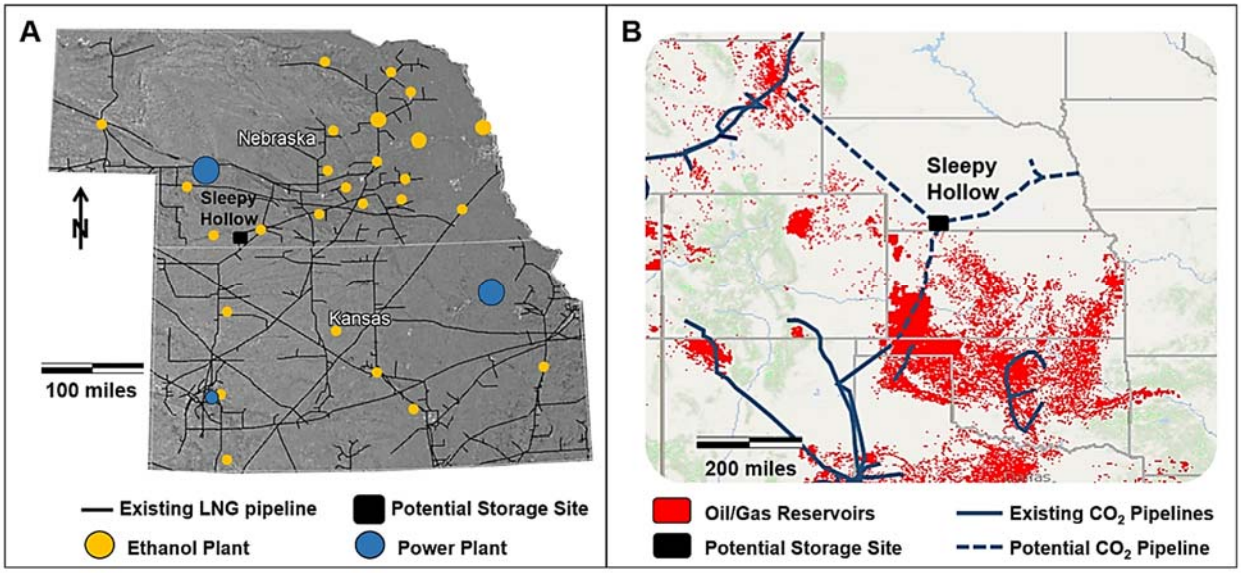

Figure ES-8. (A) Map showing existing natural gas pipelines in Nebraska and Kansas along with locations of ethanol plants, power plants, and the potential Sleepy Hollow storage site;(B) Map showing the Sleepy Hollow site alongside oil/gas fields and existing and potential CO_2 pipelines in the United States (map data from EIA, 2016; NATCARB, 2017).

The economic incentives for construction of the proposed pipeline will be further evaluated in Phase II, including consideration of CO_2-EOR, 45Q, and the ethanol industry. Low population density, and widespread agricultural land use suggests rural areas aren't likely to undergo significant development in the next 20 years, ensuring opportunities will remain for the IMSCS-HUB to expand and access existing CO_2 pipeline networks.

A distinct advantage of the IMSCS-HUB project is that the technology for ethanol-based CO_2 capture and transport for EOR is currently economically feasible and can be commercially deployed today to subsidize ethanol CO_2 saline storage, and provide scalable infrastructure needed to integrate CO_2 capture from power plants in the future. For saline storage costs and credits, the 45Q tax credit can only be claimed for 12 years after the beginning of capture but is spread across the total amount of CO_2 stored for the entire project. Despite the positive net present values with the 45Q tax credit, the discounted net profit from saline storage (~ \$9/tonne CO_2) is still less than the combined capture and transport costs estimated for each scenario (\$40 - \$76/tonne CO_2), suggesting the 45Q tax credit is not enough alone to pay for capture, transport, and saline storage costs associated with an integrated CCS operation in the IMCSCS-HUB

The per pattern economic scenario results with and without 45Q EOR storage credits show a positive net present value for the Sleepy Hollow Field study area, suggesting that profit could be made to help offset the CO_2 capture costs at the desired rate of return for the EOR operation. Net present values of approximately \$42/tonne CO_2 for CO_2-EOR operations with 45Q storage credits suggests the tax credit can be used in conjunction with EOR to close the deficit and pay for the capture, transport, and storage components of the CCS project in the IMSCS-HUB. The economic analysis provides evidence of the need for stacked storage in oil-producing areas where CO_2-EOR and the 45Q tax credit can be used subsidize the capture and transport infrastructure needed to collect and move CO_2 and then saline projects can take advantage of the infrastructure to store additional CO_2.

The assessment of the liabilities identified for the project are generally similar to those of oil and gas or other subsurface projects and that they can be addressed through regulatory, contractual, and insurance mechanisms. The analysis of the potential for problems with rights of way and environmentally sensitive areas do not look insurmountable because the pipeline and field sites are likely in sparsely populated locations with few sensitive areas. In addition, problems arising from injection operations are likely to be minimized due to the colocation of the storage site with oil and gas operations, better ensuring the public in the area are familiar with drilling and injection equipment and operations.

Existing hydrocarbon resources in the Sleepy Hollow study area and the potential for a hybrid of CO_2-EOR and geologic storage may provide technical advantages, infrastructure, and economic incentives needed to successfully commercialize CCS in the region. Saline storage alone cannot be fully supported by the 45Q tax credit under a saline scenario or a CO_2-EOR scenario. However, the use of EOR as a business case for storage provides an income from oil production that can help subsidize the construction and operation of storage projects allowing future projects to take advantage of the infrastructure, lowering costs.

The IMSCS HUB project is a significant opportunity to implement a commercial CCS project for many reasons, not the least of which is the potential to link saline storage aquifers and oilfields in southwestern Nebraska and eastern Kansas to ethanol sources in Nebraska and, potentially, the rest of the Midcontinent region. Ethanol-derived-CO_2 provides a relatively pure stream of CO_2 that can be easily captured at commercial volumes with off-the-shelf equipment. The cost of capture at ethanol CO_2 sources is relatively low compared to other industrial sources. Both of these factors allow for early implementation of a commercial carbon storage hub.

1 Introduction

Battelle, Archer Daniels Midland (ADM), Schlumberger, the Geological Survey of the Nebraska Conservation and Survey Division (CSD), and Great Plains Energy are developing the Integrated Midcontinent Stacked Carbon Storage Hub (IMSCS-HUB) in Nebraska and Kansas. The hub will gather CO_2 along a corridor running between eastern Nebraska (approximately Washington County) and transport it southwest to, approximately, Red Willow County, NE. ADM's corn-ethanol production plant at Columbus, NE will anchor the source corridor pipeline. At the end of the source corridor, the CO_2 will be utilized in local stacked-storage and piped southeast into central Kansas along a stacked-storage corridor for additional stacked-storage. Stacked-storage will be employed using CO_2 enhanced oil recovery (EOR) as a bridge to monetize the CO_2 and offset project costs. The project area (Figure 1-1) includes central and southwest Nebraska and central Kansas. This report covers the first phase, Phase I, of the project.

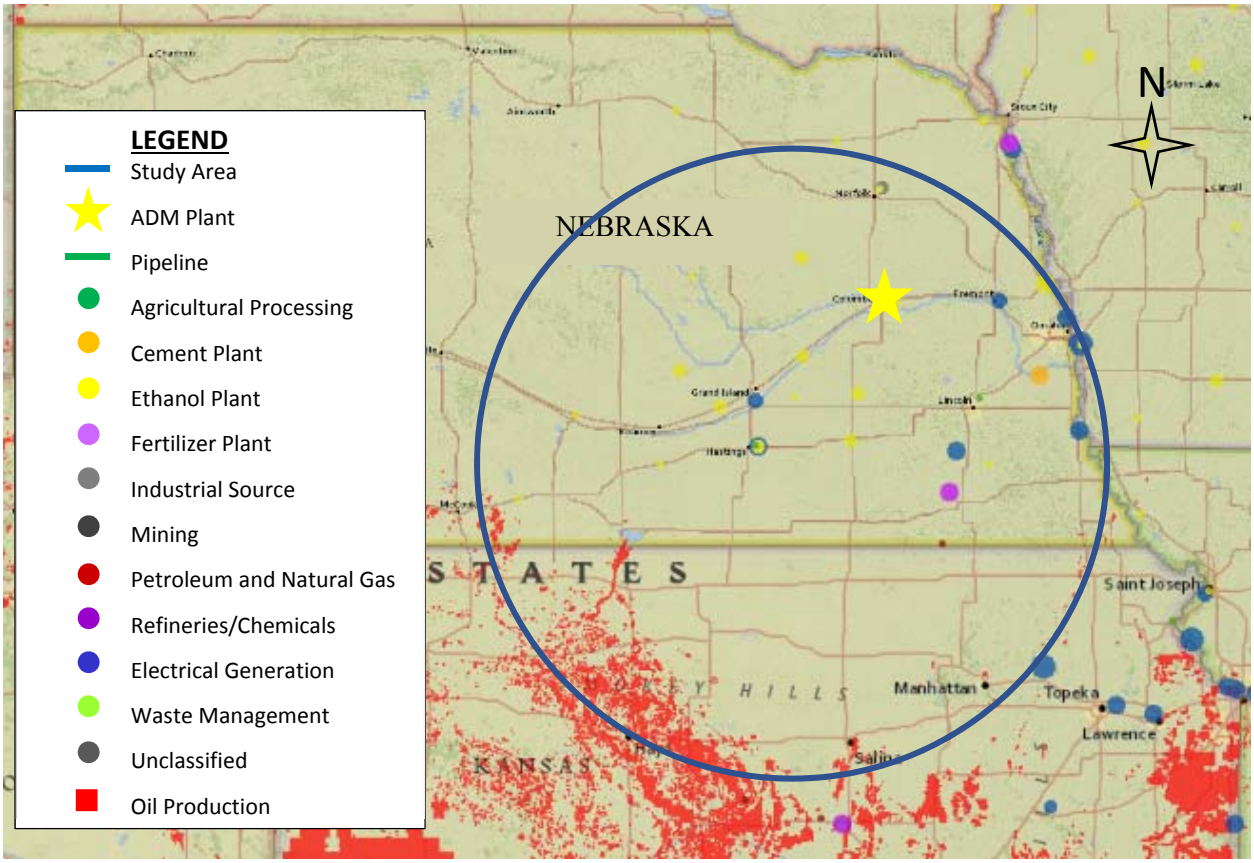

Figure 1-1. Study area showing CO_2 sources and oil fields.

The objectives of Phase I of this project were:

- to establish that a site or sites within the study area will likely be feasible for commercial-scale storage by 2025, and
- To create a coordination team capable of completing future phases of the project.

Team building activities during the project led to the development of a larger team moving into Phase II. As a result, the IMSCS-HUB project combined with the Nebraska Integrated Carbon Capture and Storage Pre-Feasibility Study led by Energy and Environment Research Center at the University of North Dakota (EERC), and the Integrated Carbon Capture and Storage for Kansas (ICKan) led by the Kansas Geologic Survey (KGS). As a result of combining teams some sources mentioned in Section 8 were not included in the initial source assessment described in Section 2.

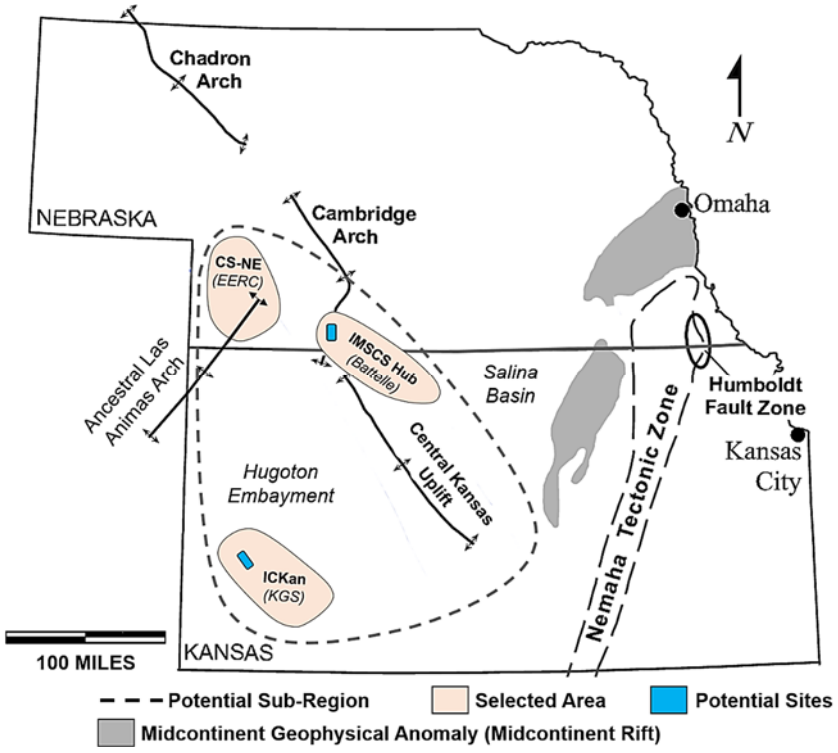

Figure 1-2. Phase I projects represented going forward in Phase II.

The Nebraska-Kansas area offers a unique opportunity for early development of a stacked storage hub due to a high density of ethanol plants which have relatively low capture costs in comparison to other CO_2 sources. This project examined the pre-feasibility of an integrated, geologic CO_2 storage hub in the Mid-Continent Region of the United States (U.S.). The project consisted of six main technical tasks:

- Task 2 – CO_2 Source Identification
- Task 3 – Sub-Basinal Geologic Assessment
- Task 4 – CO_2 Injection/Storage Assessment
- Task 5 – CO_2 Capture and Transportation Assessment
- Task 6 – Economic and Liability Assessment
- Task 7 – Policy, Outreach, and Permitting
- Task 8 – Phase II Planning

This report describes the results of these tasks and the task-specific objectives, methodologies, and results and how they relate to the next phase, Phase II, of the project. This report contains the following

sections: 2 CO_2 Sources, 3 Geology, 4 Reservoir Simulation, 5 5 Assessment of the Area of Review for the Sleepy Hollow Field using the NRAP-IAM-CS, 6 CO_2 Capture and Transport, 7 Economics and Liability, 8 Phase II planning, and 9 Conclusions.

2 CO_2 Sources

2.1 Background

The IMSCS-HUB identified two corridors in the study area; a CO_2 collection corridor (source corridor), and a stacked-storage corridor (Figure 1-1). The source corridor could run from the Cargill Ethanol plant in Blair, NE west to the ADM's corn ethanol plant at Columbus, NE and then southwest to the oil fields in and around Red Willow County, NE. The largest ethanol source for the storage complex is ADM's ethanol production facility. ADM's ethanol plant in Columbus, NE, processes corn into a variety of feed and food products. The facility processes about 550,000 bushels of corn per day, primarily sourced within a hundred miles of the facility. The two ethanol plants (wet and dry mill) have the capacity to produce a total of 1.13 million gallons of ethanol per day making this facility the largest ethanol producer in the state of Nebraska. The facility produces about 3,250 metric tonnes (Mt) per day of high purity CO_2 as a byproduct of ethanol production. Capture and conditioning of the CO_2 for the project do not require novel technology development. Capture will be accomplished using the same techniques being used at the Illinois Basin Decatur Project and the Illinois Industrial Carbon Capture and Storage Project. The CO_2 is greater than 99% pure after dehydration. Before dehydration, it contains less than 3% water by weight. The CO_2 will be collected from the corn-to-ethanol fermenters at atmospheric pressure and processed using inter-stage coolers and knock-out vessels to decrease temperature and remove moisture, leaving it dehydrated (less than 0.005% water by weight), making it ready for compression and pipeline transport. In Illinois, ADM uses a 3250 horsepower, 4-stage reciprocating compressor and a dehydration system that uses a triethylene glycol contactor (absorber)-regenerator, we expect a similar system will be employed in Nebraska. Other ethanol sources in the project area are expected to have similarly pure streams of CO_2 after capture and dehydration. More detail on the capture process is presented in Section 5.

2.2 Methods

Information about emissions from facilities of interest was obtained from the United States Environmental Protection Agency Greenhouse Gas Reporting Program (US EPA GHGRP), which collects greenhouse gas emissions data from larger emitters (i.e., sources that generally emit more than 25,000 metric tons of CO_2 a year, per 40 CFR Part 98). Established in 2009, the GHGRP contains data from 2010 through 2015, the latest year with reported emissions (US EPA, 2016a). For this analysis, data from 2011 through 2015 was used because the EPA states that changes to the reporting program made after the first reporting year (2010) do not represent the same scope of emissions and are, therefore, not necessarily comparable (US EPA, 2016b).

The source corridor study area spans 44 counties across Nebraska (Figure 2-1). The general shape of source corridor is defined from the location of the anchor source and the location of the fields that will act as stacked storage locations. The study area contains most of the potential sources reporting emissions. The emissions data were downloaded from the US GHGRP website and grouped by sorted by county, facility, and reporting year. After sorting the data, the sources inside the study area were selected for calculation of average emissions, standard deviation emissions, and total emissions over the five-year period between 2011 and 2015. The data were also sorted into three categories: Ethanol Plants, Electric Power, and Other. Ethanol Plants are plants that primarily produce ethanol, including the ADM plant in Columbus, NE. Electric Power consists of coal burning power plants. The "Other" category includes all other sources. It is important to note that the landfill and meat sources may be

emitting methane instead of CO_2, emissions were reported as CO_2-equivelant (CO_2e). However, landfills are not considered as potential sources for this project.

2.3 Results

A total of 46 reporting facilities are in the source corridor study area (Figure 2-1). These sources were split into groups by facility type. The facilities included 18 ethanol plants, five power plants, and 23 other facilities. Other sources in the area included meat processing, landfill, steel, natural gas, and chemical facilities. The resulting data were mapped and tabulated and allowed the project team to identify the most likely sources for the project allowing outreach to bring them into future phases of the project.

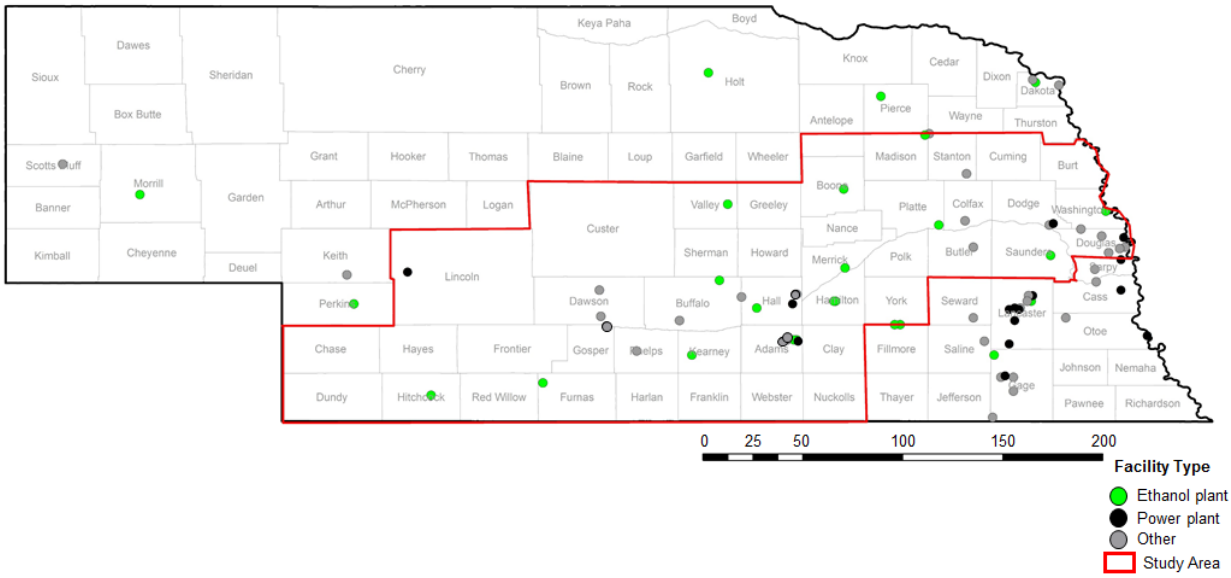

Figure 2-1. Locations of Nebraska facilities reporting in the US EPA GHGRP (US EPA, 2016).

2.3.1 General Results

The results of the analyses indicate that the study area contains around 59% of the total emissions reported in Nebraska between 2011 and 2015. The study area total emissions 2011-2015 were around 96.8 million metric tonnes [MMt] CO_2e. Nebraska's total emissions over this period were around 163 MMt CO_2e. The annual average emissions of the study area were around 19.4 MMt CO_2e.

Table 2-1, Table 2-2 and Figure 2-2 present the emissions data from 2011 through 2015 for all the facilities in the study area. In general, emissions are highest in and around larger urban centers. For instance, the counties that make up Omaha and its suburbs (Douglas, Washington, and Dodge Counties) are three of the top six counties by average annual reported emissions, accounting for a combined total of around 4.8 MMt CO_2e of the approximately 19.4 MMt CO_2e average annual emissions from the study area (around 25%). Adams and Hall Counties have the second and fourth highest average annual emissions for all counties in the study area, accounting for 2.0 MMt CO_2e and 0.84 MMt CO_2e, respectively (approximately 15% of the average annual emissions). Most of the reporting sources in Adams and Hall Counties are in and around the towns of Hastings and Grand Island, respectively. Platte County, where ADM's corn-ethanol production plant at Columbus is the sole reporting source, has the third highest average annual emissions per county. The average annual emissions from this facility account for a little more than 6% of the average annual emissions in the study area.

Table 2-3 presents the total emissions per year in the study area for each facility type. Power plants had the highest total (2011-2015) and annual emissions for all years. Power plant facilities accounted for 77% of the total and average annual emissions in the study area. Ethanol facilities made up around 17% of total and average annual emissions in the study area.

Table 2-1. Reported emissions (Mt CO_2e), 2011-2015, for facilities in study area (US EPA, 2016). Facilities are organized by descending average annual emissions (2011-2015).

Facility	County	Rank Based on Annual Emissions	Facility Category	2011-2015 Total Emissions (Mt CO_2e)	Average Emissions 2011-2015 (Mt CO_2e)	Standard Deviation of Emissions 2011-2015 (Mt CO_2e)
Gerald Gentleman Station	Lincoln	1	Power	43,809,788	8,761,958	451,204
North Omaha Station	Douglas	2	Power	17,417,691	3,483,538	162,037
Gerald Whelan Energy Center	Adams	3	Power	8,090,335	1,618,067	215,583
Archer Daniel Midland	Platte	4	Ethanol	5,863,690	1,172,738	38,824
Platte	Hall	5	Power	3,112,432	622,486	51,921
Lon D Wright Power Plant	Dodge	6	Power	2,747,683	549,537	23,907
Cargill Corn Milling North America	Washington	7	Ethanol	2,237,276	447,455	71,799
AGP Soy/Corn Processing	Adams	8	Ethanol	1,021,652	204,330	53,361
Nucor Steel Nebraska	Madison	9	Other	926,325	185,265	24,583
Green Plains Wood River, LLC.	Hall	10	Ethanol	826,192	165,238	49,478
Chief Ethanol Fuels, Inc.	Adams	11	Ethanol	817,142	163,428	8,100
Flint Hills Resources, Fairmont, LLC	York	12	Ethanol	798,112	159,622	6,872
Valero Albion Plant	Boone	13	Ethanol	778,630	155,726	32,397
Butler Co. Landfill.	Butler	14	Other	642,854	128,571	33,572
Green Plains Central City	Merrick	15	Ethanol	624,058	124,812	2,477
Abengoa Bioenergy of Nebraska, LLC	Buffalo	16	Ethanol	573,838	114,768	13,523
Metropolitan Utilities District of Omaha	Douglas	17	Other	567,854	113,571	39,759
Abengoa Bioenergy Co., LLC[1]	Fillmore	18	Ethanol	508,180	101,636	6,488
Green Plains ORD	Valley	19	Ethanol	403,842	80,768	2,265
Grand Island Regional Landfill	Buffalo	20	Other	385,605	77,121	3,291
Bertrand Compressor Station	Phelps	21	Other	359,640	71,928	15,974
Pacific Ethanol Aurora West LLC	Hamilton	22	Ethanol	212,985	70,995	69,297
Douglas County Recycling Landfill	Douglas	23	Other	342,070	68,414	14,256
Elkhorn Valley Ethanol, LLC	Madison	24	Ethanol	316,339	63,268	5,773
Cargill Meat Solutions	Colfax	25	Other	308,626	61,725	19,713
Kaapa Ethanol, LLC	Kearney	26	Ethanol	304,608	60,922	4,099
NRG Energy Center Omaha, LLC	Douglas	27	Other	279,545	55,909	3,161

Facility	County	Rank Based on Annual Emissions	Facility Category	2011-2015 Total Emissions (Mt CO_2e)	Average Emissions 2011-2015 (Mt CO_2e)	Standard Deviation of Emissions 2011-2015 (Mt CO_2e)
NNSWC Landfill	Stanton	28	Other	279,375	55,875	4,341
AltEn, LLC	Saunders	29	Ethanol	51,140	51,140	-
Nebraska Corn Processing	Furnas	30	Ethanol	254,590	50,918	2,474
Swift Beef Company	Hall	31	Other	246,321	49,264	3,804
Trenton Agri Products	Hitchcock	32	Ethanol	224,025	44,805	2,806
Tyson Fresh Meats	Dawson	33	Other	210,086	42,017	1,015
Hastings Landfill	Adams	34	Other	207,874	41,575	4,059
Pacific Ethanol Aurora East, LLC	Hamilton	35	Ethanol	178,059	35,612	24,449
Kellogg USA, Inc.	Douglas	36	Other	175,175	35,035	2,597
University of Nebraska Medical Center	Douglas	37	Other	147,117	29,423	2,331
Douglas County Landfill	Douglas	38	Other	133,396	26,679	34,927
Hormel Foods	Dodge	39	Other	132,913	26,583	1,571
Lexington Area Solid Waste Agency	Dawson	40	Other	77,388	25,796	3,321
Kearney Area Solid Waste Agency	Buffalo	41	Other	79,462	19,866	2,278
NatureWorks LLC	Washington	42	Other	82,457	16,491	22,582
Canaday	Gosper	43	Other	41,534	8,307	11,995
C W Burdick	Hall	44	Other	11,606	2,321	1,892
North Denver Station	Adams	45	Other	2,432	486	453
Don Henry Power Center	Adams	46	Other	870	174	214
All Facilities				**96,812,812**	**19,446,164**	**-**

Notes: 1. While Abengoa Bioenergy is technically located in the county south of York (Fillmore County), it is right on the border of York County.

Table 2-2. Reported emissions (Mt CO_2e), 2011-2015, for counties in study area (US EPA, 2016).

County	No. Facilities	Sum, 2011-2015	Average Annual, 2011-2015 (by Co.)[1]	Average Annual, 2011-2015 (by Fac.)[2]	2015 Emissions
Adams	6	10,140,305	2,028,061	338,010	1,784,148
Boone	1	778,630	155,726	155,726	178,809
Buffalo	3	1,038,905	207,781	74,208	202,374
Butler	1	642,854	128,571	128,571	160,224
Colfax	1	308,626	61,725	61,725	39,154
Dawson	2	287,474	57,495	35,934	66,856
Dodge	2	2,880,596	576,119	288,060	548,616
Douglas	7	19,062,848	3,812,570	544,653	3,695,797
Furnas	1	254,590	50,918	50,918	52,744
Gosper	1	41,534	8,307	8,307	3,805
Hall	4	4,196,551	839,310	209,828	804,105
Hamilton	2	391,044	78,209	48,881	203,596
Hitchcock	1	224,025	44,805	44,805	47,226
Kearney	1	304,608	60,922	60,922	58,621
Lincoln	1	43,809,788	8,761,958	8,761,958	8,331,468
Madison	2	1,242,664	248,533	124,266	207,673
Merrick	1	624,058	124,812	124,812	121,624
Phelps	1	359,640	71,928	71,928	60,113
Platte	1	5,863,690	1,172,738	1,172,738	1,160,743
Saunders	1	51,140	51,140	51,140	51,140
Stanton	1	279,375	55,875	55,875	61,268
Valley	1	403,842	80,768	80,768	79,476
Washington	2	2,319,733	463,947	231,973	506,338
York[3]	2	1,306,292	261,258	130,629	252,263

Notes: 1. Average yearly emissions for entire county (i.e., sum of emissions for all years for all sources in the county divided by number of years). 2. Average yearly emissions for a single average facility in the county. 3. The Abengoa Bioenergy is included in York County. Though located in the Fillmore County to the south, it is right on the border of York County.

Table 2-3. Annual, total, and average emissions by facility type, 2011-2015 (US EPA, 2016).

Facility Type	Number of Facilities	Emissions (MMt CO_2e)						
		2011	2012	2013	2014	2015	Total	Average Annual
Ethanol	18	3.1	3.2	3.1	3.3	3.3	16	3.2
Power Plants	5	15.6	14.5	16.0	14.8	14.3	75.2	15.0
Other	23	1.1	1.1	1.2	1.0	1.1	5.6	1.1
Total in study area	**46**	**19.8**	**18.8**	**20.3**	**19.1**	**18.7**	**96.8**	**19.4**
Total outside of study area		**13.7**	**13.4**	**13.6**	**13.2**	**12.6**	**66.5**	**13.3**

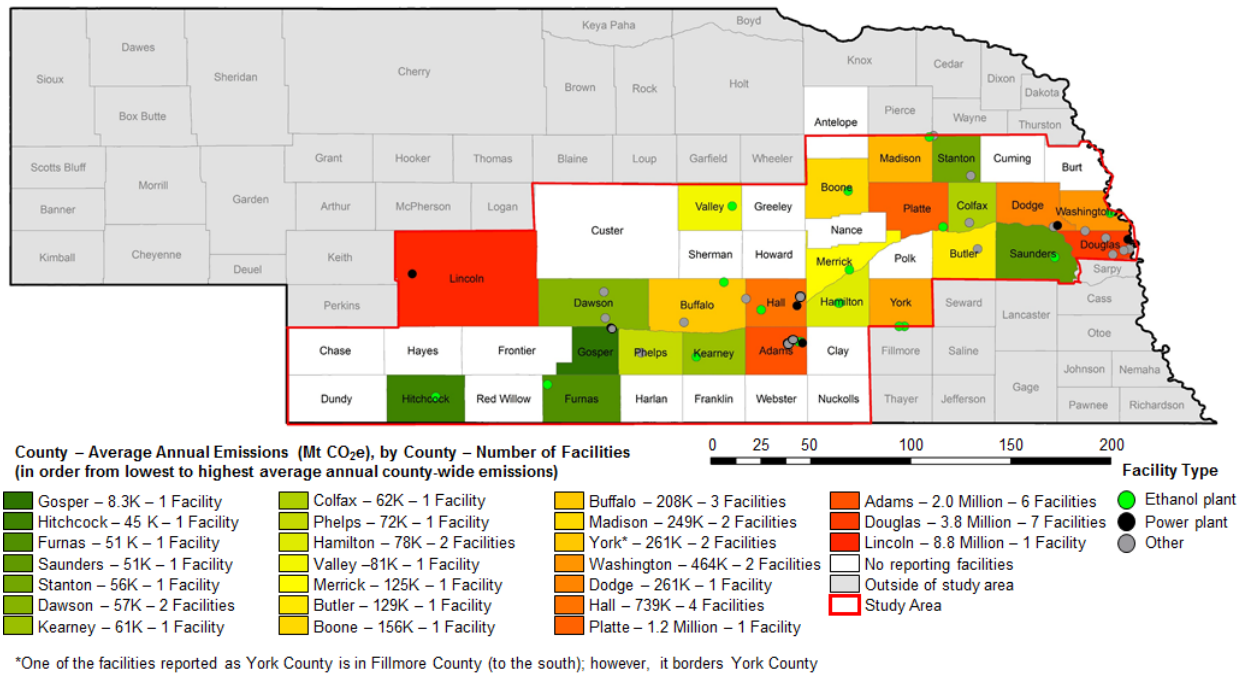

Figure 2-2. Map showing the location of all sources in the study area.

2.3.2 Electric Power

Table 2-4, Figure 2-3, and Figure 2-4 present the emissions data for the power plants in the study area. Power plants had the highest total and average annual emissions of the three source categories. The facilities were: The Gerald Gentleman Station (Lincoln County), the Gerald Whelan Energy Center (Adams County), the Lon D. Wright Power Plant (Dodge County), the North Omaha Station (Douglas County), and the Platte Power Plant (Hall County). Overall emissions fell over the period between 2011 and 2015 from 15.6 MMt CO_2e to 14.3 MMt CO_2e, respectively (Figure 2-4).

Table 2-4. Reported emissions (Mt CO_2e), 2011-2015, for power plant facilities in study area (US EPA, 2016).

Facility	County	Rank Based on Annual Emissions	Power Plant Category Rank	2011-2015 Total Emissions (Mt CO_2e)	Average Emissions 2011-2015 (Mt CO_2e)	Standard Deviation of Emissions 2011-2015 (Mt CO_2e)
Gerald Gentleman Station	Lincoln	1	1	43,809,788	8,761,958	451,204
North Omaha Station	Douglas	2	2	17,417,691	3,483,538	162,037
Gerald Whelan Energy Center	Adams	3	3	8,090,335	1,618,067	215,583
Platte	Hall	5	4	3,112,432	622,486	51,921
Lon D. Wright Power Plant	Dodge	6	5	2,747,683	549,537	23,907
All Facilities				**75,177,929**	**15,035,586**	-

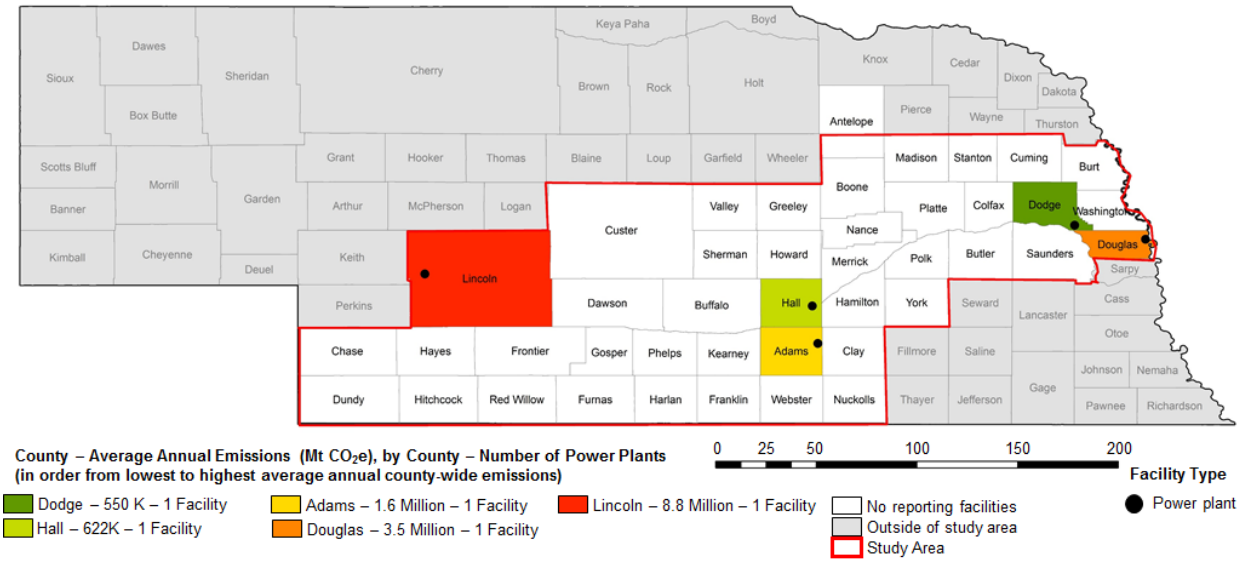

Figure 2-3. Electric power sources in the study area.

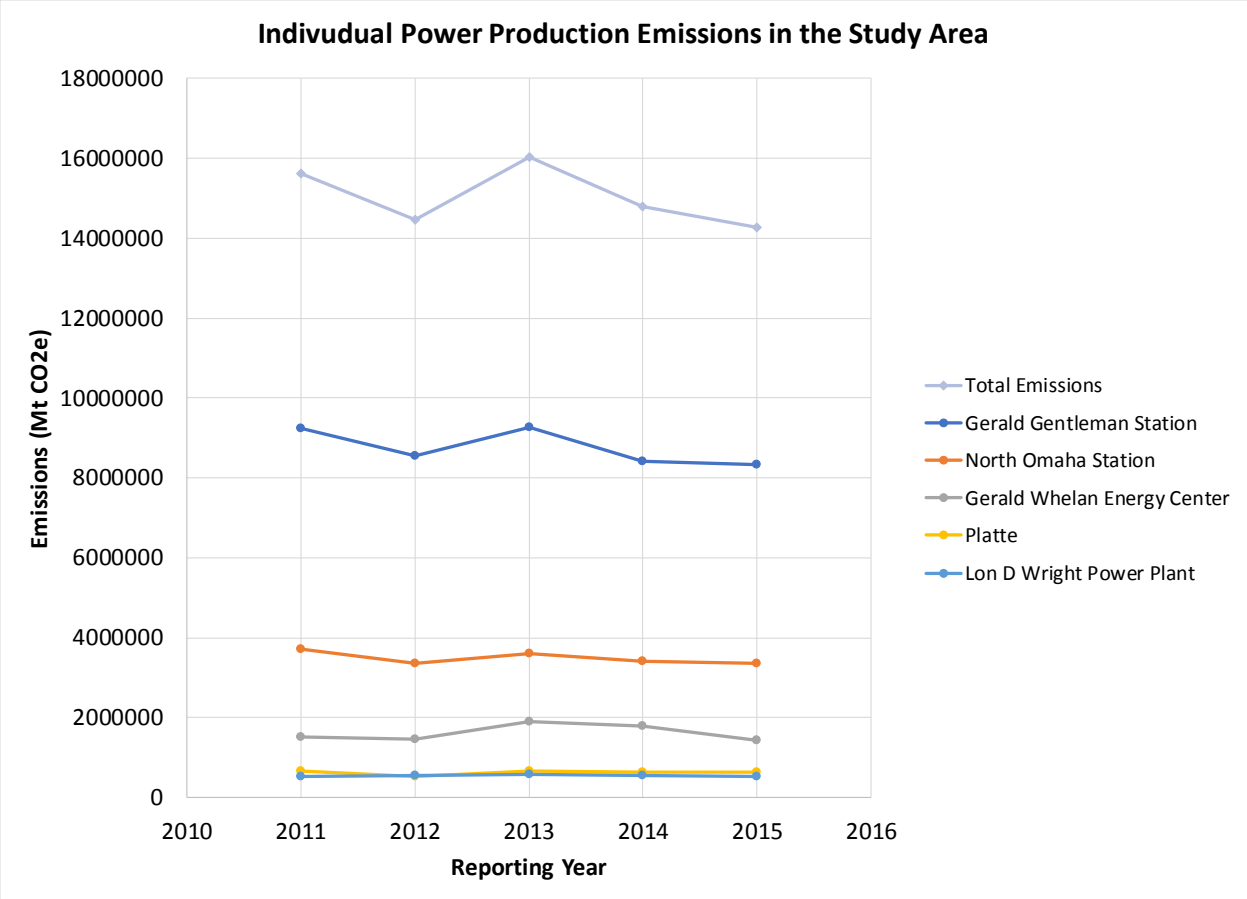

Figure 2-4. Plot showing individual facility and total power-related emissions.

2.3.3 Ethanol

Average annual emissions for the 18 ethanol production facilities in the study area are presented by facility in Table 2-5, Figure 2-5, and Figure 2-6. Several large ethanol plants exist in the study area, including the ADM facility, which is the fourth largest emitting facility in the state. Overall ethanol emissions rose between 2011 and 2015 from 3.1 MMt CO_2e to 3.3 MMt CO_2e, respectively (Figure 2-6).

Table 2-5. Reported emissions (in Mt CO_2e), 2011-2015, for ethanol facilities in study area (US EPA, 2016).

Facility	County	Rank Based on Annual Emissions	Ethanol Category Rank	2011-2015 Total Emissions (Mt CO_2e)	Average Emissions 2011-2015 (Mt CO_2e)	Standard Deviation of Emissions 2011-2015 (Mt CO_2e)
Archer Daniel Midland	Platte	4	1	5,863,690	1,172,738	38,824
Cargill Corn Milling North America	Washington	7	2	2,237,276	447,455	71,799
AGP Soy/Corn Processing	Adams	8	3	1,021,652	204,330	53,361
Green Plains Wood River, LLC.	Hall	10	4	826,192	165,238	49,478
Chief Ethanol Fuels, Inc.	Adams	11	5	817,142	163,428	8,100
Flint Hills Resources, Fairmont, LLC	York	12	6	798,112	159,622	6,872
Valero Albion Plant	Boone	13	7	778,630	155,726	32,397
Green Plains Central City	Merrick	15	8	624,058	124,812	2,477
Abengoa Bioenergy of Nebraska, LLC	Buffalo	16	9	573,838	114,768	13,523
Abengoa Bioenergy Co., LLC[1]	Fillmore	18	10	508,180	101,636	6,488
Green Plains ORD	Valley	19	11	403,842	80,768	2,265
Pacific Ethanol Aurora West LLC	Hamilton	22	12	212,985	70,995	69,297
Elkhorn Valley Ethanol, LLC	Madison	24	13	316,339	63,268	5,773
Kaapa Ethanol, LLC	Kearney	26	14	304,608	60,922	4,099
AltEn, LLC	Saunders	29	15	51,140	51,140	-
Nebraska Corn Processing	Furnas	30	16	254,590	50,918	2,474
Trenton Agri Products	Hitchcock	32	17	224,025	44,805	2,806
Pacific Ethanol Aurora East, LLC	Hamilton	35	18	178,059	35,612	24,449
All Facilities				**15,994,358**	**3,268,182**	**-**

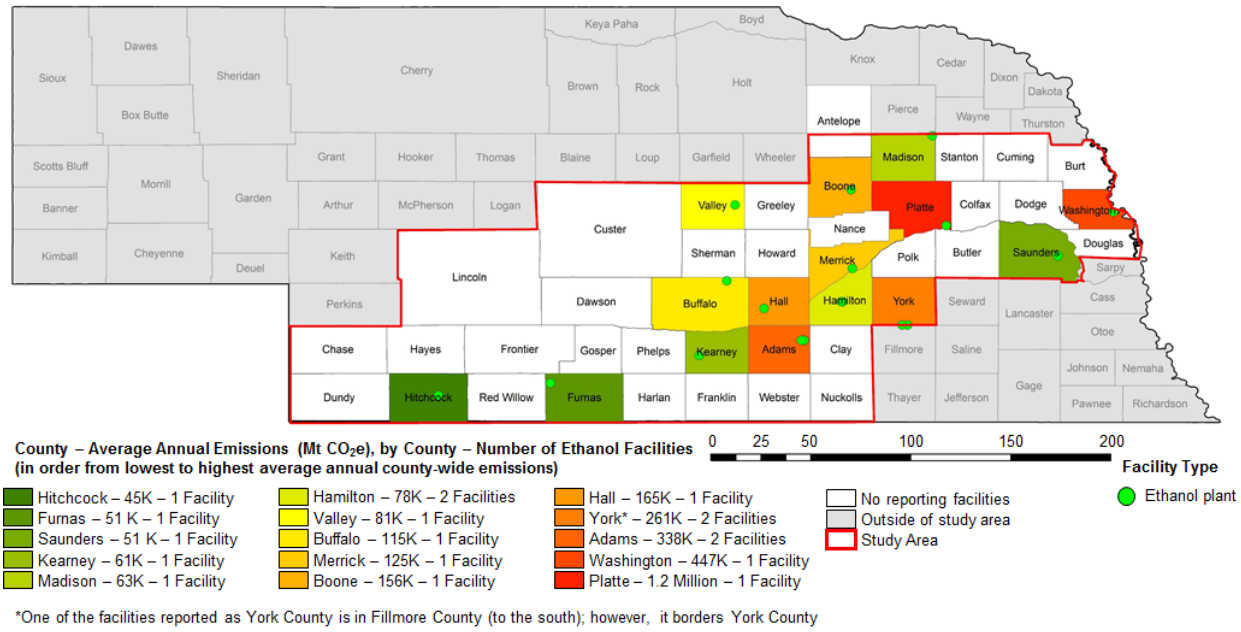

Figure 2-5. Ethanol sources in the study area.

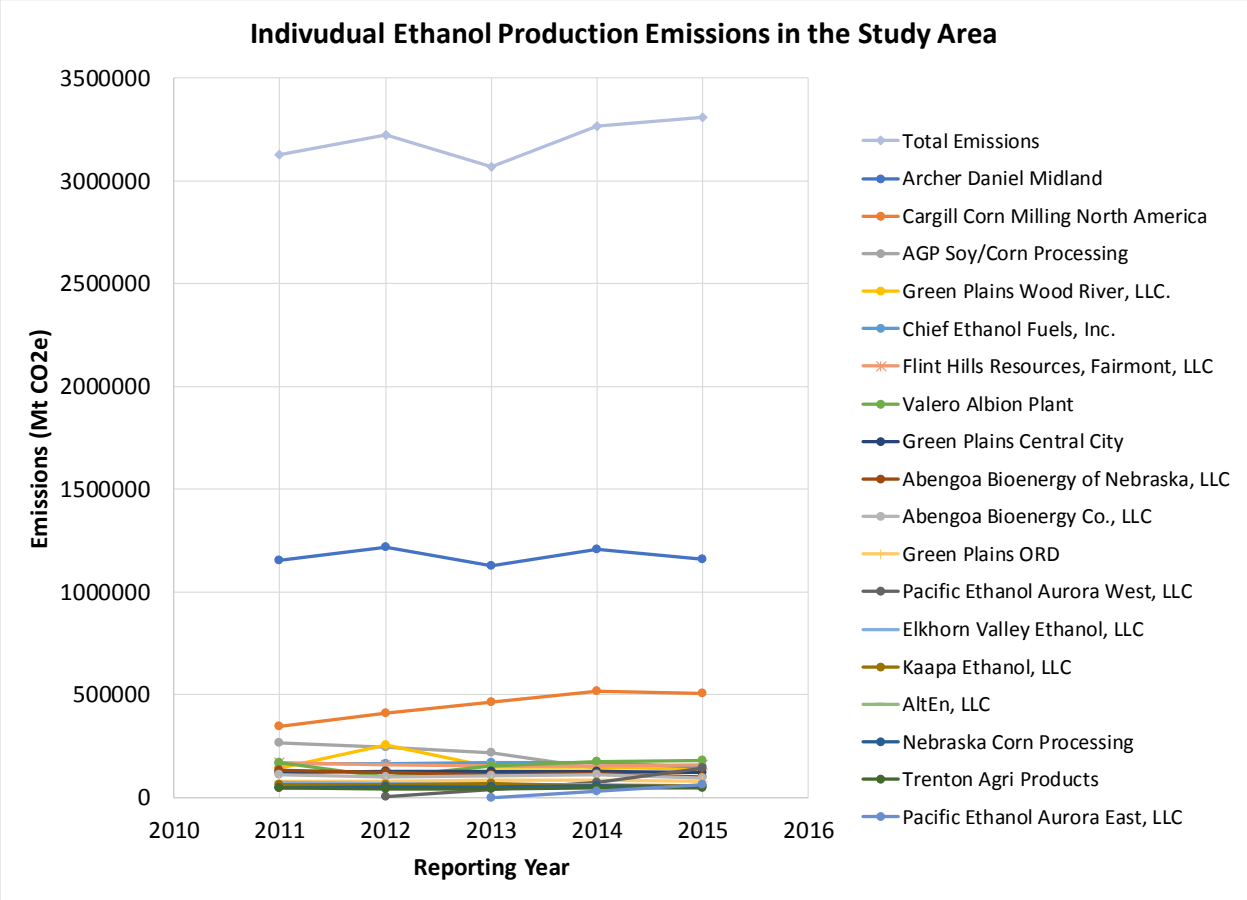

Figure 2-6. Plot showing individual facility and total ethanol-related emissions

2.3.4 Other Facilities

The analysis identified 23 other emitting facilities. The largest emitting facility was Nucor Steel with an average annual emission of 185,265 Mt CO_2e/Year. Table 2-6 and Figure 2-7 present the data and associated plots for the other sources in the study area.

Table 2-6. Reported emissions (Mt CO_2e), 2011-2015, for facilities in study area (US EPA, 2016). Facilities are organized from most to least average annual emissions (2011-2015).

Facility	County	Rank Based on Annual Emissions	Other Category Rank	2011-2015 Total Emissions (Mt CO_2e)	Average Emissions 2011-2015 (Mt CO_2e)	Standard Deviation of Emissions 2011-2015 (Mt CO_2e)
Nucor Steel Nebraska	Madison	9	1	926,325	185,265	24,583
Butler Co. Landfill.	Butler	14	2	642,854	128,571	33,572
Metropolitan Utilities District of Omaha	Douglas	17	3	567,854	113,571	39,759
Grand Island Regional Landfill	Buffalo	20	4	385,605	77,121	3,291
Bertrand Compressor Station	Phelps	21	5	359,640	71,928	15,974
Douglas County Recycling Landfill	Douglas	23	6	342,070	68,414	14,256
Cargill Meat Solutions	Colfax	25	7	308,626	61,725	19,713
NRG Energy Center Omaha, LLC	Douglas	27	8	279,545	55,909	3,161
NNSWC Landfill	Stanton	28	9	279,375	55,875	4,341
Swift Beef Company	Hall	31	10	246,321	49,264	3,804
Tyson Fresh Meats	Dawson	33	11	210,086	42,017	1,015
Hastings Landfill	Adams	34	12	207,874	41,575	4,059
Kellogg USA, Inc.	Douglas	36	13	175,175	35,035	2,597
University of Nebraska Medical Center	Douglas	37	14	147,117	29,423	2,331
Douglas County Landfill	Douglas	38	15	133,396	26,679	34,927
Hormel Foods	Dodge	39	16	132,913	26,583	1,571
Lexington Area Solid Waste Agency	Dawson	40	17	77,388	25,796	3,321
Kearney Area Solid Waste Agency	Buffalo	41	18	79,462	19,866	2,278
NatureWorks, LLC	Washington	42	19	82,457	16,491	22,582
Canaday	Gosper	43	20	41,534	8,307	11,995
C W Burdick	Hall	44	21	11,606	2,321	1,892
North Denver Station	Adams	45	22	2,432	486	453
Don Henry Power Center	Adams	46	23	870	174	214
All Facilities				**5,640,525**	**1,142,397**	**-**

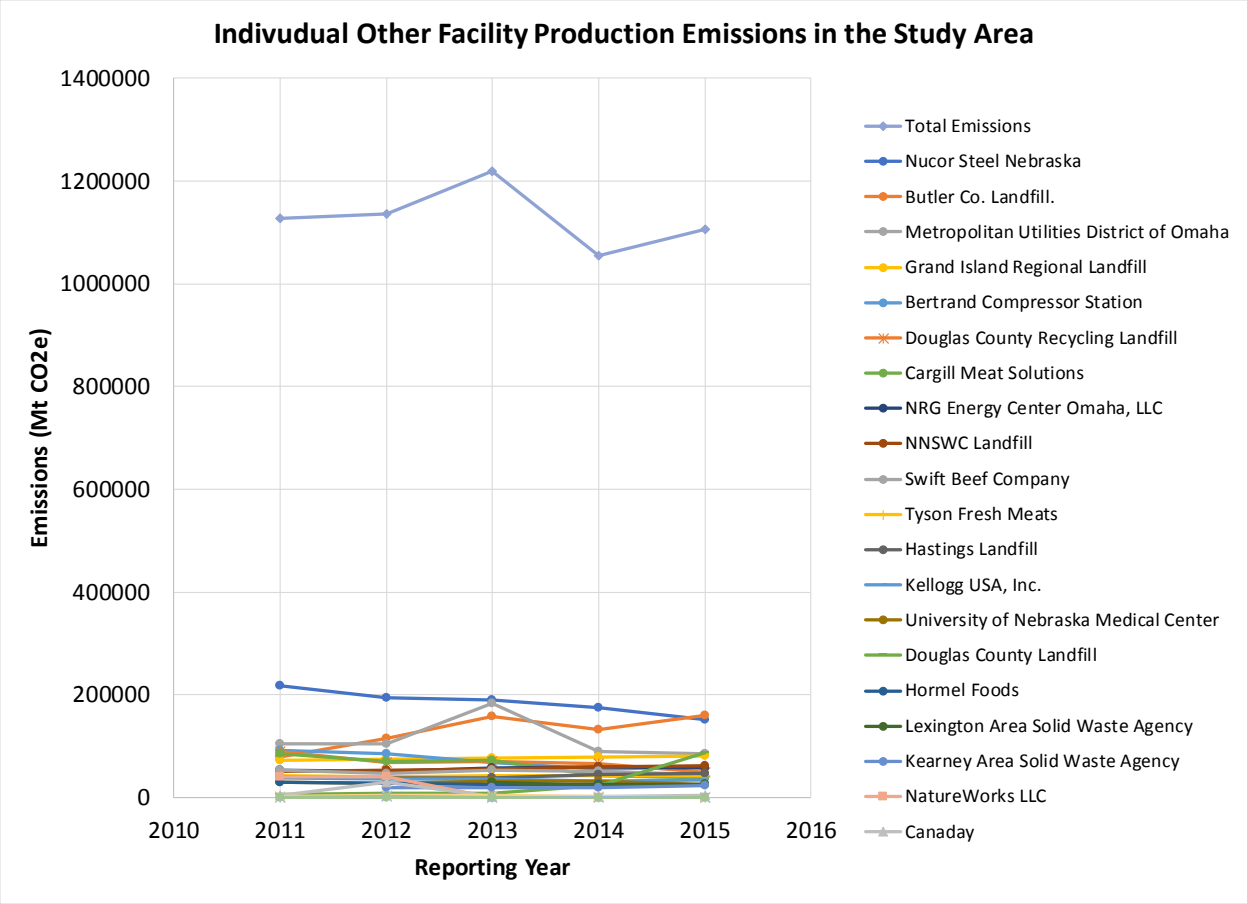

Figure 2-7. Plot showing individual and total other-facility-related emissions

2.4 Discussion

The overall annual average emissions for the study area were 19.4 MMt COe_2 during the period from 2011 through 2015. Electric power production represents the largest portion of emissions in the study area. Five power plants make up approximately 77 % of the CO_2 emissions in the study area with emissions of 15 MMt CO_2/year. Ethanol plant emissions make up the next largest portion of study-area-emissions at approximately 17 % of emissions, 3.3 MMt CO_2/year. Other CO_2 sources were the smallest portion of total emissions at approximately 6 % of total emissions, 1.1 MMt CO_2e/year. Although, electric power represents the largest portion of emissions in the study area. post-combustion capture for existing power plants is still being commercialized which likely means that CO_2 from existing power plants is not going to be a CO_2 source that engenders commercial investment in the next several years. There are many (23) Other potential sources of CO_2 in the study area. However, many of these are landfills, meat production or other natural gas related sources that may be reporting methane that appears as CO_2e. Eight of the top 10 Other sources are possibly reporting methane instead of CO_2. Only Nucor Steel and NRG Energy Center are not likely methane in the top-ten Other sources. The difficulty with post combustion capture and the likelihood that Other sources are not emitting CO_2 makes ethanol the most likely source of CO_2 to perform stacked-storage in the study area. Ethanol plants represent the largest non-power point sources for CO_2 in the study area. Ethanol emissions in the area have increased

over the last 5 years; The standard deviation of the ethanol emissions was approximately 98 thousand Mt CO_2e/year.

Focusing on ethanol as the primary CO_2 source for the project will more than meet the United States Department of Energy's (US DOE's) goals and objectives presented in DE-FOA-0001450 to construct a commercial-scale storage facility capable of storing 50 MMt CO_2 from industrial sources. Based on the annual average emissions for the existing ethanol sources in the project area there are approximately 98 MMt CO_2e for a 30-year period. Examining possible source corridor locations shows that US DOE's requirements can be easily met with only a portion of the ethanol sources. Multiple possible source corridor routes could collect commercial amounts of CO_2 for transport to the stacked-storage corridor. These hypothetical corridors do not represent specific pipeline routes and are just discussed as a tool to show that the sources in the study area can easily meet commercial-scale criteria for CO_2 supply. Three hypothetical source corridors are described here as examples. Source Corridor 1 (Figure 2-8 and Table 2-7) runs from Washington County, NE west to Platte County, NE where it turns south-southwest running through Merrick and Hamilton Counties, NE. The Corridor then turns southwest through Adams, Kearney, and Furnas Counties, NE. Source Corridor 1 could initially collect approximately 2.3 MMt CO_2/year or approximately 70 MMt CO_2e over 30 years.

Table 2-7. Sources included in Source Corridor 1.

Facility	County	Rank Based on Annual Emissions	Ethanol Category Rank	Average Emissions 2011-2015 (Mt CO_2e)
Archer Daniel Midland	Platte	4	1	1,172,738
Cargill Corn Milling North America	Washington	7	2	447,455
AGP Soy/Corn Processing	Adams	8	3	204,330
Chief Ethanol Fuels, Inc.	Adams	11	5	163,428
Green Plains Central City	Merrick	15	8	124,812
Pacific Ethanol Aurora West LLC	Hamilton	22	12	70,995
Kaapa Ethanol, LLC	Kearney	26	14	60,922
Nebraska Corn Processing	Furnas	30	16	50,918
Pacific Ethanol Aurora East, LLC	Hamilton	35	18	35,612
All Facilities				**2,331,210**

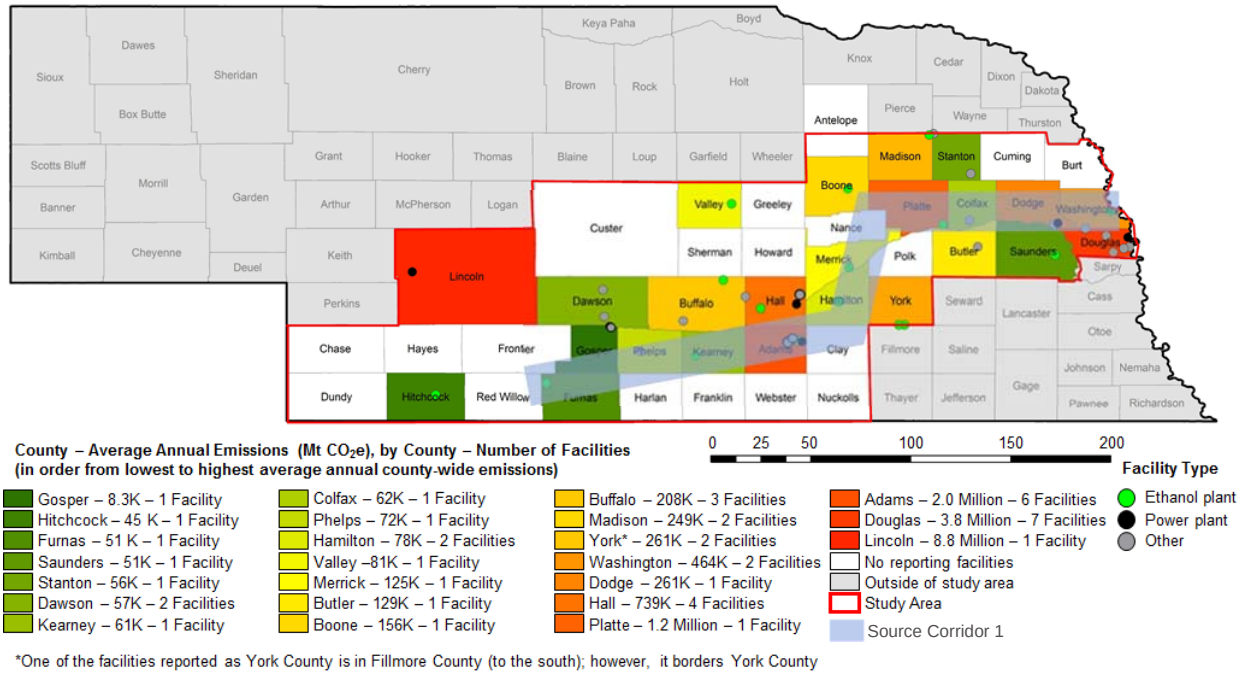

Figure 2-8. Map showing the approximate location of Source Corridor 1.

Source Corridor 2 (Figure 2-9 and Table 2-8) runs from Washington County, NE west to Platte County, NE where it turns south-southwest running to York County, NE. Source Corridor 2 then turns southwest through Adams, Kearney, and Furnas Counties, NE. Source Corridor 2 could initially collect approximately 2.4 MMt CO_2e/year or approximately 71 MMt CO_2e over 30 years.

Table 2-8. Sources included in Source Corridor 2.

Facility	County	Rank Based on Annual Emissions	Ethanol Category Rank	Average Emissions 2011-2015 (Mt CO_2e)
Archer Daniel Midland	Platte	4	1	1,172,738
Cargill Corn Milling North America	Washington	7	2	447,455
AGP Soy/Corn Processing	Adams	8	3	204,330
Chief Ethanol Fuels, Inc.	Adams	11	5	163,428
Flint Hills Resources, Fairmont, LLC	York	12	6	159,622
Abengoa Bioenergy Co., LLC[1]	Fillmore	18	10	101,636
Kaapa Ethanol, LLC	Kearney	26	14	60,922
Nebraska Corn Processing	Furnas	30	16	50,918
All Facilities				**2,361,050**

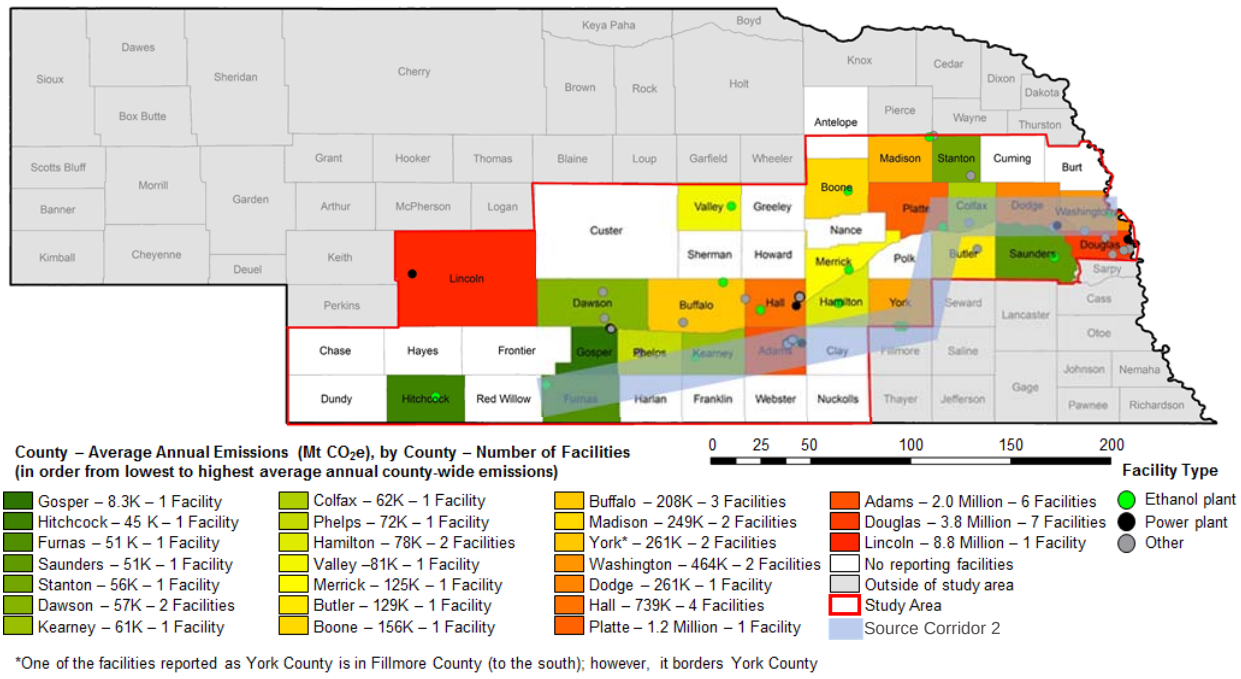

Figure 2-9. Map showing the approximate location of Source Corridor 2.

Source Corridor 3 (Figure 2-10 and Table 2-9) runs from Washington County, NE west to Platte County, NE where it turns southwest running through Merrick, Hall, Kearny Counties, NE to Furnas County, NE. Source Corridor 3 could initially collect approximately 2.1 MMt CO_2e/year or approximately 63 MMt CO_2e over 30 years.

Table 2-9. Sources included in Source Corridor 3.

Facility	County	Rank Based on Annual Emissions	Ethanol Category Rank	Average Emissions 2011-2015 (Mt CO_2e)
Archer Daniel Midland	Platte	4	1	1,172,738
Cargill Corn Milling North America	Washington	7	2	447,455
Green Plains Wood River, LLC.	Hall	10	4	165,238
Green Plains Central City	Merrick	15	8	124,812
Pacific Ethanol Aurora West LLC	Hamilton	22	12	70,995
Kaapa Ethanol, LLC	Kearney	26	14	60,922
Nebraska Corn Processing	Furnas	30	16	50,918
All Facilities				**2,093,078**

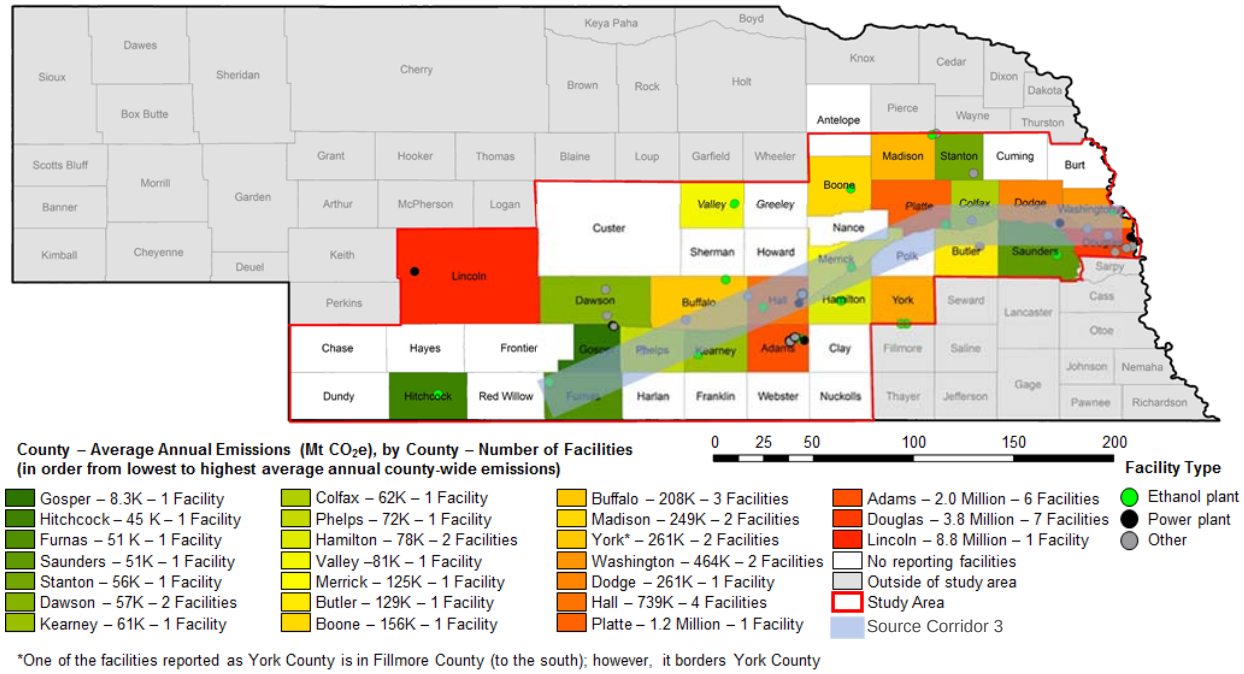

Figure 2-10. Map showing the approximate location of Source Corridor 3.

Each of these hypothetical corridors accesses commercial-scale amounts of CO_2. Each also represents an initial amount of CO_2 that may be collected; additional facilities could tap into the source corridor pipeline over time increasing the total amount transported and stored. Each source corridor scenario contained the two largest sources of ethanol-derived CO_2 in the study area; ADM's Columbus, NE facility (Platte County) and Cargill's Blair, NE facility (Washington County). These two plants are responsible for almost half (49.6%) of the total annual average ethanol-derived CO_2 emissions in the study area. These sources alone represent approximately 49 MMt CO_2 over a 30-year period.

Ethanol plants are the initial focus of this project because they include some of the largest point sources in the area and have relatively pure CO_2 streams. The nine electric power generating facilities in the study area are also large point sources; however, they are considered secondary potential sources in this study because of the low technical readiness level of low-cost capture. The ready availability of ethanol-derived CO_2 will allow for commercial development while post combustion capture costs come down.

Nearly 45 % of the total emissions (2011-2015) in the study area come from one power plant facility, Gerald Gentleman Station, on the northern end of the proposed stacked-storage corridor (Red Willow and surrounding counties). Two of the other power plant facilities, the North Omaha Station, which accounts for around a 18% of the total emissions in the study area, and the Gerald Whelan Energy Center, which accounts for around 8% of the total emissions in the study area, complete the top three sources in the state. These large sources will be able to take advantage of the infrastructure developed based on ethanol-derived CO_2 as capture comes online allowing further commercialization and stacked-storage.

The hypothetical storage corridors (Storage Corridor 1 to 3) help focus the priorities for ethanol plant outreach; mainly through the center of the study area running west from Washington County to Platte County and then southwest to Furnas County. This route contains 11 ethanol facilities with emissions of approximately 1.5 MMt CO_2e/year (Table 2-10).

Table 2-10. Likely ethanol plants for project outreach.

Facility	County	Map Code (Rank) Based on Annual Emissions)	Ethanol Category Rank	Average Emissions 2011-2015 (Mt CO_2e)
Cargill Corn Milling North America	Washington	7	2	447,455
AGP Soy/Corn Processing	Adams	8	3	204,330
Green Plains Wood River, LLC.	Hall	10	4	165,238
Chief Ethanol Fuels, Inc.	Adams	11	5	163,428
Flint Hills Resources, Fairmont, LLC	York	12	6	159,622
Green Plains Central City	Merrick	15	8	124,812
Abengoa Bioenergy Co., LLC[1]	Fillmore	18	10	101,636
Pacific Ethanol Aurora West LLC	Hamilton	22	12	70,995
Kaapa Ethanol, LLC	Kearney	26	14	60,922
Nebraska Corn Processing	Furnas	30	16	50,918
Pacific Ethanol Aurora East, LLC	Hamilton	35	18	35,612
All Facilities				**1,584,969**

2.5 Conclusions

The source identification and assessment examined a 44-county study area running from eastern to southwestern Nebraska comprising 46 point sources with annual average emissions of approximately 19.4 MMt CO_2e/year. The sources included five large electric power plants (15.0 MMt CO_2e/year), 18 ethanol plants (3.3 MMt CO_2e/year), and 23 other sources (1.1 MMt CO_2e/year). Considering the simpler capture associated with ethanol-derived CO_2, ethanol plants were focus of the source identification with respect to outreach for future phases. Three hypothetical source corridor routes connecting ethanol plants were discussed, each possible corridor had commercial-scale CO_2 emissions, between 2.1 and 2.4 MMt CO_2e/year. Based on the hypothetical corridors, 11 ethanol plants in the study area were identified as priorities for outreach because they are likely to be along the eventual source corridor. These facilities represent almost 1.6 MMt CO_2e/year emissions in addition to the almost 1.2 MMt CO_2e/year from the ADM plant at Columbus, NE. Combined the ADM Columbus Plant and the 11 facilities identified above account for approximately 2.7 MMt CO_2e/year.

3 Geology

3.1 Introduction

The suitability of the Pennsylvanian-Permian geologic interval in the Midcontinent to act as a commercial-scale CO_2 storage complex was evaluated for two potential sites at the northern end of the

stacked-storage corridor (Figure 1-1). The selected areas were identified for site-specific geologic characterization based on the following screening criteria:

- Favorable geologic conditions for vertically-stacked storage in repeating, well-isolated intervals of deep saline sandstone, limestone, and oil-bearing bearing units
- Sufficient depths to ensure subsurface pressures and temperatures are adequate for storage of supercritical CO_2
- The presence of regionally extensive caprocks to prevent vertical migration of the CO_2, reinforced by a proven confining system that has effectively trapped oil within the storage complex
- Existing resource development and the potential for a hybrid of CO_2 - enhanced oil recovery (EOR) and geologic storage to support commercialization of CCS

The first study area encompasses the Sleepy Hollow oil field in Red Willow County, southwestern Nebraska (Figure 3-1). The second selected study area is the Huffstutter oil field in Phillips County, north-central Kansas, approximately 50 miles (mi) east-southeast of the Sleepy Hollow study area. In both study areas, the middle-to-lower interval of the Pennsylvanian System hosts deep saline formations and oil-bearing zones that are overlain by a confining system of regionally extensive Upper Pennsylvanian and Permian-age shales, carbonates, and evaporites.

3.2 Methods

The workflow employed for characterization and assessment of site-scale geologic CO_2 storage resource for the two selected study areas consists of five main components:

1) A comprehensive review of basin framework and regional stratigraphy in the Mid-Continent, including assessment of structural features and crustal stresses pertinent to caprock integrity
2) Site-specific petrophysical analysis and quantification of reservoir properties and pore volumes
3) Development of three-dimensional (3D) static earth models (SEMs) representing the structure and properties of the Pennsylvanian-Permian storage complex at each study area
4) Construction of site-scale geologic maps and cross-sections depicting the vertical and lateral extent of caprocks and deep saline formations
5) Calculation of site-specific prospective CO_2 storage resource and storage efficiency for the deep saline formations of interest

The structural setting and stratigraphic succession of the Midcontinent Region is briefly described, with a focus on the geologic intervals of interest in the Pennsylvanian and Permian systems. Geologic maps and cross-sections are used to define the depth, thickness, and lateral extent of deep saline formations and caprocks. The nature and extent of the confining system between the potential injection zone(s) and underground sources of drinking water (USDWs) are also described, including an evaluation of geologic structures, crustal stresses, and seismicity that could impact caprock integrity in the study region. Storage reservoir properties, geometries, and pore volumes are evaluated via petrophysical analysis and development of SEMs in both study areas. Finally, volumetric calculations are conducted to estimate the prospective storage resource of the deep saline intervals of interest.

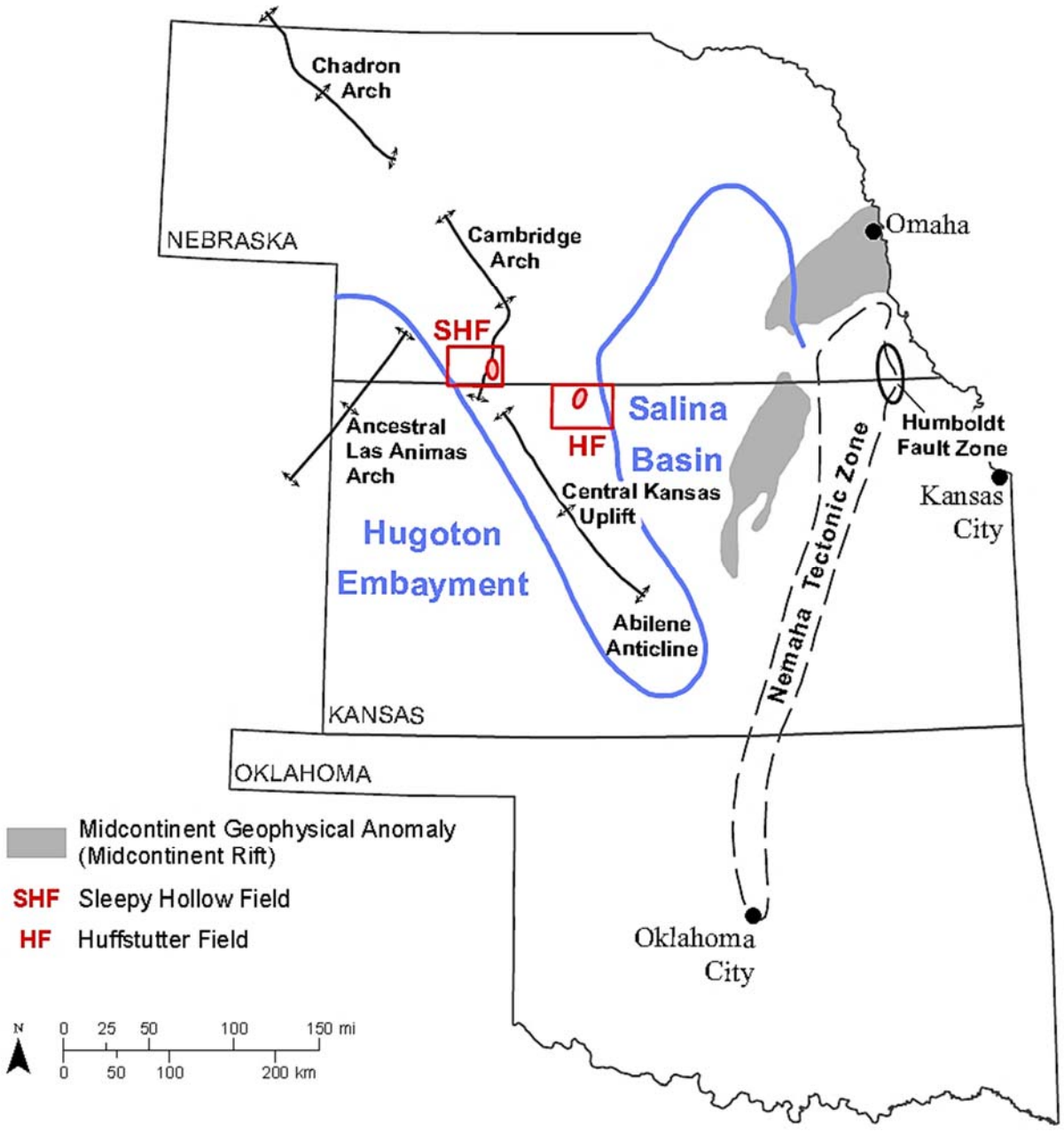

Figure 3-1. Regional map showing the Sleepy Hollow Field (SHF) in Red Willow County, Nebraska and the Huffstutter Field (HF) in Phillips County, Kansas. Image modified from Steeples (1982).

3.3 Pennsylvanian-Permian Storage Complex

Four main lithostratigraphic groups in the Pennsylvanian System were evaluated for deep saline CO_2 storage in the two study areas. In ascending order, they include: the Pleasanton-Marmaton, the Lansing-Kansas City, the Shawnee-Douglas, and the Wabaunsee groups (Figure 3-2). Potential storage targets within each group include sandstone intervals (5-20 feet [ft]) in the Wabaunsee and Pleasanton-Marmaton groups, and porous limestones (5-25 ft) in the Shawnee-Douglas and Lansing-Kansas City groups. The deep saline zones of interest in the Lansing-Kansas City occur at the top and the base of the unit; and are separated by productive oil-bearing zones.

Directly overlying the Wabaunsee Group, shales, carbonates, and evaporites deposited during the Late Pennsylvanian and Permian have potential to act as caprocks for the underlying storage reservoirs (Carlson et al., 1986; Condra and Reed, 1959; Sawin et al., 2009). These potential caprocks include, in ascending order: Admire, Council Grove, Sumner, and lower Nippewalla groups (Figure 3-2).

Secondary confining units are present at shallower depths in each study area (200-400 ft), and include the Dakota Formation (Dakota Group in Nebraska), Graneros shale, Greenhorn limestone, and Carlile shale (Condra and Reed, 1959). This stratigraphic interval was deposited from the Albian into the Turonian stages during the Cretaceous, between approximately 113 and 90 million years ago (Ma).

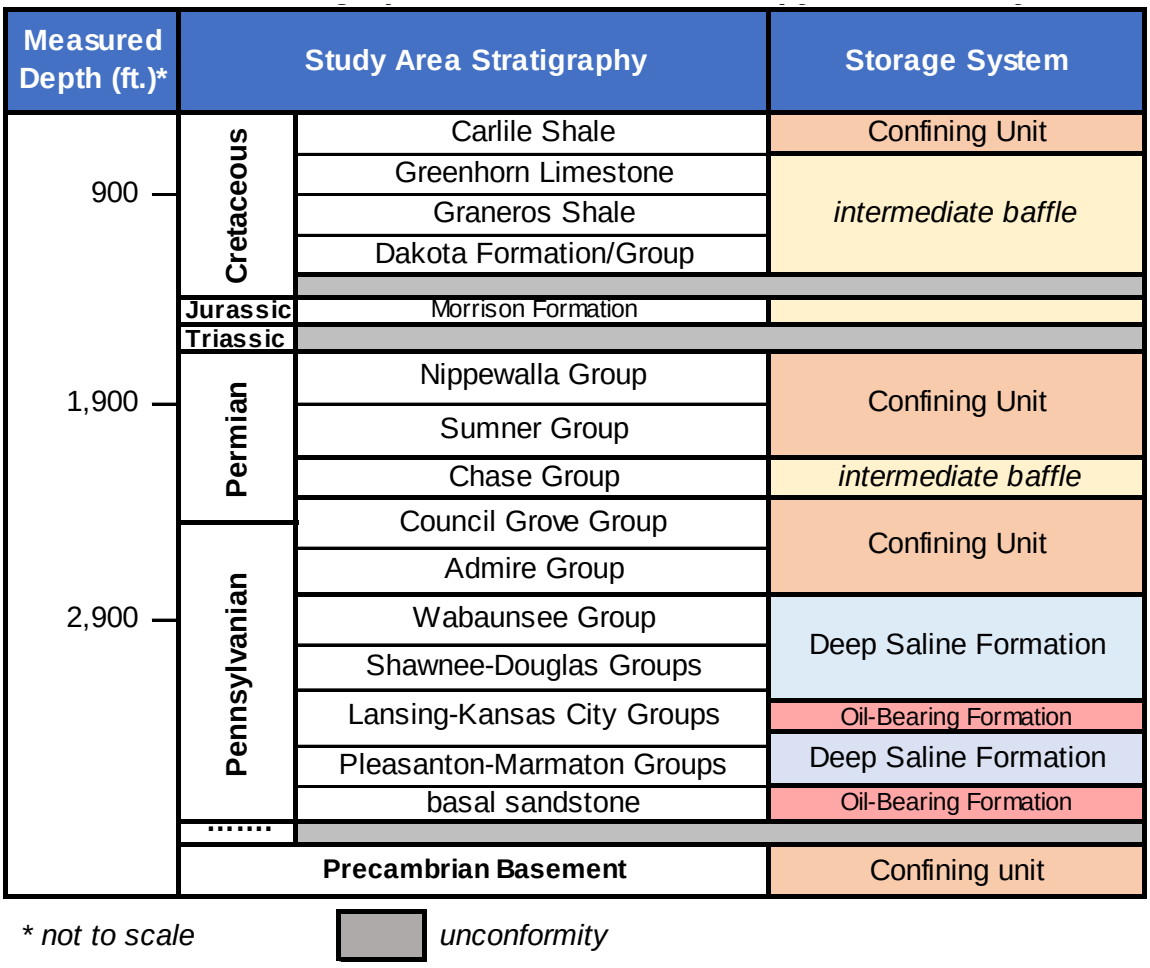

Figure 3-2. Simplified stratigraphic column showing the deep saline formations of interest and overlying caprocks evaluated in both study areas.

Alternating stratigraphic successions of marine and non-marine sediments are a distinguishing feature of the Pennsylvanian-Permian sequence in the Midcontinent. These stratigraphic successions are unique to the study region and have critical importance in the development of geologic conditions conducive to commercial-scale CO_2 injection and storage.

3.4 Geologic Background and Selected Study Areas

3.4.1 Overview

Knowledge of basin development and regional stratigraphy in the Midcontinent Region is needed to interpret and quality-check subsurface data, informing geologic models and analyses, and integrating results along various stages of site characterization. The structural and stratigraphic framework of Nebraska and Kansas was defined to help guide subsequent site characterization efforts. The role of basin evolution and stratigraphy in the development of hydrocarbon resources at each study area was evaluated in the context of geologic CO_2 storage feasibility.

3.4.2 Basin Framework of the Midcontinent Region

Nebraska and Kansas are both on the North American platform, where accumulations of Phanerozoic sedimentary rocks and sediments cover basement rocks (mostly of Proterozoic age) that are a few hundred to thousands of feet below the land surface. Nebraska and Kansas are on what was the shoreward portion of an extensive, low-relief, gently southward-dipping platform (Rascoe and Adler, 1983; Dubois, 1985) at approximately 10° north latitude during the Late Pennsylvanian (Witzke, 1990; Ziegler et al., 1997). The episodically active structural feature known as the Cambridge Arch was on this platform, but it was buried by sediments during the Late Pennsylvanian period.

The Cambridge Arch is a gentle, positive structural trend (anticlinorium) that separates the Denver or Denver-Julesburg Basin to the west from the Central Nebraska or Salina Basin to the east (Figure 3-1). Carlson (1999) considered the Cambridge Arch itself to be one of a limited number of "tectonic cores" which persisted as highs or were tectonically rejuvenated at times during the Phanerozoic. The Cambridge Arch is effectively continuous northwestward as the Chadron Arch, such that the two features have been dealt with as a single trend by some authors (e.g., Moore and Nelson, 1974). The Chadron Arch also abuts the Black Hills uplift to the northwest. To the south, the Central Kansas Uplift extends northwestward from south-central Kansas into the Cambridge Arch (Figure 3-1). Thus, there is a prominent northwesterly geographical trend of Phanerozoic uplifts from Kansas into eastern Wyoming. The four structural features making up this trend were active at different times during the Phanerozoic, however, and their dynamic relationships are by no means fully resolved (Stix, 1982). The Cambridge Arch and Central Kansas Uplift have a structural saddle between them (Rothe and Lui, 1983), but they are still reported as component parts of the same province (e.g., Higley, 1987; 1995).

These uplifts and their associated basins likely formed through a variety of mechanisms, including mantle dynamics, plate tectonics, and ancient patterns of erosion and deposition (e.g., Sloss 1988; Miller et al. 2005; Burgess 2008; Liu et al., 2014). Accommodation space was episodically generated in the Midcontinent from the Cambrian into the Late Cretaceous, and possibly even the earliest Paleocene (cf. Peppe et al., 2009; Boyd and Lillegraven, 2011). The past interactions of far-field tectonics and flexure-inducing mantle dynamics in the study areas combined with global sea-level change are partially understood at the very best. The concept of cratonic sequences has been a useful framework for understanding the depositional history of the Midcontinent (Bunker et al., 1988; Sloss, 1988), although the recapitulation of the primacy of eustatic sea-level control has tended to deflect attention from the other aspects of basin history.

Basinal areas of the Midcontinent were connected to the Illinois and Appalachian basins during highstands of Pennsylvanian sea level. They were also connected, through a series of smaller, deeper basins, to the Panthalassan Ocean on the western side of the supercontinent Pangea, of which present North America was a part (Heckel, 2008). Nearly identical conodont faunas have allowed direct

correlation of the cyclothems of the Midcontinent with those of north-central Texas (Boardman and Heckel, 1989), the Illinois Basin (Heckel and Weibel, 1991), Appalachian Basin (Heckel, 1994), and the Paradox Basin (Ritter et al., 2002).

3.4.3 Regional Stratigraphy

In southwest Nebraska and northwest Kansas, Precambrian granitic basement in the core of the Cambridge Arch lies at the base of the stratigraphic succession in the Midcontinent. In the Sleepy Hollow study area, a Pennsylvanian-age sandstone unconformably overlies the Precambrian basement (Carlson, 1993). In the Huffstutter study area, the Cambrian Arbuckle Group dolomites overlie the Precambrian basement. Ordovician through Mississippian strata are absent atop the Cambridge Arch in both study areas, reappearing approximately 80 mi (130 km) eastward into the Salina/Central Nebraska basin and also approximately 30 mi (50 km) west of the arch in the Denver (Denver-Julesburg) Basin.

The lithostratigraphic units within the Pennsylvanian System host the deep saline formations of primary interest for geologic CO_2 storage. These potential storage zones consist of sandstones and limestones with varying degrees of dolomitization, and are interbedded with thin intervals of mudrock, phosphatic shale, and minor evaporite strata that act as vertical barriers to flow, isolating oil-bearing zones from non-oil-bearing zones. The Pennsylvanian succession in Nebraska and Kansas thickens southward toward the southern margin of the Midcontinent marine shelf and the northern edge of the Anadarko Basin in Oklahoma-Texas.

Both the Pennsylvanian and Lower Permian systems across the Midcontinent have long been characterized as a succession of cyclothems. These cyclothems have salient importance in the development of deep saline, oil-bearing, and confining zones pertinent to CO_2 injection and storage in the study areas. A typical Pennsylvanian-to-Lower Permian cyclothem is defined as the following sequence of lithofacies, in ascending stratigraphic order: (1) a thin, typically dark transgressive limestone; (2) a thin, offshore, black phosphatic shale; (3) a thick, relatively light colored regressive limestone; and (4) a relatively thick siliciclastic mixture of nearshore sandstone, shale, and/or mudstone that is generally capped by a laterally extensive paleosol (e.g., Heckel, 2008; Joeckel, 1994). Many nearshore shales exhibit non-marine features such as channel sandstones, deltaic deposits, red beds, and terrestrial plant fossils. These features represent times of increased detrital influx when the shoreline prograded into the shallow sea (Heckel, 1977). The thin transgressive limestone members are fine-grained, dense, and dark with diverse biota that suggest deposition in open-marine environments (Heckel, 1977; 1994; 2008). Black phosphatic shales are typically thin and laterally extensive, marking the transgressive maximum (Heckel, 1977; 2008). Regressive limestones frequently coarsen upward into calcarenite and show evidence of upward shallowing (Heckel, 1977; 1986; Young, 2013). Paleosols are common in Pennsylvanian cyclothems in Nebraska and Kansas, and those developed in mudrocks (typically reddish ones) overlying regressive limestones within cyclothems indicate prolonged subaerial exposure during complete regressions (Prather, 1985; Joeckel, 1989; 1994; 1995; 1995b; 1999). Incomplete regressions may be recorded by less well-developed paleosols in mudrocks.

High-frequency, high-amplitude changes in eustatic sea-level and climate occurred during the Late Pennsylvanian and Early Permian. Ice caps on Gondwana melted rapidly, driving rapid marine transgressions elsewhere around the globe, and then slowly accumulated again, driving slow and interrupted regressions (Veevers and Powell, 1987; Read, 1995; Fielding et al., 2008; Heckel, 1986). Wanless and Shepard (1936) first proposed glacioeustasy as the primary control on Pennsylvanian cyclothems. Since that time other mechanisms such as plate tectonics and deltaic migration have been proposed as controlling factors, but glacioeustasy is still considered to be the primary control on the

deposition of Pennsylvanian cyclothems (Heckel, 1986; 1994). The estimated period of cyclothems ranges from approximately 20,000 to 400,000 years, which corresponds to the frequency band Milankovitch orbital parameters, rather than the general time range for tectonically-driven transgression and regression (Heckel, 1994; Miller et al., 2005). Heckel (1994) maintained that sea-level rises and falls of at least 100 meters (m) were necessary to produce the black shale and paleosols in the same sequence, although other authors have cited significantly smaller estimates (Rygel et. al., 2008). The motif of carbonate and mudrock-dominated cyclothems gives way upward through the Permian System as proportions of shales, evaporites, and dolostones increase.

Triassic and Jurassic strata are comparatively thin and limited in spatial extent in the Midcontinent. In contrast, the Cretaceous succession is regionally extensive and thick, although it does thin slightly across the Cambridge Arch. In ascending stratigraphic order, this succession is: Dakota Formation/Group, Graneros ("Belle Fouche") Shale, Greenhorn Limestone, Carlile Shale, Niobrara Formation, and Pierre Shale (Hattin et al., 1964), with the shale formations having potential to serve as secondary caprocks for the potential CO_2 injection and storage zones in the Pennsylvanian. The Dakota Formation/Group in the lower part of this succession consists of fluvial to estuarine sandstones and mudrocks. The upper part of the Cretaceous succession consists mostly of marine shales, chalky shales, and chalky limestones. The bedrock geologic map of Nebraska (Burchett, 1986) indicates that the Pierre Shale has been eroded in the west-southwest-to-east-northeast-trending valley of the Republican River between Arapahoe in Furnas County and McCook in Red Willow County; this area coincides with the crest of the Cambridge Arch, which trends north-northwest there. Nevertheless, at least part of the Pierre Shale is probably present in the uplands south of the river, where the Sleepy Hollow study area is located. Approximately 2 mi south of the study area the top of the Pierre Shale is present at a depth of 2,330 ft. The Pierre Shale is widespread on the east and west flanks of the arch, within approximately 15 mi of its axis.

Cenozoic sediments and sedimentary rocks, characteristically consisting of fluvial and, to a lesser degree eolian sediments, are important from the perspective of regional hydrogeology and the composition of the High Plains aquifer system, the primary source of freshwater in the region. Paleogene sedimentary rocks—specifically the upper Eocene-Oligocene strata of the White River Group and lower Arikaree Group—as well as lower Miocene strata of the latter, which are present elsewhere in the western half of Nebraska, are absent in Red Willow County, Nebraska as well as the surrounding counties of Furnas, Frontier, Gosper, Hayes, and Hitchcock (Cast, 2000; Eversoll, 2000a, b, 2003, 2004; Smith, 2003). Instead, strata of the Miocene Ogallala Group directly overlie Upper Cretaceous strata (Niobrara Formation or Pierre Shale) in the aforementioned counties. The Ogallala Group attains a maximum total thickness of approximately 220 ft in Red Willow County and it consists chiefly of sand/sandstone, silty sand/sandstone, and silt/siltstone, with minor gravel and silty clay (Eversoll, 2003). Likewise, the Ogallala Group directly overlies Upper Cretaceous sedimentary rocks in Phillips County, Kansas, the location of the Huffstutter study area, as well (Johnson, 1993). Quaternary fluvial sediments (dominantly sands and gravels) and loesses are widespread in both study areas and overlie either Upper Cretaceous strata or the Ogallala Group in the study areas (Johnson, 1993; Eversoll, 2003). Cenozoic strata would not be involved in the injection or storage of CO_2 in either of the study areas, and are separated from the potential injection zones by the secondary confining system of thick Cretaceous shales, and up to 1,000 additional feet of underlying rock comprised of intermediate baffles and caprocks of the primary Pennsylvanian-Permian confining system.

3.4.4 Existing Hydrocarbon Resources

Sleepy Hollow Study Area

The Sleepy Hollow study area is approximately 28 mi^2, and encompasses the Sleepy Hollow oil field in eastern Red Willow County, Nebraska (Figure 3-3). Sleepy Hollow is the most productive oil field in Nebraska and is located on the southwestern flank of the Cambridge Arch near the western margin of the Hugoton Embayment (e.g., Figure 3-1). The primary area of review is delineated by a high-density cluster of wells (approximately 1 well per 40 acres over 7,360 acres) producing primarily from the Pennsylvanian-age sandstone overlying the Precambrian basement.

Discovered in 1960, the first oil-producing unit developed at the Sleepy Hollow Field is a Desmoinesian (315 to 307 Ma) sandstone at the base of the Pennsylvanian System, herein referred to as the basal Pennsylvanian sandstone (Rogers, 1977), or basal sandstone for short. The Sleepy Hollow oil field has produced more than 48 million barrels of oil, with at least 38 million barrels produced from the basal sandstone (cf. Rogers, 1977; Standerford, 1986; Carlson, 1989). The volume of original oil-in-place in the basal sandstone is estimated at more than 1.03 billion barrels (Standerford, 1986). The average depth of the basal sandstone is 3,450 ft at the Sleepy Hollow study area, and the original reservoir pressure was approximately 900 pounds per square inch (psi) (Standerford, 1986). The sandstone is composed almost exclusively of rounded to subrounded, frosted, and pitted grains of quartz, similar to the Reagan (Cambrian) Sandstone of central and western Kansas. This unit probably developed when the Precambrian surface along the crest of the arch, which had been exposed at least since early Pennsylvanian times, was incised by fluvial channels that filled with granitic detritus. Fluvial and marine processes reworked this “granite wash,” gradually removing feldspar grains by abrasion and weathering, then reworking the remaining quartz fragments into lobate sand bodies (Rogers, 1977). There is a coarsening upward sequence within each sand body, and genetically distinct sandstone bodies may be stacked. Sedimentary structures include massive bedding, low-angle planar cross-lamination, and low-amplitude ripple lamination. Invertebrate burrows are also common (Rogers, 1977). The basal sandstone is absent east of the Sleepy Hollow study area, probably because of dominant westward longshore drift when its constituent sands were deposited (Rogers, 1977). The reservoir is limited to the north and south of the study area because of subtleties in sea level changes that restricted sand accumulation to several east-west shoreline or shallow marine trends. The upper and middle zones of the Lansing and Kansas City Groups are also oil-bearing in the Sleepy Hollow Field. Oil accumulation in the study area has been attributed to a combination of structural and stratigraphic trapping mechanisms (Rogers, 1977).

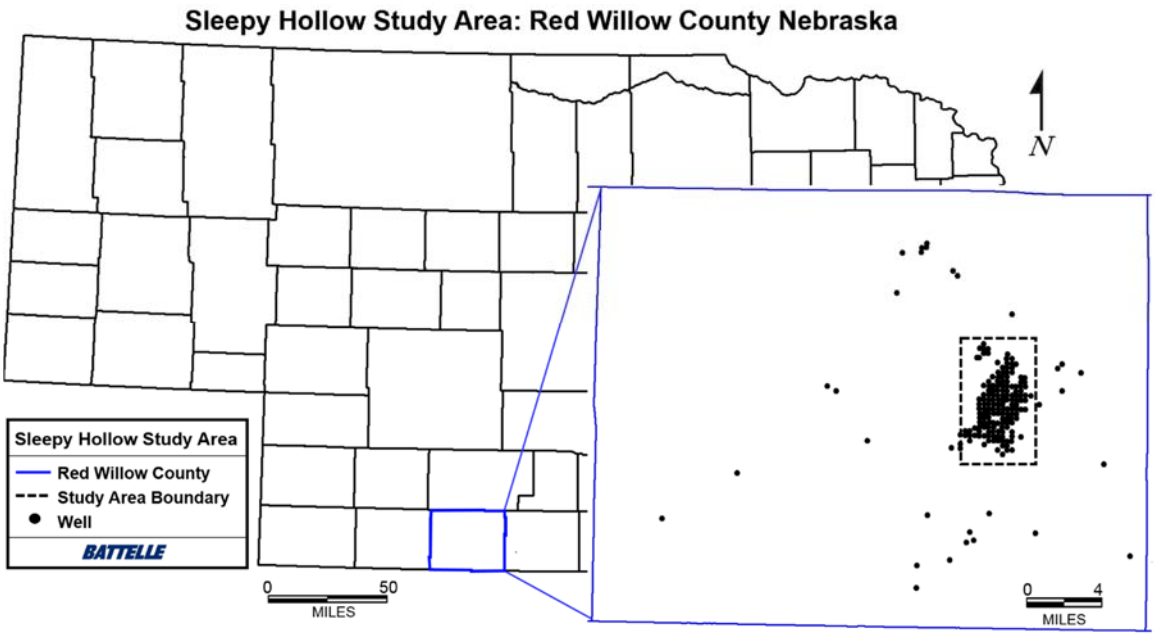

Figure 3-3. Map of Nebraska showing the outline of the Sleepy Hollow study area in Red Willow County along with the location of 205 wells with logs used for petrophysical analysis, SEM development, and storage resource calculations.

Huffstutter Study Area

The geologic storage potential of the Pennsylvanian-Permian system was evaluated at a second selected area centered around the Huffstutter oil field in Philips County Kansas (Figure 3-4). The study area is positioned on the crest of the Huffstutter-Stuttgart anticline, where it locally trends northeast-southwest. The primary area of review is delineated by the outline of the oil field that produces from the Pennsylvanian-age limestones of the Lansing-Kansas City groups.

Discovered in 1943, the Huffstutter oil field has produced over 12.5 million barrels of oil out of the Lansing-Kansas City at a depth of approximately 3,450 ft (Harris and Larsh, 1979), and the producing zones may be extensively fractured (Parkhurst, 1962). Similar to the Sleepy Hollow Field, the Huffstutter field has been described as a combination structural-stratigraphic trap (Parkhurst, 1962). Herman (1953) presented evidence of a fault on the anticline and estimated 130 ft offset in the Lansing-Kansas City unit. Herman (1953) also suggested that the oil was trapped on the structural high against the fault.

Multiple detailed studies of Lansing-Kansas City cyclothems in oil-producing areas have been conducted (e.g., Watney, 1980; Frankforter, 1982; Prather, 1984, 1985, 1985b; Watney and French, 1988; Phares, 1991; Salahuddin, 1993; Heckel and Watney, 2002; Young, 2013). Lithofacies and their diagenetic trends can be associated directly with the occurrence of oil in successions of Midcontinent cyclothems (e.g., Watney, 1980; Prather, 1985; Phares, 1991; Young, 2013). The Lansing-Kansas City oil pay zones are typically developed at the tops of regressive limestones where packstones or grainstones were subaerially weathered and meteoric dissolution produced secondary porosity (Watney, 1980; Young, 2013). Overall, oil-bearing zones are isolated from adjacent strata by mudrocks (e.g., Watney, 1980; Heckel, 1997) and, in complete cyclothems, the oil-bearing grainstones are overlain by paleosols developed in red mudstones (Prather, 1985; Young, 2013).

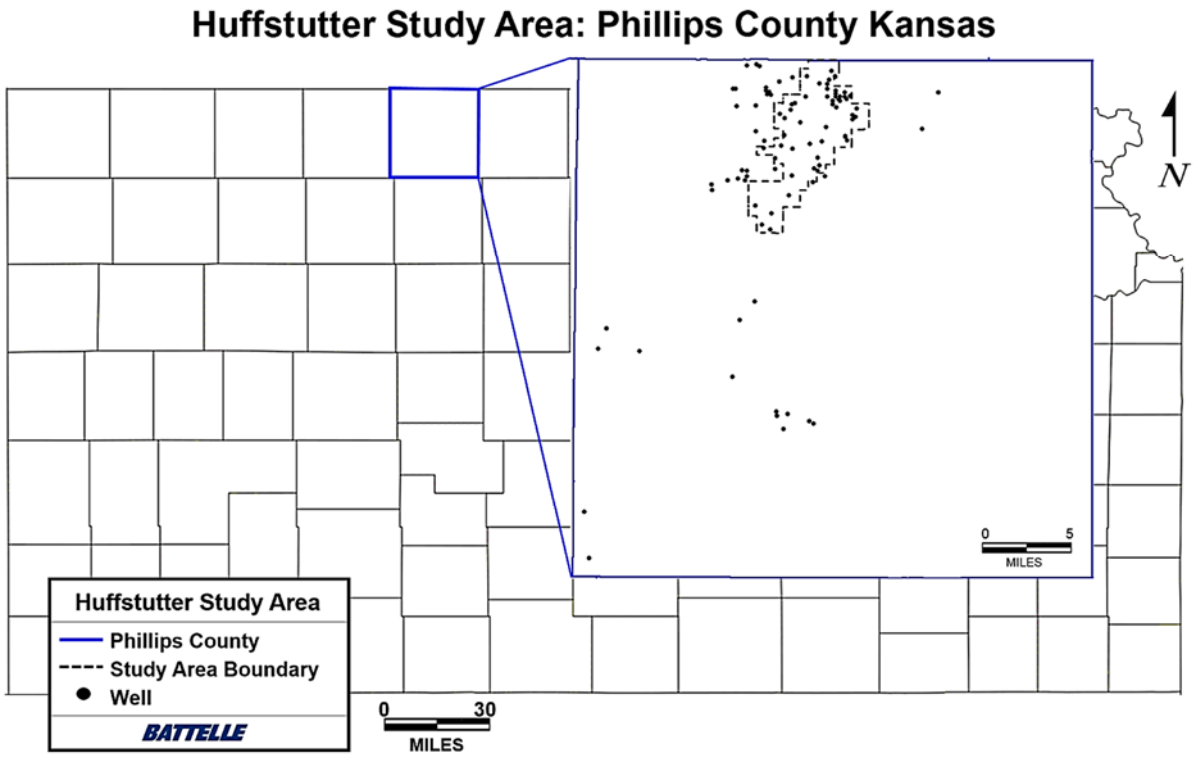

Figure 3-4. Map of Kansas showing the outline of the Huffstutter study area in Phillips County along with the location of 96 wells with logs used for petrophysical analysis, SEM development, and storage resource calculations.

Note on Stratigraphic Nomenclature

Formal stratigraphic nomenclature and classification systems have been proposed for the Lansing-Kansas City groups by multiple authors (e.g., Zeller, 1968; Dubois, 1985; Heckel and Watney, 2002), with up to eighteen formal formation names assigned to the combined lithostratigraphic unit. An additional complication is that the formal stratigraphic terminology for the Pennsylvanian System was developed in the outcrop belt in eastern Nebraska and Kansas, approximately 190 to 250 mi east of the two study areas, and is not entirely applicable in the petroleum-producing parts of Nebraska and Kansas. As such, two informal alphabetic systems of nomenclature have been applied to oil-bearing zones in the Lansing-Kansas City interval by petroleum geologists in Nebraska and Kansas. In both systems, the uppermost oil-bearing zone is labeled “A” and successive letters in the alphabet are applied to successively deeper oil-bearing zones. The Nebraska system employs letters “A” through “G” and the Kansas system employs “A” through “M.” Unfortunately, the two systems are different, and they are not directly correlative (Dubois, 1985). For the purpose of consistency, the informal lettering system used in Nebraska was used in this study to designate the zone tops within the Lansing-Kansas City, and log signatures distinguishing each zone were correlated across the two study areas to delineate deep saline intervals from oil-bearing zones within the group.

3.5 Sub-Basin Evaluation

3.5.1 Data Compilation and Management

Well Log and Core Data

To characterize the Pennsylvanian-Permian storage complex in the Sleepy Hollow study area, subsurface data was compiled from 205 wells over approximately 120 mi^2 in eastern Red Willow County, Nebraska. Of the 205 wells examined in the Sleepy Hollow study area, 171 of them occur on a 40-acre pattern spacing over approximately 7,360 acres (11.5 mi^2) in the oil field. In the Huffstutter study area, data was acquired from a total of 96 wells over 100 mi^2, with 28 wells occurring outside the boundary of the oil field.

Existing well information, core data, and log files (digital and raster) were compiled from publicly available databases and imported into Petra® and the Petrel* E&P software platform for data management and analysis. Existing seismic data was not available in either of the two study areas. The Petra® database was used for data compilation, quality assurance/quality control (QA/QC), petrophysical analysis, and geologic mapping. After QA/QC procedures and processing were completed in Petra®, the log data was imported into the Petrel database to construct the SEMs for the two study areas. Well logs in both digital and raster file format were acquired from the Nebraska Oil and Gas Conservation Commission for the Sleepy Hollow study area (http://www.nogcc.ne.gov/NOGCCPublications.aspx), and the Kansas Geological Survey Oil and Gas Well Database (http://www.kgs.ku.edu/PRS/petroDB.html#ASCII) for the Huffstutter study area. Table 3-1 provides a description of the main log types compiled and used to characterize deep saline storage reservoirs and caprocks in the two study areas.

Table 3-1. Inventory of log data available in the Sleepy Hollow and Huffstutter study areas.

Log Code	Description	Data Uses	Sleepy Hollow Well Count	Huffstutter Well Count
GR	Gamma Ray	GR was used to correlate formation tops and intraformational sedimentary sequences across the study area. The GR log was also used as a shale/clay index to determine the reservoir fraction of the deep saline formation.	212	96
NPHI	Neutron Porosity	NPHI was used to estimate porosity.	25	91
RHOB	Bulk Density	RHOB was used to estimate density porosity.	24	55
DT	Sonic (delta T)	Sonic log wave velocity responses were used to derive porosity estimates from acoustic properties and travel times.	184	20
RT	Resistivity	Resistivity logs were used to identify and correlate lithologic tops and stacking patterns, and evaluate the nature of formation fluids.	190	56

Core data from 13 wells was acquired from the Nebraska Oil and Gas Conservation Commission for the Sleepy Hollow study area (http://www.nogcc.ne.gov/NOGCCPublications.aspx). Porosity, permeability, and grain density data for all wells was compiled as tabulated data in spreadsheet format and uploaded into Petra®. An inventory of core data available for Pennsylvanian-age formations in the Sleepy Hollow study area is provided in Table 3-2. Core data from the Huffstutter study area was not available for analysis.

A total of 267 porosity values, 219 permeability values, and 13 grain density measurements were compiled for the Shawnee-Douglas groups, the Lansing-Kansas City groups, and the basal Pennsylvanian sandstone (Table 3-2). Out of 267 core porosity values, 44 were from deep saline intervals and 223 were from oil-bearing intervals in the Lansing (B and C zones) and the basal Pennsylvanian sandstone. Out of 219 permeability values available,192 were from core in potential oil-bearing zones, and 27 values were from cores in deep saline formations. The 13 grain density measurements were all from oil-bearing zones in the Lansing-Kansas City.

Table 3-2. Inventory of core data available for Pennsylvanian-age formations in the Sleepy Hollow study area.

Group/Formation	Core Data Count		
	Porosity	Permeability	Grain Density
Shawnee-Douglas groups	28	13	NA*
Lansing-Kansas City groups	154	140	13
Basal Pennsylvanian sandstone	85	66	NA*
All (Pennsylvanian interval)	**267**	**219**	**13**

*Not available

Means and ranges were calculated for the porosity, permeability and grain density measurements in each of the lithostratigraphic units using core data. Average grain density values, shown in Table 3-3, were used to calculate density porosity curves for the Lansing-Kansas City. Porosity minimum, maximum, and mean values were used for comparison with and calibration of porosity logs over the intervals evaluated (Table 3-4). The permeability values summarized in Table 3-5 were used in conjunction with core porosity data to develop three zone-specific permeability transforms and generate a composite permeability curve for the entire Pennsylvanian interval of interest.

Table 3-3. Minimum, maximum, and mean core grain density values for Pennsylvanian-age formations in the Sleepy Hollow study area.

Group/Formation	Grain Density (g/cm^3)		
	Minimum	Maximum	Mean
Lansing-Kansas City groups	2.64	2.72	2.70

Table 3-4. Minimum, maximum, and mean core porosity values for Pennsylvanian-age formations in the Sleepy Hollow study area.

Group/Formation	Porosity (%)		
	Minimum	Maximum	Mean
Shawnee-Douglas groups	1	16	7
Lansing-Kansas City groups	1	32	11
Basal Pennsylvanian sandstone	8	30	21
All (Pennsylvanian interval)	1	32	13

Table 3-5. Minimum, maximum, and mean core permeability values for Pennsylvanian-age formations in the Sleepy Hollow study area.

Group/Formation	Permeability (mD)		
	Minimum	Maximum	Mean
Shawnee-Douglas groups	0.01	1	0.1[a]
Lansing-Kansas City groups	0.01	5,900	2[a]
Basal Pennsylvanian sandstone	0.10	13,260	2,042[b]
All (Pennsylvanian interval)	0.01	13,260	9[a]

a. Geometric mean
b. Arithmetic mean

Formation Tops

Selection and correlation of Pennsylvanian and Permian formation tops for the two study areas were conducted for all potential caprocks and storage reservoirs in order to map formation depths (structure maps) and thicknesses, and define the structural framework of the SEMs for the selected areas. Tops and bases were selected for the Admire Group, the Council Grove Group, the Sumner Group, and the Nippewalla shale to represent caprock depths. Tops and bases were selected for twelve formations/zones within the deep saline interval extending from the Wabaunsee Group (top) to the Precambrian basement (base).

The stratigraphic framework developed by Heckel (1977; 1994; 2008) Dubois (1985), Joeckel (1994) and Heckel and Watney (2002) for Midcontinent Pennsylvanian-Permian strata was used to inform and guide formation top picks and interpretations in both study areas. Formal stratigraphic nomenclature is used for the major lithostratigraphic groups, and both formal and informal nomenclature is used for individual formation and zone names. Lithostratigraphic tops where assigned principally on recognition of formational patterns identified in gamma, neutron, density, resistivity, and sonic log signatures. Regional shale marker beds in the Shawnee-Douglas (e.g., Heebner Shale) and Lansing-Kansas City groups were also used as local reference points to aid stratigraphic correlations in each study area.

Tops and bases from a total of 205 wells with wireline logs were used to define the Pennsylvanian-Permian storage complex in the Sleepy Hollow study area, with tops largely acquired from the Nebraska Oil and Gas Conservation Commission's online database

(http://www.nogcc.ne.gov/NOGCCPublications.aspx). Minor adjustments and additional picks were made to this initial dataset to establish a consistent and complete set of tops and bases for the Sleepy Hollow study area.

Tops for the Huffstutter study area were acquired from the Kansas Geological Survey Oil and Gas Well Database, when available (http://www.kgs.ku.edu/PRS/petroDB.html#ASCII). A majority of the tops were selected by the Project Team, with tops and bases from a total of 96 wells with wireline logs used to define the Pennsylvanian-Permian formations of interest in the Huffstutter study area.

Data Quality Assurance/Quality Control (QA/QC)

Raster logs (i.e. electronic image files) were digitized and converted to Log ASCII Standard file format (LAS) when necessary, and all digital logs were uploaded into Petra® to undergo data QA/QC prior to petrophysical analysis and integration in SEMs. All digital logs to be used for quantitative analysis (GR, NPHI, RHOB, DT) in each study area underwent an initial processing/screening procedure consisting of the following steps:

- Logs were clipped to removed erroneous data at the beginning and end of log curves
- Log data segmented over different depth intervals of a well were spliced together to create continuous (in most cases) composite curves.
- Log curves for all wells were resampled to an equal to step rate of 0.5 ft to facilitate petrophysical calculations and analysis
- All log porosities were transformed to decimal units
- Log data statistics (e.g., minimum, maximum, mean) were calculated for all wells to evaluate the distribution in each study area and identify geologically unreasonable outliers

When outliers were identified, the log data was compared with that of the original LAS file and raster file to determine and correct the problem, if possible. If the data could not be corrected, it was spliced out of the log curve to remove it from subsequent calculations.

Gamma Ray Normalization

Gamma ray curves were normalized by zone to eliminate varying signal intensities and establish consistent readings for sandstone, carbonate, and shale lithologies. Gamma ray logs were normalized using two-to-three type wells in each study area that exhibited gamma ray values characteristic of sandstone, carbonate, and shale in intervals where these lithologies where known to exist (e.g., basal sandstone, Topeka Limestone, Carlile Shale). The mean and range of gamma ray values in each zone were normalized to the mean values and ranges calculated in type wells. Normalization by mean was conducted via Equation 3-1:

$$GR_{norm} = GR_{log} - GR_{zonemean} + GR_{normmean} \qquad \textbf{Equation 3-1}$$

Where:

- GR_{norm} = the normalized gamma ray log
- GR_{log} = the original gamma ray log value
- $GR_{zonemean}$ = the mean gamma ray value for the zone of interest in the non-type well
- $GR_{normmean}$ = the mean gamma ray value for the zone of interest in the type well

The ranges of the normalized gamma ray curves were then calculated for each zone to identify outliers in the dataset requiring additional normalization using the minimum and maximum values observed in type wells. Normalization by minimum and maximum values was conducted via Equation 3-2:

$$GR_{norm} = GR_{normmin} + (GR_{log} - GR_{zonemin}) \times (GR_{normmax} - GR_{normmin})/(GR_{zonemax} - GR_{zonemin}) \quad \textbf{Equation 3-2}$$

Where:

- GR_{norm} = the normalized gamma ray log
- $GR_{normmin}$ = the minimum gamma ray value for the zone of interest in the type well
- GR_{log} = the original gamma ray log value
- $GR_{zonemin}$ = the minimum gamma ray value for the zone of interest in the non-type well
- $GR_{zonemax}$ = the maximum gamma ray value for the zone of interest in the non-type well

This normalization procedure ensured mineralogically homogenous (i.e. clean) sandstones and carbonates had gamma ray values less than 65 gAPI (American Petroleum Institute gamma ray units) and shale/clay-rich intervals had values above 65 gAPI. The normalized gamma ray log was then used to estimate the reservoir and shale fraction of each potential storage zone, and facilitate reservoir pore volume calculations.

3.5.2 Petrophysical Calculations

Workflow

Petrophysical analysis was conducted to generate the final porosity and permeability logs curves needed to populate the SEM and characterize reservoir properties of the deep saline formations. All petrophysical calculations were conducted in Petra®.

The workflow for generating the total porosity, effective porosity, and permeability curves used for property population in the SEMs is shown in Figure 3-5. This general workflow was employed in both the Sleepy Hollow and Huffstutter study areas, with the exception being that core data was not available for integration with log data in the Huffstutter study area.

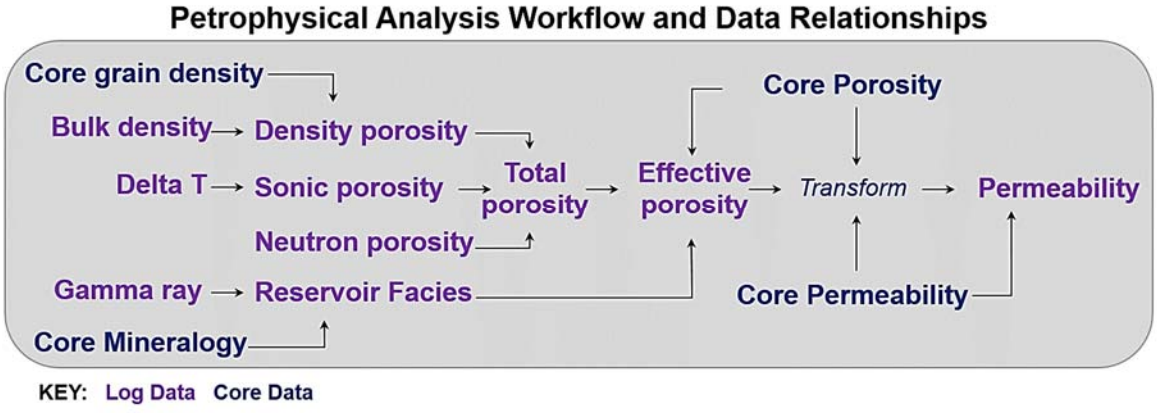

Figure 3-5. Flow chart illustrating data relationships and integration procedures used for generating total porosity, effective porosity, and permeability curves.

Shale Volume Calculations

Lithologic profiles can be developed via integration of various data types to better determine the reservoir facies of a subsurface interval. This analysis often includes a combination of routine gamma ray, neutron porosity, and bulk density logs, supplemented with grain density measurements, mineralogical data, elemental spectroscopy logs, and photoelectric logs.

In each study area, the variety of data available to thoroughly resolve lithologic heterogeneity in each well was often limited, with most wells having a gamma ray log and no more than one or two types of porosity logs. This limitation made it difficult to establish a consistent, comprehensive approach that could be applied to develop a robust reservoir facies profile for all wells in each study area. The normalized gamma ray curve was therefore used as a basic index for shale volume to derive effective porosity curves and estimate the reservoir and non-reservoir fraction of each potential storage zone via Equation 3-3:

$$V_{shale} = (GR_{log} - GR_{res}) \,/\, (GR_{shale} - GR_{res}) \qquad \textbf{Equation 3-3}$$

Where:

- V_{shale} = shale fraction (i.e. non-reservoir)
- GR_{log} = gamma ray log value
- GR_{res} = gamma ray value of clean sandstone and/or carbonate in each zone
- GR_{shale} = gamma ray value from a nearby shale interval
- 1-V_{shale} = clean sandstone and/or carbonate fraction (i.e. reservoir)

Minimum gamma ray values calculated in each zone were used as input for GR_{res}. The mean gamma ray values calculated in each well for the Carlile Shale was used as input for the GR_{shale} parameter in the Sleepy Hollow study area, and the gamma ray mean for the Heebner Shale was used for GR_{shale} in the Huffstutter study area. The estimated reservoir fraction (1-V_{shale}) was then used to correct for shale/clay-bound porosity and calculate effective log porosities for the deep saline formations of interest.

Porosity Calculations

Total porosity, effective porosity, and reservoir facies were evaluated by assuming clean carbonate and sandstone represents the potential storage reservoir, and shale represents the non-reservoir fraction of the deep saline formation. Total porosity is defined as the combined percentage of interconnected, isolated, and clay-bound porosity of the total formation. Effective porosity is defined as the combined percentage of interconnected and isolated porosity in sandstone and/or carbonate reservoirs, and does not include the clay-bound porosity associated with the non-reservoir, shale fraction. Total and effective porosity were calculated using bulk density logs, neutron porosity logs, sonic logs, and core porosity data.

Density porosity was calculated from bulk density logs via Equation 3-4.

$$DPHI = (\rho_{matrix} - RHOB_{log}) \,/ (\rho_{matrix} - \rho_{fluid}) \qquad \textbf{Equation 3-4}$$

Where:

- *DPHI* = density porosity
- ρ_{matrix} = density of rock matrix (i.e. grain density)
- $RHOB_{log}$ = bulk density log value
- ρ_{fluid} = density of pore fluids

An average grain density value of 2.70 g/cm^3 was derived from core data (e.g., Table 3-2) and used as ρ_{matrix} input for the Lansing-Kansas City. An empirically-derived industry standard calcite/limestone matrix density of 2.71 g/cm^3 was used to calculate density porosity for the Shawnee-Douglas, and a standard quartz/sandstone matrix value of 2.65 g/cm^3 was used in calculations for the basal sandstone, the Wabaunsee, and the Pleasanton-Marmaton groups. The density of pore fluids in deep saline formations was assumed to be 1.1 g/cm^3 for saltwater.

Sonic porosity was calculated using Equation 3-5:

$$SPHI = (\Delta T_{log} - \Delta T_{matrix}) / (\Delta T_{fluid} - \Delta T_{matrix}) \quad \textbf{Equation 3-5}$$

Where:

- *SPHI* = acoustic (sonic) porosity
- ΔT_{log} = acoustic travel time log value
- ΔT_{matrix} = acoustic travel time of rock matrix
- ΔT_{fluid} = acoustic travel time of pore fluids

A standard acoustic travel time of 47.6 microseconds per foot (µsec/ft) in a limestone matrix was assumed for ΔT_{matrix} in calculations for the Shawnee-Douglas and Lansing-Kansas City groups, and a ΔT_{matrix} value of 52.6 µsec/ft for consolidated sandstone was assumed for the basal sandstone, Wabaunsee, and Pleasanton-Marmaton groups (Carmichael, 1982). The ΔT_{fluid} value was assumed to be that of salt water, with an acoustic travel time of 189 µsec/ft (Carmichael, 1982).

The resulting DPHI and SPHI logs were used along with NPHI logs to estimate total porosity (PHI_t). When more than one porosity log was available, the curves were averaged to derive a total porosity curve.

The estimated reservoir fraction (1-V_{shale}) was then used to correct the total porosity curve for shale/clay effects and generate effective porosity logs. Effective porosity was estimated by calculating the porosity associated with the reservoir fraction via Equation 3-6:

$$PHIe = PHI_t \times (1 - V_{shale}) \quad \textbf{Equation 3-6}$$

Where:

- PHI_e = effective porosity
- PHI_t= total porosity (uncorrected)
- 1-V_{shale} = sandstone and/or carbonate fraction (i.e. reservoir fraction)

The minimum, maximum, and mean of the PHI_e curve in the Shawnee-Douglas, Lansing-Kansas City, and basal sandstone were then calculated and individual well results were compared to the mean and range of the porosity calculated using all available core data for each of those intervals (e.g., Table3-4). If the difference between the PHI_e mean and the core data mean was greater than 50% and/or the range of core porosities was outside of the calculated range of PHI_e values, the PHI_e log was normalized to the mean and range of the core data for the zone of interest.

Porosity-Permeability Transforms

Permeability was plotted as a function of porosity to determine the relationship between the two parameters, and derive transform equations to estimate permeability from porosity log data. Transforms were developed using core data from the Shawnee-Douglas groups, the Lansing-Kansas City groups, and the basal Pennsylvanian sandstone. Out of 219 porosity-permeability values available,192 were from core in potential oil-bearing intervals in the Lansing (B and C zones) and the basal Pennsylvanian sandstone, and 27 values were from cores in deep saline formations.

Two transforms equations were derived: (1) one for the Lansing-Kansas City, and (2) one for the Pennsylvanian interval extending from the top of the Wabaunsee to the base of the basal sandstone. Porosity and permeability values from 140 core samples were plotted to establish the transform for the Lansing-Kansas City groups shown in Figure 3-6. Due to the limited amount of core data for the Shawnee-Douglas groups and absence of data in the Wabaunsee and Pleasanton-Marmaton groups, all available core data in the Sleepy Hollow study area was combined to derive a porosity-permeability transform for the entire Pennsylvanian interval. The resulting transform, shown in Figure 3-7, was used to estimate permeability for the Wabaunsee, Shawnee-Douglas, and Pleasanton-Marmaton groups.

The two permeability transforms were applied to the total porosity (PHI_t) curve over the intervals of interest to derive a permeability curve for each well. The low R-squared value observed in the regression for the Lansing-Kansas City, and the incorporation of data from oil-bearing formations represent potential sources of inaccuracy and uncertainty in the permeability curves for the deep saline formations.

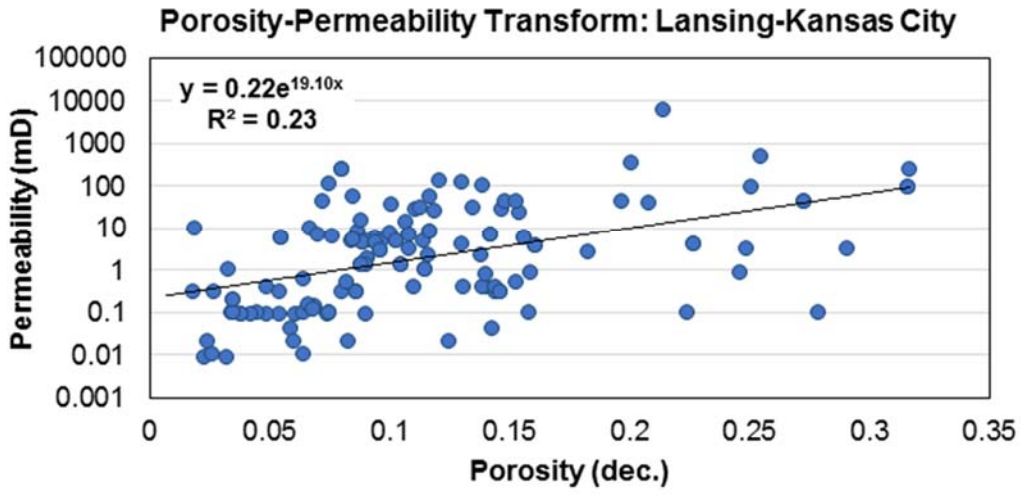

Figure 3-6. Porosity-permeability transform derived from core data from the Lansing-Kansas City groups in the Sleepy Hollow study area.

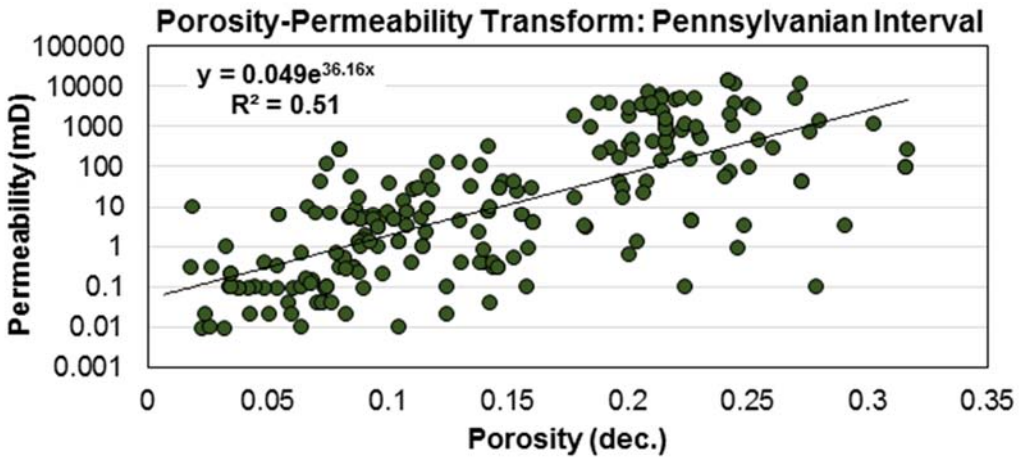

Figure 3-7. Porosity-permeability transform derived from core data from the Pennsylvanian Interval groups in the Sleepy Hollow study area.

Total and Net Reservoir Calculations

Evaluation of reservoir petrophysical properties included calculation and mapping of porosity-feet, and calculation of net-to-gross reservoir pore volumes to derive site-specific storage efficiency values for the deep saline intervals of interest.

Data availability and resolution in the Sleepy Hollow study area were sufficient to identify and remove portions of the deep saline interval associated with shale and clay-rich components. These components exhibit unconventional reservoir properties that are not conducive to deep saline CO_2 storage. Unlike storage estimates associated with total formation volume, commonly derived from average gross formation properties in circumstances of limited data availability, the deep saline interval evaluated for storage in the Sleepy Hollow study area was better constrained to "total reservoir" and "net reservoir" volumes (Table 3-6). Total reservoir was defined in this study as the fraction of the deep saline formation that is composed of sedimentary lithologies with conventional reservoir properties, such as sandstone and carbonate. Net reservoir was defined as the fraction of the total reservoir that is associated with effective, interconnected porosity, as these pore volumes are more likely to be accessible to injected CO_2 during storage.

Table 3-6. Definitions of total and net reservoir and associated data used in this study to quantify each.

Definition		Data Input/Quantification
Total reservoir volume	Portion of the deep saline formation composed of sedimentary lithologies with conventional reservoir properties (e.g., sandstone and carbonate)	Bulk volume of the subsurface unit estimated to have gamma ray values ≤ 65 gAPI
Net reservoir volume	Portion of the total reservoir associated with interconnected porosity that is potentially accessible to injected CO_2	Bulk volume of the subsurface unit estimated to have gamma ray values ≤ 65 gAPI and permeability values ≥ 1 mD

To quantify the total reservoir volume of the deep saline formation, known oil-bearing and shale intervals distinguished by formation tops and bases were excluded from the analysis. In instances where shale and/or clay was interbedded with sandstone and carbonate reservoirs, a maximum gamma ray cut-off of 65 gAPI was used to distinguish clean reservoir lithologies from shale and clay-rich intervals. A maximum gamma ray cut-off of 75 gAPI is an industry standard for distinguishing between non-reservoir and reservoir intervals (e.g., Slatt, 2006). This cut-off helps to delineate clean sandstones and carbonates with low amounts of radioactive components (GR <75 gAPI) from shale and clay-bearing rocks with higher proportions of radioactive constituents (GR >75 gAPI). A comparison of the gamma ray signatures in known shale intervals (Carlile and Heebner shales) versus gamma ray signatures in clean carbonate zones of the Lansing-Kansas City and Shawnee-Douglas groups determined a more conservative gamma ray cut-off of 65 gAPI better delineated clean carbonate reservoir from non-reservoir shale intervals in the Sleepy Hollow and Huffstutter study areas.

The net reservoir volume was determined via a minimum permeability cut-off of 1 millidarcy (mD) in addition to the maximum GR cut-off of 65 gAPI. The permeability cut-off assumes pore volume associated with any non-zero permeability measurement is, by definition, interconnected, and a minimum permeability of 1 mD is a common standard used in industry to define net intervals in oil reservoirs (Worthington and Cosentino, 2005).

3.5.3 Three-Dimensional (3D) Static Earth Model (SEM) Development

SEM Objectives and Workflow

A key factor in the success of the site-scale geologic characterization depends on understanding subsurface geologic features. In particular, an understanding of reservoir and caprock characteristics are necessary. To accomplish this, available subsurface data was integrated into a three-dimensional (3D) SEM to represent the geologic storage framework of the two study areas.

The specific objectives of the SEM are:

- Between well locations, use geologic concepts to integrate data.
- Develop surfaces from well tops and, if available, interpreted horizons (formation tops) from seismic lines.
- Create a framework representing geology of reservoirs and caprocks.
- Populate model with petrophysical data to describe reservoir characteristics (i.e. porosity and permeability).

To meet these goals, the work began with data acquisition and extensive data QA/QC, followed by petrophysical calculations, as described in Sections 3.1 and 3.2 of this report. To build a comprehensive SEM for each study area, the following subsurface data types were gathered and interpreted:

- Well locations and their trajectories
- Well drilling and completion reports
- Well logs (examples include: gamma ray, density, sonic, porosity, and permeability)
- Formation top picks from wells
- Core sample collection and analysis, if available

The regional geologic and petrophysical reservoir data compiled during this characterization phase of the project was integrated into a conceptual geologic model or SEM using the Petrel geologic modeling software. The goal of the SEM is to provide a representative model with sufficient resolution of vertical and lateral heterogeneity to honor the geology. Then, the SEM is used as a tool to evaluate the reservoir(s) and estimate prospective CO_2 storage resource. Furthermore, the SEM is used to conduct dynamic earth modeling and flow simulations to evaluate and optimize injection strategies at each selected study area.

SEMs have been prepared for two sites; the first, in Red Willow County, Nebraska focused on Sleepy Hollow study area and is on the western flank of the Cambridge Arch. The second SEM was centered on Huffstutter study area in Phillips County, Kansas and is positioned on the eastern portion of the Central Kansas Uplift (Figure 3-1).

For both sites, petrophysical SEMs were prepared and cover formations from the Upper Pennsylvanian Wabaunsee Group down to the Precambrian basement rock. The names of lithostratigraphic groups, formations, members, and informal zones incorporated into the SEMs are listed in Table 3-7.

Table 3-7. Names of formations, members, and informal zones associated with each of the four major lithostratigraphic groups evaluated in this study (in stratigraphic order).

Group(s)	Formation(s)	Member	Informal Zone Designation
Wabaunsee	*	*	*
Shawnee-Douglas	Topeka	*	*
	Deer Creek	*	*
	Lecompton	*	*
	Oread	Heebner Shale[a]	*
		Levenworth Limestone[a]	*
		Toronto Limestone[a]	*
Lansing-Kansas City	*	*	LKC A
	*	*	LKC B
	*	*	LKC C
	*	*	LKC D
	*	*	LKC E
	*	*	LKC F
	*	*	LKC G[a]
Pleasanton-Marmaton	*	*	*

*Not Designated

a. Only designated in the Huffstutter study area

A simplified linear SEM workflow is presented in Figure 3-8. Formation top data and well logs were quality checked and imported to Petrel as model inputs for structural surfaces and isopach maps.

Structural surfaces were used to delineate the model's framework which was composed of stratigraphic intervals (zones), and layers. Well log data were interpreted for potential reservoir rock and seals, and upscaled to the desired resolution. A lithofacies model consisting of carbonates, shale, and sandstone was used to guide the porosity model. The porosity model was then used to guide the permeability model. Thus, the 3D geocellular framework was populated with petrophysical properties consistent with their stratigraphic zones.

The following sections will address three topics in the SEM development:

- Showcase the data that was used to inform the SEM.
- Describe the geomodeling assumptions and critical workflow elements used in SEM construction.
- Provide details and characteristics of the SEM.

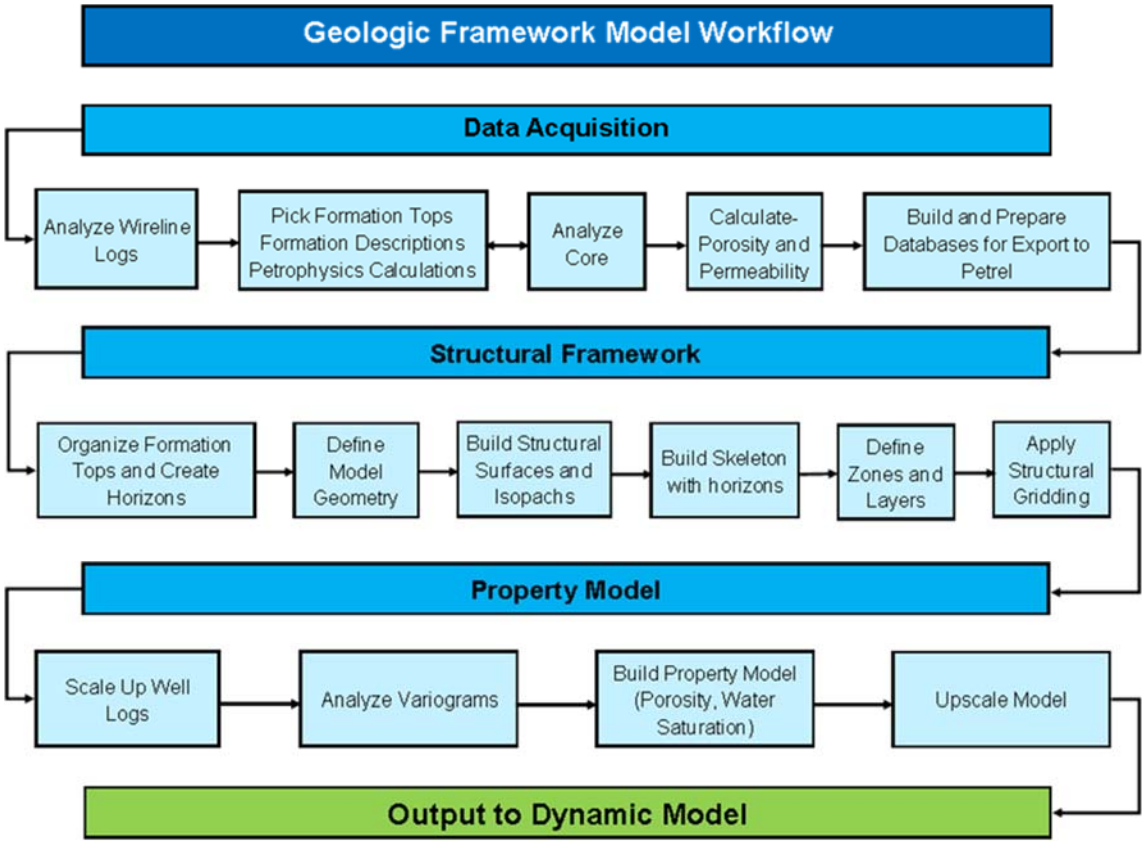

Figure 3-8. Generalized static earth modeling workflow.

Structural Framework

Two SEMs were prepared, one for the Sleepy Hollow study area, the other for the Huffstutter study area. Both SEMs covered an area of 10 mi x 10 mi and were centered on these oil fields where many wells were present. Working with existing well data, certain geologic assumptions and simplifications were implemented during construction of the models to honor geologic interpretations.

Assumptions

With Sleepy Hollow study area positioned on the western flank of the Cambridge Arch, the regional structural dip was assumed to dip to the southwest toward the Hugoton Embayment. A structural dip of 0.17-degrees with azimuth of 254-degress was interpreted from three surfaces: the top of the Lansing-Kansas City (LKC A), the base of the Lansing-Kansas City (Kansas City Base), and the top of the basal sandstone. This general trend was used to guide surface interpolation where well control was limited.

The Huffstutter study area is positioned on the eastern portion of the Central Kansas Uplift with the Salina Basin to the east. The Heebner Shale correlates nicely among well logs and represents a favorable surface that provides a general structural trend over the study area. This trend, the Heebner Shale surface, was used to guide the construction of other surfaces where well control was limited.

The SEM frameworks assumed simple surfaces without the incorporation of faults. Both Sleepy Hollow and Huffstutter Fields reside over subtle anticlinal structures as revealed by well top data across their fields. Faults, if present, are best imaged by 3D seismic or a high-density grid of 2D seismic data. This data either did not exist or was not available during this phase of the project.

The dataset used to construct the structural framework consisted of formation tops. Given their number, density, and the apparent trend of interpreted tops, the creation of surfaces was well defined over the fields. Structural surfaces and isopach maps were created in Petrel using convergent interpolation. The convergent interpolation algorithm uses a series of refinements to locally tune the surface to neighboring data while reducing anomalous extrapolations. With a number of these surfaces being relatively close together, it is not uncommon for surfaces to overlap, especially where well control is poor. This is generally observed during the QA / QC process where surfaces are inspected for conformability. To reconcile the development of overlapping surfaces, an existing surface is used as a secondary input for guiding structural trends during the surface interpolation process. As per the assumptions above, the implementation of structural trend surfaces during the process was very effective at mitigating “surface-overlapping” issues.

Facies Modeling

For simplicity, each formation was assumed to consist of four or fewer lithofacies, and lithologic heterogeneity was incorporated into the model through the development and use of facies models. Two general facies themes were implemented, one for the cyclic carbonates present in both study areas, the other for the basal sandstone.

Gamma ray logs in the area have a cyclic character, and this response is consistent with the cyclic nature of the Pennsylvanian carbonates. The cycles are attributed to variations in sea level where the corresponding sediments occur in environments of varying energy.

Cyclic Carbonates Assumptions

For the cyclic carbonates of the Shawnee-Douglas and Lansing-Kansas City groups, facies modeling for the SEM used gamma ray logs as the key indicator to estimate lithofacies.

Low gamma ray response was attributed to near shore, higher energy depositional environments where carbonates are dominate, and porosity is more favorable than deeper environments. High gamma ray response was associated with deeper, offshore sediments that have greater composition of silt and muds.

Core analysis has shown that shallow, high energy environments, especially those that were subjected to aerial exposure, have better porosity development, (Young, 2011). Thus, a simplified facies model was developed for these cyclic carbonates, and consists of three facies corresponding to the energy of their environment: high energy, moderate energy, and low energy. The gamma logs were used to delineate these three groups (Table 3-8). Gamma ray logs had been normalized previously as part of the log QA/ QC process. A fourth group was also identified for gamma ray values that were very large. Core testing has indicated that these intervals are due to phosphatic enrichment likely due to biological remains. These high gamma ray phosphatic zones were associated with high effective log porosities, and it was assumed that this was due to uncertainty and/or error introduced by data limitations in the calculation v_{shale} and associated effective porosity logs (Section 3.2.3). The intervals associated with higher gamma ray values (> 65 gAPI) were therefore treated as tight formations for modeling purposes. The consequence of this choice is potentially underestimating formation porosity in these high-phosphatic carbonate zones.

Table 3-8. Gamma ray intervals used to delineate facies from the well logs.

Gamma Ray (from well logs)	Depositional Environment	Facies Code	Notes
0-65	High Energy	0	Good porosity development
65-100	Moderate Energy	1	Poor to fair porosity development
100-150	Low Energy	2	Low Porosity
150+	Phosphatic intervals	3	Possibly good, but treated as low porosity

Given the cyclic nature of the carbonates, low energy depositional settings dominated by tight, carbonate mudstone present low permeability baffles and compliment potential storage intervals comprised of porous carbonates. These low permeability baffles would inhibit vertical CO_2 migration.

The cyclic carbonates facies model was prepared in a three-step process: 1) a discrete facies log was created for each well using its gamma ray log and the ranges indicated in Table 3-8. 2) The discrete facies logs were upscaled into the geocellular grid along their well trajectories. 3) These facies were interpolated among the wells using Gaussian Random Function Simulation (GRFS). Due to the regional extent and correlation among the wells, no lateral anisotropy was introduced to the facies model. Later, the facies model was used to condition the effective porosity distribution.

Basal Pennsylvanian Sandstone Assumptions

The basal sandstone is a local basal Pennsylvanian sandstone at Sleepy Hollow study area. The following assumptions regarding this reservoir rock are informed from a paper by Rogers (1977) and include:

- The basal sandstone is stratigraphically equivalent to the Cambrian-age Reagan Sandstone in other parts of the region.

- This sandstone package is a local feature that was deposited into shallow marine water and was sourced from the north.
- Longshore drift at the time of deposition was toward the west, with limited sand transport further to the south.
- Due to source location, structural uplift, and erosion, the basal sandstone pinches out to the east.
- Locally, the thickness of the basal sandstone varies due to basement topography. The sandstone is thicker where the weathered basement thins.
- The sandstone unit is capped by shale which is present in the overlying Marmaton Group.
- The basal sandstone has more favorable reservoir properties than facies that may exist adjacent to it.

These assumptions were used as part of the facies modeling workflow to estimate the limits and shape of the basal sand's occurrence in and around the Sleepy Hollow study area. This workflow was not implement for the Huffstutter area because no comparable basal sandstone unit was identified.

Log Adjustments and Upscaling

Porosity and permeability are the two key petrophysical properties distributed in the SEM which are directly used for dynamic modeling purposes. Petrophysical logs from both study areas were adjusted as described below prior to upscaling for property modeling.

Many intervals exhibited inflated porosity on the effective porosity logs for units that have historically been interpreted as low porosity and low permeability (i.e. tight). An explanation for this stems from the fact that these are computed logs based on a limited, existing log set where determination of shale volume may be underestimated or inaccurate. For example, Figure 3-9 shows regressive limestone sequences where favorable porosity development should occur at the top of the sequence (Young, 2011); and tighter rocks occur lower in the cycle. However, higher effective porosity values were also observed in the lower cycles of the Lansing-Kansas City interval associated with higher gamma ray values and these higher effective porosity values were considered inaccurate.

Effective Porosity Adjustment Justification

- The higher log porosities associated with the low energy facies may be due to uncertainty/error in calculation of the shale fraction (v_{shale}) and generation of the effective porosity log (see Sections 3.2.2 and 3.2.3).
- Available porosity is commonly found in the upper portion of these cycles where limestone is the dominate lithology, and where reservoir quality was enhanced when carbonate units were subjected to periods of aerial and subaerial exposure.

For modeling purposes, given the effective porosity mismatch with tighter rock units, it was necessary to attenuate the effective porosity logs for moderate and low energy depositional environments. Using the facies codes originating from the gamma ray logs, the effective porosity and permeability logs were adjusted with the coefficients (multipliers) given in Table 3-9. Figure 3-9 shows the attenuated porosity curve in black. The permeability logs also required adjustments because they originated from a porosity-permeability transform.

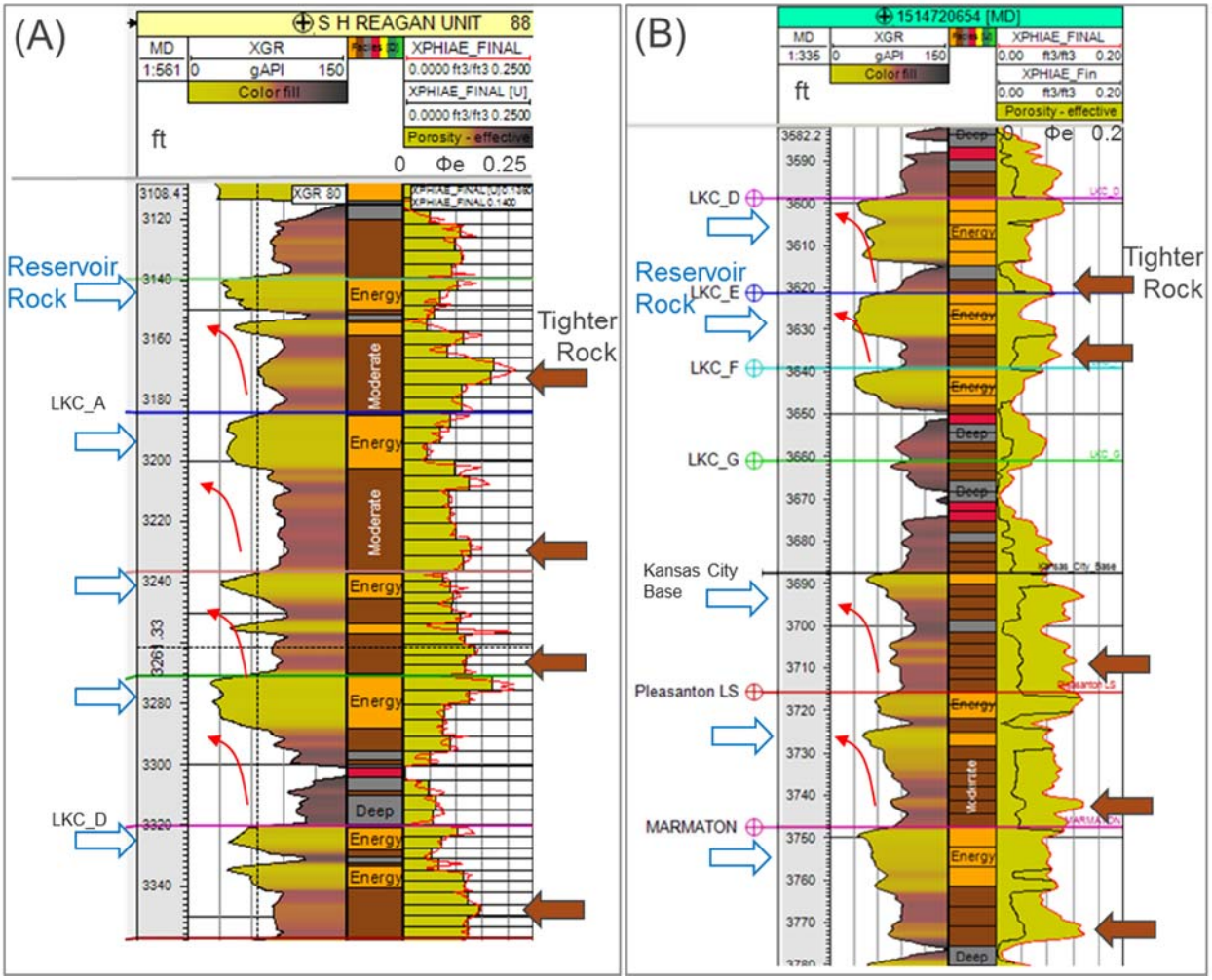

Figure 3-9. Gamma ray and effective porosity log from (A) Sleepy Hollow Field and (B) Huffstutter Field.

Red arrows depict regressive limestone sequences on the gamma ray log. Brown arrows at right point to suspect porosity intervals where computed effective porosity is overestimated due to inaccurate shale volume estimates.

Table 3-9. Gamma ray intervals used to delineate facies from the well logs.

Gamma Ray (from well logs)	Facies Code	Depositional Environment	Porosity Adjustment	Permeability Adjustment
0-65	0	High Energy	1 x Φe	1 x K
65-100	1	Moderate Energy	1/4 x Φe	1/50 x K
100-150	2	Low Energy	1/8 x Φe	1/500 x K
150+	3	Phosphatic intervals	1/8 x Φe	1/500 x K

The adjusted effective porosity well log data was upscaled to the cells along well trajectories. The upscaled values occur at the vertical resolution of the model's grid using the arithmetic averaging method which is commonly employed for additive properties such as porosity. The permeability logs were upscaled in a similar fashion, but used a geometric averaging method which better represents logarithmic character.

Property Model

The workflow for developing the porosity model involved upscaling the effective porosity log values to the vertical grid resolution along well trajectories. Distributing the upscaled data away from well control often involves variogram analysis to understand a formation's lateral heterogeneity. With significant lateral continuity among the well log signatures, a variogram analysis was not conducted during this phase of the project. Instead, the facies model was used to delineate the different reservoir flow units: high energy carbonates with porosity development versus tighter units that would behave more like confining units. A GRFS was chosen for the generation of the 3D porosity distribution in the SEM and was conditioned by the facies model. This stochastic algorithm used a range of values as observed from the upscaled well log data with a maximum effective porosity of 25%.

The 3D permeability distribution in the SEM was simulated by conditioning it to the porosity model. It assumes that permeability is related to porosity, and that high porosity cells would yield good permeability. Conversely, low permeability cells would be associated with tight, low porosity cells. The permeability modeling method works with the upscaled permeability log and uses GRFS. However, the simulation is guided by the porosity model as a secondary variable through a collocation, co-kriging method and normal score transform.

Modeling results were assessed by comparing histograms of the well logs with upscaled values and the property model values. These histograms can reveal where upscaling and modeling has been successful or where the workflow does not represent original data. Frequently, it shows where there are simple limitations to upscaling, especially when formations have significant vertical heterogeneity. Log sampling accuracy is enhanced with finer grid layers, but comes at the expense of model cell counts that can range in the hundreds of millions.

3.5.4 Geologic Mapping

Caprock Maps

Structure (top depth) and isopach (gross thickness) were generated from well data to evaluate the vertical and lateral distribution of potential caprocks in both study areas. All caprock maps were created in Petra® in the Universal Transverse Mercator (UTM) coordinate system (zone 14N) using the Geodetic Reference Spheroid of 1980 (GRS 1980) and the North American Datum of 1983 (NAD83). Caprock structure and isopach maps were gridded using a minimum curvature surface style without faults. All maps were gridded using an average grid size estimate for interpolation, with grid limits defined by the SEM boundary surrounding each study area (e.g Section 3.3). The number of well data points used to generate caprock structure and isopach maps is shown in Table 3-10 for the Sleepy Hollow study area, and Table 3-11 for the Huffstutter study area.

Table 3-10. Number of well data points used to generate structure and isopach maps for caprocks in the Sleepy Hollow study area (in stratigraphic order).

Caprock Group Name	Structure Map Well Data Count*	Isopach Map Well Data Count*
Nippewalla	33	27
Sumner	32	26
Council Grove	32	26
Admire	33	27

*Three wells outside of the study area were used as control points

Table 3-11. Number of well data points used to generate structure and isopach maps for caprocks in the Huffstutter study area.

Caprock Group Name	Structure Map Well Data Count	Isopach Map Well Data Count
Nippewalla	52	55
Sumner	58	54
Council Grove	59	55
Admire	60	59

Deep Saline Formation Maps

Structural surfaces were created for potential storage zones in the SEMs using well tops from each study area and a convergent interpolation algorithm in Petrel®. This gridding algorithm employs a series of refinements to locally tune a surface to neighboring data while reducing anomalous extrapolations.

In some cases, the individual formations and members comprising stratigraphic groups were combined to generate structure, isopach, and porosity-footage maps for each group using grid data from the SEM. These groups reflect deep saline Pennsylvanian strata that exhibit regional-scale lithostratigraphic similarities in the Midcontinent. The names of formations and members assigned to each lithostratigraphic group are listed in Table 3-12. The top structural surface for each group was used to generate structure maps. Isopach maps were generated by computing the vertical difference between the structural top and bases for each group. The number of wells used to generate structure and isopach maps for the deep saline formations in the Sleepy Hollow and Huffstutter study areas is listed in Table 3-13 and Table 3-14, respectively.

Table 3-12. Names of formations, members, and informal zones associated with each of the four major lithostratigraphic groups evaluated in this study (in stratigraphic order).

Group(s)	Formation(s)	Member	Informal Zone Designation
Wabaunsee	*	*	*
Shawnee-Douglas	Topeka	*	*
	Deer Creek	*	*
	Lecompton	*	*
	Oread	Heebner Shale[a]	*
		Levenworth Limestone[a]	*
		Toronto Limestone[a]	*
Lansing-Kansas City	*	*	LKC A
	*	*	LKC B
	*	*	LKC C
	*	*	LKC D
	*	*	LKC E
	*	*	LKC F
	*	*	LKC G[a]
Pleasanton-Marmaton	*	*	*

*Not Designated

a. Only present in the Huffstutter study area

Table 3-13. Number of well data points used to generate structure and isopach maps for deep saline formations in the Sleepy Hollow study area.

Group(s)	Structure Map Well Data Count*
Wabaunsee	117
Shawnee-Douglas	153
Lansing-Kansas City	180
Pleasanton-Marmaton	178

*4 wells outside of the study area were used as control points for the Wabaunsee Group, 53 for the Shawnee-Douglas groups, 9 for the Lansing-Kansas City groups, and 5 for the Pleasanton-Marmaton groups.

Table 3-14. Number of well data points used to generate structure and isopach maps for deep saline formations in the Huffstutter study area.

Group(s)	Isopach Map Well Data Count
Wabaunsee	58
Shawnee-Douglas	70
Lansing-Kansas City	24
Pleasanton-Marmaton	23

*2 wells outside of the study area were used as control points for the Shawnee-Douglas groups, 2 for the Lansing-Kansas City groups, and 1 for the Pleasanton-Marmaton groups

Porosity-footage was calculated and mapped for the Wabaunsee, Shawnee-Douglas, Lansing-Kansas City and Pleasanton-Marmaton groups in both study areas to gauge the thickness of the pore volume within the total reservoir interval. The maps were generated in Petrel® from the porosity distributions of the "energy" or reservoir facies within each saline storage layer in the SEMs using the following equation (Equation 3-7):

$$Porosity\text{-}Footage = \Sigma(\phi_{Reservoir} * h_{Reservoir}) \qquad \textbf{Equation 3-7}$$

Where:

- *Porosity-Footage* = the cumulative thickness of pore space
- $\phi_{Reservoir}$ = the porosity of the total reservoir interval in a given zone as determined by the maximum gamma ray cut-off of ≤ 65 gAPI (i.e. high energy facies)
- $h_{Reservoir}$ = the total thickness of the reservoir interval in a given zone as determined by the maximum gamma ray cut-off of ≤ 65 gAPI (i.e. high energy facies)

The porosity-footage maps were gridded with a convergent interpolation algorithm and grid cells of 492 ft x 492 ft with grid limits defined by the SEM boundary surrounding each study area (see Section 3.3). The number of well data points used to generate saline storage zone porosity-footage maps is shown in Table 3-15 for the Sleepy Hollow study area, and Table 3-16 for the Huffstutter study area.

Table 3-15. Number of well data points used to generate porosity-footage maps for deep saline formations in the Sleepy Hollow study area.

Saline Group Name	Porosity-Footage Map Well Data Count
Wabaunsee	195
Shawnee-Douglas	199
Lansing-Kansas City	198
Pleasanton-Marmaton	182

Table 3-16. Number of well data points used to generate porosity-footage maps for deep saline formations in the Huffstutter study area.

Saline Group Name	Porosity-Footage Map Well Data Count
Wabaunsee	66
Shawnee-Douglas	70
Lansing-Kansas City	70
Pleasanton-Marmaton	17

3.5.5 Prospective Storage Resource Calculations

DOE-NETL Static (Volumetric) Method

The static (volumetric) methodology developed by the U.S. Department of Energy (DOE) National Energy Technology Laboratory (DOE-NETL, 2008; 2010; Goodman et al., 2011; 2016) was used to quantify and map the prospective CO_2 storage resource of the deep saline formations of interest for storage in the Sleepy Hollow and Huffstutter study areas.

Static methods for estimating CO_2 storage involve calculation of subsurface pore volumes and substitution of in-situ fluid volumes in a given formation to derive an equivalent mass of CO_2 that could be stored in that formation. This method is similar to the standard equation used in the oil and gas industry to estimate original oil-in-place (OOIP) (Calhoun, 1982; Lake, 1989). Static estimates do not account for economic or dynamic operational constraints associated with a potential CO_2 storage project.

The static assessment employed in this study is classified as a storage resource assessment (e.g., DOE-NETL, 2010; Goodman et al., 2011; 2013). At the highest level, the theoretical maximum storage resource is the maximum amount of CO_2 that could be stored in the total pore volume of the formation. This represents an upper limit on storage resource that will not likely be fully accessed due to geologic, physical, operational, and economic constraints encountered in practice. The storage resource can be further organized into subclasses as shown in the DOE-NETL classification system (Figure 3-10). The prospective storage resource calculation incorporates a storage efficiency factor to represent the net reservoir pore volume having geologic properties and subsurface hydrogeologic conditions favorable for CO_2 storage, eliminating the technically inaccessible pore volume from the static estimate. As a project continues to evolve and additional site-specific information is incorporated into the estimate, the storage assessment classification progresses to contingent storage resource and then storage capacity, and the range and uncertainty in storage estimates will decrease.

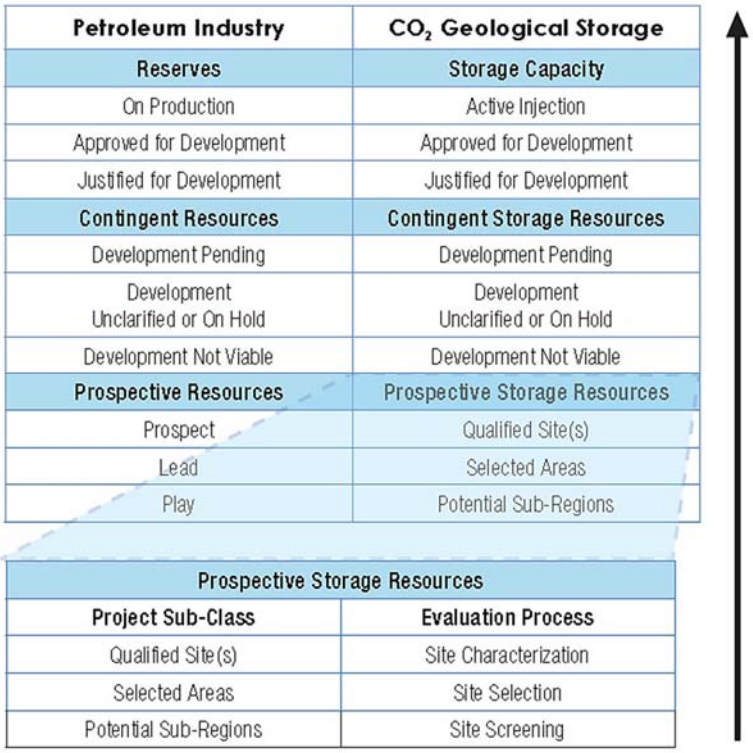

Figure 3-10. Comparison of CO_2 storage and petroleum industry classification systems as defined by the U.S. DOE-NETL (2017), and adapted from the SPE/WPC/AAPG/SPEE Resource Classification System (© Society of Petroleum Engineers, Petroleum Resources Management System).

The storage resources evaluated in this work are classified as prospective storage resources. The static volumetric equation developed by DOE-NETL for estimating CO_2 storage resource in deep saline formations is shown in Equation 3-8:

$$G_{CO2} = A_t \, h_g \, \phi_t \, \rho_{CO2res} \, E_{saline} \qquad \textbf{Equation 3-8}$$

The equation includes total area (A_t), gross formation thickness (h_g), and total porosity (ϕ_t) to represent the total pore volume of a formation. The storage efficiency factor (E_{saline}) is then used to derive the net reservoir fraction of the total pore volume that will potentially be accessible to CO_2 (Goodman et al., 2011, 2016). This pore volume is equated to a CO_2 storage volume and the calculated CO_2 density at reservoir conditions (ρ_{CO2res}) is then used to derive a mass of CO_2 stored (G_{CO2}), representing the prospective storage resource.

Heterogeneous grid data from the SEM was used for site-specific calculation of storage efficiency and prospective storage resource in the Sleepy Hollow study area. Grid data was not directly used in calculations for the Huffstutter study area due to fewer wells and a more geographically dispersed dataset in the field. Instead, data from the Huffstutter SEM grid was averaged and mean values were used as input for parameters in the Huffstutter study area.

Data from the total reservoir volume was used as input for the A_t, h_g, ϕ_t, ρ_{CO2res}, parameters, and data from the net reservoir volume was used to derive net-to-total reservoir values in the Sleepy Hollow study area to facilitate site-specific efficiency calculations. The definitions of parameters in Equation 3-8

are provided in Table 3-17 along with the associated data input and methods used in this study to quantify each parameter.

Table 3-17. Definitions and data input used in this study to quantify parameters in the DOE-NETL Prospective storage resource equation for deep saline formations.[a]

Parameter	Symbol[b]	Definition	Data Input/Quantification
CO_2 Mass	G_{CO2}	Mass estimate of CO_2 storage resource	See parameters below
Total Reservoir Area	A_t	Total area of the deep saline formation that is predominately sandstone and carbonate	Areal extent of sandstone and/or carbonate reservoir with gamma ray values ≤ 65 gAPI
Total Reservoir Thickness	h_g	Thickness of the deep saline formation that is predominately sandstone and carbonate	Total thickness of sandstone and/or carbonate reservoir with gamma ray values ≤ 65 gAPI
Total Reservoir Porosity	ϕ_t	Porosity of the sandstone and carbonate reservoir that is both isolated (inaccessible) and interconnected (accessible)	Average porosity (e.g., log and core porosity) of sandstone and/or carbonate reservoir with gamma ray values ≤ 65 gAPI
CO_2 Density	ρ_{CO2res}	Density of CO_2 at in-situ reservoir conditions	Density of CO_2 (Duan and Sun, 2003) at temperatures and pressures based on depth of reservoir, a geothermal gradient of 0.014°F/ft, and pressure gradient of 0.470 psi/ft
Storage Efficiency	E_{saline}^{s}	Fraction of the total reservoir pore volume that is filled by CO_2	Comprised of individual parameters shown in Table 3-18 and calculated stochastically in CO_2-SCREEN

a. DOE-NETL (2010); Goodman et al. (2011; 2016)

b. "s" superscript denotes stochastically calculated parameter (Goodman et al., 2016)

3.5.2 Site-Specific CO_2 Storage Efficiency

Storage efficiency factors account for geologic and physical limitations encountered during storage that will reduce access to the total pore volume of the deep saline formation during CO_2 injection. The E_{saline} parameter defined by DOE-NETL is the product of five individual efficiency factors shown in Equation 3-9 (DOE-NETL 2008, 2010, 2012; Goodman et al., 2011). Three efficiency factors are geologic terms that represent the net effective pore volume of the saline formation: net-to-total area ($E_{An/At}$), net-to-gross thickness ($E_{hn/hg}$), and effective-to-total porosity ($E\phi_e/\phi_t$). The two remaining efficiency factors are fluid displacement terms. The volumetric displacement efficiency (E_V) accounts for the effects of fluid density and buoyancy (sweep efficiency) in the volume of rock contacted by CO_2 surrounding an injection well. Microscopic displacement efficiency (E_d) accounts for irreducible water saturation. Definitions of the parameters in Equation 3-9 are provided in Table 3-18.

$$E_{saline} = E_{An/At}\, E_{hn/hg}\, E\phi_e/\phi_t\, E_V\, E_d \qquad \textbf{Equation 3-9}$$

Table 3-18. Definitions and data input used in this study to quantify storage efficiency parameters[a] for deep saline formations in the Sleepy Hollow study area.

Parameter	Symbol[b]	Definition	Data Input/Quantification
Net Reservoir Area	A_n^s	Area of the sandstone and/or carbonate reservoir associated with interconnected pore volumes	areal extent of sandstone and/or carbonate reservoir with gamma ray values ≤ 65 gAPI and permeability values ≥ 1 mD
Net Reservoir Thickness	h_n^s	Thickness of the sandstone and/or carbonate reservoir associated with interconnected pore volumes	thickness of sandstone and/or carbonate reservoir with gamma ray values ≤ 65 gAPI and permeability values ≥ 1 mD
Effective Reservoir Porosity	ϕ_e^s	Porosity of the sandstone and/or carbonate reservoir associated with interconnected pore volumes	average porosity (e.g., log and core porosity) of sandstone and/or carbonate reservoir with gamma ray values ≤ 65 gAPI and permeability values ≥ 1 mD
Net-to-Total Pore Volume Efficiency[c]	$E_{PVn/PVt}^s$	Net fraction of the total reservoir pore volume that is interconnected	$(A_n h_n \phi_e) / (A_t h_g \phi_t)$
Volumetric Displacement Efficiency	E_V	Combined fraction of the immediate volume surrounding an injection well and net thickness fraction that is contacted by CO_2 due to density differences between CO_2 and in-situ water	default values[d] based on sandstone and carbonate lithologies and their inferred depositional environments (IEAGHG, 2009)
Microscopic Displacement Efficiency	E_d	The fraction of pore volume containing mobile water that can be displaced by the contacted CO_2	default values[d] based on sandstone and carbonate lithologies and their inferred depositional environments (IEAGHG, 2009)

a. DOE-NETL (2010); Goodman et al. (2011; 2016)
b. "s" superscript denotes stochastically calculated parameter (Goodman et al., 2016)
c. parameter developed for this study; not a DOE-NETL equation parameter
d. in CO_2-SCREEN tool (Sanguinito et al., 2016; https://edx.netl.doe.gov/organization/co2-screen)

To better facilitate the use of site-specific data to define storage efficiency inputs, the $E_{An/At}$, $E_{hn/hg}$, and $E\phi_e/\phi_t$ parameters were combined into one term to represent the net-to-total reservoir pore volume efficiency such that:

$$E_{PVn/PVt} = E_{An/At}\, E_{hn/hg}\, E\phi_e/\phi_t \qquad \textbf{Equation 3-10}$$

and Equation 3-9 can be rewritten as:

$$E_{saline} = E_{PVn/PVt}^s\, E_V\, E_d \qquad \textbf{Equation 3-11}$$

Where the "s" superscript is added to the $E_{PVn/PVt}$ parameter to denote it as a stochastic calculation parameter defined by site-specific data (Goodman et al., 2016).

Site-specific high and low probability (*P*) values were assigned to the $E_{PVn/PVt}$ parameter based on the P_{10} and P_{90} percentiles of the net-to-total pore volumes calculated using the methods in Table 3-18 and petrophysical data from total and net reservoir intervals in each potential storage zone (e.g. Table 3-6). Due to data limitations in the Huffstutter study area, the P_{10} and P_{90} values derived from Pennsylvanian formations in the Sleepy Hollow study area were used as input for deep saline $E_{PVn/PVt}$ efficiency parameters in the Huffstutter study area.

High and low probability values for the E_v and E_d parameters were assumed from P_{10} and P_{90} values reported as regional-scale defaults based on lithology and depositional environment of the potential storage zone (IEAGHG, 2009). The final prospective storage resource (GCO_2) and storage efficiency (E_{saline}) results were calculated stochastically using the DOE-NETL CO_2-SCREEN tool to derive estimates at the P_{10} (low), P_{50} (median), and P_{90} (high) probabilities (e.g., Goodman et al., 2011; 2016; Sanguinito et a., 2016).

U.S. DOE-NETL CO_2-SCREEN Tool

The CO_2-SCREEN tool (beta v.2) developed by DOE-NETL (Sanguinito et al., 2016) was used to calculate prospective storage resource estimates for the deep saline formations in the two study areas. The tool employs the static volumetric method developed by DOE-NETL to estimate the storage resource of open-system deep saline formations (DOE-NETL, 2010; Goodman et al., 2011; DOE-NETL, 2012; Goodman et al., 2016). The tool is intended to provide the Regional Carbon Sequestration Partnerships and future CCS project developers with a consistent method for estimating the prospective CO_2 storage resource of deep saline formations, and facilitate comparison of results across different partnerships and research efforts (Sanguinito et al., 2016). The tool consists of an Excel interface for entering data viewing results, integrated with a GoldSim® module for stochastic calculations. The tool is publicly available through the DOE-NETL Energy Data eXchange (EDX) website (https://edx.netl.doe.gov/organization/co2-screen).

The prospective storage resource (GCO_2) and storage efficiency (E_{saline}) results were calculated stochastically in CO_2-SCREEN to derive P_{10} (low), P_{50} (median), and P_{90} (high) probability estimates (e.g., Goodman et al., 2011; 2016; Sanguinito et al., 2016). The p-values reported for individual storage efficiency parameters and calculated in CO_2-SCREEN are statistical confidence levels derived from cumulative probability values, with results interpreted to represent a 90% chance that the true CO_2 storage resource will be greater than the calculated P_{10} value and less than the P_{90} value (Goodman et al., 2011). As such, P_{10} represents the lowest estimated value with the highest confidence level, and P_{90} is the highest value with the lowest confidence level. This definition is in contrast with common industry usage of p-values as exceedance probabilities, where P_{10} is the high and P_{90} is the low estimate and results imply there is a 90% probability that a given value will be greater than the reported P_{90} value and less than the P_{10}. The P_{50} value is the median of the data derived from the 10,000 realizations from Monte Carlo sampling in the GoldSim® module.

Data from the SEM was used as input in CO_2-SCREEN to define the total reservoir area (A_t), total reservoir thickness (h_g), and total reservoir porosity (ϕ_t). Formation depth was also exported from the SEM grid and used to derive reservoir pressure and temperature based on a pressure gradient of 0.470 psi/ft and a geothermal gradient of 0.014°F/ft calculated for the Midcontinent Region (Table 3-17). CO_2 density (ρ_{CO2res}) was calculated in CO_2-SCREEN using reservoir pressure and temperature input.

Up to 300 cells are available for data input in CO_2-SCREEN. To conduct heterogenous, grid-based calculations of storage resource in the Sleepy Hollow study area, data from the SEM was re-gridded to a coarser resolution. The number of CO_2-SCREEN input cells assigned to each deep saline interval was weighted by gross thickness (Table 3-19). The SEM data for each potential storage zone was then re-gridded to the associated cell resolution shown in Table 3-19 for each zone, and the cell data was entered in CO_2-SCREEN.

The site-specific p-values calculated for the $E_{PVn/PVt}$ parameter, and the default values for E_v and E_d were also entered on a cell-by-cell basis for each of the potential storage zones. The default E_v and E_d values used for each deep saline storage zone are shown in Table 3-20.

The p-values were used in CO_2-SCREEN to generate a distribution that is randomly sampled using Monte Carlo sampling techniques. The sampling results were then used to derive the P_{10}, P_{50}, and P_{90} estimates for storage efficiency (E_{saline}) and prospective storage resource (G_{CO2}). More detailed information on the stochastic calculation method employed for prospective storage resource calculations in CO_2-SCREEN can be found in Goodman et al. (2011; 2016) and Sanguinito et al. (2016).

Table 3-19. Total number of cells and cell area (At), used in heterogenous CO_2-SCREEN calculations for the Sleepy Hollow study area. Also shown are averages for total reservoir thickness (hg) and total reservoir porosity (ϕt) calculated from cell data.

Group(s)	Formations/ zones	No. of Cells	Area per Cell (mi^2)	Total Reservoir Thickness Mean (ft)	Total Reservoir Porosity Mean (%)
Wabaunsee	*	82	1.4	68	6
Shawnee-Douglas	Topeka	33	3.5	30	5
	Deer Creek-Oread	52	2.2	44	5
Lansing-Kansas City	A	31	3.8	28	4
	D-F	70	1.7	62	5
Pleasanton-Marmaton	*	32	3.6	25	6

*Values represent all formations in the group

Table 3-20. Default p-values used as input in CO_2-SCREEN for *Ev* and Ed in both study areas.

Group	Formations/zones	E_v		E_d	
		P_{10}	P_{90}	P_{10}	P_{90}
Wabaunsee	*	0.16	0.39	0.35	0.76
Shawnee-Douglas	Topeka, Deer Creek, Oread	0.44	0.72	0.31	0.42
Lansing-Kansas City	A, D, E, F	0.44	0.72	0.31	0.42
Pleasanton-Marmaton	*	0.16	0.39	0.35	0.76

*Values reported were used for all formations in the group

For CO_2-SCREEN calculations in the Huffstutter study area, data from the SEM grid was averaged and mean values from each potential deep saline storage zone were used as input for total reservoir area

(A_t), total reservoir thickness (h_g), and total reservoir porosity (ϕ_t). The mean values calculated for each potential storage zone in Huffstutter, and used for single-cell CO_2-SCREEN calculations are shown in Table 3-21. Storage efficiency calculations in for the Huffstutter study area were based on the P_{10} and P_{90} values derived for the $E_{PVn/PVt}$ parameter in the Sleepy Hollow study area, and the CO_2-SCREEN defaults for E_V and E_d (Table 3-20).

Table 3-21. Mean values for total reservoir area (At), total reservoir thickness (hg), and total reservoir porosity (ϕt) used in single-cell CO_2-SCREEN calculations for the Huffstutter study area.

Group(s)	Total Reservoir Area (mi^2)	Total Reservoir Thickness Mean (ft)	Total Reservoir Porosity Mean (%)
Wabaunsee	32	179	6%
Shawnee-Douglas	32	134	6%
Lansing -Kansas City	32	81	5%
Pleasanton-Marmaton	32	69	5%

3.6 Results

3.6.1 Regional Geologic Structures, Crustal Stress, and Seismicity

Structures

Similar to oil and gas reservoirs, regional geologic structure exerts control on the development of subsurface features and conditions important for evaluating geologic storage feasibility, such as reservoir porosity and flow zones, trapping mechanisms, stress regimes, and caprock integrity. Understanding of regional geologic structure in the study areas is rooted in an interpretation of late Paleoproterozoic accretional tectonics. Basement rocks under the present study areas—and under almost all of Nebraska and northwestern Kansas—are part of the northeast-trending Yavapai province, a basement rock terrane that was produced by the accretion of dominantly juvenile arc crust to the southern border of Archean and tectonically-reworked Archean crust (e.g., Wyoming and Superior provinces, plus the Trans-Hudson Orogen) of the North American craton (Whitmeyer and Karlstrom, 2007). According to Karlstrom and Humphreys (1998), the northern edge of deformation that occurred about 1.65 billion years ago from contractional tectonics in regional basement rocks trends from just south of the southwestern corner of present Nebraska roughly along the Nebraska-Kansas border. Doubtless, accreted basement terrains bear their own tectonic fabric, and there is a general indication that at least some geologic structures in Proterozoic basement rocks under Nebraska and Kansas exert tectonic influence even to the present day, but the assessment of specific cases involves considerable speculation. Long after the accretion of the Yavapai province, intracontinental extension during the assembly of the supercontinent Rodinia at 1.1-1.2 Ga led to the development of the Midcontinent Rift approximately 400 km to the east of the study areas, but there are no known extensional structures from this episode in the two study areas (Whitmeyer and Karlstrom, 2007).

This report has previously discussed the roles of the Cambridge and Chadron arches, the Black Hills, and the Central Kansas Uplift in relation to basin history (Figure 3-1). The ancestral Las Animas Arch, another cratonic structure in the region surrounding the study areas, also bears mention. This arch extended north-northeastward from eastern Colorado to the Cambridge Arch in Nebraska during the Pennsylvanian and Permian periods, rising as it approached the latter (Rascoe, 1978); its position differed slightly from the current position of the Las Animas Arch (Figure 3-1). The Las Animas Arch affected both the thicknesses and lithofacies distributions of lower Pennsylvanian to middle Permian

strata. Some manifestation of those effects appears to have extended into present Dundy, Hitchcock, Chase, and Hayes counties in southwestern Nebraska (Rascoe, 1978).

There is widespread agreement that the Cambridge Arch, the Las Animas Arch, and other structural features east of the present Rocky Mountain front were reactivated by transpressional lithospheric buckling during the Laramide Orogeny in the Late Cretaceous and early Paleogene (Stix, 1982; Bunker et al., 1988; Tikoff and Madsen, 2001). Thus, both Paleozoic and Mesozoic strata dip very gently (~0.5°) away from the axis of the Cambridge Arch (Higley, 1987).

Moore and Nelson (1974) said that the Cambridge and Chadron arches together "had a profound influence on depositional and erosional patterns during most of Paleozoic and Mesozoic time" in Nebraska. It is likely that multiple uplifts of the Cambridge Arch occurred during the Phanerozoic. Stix (1982) compiled multiple accounts and proposed separate intervals of uplift during the Early Ordovician, latest Devonian, Mississippian, Pennsylvanian, latest Permian and Triassic, Early Cretaceous, Late Cretaceous and early Paleogene, Oligocene, and Pleistocene. Evidence for some of these episodes of uplift is in the regional distribution of strata of particular ages include: certain strata present in one or more of the adjacent basins are absent atop the arch, and other strata that thin over the arch. Trends in the geography and deposits of fluvial systems provide the basis for a proposed Pleistocene episode of reactivation (Stanley and Wayne, 1972; Rothe and Lui, 1983).

Uplift of the Cambridge Arch during the late Middle Mississippian to Middle Pennsylvanian periods (late Visean to Moscovian) occurred in concert with the formation of the Ancestral Rocky Mountains, which experienced additional tectonism until the middle of the Permian Period (Rascoe and Adler 1983; Kluth, 1986; Ye et al., 1996). Extensive erosion of pre-Pennsylvanian Paleozoic strata occurred atop the Cambridge Arch. Atokan-Desmoinesians strata onlap the arch (Adler et al., 1971; Higley, 1987; Rascoe and Adler, 1983). Rascoe and Adler (1983, fig. 8) depicted parts of both the Cambridge Arch and Central Kansas Uplift as emergent during the Desmoinesian. Post-Desmoinesian Pennsylvanian and Permian strata extend over the arch. The nearshore platform during the deposition of Pennsylvanian and Permian strata in the Midcontinent was nearly flat with a gentle southward dip toward the deepest part of the basin in present Oklahoma (Feldman et al., 2005).

Smaller-scale geologic structures in the vicinity of the Sleepy Hollow and Huffstutter study areas are not well-represented in published literature. In a study of satellite imagery that compiled different kinds of data from multiple sources, Stix (1982, plate 2) mapped "known" structural features in the northern part of northwestern Kansas and southwestern Nebraska from the approximate location of the Cambridge Arch westward to the Colorado state line. He depicted five broad, gentle folds in the general vicinities of Perkins and Chase counties in Nebraska, west of 101° West longitude. The axes of these folds trend roughly east-west and plunge westward. Stix (1982) attributed these folds to salt tectonics involving lower Permian strata. Stix (1982, plate 2) also depicted six north-to-northwest-plunging, broad, gentle folds south of the state line in northwestern Kansas that are subparallel to the trend of the Cambridge Arch. Stix (1982, plate 2) also mapped a few faults in the vicinity pf the Cambridge Arch. Polygonal faults (sensu Cartwright et al., 2003) appear to be very common in Cretaceous strata under the Great Plains, including both study areas. Numerous, small, normal faults exhibiting limited throw, and recently characterized as polygonal faults (Maher, 2014; St-Onge, 2017), are present in the Cretaceous Niobrara Formation and Pierre Shale in Nebraska and Kansas, although they are not adequately mapped. Maher (2014) interpreted these faults as the potential results of diagenesis during either the Late Cretaceous Period or the Miocene Epoch. Likewise, chalcedony veins and clastic dykes in Paleogene rocks on the Great Plains may also result from diagenesis (Maher and Shuster, 2012).

Crustal Stresses

Exceedingly few data characterize present crustal stresses in the northern Midcontinent, especially in comparison with the Appalachian region, Western Cordillera, and Oklahoma-Texas (Zoback, 1992; Zoback and Zoback, 1980, 1989; Haimson, 1990; Heidback et al., 2016). The crust in the "midplate central United States," which includes the present study areas, has been characterized as having maximum horizontal compressional stresses of comparatively uniform magnitude oriented east-northeast- to northeastward (Zoback and Zoback, 1980, 1989). Haimson (1990), however, reported maximum horizontal stresses oriented approximately N30°W in the Proterozoic Sioux Quartzite near Sioux Falls, South Dakota (nearly 500 km northeast of the present study areas) and related it to a 1989 earthquake in north-central Kansas, which he also interpreted to reflect northwest-oriented maximum horizontal stresses. Haimson (1990) speculated that these apparently anomalous stresses relate to activity along the bounding faults of the buried Midcontinent Rift.

The general east-west orientation of maximum horizontal stress (i.e., compression) has likely existed in the Midcontinent for tens of millions of years. Sevier-Laramide (Cretaceous-early Paleogene) crustal stresses in the interior of North America are determined to have been roughly east-west—parallel to today's principal compressive stress—through the analysis of mechanically twinned calcite crystals in sedimentary carbonate rocks (Craddock and van der Pluijm, 1999). Furthermore, although Cretaceous carbonate rocks in the northern Midcontinent preserve the aforementioned, roughly east- west calcite-twinning fabric, Paleozoic carbonates in the same area preserve a fabric that is roughly perpendicular and presumed to be related to the much earlier deformation of the Ouachita and Appalachian orogens (van der Pluijm et al., 1997). Therefore, crustal stress regimes changed markedly over a large part of the continental interior during the Phanerozoic. Today, an extensional regime with north-northwestward maximum horizontal stresses is apparent in the Rocky Mountain front in adjacent Colorado; therefore, a transition between compressional regimes in the east and extensional regimes to the west may exist somewhere between eastern Kansas-Nebraska and northeastern Colorado (cf. Zoback and Zoback, 1980, 1989).

Seismicity

Seismicity in southwestern Nebraska and adjacent areas has been mild throughout the historic recorded beginning ca. 1854 and the overall seismic hazard is low. Maps in Petersen et al. (2016, Figure 7) suggest that southwestern Nebraska has a 1% probability of an event exceeding MMI III-IV in any given year and placed the chance of a damaging earthquake in the area during 2016 at less than 1%, the same value that characterized almost all of the USA east of the Rocky Mountains. Indeed, there was no earthquake of that range of magnitude or greater in the area during that year. The hazard map based on the USGS 2014 long-term model indicates a slightly elevated peak ground acceleration around the southern Cambridge Arch and Central Kansas Uplift in comparison with immediately surrounding areas (0.04-0.06 g vs. 0.02g-0.04g) at a 2% probability of exceedance in 50 years (U.S. Geological Survey, 2014). The spectral response acceleration for 0.2g around the arch and uplift under the aforementioned conditions would be 0.08 to 0.12g (U.S. Geological Survey, 2014b). Multiple historical earthquakes in Kansas were associated by Steeples et al. (1990) with tectonism in the Central Kansas Uplift, which they considered to present a risk similar to that of the northern Nemaha Tectonic Zone (i.e., Humboldt Fault, etc.) in southeastern Nebraska and eastern Kansas.

Despite these low seismic risks, Wollard (1958) presented data effectively suggesting that the entire Central Kansas Uplift-Cambridge Arch system, while geologically old, remains seismically active. Microearthquakes detected in the area of the Sleepy Hollow oil field during a monitoring program in the late 1970s and 1980s have been interpreted as the results of both waterflood-induced events and as

manifestations of natural seismicity (Rothe and Lui, 1983; Hillebrand et al., 1988; Steeples et al., 1990). It is important to point out that the events started well after waterflood started and have stopped even though waterflood continues, making links between seismicity tenuous. However, these results should be remembered in the light of increased vigilance regarding induced seismicity in the interior of the United States.

3.6.2 SEM Results

Sleepy Hollow Study Area

A 3D SEM was created and focused on Sleepy Hollow Field in Red Willow County, NE. In this study, existing, high-density well data was obtained for the field, with lesser well sampling at distances away from the field. The SEM was expanded out beyond the field to cover an area of 10 miles by 10 miles. The model is comprised of approximately 10 million cells; cell size is 230 ft by 230 ft. Around 620 feet thick, the petrophysical SEM was developed for 13 zones from the Wabaunsee Group down to Precambrian basement at approximately 3,500 feet.

The 3D framework of the SEM created for the Sleepy Hollow study area in Red Willow County, Nebraska consisted of surfaces developed from formation tops interpreted from well logs in 212 wells (Figure 3-11). Many of these wells focused on the Sleepy Hollow Field which was central to the 10 mi x 10 mi model area used for the SEM. Tops relevant to the SEM were from the Wabaunsee Group down to the Precambrian basement rock. Average depths to these tops are listed in Table 3-22. Figure 3-12 shows these formation tops in SH Reagan Units 100 and 101 which are central to the Sleepy Hollow Field. The vertical extent of the SEM based on these two wells from the Wabaunsee Group down to the weathered Precambrian basement is approximately 590 ft.

Table 3-22. Average depth and total thickness values derived from gridded SEM surfaces for the Pennsylvanian intervals of interest in the Sleepy Hollow study area.

Group(s)	Formation/Zone	Depth (ft)		Gross Thickness (ft)	
		Mean	σ	Mean	σ
Wabaunsee	*	2,862	116	137	8
Shawnee-Douglas	Topeka	2,999	118	55	8
	Deer Creek	3,054	114	86	7
	Oread	3,095	119	45	6
Lansing-Kansas City	LKC A	3,140	115	52	3
	LKC B	3,191	117	36	4
	LKC C	3,228	116	47	4
	LKC D	3,274	117	44	4
	LKC E	3,318	116	27	3
	LKC F	3,345	117	45	6
Pleasanton - Marmaton	*	3,390	118	53	9
Basal Pennsylvanian sandstone		3,443	117	17	15
Weathered Precambrian		3,460	111	23	10
Precambrian		3,482	110	-	-

*Values reported for all formations in the group

A regional dip of 0.17° (azimuth 254°) for the area was estimated from well tops and used to guide surface trends in areas with limited or no well control points. This field has a high concentration of wells that were drilled to basement which enabled picking the basal sand unit.

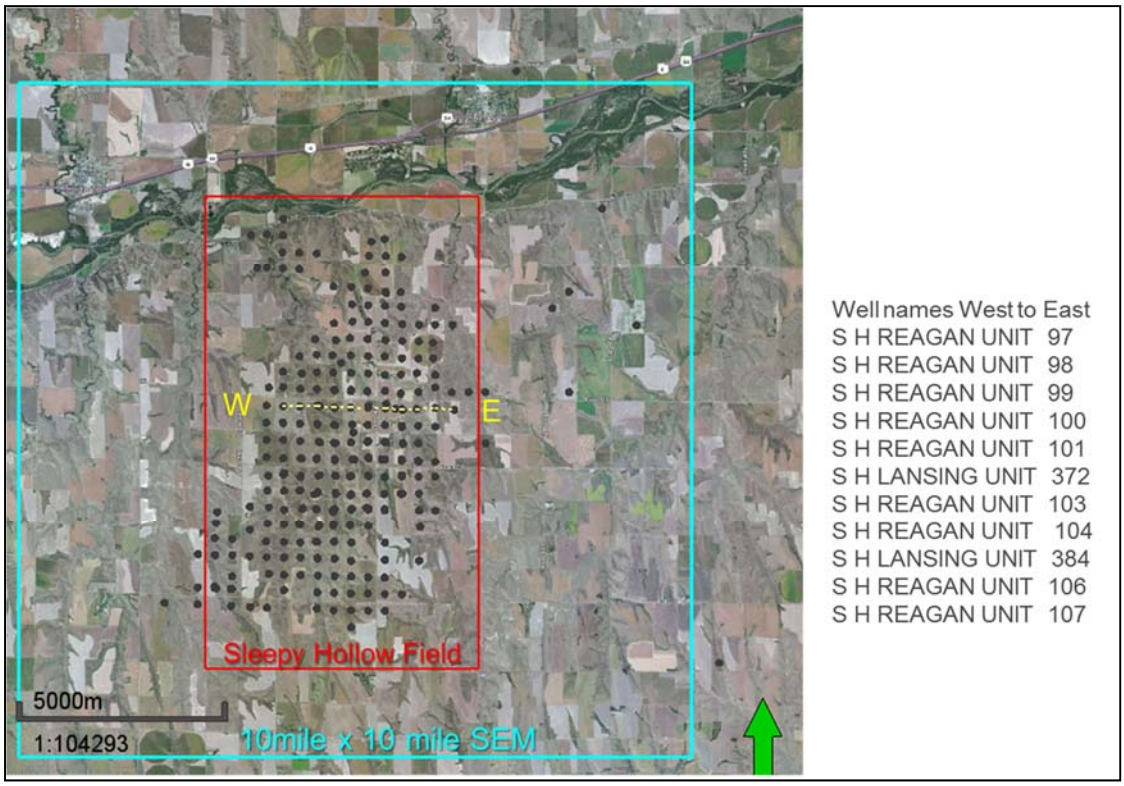

Figure 3-11. Well locations (gray dots) with well tops in and around the Sleepy Hollow study area

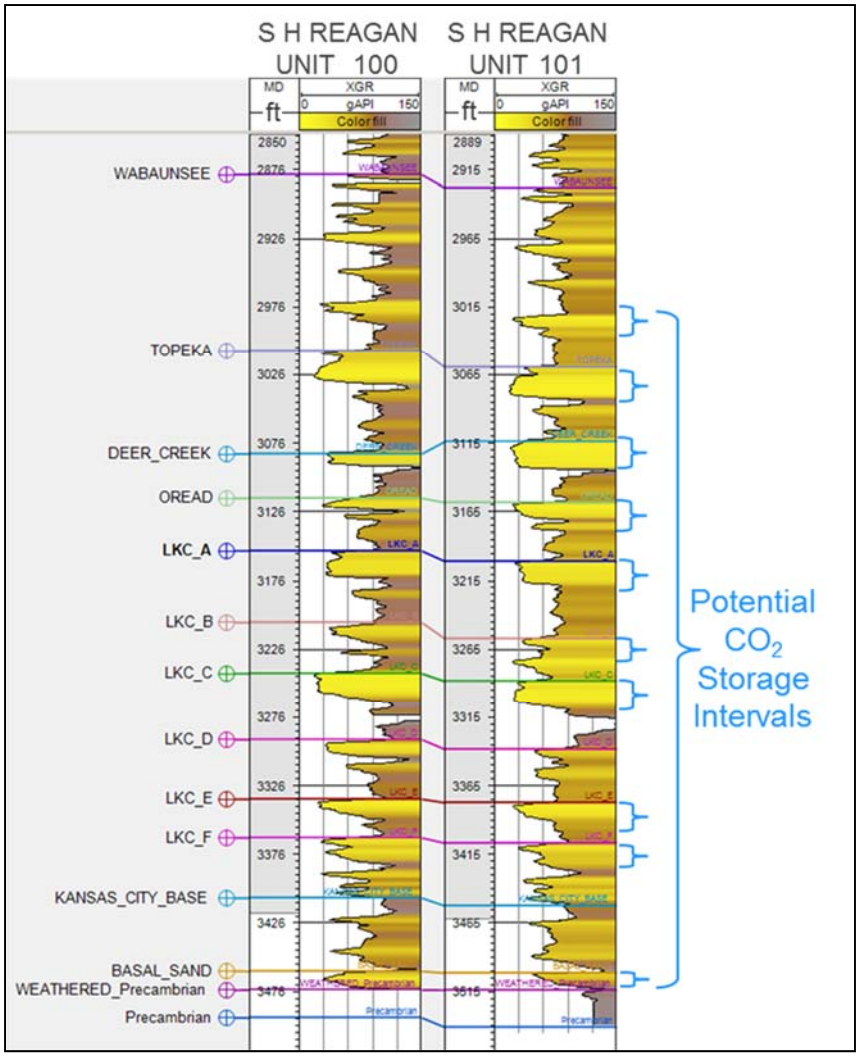

Figure 3-12. Example formation tops from the center of Sleepy Hollow Field. Potential storage intervals are in areas of low GR response and are separated by zones that are considered tighter.

Gamma ray logs appeared in 212 wells. The gamma ray data enabled the picking of well tops, correlating the wells, and producing structural surfaces from interpreted formation tops. Several logs started just above the Wabaunsee Group and went down to basement rock. Most well log data originated from paper hardcopies, and these were digitized and corrected or normalized where necessary. Effective porosity and permeability logs were derived from existing well logs; see Section 3.1.1 and 3.1.2 for details. Fewer wells had logs extending up through the shallower sections above the Wabaunsee Group. Figure 3-13 shows example logs from the SH Reagan Unit 98 well. The W-to-E cross-section (Map view, Figure 3-11) is shown as a well section in Figure 3-14 and reveals the correlation among stratigraphic units across the field. The gamma ray log indicates significant continuity for most stratigraphic features, especially for the “cleaner” subunits. The gamma ray logs reveal the carbonate cycles, with higher porosity generally found in areas of low GR response.

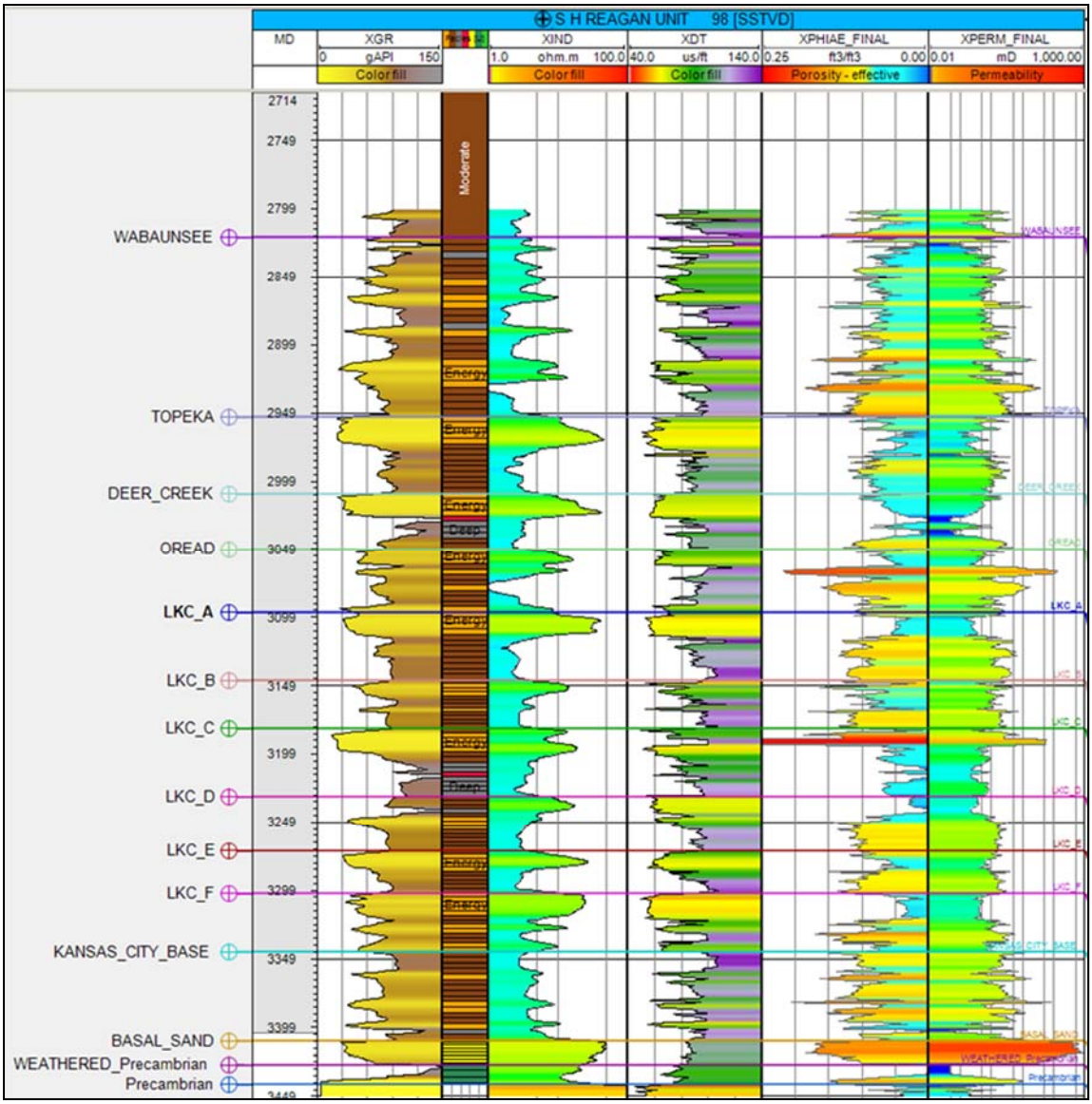

Figure 3-13. Example well logs from the SH Reagan 98 well. From left to right: GR, facies, resistivity, sonic, porosity, and permeability.

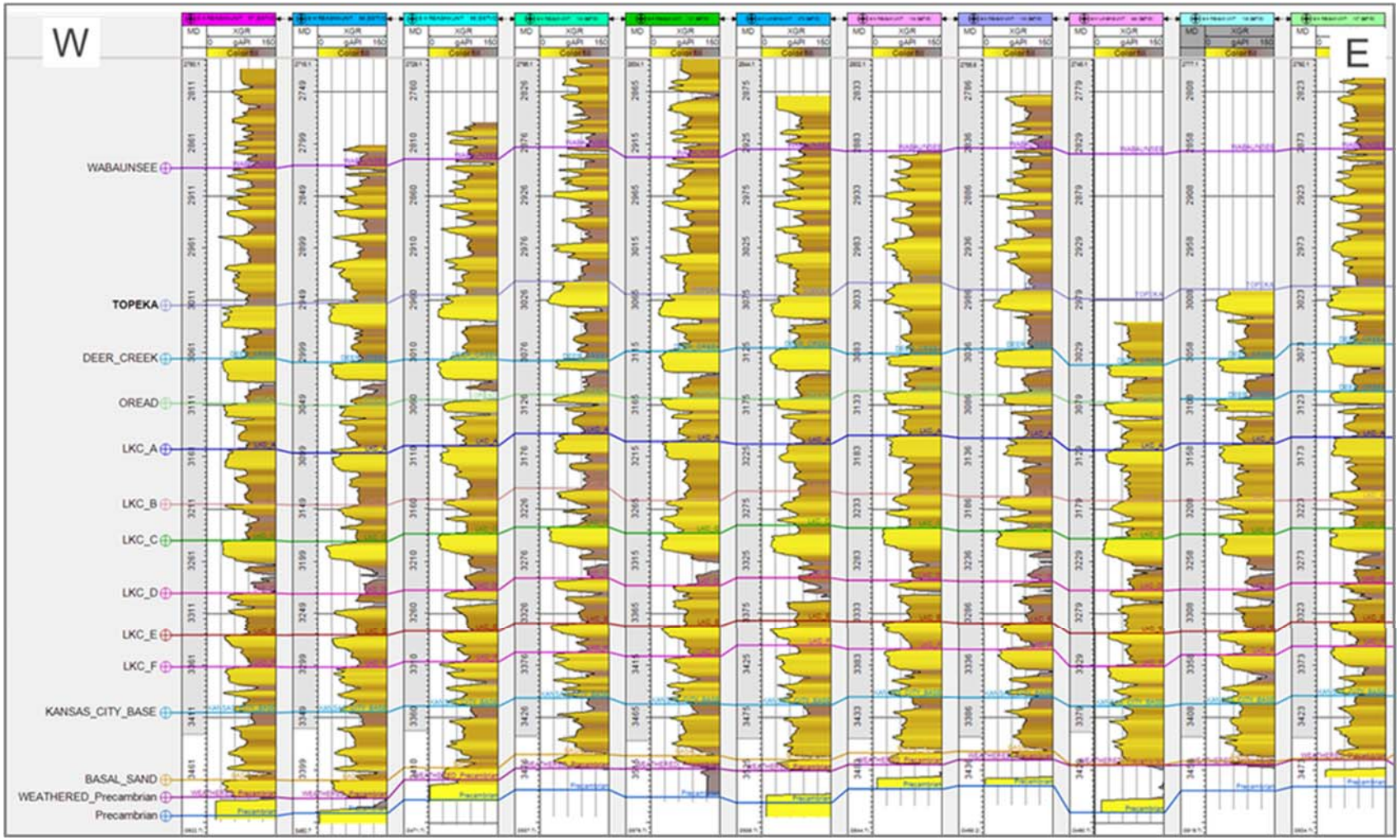

Figure 3-14. Example of the carbonate cyclicity observed in gamma ray well log correlated across the Sleepy Hollow Field. Log signatures indicate significant continuity of formations. Section appears on map in Figure 3-11.

Structural Framework

A total of 22 surfaces were used in developing the structural framework of the Sleepy Hollow SEM from ground level to basement (Figure 3-15). Of these, 13 surfaces from the Wabaunsee Group downward were used for delineating the zones for petrophysical modeling (Figure 3-16).

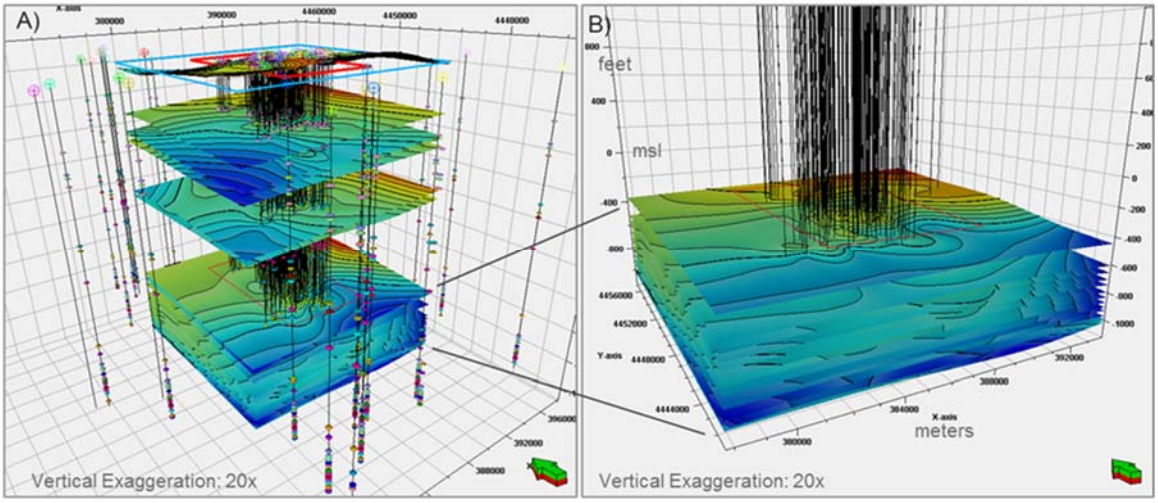

Figure 3-15. Oblique view of SEM area with wells, well tops, and surfaces. A) Well tops appear as colored disks along the wells. B) Close-up of the lower 13 surfaces used to define the framework for the petrophysical modeling.

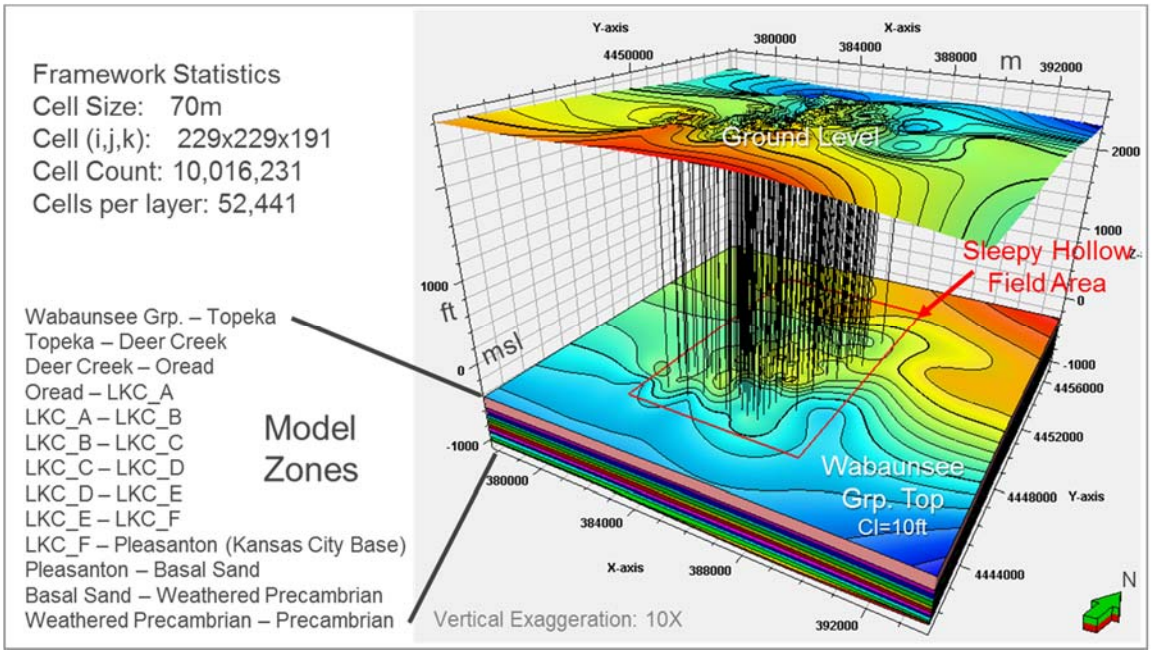

Figure 3-16. The structural framework of the Sleepy Hollow study area. Population of petrophysical properties was conducted for zones from the Wabaunsee Group down to Precambrian basement top.

The SEM has a horizontal resolution defined by a grid cell XY-increment of 70 m. The surfaces define stratigraphic zones which were subsequently layered. Each zone was given a zone division which consists of layer type and a layer count or cell thickness. The layer type used in this SEM was "proportional," which divides the zone into a set number of layers (Table 3-23). Depending on the thickness of the zone, cell heights will vary. Average layer (cell height) thickness is provided in Table 3-23. The SEM layers were generated to follow the corresponding structural surface in each zone, with their respective cell thicknesses chosen to capture vertical heterogeneity apparent in the permeability log. Each model layer had 229 x 229 cells for a total of 52,411 cells.

Table 3-23. SEM zone layering types and divisions for the Sleepy Hollow study area.

Zone Reference	Zone Division	Number of Layers	Average Layer Thickness (ft/layer)
Ground Level – Carlile	Proportional	1	NA[a]
Carlile – Greenhorn	Proportional	1	NA[a]
Greenhorn – Nippewalla	Proportional	4	NA[a]
Nippewalla – Admire	Proportional	2	NA[a]
Admire – Wabaunsee	Proportional	1	NA[a]
Wabaunsee – Topeka	Proportional	25	5.48
Topeka – Deer Creek	Proportional	14	3.93
Deer Creek – Oread	Proportional	10	4.09
Oread – LKC A	Proportional	12	3.73
LKC A – LKC B	Proportional	12	4.30
LKC B – LKC C	Proportional	12	3.03
LKC C – LKC D	Proportional	14	3.33
LKC D – LKC E	Proportional	13	3.36
LKC E – LKC F	Proportional	10	2.72
LKC F – Pleasanton-Marmaton	Proportional	13	3.45
Pleasanton-Marmaton – Basal Sandstone	Proportional	16	3.30
Basal Sandstone – Weathered Precambrian	Follow surface	(2.5 ft)[b]	2.50
Weathered Precambrian – Precambrian	Proportional	3	7.57

a. Detailed layering was not performed for caprock units

b. The basal sandstone layering is in 2.5-foot increments (cell thickness)

Facies Model

A cross-section through the cyclic carbonate facies model is given in Figure 3-17. The basal sandstone facies appear as a thin yellow streak and pinches out on the eastern side of the field. The oblique view of this basal sandstone facies model shows its extent where highly favorable reservoir conditions are believed to be present (Figure 3-17c). Holes in this portion of the facies model are where the basal sandstone unit pinches out against the basement or tight, weathered basement rock.

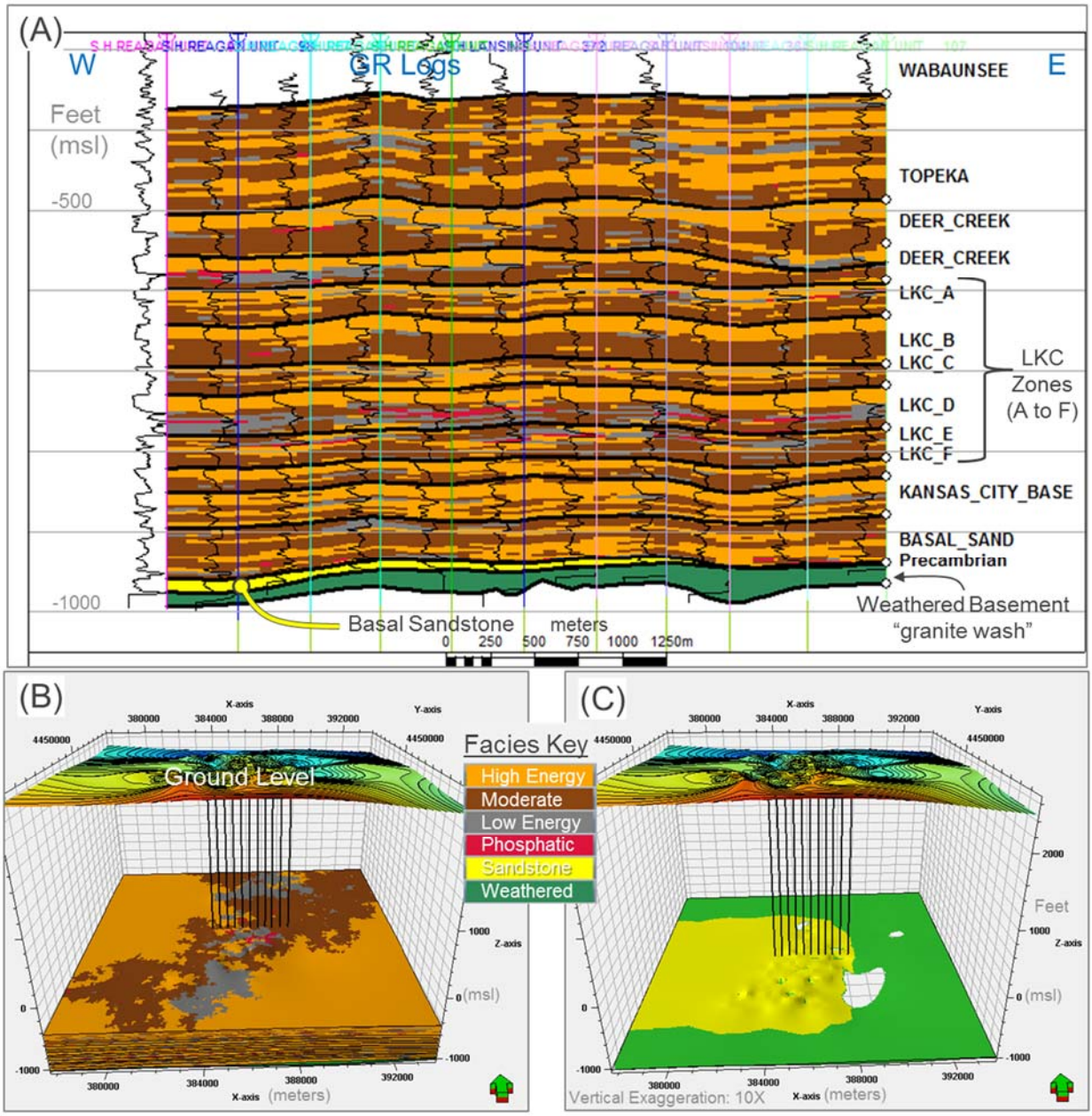

Figure 3-17. Facies model for the Sleepy Hollow study area. A) Cross-section of facies model through Sleepy Hollow Field. B) Oblique view of the facies model showing the top of the Wabaunsee Group and underlying units. Wells correspond to cross-section above. C) Basal Sand facies model with basal sandstone being bounded by either weather basement rock or laterally by less porous rock.

Petrophysical Properties

As discussed in the SEM methods Section 3.1.3, the derived effective porosity logs required adjustments to account for known porosity and permeability trends in lithologic sequences of the Lansing-Kansas City. Permeability logs were calculated based on effective porosity and were also affected. The original and adjusted porosity and permeability logs are shown for two wells in the Sleepy Hollow study area in Figure 3-18, along with their upscaled values. The upscaled values have favorable porosity and permeability values that align with the higher energy depositional environments where good porosity

development occurs, (Young, 2011). More importantly, porosity and permeability logs and their upscaled counterparts have been attenuated across the lower-energy portions of the regressive limestone sequences.

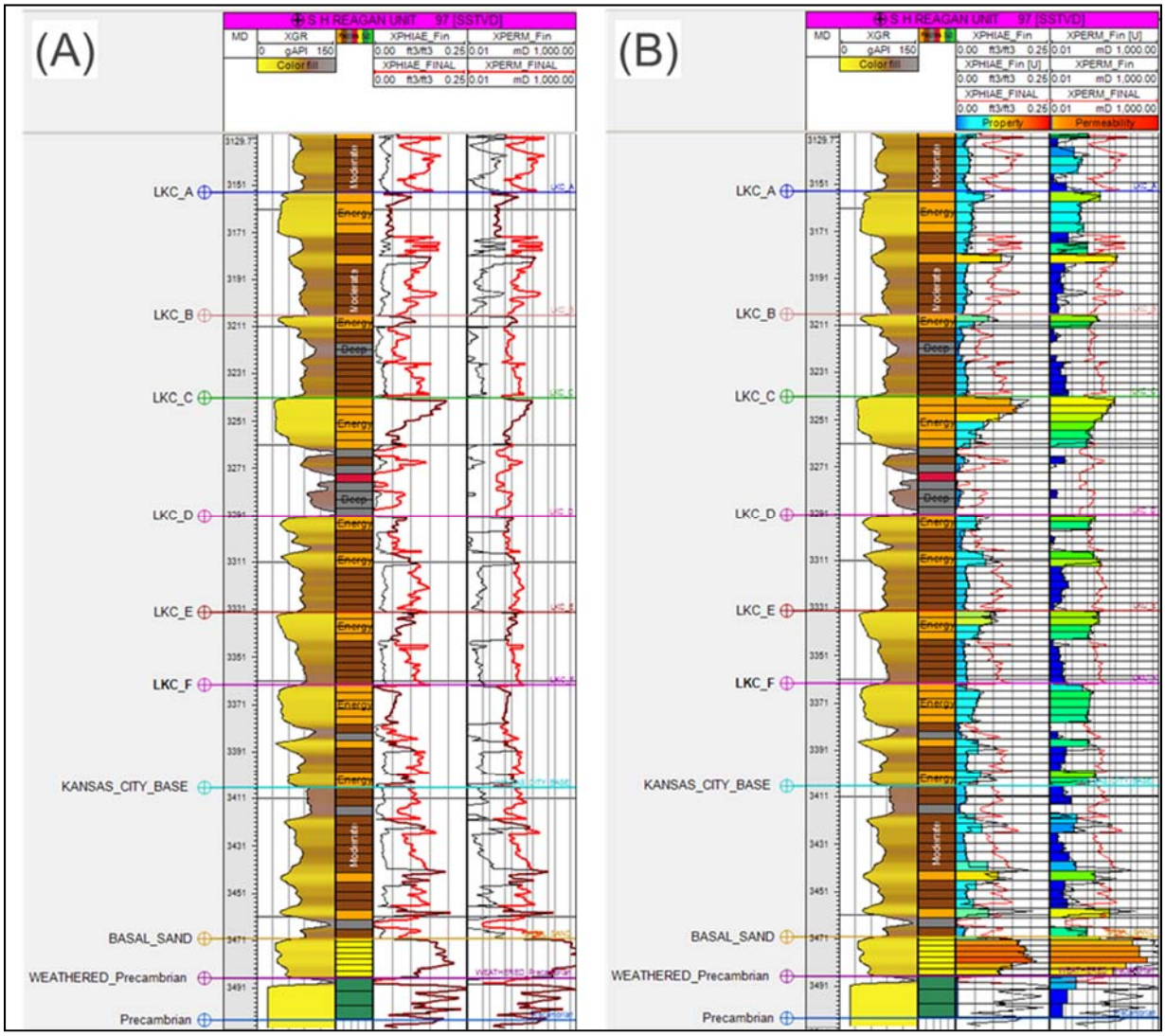

Figure 3-18. Example porosity and permeability log adjustments. A) Original effective porosity and permeability logs in red, with adjusted (attenuated) log values in black. B) Same logs as on left, but showing upscaled values into SEM cells along well path.

The petrophysical properties of the potential storage intervals are shown in Figure 3-19 and Figure 3-20. The effective porosity and permeability from the top of the LKC A Zone are given in map view in Figure 3-19a and Figure 3-19b, respectively. Because the permeability model was generated through co-located, cokriging with the porosity model, it has a similar distribution with the porosity model. This type of texture is common throughout the cyclic carbonate section, and reduced values associated with tighter intervals appear as darker blue streaks in the SEM cross-sections (Figure 3-20). The cyclic nature of the carbonate units produces alternating zones of favorable storage intervals among much tighter, low permeability units. Thus, the potential injections zones have their own confining units due to the presence of tight, intervening, deeper-basin sediments.

The basal sandstone was treated separately as its own facies to control its areal extent in the SEM. An anisotropic component was introduced in the porosity modeling to generate the appearance of sandbars trending with the longshore drift in a westward direction (Figure 3-19c) (Rogers,1977). The porosity and permeability for the basal sandstone is also shown in Figure 3-20 and appears as a thin unit pinching out to the east.

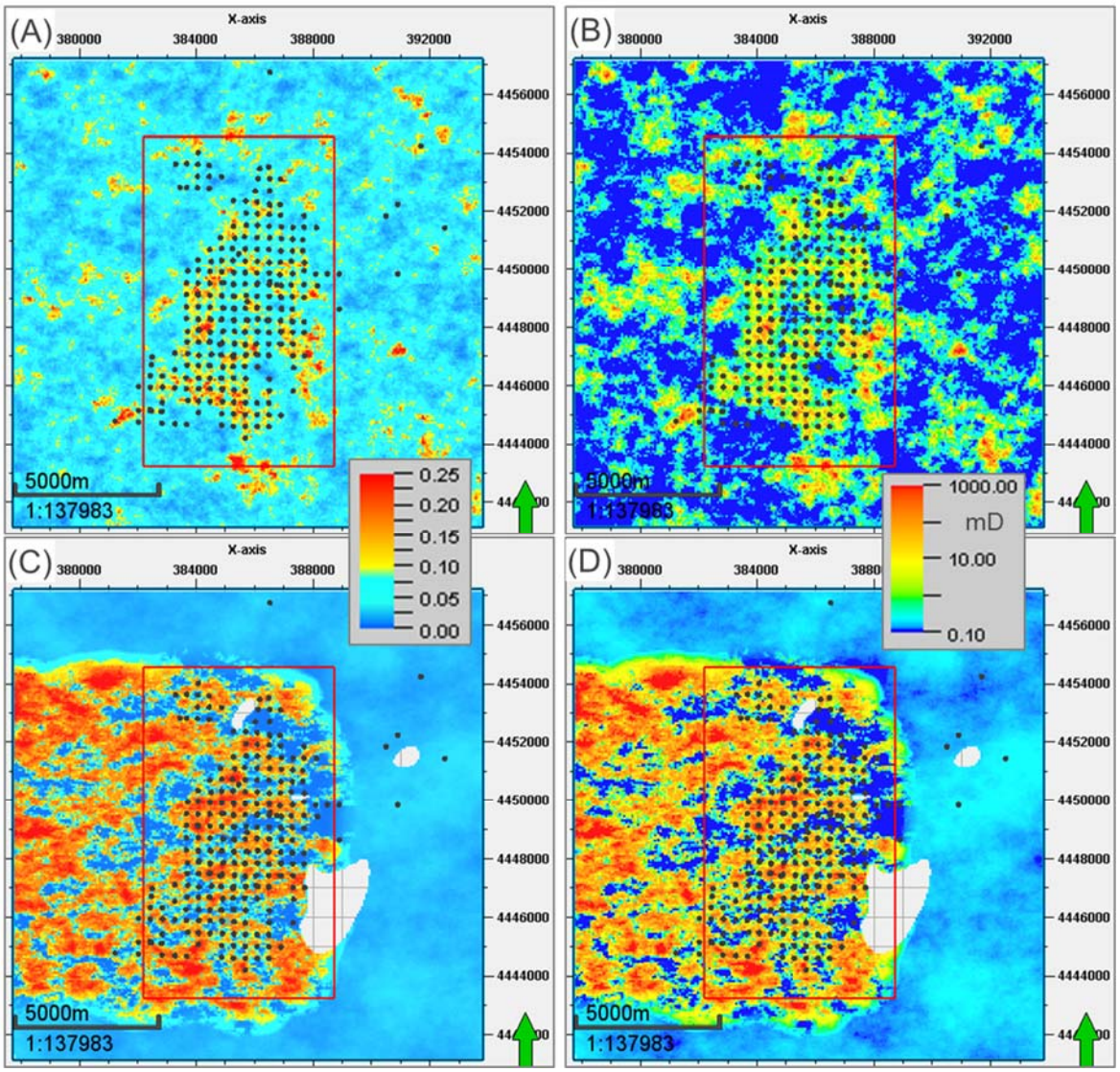

Figure 3-19. Property distribution maps spanning the 10mi x 10mi SEM. A) Effective porosity on top of the LKC A Zone. (B) Permeability on top of the LKC A Zone. (C) Effective porosity on top of the basal sandstone. (D) Permeability on top of the basal sandstone. Red rectangle is approximate location of the Sleepy Hollow Field. Black Dots are well locations with petrophysical logs.

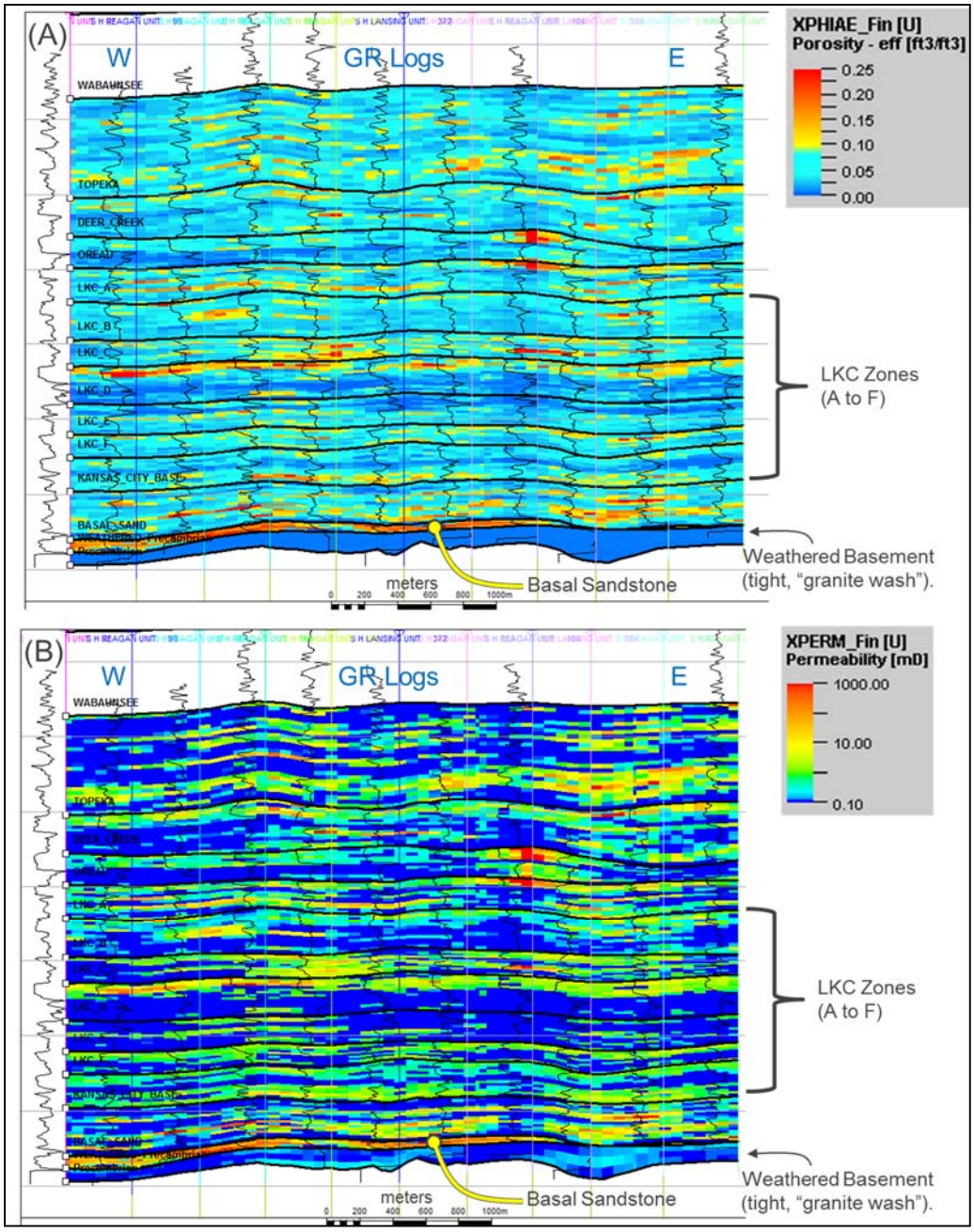

Figure 3-20. Cross-sections through the property models. A) Effective porosity model. B) Permeability model. Cross-section appears in map view in Figure 3-11.

Except for the weathered Precambrian that was poorly informed with well data, Figure 3-21 shows the histograms for effective porosity and permeability for all SEM zones where petrophysical modeling was performed. This includes the Wabaunsee Group down through the base of the basal sandstone. There is good agreement between the well logs and upscaled log properties, and with the final property models which are comprised of millions of cells. Under-representation of high porosity (and high permeability) values is a common occurrence due to sampling and averaging data across a cell's height. This can be seen in the porosity histogram where there is a slight inflation in porosity estimates in the 7.5% (0.075 decimal) range at the expense of higher values. The permeability histogram shows very good agreement

between the permeability logs and the final permeability model. There is a bimodal distribution, and this may be in part due to the basal sand unit offering good permeability. The permeability model spike at 0.001 mD is attributed to some model zone(s) where values were truncated at that lower limit.

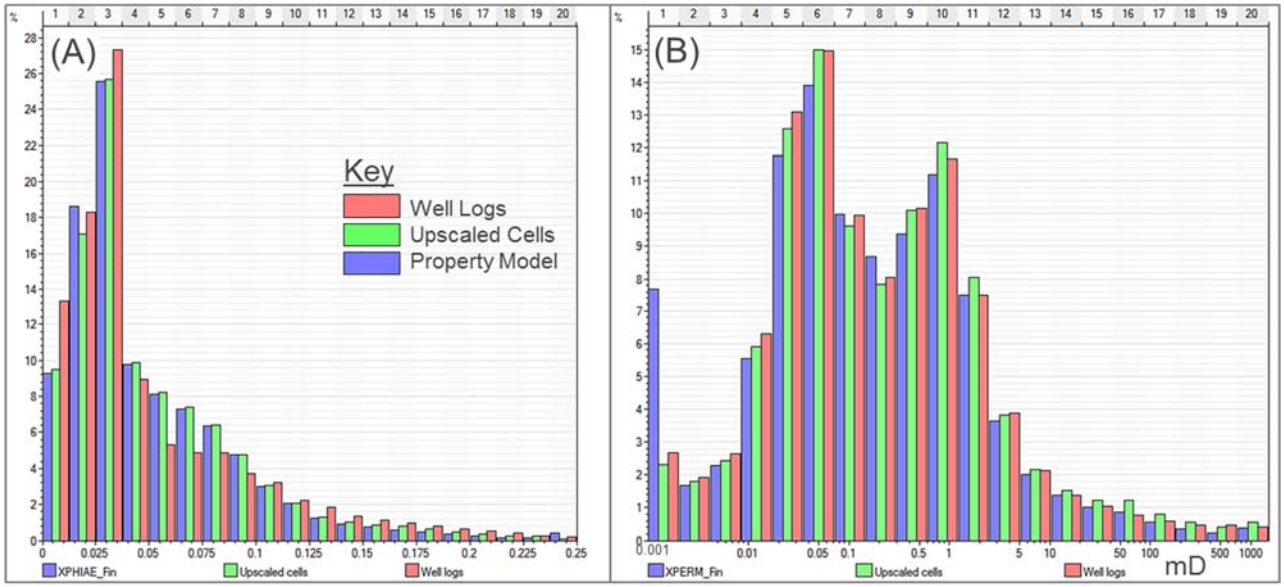

Figure 3-21. Histograms depicting property distributions of the SEM for the Sleepy Hollow study area. A) Effective porosity (XPHIAE_Fin) and B) Permeability (XPERM_Fin).

Huffstutter Study Area

A 3-Dimensional SEM was created and focused on Huffstutter Field in Phillips County, Kansas. In this study, existing well log data was obtained for approximately 96 wells, with lesser well sampling at distances away from the field. The model's framework consists of surfaces developed from formation tops interpreted from well logs in the 96 wells. This study area had a limited number of wells drilled to basement. The SEM was expanded out beyond the field to cover an area of 10 miles by 10 miles. The model is comprised of approximately 13.75 million cells; cell size is 70 meters by 70 meters. Around 1,060 feet thick, the petrophysical SEM was developed for 18 zones from the Wabaunsee Group down to Precambrian basement at approximately 3,800 feet.

Well tops from 96 wells were imported to the SEM for the Huffstutter study area. Many of these wells focused on the Huffstutter oil field, which was central to the 10 mi x 10 mi model area used for the SEM (Figure 3-22). Tops relevant to the SEM were from the Wabaunsee Group down to the Precambrian basement rock. Figure 3-23 shows the formation tops in one well from the Huffstutter study area. Of special interest were the Pennsylvanian cyclic carbonates of the Lansing-Kansas section. Approximate depths to these tops are listed in Table 3-24. Figure 3-24 shows these formation tops in the 1514720612 well. The vertical extent of the SEM from the Wabaunsee Group down to the top of the Arbuckle is approximately 950 feet.

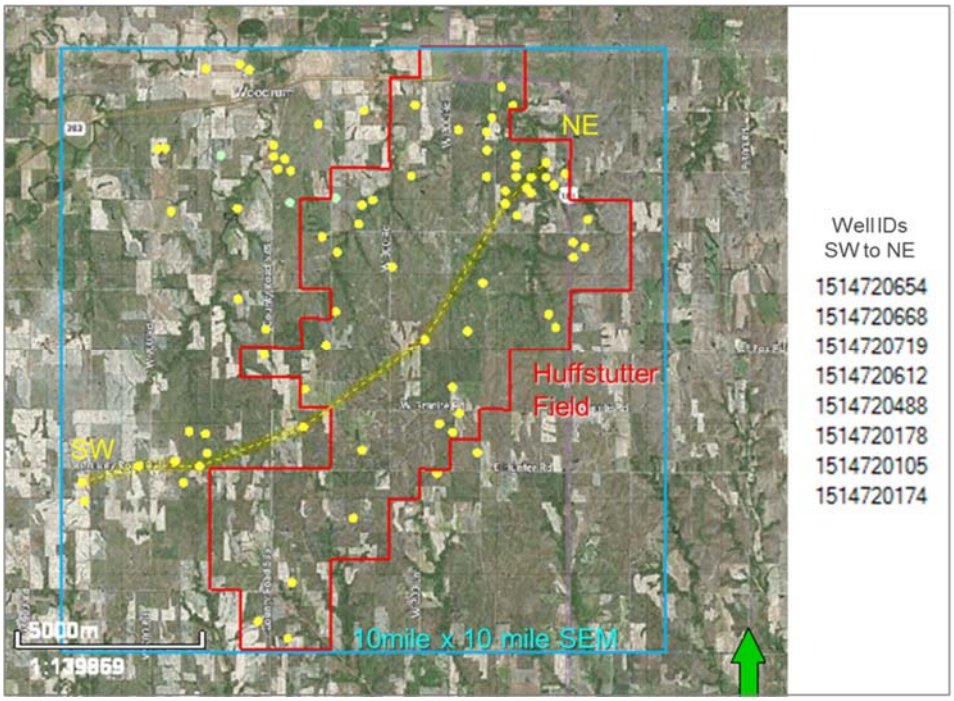

Figure 3-22. Wells location (yellow) with well tops in and around the Huffstutter study area.

Table 3-24 Average depth and total thickness values derived from gridded SEM surfaces for the Pennsylvanian intervals of interest in the Huffstutter study area.

Group(s)	Formation/Zone	Depth (ft)		Gross Thickness (ft)	
		Mean	σ	Mean	[illegible]
Wabaunsee	*	2,741	58	353	9
Shawnee-Douglas	Topeka	3,094	57	64	6
	Deer Creek	3,158	55	74	7
	Lecompton[a]	3,232	58	71	12
	Heebner[a]	3,303	59	4	1
	Levenworth[a]	3,307	59	24	2
	Toronto[a]	3,331	59	17	2
Lansing-Kansas City	LKC A	3,349	59	33	2
	LKC B	3,382	59	36	4
	LKC C	3,418	60	55	4
	LKC D	3,473	58	24	2
	LKC E	3,496	58	18	2
	LKC F	3,514	58	25	2
	LKC G	3,540	57	23	3
Pleasanton-Marmaton	*	3,562	58	55	37
Arbuckle Group	*	3,727	61	-	-
Precambrian		3,802	75	-	-

* Values reported for all formations in the group

Most of the gamma ray logs used in the Huffstutter SEM started just above the Wabaunsee Group and went down to Pleasanton-Marmaton groups. Only about 5 wells in this study have data that penetrates the basement rock. Fewer wells had logs extending up through the shallower sections above the Wabaunsee Group. Figure 3-23 shows example logs from the 1514720612 well. The SW-to-NE cross-section is shown as a well log section in Figure 3-25 and reveals the correlation among stratigraphic units across the field. The gamma ray signature indicates significant continuity for most stratigraphic features, especially for the “cleaner” subunits.

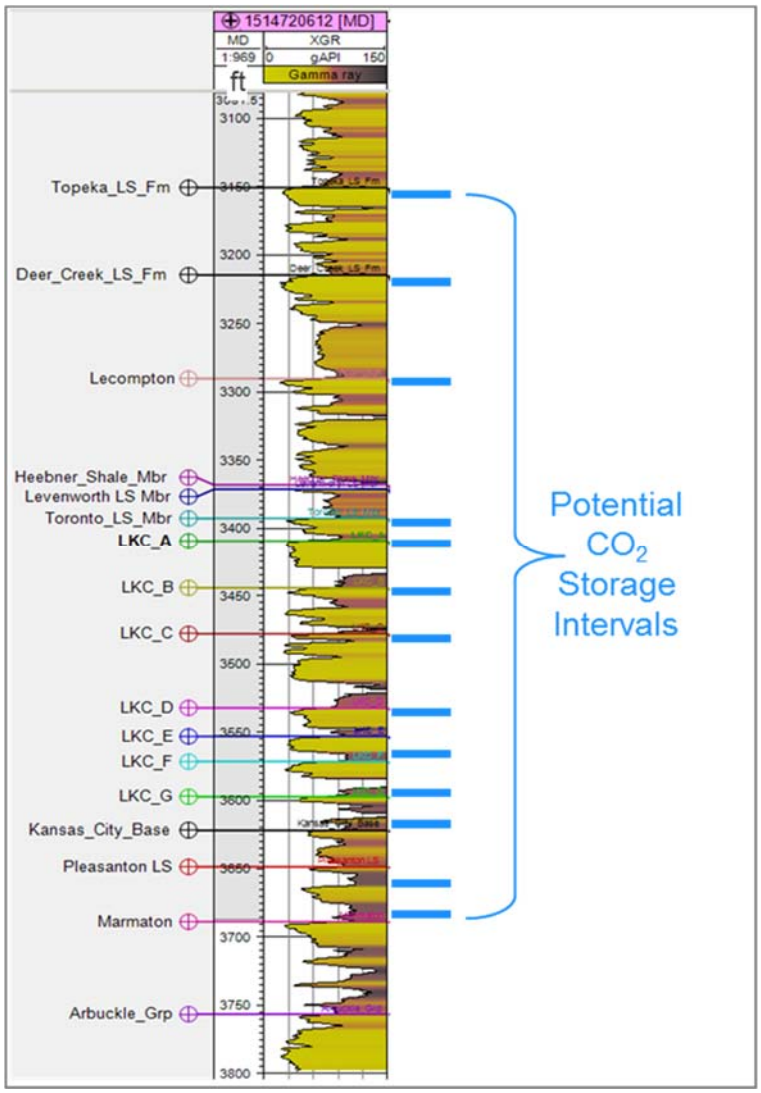

Figure 3-23. Formation tops in one well from the Huffstutter study area. The gamma ray log reveals the carbonate cycles. Potential storage intervals are in areas of low GR response and are separated.

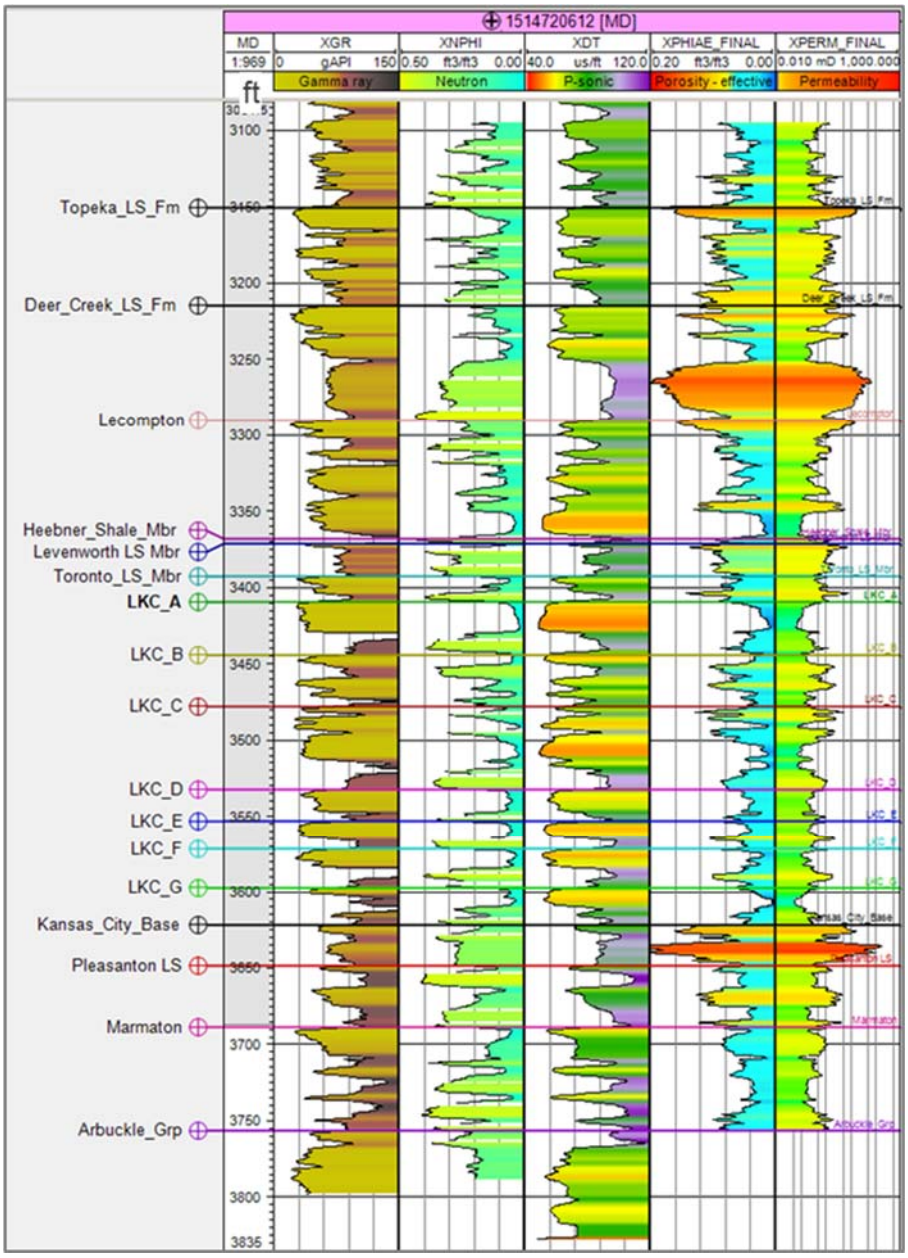

Figure 3-24. Example well logs from the 1514720612 well. From left to right: GR, facies, resistivity, sonic, porosity, and permeability.

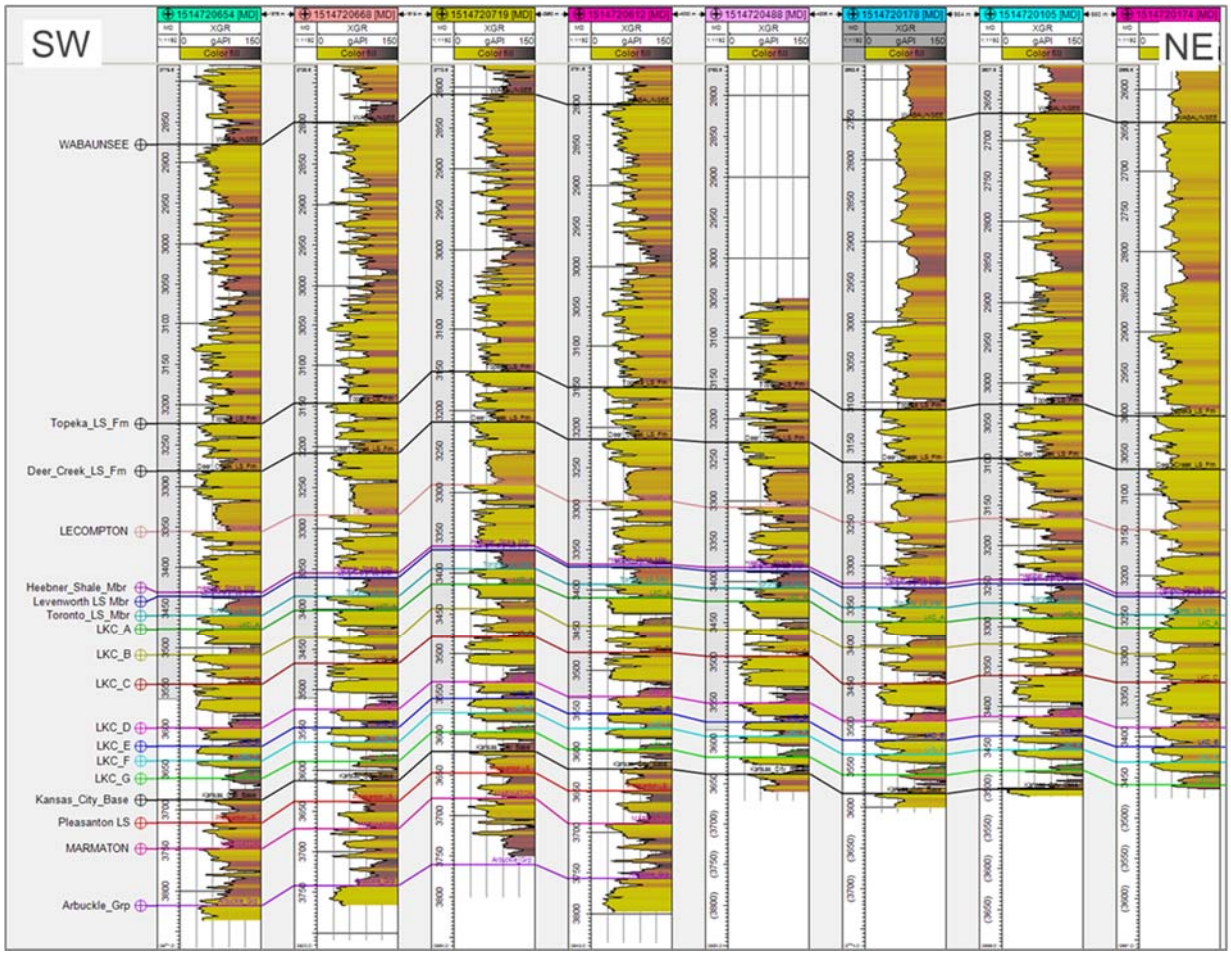

Figure 3-25. Log cross-section showing carbonate cyclicity observed in gamma ray well logs correlated across the Huffstutter study area. Log signatures indicate significant continuity of formations. Cross-section on map in Figure 3-22.

Structural Framework

A total of 26 surfaces were used in developing the framework from ground level to basement (Figure 3-26). Of these, 19 surfaces from the Wabaunsee Group downward were used for delineating the 18 zones for petrophysical modeling (Figure 3-27).

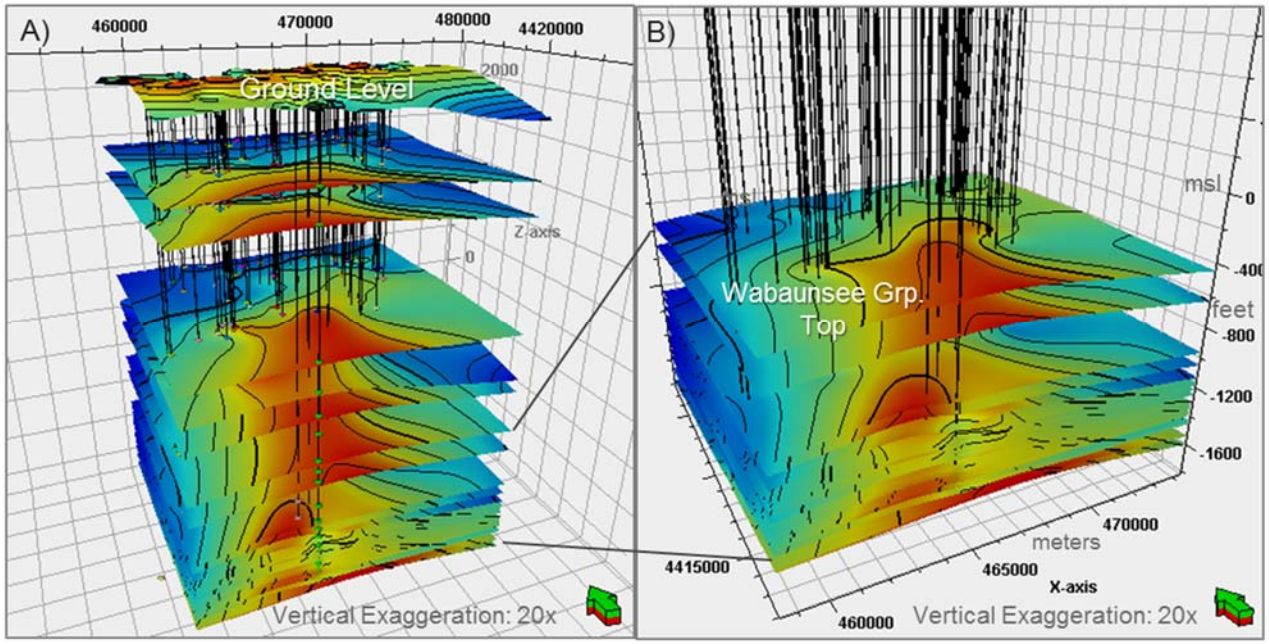

Figure 3-26. Oblique view of SEM area with wells, well tops, and surfaces. A) Well tops appear as beads along the wells. B) Close-up of the lower 19 surfaces used to define the framework for the petrophysical modeling.

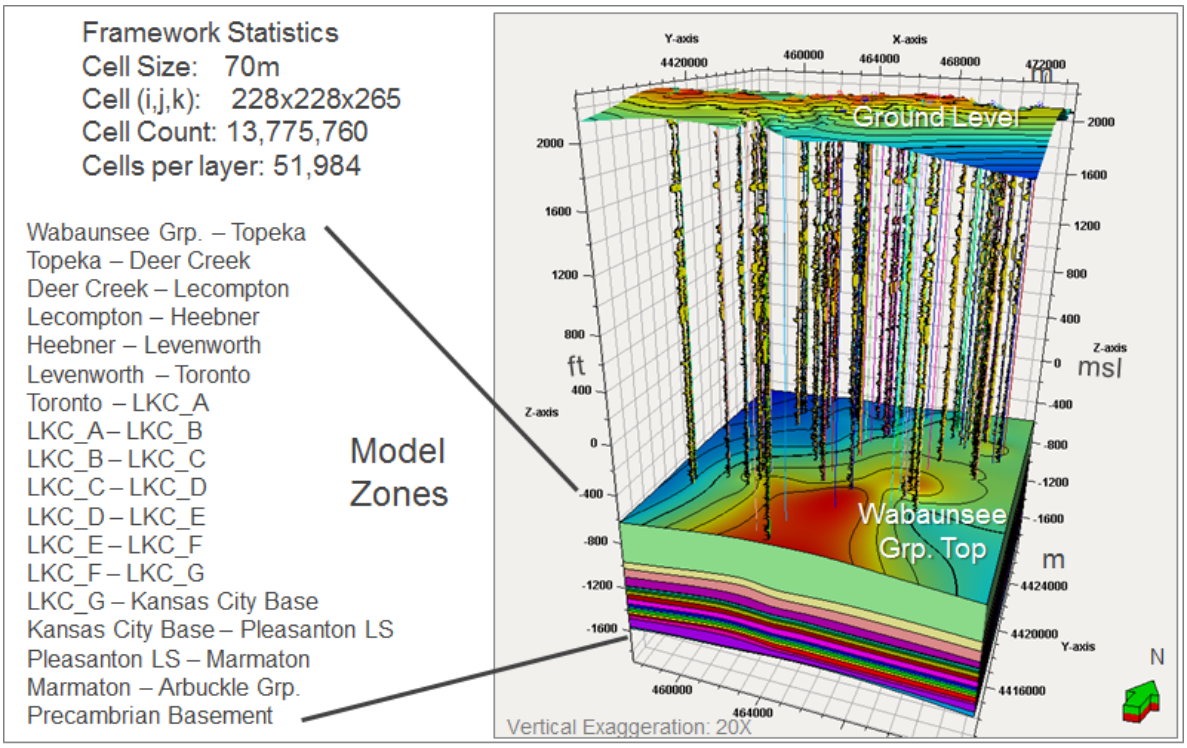

Figure 3-27. The structural framework of the Huffstutter Field study area. SEM is 10 miles by 10 miles. Petrophysical modeling was conducted for zones from the Wabaunsee Group down to Precambrian basement top.

The SEM for the Huffstutter study area has a horizontal resolution defined by a grid cell XY-increment of 230 ft (70 m). The surfaces define stratigraphic zones which were subsequently layered. Each zone was given a zone division which consists of layer type and a layer count or cell thickness (Figure 3-27). The layer type used in this SEM was "proportional," which divides the zone into a set number of layers (Table 3-25). Depending on the thickness of the zone, cell heights will vary. The SEM layers were generated to follow the corresponding structural surface in each zone, with their respective cell thicknesses chosen to capture vertical heterogeneity apparent in the permeability log. Each model layer had 229 x 229 cells for a total of 52,411 cells.

Table 3-25 SEM zone layering types and divisions For the Huffstutter study area.

Zone Reference	Zone division	Number of Layers	Average Layer Thickness (feet/layer)
Ground Level – Carlile	Proportional	1	NA*
Carlile – Greenhorn	Proportional	1	NA*
Greenhorn – Sumner	Proportional	1	NA*
Sumner – Chase	Proportional	1	NA*
Chase – Council Grove	Proportional	1	NA*
Council Grove – Admire	Proportional	1	NA*
Admire – Wabaunsee	Proportional	1	NA*
Wabaunsee – Topeka	Proportional	50	7.05
Topeka – Deer Creek	Proportional	20	3.22
Deer Creek – Lecompton	Proportional	25	2.98
Lecompton – Heebner	Proportional	18	3.92
Heebner – Levenworth	Proportional	3	1.47
Levenworth – Toronto	Proportional	8	3.00
Toronto – LKC A	Proportional	8	2.18
LKC A – LKC B	Proportional	12	2.78
LKC B – LKC C	Proportional	14	2.57
LKC C – LKC D	Proportional	18	3.03
LKC D – LKC E	Proportional	7	3.36
LKC E – LKC F	Proportional	7	2.57
LKC F – LKC G	Proportional	10	2.52
LKC G – Kansas City Base	Proportional	11	2.05
Kansas City Base – Pleasanton	Proportional	10	2.64
Pleasanton – Marmaton	Proportional	10	3.43
Marmaton – Arbuckle	Proportional	15	6.94
Arbuckle – Precambrian Basement	Proportional	12	6.29

***Detailed layering was not performed for caprock units**

Facies Model

A cross-section through the cyclic carbonate facies model for the Lansing-Kansas City interval is given in Figure 3-28. Well control for Pleasanton Group through Arbuckle Group is limited. An oblique view of the facies model is shown in Figure 3-28b. The upper surface is the top of the Wabaunsee Group.

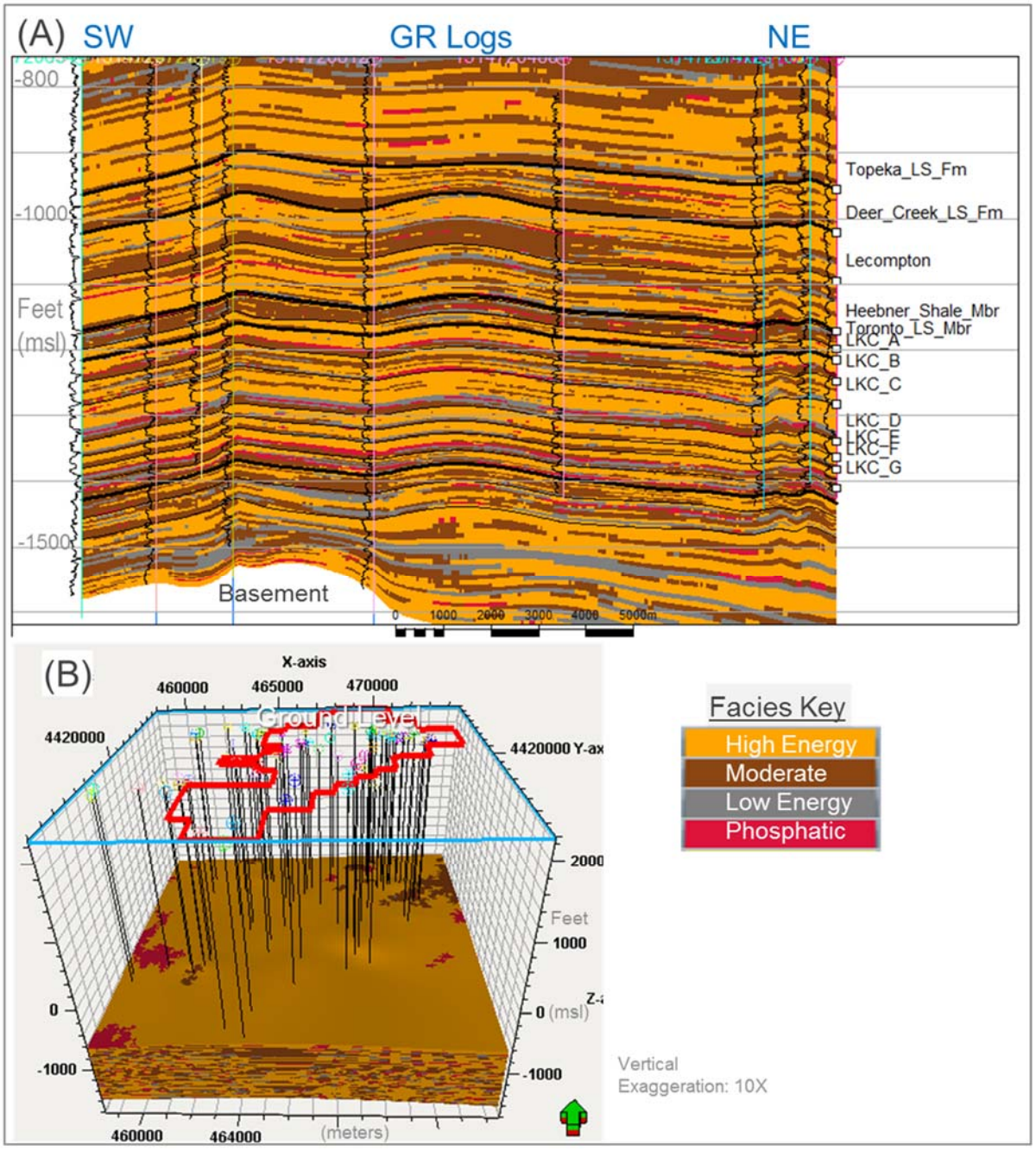

Figure 3-28 Facies Model for the Huffstutter study area. A) Well section of facies model through Huffstutter Field. Well section is mapped in Figure 3-22B) Oblique view of facies model showing the top of the Wabaunsee Group. Wells correspond to cross-section above.

Petrophysical Properties

As discussed in the SEM methods Section 3.1.3, the derived effective porosity logs required adjustments to account for known porosity and permeability trends in lithologic sequences of the Lansing-Kansas City. Permeability logs were calculated based on effective porosity and were also affected. As example of the original and adjusted porosity and permeability logs are shown for well 1514720654, along with their upscaled values, Figure 3-29. The upscaled values have favorable porosity and permeability values that align with the higher energy depositional environments where good porosity development occurs, (Young, 2011). More importantly, porosity and permeability logs and their upscaled counterparts have been attenuated across the lower-energy portions of the regressive limestone sequences.

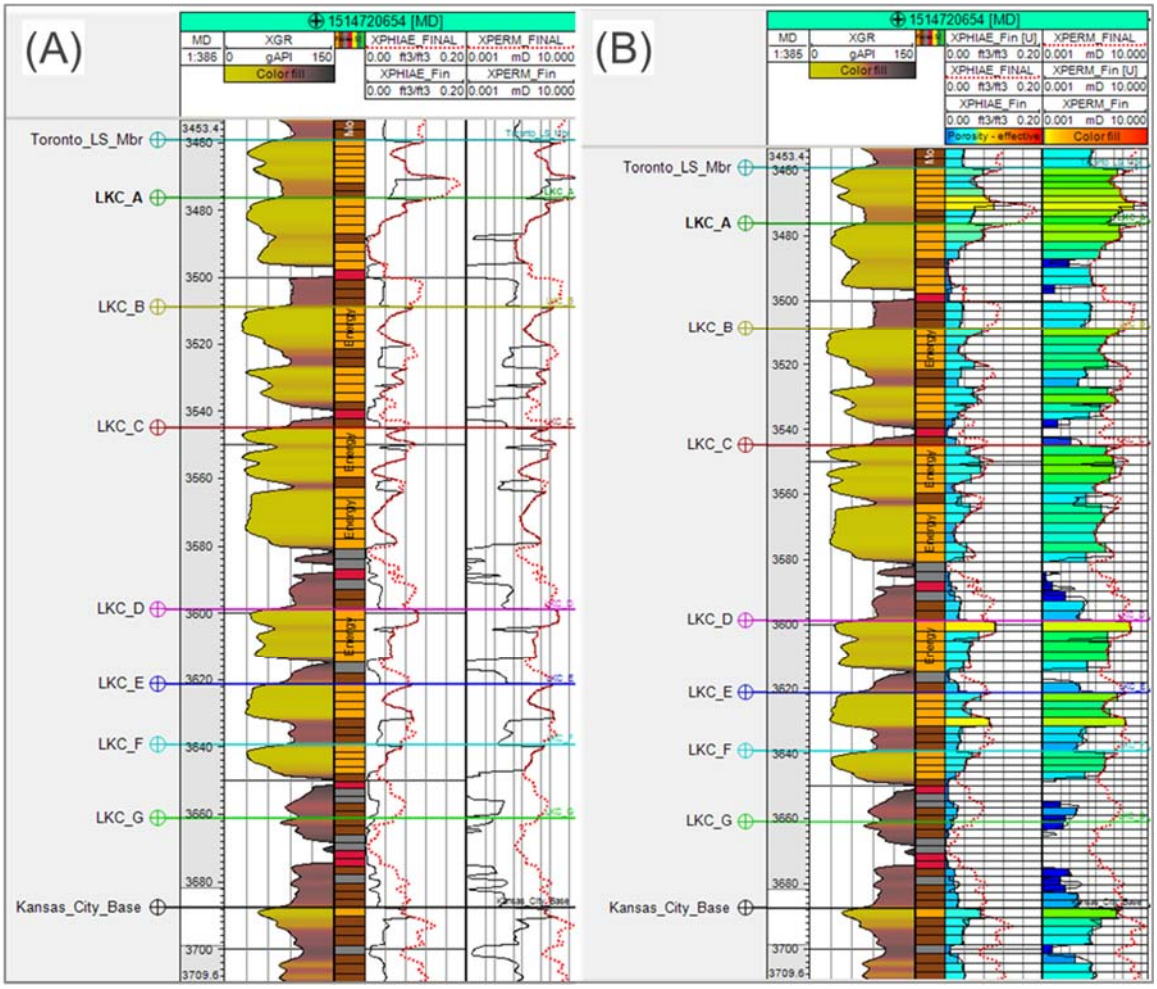

Figure 3-29. Example porosity and permeability log adjustments for the Huffstutter SEM. A) Original effective porosity and permeability logs in red, with adjusted (attenuated) log values in black. B) Same logs as on left, but showing upscaled values into SEM cells along the well path.

The resulting property models are shown in Figure 3-30 and Figure 3-31. An example of the effective porosity and permeability models from the top of the LKC A Zone is given in map view in Figure 3-30a and b, respectively. Because the permeability model was generated through co-located, cokriging with the porosity model, it has a similar distribution with the porosity model. This type of texture is common throughout the cyclic carbonate section, with reduced values for tighter intervals as seen in the cross-

sections in Figure 3-31. Tighter intervals appear as darker blue streaks in the cross-section and are generally related to lower section of each regressive carbonate cycle.

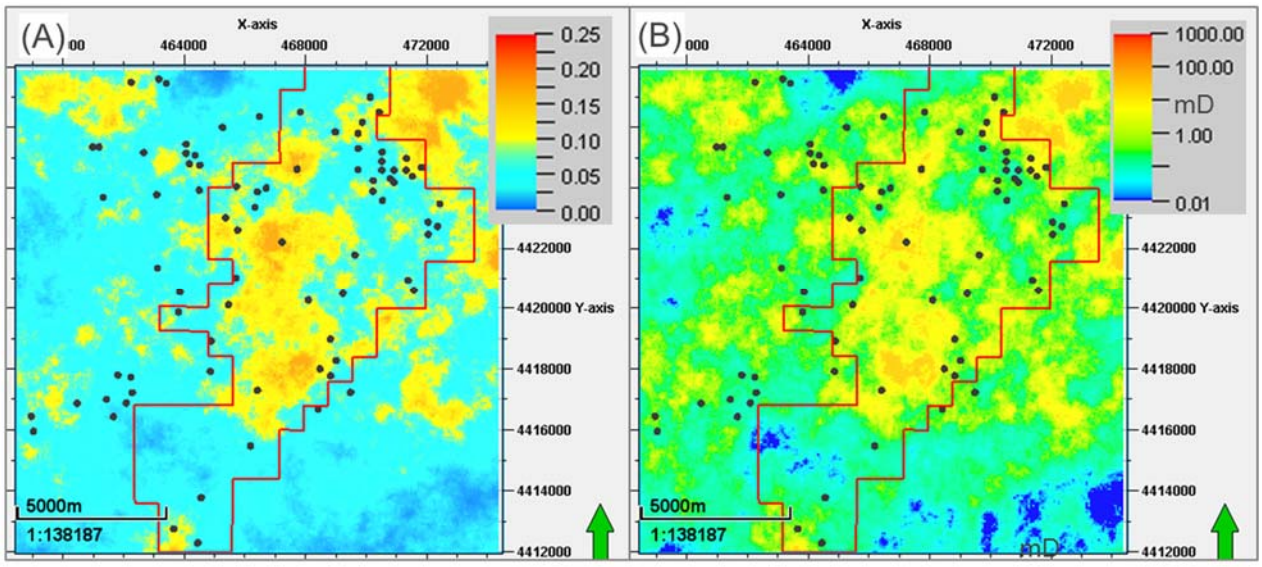

Figure 3-30. Property distribution maps spanning the 10 mi x 10 mi SEM. A) Effective porosity on top of the LKC A Zone. B) Permeability on top of the LKC A Zone. Red polygon demarks the Huffstutter Field. Black dots are well locations with petrophysical logs.

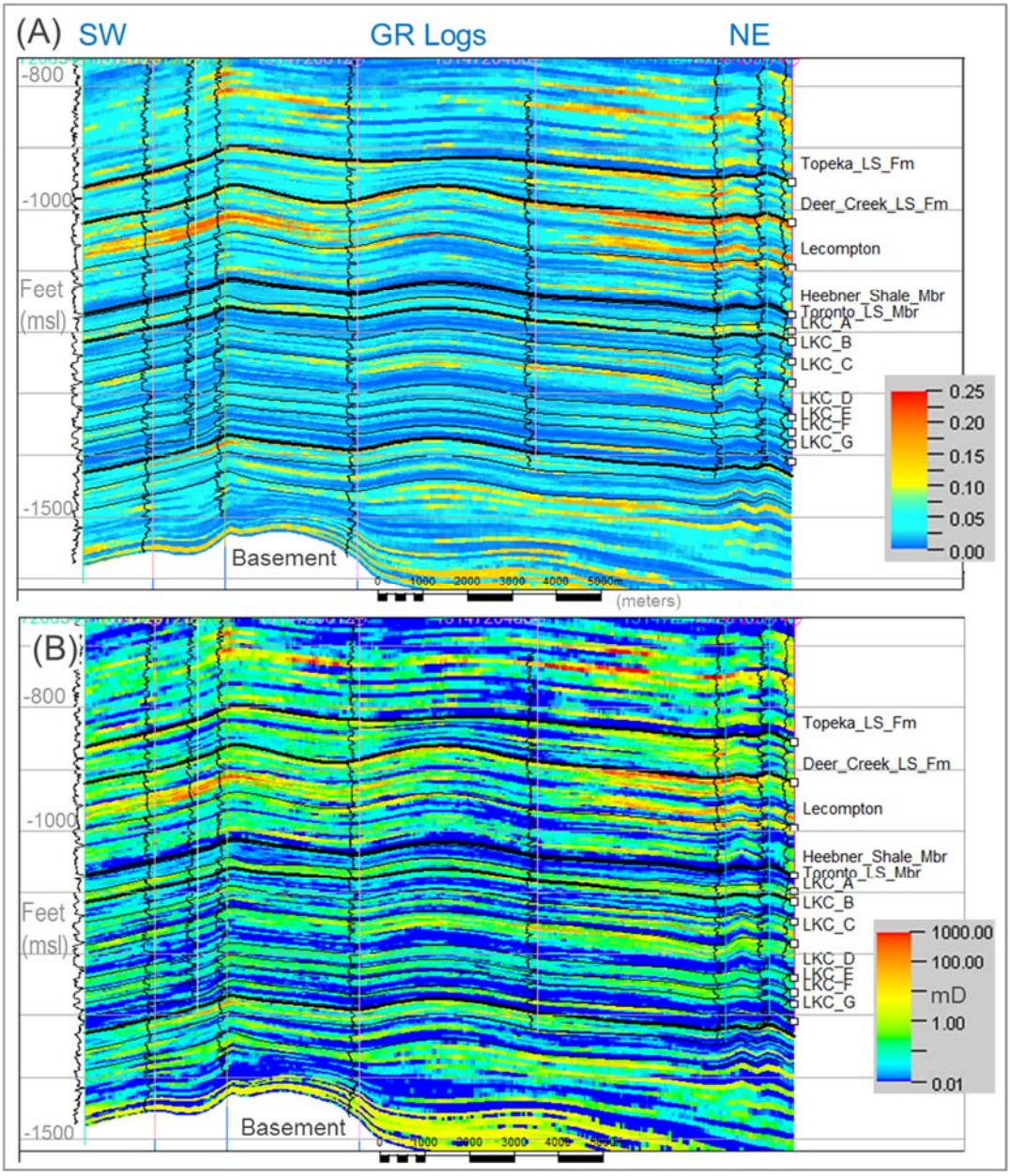

Figure 3-31. Cross-sections through the property models. A) Effective porosity model (XPHIAE_Fin). B) Permeability model (XPERM_Fin).

Figure 3-32 shows the histograms for effective porosity and permeability for all SEM zones where petrophysical modeling was performed. This includes the Wabaunsee Group down through the base of the Arbuckle Group. With limited well penetration, the Arbuckle Group was poorly sampled. There is agreement going from the well logs to the upscaled log properties and then to the property models, which are comprised of millions of cells. Under-representation of high porosity (and high permeability) values is a common occurrence due to sampling and averaging data across a cell's height. This can be seen in the porosity histogram where there is an inflation in porosity estimates in the 4% (0.04 decimal) range at the expense of higher values. The permeability histogram shows moderate agreement between the permeability logs and the final permeability model. Deviations here may be due to the limited log coverage in the thick Wabaunsee Group and in the Arbuckle Group.

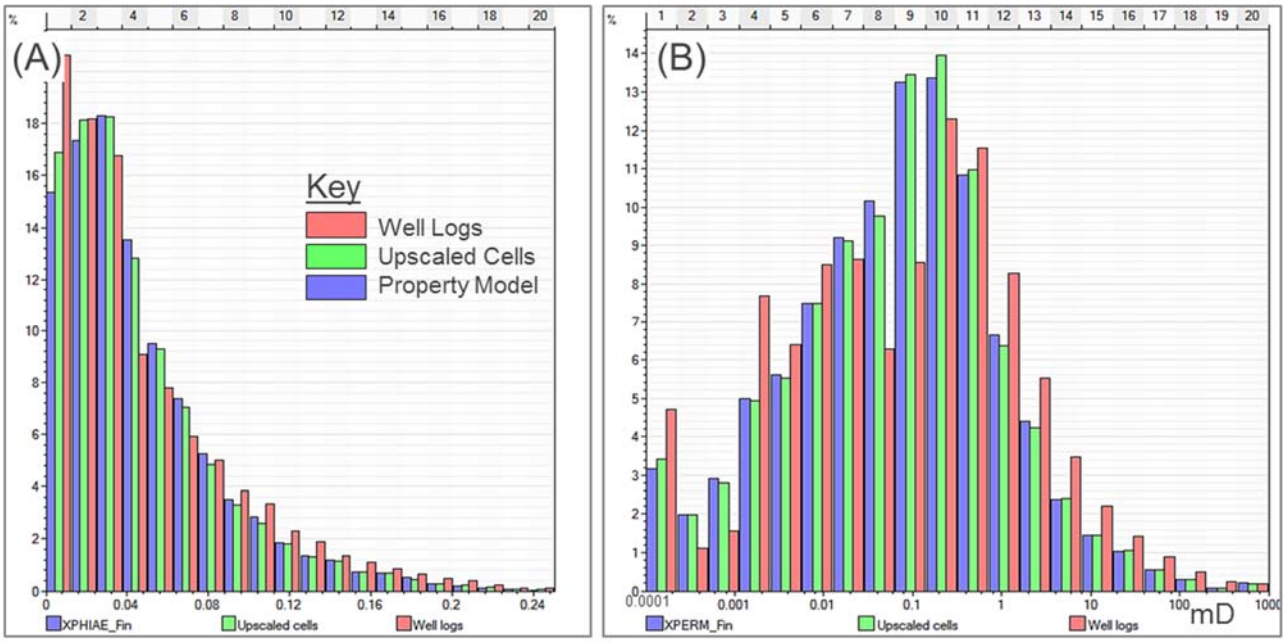

Figure 3-32. Histograms depicting property distributions. A) Effective porosity (XPHIAE_Fin) and B) Permeability (XPERM_Fin).

3.6.3 Site-Specific Characterization and Geologic Maps

Sleepy Hollow Study Area

Caprocks

Upper Pennsylvanian and Lower Permian shale, evaporite, and carbonate formations were evaluated as primary caprocks for the underlying storage complex. In ascending order, these lithostratigraphic units include: Admire, Council Grove, Sumner, and lower Nippewalla groups. These units exhibit log responses consistent with tight (i.e., low porosity) non-reservoir lithologies, such as gamma ray values greater than 65 gAPI for shale and/or effective log porosities less than 5%. Directly overlying the Wabaunsee Group in both the Sleepy Hollow and Huffstutter study areas, the shale and siltstone formations of the Admire Group represent the base of the primary caprock sequence. A shale unit characterized by high gamma ray log response (> 65 gAPI) was identified in the lower portion of the Nippewalla Group, and represents the top of the Pennsylvanian-Permian caprock complex. Structure maps were generated for each study area to evaluate depth and areal extent of potential caprocks. Isopach maps were produced to assess gross thicknesses.

In the Sleepy Hollow study area, gamma ray logs penetrating the entire Pennsylvanian-Permian caprock complex were available from 32 to 33 wells, depending on the unit, to quantify and map caprock structure and thickness (Table 3-26). Average depths, gross thicknesses, and associated standard deviations measured for caprock units in the Sleepy Hollow study area are shown in Table 3-26. The depths of all four caprock units appear to generally increase from the east to the west (Figure 3-33a, Figure 3-34a, Figure 3-35a, and Figure 3-36a). The shale interval at the base of the Nippewalla Group occurs at an average depth of 1,772 ft and has an average gross thickness of 221 ft, with the greatest thicknesses occurring in the northwest portion of the study area (Figure 3-33b). The underlying Sumner Group, comprised of shale and evaporite formations, has an average depth and gross thickness of 1,986 ft, and 286 ft, respectively. The gross thickness of the Sumner Group generally increases from the northwest to the southeast (Figure 3-34b). The shale, sandstone, and carbonate formations of the Chase

Group separate the Sumner Group from the underlying Council Grove Group, and was not evaluated as a potential caprock due to thin, localized intervals of porosity greater than 5% observed on logs. The Lower Permian Council Grove Group is present at an average depth of 2,468 ft, and is the thickest of the four main caprock units evaluated in the study area, with an average gross thickness of 325 ft. The Upper Pennsylvanian Admire Group occurs at an average depth of 2,784 ft, and has an average gross thickness of 110 ft. Gross thicknesses of the Council Grove and Admire are highest in the east-central portion of the study area (Figure 3-35b, and Figure 3-36b, respectively).

Variation observed in caprock depth is represented by standard deviations that range from 82 ft to 92 ft (Table 3-26). Standard deviations in gross thickness range from 9 ft to 19 ft. Caprock depths and gross thicknesses are poorly constrained in the northern and southern extremes of the Sleepy Hollow study area where well density is low. Structural cross-sections constructed along broad transects were used to further characterize the vertical and lateral extent of caprocks, and evaluate site-specific stratigraphic trends.

Table 3-26. Mean and standard deviation (σ) of caprock depth and gross thickness of caprocks along with the associated well count (n) for the Sleepy Hollow study area.

Group	Depth (ft md*)			Gross Thickness (ft)		
	Mean	σ	*n*	Mean	*Σ*	*n*
Lower Nippewalla	1,772	92	33	221	9	33
Sumner	1,986	83	32	286	19	32
Council Grove	2,468	86	32	325	11	32
Admire	2,784	82	33	110	9	33

*Values reported in measured depth (md) for the purposes of CO_2 storage assessment; refer to caprock structure maps for depths relative to mean sea level.

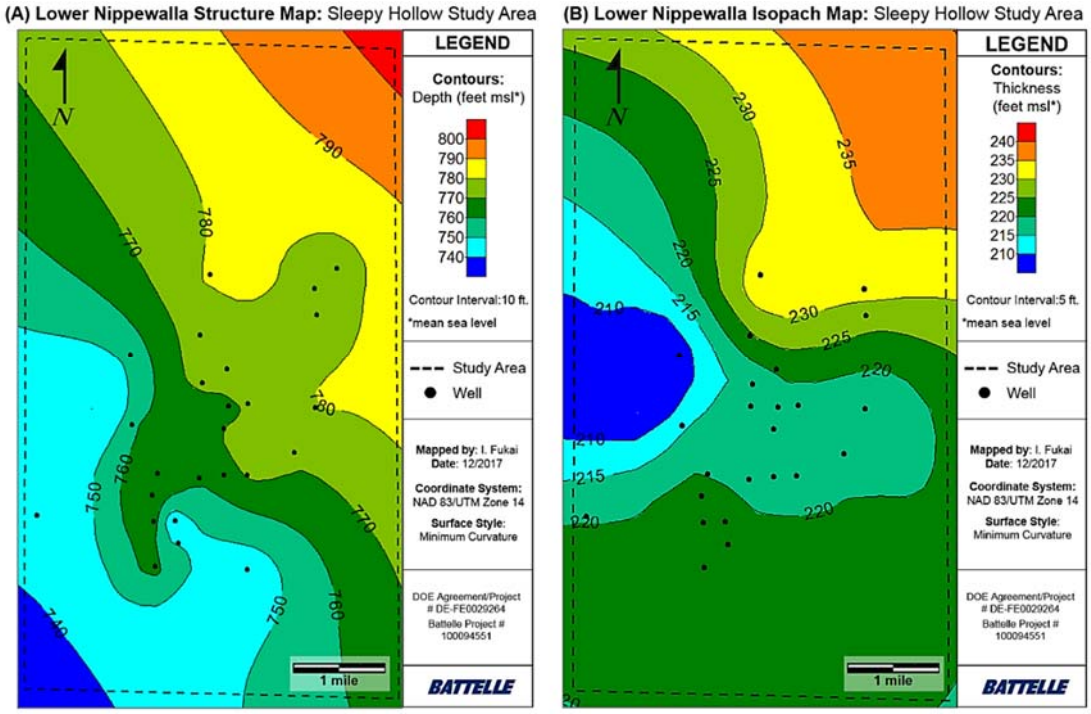

Figure 3-33. (A) Structure and (B) isopach map for the lower Nippewalla shale in the Sleepy Hollow study area.

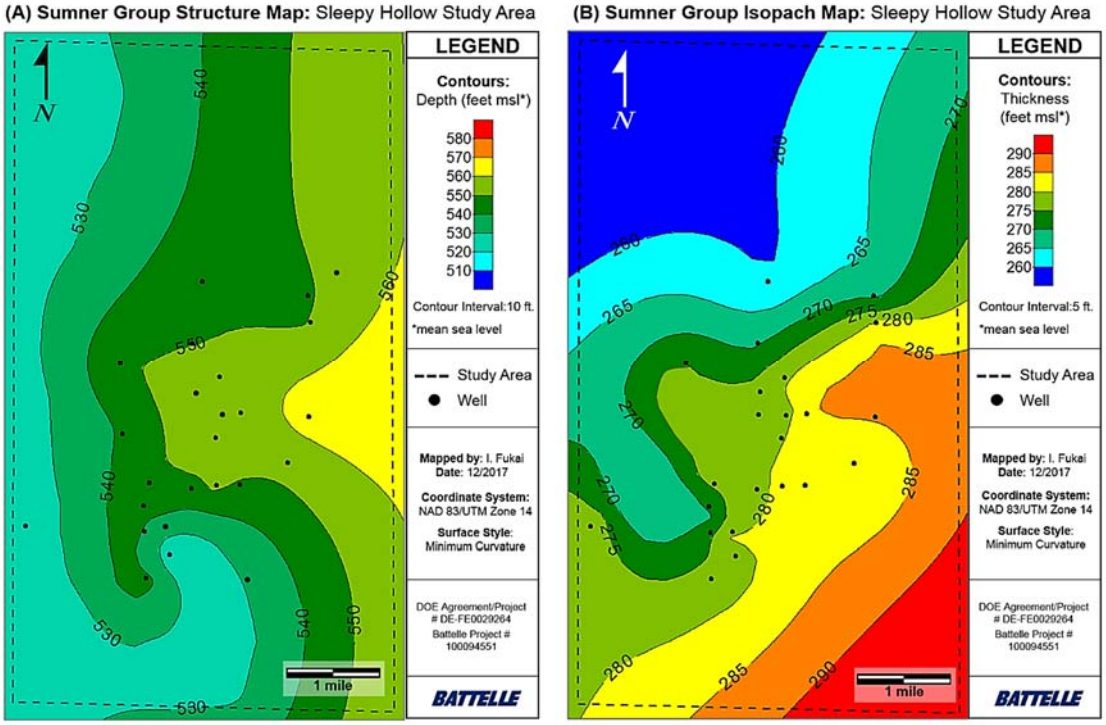

Figure 3-34. (A) Structure and (B) isopach map for the Sumner Group in the Sleepy Hollow study area.

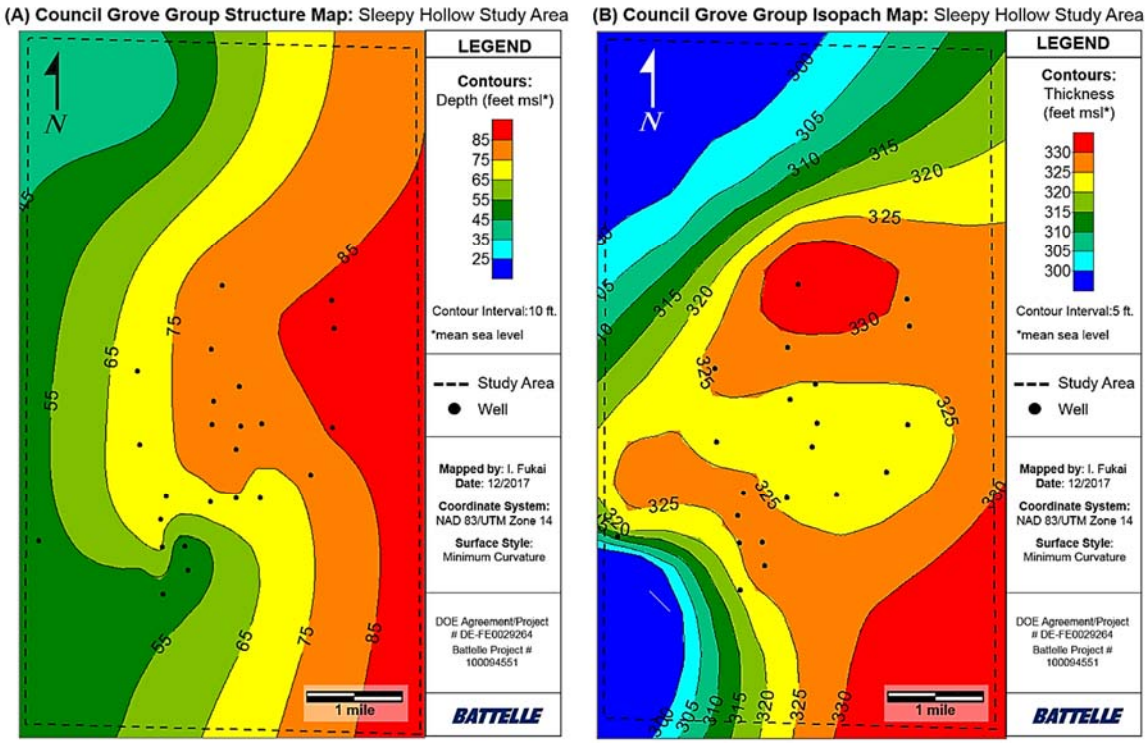

Figure 3-35. (A) Structure and (B) isopach map for the Council Grove Group in the Sleepy Hollow study area.

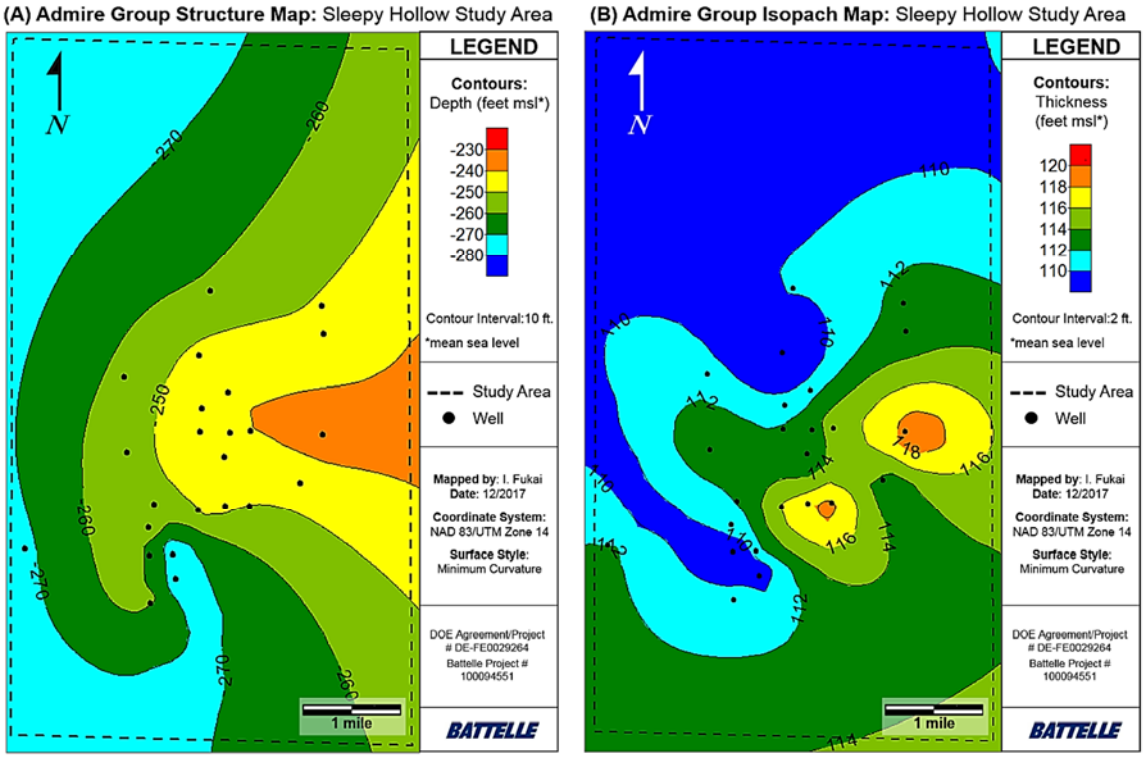

Figure 3-36. (A) Structure and (B) isopach map for the Admire Group in the Sleepy Hollow study area.

Structural cross-sections were constructed to examine the vertical and lateral continuity of caprocks, and evaluate the potential impact of faults/fold on the lithologic configuration of caprock units at each study area. The A-A' cross-section shown in Figure 3-37 was generated to examine the interval extending from the lower Nippewalla to the Wabaunsee Group along a general west-to-east transect in the Sleepy Hollow study area. The depths and gross thicknesses of caprocks appear to be relatively consistent from west to east, with depth variations less than ± 25 ft observed in all lithostratigraphic units evaluated. Similarly, variations of approximately 10 ft or less are observed in gross thicknesses of caprocks. The gross thickness of the Chase Group, separating the lower Nippewalla and Sumner groups from the underlying Council Grove and Admire groups, is approximately 150 ft in the A-A' cross-section. There are no major offsets in lithostratigraphic tops or drastic thickness changes to indicate significant faulting or folding along the west-to-east transect in the study area.

The B-B' cross-section shown in Figure 3-38 was generated to examine the Pennsylvanian-Permian caprock complex along a general south-to-north transect in the Sleepy Hollow study area. Depth variation of ± 25 ft was observed in all caprock units along this transect. This variation is best expressed in the central portion of the transect between well number 2614505429 and well number 2614521500. Gross thicknesses appear to be relatively consistent from south to north, with variations less than approximately 20 ft observed in caprocks. Similar to the A-A' cross-section, there do not appear to be any major faults impacting the vertical and lateral continuity or configuration of caprock units in the B-B' cross-section for the Sleepy Hollow study area.

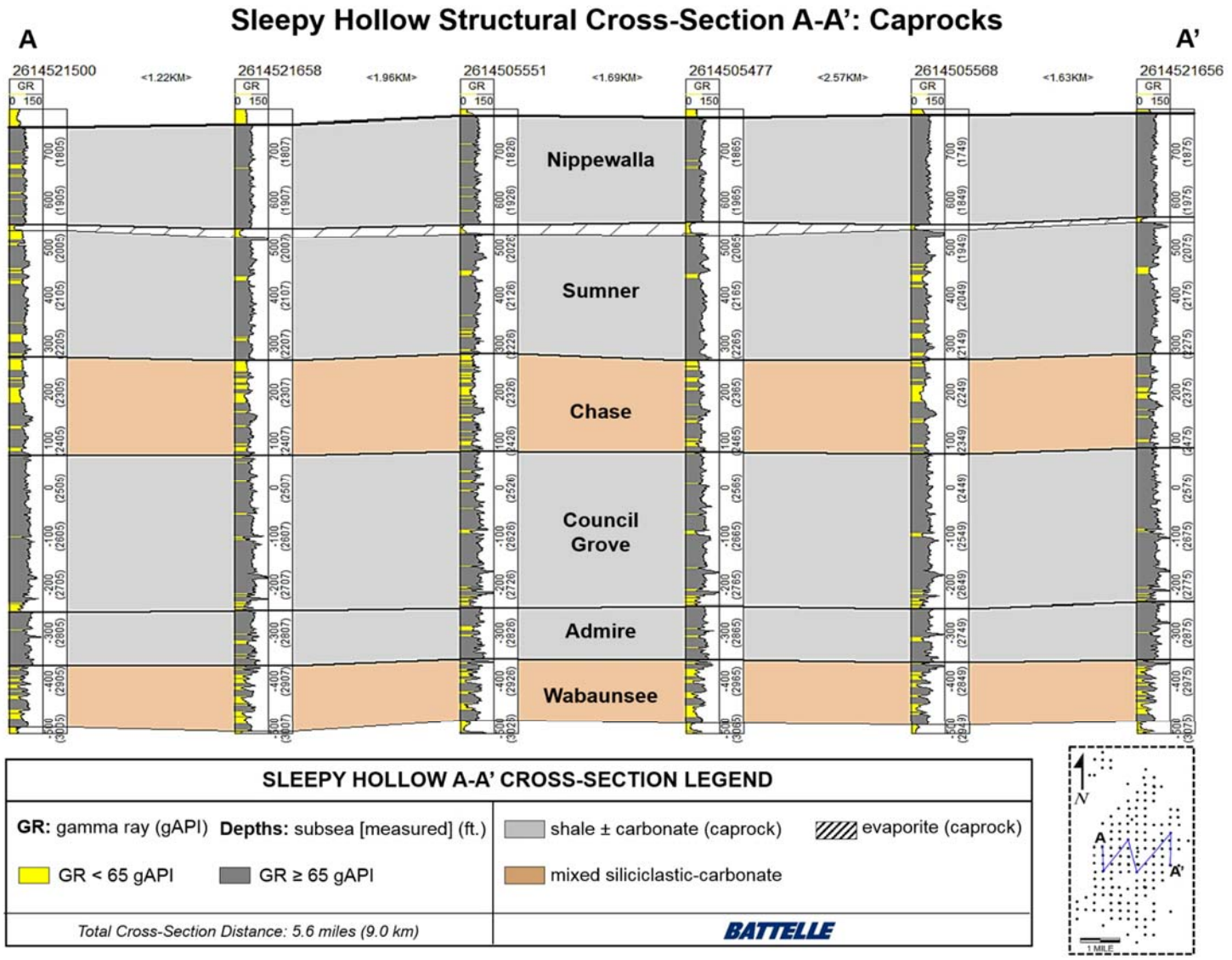

Figure 3-37. Structural cross-section showing lateral extent and thickness of the primary caprock units along a general west-to-east transect in the Sleepy Hollow study area.

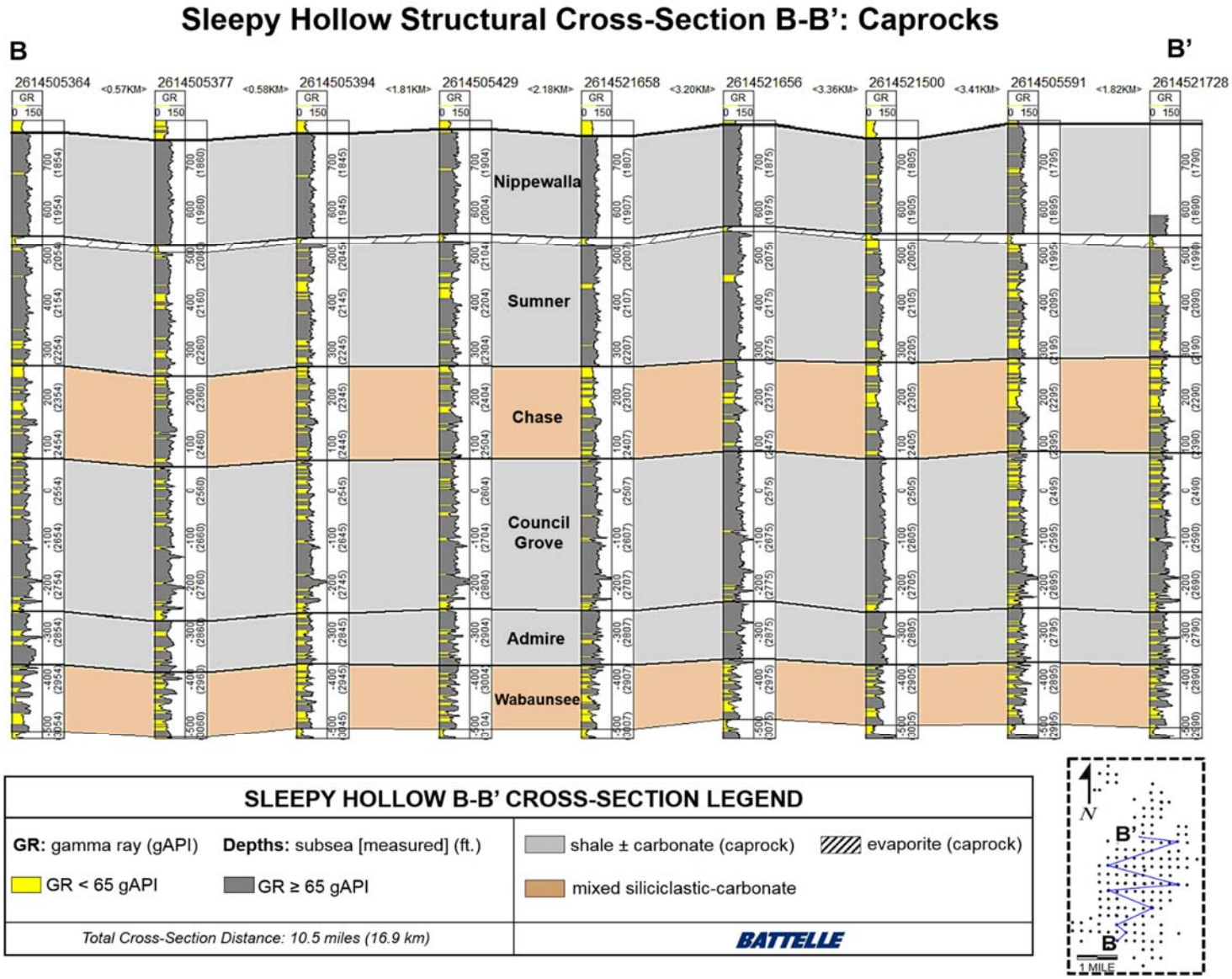

Figure 3-38. Structural cross-section showing lateral extent and thickness of the primary caprock units along a general south-to-north transect in the Sleepy Hollow study area.

Deep Saline Formations

Structural maps showing depths of the Pennsylvanian-age lithostratigraphic units indicate deep saline intervals of interest are laterally extensive throughout the Sleepy Hollow study area, with the Wabaunsee Group occurring at average depths of 2,862 ft. Average depths of 2,862 ft and greater for the deep saline intervals are associated with adequate subsurface pressures and temperatures for supercritical CO_2 storage.

Structural maps for deep saline formations show the presence of a northeastward trending, gentle, anticlinal structure that shallows to the northeast (Figure 3-39a to Figure 3-42a), likely reflecting the underlying structure of the Cambridge Arch. The southeast limb of the anticline appears to dip more strongly than the northwest side. However, there are lesser well control points on the northwestern limb and this may result in a more relaxed dip in that area.

The isopach maps show 15ft +/- 5ft of difference in gross thickness of the four groups in the Sleepy Hollow study area Figure 3-39b to Figure 3-42b. Some thickness variations may reflect local fluctuations in deposition and erosion. Differences observed in the northeastern and southeastern portions of the study area may be due to limited well control in these areas.

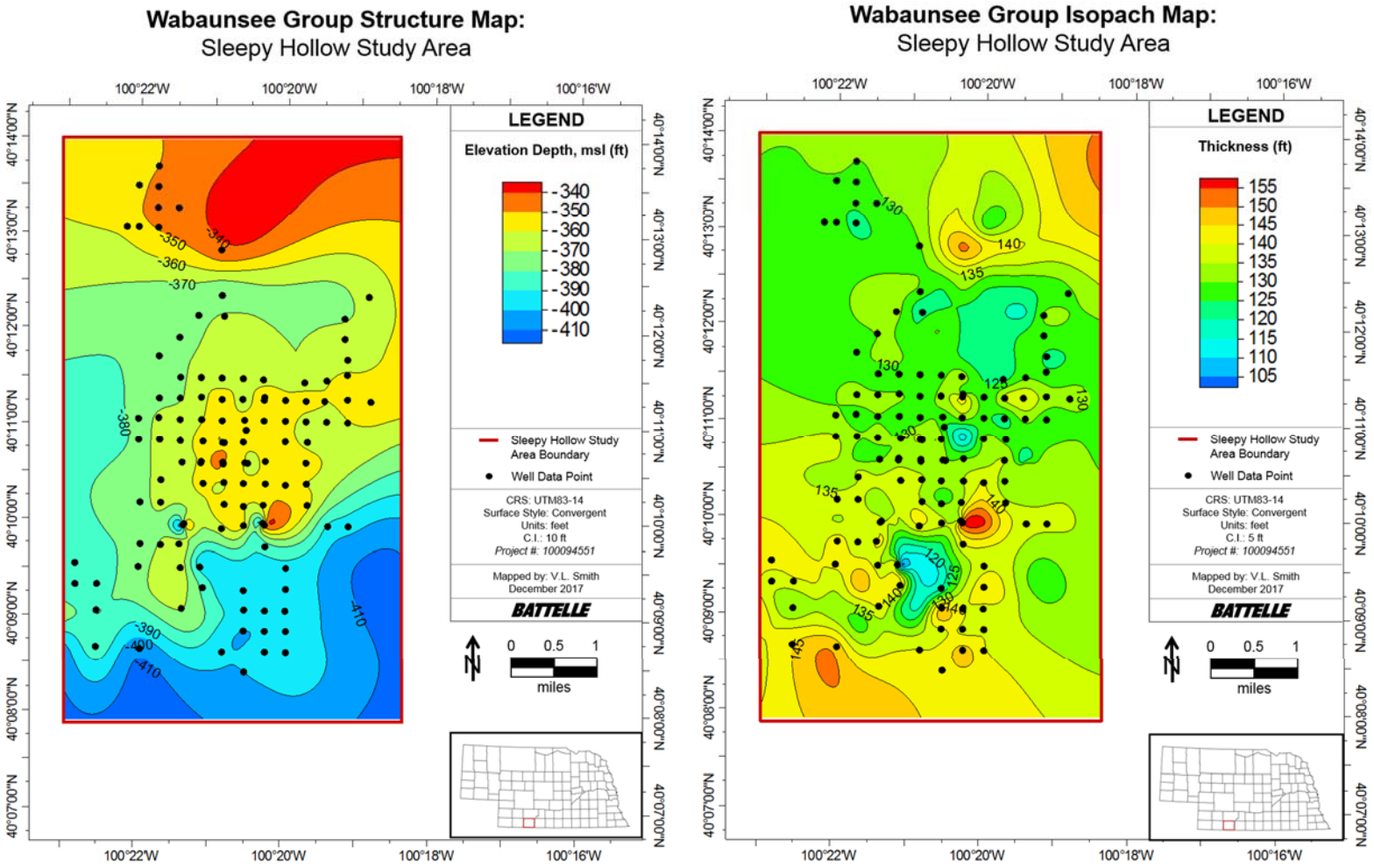

Figure 3-39. (A) Structure and (B) isopach of the Wabaunsee Group in the Sleepy Hollow study area.

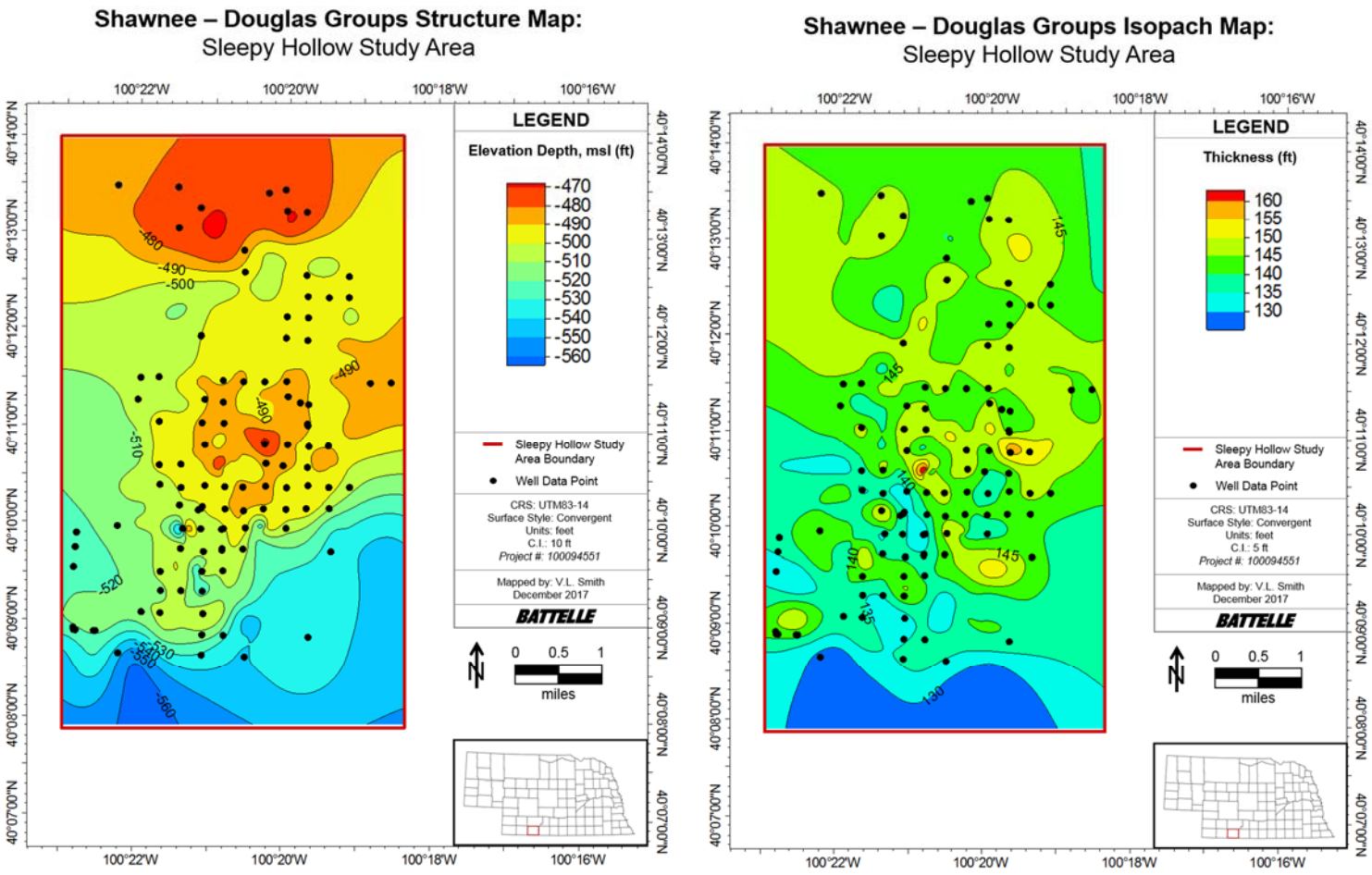

Figure 3-40. (A) Structure and (B) isopach of the Shawnee-Douglas groups in the Sleepy Hollow study area.

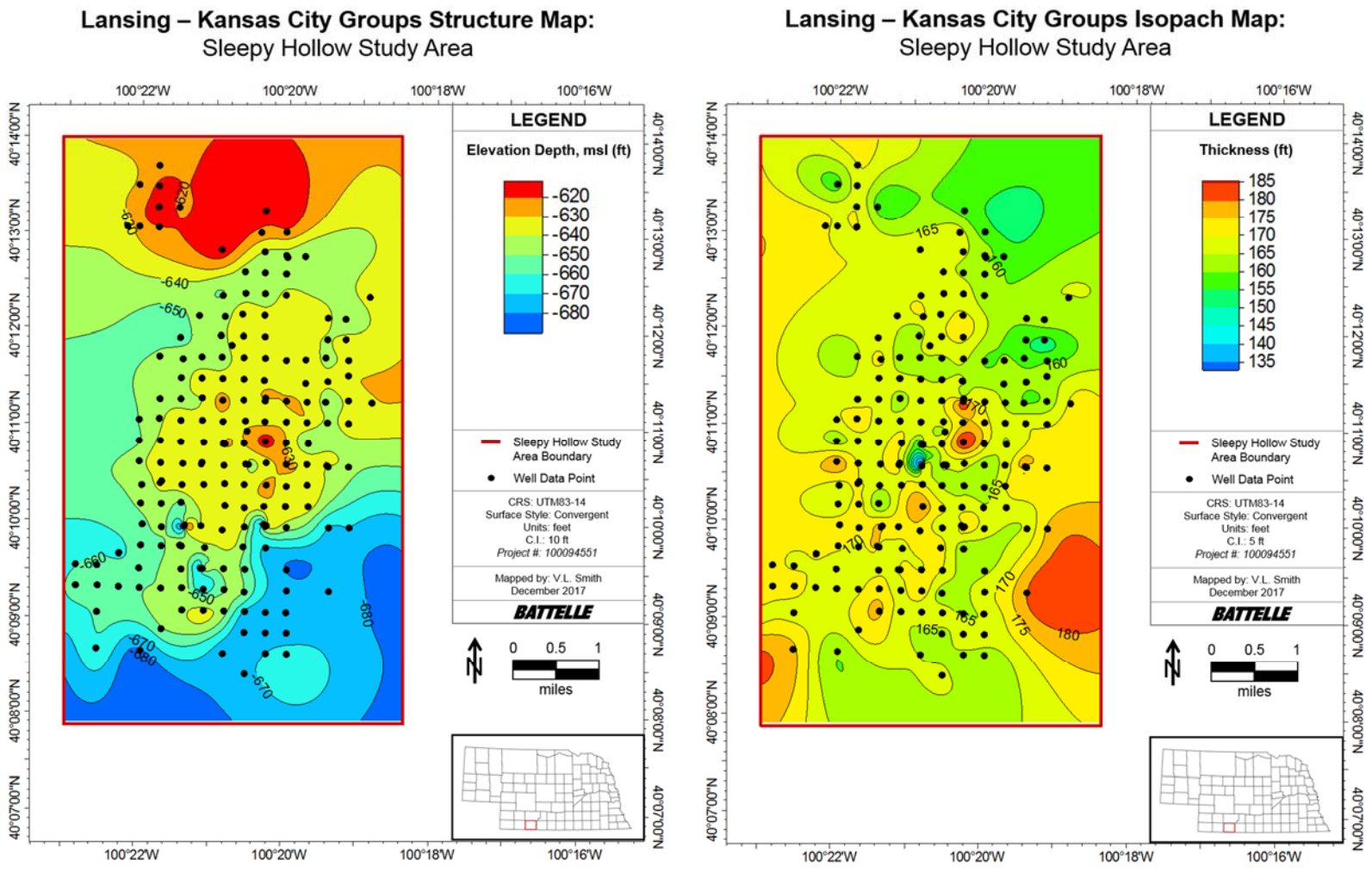

Figure 3-41. (A) Structure and (B) isopach map of the Lansing-Kansas City groups in the Sleepy Hollow study area.

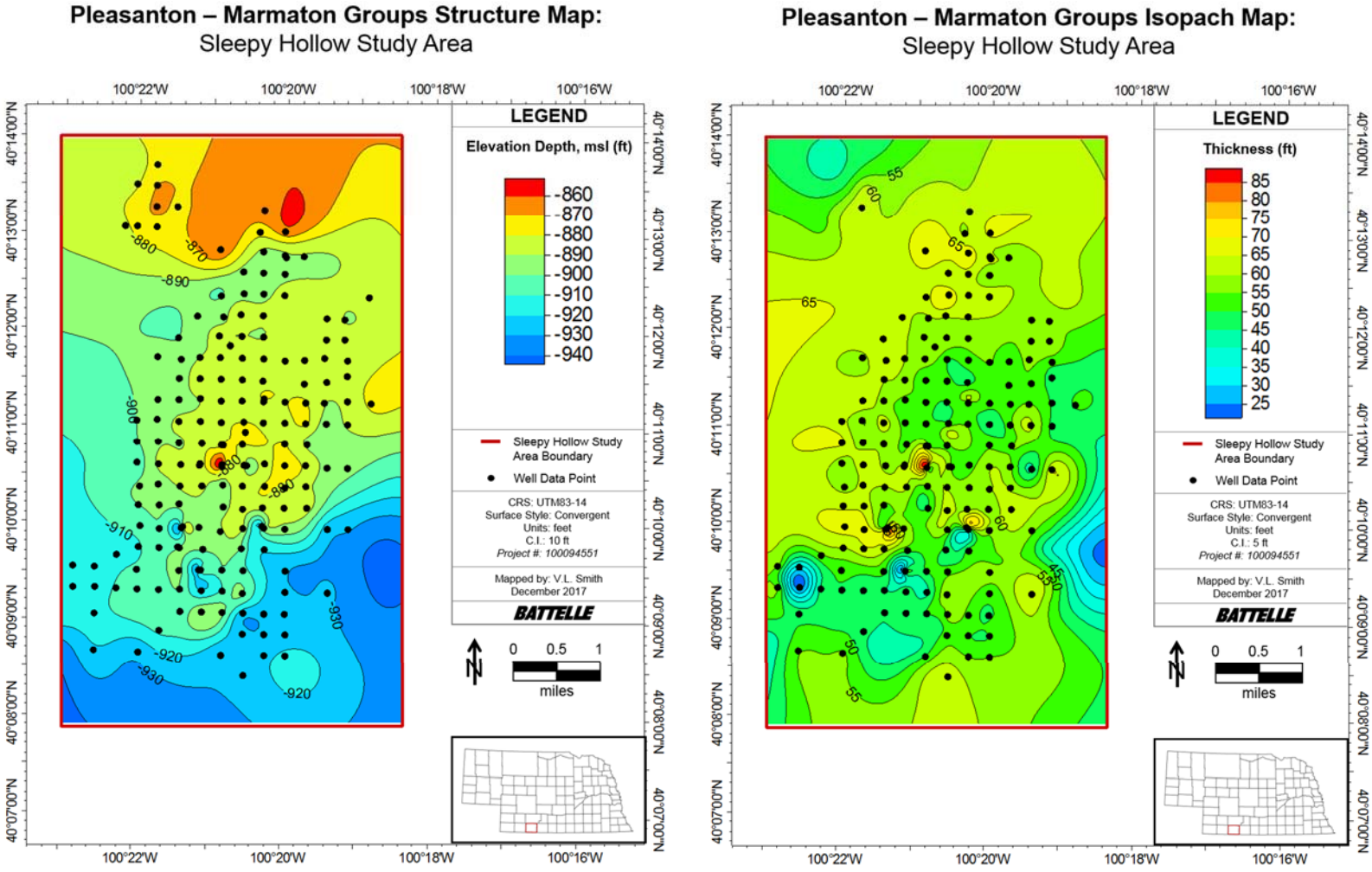

Figure 3-42. (A) Structure and (B) isopach map of the Pleasanton-Marmaton groups in the Sleepy Hollow study area.

Structural cross-sections were constructed to examine the vertical and lateral continuity of deep saline formations, and evaluate the potential impact of faults/fold on potential storage intervals at each study area. The C-C' cross-section shown in Figure 3-43 was generated to examine the interval extending from the Wabaunsee Group to the basal Pennsylvanian sandstone along a west-to-east transect in the Sleepy Hollow study area. The depths and gross thicknesses of the lithostratigraphic groups appear to be relatively consistent from west to east, with variations less than ± 25 ft observed in most of the units evaluated. The exception to this is the basal Pennsylvanian sandstone, which pinches out toward the east. Net thickness of potential storage intervals appears to be greatest on western side of the transect (green intervals, Figure 3-43). Distinct, laterally continuous net intervals are observed in the upper and lower sections of the Wabaunsee, in the middle of the oil-bearing zone of the Lansing-Kansas City, and in the middle of the Pleasanton-Marmaton groups. There are no major offsets in lithostratigraphic tops or drastic thickness changes to indicate significant faulting or folding along the west-to-east transect in the Sleepy Hollow study area.

The D-D' cross-section shown in Figure 3-44 was generated to examine the Pennsylvanian deep saline formations along a south-to-north transect in the Sleepy Hollow study area. Depths appear to generally increase by 25 ft from the south to the central portion of the study area, and then decrease slightly by approximately 15 ft from the central to the northern portion of the transect. This trend coincides with basement highs and lows observed in the Precambrian structural surface. Gross thicknesses are largely consistent from south to north, with the exception that basal Pennsylvanian sandstone pinching out completely in the northernmost well on the transect. Net thickness intervals appear to be greater in wells situated on basement highs, such as well 2614505501 and well 2614505551. Similar to trends observed along the west-to-east transect, laterally continuous net intervals are observed in the D-D' cross-section in the upper and lower sections of the Wabaunsee, in the middle of the oil-bearing zone of the Lansing-Kansas City, and in the middle of the Pleasanton-Marmaton groups. There are no major offsets in lithostratigraphic tops or drastic thickness changes to indicate significant faulting is present along the south-to-north transect in the Sleepy Hollow study area.

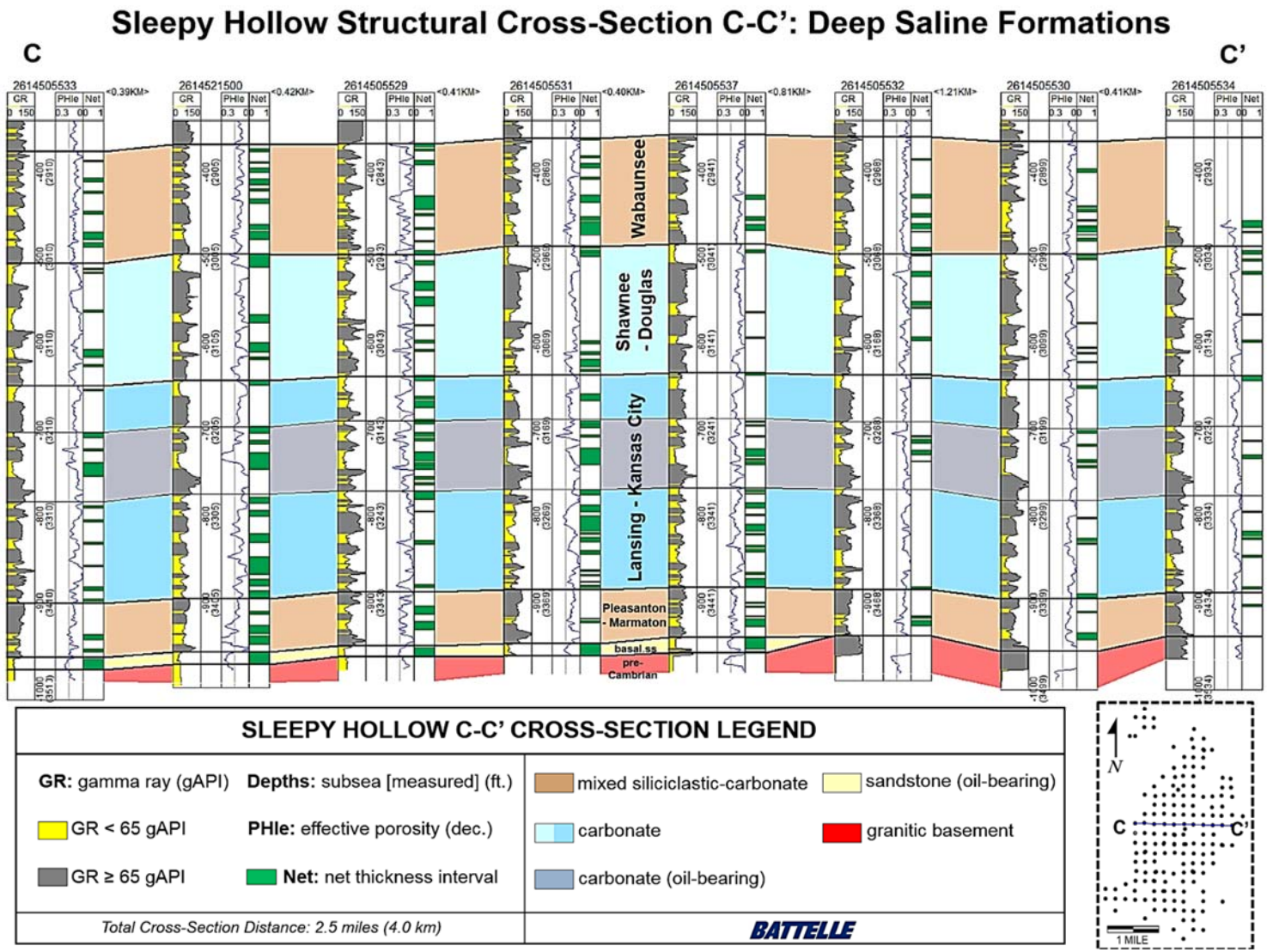

Figure 3-43. Structural cross-section showing lateral extent, gross thickness, and net reservoir intervals of the deep saline formations and oil-bearing zones along a west-to-east transect in the Sleepy Hollow study area.

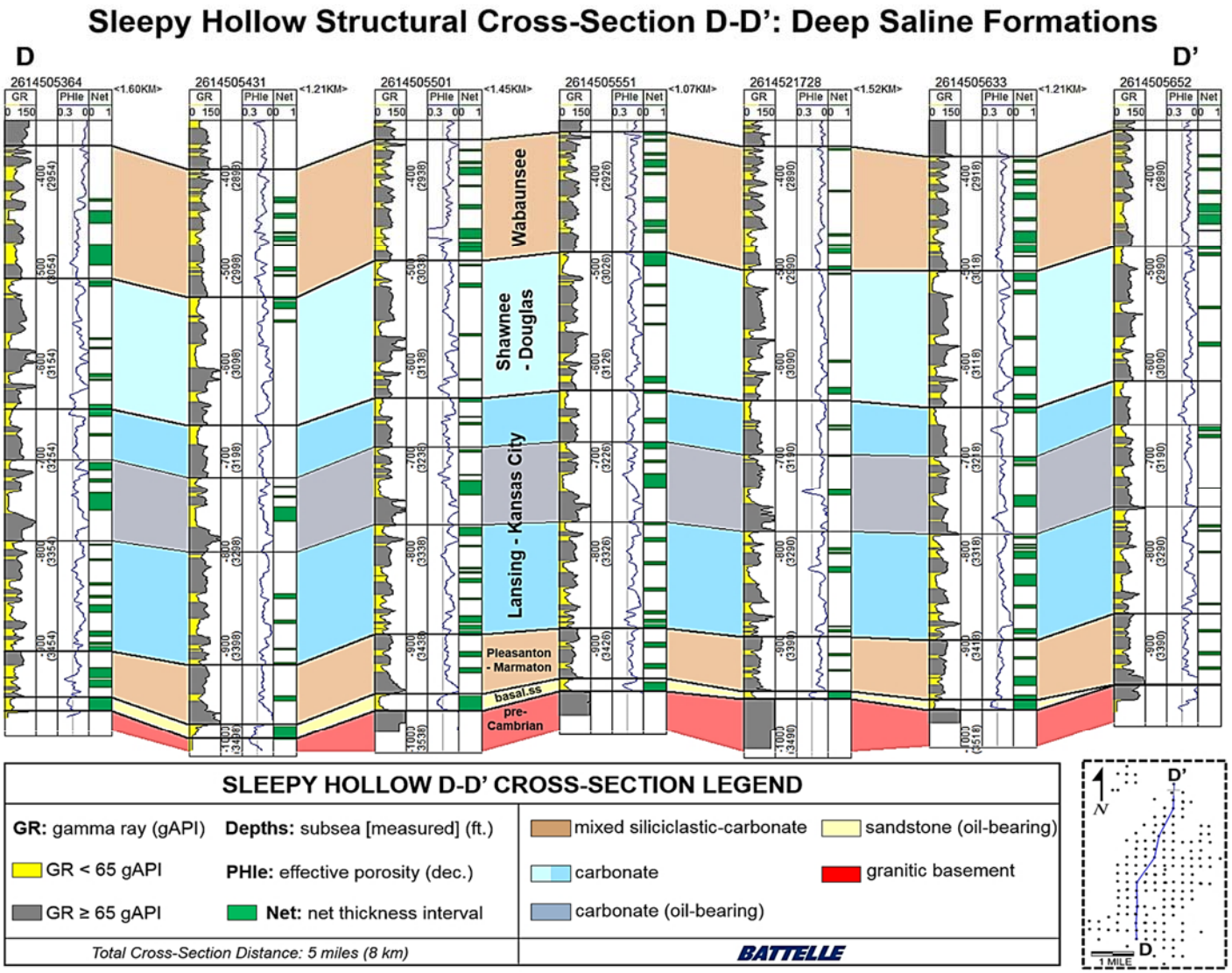

Figure 3-44. Structural cross-section showing lateral extent, gross thickness, and net reservoir intervals of the deep saline formations and oil-bearing zones along a general south-to-north transect in the Sleepy Hollow study area.

The heterogenous grid data of the SEM was used to quantify and map total and net reservoir properties of the deep saline formations of interest in the Sleepy Hollow study area (refer to Table 3-6 in Section 3.1.2 for an explanation of "total reservoir" and "net reservoir" distinctions). Total reservoir thickness, total reservoir porosity and permeability, and total reservoir pore volume is listed in Table 3-27 along with average net-to-total reservoir pore volume ratios calculated for the lithostratigraphic units of interest in the Sleepy Hollow study area.

Table 3-27. Average total reservoir thickness, total reservoir porosity and permeability, and total reservoir pore volume along with net-to-total reservoir pore volume ratio for the Sleepy Hollow study area.

Group/Formation/Zone	Total Reservoir Thickness (ft)		Total Reservoir Porosity (%)		Total Reservoir Permeability (mD)		Total Reservoir Pore Volume (million ft^3)	Net-to-Total Reservoir Pore Volume
	Mean	σ	Mean	σ	Mean	Σ		Mean
Wabaunsee	68	19	6	0.5	9	14	11,026	0.77
Topeka	30	8	5	0.5	11	26	4,162	0.55
Deer Creek-Oread	44	11	5	0.6	6	14	6,198	0.52
A Zone	28	8	4	0.5	6	17	3,903	0.43
D-F Zones	62	12	5	0.5	2	5	8,925	0.60
Pleasanton-Marmaton	25	9	6	0.6	11	21	3,947	0.82

The porosity-feet, or the cumulative thickness of pore space, of the Wabaunsee Group in the Sleepy Hollow study area exceeds 7 feet in some locations. Figure 3-45 demonstrates the geographic trends of the porosity footage within the Wabaunsee. A north-south trend of high porosity footage within the Wabaunsee exists left of center of the Sleepy Hollow study area. Additionally, the high porosity footage in the center of the study area extends west-northwest and east-southeast. High porosity footage in the Wabaunsee also occurs in the southeast corner of the study area.

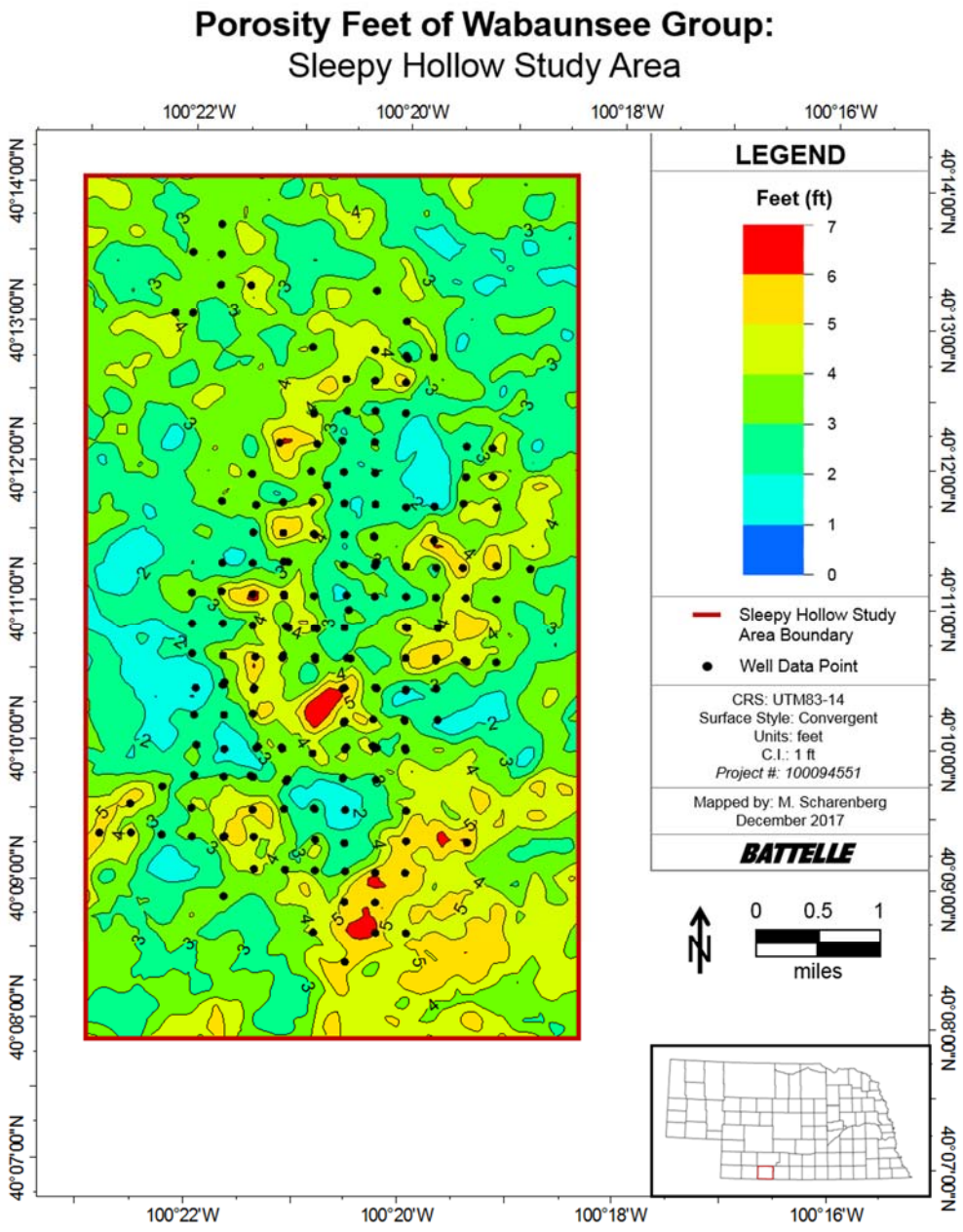

Figure 3-45. Porosity footage map of the Wabaunsee Group in the Sleepy Hollow study area.

The porosity footage map of the Shawnee-Douglas groups (Figure 3-46) demonstrates similar trends to the Wabaunsee Group; high porosity footage left of center trending north-south, high porosity footage in the southeast corner of the study area, and in the center extending west-northwest and east-southeast. The west-northwest and east-southeast trend of high porosity footage is more prominent in the Shawnee-Douglas groups than in the Wabaunsee.

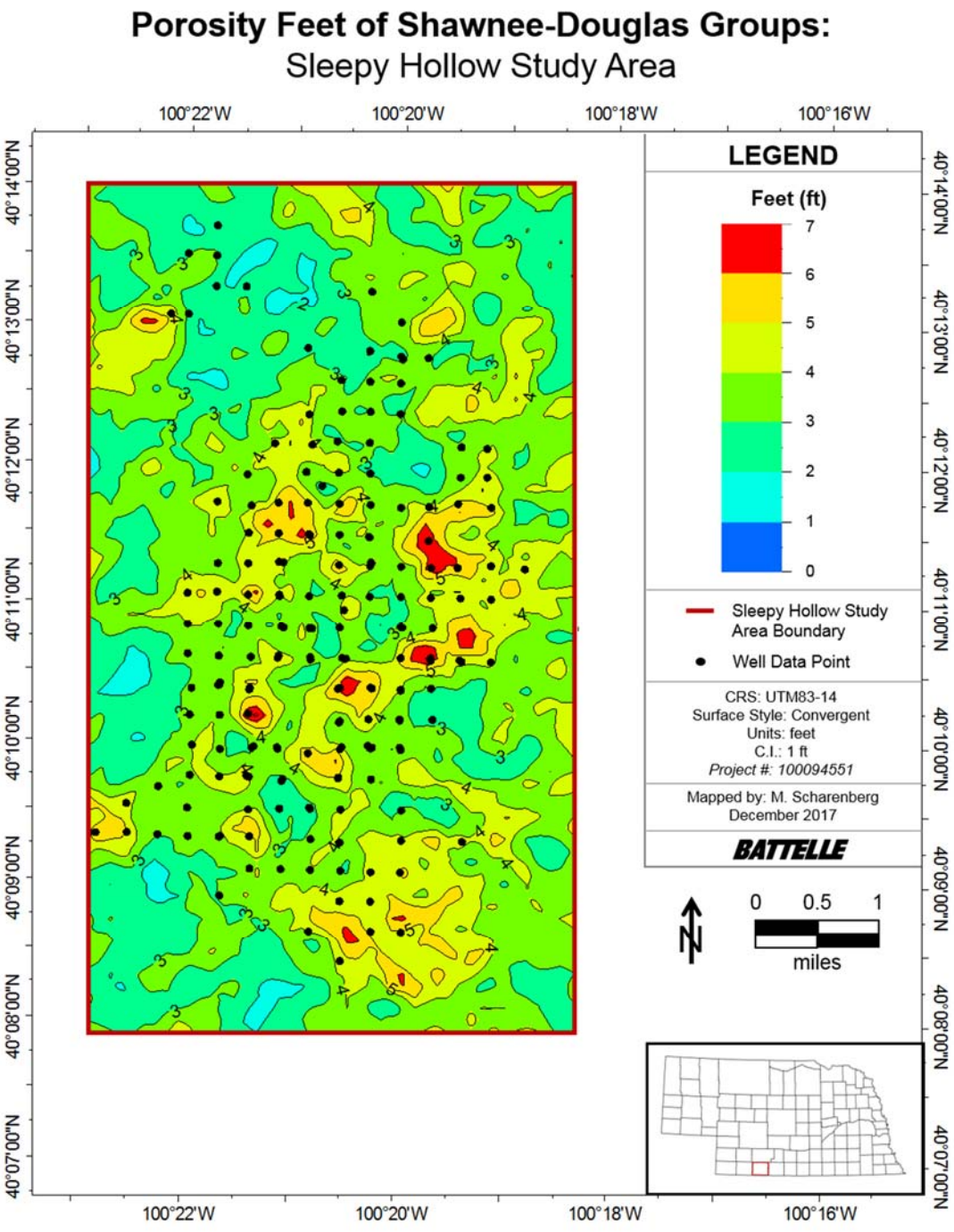

Figure 3-46. Porosity footage map of the Shawnee-Douglas groups in the Sleepy Hollow study area.

The same overall geographic trends are visible in the porosity footage map of Lansing-Kansas City groups in the Sleepy Hollow study area as are seen in the Wabaunsee and Shawnee-Douglas groups (Figure 3-47). The northern end of the high porosity-footage trend that exists left of center which runs north-south is more distinct in Lansing-Kansas City groups.

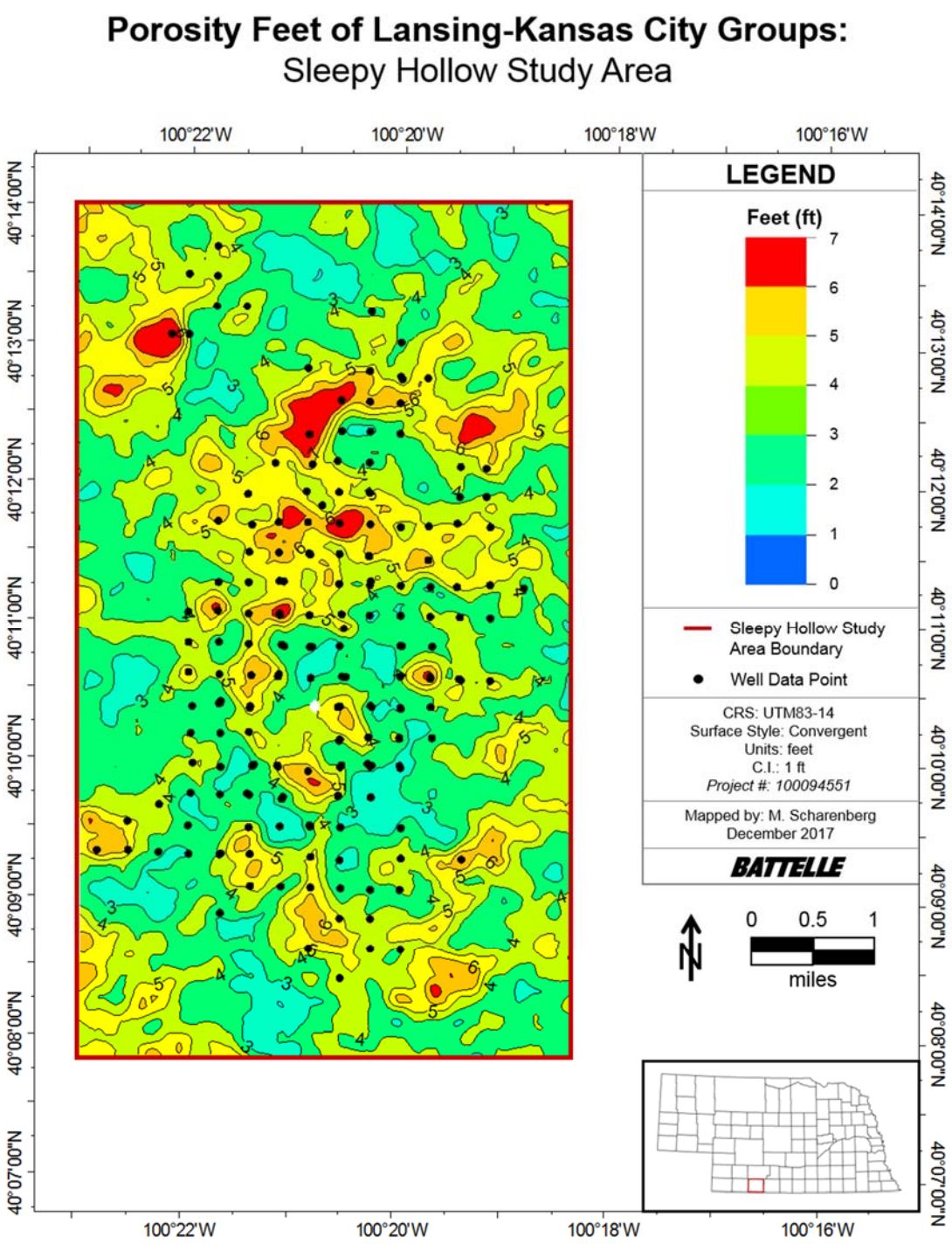

Figure 3-47. Porosity footage map of the Lansing-Kansas City groups in the Sleepy Hollow study area.

The Pleasanton-Marmaton groups display high porosity footage left of center in a mostly northern north-south trend which is similar to the trend observed in the other three storage zones (Figure 3-48). The localized high in the southeast corner of the study area also exists in the Pleasanton-Marmaton groups porosity footage map.

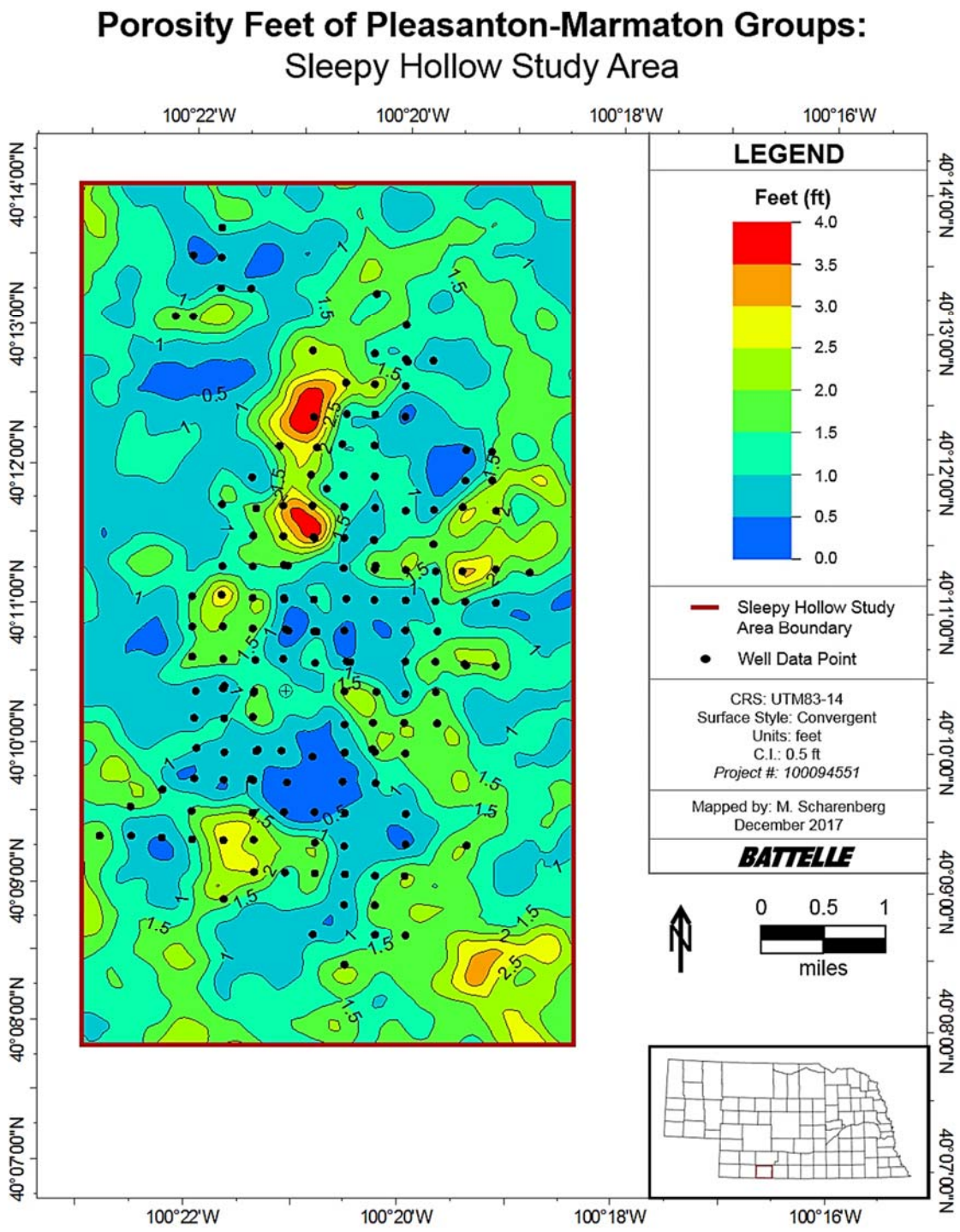

Figure 3-48. Porosity footage map of the Pleasanton-Marmaton groups in the Sleepy Hollow study area.

The spatial trends observed in the four saline storage zones are preserved when the zones are combined into a stacked saline storage porosity-feet map (Figure 3-49). Localized high porosity-feet values in the northwest corner of the Sleepy Hollow study area are emphasized in the combined saline storage zones porosity footage map.

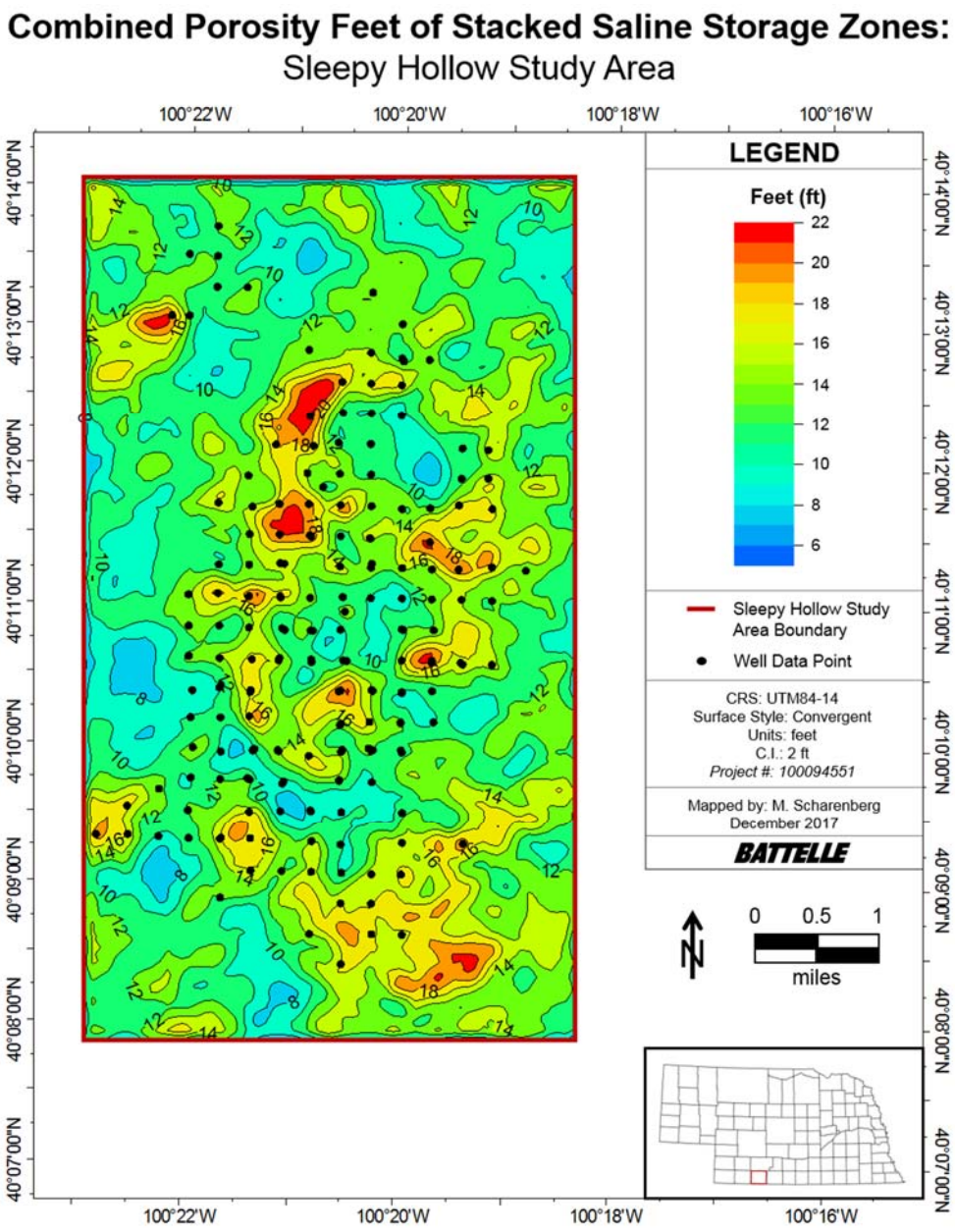

Figure 3-49. Porosity footage map of the four saline storage zones in the Sleepy Hollow study area.

Huffstutter Study Area

Caprocks

In the Huffstutter study area, gamma ray logs penetrating the entire Pennsylvanian-Permian caprock complex were available from 52 to 60 wells, depending on the unit, to quantify and map caprock structure and thickness (Table 3-28). Average depths, gross thicknesses, and associated standard deviations measured for caprock units in the Huffstutter study area are shown in Table 3-28. The depths of all four caprock units appear to generally increase from the southeast to the northwest portion of the study area (Figure 3-50a, Figure 3-51a, Figure 3-52a, and Figure 3-53a). The shale interval at the base of the Nippewalla Group occurs at an average depth of 1,446 ft and has an average gross thickness of 291 ft, with the greatest thicknesses occurring in the north east and southeast corners of the study area

(Figure 3-50b). The underlying Sumner Group has an average depth and gross thickness of 1,741 ft, and 237 ft, respectively. The highest gross thicknesses of the Sumner Group are observed in wells located along the northern and east-central portions of the study area (Figure 3-51b). The Council Grove Group is present at an average depth of 2,156 ft, and similar to the Sleepy Hollow study area, is the thickest of the four main caprock units evaluated in the Huffstutter study area. It has an average gross thickness of 391 ft. A local high is observed in gross thicknesses greater than 380 ft for the Council Grove in the northeast (Figure 3-52b). The Upper Pennsylvanian Admire Group occurs at an average depth of 2,544 ft, and has an average gross thickness of 184 ft. Gross thicknesses of the Admire are highest in localized areas in the northeast and south-central portions of the Huffstutter study area (Figure 3-53b). Variation in caprock depth is represented by standard deviations that range from 58 ft to 75 ft (Table 3-28). Standard deviations in gross thickness range from 3 ft to 37 ft. Caprock depths and gross thicknesses are poorly constrained in the central and southeast where well density is low in the study area.

Table 3-28. Mean and standard deviation (σ) of caprock depth and gross thickness along with the associated well count (n) for the Huffstutter study area.

Group	Depth (ft md*)			Gross Thickness (ft)		
	Mean	σ	*n*	Mean	*σ*	*n*
Lower Nippewalla	1,446	60	52	291	7	52
Sumner	1,741	58	58	237	37	56
Council Grove	2,156	75	59	391	16	59
Admire	2,544	70	60	184	3	59

*Values reported in measured depth (md) for the purposes of CO_2 storage assessment; refer to caprock structure maps for depths relative to mean sea level.

Structural cross-sections were constructed for the Huffstutter study area to facilitate site-scale characterization of the vertical and lateral continuity of caprocks, and evaluate the potential impact of faults/fold on caprock configuration. The A-A' cross-section shown in Figure 3-54 was generated to examine the interval extending from the lower Nippewalla to the Wabaunsee Group along a south-to-north transect in the Huffstutter study area. Consistent with trends observed on structure maps, caprock depths appear to increase by approximately 25 ft from the south to the north. This trend can be observed in all lithostratigraphic units, and coincides with pinching out of the evaporite unit at the top of the Sumner Group, an increase in the gross thickness of the overall Sumner Group, and a decrease in thickness of the Chase Group. The gross thickness of the Council Grove and Admire groups appear to be relatively consistent across the transect. Changes in caprock depth and gross thickness are most pronounced near the northeast corner of the Huffstutter study area, between well 1514720405 and well 1514720207.

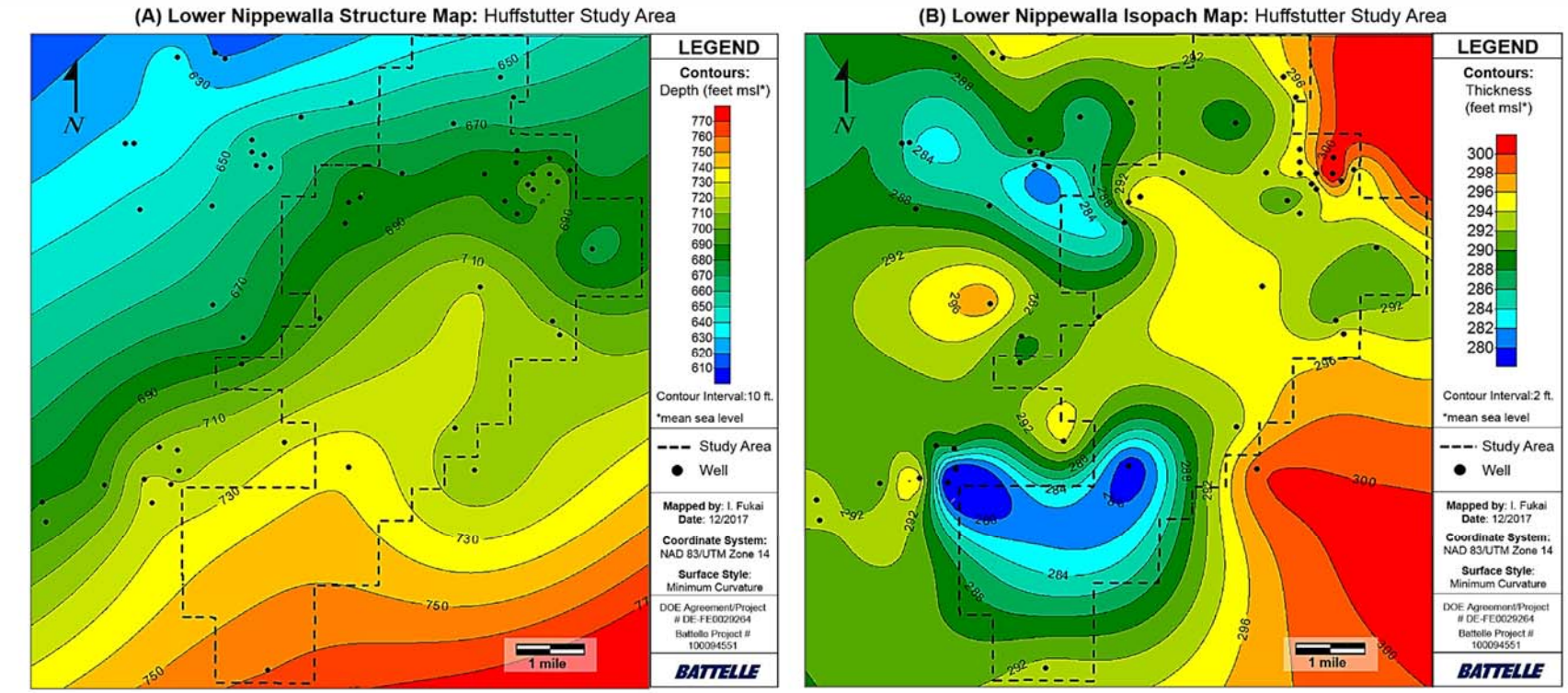

Figure 3-50. (A) Structure and (B) isopach map for the lower Nippewalla Group in the Huffstutter study area.

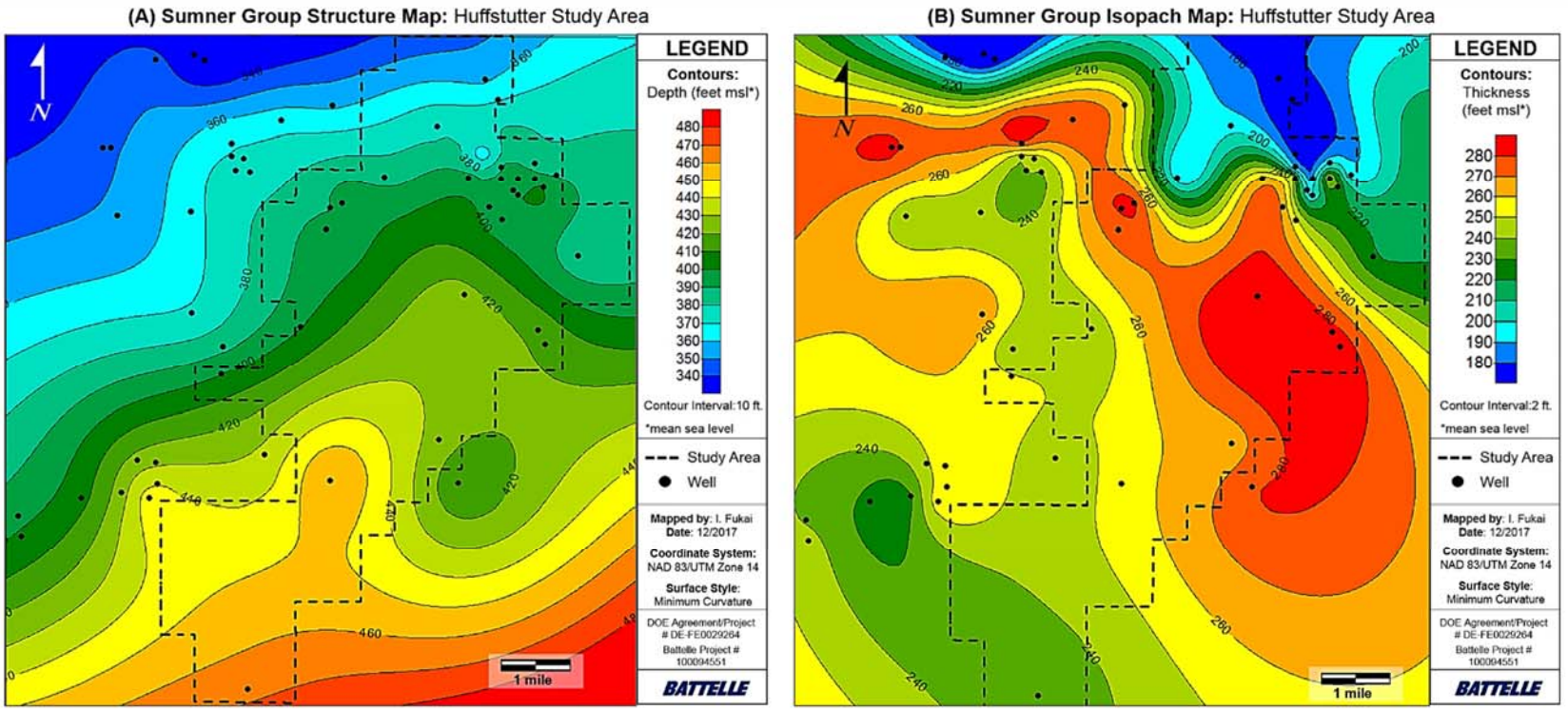

Figure 3-51. (A) Structure and (B) isopach map for the Sumner Group in the Huffstutter study area.

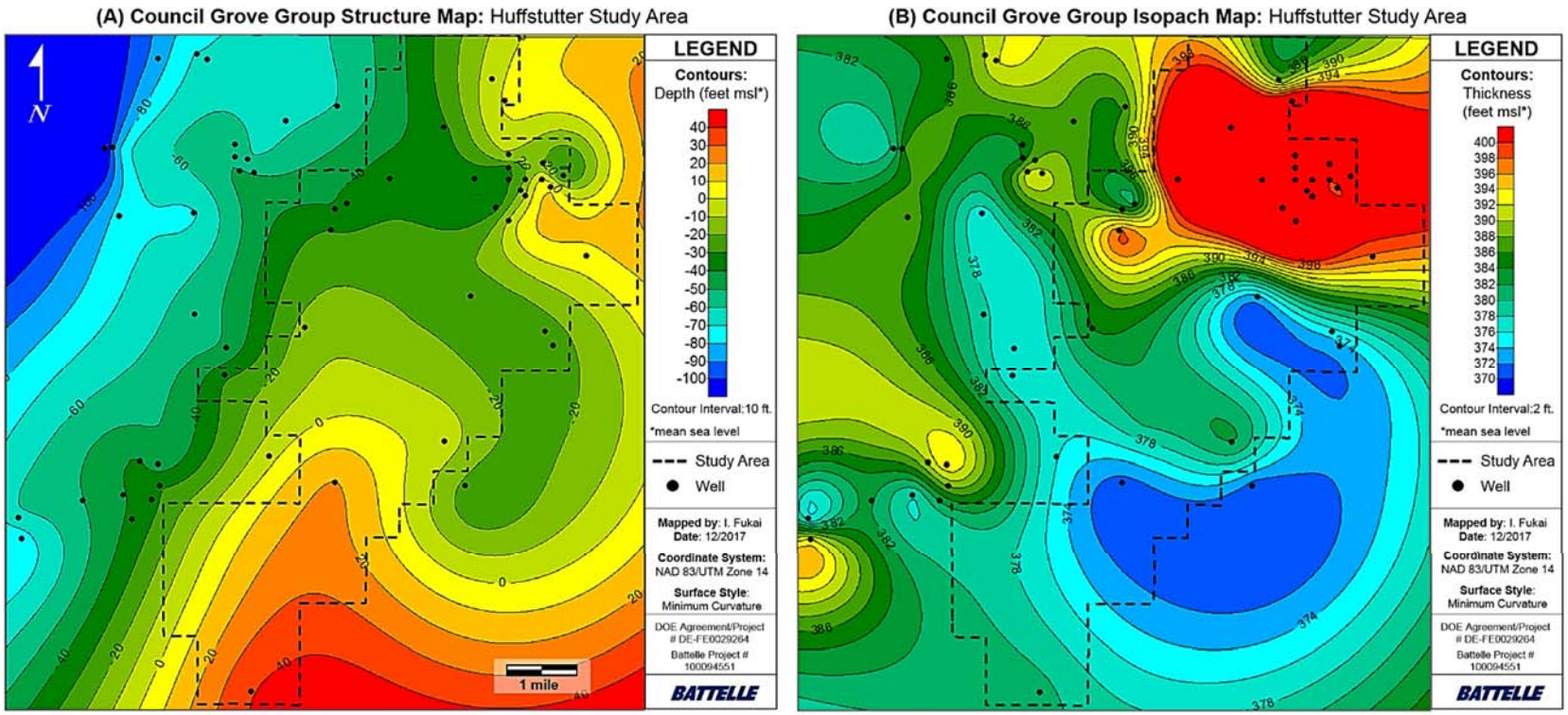

Figure 3-52. (A) Structure and (B) isopach map for the Council Grove Group in the Huffstutter study area.

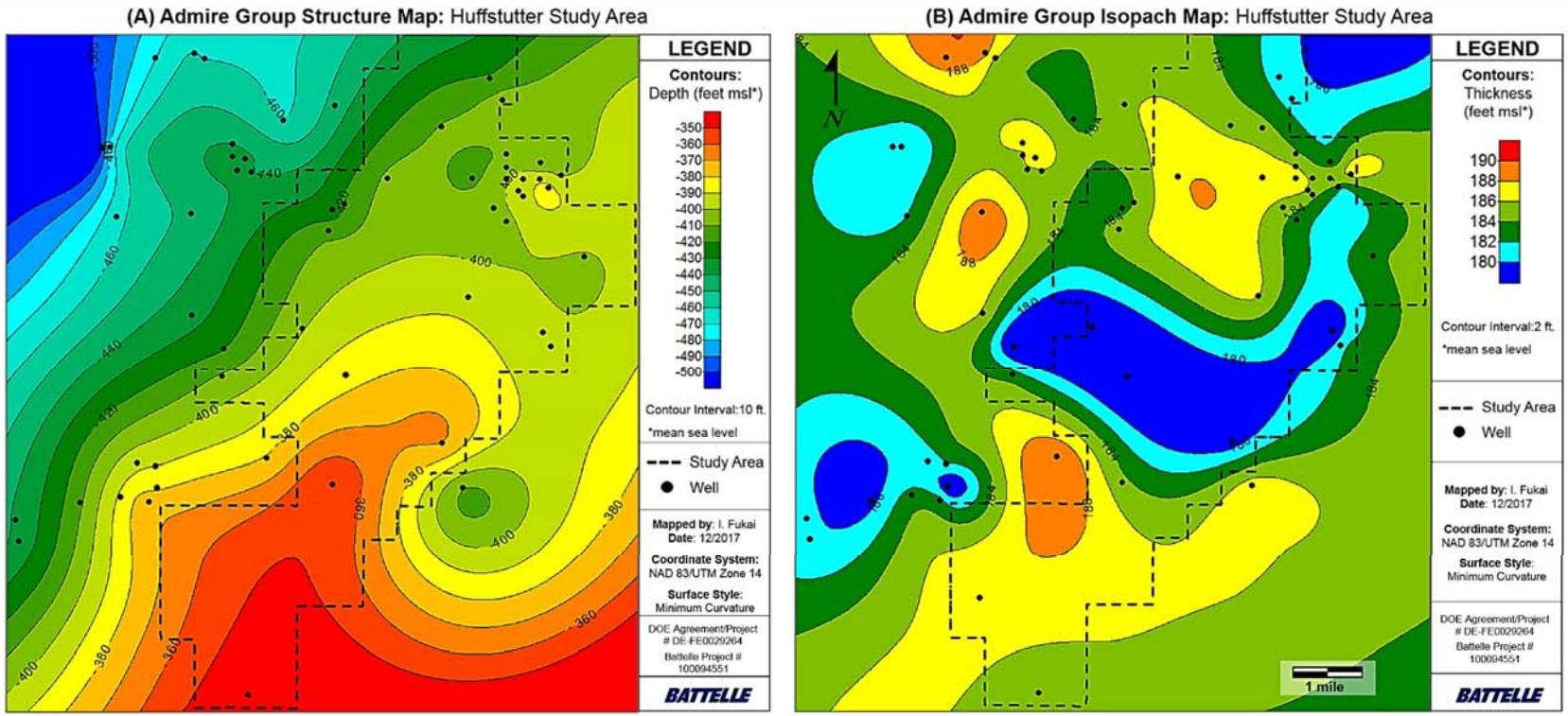

Figure 3-53. (A) Structure and (B) isopach map for the Admire Group in the Huffstutter study area.

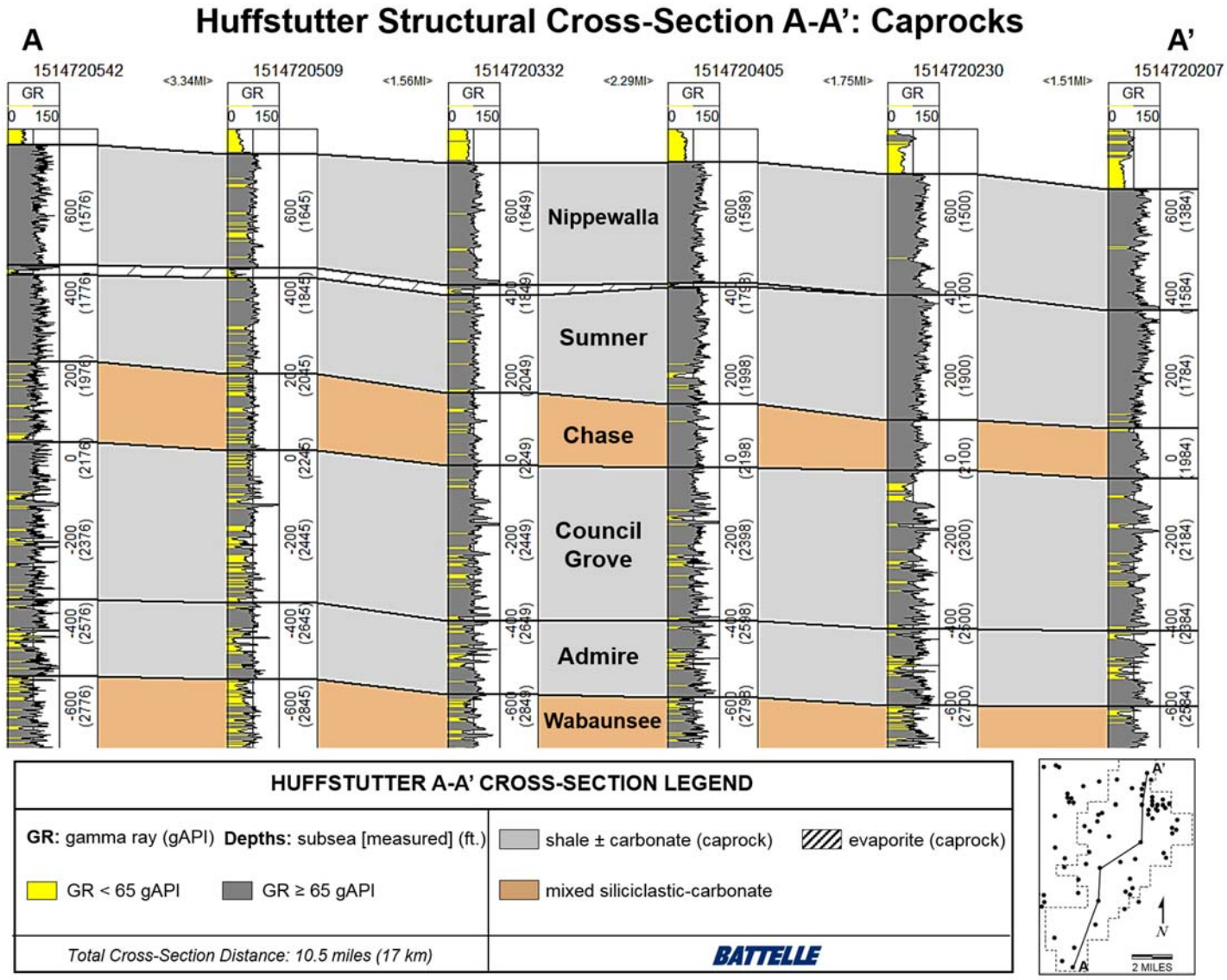

Figure 3-54. Structural cross-section showing lateral extent and thickness of the primary caprock units along a general west-to-east transect in the Huffstutter study area.

Deep Saline Formations

The Huffstutter structural maps show a structural high near the southwest portion of the field that is likely related to the Cambridge Arch (Figure 3-55a to Figure 3-58a). The northwestern limb of the anticline has better well control for delineating structural dip, and structural contours in this location are likely more accurate than those found on the southeast limb.

The isopach maps show a difference of 15ft +/- 5ft in the thickness of four lithostratigraphic groups in the Huffstutter study area (Figure 3-55b to Figure 3-58b). Thickness differences observed in the Pleasanton – Marmaton groups (Figure 3-58b) are much more significant, which is likely due to limited well penetration to the base of the group.

Structural cross-sections were constructed for the interval extending from the Wabaunsee Group to the base of the Pleasanton-Marmaton groups to examine the vertical and lateral continuity of deep saline

formations, and evaluate the potential impact of faults/fold on potential storage intervals in the Huffstutter study area. The B-B' cross-section shown in Figure 3-59 was generated to facilitate site-scale characterization of deep saline formations along a general west-to-east transect in the study area. Depth variations of approximately ± 100 ft are observed in all Pennsylvanian units evaluated, and occur primarily as a decrease in depth from the west to the east. This change in depth is most pronounced between well 1514720653 and well 1514720613. Gross thicknesses appear to be relatively constant across the transect. Laterally continuous net thickness intervals are observed in the upper and lower Wabaunsee, the middle of the Shawnee-Douglas, and the middle of the Pleasanton-Marmaton groups.

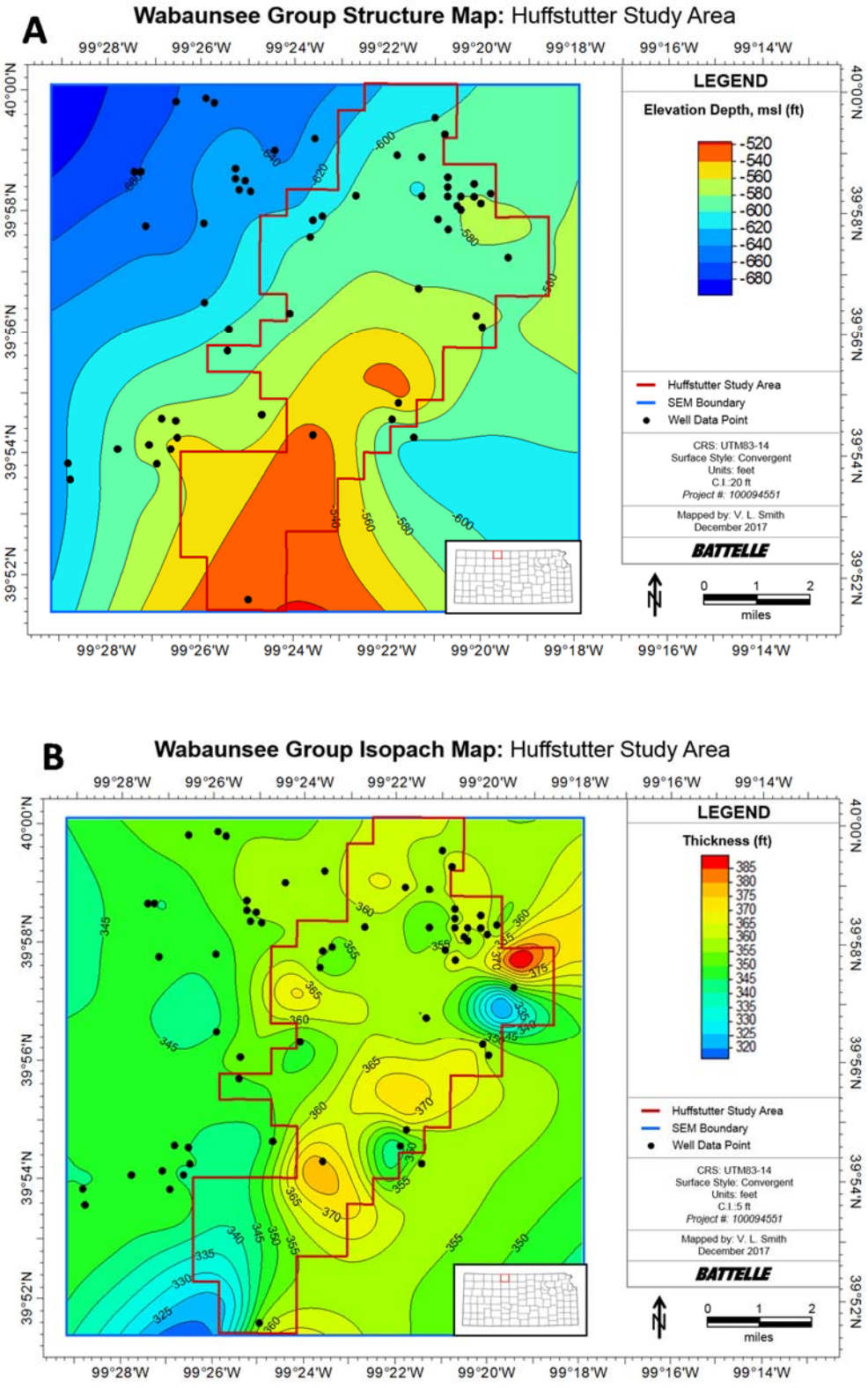

Figure 3-55. (A) Structure and (B) isopach map of the Wabaunsee Group in the Huffstutter study area.

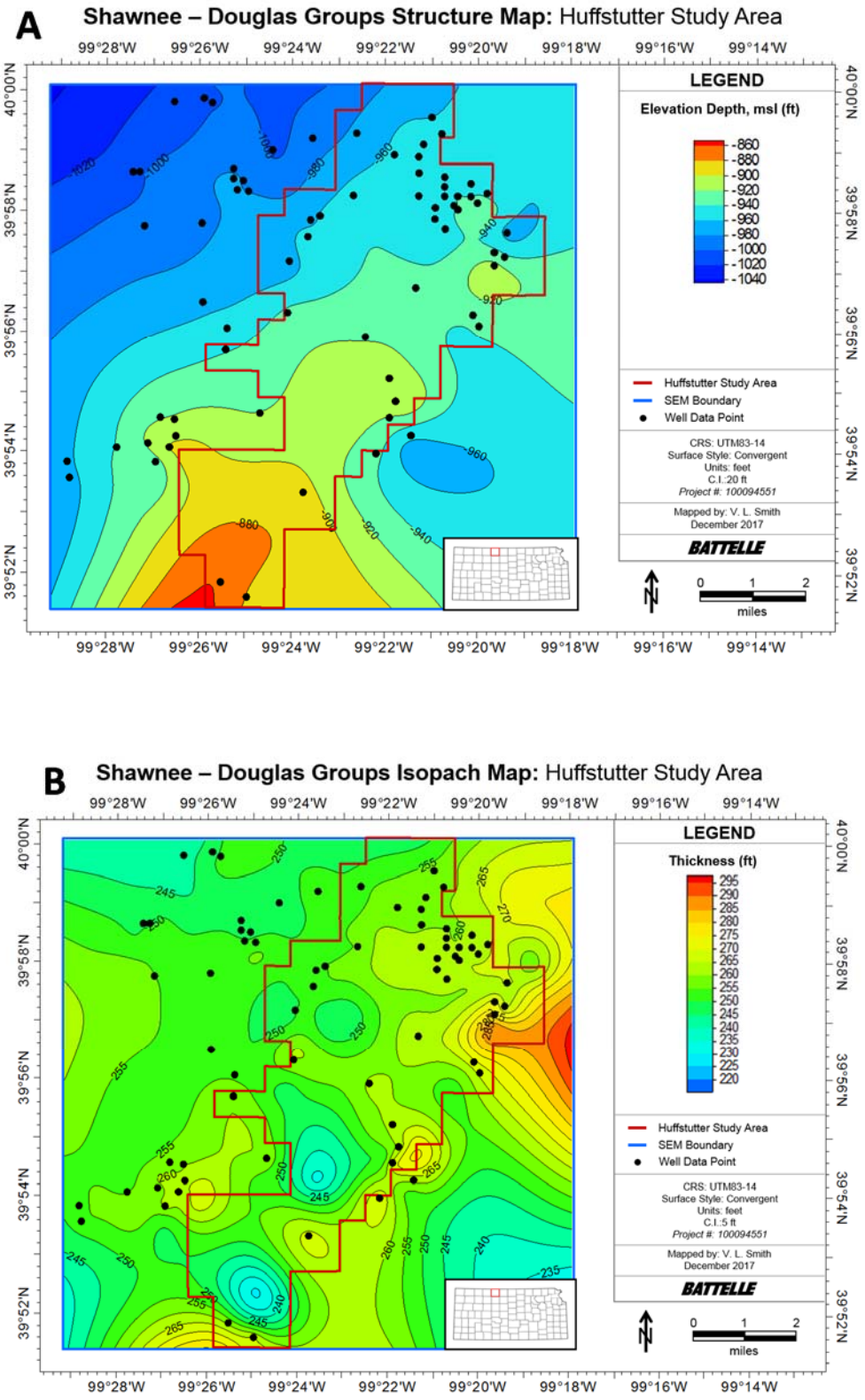

Figure 3-56. (A) Structure and (B) isopach map of the Shawnee-Douglas groups in the Huffstutter study area.

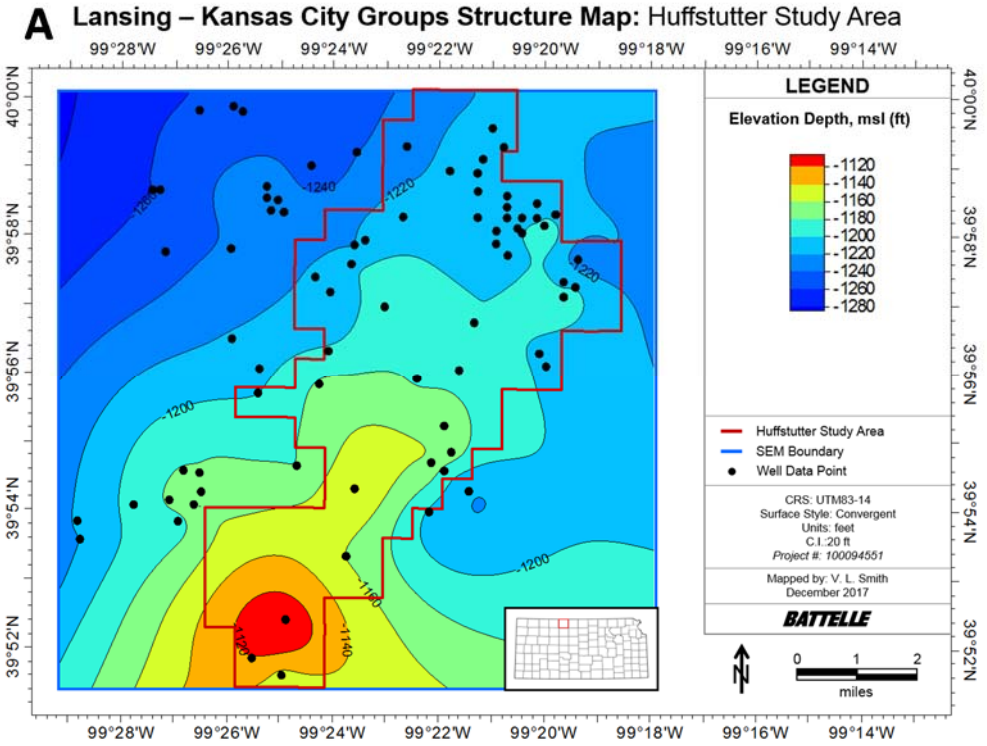

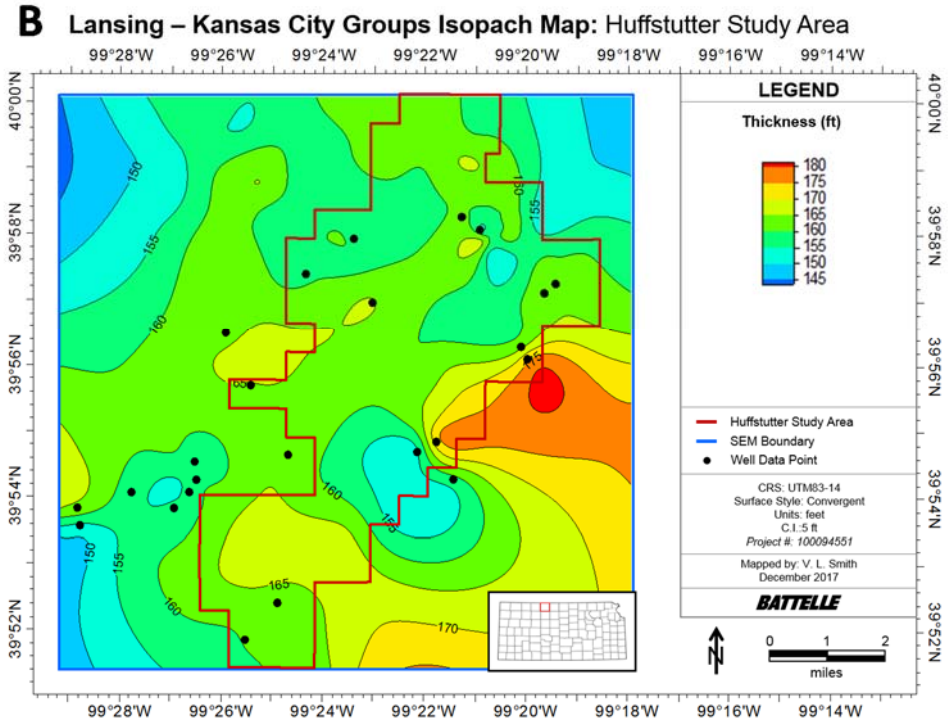

Figure 3-57. (A) Structure and (B) isopach map of the Lansing-Kansas City groups in the Huffstutter study area.

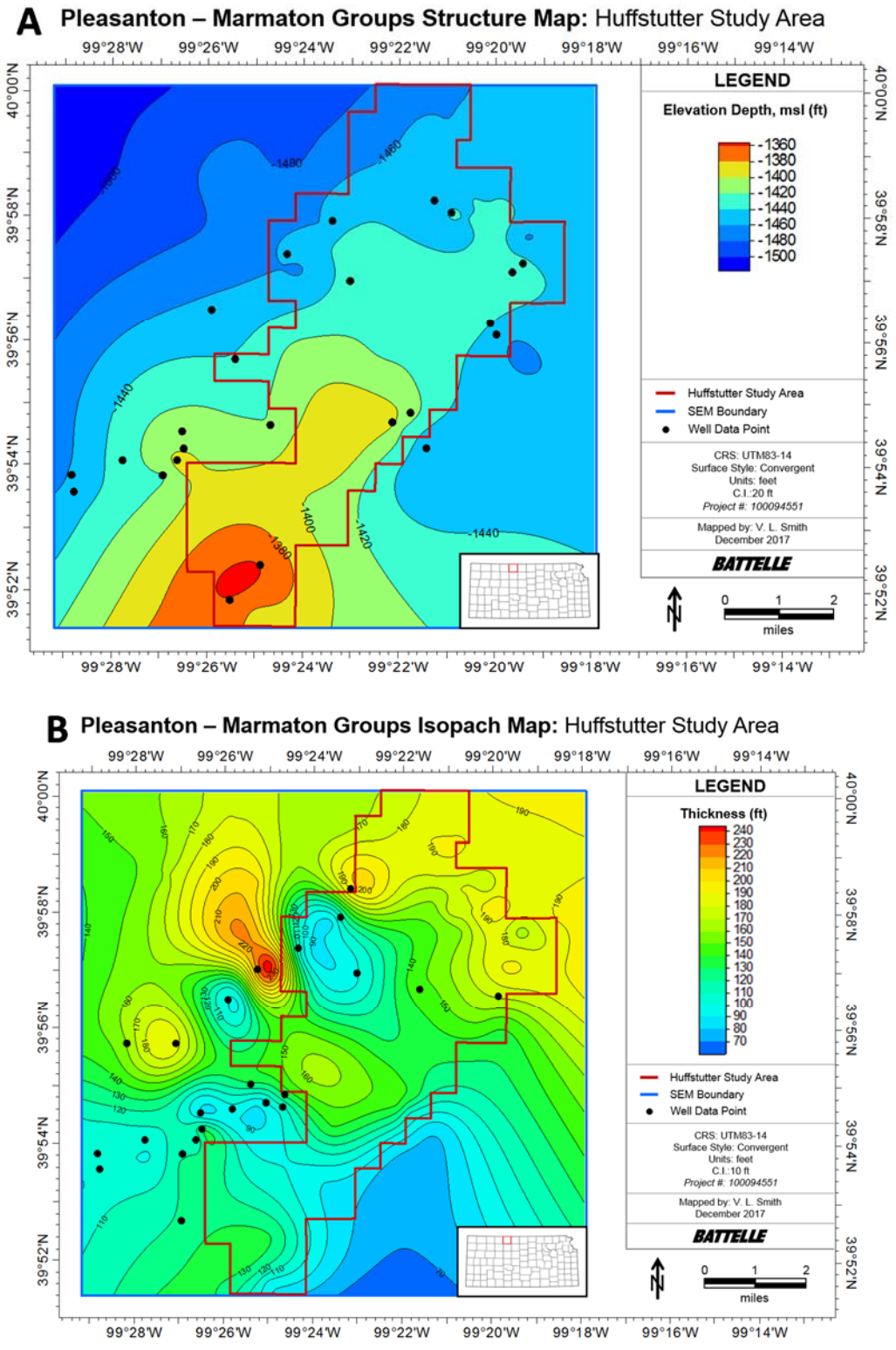

Figure 3-58. (A) Structure and (B) isopach map of the Pleasanton-Marmaton groups in the Huffstutter study area.

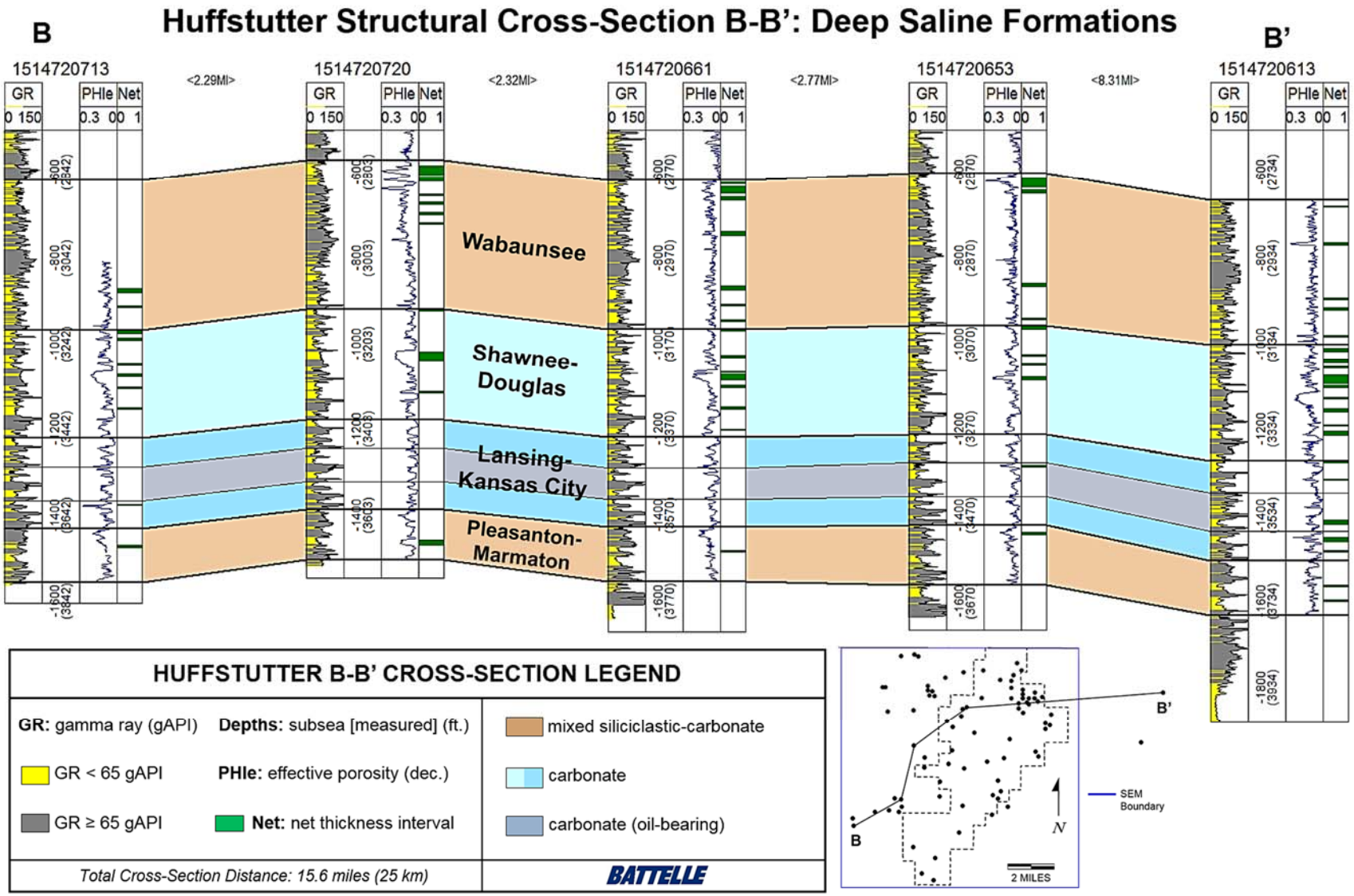

Figure 3-59. Structural cross-section showing lateral extent, gross thickness, and net reservoir intervals of the deep saline formations and oil-bearing zones along a west-to-east transect in the Huffstutter study area.

The heterogenous grid data of the SEM was used to quantify and map total and net reservoir properties of the deep saline formations of interest in the Huffstutter study area (refer to Table 3-6 in Section 3.1.2 for an explanation of "total reservoir" and "net reservoir" distinctions). Gross reservoir thickness, total reservoir porosity and permeability, and total reservoir pore volume is listed in Table 3-29 along with average net-to-total reservoir pore volume ratios calculated for the lithostratigraphic units of interest in the Huffstutter study area.

Table 3-29. Average total reservoir thickness, total reservoir porosity and permeability, and total reservoir pore volume for the Huffstutter study area.

Group(s)	Total Reservoir Thickness (ft)		Total Reservoir Porosity (%)		Total Reservoir Permeability (mD)		Total Reservoir Pore Volume (million ft^3)
	Mean	σ	Mean	σ	Mean	[illegible]	
Wabaunsee	179	22	6	1.3	16.6	22.3	29,960
Shawnee-Douglas	134	18	7	1.5	4.0	3.4	20,563
Lansing-Kansas City	81	14	4	1.0	0.8	1.0	10,212
Pleasanton-Marmaton	69	21	5	1.1	0.5	0.8	9,619

The porosity footage of the Wabaunsee in the Huffstutter study area exceeds 24 feet in the northeast corner of the Huffstutter field (Figure 3-60). In the north-central region, a trend of increased porosity footage is observed which extends to the southwest.

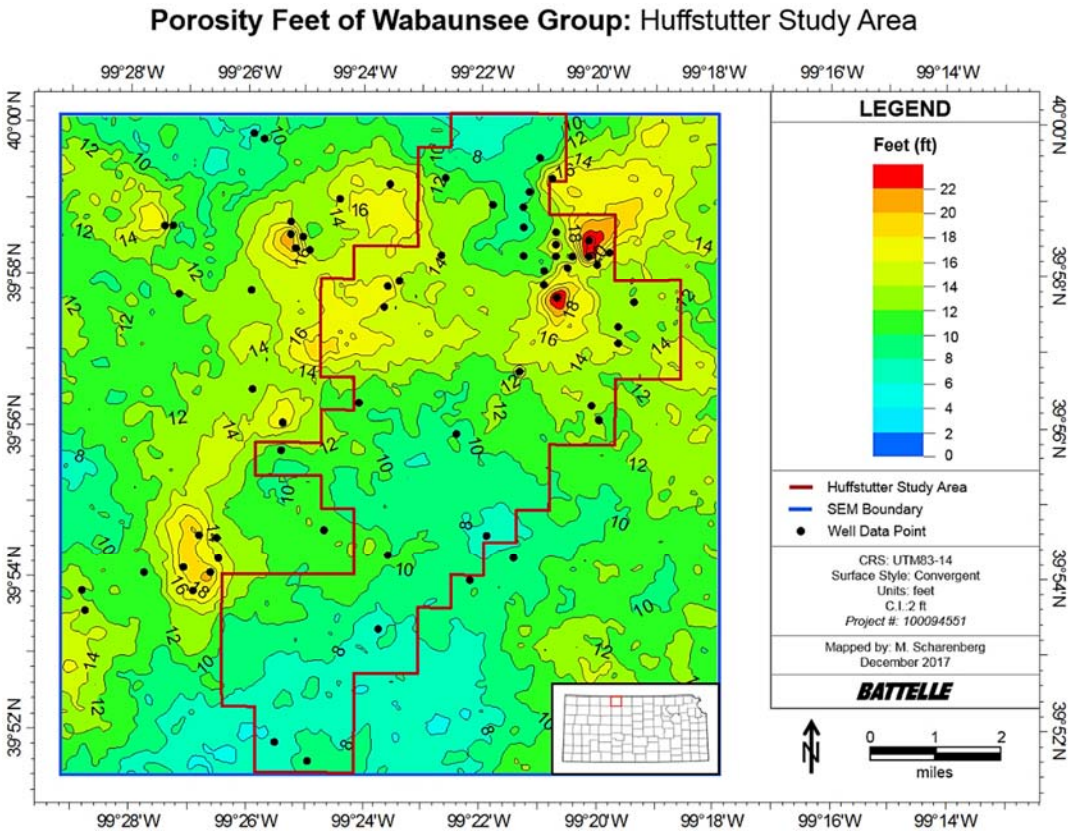

Figure 3-60. Porosity footage map of the Wabaunsee Group in the Huffstutter study area.

The Shawnee-Douglas groups exhibit a local high in porosity footage in the northeast corner of the Huffstutter field similar to that which is observed in the Wabaunsee Group (Figure 3-61). In the Shawnee-Douglas groups, this local high extends southward create a large, high porosity footage zone on the eastern third of the study area with porosity footage values exceeding 13 ft. The trend of increased porosity footage observed on the western side of the study area trending north-northeast to southwest is also observed in the Shawnee-Douglas groups. Additionally, a northwest-southeast trend of increased porosity footage that runs south of center is observed in the Shawnee-Douglas groups.

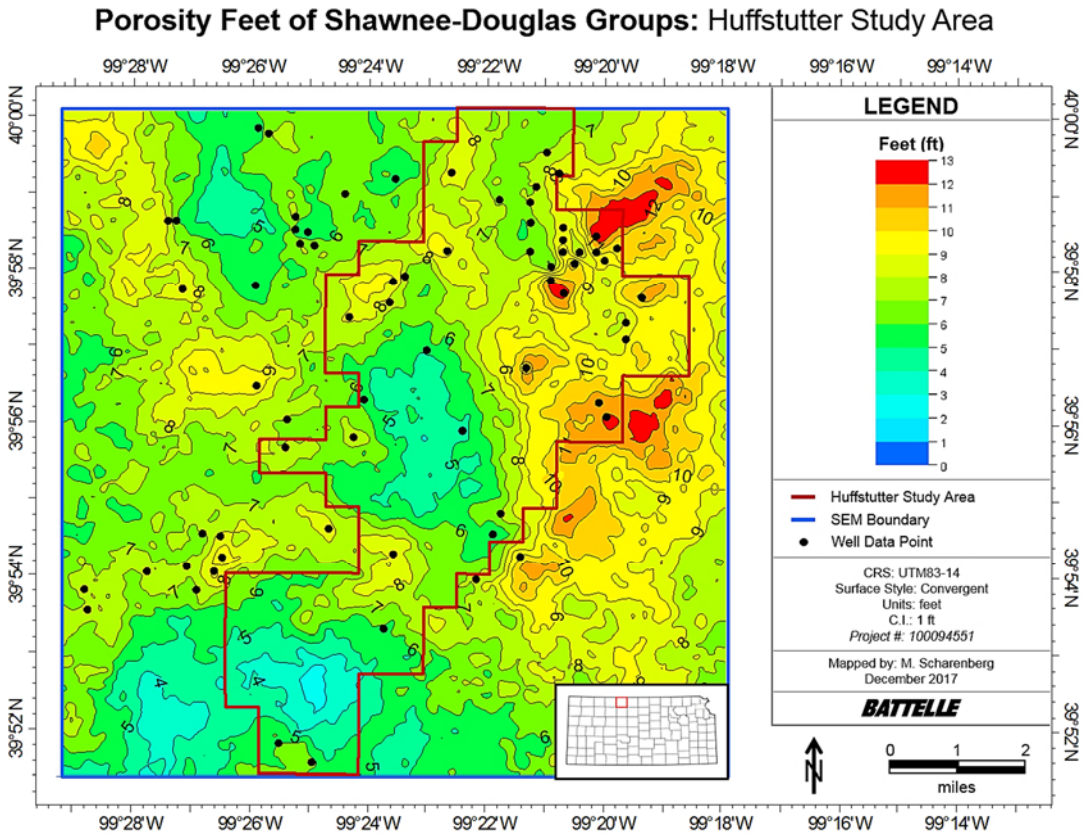

Figure 3-61. Porosity footage map of the Shawnee-Douglas groups in the Huffstutter study area.

The porosity footage map of the Lansing-Kansas City groups demonstrates a trend of increased porosity footage north of center which is interpolated as extending to the southeast (Figure 3-62). The northwest-southeast trend of increased porosity footage that runs south of center is also observed in the Lansing-Kansas City groups.

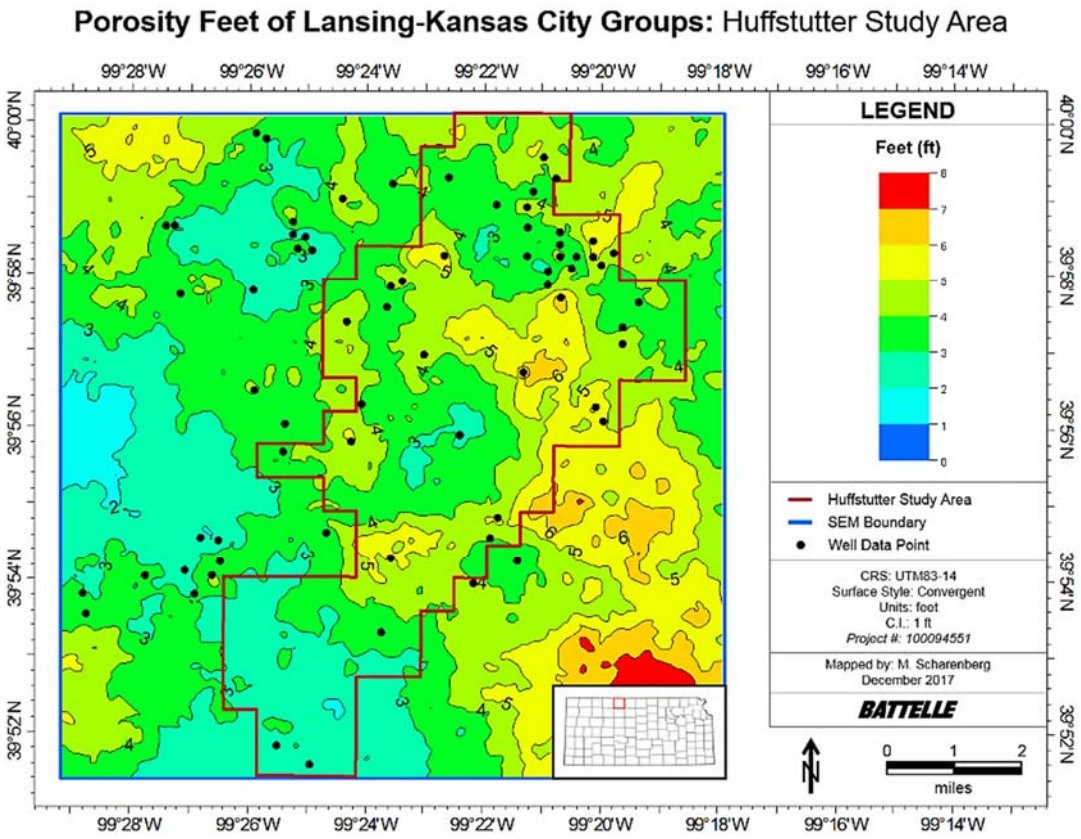

Figure 3-62. Porosity footage map of the Lansing-Kansas City groups in the Huffstutter study area.

The Pleasanton-Marmaton groups exhibit high porosity footage in the center of the Huffstutter study area (Figure 3-63). This localized high extends to the northwest and the northeast. This storage zone is not as well-constrained by borehole data points as the overlying storage zones, therefore a larger amount of interpolation and extrapolation occurred when characterizing this zone. This may explain why the trends in the porosity-footage map for the Pleasanton-Marmaton do not correlate as well with the other storage zones in the Huffstutter field.

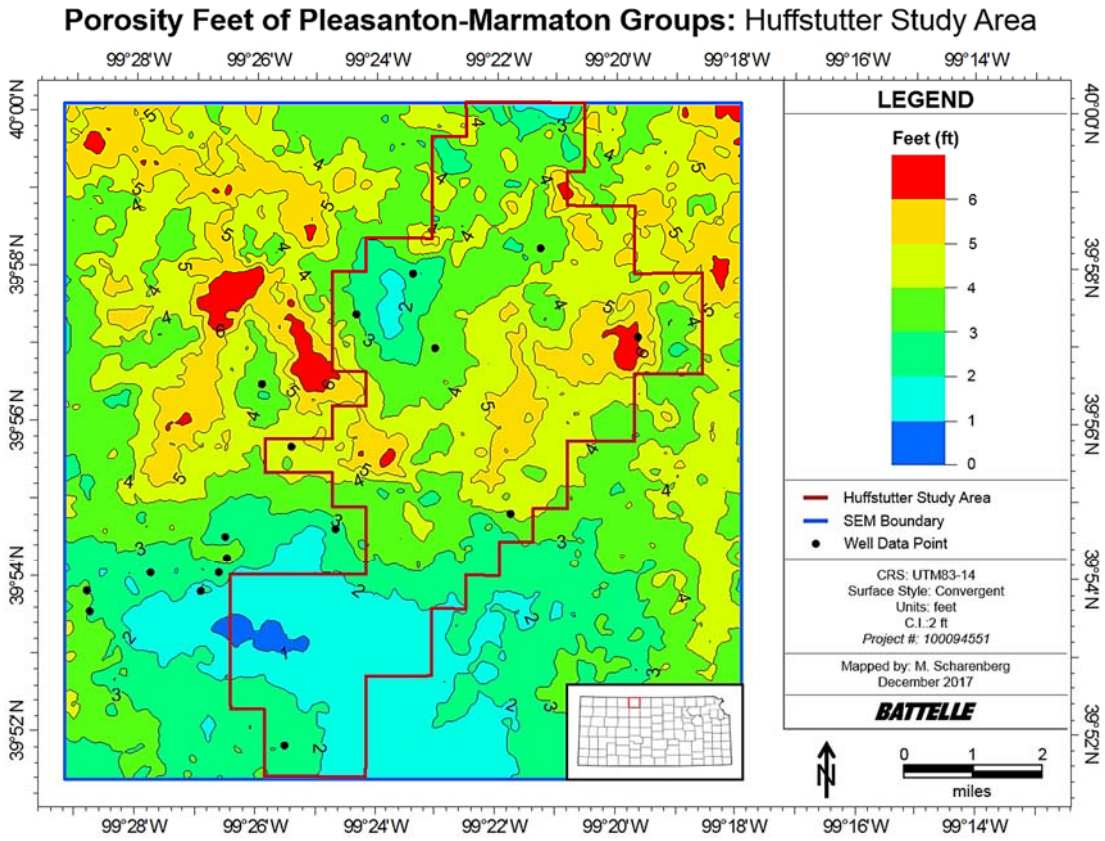

Figure 3-63. Porosity footage map of the Pleasanton-Marmaton groups in the Huffstutter study area.

The spatial trends observed in the four saline storage zones are represented in the map of combined porosity-feet for the saline storage zones in the Huffstutter (Figure 3-64). Porosity footage values nearly reach 50 ft in the northeast corner of the field. The northwest-southeast trend of increased porosity footage that runs south of center is observed in the stacked saline porosity footage map. Values of porosity-feet exceeding 32 ft are observed within the north-northeast to southwest trend along the western side of the study area.

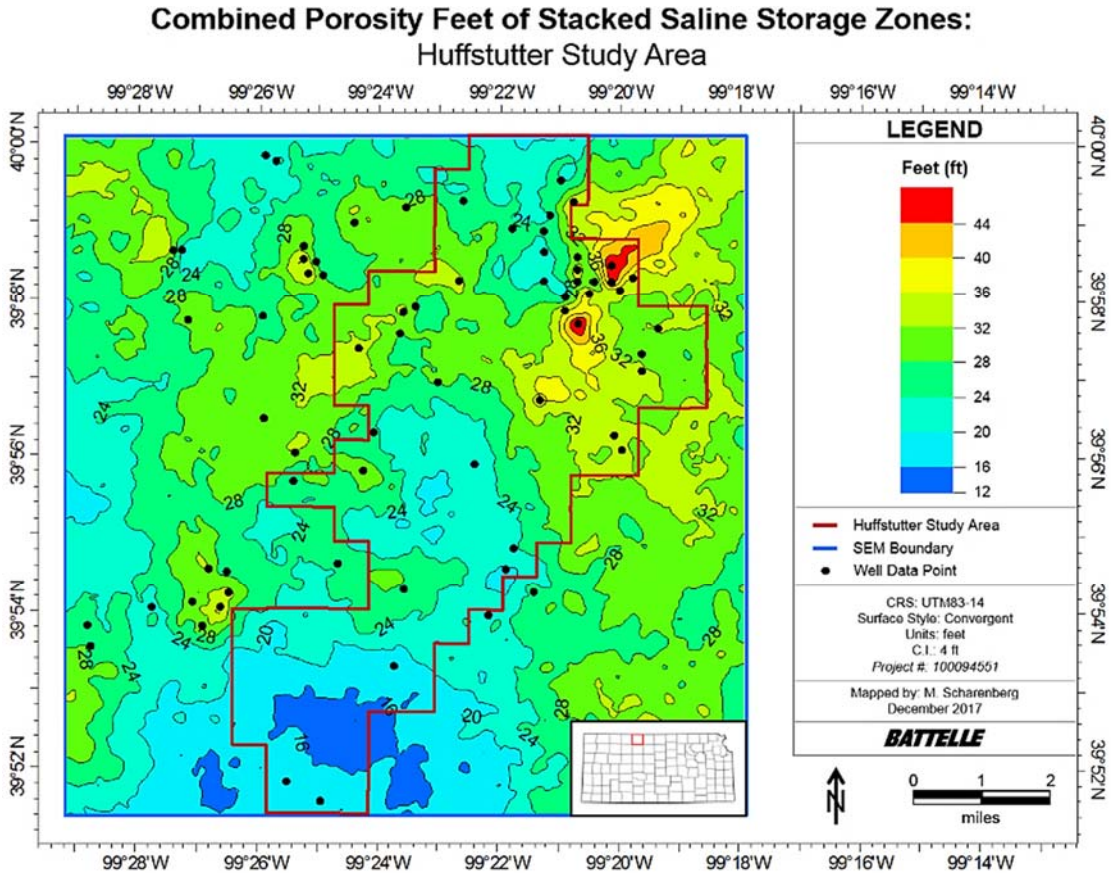

Figure 3-64. Combined porosity footage map of the stacked saline storage zones in the Huffstutter study area.

3.6.4 Prospective Storage Resource Estimates

Sleepy Hollow Study Area

Areal extent, thickness, and average porosity calculated for the total and net reservoir volumes were used to derive site-specific p-values for the net-to-total reservoir pore volume ($E_{PVn/PVt}$) for storage efficiency and prospective storage resource calculations in the Sleepy Hollow study area. The P_{10} and P_{90} values calculated for the lithostratigraphic units of interest for deep saline CO_2 storage are shown in Table 3-30, along with the CO_2-SCREEN default values used as input for the volumetric displacement (E_V) and microscopic displacement (E_d) efficiency parameters.

Using the P_{10} and P_{90} values in Table 3-30 as input for storage efficiency parameters (e.g., Equation 3-10, 3-11) the prospective storage resource was calculated in CO_2-SCREEN for each of the deep saline intervals of interest in the Sleepy Hollow study area. The Wabaunsee has the highest median (P_{50}) prospective G_{CO2} value of the six storage zones at 27.7 Mt followed by the LKC D-F Zone at 25.9 Mt, the Deer Creek-Oread at 11.7 Mt, the Topeka at 11.0 Mt, the Marmaton at 10.7 Mt, and the LKC A Zone at 7.0 Mt (Table 3-31). The P_{10} prospective storage resource for the geologic complex comprised of the six storage zones of stacked saline formations in the Sleepy Hollow study area is 49.7 Mt. The P_{50} prospective storage resource of the stacked saline formations is 94.0 Mt and the P_{90} is 159.6 Mt.

The storage efficiency factors (E_{saline}) for each storage zone reduce the fraction of the total pore volume that is technically accessible for CO_2 storage. The average P_{50} E_{saline} of the storage zones range from 4.2% to 6.7% with a mean of 5.8%. The storage zones in descending order of P_{50} storage efficiency are LKC D-F Zone (6.7%), Marmaton (6.2%), Topeka (6.1%), Wabaunsee (5.8%), Deer Creek-Oread (5.7%), and the LKC A Zone (4.2%).

While the Wabaunsee Group has the third highest storage efficiency, it has the highest CO_2 storage resource estimate as a result of its relatively high average porosity (6%) and high total reservoir thickness (68 ft). The LKC D-F Zone has the second highest G_{CO2} due to the combined effects of its high storage efficiency (P_{50} of 6.7%), total reservoir thickness (62 ft), and porosity of 5%.

Table 3-30. Site-specific EPVn/PVt values calculated from well data in the Sleepy Hollow study area and default EV and Ed values used in CO_2-SCREEN calculations.

Group(s)	Formations / zones	$E_{PVn/PVt}$		E_V		E_d	
		P_{10}	P_{90}	P_{10}	P_{90}	P_{10}	P_{90}
Wabaunsee	*	0.63	0.90	0.16	0.39	0.35	0.76
Shawnee-Douglas	Topeka	0.32	0.77	0.44	0.72	0.31	0.42
	Deer Creek, Oread	0.28	0.75	0.44	0.72	0.31	0.42
Lansing-Kansas City	A	0.14	0.70	0.44	0.72	0.31	0.42
	D-F	0.43	0.76	0.44	0.72	0.31	0.42
Pleasanton-Marmaton	*	0.64	0.97	0.16	0.39	0.35	0.76

*Values reported for all formations in the group

Table 3-31. Prospective storage resource and storage efficiency estimates for the deep saline formations of interest in the Sleepy Hollow study area.

Group(s)	Formation / Zone	Avg. E_{saline} Results (%)			Prospective Storage Resource (Mt)		
		P_{10}	P_{50}	P_{90}	P_{10}	P_{50}	P_{90}
Wabaunsee	*	2.9	5.8	10.2	14.0	27.7	48.9
Shawnee-Douglas	Topeka	3.3	6.1	9.5	5.9	11.0	17.2
	Deer Creek-Oread	2.9	5.7	9.1	5.7	11.7	23.3
Lansing-Kansas City	A zone	1.5	4.2	8.2	2.5	7.0	13.9
	D-F zones	4.2	6.7	9.6	16.4	25.9	37.4
Pleasanton-Marmaton	*	3.0	6.2	11.1	5.2	10.7	19.0
Total					**49.7**	**94.0**	**159.6**

*Values reported for all formations in the group

Huffstutter Study Area

Using the total reservoir properties quantified for each of the deep saline intervals of interest in the Huffstutter study area, and the storage efficiency p-values reported in Table 3-32, the prospective storage resource was calculated in CO_2-SCREEN for four main lithostratigraphic groups in the study area.

The four lithostratigraphic units represent potential deep saline storage zones in the Huffstutter, and include: (1) the Wabaunsee Group, (2) the Shawnee and the Douglas groups, (3) the Lansing-Kansas City groups, and (4) the Pleasanton and the Marmaton groups. The Wabaunsee has the highest median (P_{50}) prospective G_{CO2} value of the four storage zones at 68.7 Mt followed by the Shawnee-Douglas groups at 48.9 Mt, the Lansing-Kansas City groups at 24.1 Mt, and the Pleasanton-Marmaton groups at 20.4 Mt (Table 3-33). The P_{10} prospective storage resource for the geologic complex comprised of the six storage zones of stacked saline formations in the Sleepy Hollow study area is 80.8 Mt. The P_{50} prospective storage resource of the stacked saline formations is 159.2 Mt and the P_{90} is 269.7 Mt.

The storage efficiency factors (E_{saline}) for each storage zone reduce the fraction of the total pore volume that is technically accessible for CO_2 storage. The average P_{50} E_{saline} of the storage zones in the Huffstutter study area range from 5.2% to 5.9% with a mean of 5.6%. The storage zones in descending order of P_{50} storage efficiency are Shawnee-Douglas groups (5.9%), Wabaunsee (5.8%), Pleasanton-Marmaton groups (5.3%), and the Lansing-Kansas City groups (5.2%) (Table 3-33).

Table 3-32. EPVn/PVt values calculated from well data in the Sleepy Hollow study area and default EV and Ed values used in CO_2-SCREEN calculations for the Huffstutter Study area.

Group	$E_{PVn/PVt}$		E_v		E_d	
	P_{10}	P_{90}	P_{10}	P_{90}	P_{10}	P_{90}
Wabaunsee	0.63	0.90	0.16	0.39	0.35	0.76
Shawnee-Douglas	0.30	0.77	0.44	0.72	0.31	0.42
Lansing-Kansas City	0.23	0.74	0.44	0.72	0.31	0.42
Pleasanton-Marmaton	0.64	0.77	0.16	0.39	0.35	0.76

Table 3-33. Prospective storage resource and storage efficiency estimates for the deep saline formations of interest in the Huffstutter study area.

Group(s)	Avg. E_{saline} Results (%)			Prospective Storage Resource (Mt)		
	P_{10}	P_{50}	P_{90}	P_{10}	P_{50}	P_{90}
Wabaunsee	2.9	5.8	10.2	34.8	68.7	120.6
Shawnee-Douglas	3.1	5.9	9.4	25.5	48.9	77.7
LKC	2.4	5.2	8.9	9.8	21.2	36.2
Pleasanton-Marmaton	2.8	5.3	9.1	10.6	20.4	35.2
Total				**80.8**	**159.2**	**269.7**

3.7 Discussion

3.7.1 Structural and Stratigraphic Framework of the Selected Study Areas

Basin evolution and regional stratigraphy have played an important role in the development of Pennsylvanian and Permian-age geologic CO_2 storage resources, hydrocarbon reservoirs, and caprocks in Nebraska and Kansas. Alternating stratigraphic successions of marine (e.g., limestone and shale) and non-marine (e.g., paleosols and sandstones) sediments are unique to the Pennsylvanian System in the study region, and are related to the development of geologic conditions conducive to commercial-scale CO_2 injection and storage.

Due to extensive erosion above the Cambridge Arch, the deepest section of Paleozoic strata overlying the Precambrian basement in both study areas is primarily comprised of Pennsylvanian-age rocks. Between the two selected study areas, deep saline intervals extending from the Wabaunsee (top) to the Pleasanton-Marmaton groups (base) occur with oil-bearing zones (e.g., Lansing-Kansas City) at depths ranging from approximately 2,700 ft to 3,700 ft. These depths are sufficient for storage of supercritical CO_2 at relatively low costs for well drilling, operation, and maintenance.

The oil-bearing zones occur between and/or adjacent to the deep saline formations evaluated for CO_2 storage rather than hundreds-to-thousands of feet above them, as is often the case in other U.S. basins (e.g., Appalachian basin, Permian basin). This scenario enhances the potential for synergy between EOR operations in the petroleum industry and geologic storage projects. Throughout the Pennsylvanian interval of interest, isolation of oil-bearing zones from deep saline formations is demonstrated by hydrocarbon trapping mechanisms and laterally continuous interbeds of shale and mudrock. The structural and stratigraphic relationships between hydrocarbon reservoirs and deep saline storage interval in the Pennsylvanian create ideal conditions for optimizing the efficiency of CO_2 of injection and storage operations while improving overall CCS project economics.

3.7.2 Pennsylvanian-Permian Confining System

The Pennsylvanian-Permian confining system separating the potential CO_2 storage intervals from USDWs at both study areas is comprised of three main components: (1) structural-stratigraphic hydrocarbon trapping mechanisms; (2) primary caprocks consisting of the Admire, Council Grove, Sumner, and Nippewalla groups; and (3) secondary caprocks consisting of the Cretaceous-age Carlile Shale, Greenhorn Limestone, and Graneros Shale.

The impact of geologic structures, crustal stresses, and seismicity on the integrity of the confining system at the two study areas is not well known. Aside from faults reported within the Lansing-Kansas City in the Huffstutter field (e.g., Herman, 1952; Parkhurst, 1962), the vertical extent and stratigraphic position of potential faults have not been clearly mapped or defined in the two study areas. Similarly, no studies have been conducted to characterize site-specific stress regimes in or near the two selected study areas. A maximum horizontal stress of relatively uniform magnitude has been reported for the Midcontinent Region, with present-day principal compressive stresses oriented roughly east-to-west, parallel to crustal stresses associated with the Sevier-Laramide orogeny. Recent hazard mapping indicates low seismic hazard in southwest Nebraska, with a 1% probability reported for the likelihood of a seismic event exceeding a Peak Modified Mercalli Intensity rating of IV (light shaking) in any given year (Petersen et al., 2016). However, microseismic events detected near the study areas and elevated peak ground acceleration near the Central Kansas Uplift have resulted in the development of microseismic monitoring networks in the region, as well as increased vigilance and precautionary measures to reduce the risk of induced seismicity during injection/water-flood operations.

Examination of structural cross-sections, structure maps, and isopach maps suggests the primary caprocks are vertically and laterally continuous in both study areas. Directly overlying the Pennsylvanian interval of interest for storage, the four lithostratigraphic units comprising the Pennsylvanian-Permian caprock complex occur at depths ranging from 1,500 ft (top) to 2,800 ft. (base) in both study areas. These units have a combined average gross thickness of 942 ft in the Sleepy Hollow study area and 1,103 ft in Huffstutter. Minor variation was observed in depths ($\sigma \leq 92$ ft) and gross thicknesses ($\sigma \leq 37$ ft) of caprocks in both study areas. There were no faults or structural discontinuities observed along the two cross-section transects for caprocks in the Sleepy Hollow study area (Figure 3-37; Figure 3-38).

3.7.3 Site-Scale Reservoir Characterization and Comparison of Study Areas

Distinct and laterally continuous net reservoir intervals were consistently observed in four lithostratigraphic units on cross-sections in the Sleepy Hollow study area: (1) the Wabaunsee Group (upper and lower sections); (2) the Lansing-Kansas City groups (oil-bearing zone); (3) the Pleasanton-Marmaton groups (middle section); and (4) the basal sandstone (e.g., Figure 3-43; Figure 3-44). The net intervals identified within the Wabaunsee and Pleasanton-Marmaton in Sleepy Hollow were also observed on the B-B' cross-section of the Huffstutter study area (Figure 3-59), suggesting some net reservoir zones may be traceable between the two study areas. Relatively thick net reservoir intervals (20-30 ft) observed in the oil-bearing zones of the Lansing-Kansas City and basal sandstone further support the potential for a hybrid of vertically-stacked CO_2-EOR and geologic storage operations that could provide technical and economic advantages needed to successfully commercialize CCS in the Midcontinent region.

In the Sleepy Hollow study area, porosity-feet highs (≥ 16 ft) occur along a north-south trend in the west-central portion of the field, and in the southeast corner of the study area (Figure 3-49). These trends are consistent with relatively thick net reservoir intervals observed on cross-sections (e.g., Figure 3-43). Porosity-feet highs in the west-central portion of the field appear to correlate with greater depth and, to a lesser extent, greater gross thickness on structure and isopach maps for the deep saline intervals (e.g., Figure 3-42; Figure 3-49). The porosity-feet high in the southeast corner of the Sleepy Hollow study area exhibits a notable positive correlation with depth on all structure maps and does not show an obvious correlation with gross thickness of the Pennsylvanian units. The apparent positive correlation between depth and porosity-feet was also observed on cross-sections generated for the Sleepy Hollow study area, with a thicker net reservoir interval in wells located on structural highs (e.g., Figure 3-44).

In the Huffstutter study area, porosity-feet highs (≥ 28 ft) were observed in the northeastern and, to a lesser extent, along the western margin of the study area (Figure 3-64). Similar to the Sleepy Hollow study area, porosity-feet highs appear to correlate with greater depths on structure maps of the deep saline intervals of interest (e.g., Figure 3-56a; Figure 3-60).

Gross thickness of the Wabaunsee, Shawnee-Douglas, and Lansing-Kansas City were approximately 150-200 ft greater in the Huffstutter study area than those in Sleepy Hollow. Similarly, the combined porosity-footage of deep saline Pennsylvanian intervals was, on average, approximately twice as high in the Huffstutter study area relative to Sleepy Hollow. The highest porosity-footage in the Huffstutter study area occur in an isolated area in the northeast corner of the field and appear to correlate with notable gross thickness variations (± 20 to ± 40 ft) on isopach maps of caprocks and deep saline intervals (e.g., Figure 3-51b; Figure 3-55b; Figure 3-64). These thickness variations may reflect potential faulting and/or structural discontinuities in the northeast portion of the Huffstutter field.

On average, the site-specific P_{10} storage efficiency estimates (E_{saline}) from this study are approximately 6 times higher than the average P_{10} value (0.5%) reported for deep saline formations at the regional scale in the DOE-NETL's Carbon Storage Atlas V (2015). The P_{50} and P_{90} values calculated for storage efficiency in this study are approximately 1.5 to 3 times higher than the P_{50} (2.0%) and P_{90} (5.5) values published in DOE-NETL's Carbon Storage Atlas V (2015). This suggests that relative to estimates from regional-scale assessments, the use of site-specific data and stochastic calculation methods may result in higher storage efficiency P_{10} values and a narrower range of prospective storage resource estimates.

The P_{10} (low) values reported in this study indicate a 90% probability of exceeding the P_{10} value, and as such, it represents a high-confidence estimate for Prospective storage resource calculations. Prospective CO_2 storage resource estimates of 49.7 - 80.8 Mt calculated at the P_{10} percentile suggest the net reservoir pore volume of Pennsylvanian-age deep saline intervals in each study area are likely capable of storing commercial-scale CO_2 quantities. Site-specific geologic storage resource and CO_2 storage efficiency was better constrained at the Sleepy Hollow study area relative to the Huffstutter study area due to increased data availability and coverage. Evaluation of geologic structures in the region also suggests the Sleepy Hollow study area may be better suited for long-term geologic storage, with minimal faulting, crustal stress, and seismicity to impact potential storage zones and confining systems in the selected study area.

Despite the data limitations and potential presence of faults in the Huffstutter study area, preliminary estimates of porosity-footage and prospective storage resource warrant further investigation of reservoir properties and deep geologic storage resources in Kansas.

3.7.4 Data Gaps and Future Work

In each study area, the variety of data available to thoroughly resolve lithologic heterogeneity in each well was often limited, with most wells having a gamma ray log and no more than one or two types of porosity logs. This limitation made it difficult to establish a consistent, comprehensive approach that could be applied to develop a robust reservoir facies profile for all wells in each study area. Additional lithologic data, such as mineralogical analyses, geochemical logs, and photoelectric logs, is needed to better quantify reservoir facies and effective porosity.

Petrophysical calculations and correction and calibration of log porosity was limited by the scarcity of core data over the deep saline intervals of interest. In the Sleepy Hollow study area, grain density core data was available only for the Lansing-Kansas City groups, and only 12% (27 out of 219 values) of the available core permeability measurements were from the deep saline Pennsylvanian interval.

Poor well control was observed on caprock structure and isopach maps in the northern and southern portions of the Sleepy Hollow study area. Subsurface analysis in the Huffstutter study area was limited to log data from 96 wells, with only 23-70 wells available to characterize each of the caprock and deep saline units. More deep well data is also needed in the Huffstutter study area to characterize the Arbuckle Group and Precambrian basement. Other potential sources of error and uncertainty in geologic maps and analyses in both study areas may arise from depth datums based on ambiguous or erroneous Kelly Bushing (KB) values, and/or instances where tops could not be clearly resolved. Seismic data would help to better constrain the structural and stratigraphic framework of the two selected study areas.

As more data becomes available, the geologic models and analysis workflows established in this work can be updated and applied to ensure a potential CCS project successfully advances from site selection and characterization to site construction, operation, monitoring, and closure phases.

3.8 Conclusions

As part of a pre-feasibility assessment of a commercial-scale geologic CO_2 storage hub in the Midcontinent, this section evaluated the suitability of the Pennsylvanian-Permian interval to serve as a geologic CO_2 storage complex at two selected areas. In both study areas, the deep saline geologic storage resource was evaluated for four major Pennsylvanian-age lithostratigraphic units: the Pleasanton-Marmaton, the Lansing-Kansas City, the Shawnee-Douglas, and the Wabaunsee groups. The deep saline interval of interest is interbedded with oil-bearing zones, and are directly overlain by regionally extensive Upper Pennsylvanian and Permian caprocks of the Admire, Council Grove, Sumner, and Nippewalla groups.

The structural and stratigraphic framework of Nebraska and Kansas was defined to guide data analysis and inform geologic modeling efforts. Site-specific geologic characterization was conducted via petrophysical analysis, construction of heterogenous site models and geologic maps, and calculation of prospective storage resources for the deep saline interval of the Pennsylvanian system. Results were used to identify potential qualified sites for further characterization and help establish the groundwork for commercial-scale development of geologic CO_2 storage resources in the Midcontinent Region.

The main contributions of this assessment include:

- Construction of 3D SEMs representing the geologic storage framework of the Pennsylvanian-Permian interval at each of the selected study areas
- Development of workflows to establish a consistent, repeatable methodology for site-scale geologic resource characterization that can be easily applied to other potential sites in the region
- Characterization of key confining system components including hydrocarbon trapping mechanisms, and caprock structural and stratigraphic continuity
- Quantification of site-specific storage efficiencies and prospective storage resource of the deep saline Pennsylvanian interval in both study areas

Maps of geologic structure and gross thicknesses indicate caprocks are vertically and laterally continuous at each study area, with no evidence of structural discontinuities or faulting observed on cross-sections for the Sleepy Hollow study area. Faulting of the Pennsylvanian interval in the Huffstutter field, proposed in previous studies, is supported by the presence of notable thickness variations in the northeast corner of the study area on caprock and deep saline isopach maps.

Site-specific geologic characterization and estimates of CO_2 storage resource were better constrained at the Sleepy Hollow study area relative to the Huffstutter study area due to increased data availability and spatial coverage. Site-scale analysis and mapping of potential storage zones generally show small variation in formation properties within each site, with regional structures such as the Cambridge Arch likely responsible for local map variations and the development of reservoir properties. Other key outcomes and takeaways are summarized below:

- Distinct, laterally continuous net reservoir intervals observed in the Wabaunsee and Pleasanton-Marmaton groups at both study areas suggest net reservoir zones may be traceable and continuous over distances of 50 mi or greater.

- Prospective storage resource results calculated at the P_{10} probability value (49.7 - 80.8 Mt) indicate a high level of confidence in the likelihood that the deep saline CO_2 storage resource is 50 Mt or greater at each site; sufficient for commercial-scale CO_2 storage.
- Potential qualified sites were identified in Sleepy Hollow based on the presence of thick net reservoir intervals and porosity-footage highs in the western and southeast portions of the study area.

Cyclothems comprised of marine and non-marine sediments are a distinguishing feature of the Pennsylvanian-Permian-age subsurface interval in the Midcontinent. These stratigraphic successions provide alternating sequences of deep saline formations, shale, and oil-bearing zones conducive to vertically-stacked CO_2 injection and storage in oil-bearing and deep saline storage reservoirs. Existing hydrocarbon resources at the two selected study areas, and the potential for a hybrid of CO_2-EOR and geologic storage may provide technical advantages, infrastructure, and economic incentives needed to successfully commercialize CCS in the region. A continued effort is needed to eliminate data gaps and conduct further characterization of potential qualified sites for CO_2 storage in the study region. This initial characterization shows that the Pennsylvanian-Permian interval at the selected study areas has high potential to serve as a long-term, commercial-scale geologic storage complex.

4 Reservoir Simulation

4.1 Scope

Reservoir simulation was used to evaluate strategies for injection into the Pennsylvanian-Permian geologic interval in the Midcontinent to act as a commercial-scale CO_2 storage complex using ECLISPE, Schlumberger's dynamic modeling simulator. The geologic assessment (Section 3) identified a primary injection site, Sleepy Hollow Field, in Nebraska and a secondary injection site, Huffstutter Field, in Kansas. Both sites were shown to have sufficient storage capacity to store 50 million tonnes of CO_2 over 30 years. This section describes the reservoir modeling necessary to show that injection and storage are feasible. This report describes the dynamic modeling performed to examine the pre-feasibility of an integrated, geologic CO_2 storage hub in the midcontinent region of the United States (U.S.) project. The Pennsylvanian-Permian storage complex was evaluated for CO_2 storage due to the major CO_2 storage capacity in the saline strata to meet the storage target. This study assesses the storage capacity and injectivity in terms of storage target within the study area. CO_2 plume migration and containment associated with the area of review (AoR) are also investigated.

In Sleepy Hollow Field in Red Willow County, southwestern Nebraska (Figure 3-1) the middle-to-lower interval of the Pennsylvanian System hosts deep saline formations and oil-bearing zones that are overlain by a confining system of regionally extensive Upper Pennsylvanian and Permian-age shales, carbonates, and evaporites. These strata are regionally extensive and are expected to be present at multiple storage sites in the region.

4.2 Pennsylvanian-Permian Storage Complex

Four main lithostratigraphic groups in the Pennsylvanian System were evaluated for deep saline CO_2 storage in the two study areas. In ascending order, they include: the Pleasanton-Marmaton, the Lansing-Kansas City, the Shawnee-Douglas, and the Wabaunsee groups (Figure 3-2). Potential storage targets within each group include sandstone intervals (5-20 feet [ft]) in the Wabaunsee and Pleasanton-Marmaton groups, and porous limestones (5-25 ft) in the Shawnee-Douglas and Lansing-Kansas City groups. The deep saline zones of interest in the Lansing-Kansas City occur at the top and the base of the unit, and are separated by productive oil-bearing zones.

Directly overlying the Wabaunsee Group, shales, carbonates, and evaporites deposited during the Late Pennsylvanian and Permian have potential to act as caprocks for the underlying storage reservoirs (Carlson et al., 1986; Condra and Reed, 1959; Sawin et al., 2009). These potential caprocks include, in ascending order: Admire, Council Grove, Sumner, and lower Nippewalla groups (Figure 3-2).

4.3 ECLIPSE Model and Model Settings

4.3.1 ECLIPSE

Schlumberger's Eclipse E300 compositional reservoir simulator was used to model saline storage at Sleepy Hollow Field. With the CO_2 storage feature (CO2STORE), ECLIPSE has been specifically designed for the modeling of CO_2 storage in subsurface formations and has been successfully applied to numerous CO_2 storage projects since the commercial release in 2006. It allows the fluids in the pore space be modeled in two phases: a CO_2-rich phase (labeled gas phase), an H_2O-rich phase (labeled liquid phase) and a separate solid phase (salt contents). It can be also used to simulate non-isothermal case within the temperature range of 12-250 ?C.

4.3.2 Simulation Grid and Properties

The dynamic modeling is based on the 3D static earth model constructed in Section 3 for the development of the static model in detail]. The sub-basinal heterogeneous reservoir model covered a 16-km x 16-km (10-mile x 10-mile) area with the Sleepy Hollow oil field centered in the model domain (see Figure 4-1). The static model used for dynamic modeling includes 14 geologic zones ranging from Foraker Group to Basal Sand from top to bottom. With the original cell size of 70 m by 70 m (230 ft by 230 ft) in the static model, the 3D grid configuration is 229 x 229 x 183 (totaling 9,596,703 cells) in x, y, and z direction, respectively. Vertical thickness of each cell range depends on the vertical proportion of each formation.

Four major lithostratigraphic groups for saline CO_2 storage include Wabaunsee group, Shawnee-Douglas group (Topeka, Deer Creek, and Oread Formation), Lansing-Kanas City (LKC) group except for the oil-bearing LKC C zone, and Pleasanton-Marmaton (Kansas City Base) in descending order. During the static modeling, the effective porosity logs was attenuated for moderate and low energy depositional environments as described in Section 3. The attenuation could be appropriate for the low energy environment of LKC zones. However, this process significantly attenuated permeabilities of potential saline storage targets due to the application of porosity-permeability correlation and led to the difference in the original porosity logs and upscaled logs by one order of magnitude in the saline formations. Thus, in order to match the original and upscaled logs, permeabilities of saline formations (Wabaunsee, Topeka, Deer Creek, Oread, LKC A, and Kansas City Base) were multiplied uniformly by 10 prior to the grid coarsening.

To reduce the number of cells and speed up the simulation run times, grid/property was applied outside the 6-km x 9.5-km rectangle (see Figure 4-2) where the CO_2 injection wells were placed. Figure 4-2 shows the 3D permeability distribution after grid coarsening. Grid coarsening with 5 by 5 host cells in x and y directions was applied outside the rectangle, leading to the reduction of approximately 7 million cells. No z directional coarsening was made. Within each coarse cell, petrophysical properties were upscaled from the host cells as well. The petrophysical properties (porosity and permeability) within the rectangle (Figure 4-2) were preserved and there is no loss or modification to the petrophysical fields due to upscaling. Figure 4-3 illustrates the 3D porosity distributions within the model domain.

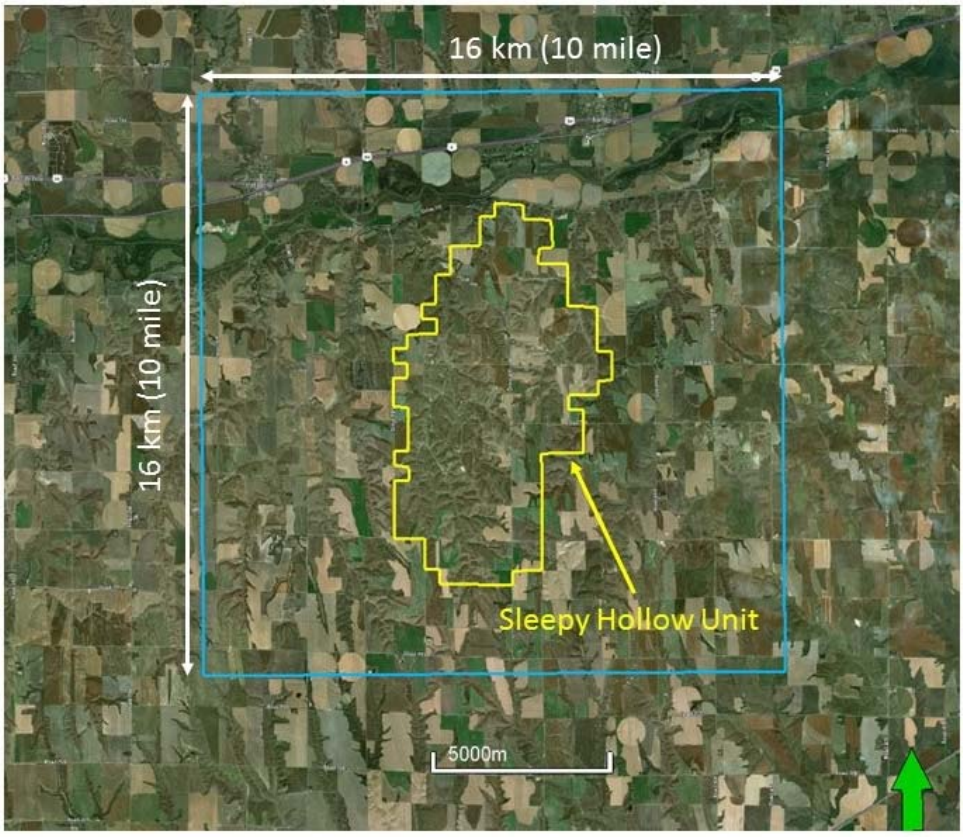

Figure 4-1. Dynamic model domain and Sleepy Hollow oil field unit boundary.

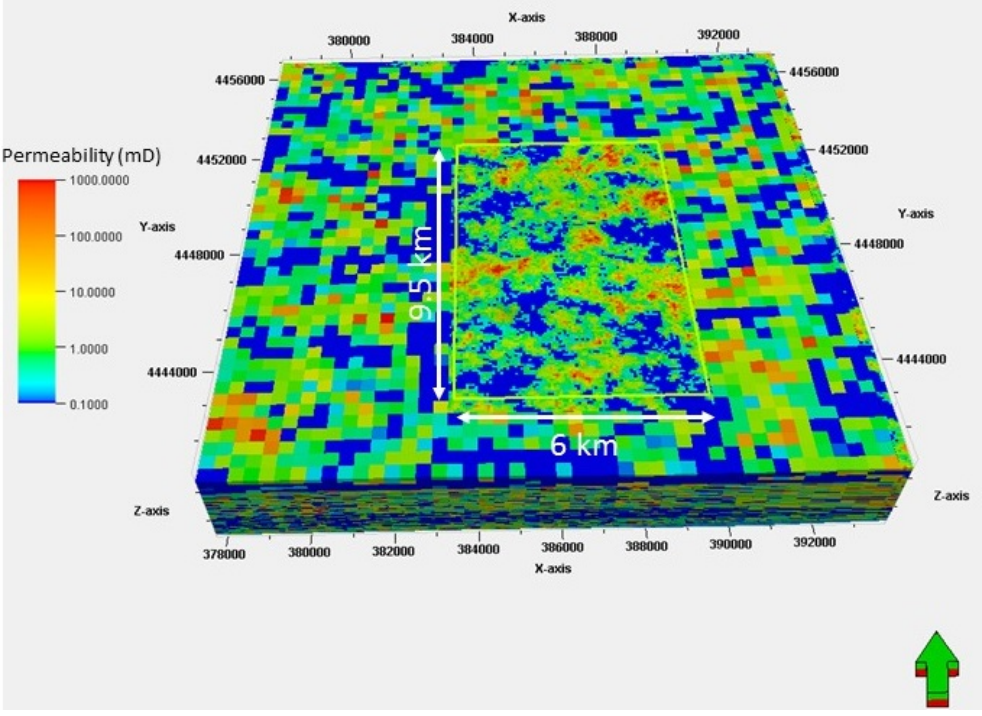

Figure 4-2. 3D permeability distribution after upscaling. Vertical exaggeration is 10x.

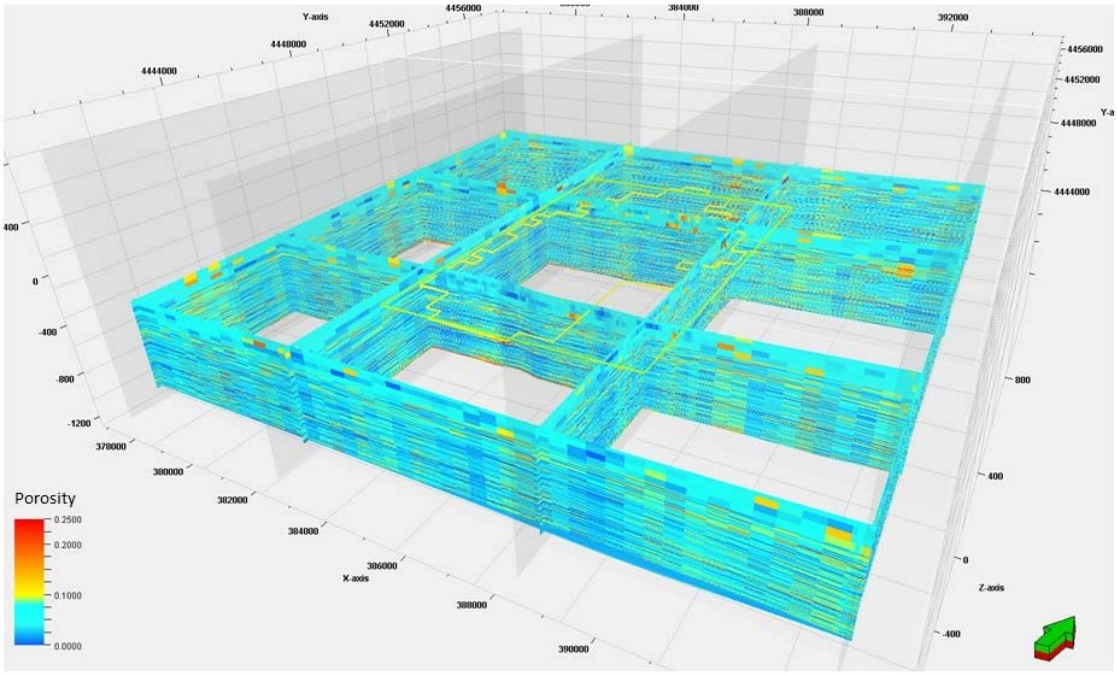

Figure 4-3. 3D porosity distribution after upscaling. Vertical exaggeration is 10x.

4.3.3 Fluid Properties

The reservoir was assumed to be 100% brine saturated with an initial formation salinity of 70,000 ppm, which is based on the water salinity from basal sand in the Sleepy Hollow Field. For modeling purposes, the injected gas is assumed to have the behavior of pure CO_2.

4.3.4 Relative Permeability

Due to the absence of special core analysis (SCAL) data and no analogous data available in the neighboring areas, the CO_2-brine relative permeability curve was modified from Bennion and Bachu (2005) and shown in Figure 4-4.

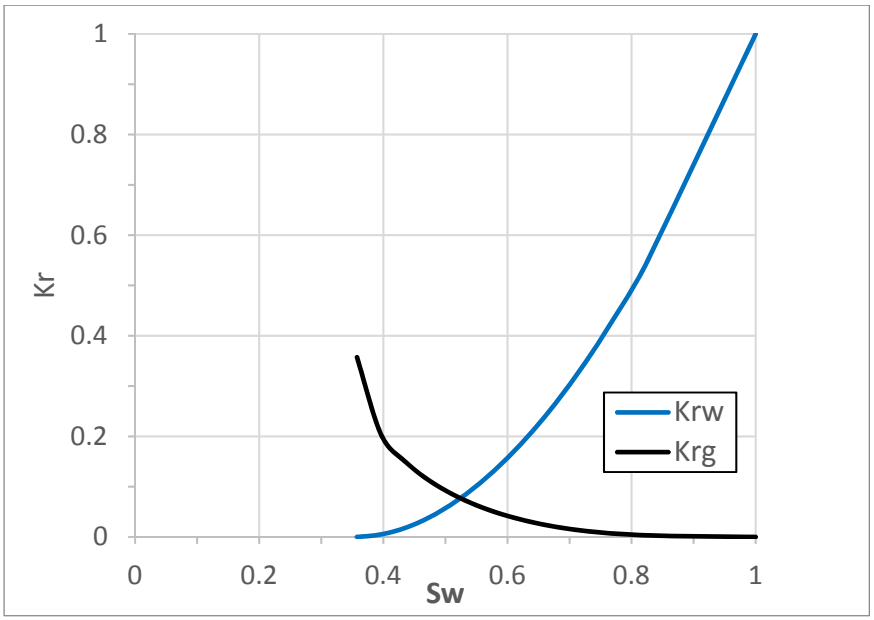

Figure 4-4. Relative permeability (Kr) curves assumed for the numerical simulations. Note: Krw is the relative permeability of brine and Krg is the relative permeability of CO_2.

4.3.5 Reservoir Boundaries

Infinite-acting conditions were assumed at the lateral boundaries of the simulation. This was modeled by applying a pore multiplier of 10^6 in the cells at the model perimeter to account for a near-infinite aquifer volume. The infinite-acting boundaries act as pressure sinks/source during and after the injection. No-flow boundaries are assumed at the top and bottom of the model.

4.3.6 Model Equilibration

The model was equilibrated as an under-pressured reservoir by approximately 16% compared to the hydrostatic gradient which was reported in Kincaid (1961). The reference datum for the reservoir pressure is at a depth of 2,899 ft with a pressure of 1,054 psi. Reservoir temperature was assumed constant in the reservoir at 93˚F.

4.3.7 Injection Well Locations

In order to determine the location of potential CO_2 injectors, the vertical cumulative KH (permeability (K) x thickness (H)) map of saline storage formations was used as a proxy to the injectivity within the study area. Figure 4-5 shows the KH map with eight injection wells inside the Sleepy Hollow Field boundary. The wells were placed near the boundaries of the field to allow maximum spacing and still take advantage of the assumed CO_2 injection infrastructure of the field.

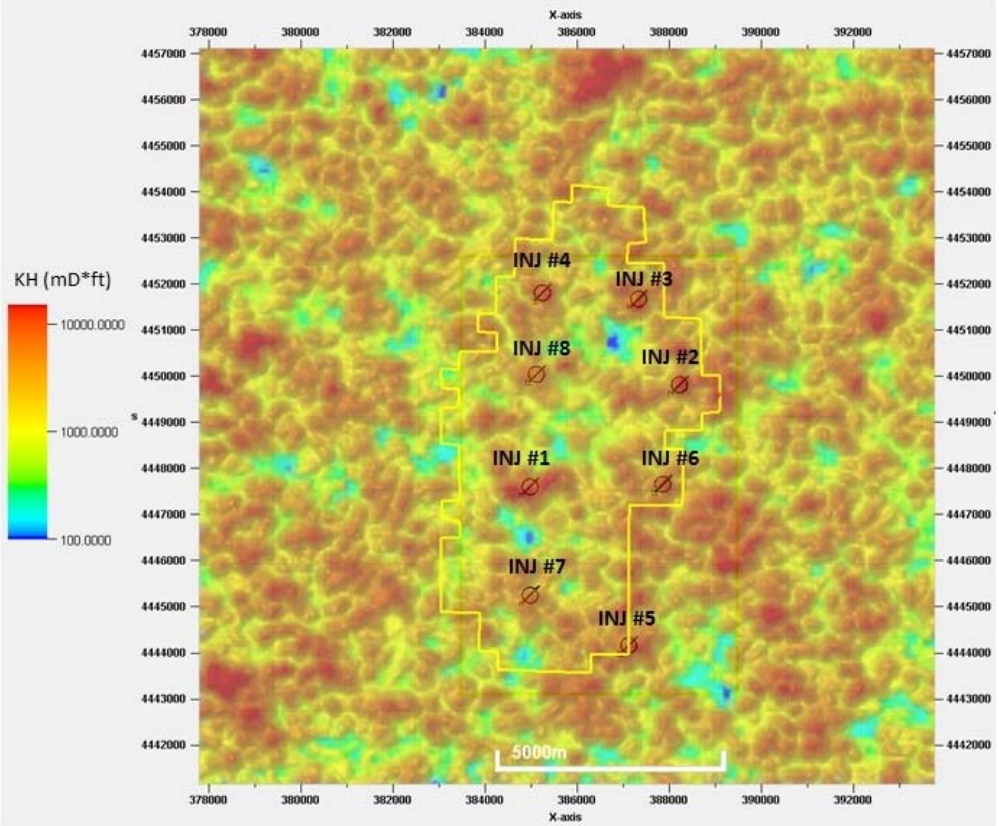

Figure 4-5. Cumulative KH map and location of 8 injection wells.

4.3.8 Injection Constraints

The CO_2 storage target is 50 million tonnes over a 30-year injection period (daily injection of 4566 tonnes). In the dynamic modeling work, a single well injection scenario was considered initially. For the modeling purpose, the CO_2 injection was carried out in the entire vertical interval (all saline formations). Figure 4-6 shows the perforation interval within the injection well (INJ) #1. Since there is no fracture pressure gradient data available in the saline formations, CO_2 injection rate is constrained by the maximum allowable bottom hole pressure (BHP) which is assumed to be 90% of lithostatic gradient.

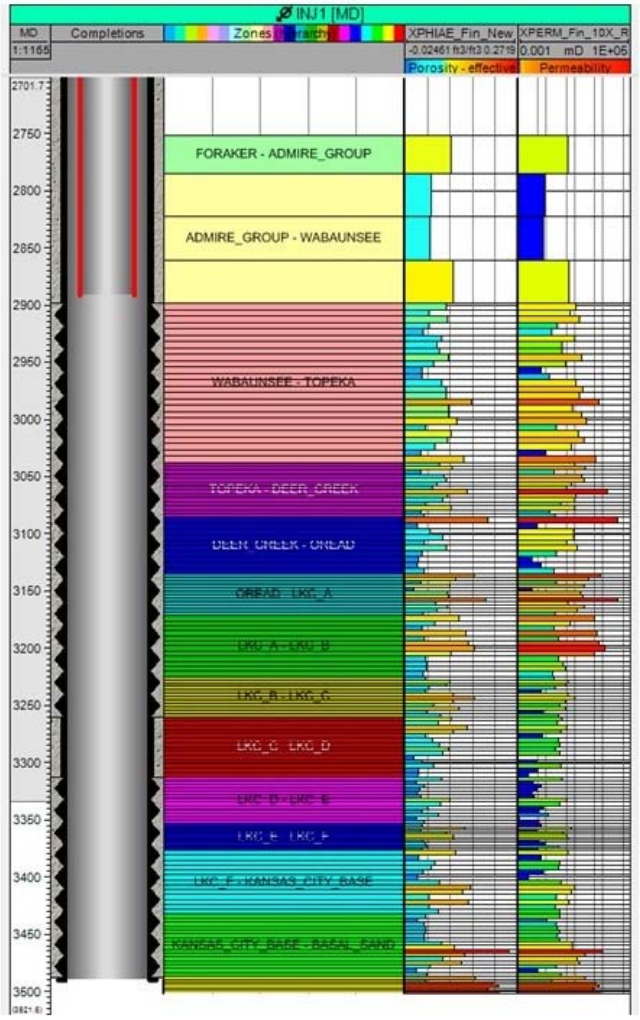

Figure 4-6. Perforation intervals and petrophysical properties (porosity and permeability) in the injector no. 1 (INJ #1). Unit of measured depth (MD) is in feet.

4.4 Dynamic Modeling

4.4.1 Single-Well Injection Cases

Using the numerical settings described in Section 4.3, a single well injection scenario with a 30-year continuous injection followed by a 10-year post injection was simulated for each of the eight wells shown in Figure 4-5.

4.4.2 Simulated Injectivity

With the continuous injection scenario subject to the maximum allowable BHP constraint, Figure 4-7 illustrates the simulated CO_2 injection rate for each injector. The initial maximum CO_2 injection rate was 4,566 metric tons per day (equivalent to injection target), decreasing significantly and stabilizing over the next several years. After the continuous 30-year injection, the greatest cumulative CO_2 storage was obtained from INJ #2 and #6 then followed by INJ #5, #1, #4, and #8. INJ #3 and #7 showed the lowest injectivity. The greatest cumulative CO_2 injection at INJ #2 was approximately 34.8 million metric tons after 30 years resulting in 30-year average injection rate of 3,177 metric tons per day (Figure 4-8). The lowest average injection rate was found at INJ #7 with a rate of 2,662 metric tons per day. The single

well simulation results show very good injectivity performance. However, no single well injection case could achieve the storage target (50 million metric tons for 30 years), which leads to the multi-well CO_2 storage system to meet the injection goal.

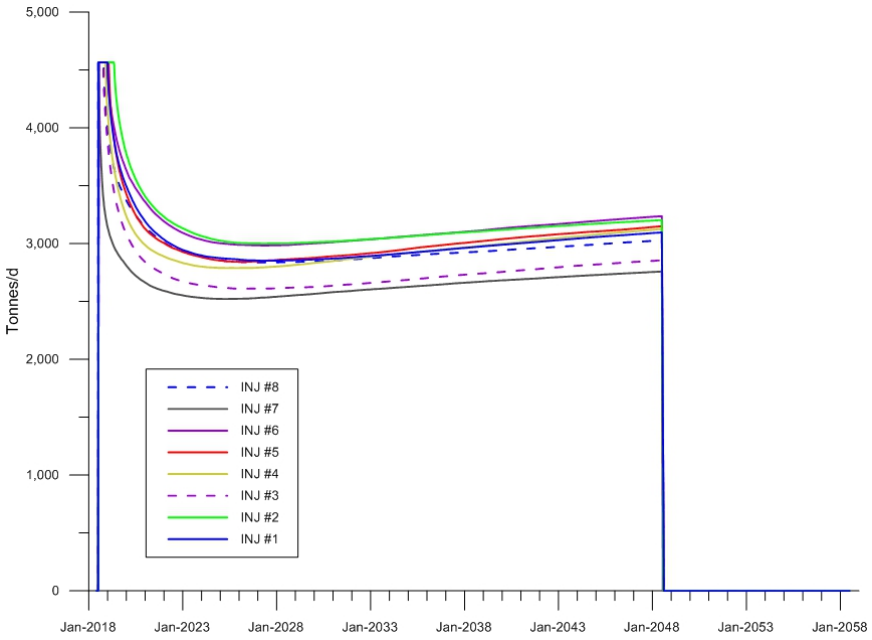

Figure 4-7. Simulated CO_2 injection rate (metric tons/d) vs. time for singe-well cases.

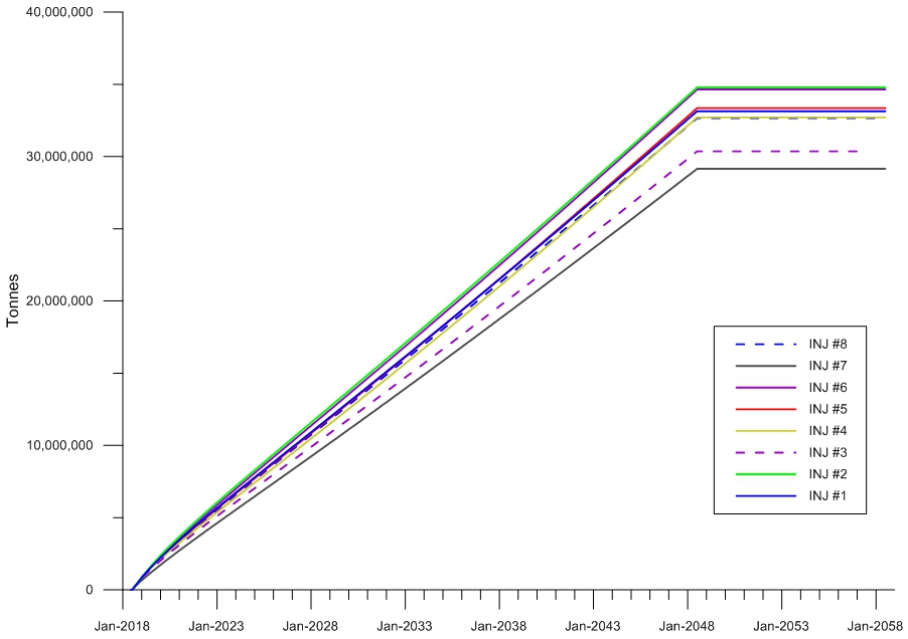

Figure 4-8. Simulated cumulative CO_2 injection (metric tons) vs. time for singe-well cases.

4.4.3 Multi-Well Injection Cases

The simulation results from single-well injection cases show that a single vertical well applied in the study area cannot achieve the CO_2 injection target. Thus, the multi-injector system with the

combination of vertical wells was investigated with respect to the storage target. First, the combination of two CO_2 injectors was examined based on the single-well injectivity results. Best possible combinations from the two highest performing injectors such as INJ #2 and #6 and INJ #2 and #5 were applied in the simulation cases. However, due to the pressure interference between two wells and BHP constraint, the combined injection rate was not able to reach the injection goal with two injectors.

Next, the multi-well system with three injectors was considered and simulated. After examining several combinations, the simulated injection rates and cumulative injection (Figure 4-9) show that a three-injector system with INJ #1, #2, and #5 maintains stable injectivity throughout the entire injection period and combined CO_2 injection satisfies the storage target successfully. This suggests that at least three vertical injection wells are required in the study area to achieve the specified injection target, given the limited data and assumptions made.

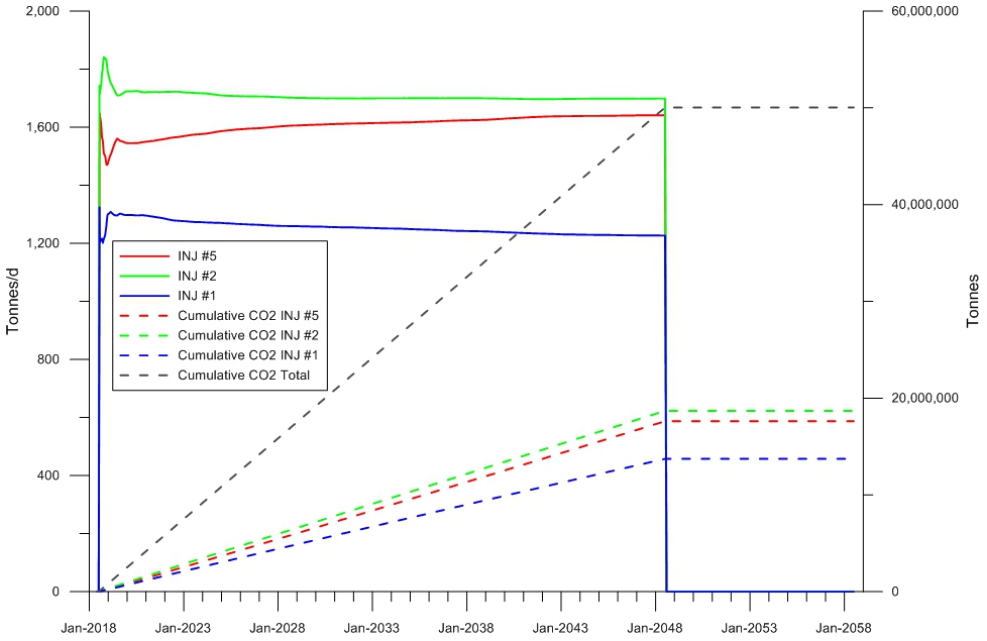

Figure 4-9. Simulated CO_2 injection rate (metric tons/d) and cumulative injection (metric tons) for INJ #1, #2, and #3.

CO_2 Plume Extent

Figure 4-10 through Figure 4-13 illustrate the temporal 3D CO_2 plume evolution with three injectors (INJ #1, #2, and #5) after a 10, 20, 30-year continuous injection and a 10-year post-injection period, respectively. It was noted that the CO_2 plume reached the coarsened cells beyond the centered fine cell area. The size and distribution of fine cells will need to be revised in the future work in order to not lose the details of the CO_2 plume with the coarse cells near the plume edge.

Detailed CO_2 saturation (Sg) profiles along the cross-section A-A' (see Figure 4-14 for the location) containing both injector INJ #1 and INJ #2 are shown in Figure 4-15 (a) – (d) after 10, 20, 30-year injection and 10-year post-injection, respectively. Similarly, Figure 4-16 (a) – (d) and Figure 4-17(a) – (d) show the 2D saturation profiles along the cross-section B-B' and C-C' after 10, 20, 30-year injection and 10-year post-injection period.

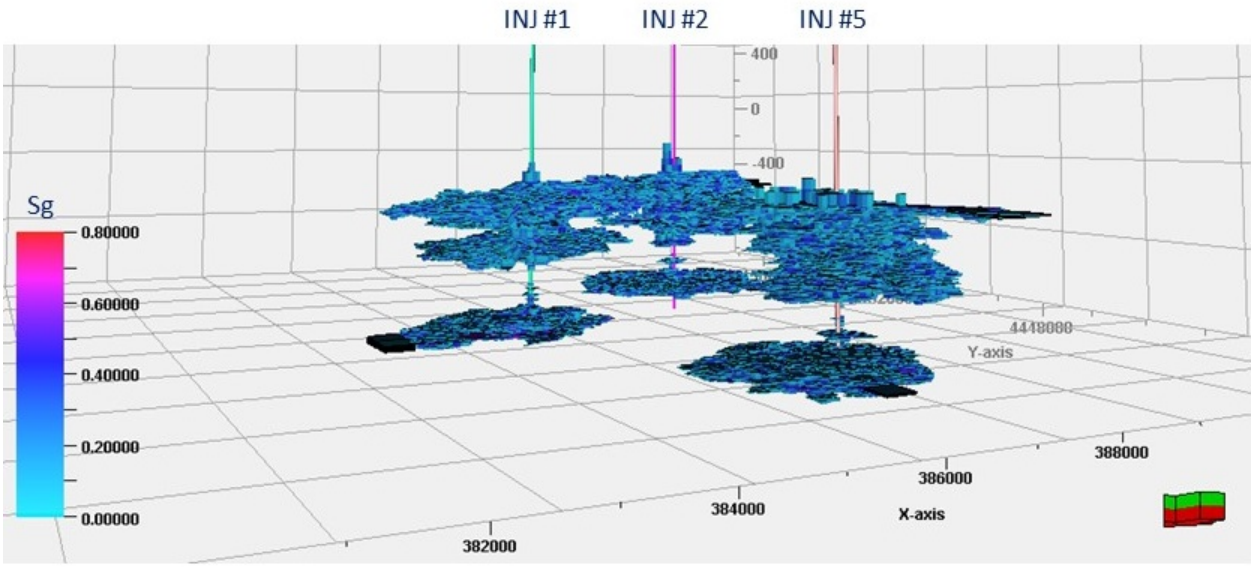

Figure 4-10. 3D simulated CO_2 plume distribution after 10 years since injection started. Vertical exaggeration is 10x.

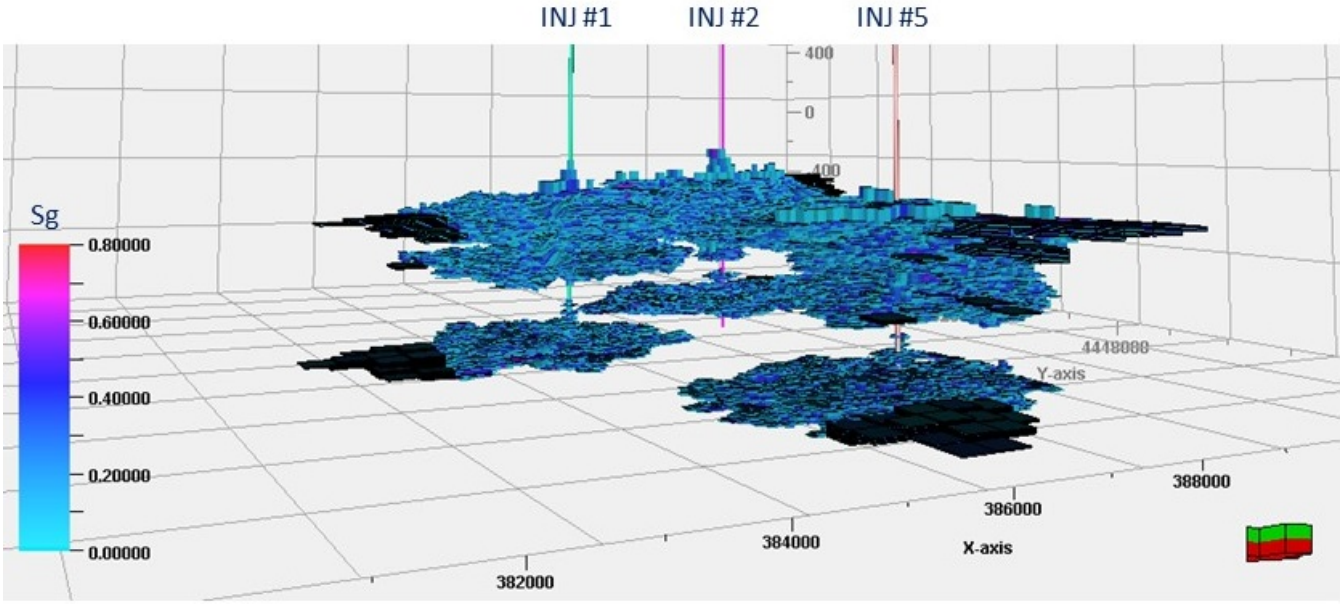

Figure 4-11. 3D simulated CO_2 plume distribution after 20 years since injection started. Vertical exaggeration is 10x.

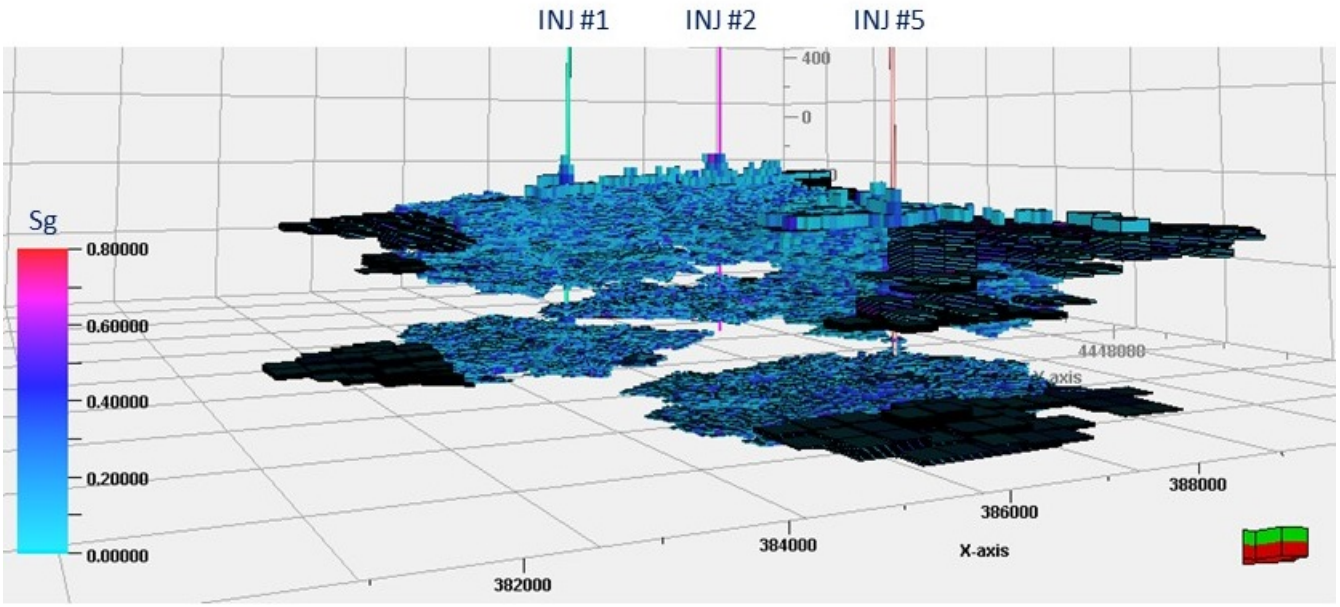

Figure 4-12. 3D simulated CO_2 plume distribution after 30 years since injection started. Vertical exaggeration is 10x.

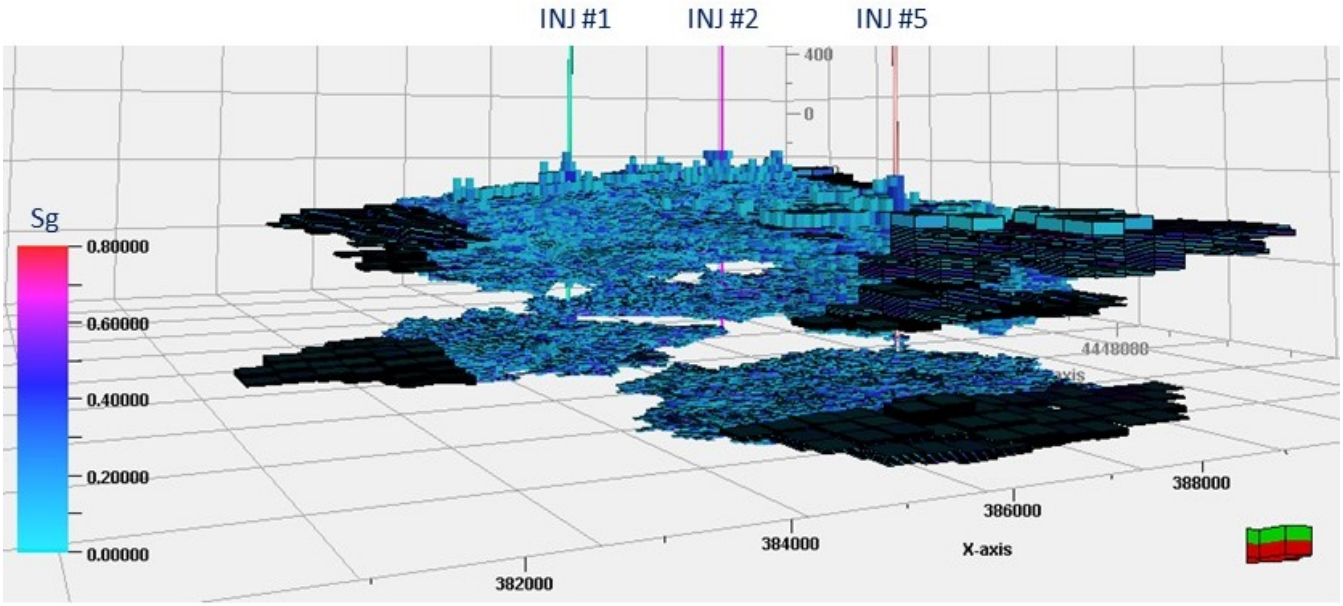

Figure 4-13. 3D simulated CO_2 plume distribution after 10 years since injection ended. Vertical exaggeration is 10x.

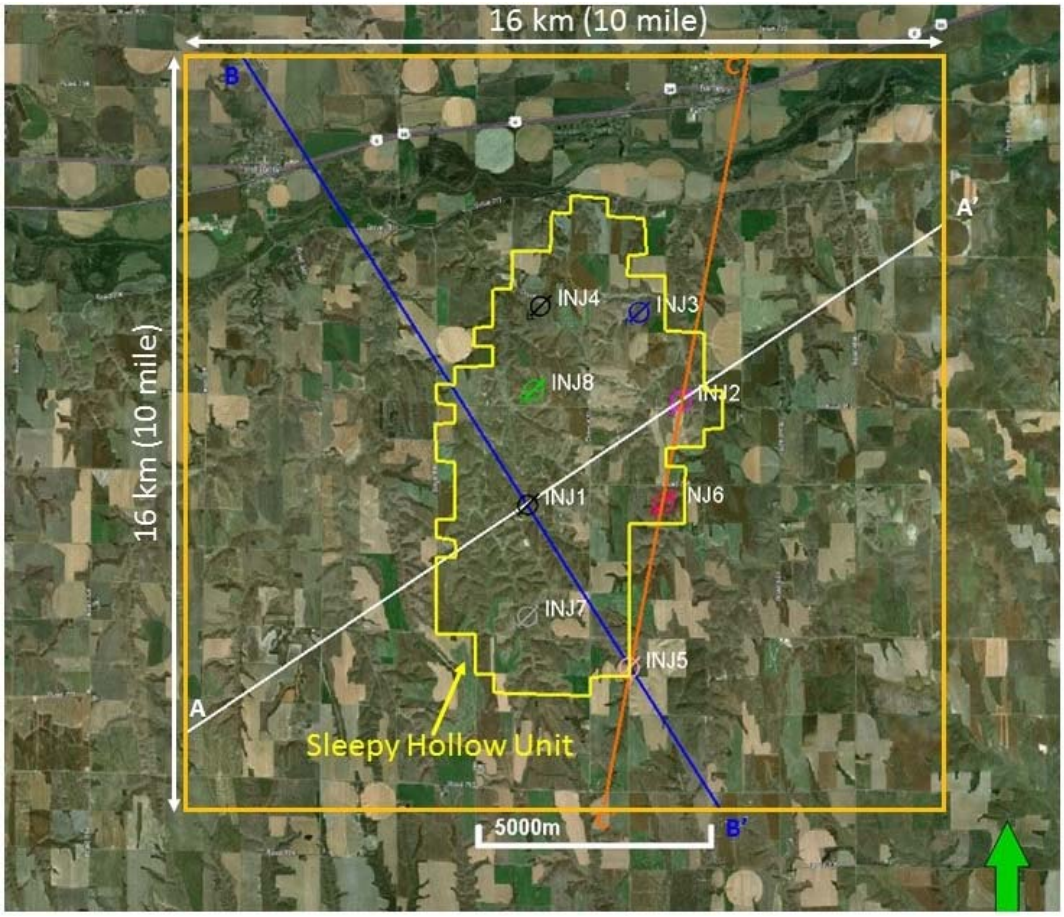

Figure 4-14. Satellite imagery showing the location of injectors (INJ #1 ~ #8). A-A' is the cross-section line including both injector INJ #1 and INJ #2. Cross-section line B-B' includes injector INJ #1 and INJ #5 which is almost perpendicular to A-A'. Third cross-section line C-C' includes injector INJ #2 and INJ #5.

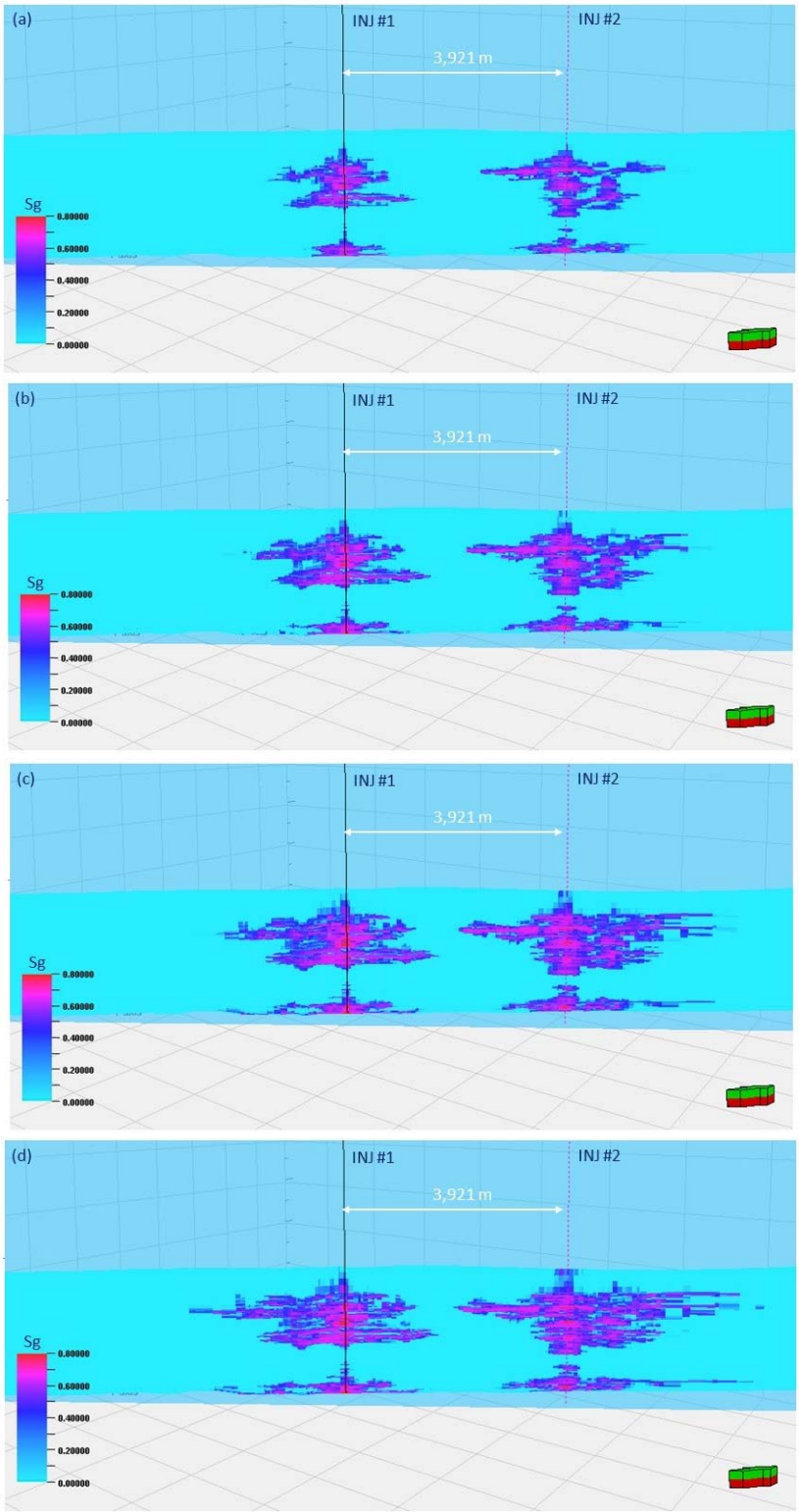

Figure 4-15. Simulated CO_2 saturation profile along the cross-section A-A' after 10- (a), 20- (b), 30-year (c) injection, and 10-year post-injection (d). Vertical exaggeration is 10x.

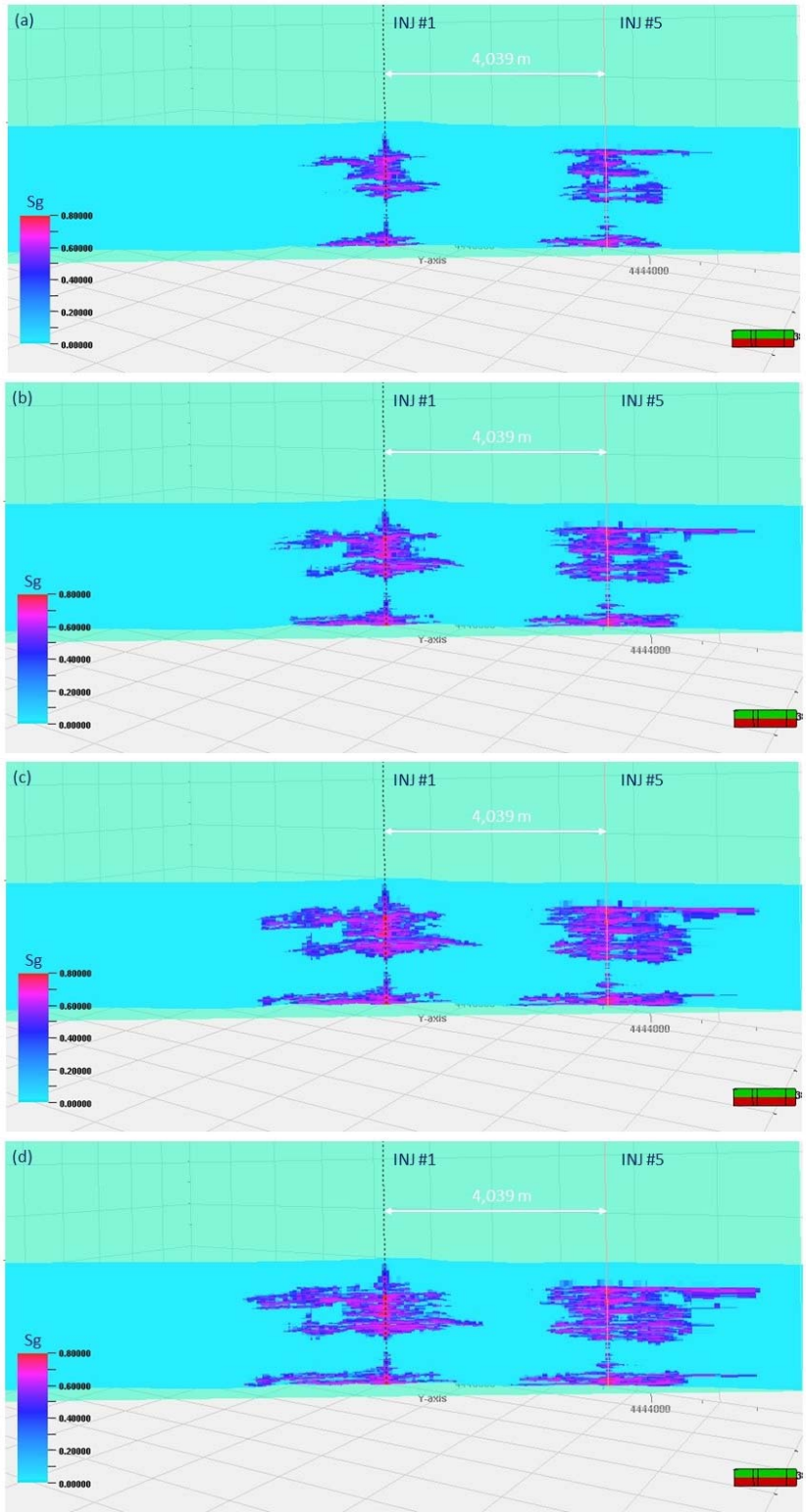

Figure 4-16. Simulated CO_2 saturation profile along the cross-section B-B' after 10- (a), 20- (b), 30-year (c) injection, and 10-year post-injection (d). Vertical exaggeration is 10x.

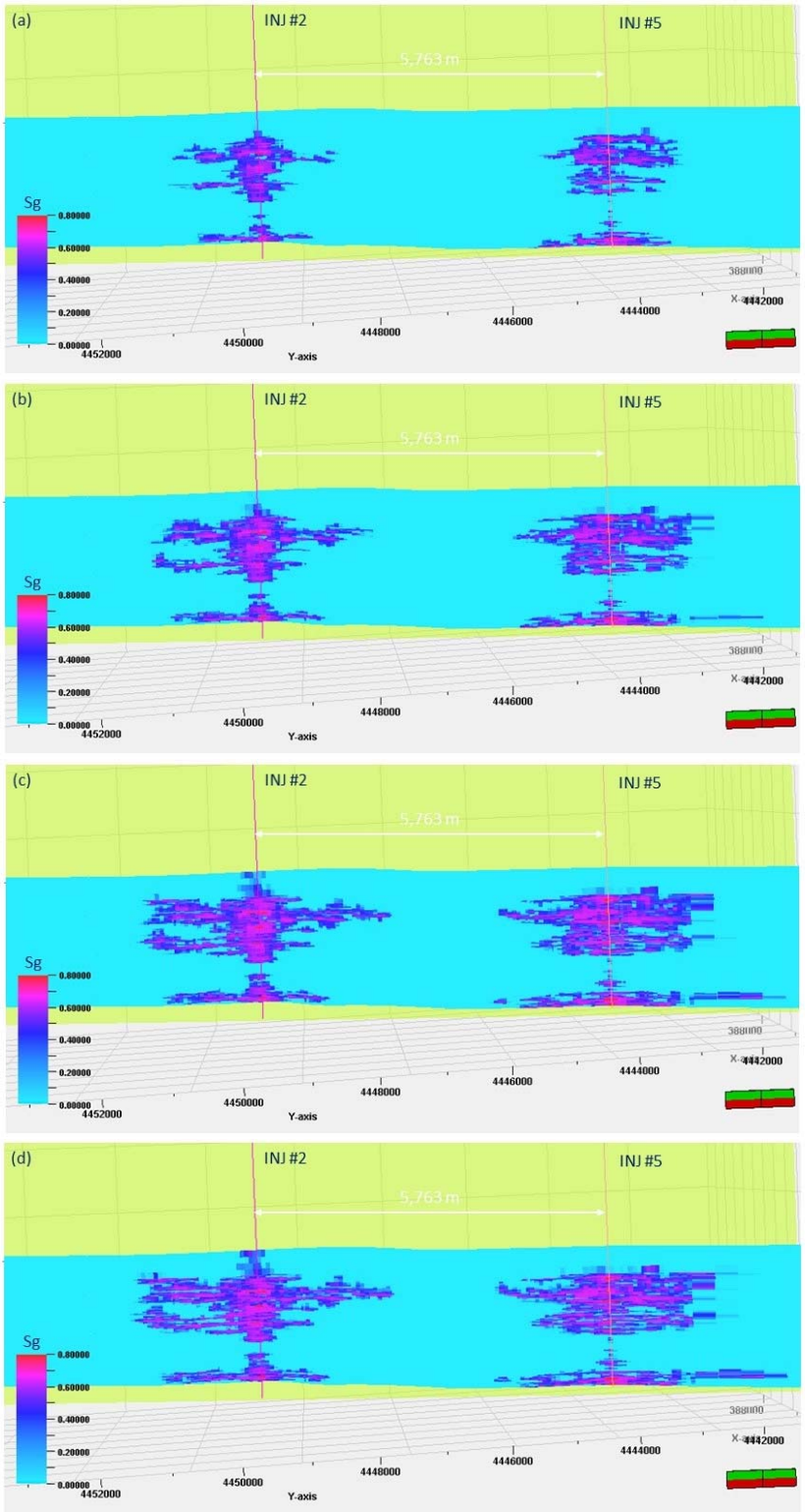

Figure 4-17. Simulated CO_2 saturation profile along the cross-section C-C' after 10- (a), 20- (b), 30-year (c) injection, and 10-year post-injection (d). Vertical exaggeration is 10x.

Figure 4-18 illustrates the temporal evolution of the CO_2 plume during and post CO_2 injection by plotting the edge of the CO_2 plume defined as CO_2 gas saturation of 0.01 (or 1%). The CO_2 plume edge centered from each injector tends to grow radially. The entire CO_2 plume from three injectors extends approximately 9 km in the East-West direction and 11 km in the North-South direction after the 30-year injection.

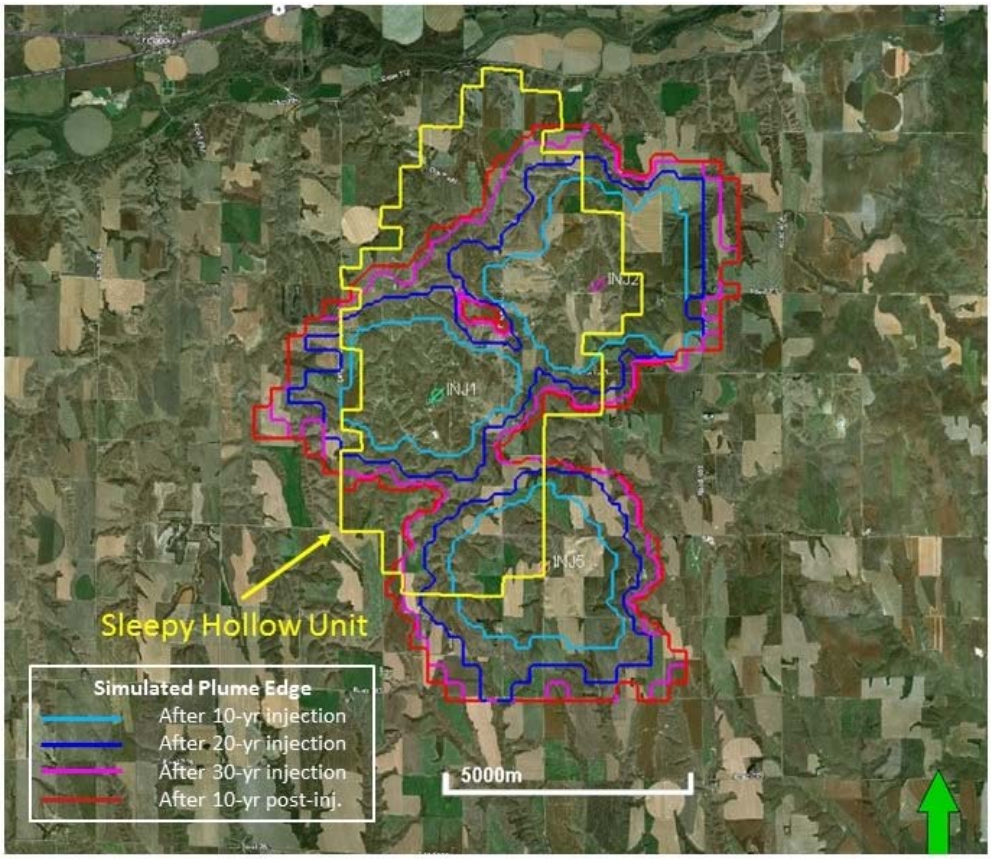

Figure 4-18. Edge of the simulated CO_2 plume after 10, 20, and 30-year injection and 10-year post-injection period.

CO_2 Storage in Target Formations

As shown in the 2D CO_2 profiles and 3D distributions, CO_2 migrates into multiple intervals. In order to evaluate the storage performance of each formation, the simulated cumulative CO_2 storage in each saline formation is plotted in Figure 4-19. Major CO_2 storage occurs at Wabaunsee (26%), Kansas City Base (19%), Topeka (18%), Oread (15%), LKC A (8%), and Deer Creek (6%). Whereas, the simulated CO_2 storage in LKC B, D, E, & F zones is minimal. It is important to note that the oil producing part of the LKC D was not perforated in these simulations.

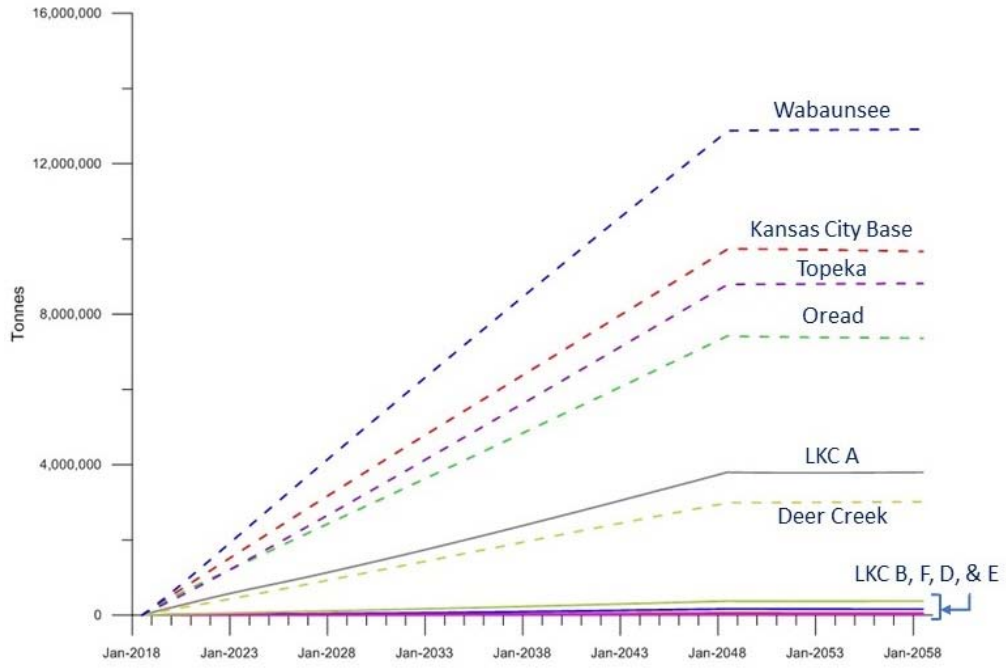

Figure 4-19. Cumulative CO_2 in each target formation.

4.4.4 Sensitivity Cases

To investigate the impact of uncertain parameters on the CO_2 storage complex, a sensitivity analysis with nine input parameters (relative permeability, vertical permeability anisotropy ratio, reservoir temperature, salinity, perforation interval, initial reservoir pressure, fracture pressure [BHP limit], porosity, and permeability) was conducted with ±10% variation for the upper and lower level in each parameter except for the perforation intervals. For this analysis, 10-year continuous injection at INJ #1 was considered as the Base Case. A list of the sensitivity cases and the simulated cumulative CO_2 injection amount after the 10-year injection are given in Table 4-1. Including the Base Case, a total of 47 simulation cases were prepared and ran by applying a simple one-factor-at-a-time approach. Figure 4-20 is a tornado chart representing the relative sensitivity of the cumulative CO_2 injection to the change in each parameter graphically.

The sensitivity analysis reveals that the CO_2 storage in this study is more sensitive to the BHP constraint, perforation of Kanas City Base, initial reservoir pressure, reservoir temperature, CO_2-brine relative permeability, and permeability of Wabaunsee. Whereas, sensitivity to ±10% porosity change appears to be negligible. Effects of vertical permeability anisotropy, salinity, and permeabilities of Topeka, Deer Creek, and Oread were also found to be less but non-negligible in terms of injectivity.

Table 4-1. Summary of sensitivity cases.

	Cumulative CO_2 Injection (metric tons) after 10-yr continuous injection
Base Case	
CO_2-Brine Relative Permeability	
Permeability Anisotropy Ratio (kv/kh): 0.3	
Reservoir Temperature: 97 °F	
BHP limit: 2608.74 psi	1.0768E+07
Initial pressure @ ref datum: 1054.04 psi	
Salinity: 70,000 ppm	
Entire perforation interval is open	
No modification in permeabilities	
No modification in porosities	
CO_2-Brine Relative Permeability	
Lower case	1.0405E+07
Upper case	1.1108E+07
Permeability Anisotropy Ratio	
kv/kh = 0.27	1.0649E+07
kv/kh = 0.33	1.0875E+07
Reservoir Temperature	
RTEMP=83.7 ºF	1.0212E+07
RTEMP=102.3 ºF	1.1277E+07
Perforation Interval	
Closure of Wabaunsee	1.0534E+07
Closure of Topeka	1.0684E+07
Closure of Deer Creek	1.0475E+07
Closure of Oread	1.0616E+07
Closure of LKC A	1.0744E+07
Closure of LKC B	1.0768E+07
Closure of LKC D	1.0768E+07
Closure of LKC E	1.0768E+07
Closure of LKC F	1.0768E+07
Closure of Kansas City Base	9.1643E+06
BHP Limit	
2347.87 psi	8.7729E+06
2869.61 psi	1.2776E+07
Initial Pressure @ reference datum	
948.6 psi	1.1524E+07
1159.4 psi	1.0011E+07

Table 4-1. continued.

Permeabilities Multiplier	
0.9 to Wabaunsee	1.0451E+07
1.1 to Wabaunsee	1.1079E+07
0.9 to Topeka	1.0633E+07
1.1 to Topeka	1.0899E+07
0.9 to Deer Creek	1.0711E+07
1.1 to Deer Creek	1.0822E+07
0.9 to Oread	1.0655E+07
1.1 to Oread	1.0881E+07
0.9 to LKC_A	1.0703E+07
1.1 to LKC_A	1.0832E+07
0.9 to KC Base	1.0645E+07
1.1 to KC Base	1.0885E+07
Salinity	
6,3000 ppm	1.0871E+07
7,7000 ppm	1.0662E+07
Porosity Multiplier	
0.9 to Wabaunsee	1.0751E+07
1.1 to Wabaunsee	1.0786E+07
0.9 to Topeka	1.0763E+07
1.1 to Topeka	1.0771E+07
0.9 to Deer Creek	1.0764E+07
1.1 to Deer Creek	1.0771E+07
0.9 to Oread	1.0775E+07
1.1 to Oread	1.0762E+07
0.9 to LKC_A	1.0761E+07
1.1 to LKC_A	1.0775E+07
0.9 to KC Base	1.0767E+07
1.1 to KC Base	1.0769E+07

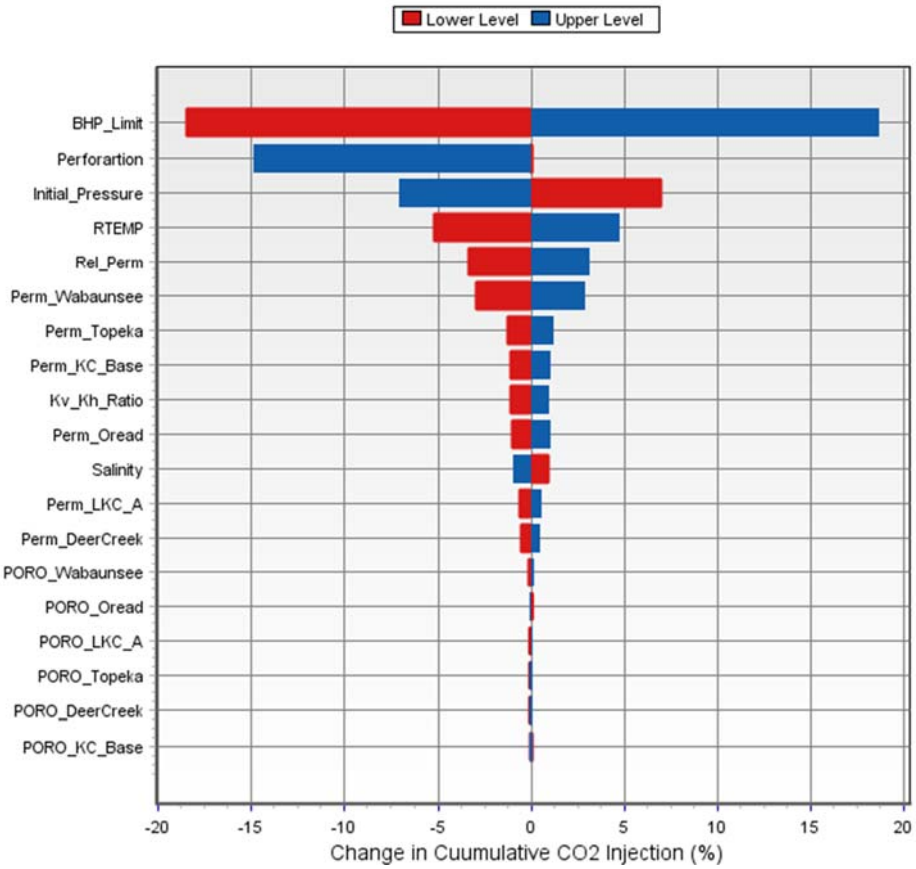

Figure 4-20. Tornado chart for sensitivity analysis. ±10% variation for the upper and lower level in each parameter except for the perforation intervals.

CO_2-Brine Relative Permeability

In terms of sensitivity to relative permeability, the CO_2-brine relative permeability curve described in Section 4.3.4 was modified to increase end-point relative permeability (Krg) at an irreducible water saturation (Sw=0.36) by ±10% from the Base Case for the Upper and Lower Case (see Figure 4-21). Brooks and Corey (1966) model was used to create the new relative permeability curves. Compared to the Base Case, this change in the relative permeability curves affected the mobility of injected CO_2 and consequently CO_2 storage in the target formations. The simulation results of both the Upper and Lower Case relative permeability curve increased and decreased the cumulative 10-year CO_2 injection by 3.2% and -3.4% from the Base Case, respectively.

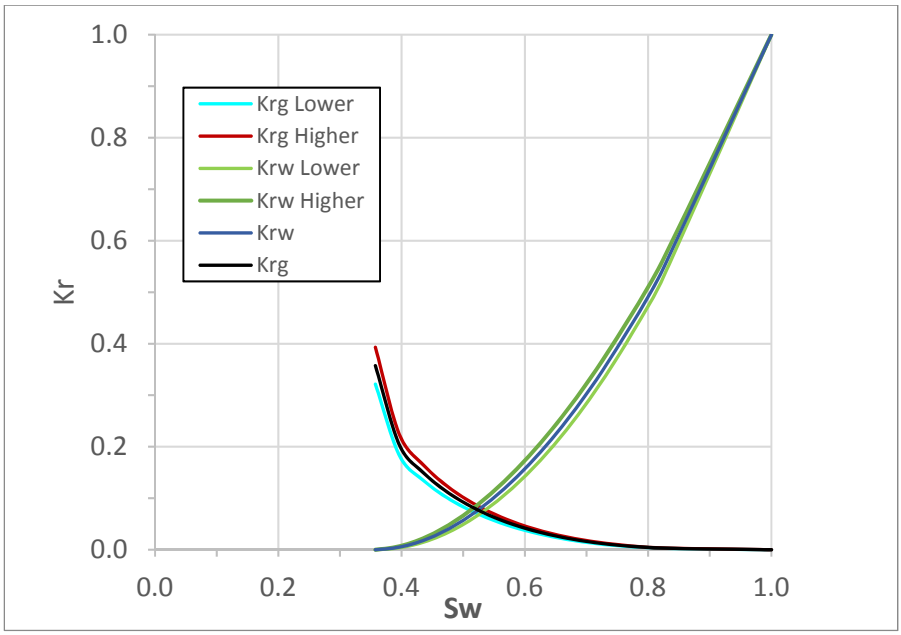

Figure 4-21. Relative permeability curves for Lower, Base, and Upper Case created by Brooks and Corey (1966) equation.

Permeability Anisotropy Ratio

The vertical anisotropy ratio (kv/kh) of permeability was assumed to be 0.3 in the Base Case. Two additional cases with the anisotropy ratios of 0.27 and 0.33 were performed to investigate the sensitivities of vertical permeability anisotropy to the results. With the anisotropy ratio of 0.27 (Lower Case), the cumulative CO_2 injection amount at the end of 10-year injection period was reduced by 1.1% from the Base Case. Similarly, the Upper Case (kv/kh=0.33) increased the injection amount by 1%.

Reservoir Temperature

The Base Case in this work assumed the isothermal reservoir temperature of 93 °F which was estimated from the geothermal gradient from the reservoir temperature of the Sleepy Hollow oil reservoir. Simulation cases with ±10% variation in the reservoir temperature of 102.3 °F (Upper) and 83.7 °F (Lower case) were run to examine the effect of reservoir temperature on the results. Given the pressure range in the model, the isothermal case with the decrease of 9.3 °F in the reservoir temperature caused the increase in CO_2 density and viscosity especially at the shallow formations, therefore leading to less buoyant force (or vertical migration) and mobility (lateral migration). As a result, decrease in injectivity occurred due to the lower reservoir temperature compared to the Base Case. The opposite occurred with the increase of reservoir temperature. The effect of reservoir temperature on the 10-year injection amount was -5% (Lower Case) and 4.7% (Upper Case) from the Base Case, which was not negligible.

Perforation Intervals

The Base Case assumed the application of perforation intervals in the entire saline formations. By excluding (or closure of) the perforation interval of each formation sequentially, the effect of each storage formation was investigated. Compared to the Base Case, the closure of perforation interval in the Kansas City Base is significant. Consistent with the simulation results with three-injector case in Section 3.2, LKC B, D, E, and F zones did not affect the results at all.

BHP Constraint

Due to no fracture pressure data available, 90% of lithostatic pressure was assumed for the BHP constraint controlling maximum injection rates in the Base Case. After ±10% change in the BHP constraint, both Lower and Upper Case with the BHP constraint caused the increase and decrease accordingly in the cumulative 10-year CO_2 storage by slightly more than 18.5%, which makes the BHP constraint the most sensitive.

Initial Reservoir Pressure

According to the under-pressured reservoir condition found at the Sleepy Hollow oil reservoir, the Base Case model assumed a 16% under-pressured reservoir compared to the hydrostatic gradient. The sensitivity runs included ±10% variation in the initial reservoir pressure at the reference datum. That is, the Lower Case represents further under-pressured reservoir and widens the injection window between the initial reservoir pressure and BHP constraint, which would allow more CO_2 injection. Whereas, the Upper Case with the 10% higher initial pressure at the reference datum would narrow the injection window. The simulated cumulative CO_2 injection showed that there is 7% increase in the Lower Case and a similar decrease in the Upper Case.

Permeabilities

The permeabilities of six major storage formations (Wabaunsee, Topeka, Deer Creek, Oread, LKC A, and Kansas City Base) were modified and examined separately. Uniform multiplication factors of 0.9 (Lower Case) and 1.1 (Upper Case) were applied to each formation. The simulation results show that there is a positive correlation between the multiplication factor and the greatest impact (±2.9%) occurred within the Wabaunsee formation. Deer Creek showed the smallest impact (±0.5%) with respect to the permeabilities.

Salinity

Compared to the Base Case (70,000 ppm), the cumulative CO_2 injection amount was negatively correlated to the change in salinity. Approximately 1% increase in the cumulative injection occurred at the end of the 10-year injection period due to the 10% decrease in salinity. The opposite took place when the salinity increased by 10%

Porosities

Similar to the sensitivity analysis of permeabilities, sensitivity analysis also included the effect of porosities in six storage formations. The porosities of each formation increased and decreased by 10% separately. According to the simulation results, a ±10% change in the porosities of each formation was the least sensitive parameter to the CO_2 injection.

4.5 Conclusions

This report has been prepared to numerically investigate the pre-feasibility of saline CO_2 sequestration in the sub-basinal area encompassing the Sleepy Hollow oil field in Red Willow County, southwestern Nebraska. Dynamic simulations were run based on the static earth model described in Section 3. The simulations included different well location configurations, and the sensitivity analysis. The following conclusions are drawn based on the results of these efforts:

- The simulation results with a single injector show very good injectivity performance. INJ #2 could inject approximately 34.8 million metric tons after 30 years resulting in an average injection rate of 3,177 metric tons per day.
- No single-well injection case could achieve the storage target (50 million metric tons for 30 years); a multi-injector system is required.
- Due to the pressure buildup and significant inter-well interference, the two-injector system was not able to meet the injection target either.
- At least three injection wells are required to satisfy the injection target in the study area. Best results were obtained when using INJ #1, #2, and #5.
- In general, the CO_2 plume tends to grow radially centered from each injector. With the injectors of #1, #2, and #5, the entire CO_2 plume extends approximately 9 km in the East-West direction and 11 km in the North-South direction after 30-year injection.
- Major CO_2 storage occurs at Wabaunsee (26%), Kansas City Base (19%), Topeka (18%), Oread (15%), LKC A (8%), and Deer Creek (6%).
- Simulated plume migration suggests that the static model should be extended further laterally in the future work with new additional data. Upscaling/coarsening should also be applied appropriately in order to not lose the details of the CO_2 plume, especially near the plume edge.
- In addition to the Base Case, the simulation work to examine the effects of various parameters reveals that simulated injectivity appears to be more sensitive to BHP constraint, perforation of Kanas City Base, initial reservoir pressure, reservoir temperature, CO_2-brine relative permeability, and permeability of Wabaunsee. Effects of vertical permeability anisotropy, salinity and permeabilities of Topeka, Deer Creek, and Oread were found to be less but non-negligible. Whereas, sensitivity to porosity seems to be negligible.
- Due to the lack of interest in the saline aquifers, there is almost no data available for the potential saline formations in the study area. Non-negligible parameters identified from the sensitivity analysis need to be taken into account in the future work in order to reduce the major uncertainties.

The output from the ECLIPSE simulations will be combined with well data collected to during the geologic modeling (Section 3) to develop a risk assessment model using the NRAP IAM CS model.

5 Assessment of the Area of Review for the Sleepy Hollow Field using the NRAP-IAM-CS

5.1 Introduction

U.S. Environmental Protection Agency's (EPA's) Class VI regulations require owners or operators of carbon storage projects to determine an Area of Review (AoR) representative of project risk to underground sources of drinking water (USDWs). The AoR is an estimate of the region potentially impacted by the CO_2 injection and is used to develop monitoring plans to ensure protection of USDWs. Estimates of the AoR need to account for the physical and chemical properties of all phases of the injected carbon dioxide stream, are based on available site characterization, monitoring, and operational data, and are to be made with computational models (40 CFR 146.84). Permitting also requires an understanding of the leakage risks from leakage pathways, such as wells and/or faults connecting the storage reservoir with any overlying underground sources of drinking water (USDWs). Environmental Protection Agency's (EPA) Class VI Rule requires groundwater geochemistry monitoring above the lowermost confining zone overlying the storage reservoir to detect changes in aqueous geochemistry resulting from fluid leakage out of the injection zone [40CFR 146.90(d)] (U.S. Environmental Protection Agency, 2012).

The NRAP-IAM-CS is a science-based toolset developed by the U.S. Department of Energy (DOE) for quantitative risk assessment of geologic sequestration of carbon dioxide (CO_2) (Pawar et al., 2016). The toolset adopts a stochastic approach in which predictions address uncertainties in storage reservoirs, leakage scenarios, and shallow groundwater impacts. It is derived from detailed physics and chemistry simulation results that are used to train more computationally efficient models, referred to here as reduced-order models (ROMs), for each component of the system. These tools can be used to help regulators and operators define the AoR and better understand the expected sizes and longevity of changes in water quality caused by CO_2 and brine leakage from a storage reservoir into drinking water aquifers.

The EPA defines the AoR as the maximum extent of the separate-phase CO_2 plume or the pressure front over the lifetime of the project as estimated by numerical model simulations. Generally, the maximum pressure front defines the AoR because it is larger than the supercritical CO_2 plume. The AoR is often delineated by the area within which the maximum pressure buildup is above the pressure needed to move the reservoir fluids up an open wellbore into the lowest USDW (U.S. EPA, 2013). This approach is conservative and assumes that any leakage will impact USDW quality regardless of the magnitude and duration of the leak.

5.2 Organization

The NRAP-IAM-CS model was used to estimate the Area of Review (AoR) for the Sleepy Hollow Field in Nebraska. The chapter is organized into the following sections:

- Section 5.3 presents an approach to a risk-based AoR based on leakage impacts to groundwater quality in a shallow drinking water aquifer overlying the storage reservoir from hypothetical open (uncemented) wells;
- Section 5.4 presents the U.S. EPA suggested critical pressure method for calculating the AoR for the Sleepy Hollow Site;

- Section 5.5 presents application of the NRAP-IAM-CS tool to the Sleepy Hollow site to determine impacts to groundwater quality in a shallow drinking water aquifer overlying the storage reservoir from leakage through hypothetical open (uncemented) wells.

5.3 Risk-Based Approach for Determining the Area of Review (AoR)

The risk-based AoR calculated using the NRAP-IAM-CS is the area where CO_2 or brine leakage from a hypothetical open borehole connecting the storage reservoir to the shallow drinking water aquifer would cause drinking water quality to change outside "no-net degradation" thresholds. For the Sleepy Hollow Field, the "no-net-degradation" threshold is pH = 6.6 and total dissolved solids (TDS) = 420 ppm (i.e., pH not less than 6.6 and TDS not greater than 420 ppm). The boundaries of the AoR are calculated by calculating pH and TDS in the shallow drinking water aquifer at hypothetical open wells located at increasing distances to the east, west, north, and south of the injection wells until no impact to the aquifer is observed. CO_2 or brine leakage at a location beyond the AoR boundary is possible, but the leaked mass may be too small to cause pH or TDS to change outside their threshold values

5.3.1 Description of NRAP-IAM-CS and Assumptions

The NRAP-IAM-CS is an integrated system model developed by the U.S. Department of Energy for use in performance and quantitative risk assessment of geologic sequestration of carbon dioxide (CO_2) (Pawar et al., 2016). The model components include a primary CO_2 injection reservoir, potential leakage pathways, and receptors such as shallow aquifers. The model is designed to perform probabilistic simulations related to the long-term fate of a CO_2 sequestration project. A stochastic framework at the system level allows NRAP-IAM-CS to be used to explore complex interactions among large numbers of uncertain variables and helps evaluate the likely performance of potential sequestration sites. The model samples values for each uncertain parameter from probability distributions, leading to estimates of global uncertainty that accumulate as the coupled processes interact during a simulation. NRAP-IAM-CS is designed to link together many different processes (e.g., subsurface injection of CO_2, CO_2 migration, leakage, and shallow aquifer impacts) required in the analysis of long-term CO_2 storage in geologic reservoirs. The underlying processes can be simulated using reduced-order models (ROMs) developed for the components in the IAM. Details of the NRAP-IAM-CS are provided in the software users manual (Stauffer, et al., 2016). The risk-based AoR calculation uses spatial and temporal distributions of CO_2 saturations and pressures within the storage reservoir from a multi-phase numerical reservoir flow simulator that was used to predict CO_2 plume evolution as input to a site-specific open wellbore ROM and a shallow groundwater ROM developed with NRAP-IAM-CS (Figure 5-1). For this project the results of the ECLIPSE simulations in Section 4 were used as inputs into the NRAP-IAM-CS

model.

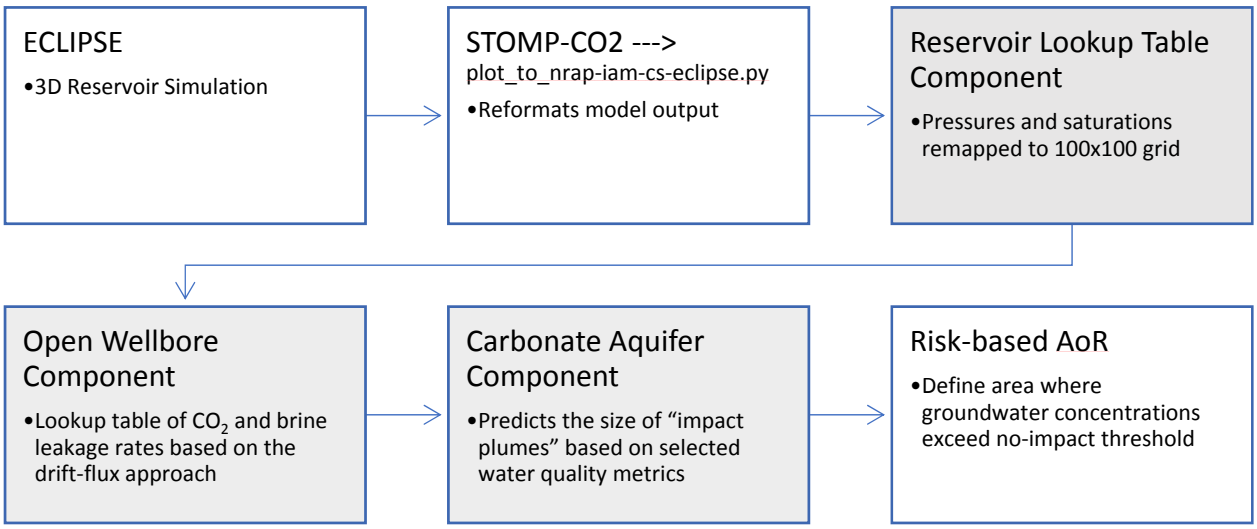

Figure 5-1. Components of the risk-based AoR approach (grey components are part of the NRAP-IAM-CS system model).

The *open wellbore model* (used to calculate CO_2 and brine leakage rates into a shallow aquifer and to the atmosphere) (Pan et al., 2011) is a multiphase and non-isothermal model that couples wellbore and reservoir flow of CO_2 and variable salinity brine. The model allows for the phase transition of CO_2 from supercritical phase to gaseous phase and accompanying Joule-Thompson cooling and exsolution of CO_2 from the brine phase. The model simulates CO_2 and/or brine leakage from the storage reservoir using inputs of pressure and CO_2 saturations from lookup tables. The CO_2 and brine fluxes from the open wellbore Reduced-Order Model (ROM) used to calculate groundwater impacts are qualitative, because leakage rates from the open wellbore ROM may exceed the range of values to which the carbonate aquifer ROM was calibrated (Table 5-1). Additional parameters needed for the wellbore leakage and aquifer impact calculations are shown in Table 5-2.

It is very important to note that *open wellbore model* assumes that the wellbore is completely open – meaning that the annular space outside the casing is completely devoid of cement or other material. The assumption of a completely open borehole that penetrates the storage reservoir and connects it to the shallow drinking water aquifer can lead to unrealistically high leakage rates (flux of brine and CO_2) and aquifer impacts (resulting from chemical constituent concentrations in the shallow drinking water aquifer). However, this assumption is consistent with EPA's guidance for calculating the Area of Review.

The *unconfined carbonate aquifer ROM* (used to estimate the impacts of CO_2 and brine leaks to the drinking water aquifer) (Keating et al., 2016a) predicts the impacted volume of shallow drinking water using nine water quality parameters. The unconfined carbonate aquifer ROM is the only USDW ROM available in NRAP-IAM-CS. NRAP is currently adding a confined alluvium aquifer ROM. In this analysis two of the nine parameters (pH and TDS) were used. pH and TDS plume volumes below the no-impact threshold were assumed to be consistent with EPA guidelines for no-net degradation. More information on how the

threshold values were determined can be found in Last et al. (2016). Adjustable input parameters, including permeability mean, variance, correlation length and anisotropy, aquifer thickness and horizontal hydraulic gradient were based on site characterization data where possible.

Table 5-1. Carbonate Aquifer ROM wellbore leakage parameter maximum values.

Parameter	Maximum Value	Unit
CO_2 leak rate	500	gram/s
Brine leak rate	75	gram/s
Cumulative CO_2 mass leaked	500	kTon
Cumulative Brine mass leaked	100	kTon

Table 5-2. NRAP-IAM-CS Input Parameters for Sleepy Hollow Field.

Parameter	Value
Surface elevation	2507 ft AMSL [764.13 m]
Depth to top of the USDW	150 ft [45.72 m]
Thickness of the USDW	100 ft [30.48 m]
Pressure in the USDW	65 psia [0.45 MPa]
Temperature in the USDW	53 ^{o}F [11.67 ^{o}C]
Mean Permeability in the USDW	5000 mD [4.93e-12 m^2]
Mean Porosity in the USDW	0.25
Salinity in the USDW	325 ppm
Depth to the top of the Reservoir	2879 ft [877.52 m]
Initial Pressure of the Reservoir	1345 psia [9.27 MPa]
Temperature of the Reservoir	91.4 ^{o}F [33 ^{o}C]
Mean Permeability of the Reservoir	78 mD [7.7e-14 m^2]
Mean Porosity of the Reservoir	0.06
Salinity of the Reservoir	100,000 ppm

For the reservoir component, lookup tables for NRAP-IAM-CS were created using the plot_to_nrap-iam-cs-eclipse.py script. Because this script expects STOMP plot files as input, the 3D reservoir simulations results performed with the Eclipse code were input to STOMP-CO2 and then written out in STOMP-CO2 plot file format. The STOMP-CO2 plot files were cropped in the horizontal direction to the 6 km by 9.5 km area representing the Sleepy Hollow Oil Field boundary. The data were then translated onto a specified grid (100x100 cells) and converted to SI units. Finally, the plot_to_nrap-iam-cs-eclipse.py script writes the data to the appropriate file format expected by the NRAP-IAM-CS. Simulated CO_2 saturations and pressures for 30-years of CO_2 injection and 10 years post-injection with a total injection of 50 MMT CO_2 were thus converted to a format acceptable to the NRAP-IAM-CS.

Only one horizontal plane is extracted from the reservoir simulation results for use in the NRAP-IAM-CS calculations. For this application, reservoir pressures and gas saturations for all nodes of the Eclipse model at two-year time steps from 0 to 10 years, 5-year times steps from 15 years to 30 years, and

yearly timesteps from 32 to 40 years were used. For Sleepy Hollow, values from Layer 21 of the Eclipse model (Layer 162 in the STOMP model) were extracted. This layer was selected because it had the highest pressure (gradient) and largest CO_2 plume. This should translate to the largest AoR. The elevation of the top of the reservoir was extracted from the grid data and translated to the new grid locations.

The initial pressure in the extracted layer of the model was 7.5 MPa (1088 psi). The initial gas saturation over the entire model domain was 0. Figure 5-2 through Figure 5-5 show the interpolated pressures and CO_2 saturations at 30 years (the end of the injection period) and 40 years (the end of the modeled post-injection period).

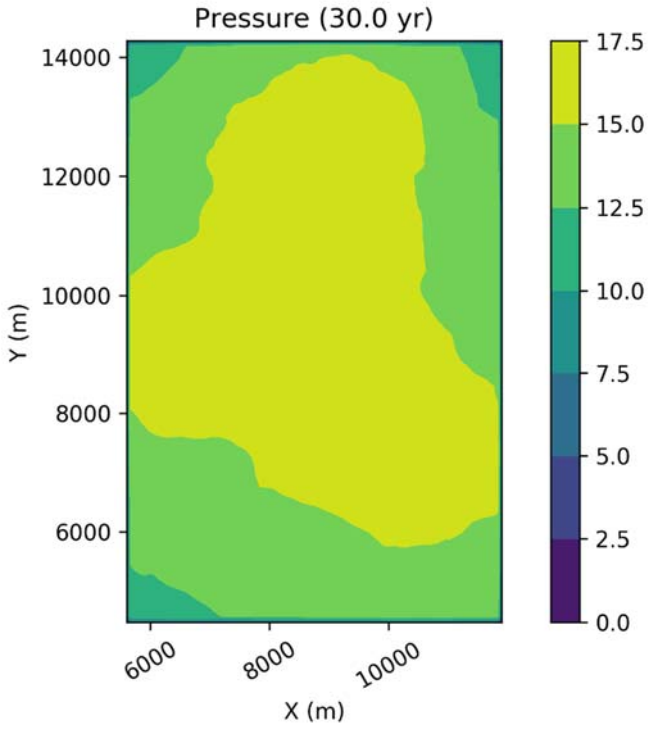

Figure 5-2. Pressure distribution in MPa for Eclipse model layer 21 at time 30 years interpolated to a 100x100 grid.

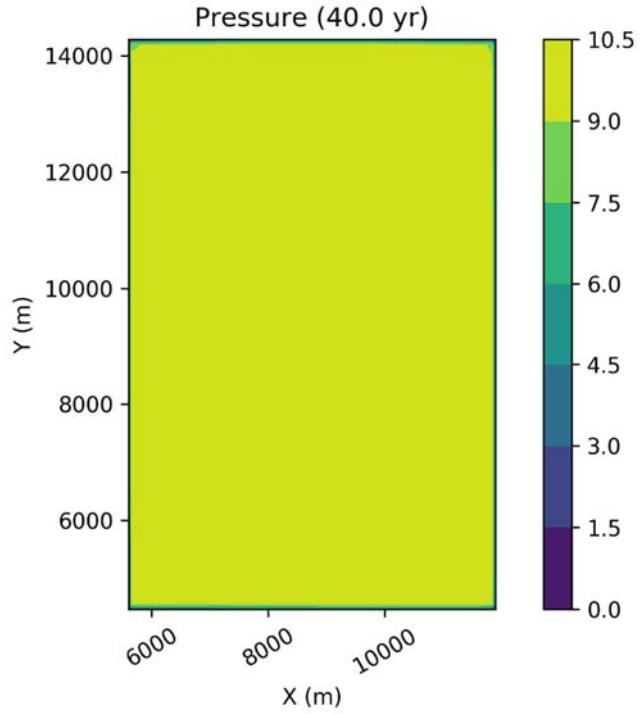

Figure 5-3. Pressure distribution in MPa for Eclipse model layer 21 at time 40 years interpolated to a 100x100 grid.

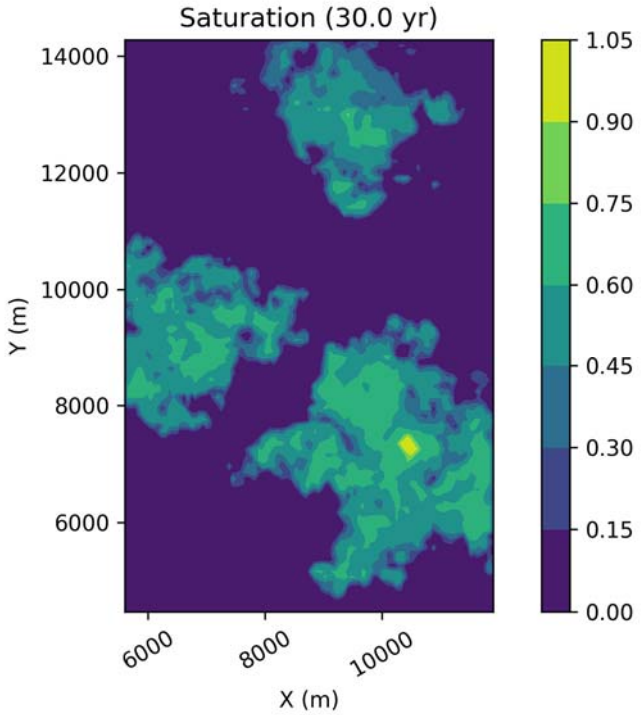

Figure 5-4. CO_2 gas saturation distribution Eclipse model layer 21 at time 30 years interpolated to a 100x100 grid.

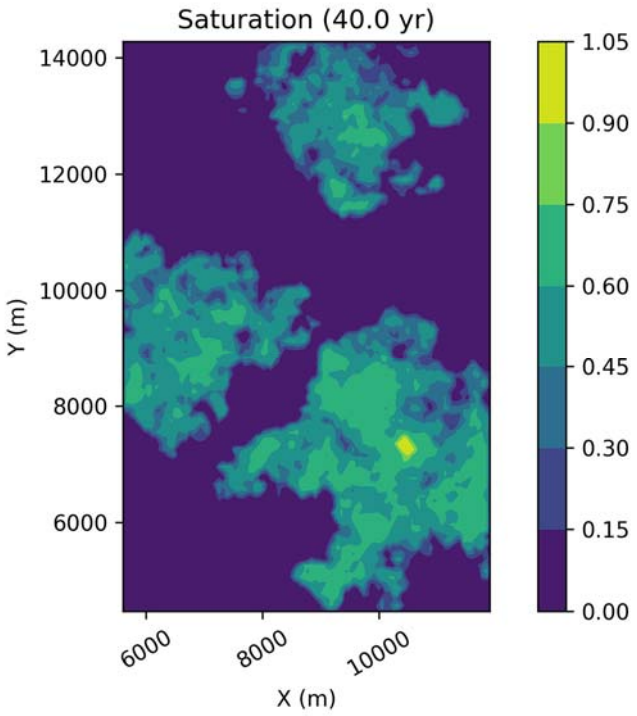

Figure 5-5. CO_2 gas saturation distribution for Eclipse model layer 21 at time 30 years interpolated to a 100x100 grid.

5.4 Critical Pressure Calculations

Currently, the EPA provides guidance to operators of CO_2 storage sites for approaches to determining the critical pressure that should be used to define the pressure front that is considered in the AoR delineation (U.S. EPA, 2012). The following approach was taken to determine a critical pressure for the Sleepy Hollow site.

The critical pressure corresponds to the critical (minimal) pressure needed to move fluids from the reservoir into a USDW through a hypothetical open conduit, such as an uncemented well (U.S. EPA, 2012). The first step is to use a method that is applicable to reservoirs that are hydrostatic or underpressurized prior to the injection of CO_2 (Birkholzer et al., 2011). This method assumes that the density of the fluid in the wellbore is uniform and equal to the density in the injection zone. Equation 5-1 can be used to calculate the necessary increase in pressure in the reservoir to equalize the hydraulic head between the injection zone and the USDW.

$$\Delta P_{if} = P_u + \rho_i g \cdot (z_u - z_i) - P_i$$

Equation 5-1

where:

P_u is the initial pressure in the USDW (Pa= kg·m^{-1}·s^{-2}),

ρ_i is the density of the injection zone fluid (kg/m^3),

g is the acceleration of gravity (m/s^2),

z_u is the depth to the base of the lowermost USDW (m),

z_i is the depth to the top of the injection zone (m), and

P_i is the initial pressure in the injection zone (Pa)

A positive value of $\Delta P_{i,f}$ (Equation 5-1) corresponds to an injection reservoir that is under-pressurized relative to the USDW (i.e., a downward hydraulic gradient exists between the USDW and the injection zone). The reservoir overpressure would need to increase to values equal to or above $\Delta P_{i,f}$ to move reservoir fluid into the drinking water aquifer. A $\Delta P_{i,f}$ value of zero corresponds to the hydrostatic case. A negative value of $\Delta P_{i,f}$ indicates an over-pressurized injection zone relative to the USDW, where reservoir brine has the potential to migrate to the drinking water aquifer prior to any CO_2 injection.

Using Equation 5-1 and the parameters in Table 5-3, a critical pressure of -0.211 MPa (-30.6 psi) was calculated for the Sleepy Hollow site. The negative critical pressure indicates that the reservoir is slightly over-pressurized relative to the USDW. Some over-pressurization within the injection zone may be allowable without causing sustained fluid leakage, owing to the density differential between the fluids in the injection zone and USDW. In such cases, a second method, shown in Equation 5-2, can be used to estimate the pressure needed to displace the existing fluid in the borehole and create leakage into the USDW. Equation 5-2 assumes that below the calculated "threshold" pressure, no leakage into the USDW will occur (Nicot et al, 2009). Using Equation 5-2, a threshold pressure of 0.303 MPa (44 psi) was calculated for the Sleepy Hollow site. Because the value of ΔP_c using Equation 5-2 is greater than the value of $\Delta P_{i,f}$ using Equation 5-1, the difference in magnitude between the two may be used as an estimate of the allowable pressure increase, subject to the assumptions used to derive Equation 5-2 (see Nicot et al, 2009). This results in an allowable pressure increase of 0.092 MPa (13.4 psi), (0.303 MPa – 0.211 MPa) which can be used to define the AoR.

$$\Delta P_c = \frac{1}{2} \cdot g \cdot \xi \cdot (z_u - z_i)^2$$

Equation 5-2

where:

g is the acceleration of gravity (m/s^2),
z_u is the depth to the base of the lowermost USDW (m),
z_i is the depth to the top of the injection zone (m),
ρ_i is the fluid density in the injection zone (kg/m^3),
ρ_u is the fluid density in the USDW (kg/m^3), and
$\xi = \frac{\rho_i - \rho_u}{z_u - z_i}$ (kg/m^2)

Table 5-3. Inputs for Critical Pressure and Threshold Pressure Calculations (Equations 5-1 and 5-2).

Input Parameter	Value
Depth to top of injection zone (m)	877.5
Depth at base of the lowermost USDW (m)	61
Initial Pressure in Injection Zone (MPa)	9.27
Initial Pressure at the base of the lowermost USDW (MPa)	0.448
Fluid Density in the Injection Zone (kg/m^3)	1,075.8
Fluid Density in the USDW (kg/m^3)	1,000
Critical Pressure from Equation 5-1 (MPa)	-0.211
Threshold Pressure Increase from Equation 5-2 (MPa)	0.303
Allowable Pressure Increase (Threshold Pressure + Critical Pressure) (MPa)	0.092

5.4.1 Application of NRAP-IAM-CS to Determine Risk of Brine Leakage at the Sleepy Hollow Site

Because the reservoir is over-pressurized relative to the USDW, brine leakage will be the controlling factor in determining the AoR. Pressure buildup from the injection activities creates increased risk for brine to migrate to the USDW. The NRAP-IAM-CS was used to determine the impact to the USDW from brine leakage through a hypothetical open wellbore at several locations within the model domain (Figure 5-6 and Table 5-4). These wells were placed at the corners of the domain where the maximum pressure is the lowest (see Figure 5-2) and there is no CO_2 plume footprint. These locations should represent those areas with the lowest risk of impact to the USDW. Figure 5-7 shows the modeled reservoir pressure with time (and the maximum pressure differential shown in parenthesis) at the four hypothetical well locations. Note that the pressure differential at all four well locations is above the allowable pressure threshold of 0.092 MPa. Therefore, there is a risk of brine leakage through an open wellbore at these well locations. Figure 5-8 shows the brine leakage rates calculated by the NRAP-IAM-CS at the four hypothetical well locations and Figure 5-9 shows the cumulative mass of brine leaked. The NRAP-IAM-CS was not able to calculate the impact to the USDW at these locations because the leakage rates and cumulative mass leaked were greater than the maximum values for which the carbonate aquifer ROM was developed. Efforts are currently underway to develop an aquifer ROM that will accept higher values for leakage rates.

In order to estimate an AoR based on the risk of brine leakage at Sleepy Hollow Field, the model domain needs to be expanded such that there are areas within the model domain where the maximum pressure buildup is less than the pressure threshold of 0.092 MPa. Hypothetical wells can be placed in these areas and the NRAP-IAM-CS can be used to determine brine leakage rates and impact to the USDW.

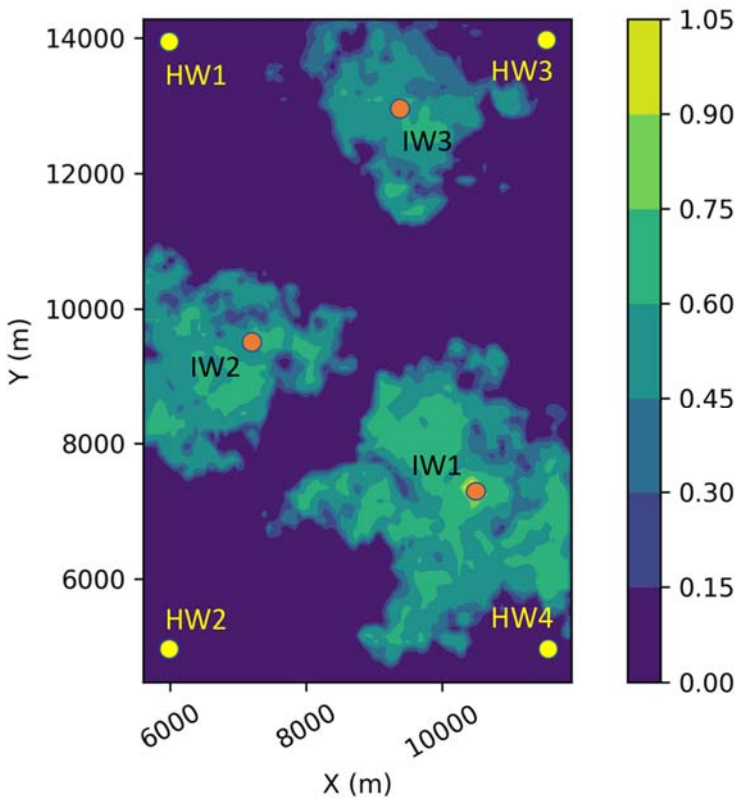

Figure 5-6. Locations of hypothetical wells superimposed on the gas saturation contour plot for year 30. The grid has units of meters.

Table 5-4. Locations of hypothetical open wells.

Hypothetical well Locations		
	x(m)	y(m)
Well 1	6000	14000
Well 2	6000	5000
Well 3	11500	14000
Well 4	11500	5000

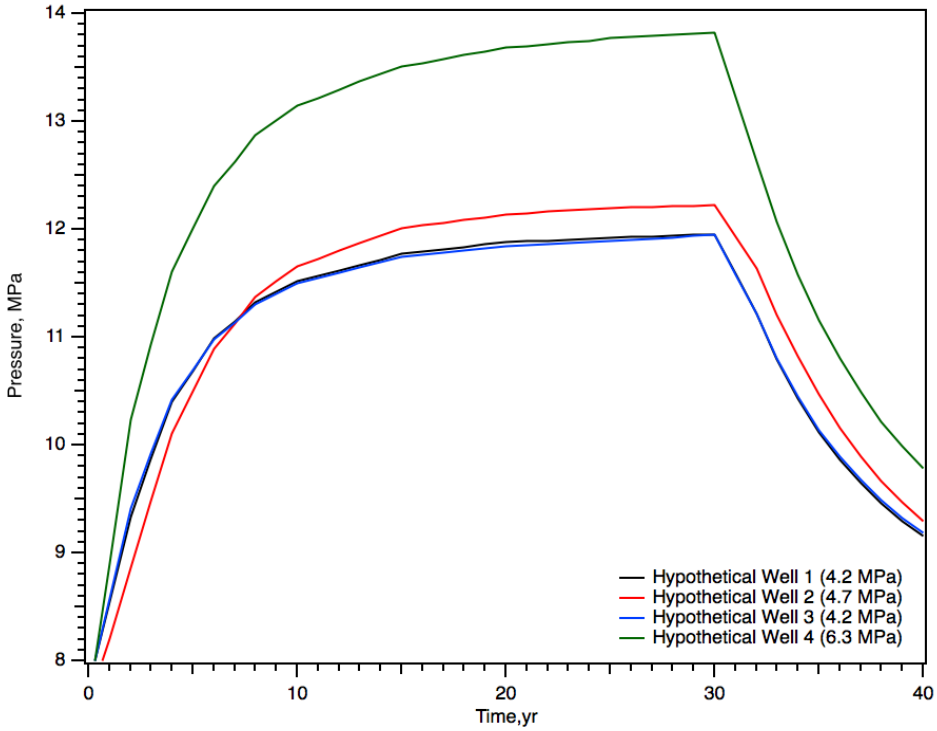

Figure 5-7. Pressure vs. time at each hypothetical well location. The maximum pressure difference is shown in parenthesis for each well.

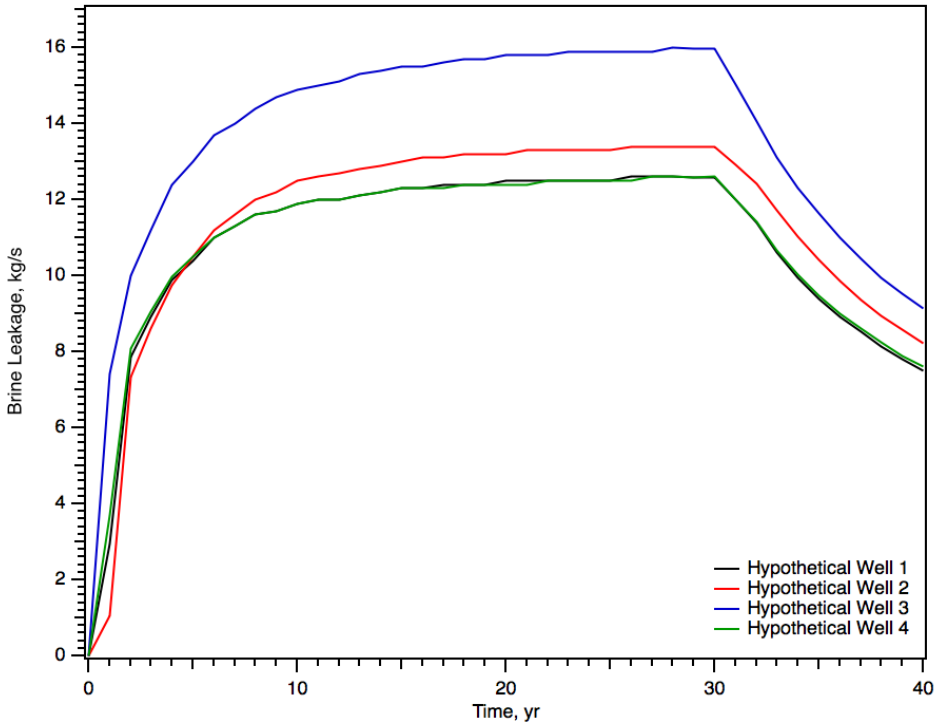

Figure 5-8 Brine leakage rates (kg/s) over time at hypothetical well.

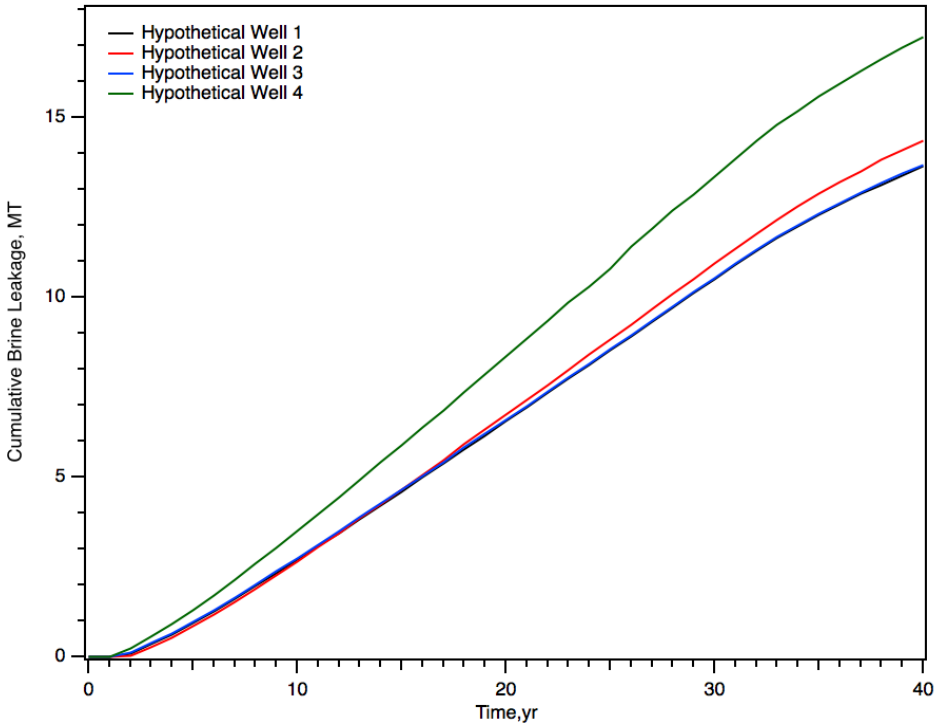

Figure 5-9. Cumulative mass of brine leakage (MT) over time at hypothetical well locations.

5.5 Summary and Conclusions

The NRAP-IAM-CS can be used to determine the AoR based on the impact to the USDW from CO_2 and/or brine leakage from the storage reservoir. In the case of the Sleepy Hollow site, estimation of the critical pressure based on EPA's suggested methods resulted in a determination that the reservoir was slightly over-pressurized relative to the USDW. Therefore, delineation of the AoR using that approach would result in an area defined by the maximum pressure buildup of 0.092 MPa. Simulation results from the Eclipse simulator provided the pressure and saturation distributions used by the NRAP-IAM-CS for determining CO_2 and brine leakage and impact to an overlying aquifer, the USDW. However, there were no locations within the Eclipse model refined area at which there was no impact to the USDW from CO_2 or brine leakage. This means that the AoR would be larger than the 9.5 km by 6 km area defined by the fine resolution grid of the Eclipse model. Extension of the model has been suggested for future simulation work and is needed to determine an AoR using both the EPA suggested approach and the risk-based approach using the NRAP-IAM-CS.

5.6 Recommendations

The NRAP-IAM-CS toolset was released in 2017. The strength of the toolset is the ability to perform probabilistic assessments that account for the uncertainty of the storage complex. This work represents some of the first applications of the tools to potential CO_2 storage sites. The following recommendations to the toolset could advance its use for the determination of probabilistic assessments of risk-based AoR and leakage from legacy wells on quality to USDWs.

- The AoR calculations would be more robust if the toolset could sample pressures and CO_2 saturations from many 2D planes within the reservoir. This is particularly important for stacked storage reservoirs where stratigraphic heterogeneity will control pressure and CO_2 gas

saturations. A ROM specific to the site reservoir would further improve a probabilistic assessment of the AoR.

- USDW ROMs need to be calibrated against the high leakage fluxes generated from open wellbores. All USDW ROMs were calculated for cemented wellbores, where leakage is controlled by the permeability of damage zones within the completed wells.
- The NRAP-IAM-CS currently has one option for a USDW ROM, the unconfined carbonate aquifer, where CO_2 leaks to the aquifer and to the atmosphere. NRAP is updating the toolset with a confined alluvium aquifer in which all CO_2 leaked stays within the aquifer system. The alluvium aquifer may be a better match for this site.

6 CO_2 Capture and Transport

6.1 Introduction

This section describes the infrastructure requirements and considerations for CO_2 capture and transport in the IMSCS-HUB study area. The general process design requirement is to compress and dehydrate a nominal 4,600 tonnes or more a day of 99%+ pure CO_2 from ethanol plant fermenters and transport the compressed CO_2 to an injection wellhead located approximately 180 to 400 miles (straight-line distance) away from the capture facility. The compressed CO_2 would then be injected into an underground formation. The goals of the capture and transport assessment were:

- Define the requirements for capturing CO_2 from the Columbus, Nebraska ADM Ethanol Plant as well as, more generally, non-ethanol sources.
- Define the infrastructure and pipeline needs for far-field (source-to-sink) transport.
- Identify sensitive areas and populations that may be affected by the IMSCS-HUB

A significant factor for the cost of a CCS project are capture costs, which generally account for 70-90% of the overall project expense (Global CCS Institute, 2014). Capture equipment is largely dependent on the type (i.e., purity) of source. The current project is focused mainly on developing a storage corridor for CO_2 derived from ethanol production, a process that generates a relatively pure form of CO_2. As a result, capture costs using existing technologies are much lower than other sources of CO_2, typically between \$21 and \$27 per tonne of CO_2, compared to \$60 to \$200 per tonne for various other industrial sources (Global CCS Institute, 2017).

CO_2 transportation involves moving CO_2 from the capture facility to the storage area(s), a process that often involves transporting CO_2 hundreds of miles. For commercial-scale CO_2 projects with sources that are far afield of the selected storage sites, the most efficient method of on shore transport of captured CO_2 is in a super critical via pipeline (Gale and Davison, 2004; Svensson et al., 2004; Zhang et al., 2006; Han et al., 2015). The Nebraska-Kansas area offers a unique opportunity for early development of a stacked storage hub due to a high density of ethanol plants which have relatively low capture costs in comparison to other CO_2 sources.

6.2 Methods

This report integrates results from pre-feasibility efforts to characterize the capture and transport requirements for the midcontinent source corridor. Capture requirements were investigated using information provided to the project team by ADM. Near-field (at the source property) transport requirements were not addressed because the project team found that the potential storage formations were too shallow for efficient storage. However, the pipeline pressures and diameters would likely be similar to those described in this report. Far-field transportation (to storage sites far from the source) was investigated using several methods to determine design, routes, potential cooperation or conflict with existing industrial activities, safety, sensitive areas and other obstacles. First, the size and operating pressure of the pipeline were estimated through a literature review and modeling using Schlumberger's PIPESIM. Pipeline routing was completed using SimCCS (Middleton and Liebecki, 2009). An overview of existing CO_2 pipelines was determined through a review of the available literature. Property ownership along the pipeline was determined using publicly available parcel information with the modeled routes in ArcGIS. Pipeline safety was researched using the available literature. Finally, protected and sensitive areas were determined by researching the area using the criteria outlined in the National Environmental Policy Act (NEPA).

6.3 Capture Requirements

The initial source for the storage complex is ADM's ethanol production facility. ADM's ethanol plant in Columbus, NE, processes corn into a variety of feed and food products. The facility processes about 550,000 bushels of corn per day, primarily sourced within a hundred miles of the facility. The two ethanol plants (wet and dry mill) have the capacity to produce a total of 1.13 million gallons of ethanol per day making this facility the largest ethanol producer in Nebraska. The facility produces about 3,250 metric tonnes (Mt) of high purity CO_2 per day as a byproduct of ethanol production. Capture and conditioning of the CO_2 for the project do not require novel technology development. Capture will be accomplished using the same techniques being used at the Illinois Basin Decatur Project and the Illinois Industrial Carbon Capture and Storage Project. The CO_2 is greater than 99% pure after dehydration. Before dehydration, it contains less than 3% water by weight. The CO_2 will be collected from the corn-to-ethanol fermenters at atmospheric pressure and processed using inter-stage coolers and knock-out vessels to decrease temperature and remove moisture, leaving it dehydrated (less than 0.005% water by weight), making it ready for compression and pipeline transport. In Illinois, ADM uses a 3250 horsepower, 4-stage reciprocating compressor and a dehydration system that uses a triethylene glycol contactor (absorber)-regenerator, the IMSCS-HUB ethanol sources expect similar systems will be employed in Nebraska. Other ethanol sources in the project area (Table 6-1) are expected to have similarly pure streams of CO_2 after capture and dehydration. Two coal fired power plants are also being investigated as potential sources for the project. These power plants were selected because they are the largest CO_2 sources in the area and thus provide a stable source of CO_2. This section provides a description of the facilities, design requirements for a capture system, and a process design for capture at an ethanol and coal fired power plant.

Table 6-1. Ethanol sources and average annual emissions between 2011 and 2015.

No.	Facility	County	Rank - All Sources	Rank - Ethanol	2011 - 2015 Emissions (Mt CO_2e)		
					Total	Mean	St. Dev.
1	Archer Daniel Midland	Platte	4	1	5,863,690	1,172,738	38,824
2	Cargill Corn Milling N America	Washington	7	2	2,237,276	447,455	71,799
3	AGP Soy/Corn Processing	Adams	8	3	1,021,652	204,330	53,361
4	Green Plains Wood River	Hall	10	4	826,192	165,238	49,478
5	Chief Ethanol Fuels, Inc.	Adams	11	5	817,142	163,428	8,100
6	Flint Hills Resources, Fairmont	Fillmore	12	6	798,112	159,622	6,872
7	Valero Albion Plant	Boone	13	7	778,630	155,726	32,397
8	Green Plains Central City	Merrick	15	8	624,058	124,812	2,477
9	Abengoa Bioenergy of NE	Buffalo	16	9	573,838	114,768	13,523
10	Abengoa Bioenergy Co.	York	18	10	508,180	101,636	6,488
11	Green Plains ORD	Valley	19	11	403,842	80,768	2,265
12	Pacific Ethanol Aurora West	Hamilton	22	12	212,985	70,995	69,297
13	Elkhorn Valley Ethanol	Madison	24	13	316,339	63,268	5,773
14	Kaapa Ethanol	Kearney	26	14	304,608	60,922	4,099
15	AltEn	Saunders	29	15	51,140	51,140	-
16	Nebraska Corn Processing	Furnas	30	16	254,590	50,918	2,474
17	Trenton Agri Products	Hitchcock	32	17	224,025	44,805	2,806
18	Pacific Ethanol Aurora East	Hamilton	35	18	178,059	35,612	24,449
19	Gerald Gentleman Station[1]	Lincoln	1	-	43,809,788	8,761,958	451,204
20	Jeffrey Energy Center[1]	Pottawatomie[2]	Not included in Section 2				
All Facilities					**15,994,358**	**3,268,182**	**-**

1. Coal-fired power plants; 2. Kansas

6.3.1 Ethanol Surface Facility Description

The initial focus on collecting CO_2 at ethanol plants in the source corridor allows the project to focus on commercially proven techniques for CO_2 capture. In this project, CO_2 will be captured from an ethanol production plant in a process similar to the successful Illinois Basin Decatur Project (IBDP) and Illinois Integrated Carbon Capture and Storage Project (ICCS). Much of the discussion in this section is informed by the topical report from IBDP on CO_2 surface facility design and operation (IBDP, 2016). Ethanol production is a prime target for CO_2 capture because the fermentation process generates a high purity CO_2 with primarily water vapor as a contaminant, eliminating the need for complex and expensive gas scrubbing and cleanup. Furthermore, the capture and compression system may be able to piggyback off existing electricity, cooling water, and other utilities commonly available at ethanol plants.

At a high level, carbon dioxide from the fermenter needs to be compressed from near ambient pressures (about 14.7 psia) to the injection pressure at the wellhead plus pressure drops in the pipeline. In practice, the compression is done in multiple stages because the CO_2 will heat up as it is compressed, and it requires cooling between stages to avoid damaging the compressor (or the need for expensive materials of construction). Additionally, water condensation will damage compressors, so condensed water is removed prior to each compressor stage using a knock-out pot. As the CO_2 is pressurized, it will eventually become a supercritical fluid. At this point other equipment, such as multistage centrifugal pumps, can be more efficient than compressors in raising the pressure.

The pressurized CO_2 needs to be dehydrated before entering the pipeline to avoid the formation of hydrates that can plug the pipeline, and dehydration prevents water condensation which can cause corrosion issues. It is common to dehydrate pipeline gases using triethylene glycol (TEG), which is a liquid with a high affinity for water. Water vapor in the gas is pulled into the TEG stream in a contacting column, producing a dry gas for the pipeline. The TEG loaded with water is heated to boil off the dissolved water, and the TEG is then recycled in the system.

The overall capture and transport process requires significant electricity supply, as well as heat for the TEG recovery system. Interstage coolers for the compressors can be water cooled or air cooled, with air cooled heat exchangers generally being larger than water cooled. By co-locating the capture and compression system with the ethanol plant, it is likely that there will be access to electricity, heat, and cooling water utilities. If booster pumps are required in remote areas along the transport pipeline, electricity is commonly supplied with remote gas turbines.

6.3.2 Design Requirements

The design requirements for the compression facility will be impacted by the injection well permit for near field storage or the pipeline requirements for far field storage. The requirements will dictate a range of surface injection pressures, injection rates, and surface temperatures for the project. It is expected that the CO_2 pressure out of the compression facility will need to be in the range of 2,000 to 2,300 psia to overcome pipeline pressure drop and meet injection pressures without the need for booster pump stations along the pipeline. Pipeline specifications for water are generally around 30 pounds of water per million standard cubic feet (about 630 parts per million by volume) to avoid hydrate formation and corrosion from water condensation. Heat loss in the pipeline will also need to be considered in order to meet the injection temperature requirements, and a heater at the injection site may be necessary.

6.3.3 Conceptual Process Design: Ethanol Plant

Figure 6-1 provides a conceptual simplified schematic of the process for compression of CO_2 and delivery to the injection well. Carbon dioxide from the fermenter passes through a knockout pot to remove condensed water. The CO_2 then enters a blower which provides the first stage of compression. Blowers are typically cheaper to operate and more efficient that compressors, and inclusion of a blower can reduce the size and operating cost for downstream compressors. After the blower there is a cooler, and knockout pot to remove condensed water before the CO_2 enters the compressor. The compressor will have multiple stages with interstage coolers and knockout pots, just as after the blower. The type of compressor will be decided upon in the design stage; with reciprocating and screw compressors offering good turndown (regulation range) flexibility and typically short lead times. A centrifugal compressor may be more economical for larger flowrates but generally has less turndown flexibility.

The dehydration step may be performed between compression stages, where the lower pressure can lead to a less capital-intensive operation but is shown after the compressors for simplicity in this case. Once the CO_2 has reached sufficient density, it can be pumped efficiently with a multistage centrifugal pump to the final target pressure. The final design of the process will depend upon factors such as permit requirements, utility availability at the site, ethanol plant factors, capital versus operating budgets and constraints, project life and scale, and many other factors, and the final process design will incorporate these considerations.

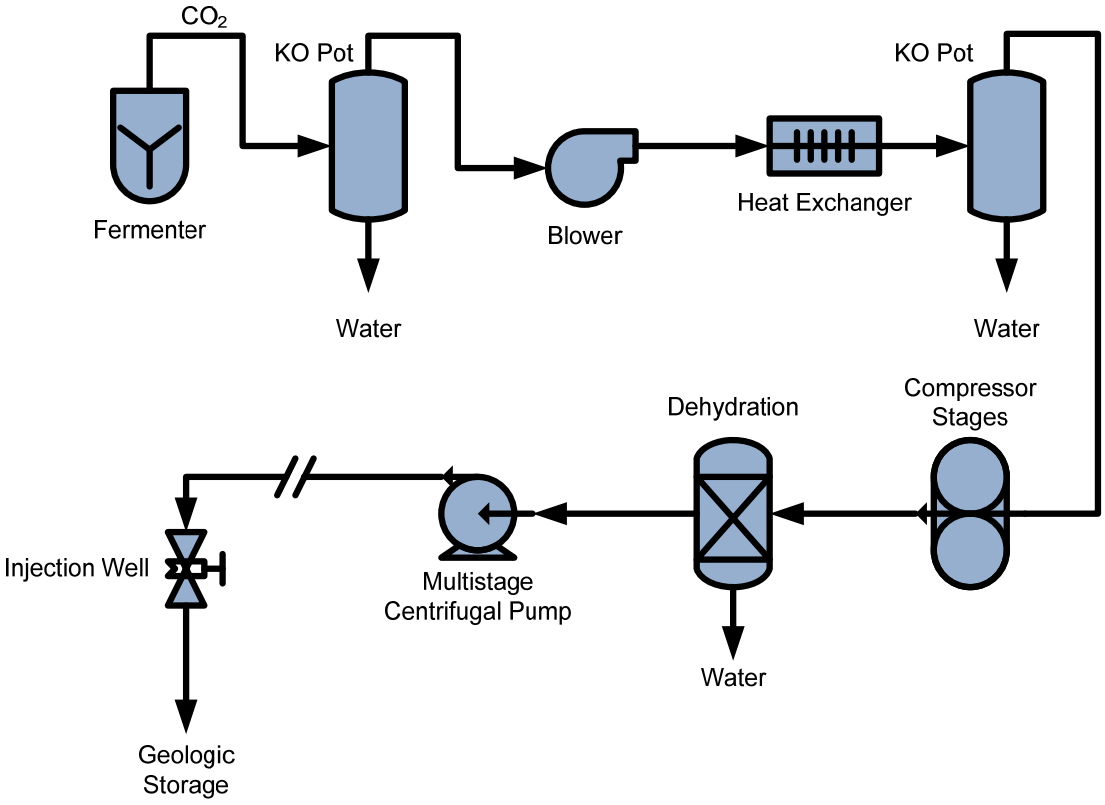

Figure 6-1. Conceptual simplified schematic illustrating the expected equipment for the CO_2 compression facilities.

6.3.4 CO_2 Capture from Coal-Fired Power Plants

The IMSCS-HUB will initially focus on CO_2 from ethanol plants in the region. However, for comparison included here is a general section here on capture from coal fired power plants which may be of interest

as the project progresses and plants such as Nebraska Public Power District's Gerald Gentleman Station add CO_2 to the IMSCS-HUB system. There are several power plant designs that could be used for both power production and simultaneous CO_2 capture. These include post-combustion capture, in which a CO_2 scrubbing system is added to the end of power plant flue gas stream (DOE/NETL, 2013); pre-combustion capture, in which fuel is converted into elemental hydrogen (H_2) and CO_2 and then separated so that the H_2 can be combusted while the CO_2 is sent to storage (DOE/NETL, 2015); and oxy-combustion capture, in which air is separated into elemental nitrogen (N_2) and elemental oxygen (O_2) and the fuel is combusted with O_2, resulting in a concentrated CO_2 stream which can be sent to storage (DOE, 2014). Each of these technologies has advantages and disadvantages under different circumstances. However, in their current state of development, these technologies are relatively expensive and have not been proven at full scale (Glier, 2015). A growing community of universities, government laboratories, and industrial partners is investigating CCS technology options in a collective effort to discover capture processes that will prove competitive with other electricity generation technologies in a carbon-constrained regulatory future. The CCS community is working to advance these technologies through pilot and demonstration phases towards commercialization.

The technology most suitable for application to the existing fleet of power plants or new pulverized coal power plants is post-combustion CO_2 capture technology. The plant configuration with post-combustion capture, shown in Figure 6-2, is the most likely to be technically viable as a retrofit option on existing power plants (DOE/NETL, 2010). This is an important consideration because a large portion of future power-sector CO_2 emissions will emanate from existing or new pulverized coal power plants, and post-combustion CO_2 capture may be a useful technology to reduce CO_2 emissions at these plants (ITFCCS, 2010). In addition, other industrial point sources account for a significant proportion (19%) of GHG emissions (IPCC, 2007) and post-combustion capture can also be applied to many of these industries, including those involved in the production of fuels, cement, pulp and paper, ammonia, iron, and steel (IPCC, 2014b; ITFCCS, 2010). Post-combustion CO_2 capture technologies are being developed in this context.

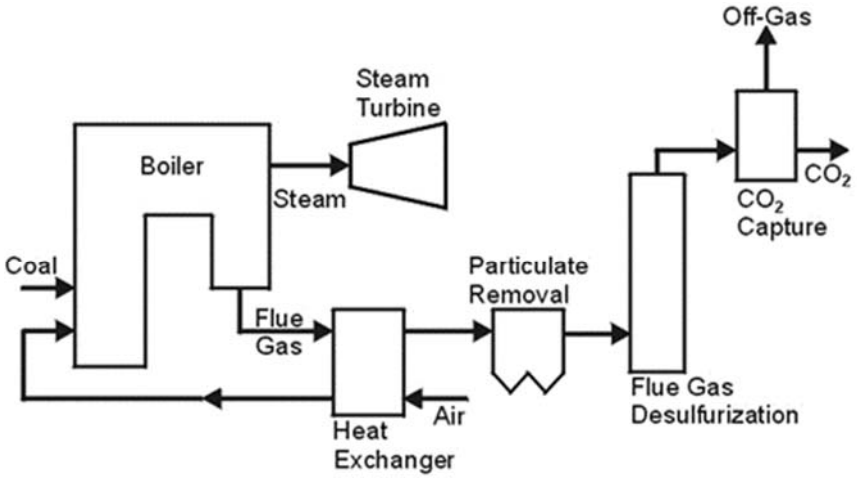

Figure 6-2. Simplified schematic of a coal-fired power plant with a generic post-combustion CO_2 capture system. Other major air pollutants (nitrogen oxides, particulate matter, and sulfur dioxide) are removed from the flue gas prior to CO_2 capture (Battelle, 2001).

Carbon capture research and development programs have expanded rapidly, this section attempts to synthesize key findings from the literature and from online databases which track and report on the status of CO_2 capture technology developments. Excellent publicly available databases and CCS project status reports are maintained by organizations such as the U.S. Department of Energy's National Energy Technology Laboratory (DOE/NETL), the International Energy Agency Greenhouse Gas Programme (IEAGHG), the Scottish Carbon Capture and Storage organization, and the Global Carbon Capture and Storage Institute. In many cases, the information from public databases and reports presented below has also been supplemented and checked by additional data from companies and research groups in capture technology development and testing. In each one of the sections below, the objective is to summarize the status of CO_2 capture technology developments.

Post-combustion CO_2 capture systems have been in use commercially for many decades, mainly in industrial processes for purifying natural gas streams; however, they have also been used on combustion-based flue gas. The first process for separating CO_2 from a gas stream was patented almost 90 years ago (USA Patent No. 1,753,901, 1930) using an amine solvent. Since that time, amine-based systems have remained the preferred method to meet CO_2 product specifications in industries ranging from natural gas production to the food and beverage industry (CO_2 Capture Project, 2008). There are hundreds of commercial aqueous systems currently in operation; most are used for removing acid gases from a product stream, and the captured CO_2 is typically vented to the atmosphere (Versteeg, 2012).

The history of commercialization has advanced liquid solvent-based scrubbing to the technological forefront in terms of readiness for CCS deployment at coal-fired power plants (Rochelle, 2009; Sintef, 2013). This commercial experience led to the first carbon capture and storage facility at the Mountaineer Power Plant in 2009. This facility captured 1.5% of the plant's emissions using Alstom Power's Chilled Ammonia Process (now owned by General Electric). Today, a number of vendors currently offer commercial post-combustion processes, including the Cansol® CO_2 capture system, the Fluor Daniel Econoamine FG Plus® process, the HTC Purenergy process, the Mitsubishi Heavy Industries KM CDR Process®, and the Shell carbonate slurry process.

Although several CO_2 capture systems have operated commercially for nearly two decades on a portion of power plant flue gases, it was not until 2014 that an integrated CO_2 capture and storage process had been applied to the full-scale flue gas stream of a modern coal-fired or natural gas-fired power plant at the Boundary Dam Integrated Carbon Capture and Storage Demonstration Project. Demonstration of post-combustion CO_2 capture at the commercial scale is widely regarded as crucial for this technology to gain acceptance by electric utility companies and by the institutions that finance and regulate power plant construction and operation.

Several large-scale CCS projects are actively injecting CO_2 into suitable geologic formations or are in the planning phase that will combine post-combustion CO_2 capture, transport, and storage. Figure 6-3 shows the name and type of major CCS projects in the power and industrial sectors throughout the world as of 2016. Several of these CO_2 capture systems will transport the captured CO_2 via pipeline to a geological storage site, often in conjunction with EOR in order to improve the project economics. Most of the projects have completed front-end engineering design studies and are awaiting final investment decisions that are expected to be announced later in 2018.

Included in this list is the Petra Nova project led by NRG Energy (NRG) in tandem with JX Nippon Oil and Gas Exploration EOR Limited (JX). This project deployed the world's largest full-scale post-combustion coal-fired CCS process and began injecting CO_2 as part of an EOR operation during the final days of 2016.

The $1 billion retrofit of an existing coal-fired unit is capable of capturing over 5000 tons of CO_2 per day or about 1.6 million tonnes per year. Figure 6-4 shows a photograph of the Petra Nova carbon capture facility located in Thompsons, Texas.

At present, the technologies that are being incorporated into the designs of initial large-scale post-combustion demonstration plants use liquid amines for CO_2 capture. These technologies represent the best available practice for post-combustion CO_2 capture and will most likely become the technologies chosen for the first generation of post-combustion CCS.

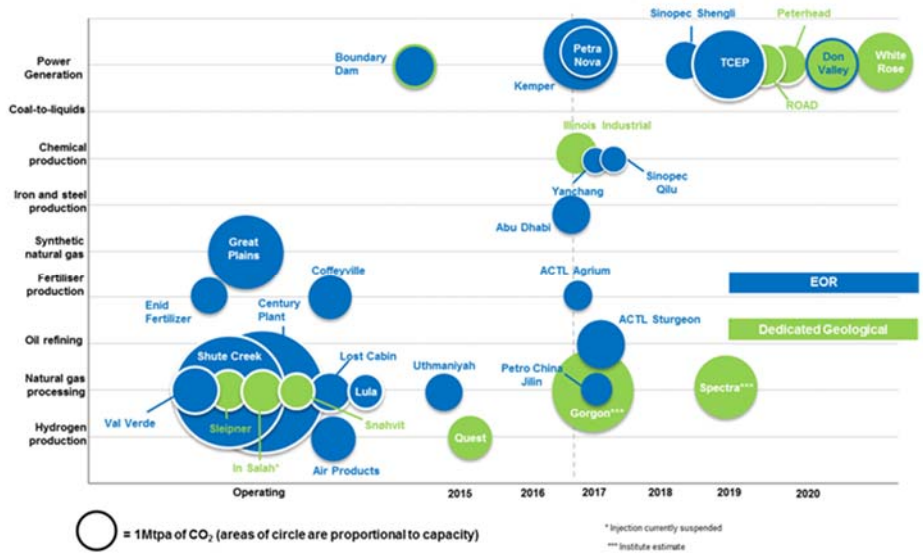

Figure 6-3. Large-scale CCS projects proceeding to operate and execute since 2011 (Global CCS Institute, 2016).

Figure 6-4. The Petra Nova CO_2 capture facility located in Thompsons, Texas. Photo courtesy of NRG Energy, Inc.

Currently, integrated gasification combined cycle (IGCC) looks less promising for power generation due to the cost of the plant even without CO_2 capture. Regarding more innovative technology, promising candidates, such as inertial extraction, chemical looping combustion, or oxy-fired CO_2 cycle, are plausible routes for the next generation of CO_2 capture technologies. However, their effective development up to full-scale deployment is not guaranteed due to the constant improvement of amine-based technology and their difficulty in retrofit integration to the current fleet.

A schematic for a pulverized coal-fired power plant using post-combustion CO_2 capture is shown above in Figure 6-2. First, coal is pulverized and combusted with air in a furnace (boiler). The heat of combustion is used to make steam at various pressure levels. The highest pressure of the steam relative to the critical point of water determines whether the system is classified as a subcritical or supercritical process. The steam produces mechanical power in steam turbines, which are attached by a shaft. The shaft is attached to a generator, which converts the mechanical power to electric power. A condenser is used to produce liquid water from the turbine exhaust, and then a pump is used to recompress the water to high pressure. The combustion exhaust leaving the furnace typically goes through an ash removal, a nitrogen oxide (NO_x) removal, and a sulfur oxide (SO_x) removal process, and there are various options for each stage. When CO_2 capture is used, the gas leaving the SO_x removal stage is sent to a solvent-based CO_2 capture process, which removes CO_2 and residual acid gases (nitrogen dioxide [NO_2] and sulfur dioxide [SO_2]). The CO_2 is then recovered for later compression, transport, and storage. The remainder of the flue gases (mostly N_2 and water) are exhausted to the atmosphere. Typical solvents for this purpose include monoethanolamine (MEA), diglycolamine (DGA), and methyldiethanolamine (MDEA), among others (Khojasteh Salkuyeh & Mofarahi, 2012; Mudhasakul, Ku, & Douglas, 2013; Closmann, Nguyen, & Rochelle, 2009; Adams II, Hoseinzade, Bhaswanth Madabhushi, & Okeke, 2017).

Amine-based post-combustion—i.e., flue gas treatment downstream from pulverized coal combustion, using chemical absorption—remains the preferred CO_2 capture technology for the short and medium terms (~year 2030). The technology readiness level (TRL) is between 6 and 7 (Kanniche, et al., 2017). There has been extensive relevant literature in recent years, including detailed CCS design studies published by the U.S. Department of Energy (DOE/NETL, 2015), the International Energy Agency (IEA) (IEAGHG, 2014), the Electric Power Research Institute (EPRI, 2013), and others. A review of recent literature finds thermal efficiency penalties ranging from 7.7 to 11.9% points for petroleum coke plants with post-combustion CCS. There are also actual efficiency penalties reported in recent amine-based CCS installations. At the fully integrated Boundary Dam project (shown above), the coal-fired unit produces 146 MW without capture and 117 MW with capture (Bruce, 2015), representing a 20% power derating or a loss of about 8% efficiency points, consistent with the recent literature range of 7.7 to 11.9% points cited above.

6.4 Near-Field Transport Requirements

At the beginning of the project, near-field transport and disposal was originally proposed as a means of sequestering a portion or all of the CO_2 generated by the Columbus, Nebraska ADM plant. Geological investigations, conducted as part of geologic assessment, revealed that there are probably no reservoirs near the ADM plant that are deep enough to act as a reservoir for CO_2 at super critical conditions (Battelle, 2018a). Thus, efforts investigating CO_2 transport were for far field transport requirements.

6.5 Far-Field Transport Requirements

Far-field transport refers to the process of transporting capture CO_2 from the source area to the storage area where it will then be injected into the ground. This can require moving large amounts of CO_2 hundreds of miles from an industrial area to a suitable storage location. As mentioned earlier, the most

efficient way to transport large amounts of CO_2 on land is in a dense (supercritical or liquid state) in a pipeline. Routing and constructing a pipeline that is several hundred miles long requires careful planning and considerations of issues including pipeline design/specifications, existing pipelines, affected property owners, safety, environmentally and culturally important/sensitive areas, and potential obstacles or barriers to pipeline construction. This section provides an initial regional assessment that can be used for input for a source corridor pipeline to deliver CO_2 to storage corridor, including size and pressure initial possible pipeline routing conducted using SimCCS, a review of the existing CO_2 pipelines in the United States, property ownership along potential pipeline routes and in the Red Willow County Storage area, pipeline safety considerations, protected/sensitive areas, and obstacles and barriers to pipeline and storage operations.

6.5.1 Pipeline design and specifications

The state of CO_2 is determined by the temperature and pressure within the pipeline. One of the complicating factors of transporting CO_2 long distances is pressure change due to friction losses in the line and elevation changes and temperature changes with weather. Pressure loss/changes are due to change in elevation and friction within the pipeline and are dependent on pipeline geometry and flow rate (Zhang et al., 2006; Vandeginste and Piessens, 2008). Temperature changes are the result of differences in temperature between the fluid in the pipeline and the surrounding soil (if buried) or atmosphere (if at surface) (Zhang et al., 2006). For longer pipelines, booster pumps may be needed to increase the pressure midstream to ensure CO_2 remains in a super critical state (Zhang et al., 2006; Leung et al., 2014). Other factors affecting pipeline requirements include the pressure at which the pipeline operates, the purity and water content of the CO_2, and safety considerations like fracture control, proper siting of pipelines, land use/human activity, and monitoring and verification (Zhang et al., 2006; Johnsen et al., 2011; Svensson et al., 2004; Han et al., 2015; Wettenhall et al., 2014;).

Optimal pipeline specifications are a function of CO_2 flow rate, density, and average viscosity (Zhang et al., 2006). Ultimately, this is determined by the amount of CO_2 needed or available (flow rate), the pressure at which the pipeline is operating and the change in temperature and pressure in the pipeline (CO_2 properties). Schlumberger's PIPESIM nodal analysis software was used to model CO_2 transport between the Cargill ethanol plant at Blair, NE and Sleepy Hollow Field, Red Willow County, NE. The route selected was based on the work described in Section 2. The ethanol plants included in the model are shown in Table 6-2. Eleven ethanol sources were included in the model with approximately 2.3 million tonnes per year of CO_2 emissions (Figure 6-5). Each of the sources was located on the map using the GIS feature in PIPESIM. Once pipelines connected each of the sources and Sleepy Hollow Field the elevations of the pipeline were imported into the model to incorporate the local topography to better model pressure changes along the route (Figure 6-6). For the modeling purposes pipe wall thickness was assumed to be 0.5 inches (12.7 mm), pipe roughness was assumed to be 0.001 in (0.0254 mm), and the heat value, U was assumed to be 0.2 Btu/(h.degF.ft^2) (1.135653 J/(s.degC.m^2). The CO_2 stream was assumed to be 100% CO_2.

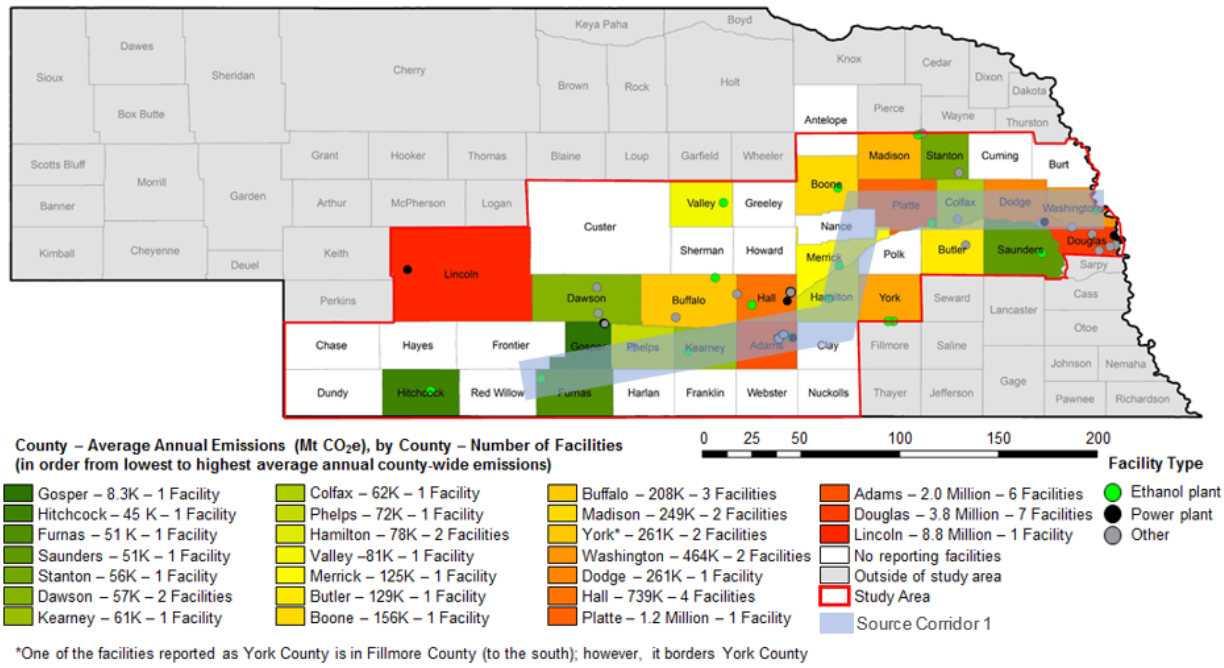

Figure 6-5. Approximate route for the source corridor pipeline from Section 2.

Table 6-2. Ethanol sources included in the source corridor pipeline model.

Facility	County	Rank Based on Annual Emissions	Ethanol Category Rank	Average Emissions 2011-2015 (Mt CO_2e)
Archer Daniel Midland	Platte	4	1	1,172,738
Cargill Corn Milling North America	Washington	7	2	447,455
AGP Soy/Corn Processing	Adams	8	3	204,330
Chief Ethanol Fuels, Inc.	Adams	11	5	163,428
Green Plains Central City	Merrick	15	8	124,812
Pacific Ethanol Aurora West LLC	Hamilton	22	12	70,995
Kaapa Ethanol, LLC	Kearney	26	14	60,922
Nebraska Corn Processing	Furnas	30	16	50,918
Pacific Ethanol Aurora East, LLC	Hamilton	35	18	35,612
All Facilities				**2,331,210**

Figure 6-6. PIPESIM pipeline model showing an approximate route and related ethanol CO_2 sources

As an initial pipe sizing exercise, a pressure profile and nodal analysis was conducted for the pipeline section running between Cargill in Blair, NE and ADM in Columbus, NE. The results of the pressure profile model show the six- and eight-inch ID pipe have significant pressure loss along the line compared to 10- and 12-inch pipe (Figure 6-7 and Table 6-3). The results of the nodal analysis show that all pipelines can transport the amount of CO_2 emitted by Cargill (1,225,904 kg/day) between Blair and Columbus, NE (Table 6-8 and Table 6-4). However, the 10- and 12-inch pipe have significantly extra capacity, even with higher outlet pressure, 1900-2100 psig; the range estimated in the pressure profile model.

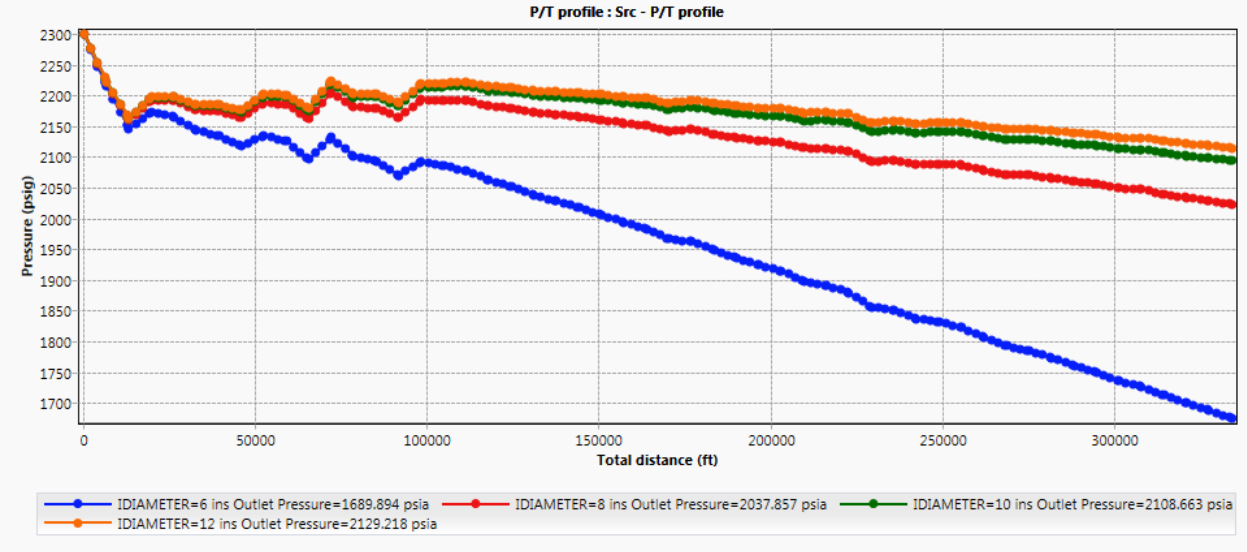

Figure 6-7. Pressure versus distance between Blair, NE and Columbus, NE for 6, 8, 10, and 12 Inside diameter pipeline.

Table 6-3. Inside diameter and system outlet pressure at ADM for 6- through 12-inch ID pipe.

Pipeline ID (in)	System outlet pressure (psig)
6	1675
8	2023
10	2094
12	2114

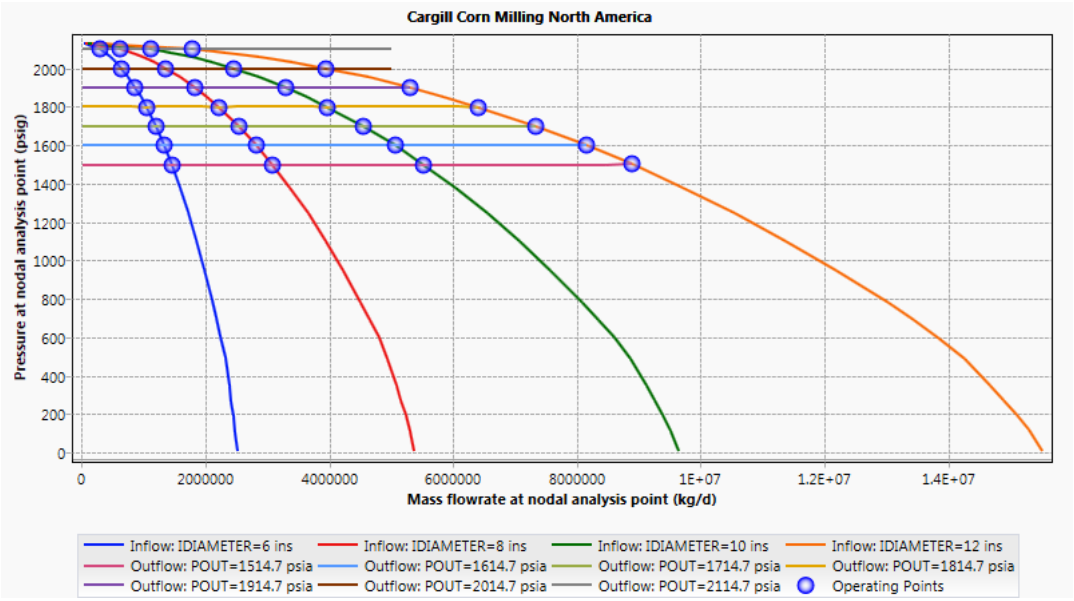

Figure 6-8. Nodal analysis showing operating points for 6- through 12-inch pipeline and 1500-2100 psi outlet pressure at ADM

Table 6-4. Flowrate at operating points for 6- through 12-inch ID pipeline segment between 1500 and 2100 psig.

Outlet Pressure (psig)	Pipeline Inside Diameter							
	6-inch		8-inch		10-inch		12-inch	
	Mass Flow Rate							
	kg/day	Million Tonne/ year	kg/day	Million Tonne/ year	kg/day	Million Tonne/ year	kg/day	Million Tonne/ year
1,500	1,448,056	0.5	3,080,165	1.1	5,523,552	2.0	8,890,894	3.2
1,600	1,326,015	0.5	2,821,006	1.0	5,060,062	1.8	8,149,717	3.0
1,700	1,191,303	0.4	2,534,952	0.9	4,547,835	1.7	7,325,679	2.7
1,800	1,039,486	0.4	2,212,548	0.8	3,970,322	1.4	6,396,677	2.3
1,900	862,421	0.3	1,836,367	0.7	3,296,234	1.2	5,311,890	1.9
2,000	638,349	0.2	1,360,150	0.5	2,442,249	0.9	3,936,509	1.4
2,100	289,029	0.1	617,534	0.2	1,110,186	0.4	1,788,778	0.7

Ten and 12-inch ID pipeline was selected for modeling the entire system. Booster stations were co-located with ethanol plants to keep the CO_2 in the pipeline in a dense phase. Figure 6-9 shows the mass flowrate increases due to each source coming into the system. Figure 6-10 shows the pipeline system with a compressor station (6 stations) at each source location compressing the CO_2 back up to the initial 2300 psi. Six stations are not necessary to keep the CO_2 in a dense phase (liquid or supercritical) in the

pipeline. Figure 6-11 shows the minimum number of compressor stations, three, needed to keep the CO_2 dense in a 10-inch ID pipeline.

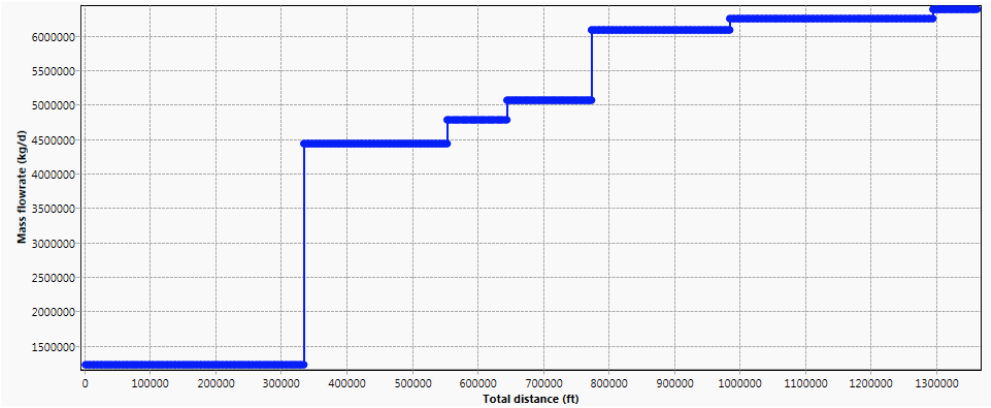

Figure 6-9. Mass flowrate versus distance between Blair, NE and Sleepy Hollow Field.

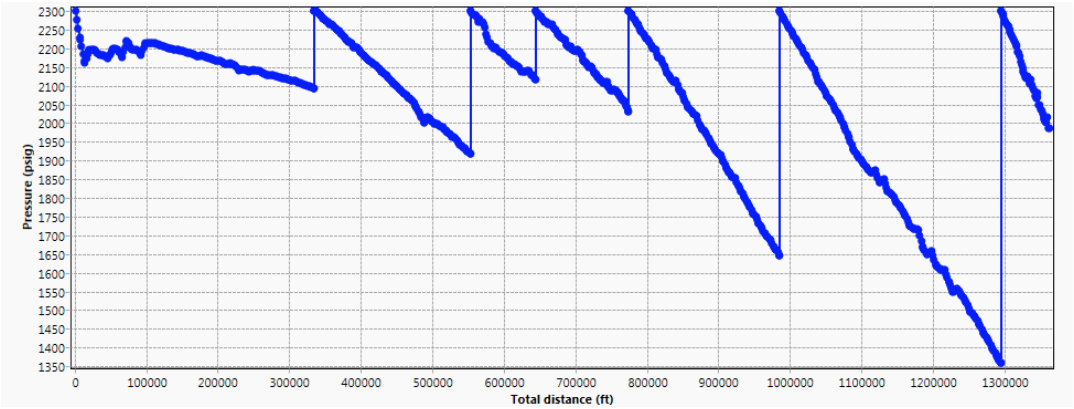

Figure 6-10. Ten-inch ID pipeline running between Blair, NE and Sleepy Hollow Field with a compressor station at each source.

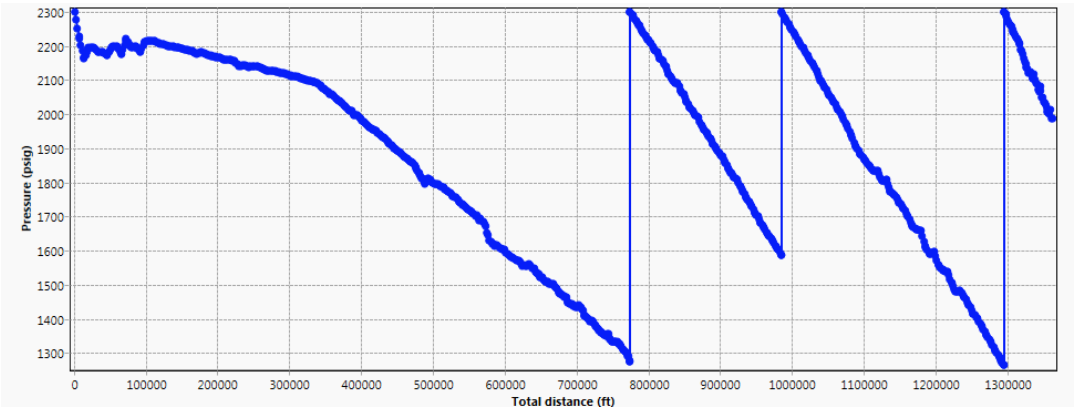

Figure 6-11. Ten-inch ID pipeline running between Blair, NE and Sleepy Hollow Field with a compressor station bringing the CO_2 keeping the pressure sufficient to keep the CO_2 in a dense phase.

Figure 6-12 shows the pressure drop using the same compressor station configuration as the 10-inch line in Figure 6-11. The friction losses on the 12-inch line are less than on the 10-inch line (hundreds of psi less at each compressor station) allowing for less compressor stations.

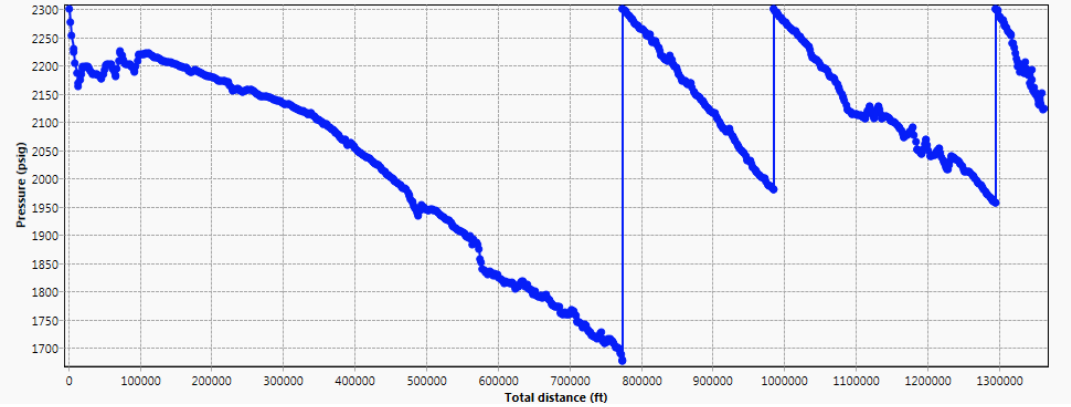

Figure 6-12. 12-inch ID pipeline running between Blair, NE and Sleepy Hollow Field with the minimum number of compressor stations from the 10-inch pipeline simulation.

Figure 6-13 shows the 12-inch line with a single compressor station at the AGP Corn Processing-Chief Ethanol node. The inclusion of a single compressor station is required to keep the CO_2 in a dense phase when it arrives at Sleepy Hollow Field.

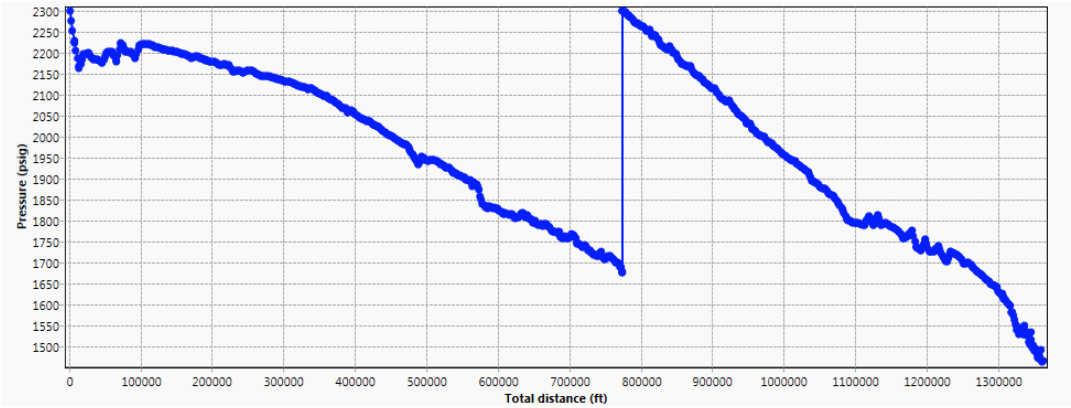

Figure 6-13. 12-inch ID pipeline running between Blair, NE and Sleepy Hollow Field with the minimum number of compressor stations.

General modeling of 8-, 10-, and 12-inch lines was conducted investigate the capacity of each line with a single compressor station. Flowrates included in the simulation were between 1,000 and 10,000 tonnes/ day (365,000 and 3,650,000 tonnes/year); Table 6-5.

Table 6-5. Flowrates for investigation of line capacity between Blair, NE and Sleepy Hollow Field. Please note that the standard English unit of lbs/s shows up in the legends for the plots below and could not be changed within PIPESIM to show up as kg/day or tones/day.

Flowrate				
Tonne/year	Tonne/day	kg/day	kg/s	lb/s
365,000	1,000	1,000,000	11.57	25.46
730,000	2,000	2,000,000	23.15	50.93
1,095,000	3,000	3,000,000	34.72	76.39
1,460,000	4,000	4,000,000	46.30	101.85
1,825,000	5,000	5,000,000	57.87	127.31
2,190,000	6,000	6,000,000	69.44	152.78
2,555,000	7,000	7,000,000	81.02	178.24
2,920,000	8,000	8,000,000	92.59	203.70
3,285,000	9,000	9,000,000	104.17	229.17
3,650,000	10,000	10,000,000	115.74	254.63

The results of the modeling, show that the 8-inch line functions between 1,000 to 3,000 tonnes/day (1,000,000 and 3,000,000 kg/day), the 10-inch line functions between 1,000 to 5,000 tonnes/day (1,000,000 and 500,000 kg/day), and the 12-inch line functions between 1,000 to 8,000 tonnes/day (1,000,000 and 8,000,000 kg/day) (Figure 6-14 and Figure 6-15). The annual emission of CO_2 is 6,387 tonnes/day for this scenario, so only the 12-inch line has extra capacity. At Sleepy Hollow Field, the pressure at Sleepy hollow field for the 8,000 tonne/ day case is 935 psi; sufficient to keep the CO_2 in a dense phase (Figure 6-16).

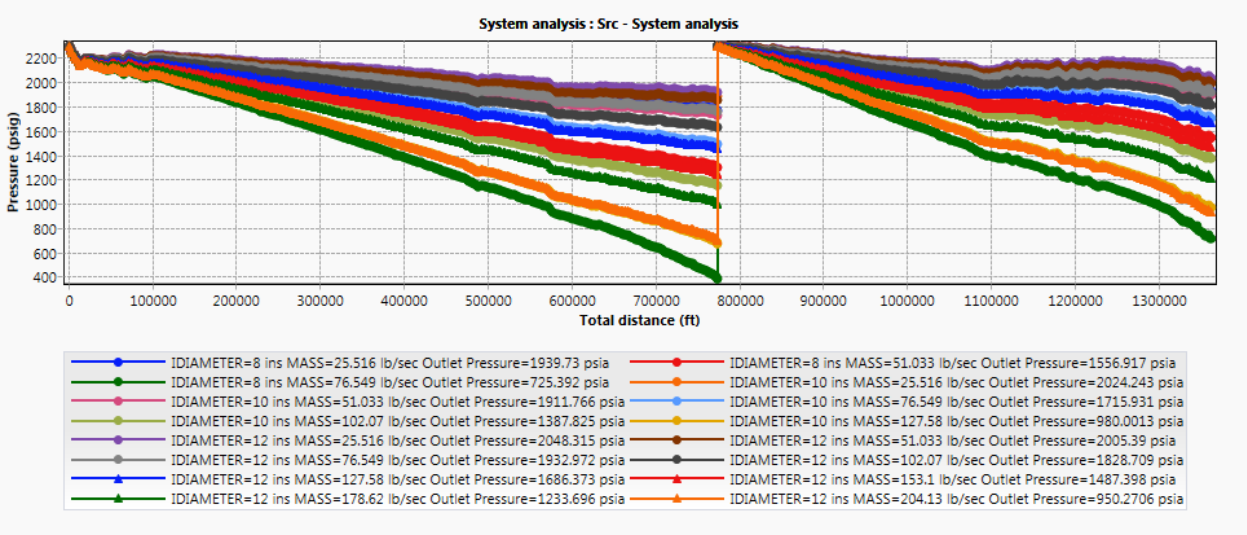

Figure 6-14. System pressure versus distance for 8-, 10-, and 12-inch lines between Blair, NE and Sleepy Hollow Field (compressor station at AGP Soy Corn Processing and Chief Ethanol).

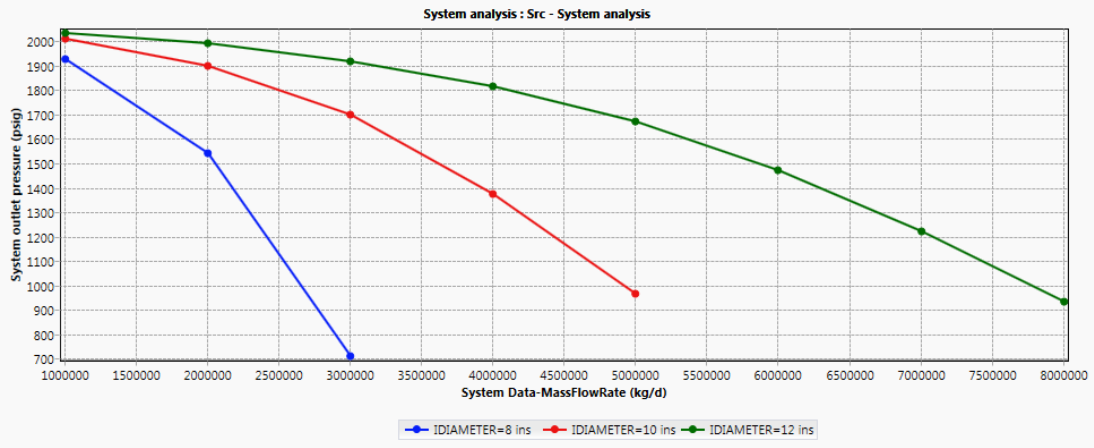

Figure 6-15. Outlet pressure versus mass flow rate for 8-, 10-, and 12-inch lines between Blair, NE and Sleepy Hollow Field (compressor station at AGP Soy Corn Processing and Chief Ethanol).

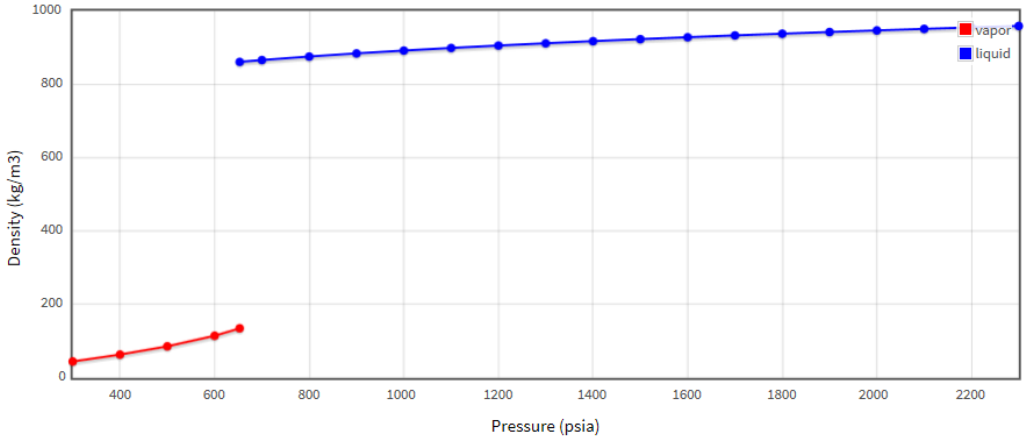

Figure 6-16. NIST REFPROP Modeling of CO_2 density versus pressure at 50 °F.

The compressor station was moved one node (source) east and one node west to examine the effect on line capacity. Moving the station to the east (from APG to Pacific) showed the line pressure before the compressor station was higher and the line pressure at Sleepy Hollow Field was lower compared to the previous simulation; the overall capacity was unchanged (Figure 6-17 and Figure 6-18). Moving the node to the west (from AGP to Kappa) resulted in less capacity (not shown).

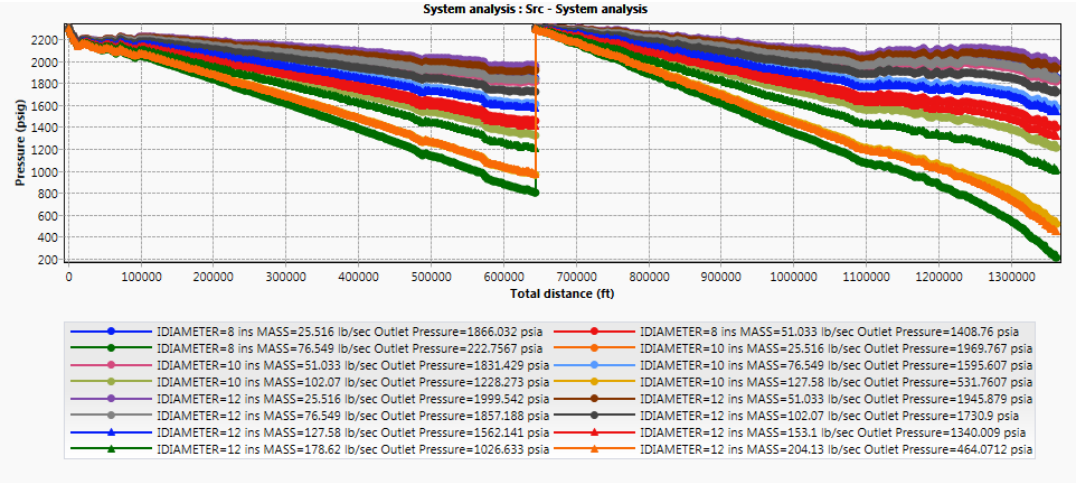

Figure 6-17. System pressure versus distance for 8-, 10-, and 12-inch lines between Blair, NE and Sleepy Hollow Field (compressor station at Pacific Ethanol).

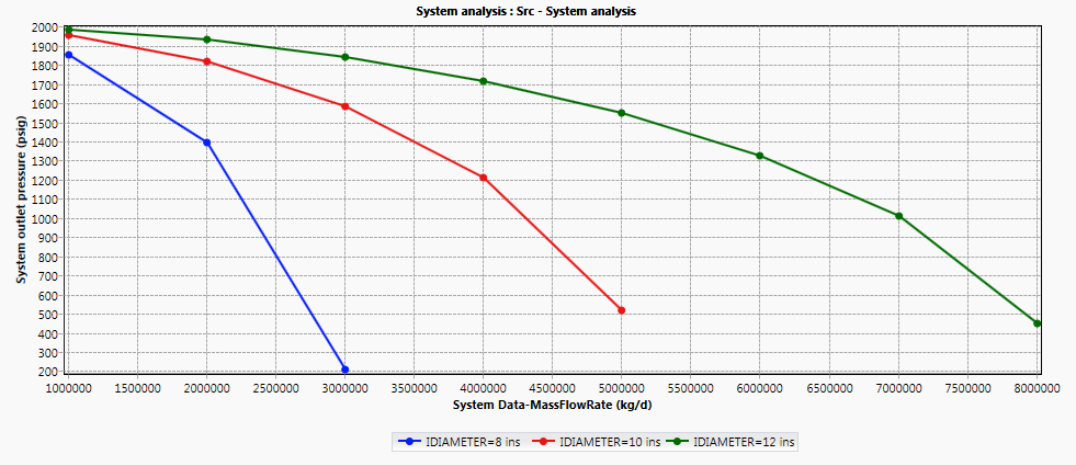

Figure 6-18. Outlet pressure versus flowrate for 8-, 10-, and 12-inch lines between Blair, NE and Sleepy Hollow Field (compressor station at Pacific Ethanol).

Two different pipe size configurations were also studied. The configurations consisted of 8-inch pipeline to the compressor node followed by 10-inch pipeline to Sleepy Hollow Field. Compressor stations were located at AGP Ethanol or Pacific Ethanol. The results of the modeling were similar to the single diameter pipeline scenarios (Figure 6-19 to Figure 6-22. However, when the compressor station is at AGP Ethanol, the pressure entering the compressor station in the 8-inch/10-inch scenario is likely too low for the 3,000,000 tonne/year case. It is possibly too low, near the liquid-gas transition for the 5,000,000 tonne/year case for the 10-inch/12-inch pipeline. When the compressor station is at Pacific Ethanol, the pressure for the 6,000,000 tone/year case is likely too low (gas phase) for the 10-inch/12-inch pipeline. The pressure is possibly too low (near the liquid-gas transition) for the 3,000,000 tonne/year case for the 8-inch/10-inch pipeline.

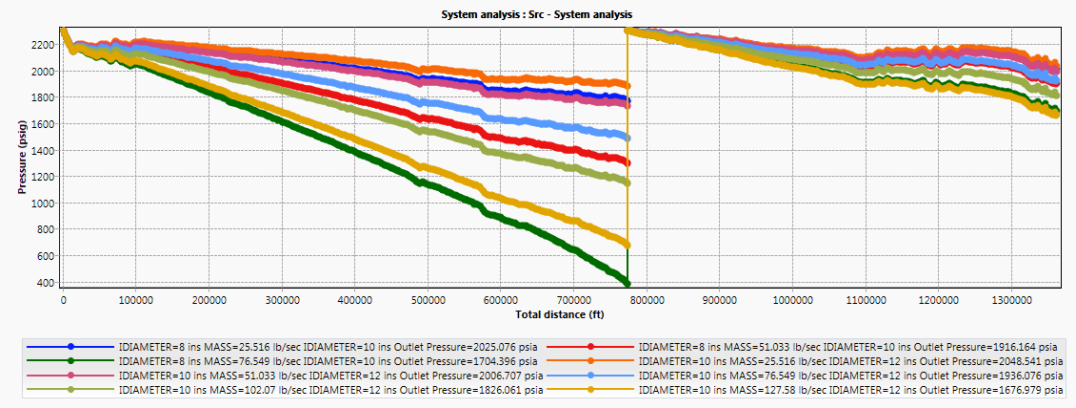

Figure 6-19. System pressure versus distance for 8-inch line to the AGP Soy Corn Processing and Chief Ethanol node followed by a 10-inch line to Sleepy Hollow Field or a 10-inch line to the AGP Soy Corn Processing and Chief Ethanol node followed by a 12-inch line to Sleepy Hollow Field.

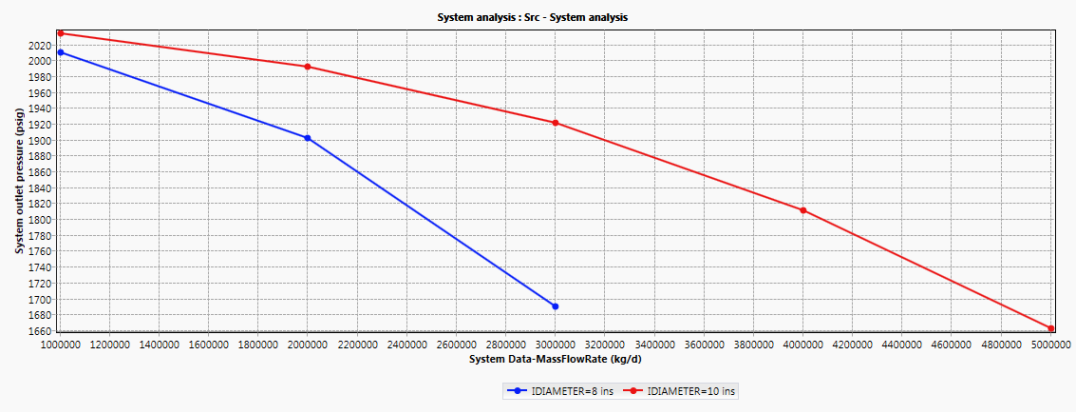

Figure 6-20. Outlet pressure versus flowrate for 8-inch line to the AGP Soy Corn Processing and Chief Ethanol node followed by a 10-inch line to Sleepy Hollow Field or a 10-inch line to the AGP Soy Corn Processing and Chief Ethanol node followed by a 12-inch line to Sleepy Hollow Field.

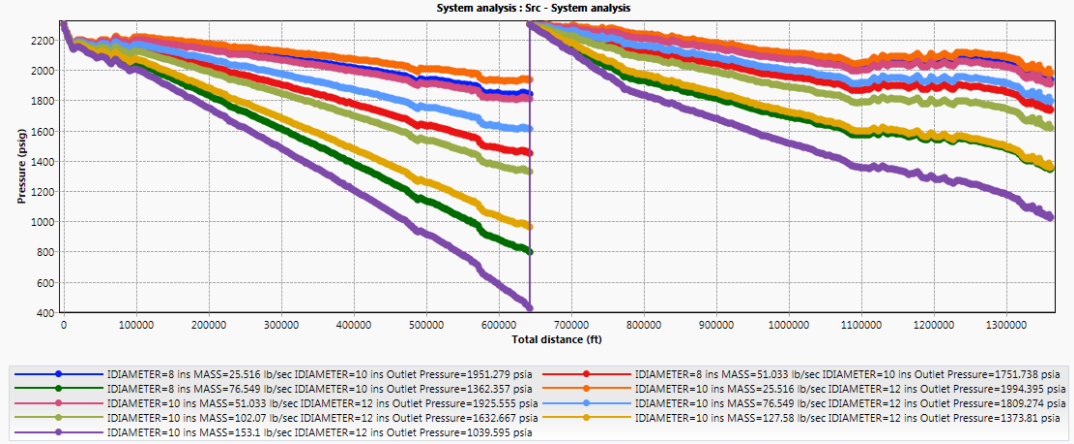

Figure 6-21. System pressure versus distance for 8-inch line to the Pacific Ethanol node followed by a 10-inch line to Sleepy Hollow Field or a 10-inch line to the Pacific Ethanol node followed by a 12-inch line to Sleepy Hollow Field.

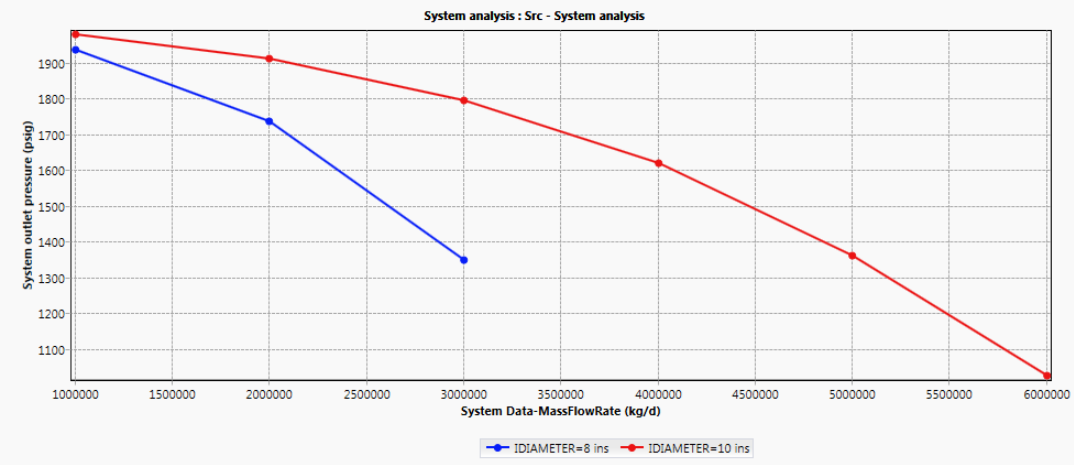

Figure 6-22. Outlet pressure versus flowrate for 8-inch line to the Pacific Ethanol node followed by a 10-inch line to Sleepy Hollow Field or a 10-inch line to the Pacific Ethanol node followed by a 12-inch line to Sleepy Hollow Field

Figure 6-23 shows the pressure versus distance profile for the 2.3 million tonne/year scenario with the compressor station at the AGP Ethanol node. There pressure at the compressor node and at Sleepy Hollow Field are sufficient to keep the CO_2 in a dense phase.

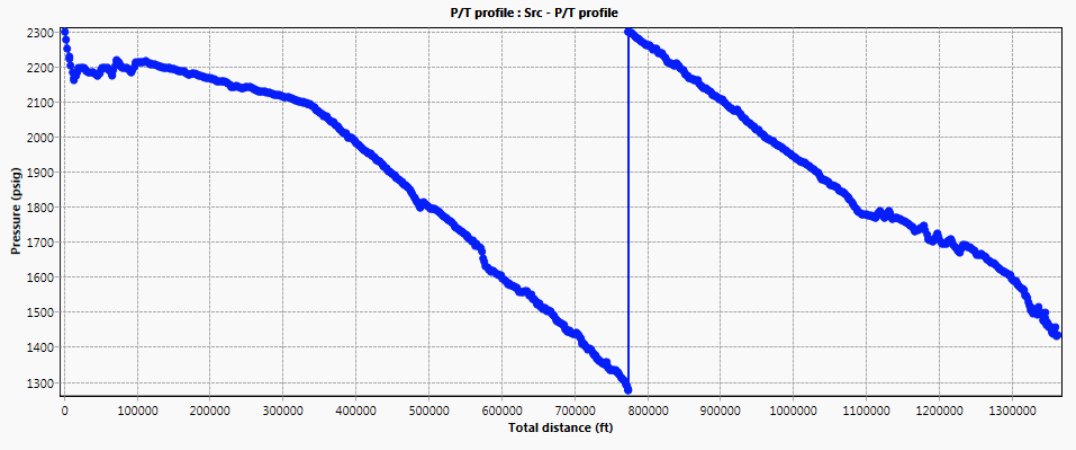

Figure 6-23. 10-inch ID pipeline running between Blair, NE and the first compressor station and 12-inch pipeline running from the first compressor station to Sleepy Hollow Field

6.5.2 Pipeline Routing: SimCCS

A study for potential pipeline routing was conducted for this study using the SimCCS software package (Middleton and Bielecki, 2009). The routes in this section of the report extend all the way through the storage corridor to examine how the total routing will work. The pipeline design work above only considered a line between Cargill and Sleepy Hollow Field because that line would likely be the largest diameter portion of the trunk line. Pipeline routes using SimCCS software are generated using a four-step process. First, the geographic area is rasterized into a weighted-cost surface that multiplies the base cost of building a CO_2 pipeline across a uniform surface to match the corresponding geography of the real world. This base cost is based on published costs for natural gas pipelines. Second, a set of potential origin-destination paths between all source/sink location pairs is calculated using a modified Dijkstra shortest-path algorithm on the weighted-cost surface. Third, a subset of these paths is selected as a candidate network by selecting edges that connect node pairs; these pairs are defined by a Delaunay triangulation of all source/sink locations. And fourth, final routes are selected by a Mixed Integer Linear Program (MILP) that aims to minimize cost while connecting source/sink locations in a way to ensure a target CO_2 storage amount is met.

Conceptually, generating the weighted-cost surface involves laying a grid overtop of the geographic area and determining the cost to traverse from one cell to a neighboring cell. Typically, with SimCCS, these cells are approximately one-kilometer square but could be much higher resolution (e.g., distribution-transport within an oilfield) or lower (e.g., the entire country of France). The cost to traverse from one cell to the other is a function of topography (slope and aspect), land ownership (10 classes), land use (16 types), crossings (rail, river, and roads), existing pipeline rights-of-way (ROW), and population density. Further, Los Alamos National Laboratory (LANL) uses separate weighted-cost surfaces for construction costs and for ROW costs; this is critical since these costs are independent. For example, a steep slope will affect construction but not ROW costs (pipelines are typically buried in trenches), while construction costs are essentially identical for cropland and grassland whereas land purchases for ROWs are not.

The weighted-cost surface can be considered as a graph, with nodes in the centers of cells and edges connecting the center to the center of each of the neighbor cells' centers. Costs to traverse cells are accounted for in edge weights. Direct moves to a diagonal cell are multiplied by a factor of √2 to account for the increased distance of the move compared with a cardinal move. This edge-weighted graph structure is then used for the rest of the pipeline route generation process. Shortest (cheapest) paths

between all source/sink locations are can be calculated using shortest path algorithms with cell-to-cell paths representing the routing of that pipeline.

A subgraph of the all source/sink location pairs graph is selected as a candidate network. There are various methods of accomplishing this, with Delaunay triangulation being one of the most robust (high quality and quick). In this method, a Delaunay triangulation of the set of source/sink locations is taken. This results in a set of source/sink pairs which are then connected with the shortest paths determined from the all source/sink location pairs shortest paths process. This candidate network is the collection of potential pipelines from which the final optimization process chooses.

The fourth and last step is to select final pipeline routes from the candidate network. This is done in conjunction with selecting which sources and sinks to open and how much to capture and inject into each location. A MILP is formulated that minimizes capture, transport, and storage costs while ensuring that enough CO_2 is captured and injected to meet project targets. From this optimization problem, a completed CCS infrastructure design is produced, that includes the necessary pipelines (of the appropriate size) to transport CO_2 from its capture location to its storage location.

Pipeline routes generated

The resulting pipeline routes are provided in Figure 6-24 and are detailed in Table 6-6. Six different scenarios were generated, focusing on the 18 ethanol sources in the area and two of the large coal-fired power plants (Figure 6-1) and two sinks of interest (Sleepy Hollow Field in Nebraska and the Patterson Heinitz Heartland Field in Kansas). The scenarios outline above are intended to act as representative examples of different scenarios possible for aggregating and transporting CO_2 to the fields of interest.

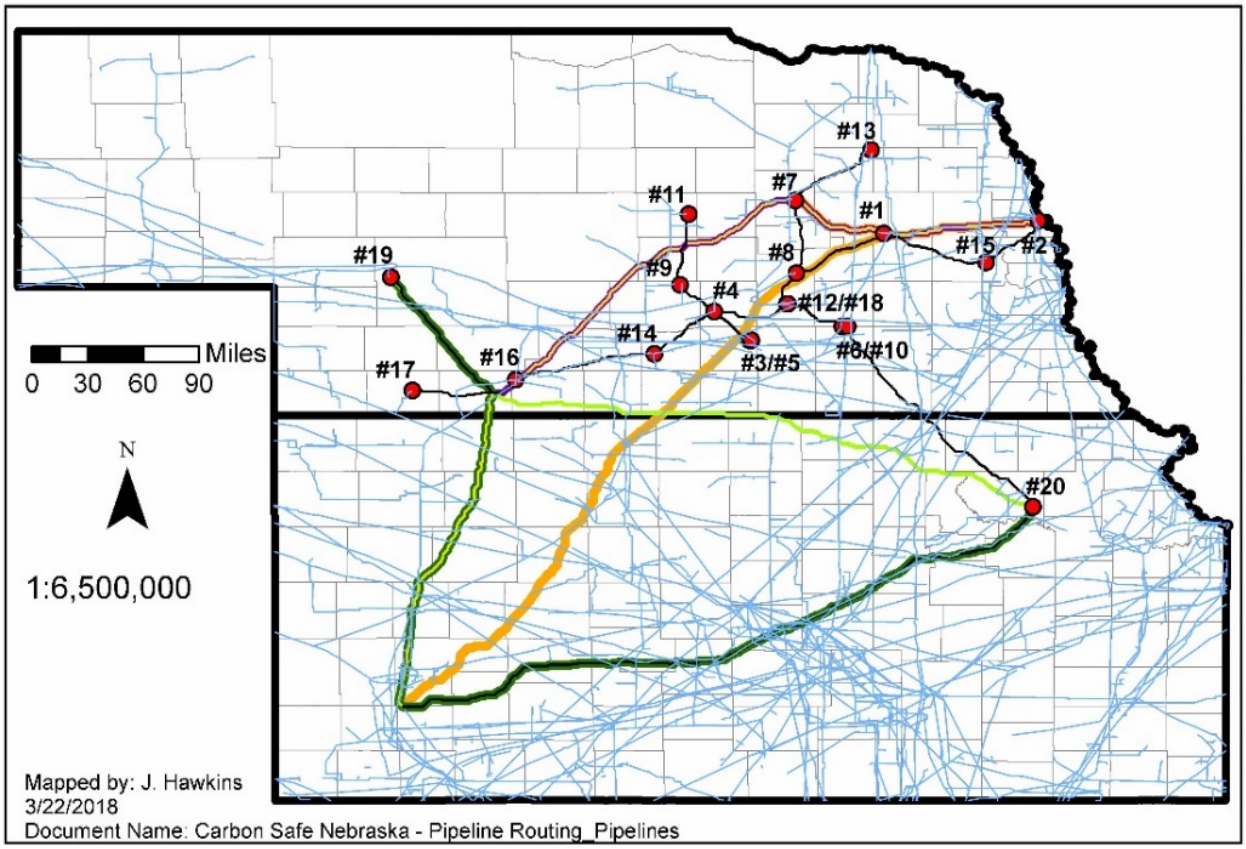

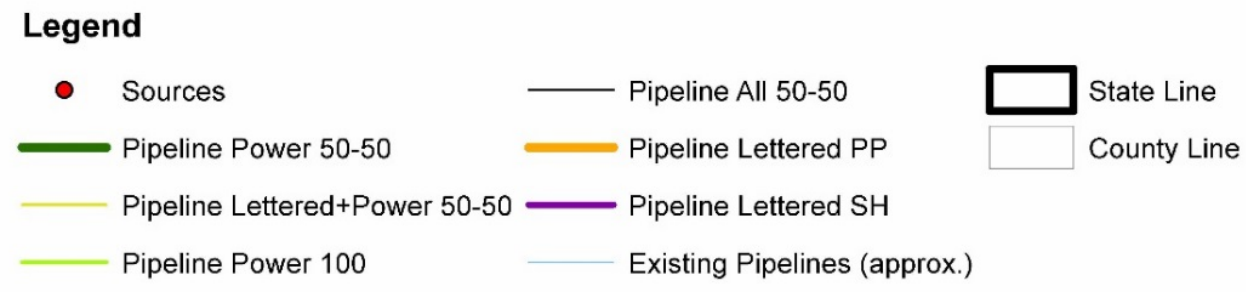

Figure 6-24. Pipeline routes generated using SimCCS (summarized in Table 6-6) overlain with existing natural gas and hazard liquid pipelines (U.S. DOT, 2018). The numbers indicate the sources and correspond with the numbers on Table 6-1.

Table 6-6. Summary of pipeline routes generated using SimCCS with overlapping existing pipeline.

Route	Length (mi)	Overlapping Existing Pipelines[1]
All 50-50	1,085	**Seg. 5**: -Source #13 to Geneva-Norfolk 8" - Madison 8-in to Norfolk (510 - Non-HVL product) south to - Tallgrass Interstate Gas Transport (TIGT) - Albion-Norfolk STBS (7500030000) SW to -TIGT - Grand Island-Albian (E. Line) (7500010000) south to - Black Hills Energy Nebraska Transmission (BHE NE) - 26792 to Source #7 **Seg. 9**: TIGT - Doniphan-York (71000500500) **Segs. 14/15**: TIGT - Holdrege to Hastings North (7100070000) WSW to -TIGT - Scott City-Holdrege (720010000) to Sleepy Hollow. **Seg. 18**: Oneok NGL pipeline - North system pipeline/11110 (553) SW to -ANR Pipeline - 8115100, 8116100, 8113100, 8112100 southwest to -Kansas Pipeline Co. - Hamston-Hudson Crude Oil to Pawnee County, KS.
Lettered + Power 50-50	899	**Seg. 1**: -BHE NE - 11696881, 11696880, and 1911346. -Northern Natural Gas Company Market Area (NNGC MA) - 179NEB53001, 52902, and 52901. **Seg. 3**: -BHE NE - 23606. **Seg. 6:** - TIGT - Scott City-Holdrege (7200010000) to -TIGT - Holcomb-Scott City (7050030000) to -Oneok NGL pipeline - Kansas Gathering System/10253 (553). **Seg. 7**: Oneok NGL pipeline - North system pipeline/11110 (553) SW to -ANR Pipeline - 8115100, 8116100, 8113100, 8112100 southwest to -Kansas Pipeline Co. - Hamston-Hudson Crude Oil to Pawnee County, KS.
Power 100	335	None.
Power 50-50	591	**Seg. 2:** - TIGT - Scott City-Holdrege (7200010000) to -TIGT - Holcomb-Scott City (7050030000) to -Oneok NGL pipeline - Kansas Gathering System/10253 (553). **Seg. 3**: Oneok NGL pipeline - North system pipeline/11110 (553) SW to -ANR Pipeline - 8115100, 8116100, 8113100, 8112100 southwest to -Kansas Pipeline Co. - Hamston-Hudson Crude Oil to Pawnee County, KS.
Lettered SH	294	**Seg. 1**: -BHE NE - 11696881, 11696880, and 1911346. -NNGC MA - 179NEB53001, 52902, and 52901. **Seg. 3**: -BHE NE - 23606.
Lettered PP	468	**Seg. 1**: -BHE NE - 11696881, 11696880, and 1911346. -NNGC MA - 179NEB53001, 52902, and 52901. **Seg. 3:** TIGT - Phillipsburg-Grand Island (7100050000 and 71000060000)

1. Existing pipelines are natural gas pipelines unless otherwise noted.

Pipeline Segments

Pipelines were split into segments to show the flow-rates and lengths of specific portions of the pipeline and to identify the portion of the pipeline that is considered the trunk-line (i.e., the large-scale pipeline that transports CO_2 through the source corridor to the storage corridor). Figure 6-25 and Table 6-7 provide an overview of the segments of each of the routes, a description of the segment, whether the segment is considered a trunk-line including the length of the segment, the flow rate through the segment. The trunk lines and smaller-scale lines are also compared by calculating the Million Tonne/year delivered to the sink per mile of pipeline. In addition, the overlapping existing pipelines are pipelines are identified, by segment, in Table 6-6. Existing pipelines (i.e., existing rights of way) are an important factor when considering pipeline routes as they can serve as an easily accessible route. Several hundred miles of natural gas or hazardous liquid pipeline transect the study area (U.S. DOT, 2018).

All 50-50

The All 50-50 route has a total of 18 segments which add to a total length of 1,085 miles. There are two main trunk-lines under this scenario, one that runs through Nebraska (Segments 3, 6, 9, and 13-15) and one that runs from the Jeffrey Energy Center (Pottawatomie County, Kansas) to the oilfields of southwestern Kansas. The Nebraska trunk line consists of the following:

- The trunk line begins at Source #1 (ADM Columbus, Nebraska Ethanol Plant) and connects to Source #8 (Green Plains Central City) in Merrick County, Sources #12/#18 (Pacific Ethanol Aurora West and East, respectively) in Hamilton County, Source #4 (Green Plains Wood River) in Hall County, Source #14 (Kaapa Ethanol) in Kearney County, Source #16 (Nebraska Corn Processing) in Furnas County, and finally to the sink in Red Willow County Nebraska.
- The total length of the trunk line is 217 miles.
- The flow rate in the trunk line increases from 1.2 million metric tonnes per year (Million Tonnes/year) at Source #1 to 1.7 Million Tonnes/year delivered to the sink when only considering emissions from sources on the main trunk line (0.008 Million Tonnes/year/mile pipeline).
- Smaller-scale lines connecting to the main trunk line include the following:
  - Segments 1 and 2, which connect Source #2 (Cargill Corn Milling North America) in Washington County and #15 (AltEn) in Saunders County to the main trunk line at Source #1, have a total flow rate of 0.5 Million Tonne/year at the trunk line and total length of 85 miles (0.006 Million Tonne year/mile pipeline).
  - Segments 4 and 5, which connect Source #7 (Valero Albion Plant) in Boone County and #13 (Elkhorn Valley Ethanol Plant) in Madison County to the main trunk line at Source #8 in Merrick County, have a combined flow rate of 0.2 Million Tonne/year at the trunk line and total length of 89 miles (0.002 Million Tonne/year/mile pipeline).
  - Segments 7 and 8, which connect Source #20 (Jeffrey Energy Center) in Pottawatomie County, Kansas and Sources #6/#10 (Flint Hills Resources, Fairmont) in Fillmore County, Nebraska to the main trunk-line at Sources #12/#18 in Hamilton County, have a combined flow rate of 1.6 Million Tonne/year and a total length of 167 miles (0.010 Million Tonne/year/mile pipeline).
  - Segment 10, which connects Sources #3/#5 (AGP Soy/Corn Processing and Chief Ethanol Fuels, Inc., respectively) in Adams County to the main trunk-line at Source #4 in Hall County, has a combined flow rate of 0.4 Million Tonne/year and a total length of 22.2 miles (0.018 Million Tonne/year/mile pipeline).
  - Segments 11 and 12, which connect Sources #11 (Green Plains ORD) in Valley County and #9 (Abengoa Bioenergy) in Buffalo County to the main trunk line at Source #4 in Hall County, has a combined flow rate of 0.2 Million Tonnes/year and a total length of 62 miles (0.003 Million Tonnes/year/mile pipeline).
  - Segment 16, Source #17 (Trenton Agri Products) in Hitchcock County to the Sleepy Hollow Field, has a flow rate of 0.04 Million Tonnes/year and a total length of 35.3 miles (0.001 Million Tonnes/year/mile pipeline).
  - Segment 17, Source #19 (Gerald Gentleman Station) in Lincoln County to the Sleepy Hollow Field, has a flow rate of 11.0 Million Tonnes/year and a total length of 79.3 miles (0.139 Million Tonnes/year/mile pipeline).

The Kansas trunk line consists of the following:

- The trunk line begins at Source #20 (Jeffrey Energy Center) in Pottawatomie County, Kansas and runs to the oilfields of southwestern Kansas (Segment 18).
- The total length of the trunk line is 326 miles.
- The flow rate in the trunk line is 15.5 Million Tonnes/year (0.048 Million Tonnes/year/mile pipeline).

Five pipeline segments have overlapping existing pipelines:

- Segment 5 is completely overlapped by existing pipelines, including the Geneva-Norfolk 8", the Tallgrass Interstate Gas Transport (TIGT), and the Black Hill Energy Nebraska (BHE NE) natural gas pipelines.
- Two-thirds to three-fourths of Segment 9 is overlapped by the TIGT natural gas pipeline.
- Segments 14 and 15 are completely overlapped by the TIGT natural gas pipeline.
- Around two-thirds of Segment 18 is overlapped by existing pipelines, including the Oneok Natural Gas Liquids (NGL) pipeline, the ANR natural gas pipeline, and the Kansas Pipeline Co. Crude Oil pipeline.

Lettered + Power 50-50

The Lettered + Power 50-50 route has a total of seven segments which add to a total length of 899 miles. There are three main trunk lines in this scenario (all but two segments are main trunk lines), one that runs through Nebraska (Segments 2-4), one runs through the storage corridor and connects the Sleepy Hollow Field (Red Willow County, Nebraska) to the Patterson Field (Finney County, Kansas) (Segment 6), and one that runs from the Jeffrey Energy Center (Pottawatomie County, Kansas) to the oilfields of southwestern Kansas (Segment 7). The Nebraska trunk line consists of the following:

- The trunk line begins at Source #1 (ADM Columbus, Nebraska Ethanol Plant) in Platte County and connects to Source #7 (Valero Albion Plant) in Boone County, Source #16 (Nebraska Corn Processing) in Furnas County, and finally to the sink in Red Willow County Nebraska.
- The total length of the trunk line is 240 miles.
- The flow rate in the trunk line increases from 1.2 million metric tonnes per year (Million Tonnes/year) at Source #1 to 1.5 Million Tonnes/year delivered to the sink when only considering emissions from sources on the main trunk line (0.006 Million Tonnes/year/mile pipeline).
- Smaller-scale lines connecting to the main trunk line include the following:
  - Segment 1, Source #2 (Cargill Corn Milling North America) in Washington County to the main trunk line at Source #1, have a total flow rate of 0.4 Million Tonnes/year at the trunk line and total length of 69.2 miles (0.006 Million Tonnes/year/mile pipeline).
  - Segment 5, Source #19 (Gerald Gentleman Station) in Lincoln County to the Sleepy Hollow Field, has a flow rate of 11.0 Million Tonnes/year and a total length of 79.3 miles (0.139 Million Tonnes/year/mile pipeline).

The storage corridor pipeline connecting the Nebraska and Kansas oilfields consists of the following:

- The trunk line begins at Sleepy Hollow Field in Red Willow County, Nebraska and ends at the Patterson Field in Finney County, Kansas.
- The total length of the trunk line is 186 miles.

- The flow rate in the trunk line is 2.1 million metric tonnes per year (0.011 Million Tonnes/year/mile pipeline).
- There are no smaller-scale pipelines connecting to the storage corridor trunk line.

The Kansas trunk line consists of the following:

- The trunk line begins at Source #20 (Jeffrey Energy Center) in Pottawatomie County, Kansas) and runs to the oilfields of southwestern Kansas (Segment 7).
- The total length of the trunk line is 326 miles.
- The flow rate in the trunk line is 16.9 Million Tonnes/year (0.052 Million Tonnes/year/mile pipeline).

Three pipeline segments have overlapping existing pipelines:

- About half of Segment 1 is overlapped by the BHE NE and Northern Natural Gas Company Market Area (NNGC MA) natural gas pipeline.
- Less than 10% of Segment 3 is overlapped by the BHE NE natural gas pipeline.
- Around a third of Segment 6 is overlapped by the TIGT natural gas pipeline and Oneok NGL pipeline.
- Around two-thirds of Segment 7 is overlapped by existing pipelines, including the Oneok NGL pipeline, the ANR natural gas pipeline, and the Kansas Pipeline Co. Crude Oil pipeline.

Power 100

The Power 100 route has two segments, both of which are main trunk lines, that add to a total length of 335 miles:

- The Nebraska trunk line (Segment 2), which begins at Source #19 (Gerald Gentleman Station) in Lincoln County to the Sleepy Hollow Field, has a flow rate of 11.0 Million Tonnes/year and a total length of 79.3 miles (0.139 Million Tonnes/year/mile pipeline).
- The Kansas trunk line (Segment 1), which begins at Source #20 (Jeffrey Energy Center) in Pottawatomie County, Kansas and runs to the Sleepy Hollow Field, has a flow rate of 16.9 Million Tonnes/year and a total length of 256 miles (0.066 Million Tonnes/year/mile pipeline).
- There are no overlapping existing pipelines in this scenario.

Power 50-50

The Power 50-50 route has three segments, all of which are main trunk lines, that add to a total length of 591 miles. The segments in this scenario include a Nebraska trunk line (Segment 1), a storage corridor trunk line (Segment 2), and a Kansas trunk line (Segment 3):

- The Nebraska trunk line, which begins at Source #19 (Gerald Gentleman Station) in Lincoln County and runs to the Sleepy Hollow Field, has a flow rate of 11.0 Million Tonnes/year and a total length of 79.3 miles (0.139 Million Tonnes/year/mile pipeline).

- The storage corridor trunk line, which begins at the Patterson Field in Finney County, Kansas and runs the length of the storage corridor to the Sleepy Hollow Field in Red Willow County, Nebraska, has a flow rate of 3.0 Million Tonnes/year and a total length of 186 miles (0.016 Million Tonnes/year/mile pipeline).
- The Kansas trunk line, which begins at Source #20 (Jeffrey Energy Center) in Pottawatomie County, Kansas and runs to the Patterson Field, has a flow rate of 16.9 Million Tonnes/year and a total length of 326 miles (0.052 Million Tonnes/year/mile pipeline).

Two pipeline segments have overlapping existing pipelines:

- Around a third of Segment 6 is overlapped by the TIGT natural gas pipeline and Oneok NGL pipeline.
- Around two-thirds of Segment 3 is overlapped by existing pipelines, including the Oneok NGL pipeline, the ANR natural gas pipeline, and the Kansas Pipeline Co. Crude Oil pipeline.

Lettered SH

The Lettered SH route has three segments that add to a total length of 294 miles. Segments 2 and 3 are considered the main trunk line with Segment 1 acting as a smaller-scale pipeline. The main trunk line consists of the following:

- The trunk line begins at Source #1 (ADM Columbus, Nebraska Ethanol Plant) in Platte County and connects to Source #7 (Valero Albion Plant) in Boone County and finally to the sink in Red Willow County, Nebraska.
- The total length of the trunk line is 225 miles.
- The flow rate in the trunk line increases from 1.2 million metric tonnes per year (Million Tonnes/year) at Source #1 to 1.4 Million Tonnes/year delivered to the sink when only considering emissions from sources on the main trunk line (0.006 Million Tonnes/year/mile pipeline).
- Smaller-scale lines connecting to the main trunk line include the following:
  - Segment 1, Source #2 (Cargill Corn Milling North America) in Washington County to the main trunk line at Source #1, have a total flow rate of 0.4 Million Tonnes/year at the trunk line and total length of 69.2 miles (0.006 Million Tonnes/year/mile pipeline).

Two pipeline segments have overlapping existing pipelines:

- About half of Segment 1 is overlapped by the BHE NE and NNGC MA natural gas pipeline.
- Less than 10% of Segment 3 is overlapped by the BHE NE natural gas pipeline.

Lettered PP

The Lettered PP route has three segments that add up to a total length of 468 miles. The main trunk line is Segment 3 with Segments 1 and 2 acting as smaller-scale pipelines. The main trunk line consists of the following

- The trunk line begins at Source #1 (ADM Columbus, Nebraska Ethanol Plant) in Platte County and run to the sink in Finney County, Kansas.
- The total length of the trunk line is 468 miles.
- The flow rate in the trunk line is 1.2 Million Tonnes/year delivered to the sink when only considering emissions from sources on the main trunk line (0.004 Million Tonnes/year/mile pipeline).
- Smaller-scale lines connecting to the main trunk line include the following:
  - Segment 1, Source #2 (Cargill Corn Milling North America) in Washington County to the main trunk line at Source #1, has a total flow rate of 0.4 Million Tonnes/year and total length of 69.2 miles (0.006 Million Tonnes/year/mile pipeline).
  - Segment 2, Source #7 (Valero Albion Plant) in Boone County to the main trunk line at Source #1, has a total flow rate of 0.2 Million Tonnes/year and a total length of 45.9 miles (0.004 Million Tonnes/year/mile pipeline).

Two pipeline segments have overlapping existing pipelines:

- About half of Segment 1 is overlapped by the BHE NE and NNGC MA natural gas pipeline.
- Less than 10% of Segment 3 is overlapped by the TIGT natural gas pipeline.

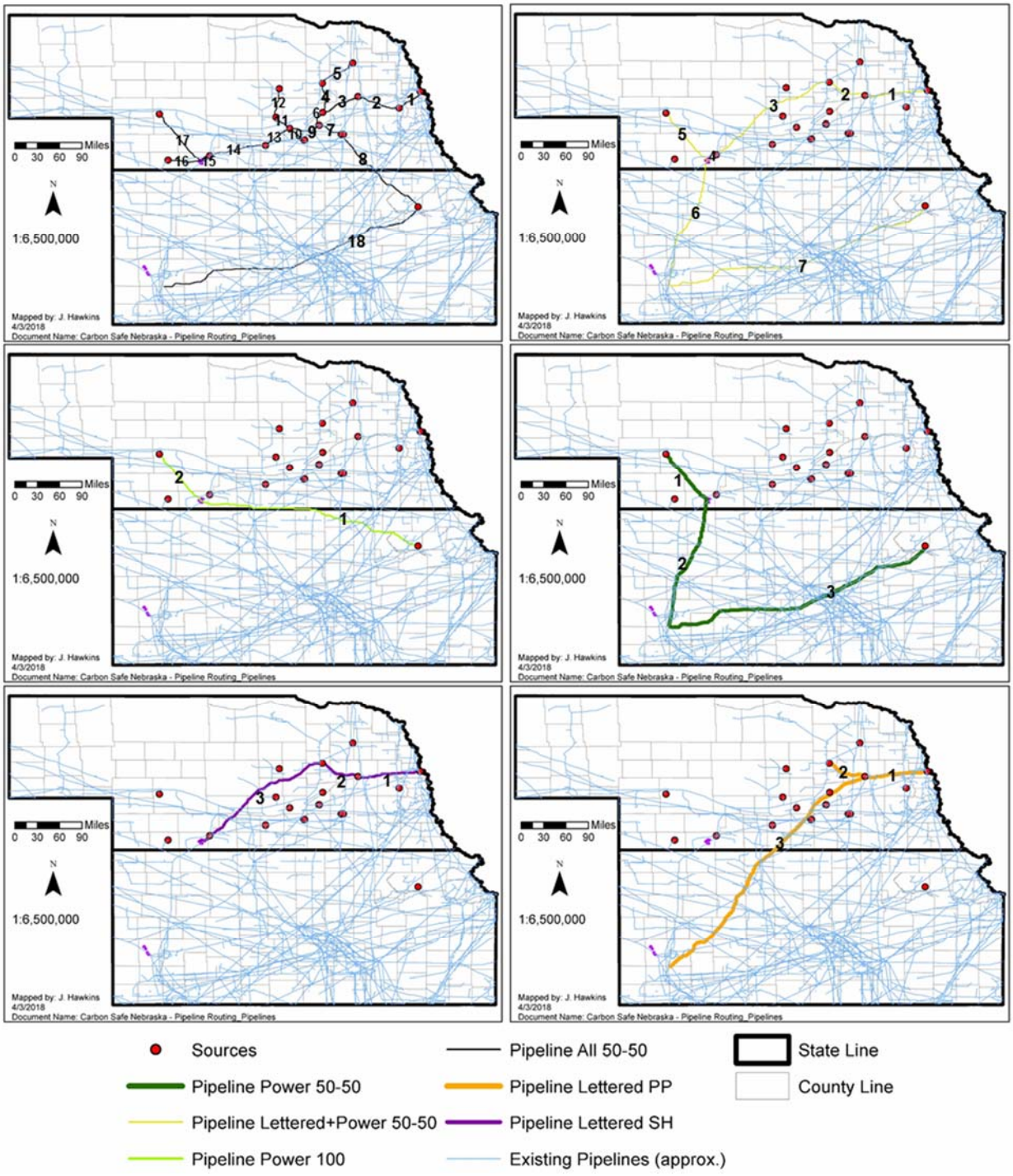

Figure 6-25. Six individual pipeline routes modeled using SimCCS. Numbers indicate segments of the pipeline that correspond with Table 6-6 and Table 6-7.

Table 6-7. Pipeline segments lengths and flow rates.

Route	Seg.	Seg. Description	TL	Length (mi)	Flow Rate (Million Tonnes/y)
All[1]	1	Source 2 to 15	--	34.7	0.4
	2	Source 15 to 1	--	49.9	0.5
	3	Source 1 to 8	Yes	47.0	1.7
	4	Source 7 to TL	--	41.6	0.2
	5	Source 13 to 7	--	46.9	0.1
	6	Source 8 to 12/18	Yes	19.8	2.0
	7	Sources 6/10 to TL	--	28.6	1.6
	8	Source 20 to 6/10	--	138	1.3
	9	Sources 12/18 to 4	Yes	34.6	3.7
	10	Sources 3/5 to TL	--	22.2	0.4
	11	Source 9 to TL	--	21.4	0.2
	12	Source 11 to 9	--	40.8	0.1
	13	Source 4 to 14	Yes	36.5	4.4
	14	Source 14 to 16	Yes	64.5	4.5
	15	Source 16 to SH	Yes	14.6	4.6
	16	Source 17 to SH	--	35.3	0.04
	17	Source 19 to SH	--	79.3	11.0
	18	Source 20 to KS sink	Yes	326	15.5

Route	Seg.	Seg. Description	TL	Length (mi)	Flow Rate (Million Tonnes/y)
Lettered + Power 50-50	1	Source 2 to 1	--	69.2	0.4
	2	Source 1 to 7	Yes	45.9	1.6
	3	Source 7 to 16	Yes	179	1.8
	4	Source 16 to SH	Yes	14.6	1.9
	5	Source 19 to SH	--	79.3	11.0
	6	Sink connection/corridor	Yes	186	2.1
	7	Source 20 to KS sink	Yes	326	16.9
Power 100	1	Source 20 to SH	Yes	256	16.9
	2	Source 19 to SH	Yes	79.3	11.0
Power 50-50	1	Source 19 to SH	Yes	79.3	11.0
	2	Sink connection/corridor	Yes	186	3.0
	3	Source 20 to KS sink	Yes	326	16.9
Lettered SH	1	Source 2 to TL	--	69.2	0.4
	2	Source 1 to 7	Yes	45.9	1.6
	3	Source 7 to SH	Yes	179	1.8
Lettered PP	1	Source 2 to TL	--	69.2	0.4
	2	Source 7 to TL	--	45.9	0.2
	3	Source 1 to KS sink	Yes	353	1.8

Notes: Million Tonnes/y - million metric tonnes/year. Seg - Segment. SH - Sleepy Hollow Field (Red Willow County, Nebraska). TL - Trunk line. Segment numbers correspond to those on Figure 6-25. Source numbers correspond to those on Figure 6-24/Table 6-1.
1. Also includes connections between Sources #18 to #12 (0.4 miles/1.6 <Mt/y), #10 to #6 (2.2 miles/1.4 Million Tonnes/year), and #5 to #3 (0.9 miles/0.2 Million Tonnes/y).

6.5.3 Overview of existing CO_2 pipelines

Existing CO_2 pipelines are of interest to the project as examples to help inform how CO_2 has been transported for other projects and how the IMSCS-HUB can connect into the larger CO_2 transport infrastructure. Table 6-8 provides an overview of 54 existing CO_2 pipelines that in the United states. CO_2 pipeline systems in the United States currently contain more than 5,100 miles of pipe and are primarily dedicated to transporting CO_2 from natural and anthropogenic sources to CO_2-EOR fields in the southwest, southeast, and Rocky Mountain regions. The proposed IMSCS-HUB is roughly located between these major CO_2 pipeline networks and has the potential to tap into existing pipelines in the south, connecting oilfields in Oklahoma, Texas, and Kansas to numerous CO_2 sources from ethanol plants in Nebraska and adjacent states in the Midwest (Figure 6-26). Low population density, and predominance of the agriculture industry in the region suggests rural areas aren't likely to undergo

significant development in the next 20 years, ensuring opportunities will remain for the IMSCS-HUB pipelines to expand and access the existing pipeline network.

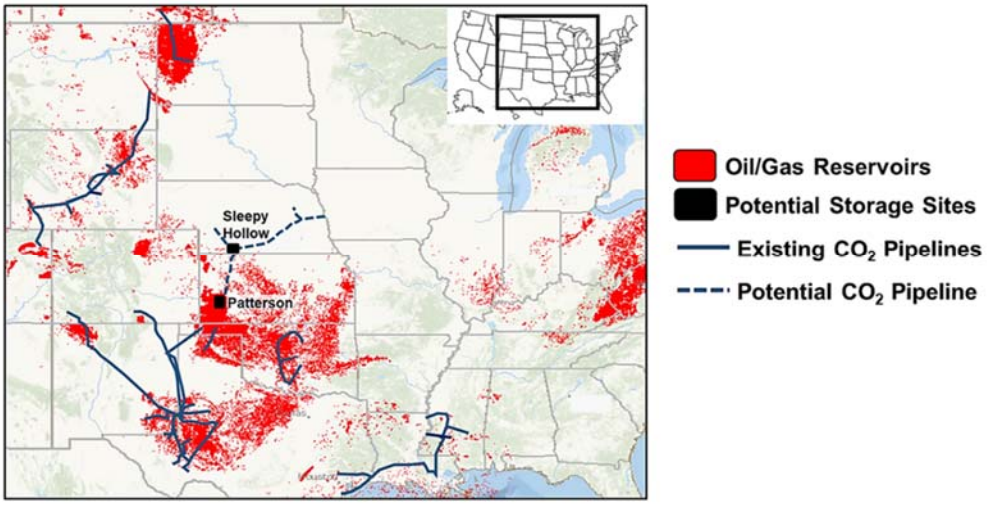

Figure 6-26. Map showing the potential storage sites and CO_2 pipeline for the IMSCS-HUB Project along with existing CO_2 pipelines and oil/gas fields in the United States (map data from NATCARB, 2017).

Table 6-8. Existing CO_2 pipelines throughout the United States.

Project	Year Const.	Pipeline Length (mi)	Pipeline Diameter (in.)	Max. Capacity (Million Tonnes)	Reported Flowrates (MMcf/yr)	State	Type
Adair	1997	15	4	1	365	TX	Small-scale distribution systems
Anton Irish	1997	40	8	1.6	29,200	TX	Small-scale distribution systems
Bairoil	1986	160	--	23	--	WY	Small-scale distribution systems
Beaver Creek	2009	53	8	1.6	10,950	WY	Small-scale distribution systems
Borger to Camrick	1972	86	6-8	1	18,250	TX, OK	Small-scale distribution systems
Bravo	1984	218	20	7	138,700	NM, TX	Large-scale trunk line
Canyon Reef Carriers	1972	170	16	4.3	80,300	TX	Large-scale trunk line
Centerline	2003	113	16	4.3	80,300	TX	Large-scale trunk line
Central basin	1985	143	16	4.3	80,300	TX	Large-scale trunk line
Chapparal	1988	23	6	1.3	--	OK	Small-scale distribution systems
Coffeyville –– Burbank	2013	68	8	1.6	29,200	KS, OK	Small-scale distribution systems
Comanche Creek	--	120	6	1.3	25,550	TX	Small-scale distribution systems
Cordona Lake	1985	7	6	1.3	25,550	TX	Small-scale distribution systems
Cortez	1984	502	30	23.6	474,500	TX	Large-scale trunk line
Souris Valley	2000	204	14	2.6	47,450	ND, SK	Other transport lines
Decatur	2011	1	--	1.1	--	IL	Pipeline to saline aquifer
Delta	2007	108	24	11.4	215,400	MS, LA	Large-scale trunk line
Dollarhide	1997	23	8	1.6	29,200	TX	Small-scale distribution systems

Project	Year Const.	Pipeline Length (mi)	Pipeline Diameter (in.)	Max. Capacity (Million Tonnes)	Reported Flowrates (MMcf/yr)	State	Type
Eastern Shelf	2011	91	10	2.1	--	TX	Small-scale distribution systems
El Mar	1994	35	6	1.3	25,550	TX	Small-scale distribution systems
Enid-Purdy	2003[1]	117	8	1.6	--	OK	Small-scale distribution systems
Este I to Welch	1997	40	14	3.4	65,700	TX	Small-scale distribution systems
Este II to Salt Creek Field	1993	45	12	2.6	47,450	TX	Small-scale distribution systems
Ford	1995	12	4	1	365	TX	Small-scale distribution systems
Free State	2006	85	20	7	131,400	MS	Small-scale distribution systems
Green Line I	2010	314	24	14	339,500	LA	Large-scale trunk line
Greencore	2013	232	22	18	282,800	WY, MT	Large-scale trunk line
Llano	--	58	8-12	1.6	29,200	NM	Small-scale distribution systems
Lost Solider/Wertz	1980s	30	16	--	15,700	WY	Small-scale distribution systems
Mabee Lateral	1992	18	10	2.1	40,150	TX	Small-scale distribution systems
McElmo Creek	1983*	40	8	1.6	29,200	CO, UT	Small-scale distribution systems
Means	1983	35	12	2.6	47,450	TX	Small-scale distribution systems
Monell	2004	33	8	1.6	29,200	WY	Small-scale distribution systems
North Cowden	1995	8	8	1.6	29,200	TX	Small-scale distribution systems
North Ward Estes	2007	26	12	2.6	47,450	TX	Small-scale distribution systems
Northeast Jackson Dome	2009	183	20	7	131,400	MS, LA	Large-scale trunk line
Pecos County	2004	26	8	1.6	29,200	TX	Small-scale distribution systems
Pikes Peak	--	40	8	1.6	29,200	TX	Small-scale distribution systems
Powder River Basin CO_2	2013	125	16	4.3	80,300	WY	Small-scale distribution systems
Raven Ridge	1985	160	16	4.3	80,300	WY, CO	Small-scale distribution systems
Rosebud	--	50	12	2.6	36,500	NM	Small-scale distribution systems
Salt Creek	2004	125	--	4.3	--		Small-scale distribution systems
Sheep Mountain	1993	408	24	11.4	215,400	TX	Large-scale trunk line
Shute Creek	2010	30	30-20	23.6	445,300	WY	Large-scale trunk line
Slaughter	1984	35	12	2.6	47,450	TX	Small-scale distribution systems
Sonat	--	50	18	3.2	62,050	MS	Small-scale distribution systems
TexOk	2009	95	4.5-6	--	25,550	OK	Small-scale distribution systems
TransPetco	1995	110	8	1.6	29,200	TX, OK	Small-scale distribution systems

Project	Year Const.	Pipeline Length (mi)	Pipeline Diameter (in.)	Max. Capacity (Million Tonnes)	Reported Flowrates (MMcf/yr)	State	Type
Val Verde	1998	83	10	2.1	40,150	TX	Small-scale distribution systems
Velma	2010	145	--	--	12,775	OK	Small-scale distribution systems
Wellman	--	27	6	1.3	25,550	TX	Small-scale distribution systems
West Texas	--	60	8-12	1.6	29,200	TX, NM	Small-scale distribution systems
White Frost	--	11	6	1.3	47,450	MI	Other transport lines
Wyoming CO_2	--	112	20	4.3	80,300	WY	Small-scale distribution systems

Notes: -- Not indicated/Unknown. 1. Indicates start of CO_2-EOR operations.
Information compiled from DOE/NETL (2015), Global CCS Institute (2014), Noothout et al. (2014), Melzer (2002), Oxy (nd), Murrell et al. (2012), Tracy (2013), Doctor et al. (2005), Thomas (2009), Mella (2002), Global CCS Institute (2011), McCollough and Stiles (1987), Dakota Gasification Company (nd), Wiseman (2010), MIT (nd), Voge (2012), Eves and Nevarez (2009), Kinder Morgan (2014), Clark (2012), Denbury (2013), Vandewater (1995), and Trinity Pipeline (2018).

6.5.4 Property ownership

Property ownership along pipeline routes

For a pipeline project, affected property owners must be considered. Parcel ownership shapefiles were obtained for the State of Nebraska[1]. These files were used in conjunction with the mapped routes to determine the property owners affected by the potential routes. Because the cost surface in the underlying SimCCS code does not consider property ownership, the results are not optimized with respect to property owners. Iterations of pipeline routing in future phases should incorporate property ownership information to minimize the number of individual property owners that are included along a route and avoid owners that would be opposed to the project.

Property ownership along each of the pipeline routes modeled using SimCCS were investigated by importing the routes generated using SimCCS into ArcGIS along with parcel ownership shapefiles supplied by the State of Nebraska. The total linear distance (in miles), aggregated by individual landowner and county, along with number of landowners affected and average length of pipeline per landowner affected are shown in Table 6-9. The following observations were made for each route:

- **All 50-50:** The 671 miles of pipeline in Nebraska transected parcels owned by 1,798 individual entities across 26 counties. Average pipeline length per landowner was 0.4 linear miles overall and ranged from 0.2 to 1.0 linear miles when split by county (Table 6-9).
- **Lettered+Power 50-50:** The 386 miles of pipeline in Nebraska transected parcels owned by 764 individual entities across 18 counties. Average pipeline length per landowner was 0.5 linear miles overall and ranged from 0.2 to 1.0 when split by county.
- **Power 50-50:** The 92.4 miles of pipeline in Nebraska transected parcels owned by 764 individual entities across four counties. Average pipeline length per landowner was 0.8 linear miles overall and ranged from 0.6 to 1.0 when split by county.

[1] Parcel ownership shape files for the State of Kansas were not readily publicly available, so the analysis was limited to the pipelines in Nebraska. During future phases of this project, parcel ownership shapefiles will be obtained from county commissioners or private brokers.

- **Power 100:** The 199 miles of pipeline in Nebraska transected parcels owned by 276 individual entities across eight counties. Average pipeline length per landowner was 0.7 linear miles overall and ranged from 0.6 to 1.0 when split by county.
- **Lettered SH:** The 323 miles of pipeline in Nebraska transected parcels owned by 654 individual entities across 15 counties. Average pipeline length per landowner was 0.5 linear miles overall and ranged from 0.2 to 0.8 when split by county.
- **Lettered PP:** The 257 miles of pipeline in Nebraska transected parcels owned by 734 individual entities across 12 counties. Average pipeline length per landowner was 0.4 linear miles overall and ranged from 0.3 to 0.5 when split by county.

Table 6-9. Summary of property ownership (in Nebraska only) for pipeline routes simulated by SimCCS (see Section 6.5.2)

County	All 50-50			Lettered+Power 50-50			Power 50-50			Power 100			Lettered SH			Lettered PP		
	PL length (mi)	No. Own-ers	Avg. length/ Owner	PL length (mi)	No. Own-ers	Avg. length/ Owner	PL length (mi)	No. Own-ers	Avg. length/ Owner	PL length (mi)	No. Own-ers	Avg. length/ Owner	PL length (mi)	No. Own-ers	Avg. length/ Owner	PL length (mi)	No. Own-ers	Avg. length/ Owner
Adams	11.8	74	0.2	---	---	---	---	---	---	---	---	---	---	---	---	30.9	125	0.4
Boone	25.2	53	0.5	30.5	77	0.4	---	---	---	---	---	---	30.5	77	0.4	11.1	31	0.6
Buffalo	23.7	60	0.4	8.1	13	0.6	---	---	---	---	---	---	8.1	13	0.6	---	---	---
Butler	20.1	71	0.3	5.1	11	0.5	---	---	---	---	---	---	5.1	11	0.5	9.4	32	0.5
Colfax	5.5	16	0.4	15.0	41	0.4	---	---	---	---	---	---	15.0	41	0.4	15.0	40	0.6
Custer	---	---	---	10.4	19	0.5	---	---	---	---	---	---	10.4	19	0.5	---	---	---
Dawson	---	---	---	22.7	49	0.5	---	---	---	---	---	---	22.7	49	0.5	---	---	---
Dodge	---	---	---	23.1	66	0.3	---	---	---	---	---	---	23.1	66	0.3	23.1	67	0.3
Douglas	12.0	76	0.2	---	---	---	---	---	---	---	---	---	---	---	---	---	---	---
Fillmore	26.2	57	0.4	---	---	---	---	---	---	---	---	---	---	---	---	---	---	---
Franklin	---	---	---	---	---	---	---	---	---	24.0	33	0.7	---	---	---	27.3	59	0.5
Frontier	26.1	32	0.8	26.1	32	0.8	26.1	32	0.8	26.1	32	0.8	---	---	---	---	---	---
Furnas	25.3	46	0.6	12.0	25	0.5	---	---	---	32.4	52	0.6	12.0	25	0.5	---	---	---
Gage	---	---	---	---	---	---	---	---	---	25.9	39	0.7	---	---	---	---	---	---
Gosper	11.1	18	0.6	33.9	62	0.5	---	---	---	---	---	---	33.9	62	0.5	---	---	---
Greeley	---	---	---	20.7	37	0.6	---	---	---	---	---	---	20.7	37	0.6	---	---	---
Hall	44.3	148	0.3	---	---	---	---	---	---	---	---	---	---	---	---	11.2	32	0.3
Hamilton	46.5	149	0.3	---	---	---	---	---	---	---	---	---	---	---	---	32.2	91	0.4
Hayes	3.1	5	0.6	3.1	5	0.6	3.1	5	0.6	3.1	5	0.6	---	---	---	---	---	---
Hitchcock	11.4	13	0.9	---	---	---	---	---	---	---	---	---	---	---	---	---	---	---
Howard	---	---	---	11.1	18	0.6	---	---	---	---	---	---	11.1	18	0.6	---	---	---
Jefferson	32.9	106	0.3	---	---	---	---	---	---	---	---	---	---	---	---	---	---	---
Kearney	25.3	63	0.4	---	---	---	---	---	---	---	---	---	---	---	---	---	---	---
Lincoln	33.5	33	1.0	33.5	33	1.0	33.5	33	1.0	33.5	33	1.0	---	---	---	---	---	---
Madison	33.8	157	0.2	---	---	---	---	---	---	---	---	---	---	---	---	---	---	---
Merrick	21.3	43	0.5	---	---	---	---	---	---	---	---	---	---	---	---	2.5	5	0.5
Nance	15.7	30	0.5	5.6	18	0.3	---	---	---	---	---	---	5.6	18	0.3	5.6	18	0.3
Nuckolls	---	---	---	---	---	---	---	---	---	3.0	4	0.7	---	---	---	---	---	---
Phelps	27.3	49	0.6	---	---	---	---	---	---	---	---	---	---	---	---	---	---	---
Platte	4.3	22	0.2	31.2	96	0.3	---	---	---	---	---	---	31.2	96	0.3	32.8	95	0.3
Polk	31.7	72	0.4	---	---	---	---	---	---	---	---	---	---	---	---	56.0	139	0.4
Red Willow	50.2	90	0.6	93.2	161	0.6	29.7	47	0.6	51.2	78	0.7	93.2	121	0.8	---	---	---
Richardson	---	---	---	0.2	1	0.2	---	---	---	---	---	---	0.2	1	0.2	---	---	---
Saline	56.7	150	0.4	---	---	---	---	---	---	---	---	---	---	---	---	---	---	---
Sarpy	46.5	165	0.3	---	---	---	---	---	---	---	---	---	---	---	---	---	---	---
TOTAL	**671**	**1798**	**0.4**	**386**	**764**	**0.5**	**92.4**	**117**	**0.8**	**199**	**276**	**0.7**	**323**	**654**	**0.5**	**257**	**734**	**0.4**

Property ownership for modeled plume in the Sleepy Hollow Field (Nebraska)

A model of the CO_2 plume development in the Sleepy Hollow Field (Battelle, 2018b). The resulting plume, after a 40-year period, was around 25 square miles. The property owners within the plume area were identified using publicly available parcel data (Table 6-10). The approximate acreage owned by each entity is also provided. The plume intersects parcels owned by 49 different entities. The number of acres owned by a single entity ranges from 2 to 1,850 acres (340 acres average). Entities include the Board of Education (635 acres), a cemetery (8 acres), two churches (417 total acres), seven farms (2,748 acres), and 38 private owners (13,026 acres).

Table 6-10. Property ownership of parcels intersected by the simulated 40-year plume in the Sleepy Hollow Field.

Owner[1]	Approximate Acreage[2]
Board of Education	635
Cemetery	8
Church #1	236
Church #2	181
Private Farm #1	438
Private Farm #2	561
Private Farm #3	313
Private Farm #4	327
Private Farm #5	403
Private Farm #6	380
Private Farm #7	326
Private Owner #1	973
Private Owner #2	437
Private Owner #3	244
Private Owner #4	1,056
Private Owner #5	81
Private Owner #6	12
Private Owner #7	166
Private Owner #8	1,247
Private Owner #9	56
Private Owner #10	91
Private Owner #11	42
Private Owner #12	325
Private Owner #13	634
Private Owner #14	80
Private Owner #15	101
Private Owner #16	765
Private Owner #17	29
Private Owner #18	408
Private Owner #19	157
Private Owner #20	2
Private Owner #21	633
Private Owner #22	473
Private Owner #23	1,850
Private Owner #24	83
Private Owner #25	204
Private Owner #26	4
Private Owner #27	7
Private Owner #28	221
Private Owner #29	405
Private Owner #30	129
Private Owner #31	40
Private Owner #32	78
Private Owner #33	484
Private Owner #34	17
Private Owner #35	33
Private Owner #36	431
Private Owner #37	318
Private Owner #38	710
TOTAL	**16,832**

1. Because the owners have not been contacted, non-public entities are identified by owner type (e.g., private farm, private owner, etc.).
2. The plume intersects fractions of some parcels at the edges. In these cases, the amount of a parcel intersected by the plume was estimated and the acreage was normalized by multiplying the total acreage of the parcel by the fraction of the parcel intersected by the plume.

6.5.5 Pipeline Safety

Safely operating pipelines is of the utmost importance when considering a project. The current literature suggests operating a natural gas or hazardous liquid pipeline is inherently more dangerous than operating a pipeline transporting CO_2 (Gale and Davison, 2004; Noothourt et al., 2014; Leung et al., 2014; Han et al., 2015); however, many of these sources caveat these results with the small sample size. The rate, severity, and causes of safety incidents with CO_2 pipelines was investigated through a review of

the available literature. Ultimately, pipeline monitoring and mitigation strategies to prevent or mediate CO_2 pipeline safety issues can be implemented to negate or reduce risk from CO_2 pipelines.

Two factors must be considered when reviewing pipeline safety issues: incident rate and incident severity. Leung et al. (2014), reviewing the available literature, found that the rate of incidents increased from the period between 1990-2001 (0.30 incidents/year/1,000 km of pipeline) to the period between 2002-2008 (0.72 incidents/year/1,000 km of pipeline), coinciding with an increase of the increase in the total length of the pipeline network from 2,800 km to 5,800 km. The authors state that while the rate of incidents is still lower than those for hazardous liquid or natural gas pipelines. The rate of incidents will likely increase as the length and complexity of the overall CO_2 pipeline network increases. In addition, Gale and Davison (2004) found that, although there is evidence to suggest the rate of safety incidents associated with CO_2 pipelines is lower than that associated with hazard liquid pipelines, it could be expected to be equivalent with that of natural gas pipelines.

Between 1972-2012, 46 safety incidents involving CO_2 pipelines were due to relief valve failure, weld/gasket/valve packing failure, corrosion, and outside force (Gale and Davison, 2004; Noothout et al., 2014; Han et al., 2015). Other potential causes of safety incidents include interval corrosion of pipelines due to contamination in the CO_2 stream, particularly water, which can mix with CO_2 and create carbonic acid, as well as human/operator error (Gale and Davison, 2004). In general, reported CO_2 safety incidents have been relatively minor compared to natural gas or hazardous liquid pipelines. Gale and Davison (2004) state that incidents involving CO_2 were less severe than those involving either hazard liquid or natural gas pipelines, causing less than half and less than 10% of the property damage (in US Dollars) per 1,000 km of pipeline compared to natural gas and hazard liquid pipelines, respectively. In addition, the safety incidents for CO_2 pipelines resulted in no fatalities or injuries compared to 58 fatalities (0.008 fatalities/1,000 km of pipeline) and 217 injuries (0.029 injuries/1,000 km of pipeline) from incidents between 1986-2001 related to natural gas pipelines and 36 fatalities (0.01 fatalities/1,000 km of pipeline) and 249 injuries (0.067 injuries/1,000 km of pipeline) from incidents between 1986-2001 related to hazardous liquid pipelines.

6.5.6 Protected and sensitive areas

The requirements outlined in the National Environmental Protection Act (NEPA) were assessed to ensure that potential adverse impacts to human health and safety, to the environment, and to culturally or historically significant places would not be significant. Site data were collected for Nebraska and Kansas to address the following categories: air quality, geology and soil, water resources, wetlands, terrestrial vegetation, wildlife, land use, parks and recreation, visual resources, cultural resources, infrastructure (specifically, dams and mining operations), and socioeconomic resources and environmental justice.

Air Quality

The National Ambient Air Quality Standards (NAAQS) Green Book Non-Attainment Areas for Criteria Pollutants was consulted (U.S. EPA, 2016). No areas within the Nebraska were designated "nonattainment" for any of the criteria pollutants (Table 6-11). Two areas within Kansas were designated as nonattainment: Kansas City, which is outside of the proposed study area, was designated as nonattainment for the 1-Hour ozone standard and part of Saline County was designated as nonattainment for the Lead standard. Proposed project activities would not require the modification of local, state, or federal air permits and would follow local and state air quality requirements.

Table 6-11. Current attainment status for criteria pollutants for Nebraska and Kansas (U.S. EPA, 2016).

Criteria Pollutant	Nebraska	Kansas
8-Hour ozone (2008 standard)	Attainment	Attainment
1-Hour ozone (1979 standard)	Attainment	Kansas City, KS[1]
Particulate matter (PM)-2.5 (2012 standard)	Attainment	Attainment
PM-10 (1987 standard)	Attainment	Attainment
SO_2 (2010 standard)	Attainment	Attainment
Lead (2008 standard)	Attainment	Saline Co.[2]
Carbon Monoxide	Attainment	Attainment
Nitrogen Dioxide	Attainment	Attainment

1. Outside of study area.
2. Part of county: "Area bounded by Schilling Rd. on the north, 1/4 mile west of S. Ohio St. on the east, Water Well Rd. on the south, and 9th Street on the west." (U.S. EPA, 2016).

Water Resources

Rivers and streams in Nebraska and northern Kansas flow eastward toward the Missouri River just east of the study area (Figure 6-27).

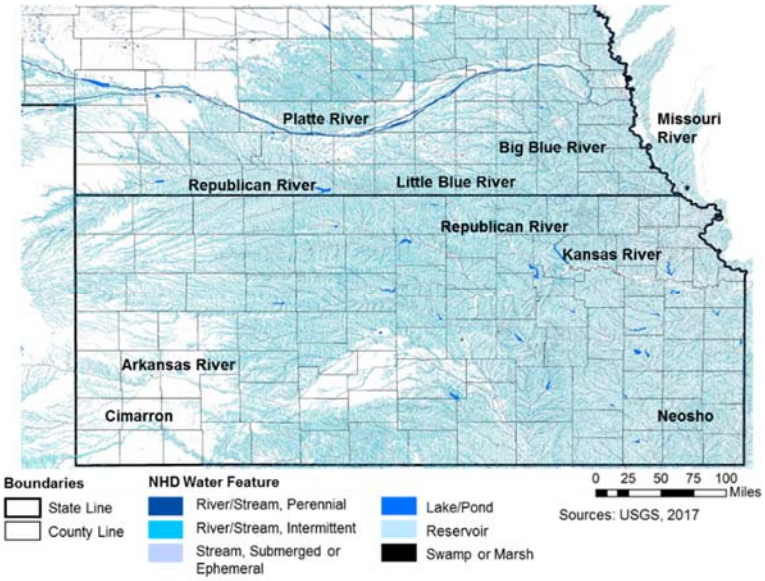

Figure 6-27. National Hydrological Database (NHD) surface waterbodies within study area.

The Missouri River flows eastward and eventually empties into the Mississippi River around St. Louis, Missouri. There are several large tributaries of the Missouri River that flow through the study area. The Platte River bisects Nebraska through the central part of the state. The Republican River flows from the southwestern corner of Nebraska into Kansas where it empties into the Kansas River. The Little Blue and Big Blue Rivers flow from the southeastern corner of Nebraska south into the Kansas River. The Kansas River flows eastward into the Missouri River around Kansas City. Rivers in southern Kansas are tributaries of toward the Arkansas River, which flows through most of the southern part of Kansas (Figure 6-27) and into the Mississippi River in southeastern Arkansas.

Wellhead protection areas or buffer zones can be found in areas around Nebraska and Kansas (NDEQ, 2011; N. LaVoie, personal communication). In addition, the Kansas Department of Health and Environment has 500 ft buffer areas around public water supply wells and surface waters protected for water supply or aquatic life (N. LaVoie, personal communication). These buffers are applicable to

sensitive activities, such as diseased animal burial pits, they are not applicable to a CCS project, per se. However, accounting for these buffer zones will help avoid public perception issues.

The principal aquifers in the study area are shown in Figure 6-28. Most of the study area is underlain by the High Plains Aquifer, also known as the Ogallala Aquifer. The High Plains Aquifer is comprised of Quaternary and Tertiary aged bedrock deposits and, in southeast Nebraska and south-central Kansas, Quaternary age unconsolidated deposits (Miller and Appel, 1997). The aquifer is an important source of irrigation waters; however, widespread irrigation using water from the High Plains Aquifer has caused significant drawdown (Miller and Appel, 1997). The depth to water can be as much as 400 feet below ground surface but is generally much shallower near larger rivers due to hydraulic connectivity of the aquifer with surface water. The principal aquifers in smaller portions of the study area are comprised of Lower Cretaceous rocks, other rocks, or unconsolidated material.

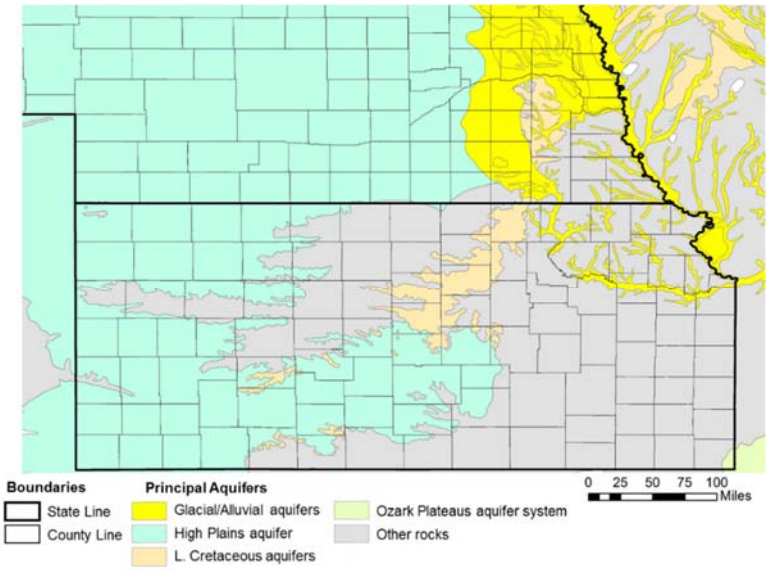

Figure 6-28. Principal aquifers of the study area.

Wetlands, Terrestrial Vegetation, and Wildlife

A number of wetlands are found in the selected study area (Figure 6-29). The largest tracts of wetlands found are found along the Platte River, bisecting the state of Nebraska. Smaller tracts of wetlands are found along the principal tributaries of the Platte, Kansas, and Arkansas Rivers. Some disconnected tracts of emergent/herbaceous wetlands can also be found in southeastern Nebraska and around lakes in central Kansas.

Native terrestrial vegetation consists largely of large swaths of grassland areas, with lesser amounts of mainly deciduous forests (Figure 6-30). Five plants species that are known to exist in Nebraska or Kansas are federally protected, including two listed as endangered (Hayden's [Blowout] penstemon and Colorado butterfly plant [both found in Nebraska only]) and three listed as threatened (Western prairie fringed orchid [found in both Kansas and Nebraska], Ute ladies'-tresses [found in Nebraska only], and Mead's milkweed [found in Kansas only]). Three of the four federally protected plant species found in Nebraska have the same protected designations by the state. The Western prairie fringed orchid, however, is listed as endangered by the State of Nebraska. Three additional plant species that are not federally protected are protected by the State of Nebraska, including one species listed as endangered (saltwort) and two listed as threatened (American ginseng and small white lady's slipper) (Table 6-12).

Kansas law does not protect plant species; thus, the federally listed species are the only plants protected in Kansas (GPNC, nd).

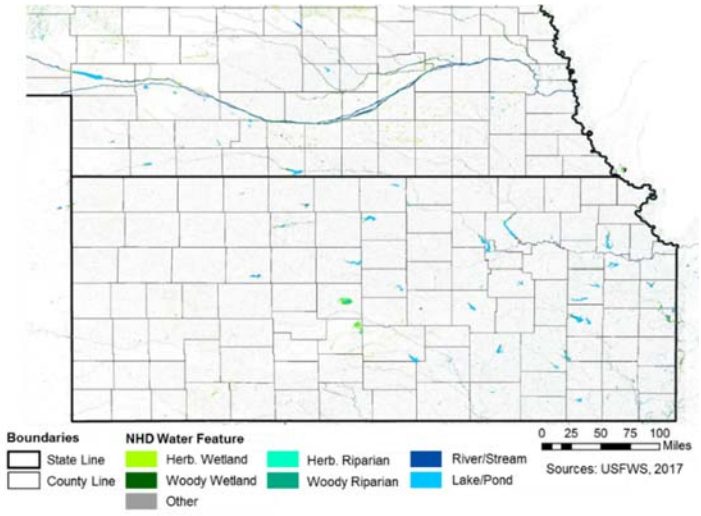

Figure 6-29. Wetlands map of study area.

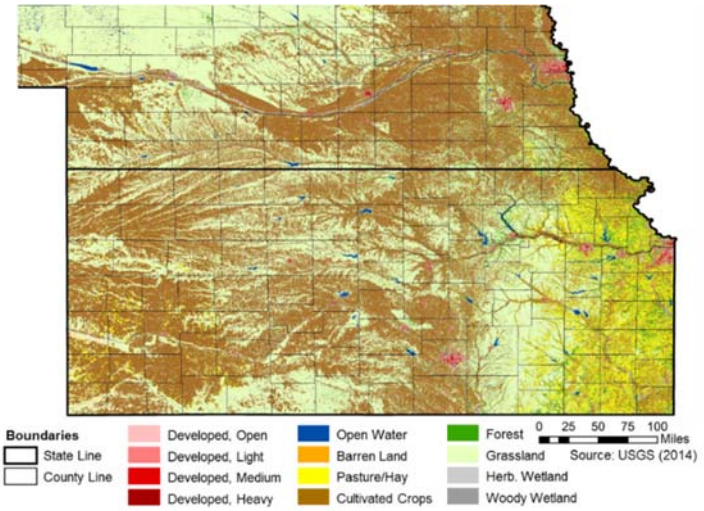

Figure 6-30. Land cover map of study area.

Seventeen federally protected wildlife species are Nebraska or Kansas (Table 6-12):

- Five bird species: Eskimo curlew (Nebraska only), and Whooping crane, Interior least tern, Piping plover, and Red knot (both states).
- Three mammals: Black-footed ferret (historically Nebraska, currently Kansas), Northern long-eared bat (both states), and Gray bat (Kansas).
- Four fish: Pallid sturgeon (both states), Topeka shiner (both states with critical habitat in east-central Arkansas), Neohso madtom (Kansas only) and Arkansas river shiner (Kansas only with critical habitat in southwest Arkansas).
- Two beetles: American burying beetle (both states) and Salt Creek tiger beetle (critical habitat both states).
- One moth: Rattlesnake-master borer moth (candidate species) (Kansas).

- Four mussels: Neosho mucket and Rabbitsfoot (Kansas with critical habitat in southeast Kansas), Scaleshell mussel (Nebraska), and Spectaclecase (Kansas).
- Five plants: Western prairie fringed orchid (both states), Hayden's (Blowout) penstemon, Colorado butterfly plant, Ute ladies'-tresses (Nebraska), and Mead's milkweed (Kansas).

Care will be taken to ensure that project activities do not exacerbate habitat loss and sedimentation and/or foster the expansion of invasive species for these and the florae and faunae protected by the state.

The federally listed species that occur in Nebraska have the same status on the state level except for the Red knot and the Northern long-eared bat, which are not listed, and the Western prairie fringed orchid, which is listed as endangered in Nebraska. The federally listed species that occur in Kansas have the same status on the state level except for the Red knot, the Northern long-eared bat, the Spectaclecase mussel, the Western prairie fringed orchid, and Mead's milkweed, which area not listed as protected on the state level, as well as the Topeka shiner, which is listed as threatened on the state level, and the Arkansas River shiner and Rabbitsfoot mussel, which are listed as endangered on the state level.

An additional 12 species are under review in Nebraska or Kansas (Table 6-12):

- Two birds: Eastern black rail (found in both states) and Lesser prairie chicken (found in Kansas).
- Three fish: Sturgeon chub (found in both states and listed as endangered in Nebraska and threatened in Kansas) and Sicklefin chub and Peppered chub (both listed as endangered in Kansas).
- Four invertebrates: Regal fritillary (found in both states), Western fanshell mussel (listed as endangered in Kansas), and Monarch butterfly and Ozark emerald (found in Kansas).
- One amphibian: Hellbender salamander (found in Kansas).
- One chelonian: Blanding's turtle (found in Nebraska).
- One plant: Hall's bulrush (found in both states).

An additional 37 wildlife species are listed as state protected species in Nebraska and Kansas, including three listed as endangered in Nebraska, nine listed as threatened in in Nebraska, nine listed as endangered in Kansas, and 26 listed as threatened in Kansas (Table 6-13).

Table 6-12. Federally listed protected species in Nebraska and Kansas (U.S. FWS, 2015a, b; Nebraska Environmental Trust, nd; Kansas Department of Wildlife, Parks, and Tourism, nd).

Common Name	Description	Fed. Status[1]	Critical Habitat[2]	Nebraska		Kansas	
				In State	State Status[1]	In State	State Status[1]
Eskimo curlew	Bird	E	Not Mapped	Yes[3]	E	No	--
Whooping crane	Bird	E	Nebraska (Platte River)	Yes	E	Yes	E
Interior least tern	Bird	E	Not Mapped	Yes	E	Yes	E
Piping plover	Bird	T		Yes	T	Yes	T
Red knot	Bird	T	Not Mapped	Yes	NL	Yes	NL
Lesser prairie chicken	Bird	UR	Not Mapped	No	--	Yes	NL
Eastern black rail	Bird	UR	Not Mapped	Yes	NL	Yes	NL
Black-footed ferret	Mammal	E	Not Mapped	Yes[3]	E	Yes	E
Gray bat	Mammal	E	Not Mapped	No	--	Yes	E
Northern long-eared bat	Mammal	E	Not Mapped	Yes	NL	Yes	NL
Pallid sturgeon	Fish	E	Not Mapped	Yes	E	Yes	E
Topeka shiner	Fish	E	East-Central Nebraska	Yes	E	Yes	T
Neosho madtom	Fish	T	Not Mapped	No	--	Yes	T
Arkansas River shiner	Fish	T	SW Kansas	No	--	Yes	E
Sturgeon chub	Fish	UR	Not Mapped	Yes	E	Yes	T
Sicklefin chub	Fish	UR	Not Mapped	No	--	Yes	E
Peppered chub	Fish	UR	Not Mapped	No	--	Yes	E
American burying beetle	Invertebrate	E	Not Mapped	Yes	E	Yes	E
Salt Creek tiger beetle	Invertebrate	E	Nebraska	Yes	E	No	--
Neosho mucket	Invertebrate	E	SE Kansas	No	--	Yes	E
Scaleshell mussel	Invertebrate	E	Not Mapped	Yes	E	No	--
Rabbitsfoot	Invertebrate	T	SE Kansas	No	--	Yes	E
Spectaclecase	Invertebrate	E	Not Mapped	No	--	Yes	NL
Western fanshell mussel	Invertebrate	UR	Not Mapped	No	--	Yes	E
Monarch butterfly	Invertebrate	UR	Not Mapped	No	--	Yes	NL
Regal fritillary	Invertebrate	UR	Not Mapped	Yes	NL	Yes	NL
Ozark emerald	Invertebrate	UR	Not Mapped	No	--	Yes	NL
Rattlesnake-master borer moth	Invertebrate	C	Not Mapped	No	--	Yes	NL
Hellbender salamander	Amphibian	UR	Not Mapped	No	--	Yes	NL
Blanding's turtle	Chelonian	UR	Not Mapped	Yes	NL	No	--
Hayden's (Blowout) penstemon	Plant	E	Not Mapped	Yes	E	No	--
Colorado butterfly plant	Plant	E	Not Mapped	Yes	E	No	--
Western prairie fringed orchid	Plant	T	Not Mapped	Yes	E	Yes	NL
Ute ladies'-tresses	Plant	T	Not Mapped	Yes	T	No	--
Mead's milkweed	Plant	T	Not Mapped	No	--	Yes	NL
Hall's bulrush	Plant	UR	Not Mapped	Yes	NL	Yes	NL

1. Status: E - Endangered, C - Candidate, UR - Under Review, T - Threatened, NL - Not listed on state resource
2. As defined by the United State Fish and Wildlife Service (US FWS) (2017).
3. Historically found in state. Listed as federally protected species on state resource.

Table 6-13. State listed protected species in the selected areas Note: 1. State Status: E - Endangered, T – Threatened (KDWPT, nd; Nebraska Environmental Trust, nd).

Common Name	Description	State Status[1]	State
Mountain plover	Bird	T	NE
Snowy plover	Bird	T	KS
Swift fox	Mammal	E	NE
River otter	Mammal	T	NE
Southern flying squirrel	Mammal	T	NE
Eastern spotted skunk	Mammal	T	KS
Blacknose shiner	Fish	E	NE
Lake sturgeon	Fish	T	NE
Northern redbelly dace	Fish	T	NE
Finescale dace	Fish	T	NE
Silver chub	Fish	E	KS
Blackside darter	Fish	T	KS
Flathead chub	Fish	T	KS
Hornyhead chub	Fish	T	KS
Arkansas darter	Fish	T	KS
Redspot chub	Fish	T	KS
Plains minnow	Fish	T	KS
Shoal chub	Fish	T	KS
Western silvery minnow	Fish	T	KS
Elktoe mussel	Invertebrate	E	KS
Sllipse mussel	Invertebrate	E	KS
Flat floater mussel	Invertebrate	E	KS
Mucket mussel	Invertebrate	E	KS
Butterfly mussel	Invertebrate	T	KS
Flutedshell mussel	Invertebrate	T	KS
Ouachita kidneyshell mussel	Invertebrate	T	KS
Rock pocketbook mussel	Invertebrate	T	KS
Scott Optioservus riffle beetle	Invertebrate	E	KS
Slender walker snail	Invertebrate	E	KS
Delta hydrobe	Invertebrate	T	KS
Sharp hornsnail	Invertebrate	T	KS
Massasauga	Reptile	T	NE
Broadhead skink	Reptile	T	KS
Checkered garter snake	Reptile	T	KS
New Mexico threadsnake	Reptile	T	KS
Northern map turtle	Chelonian	T	KS
Cave salamander	Amphibian	E	KS
Grotto salamander	Amphibian	E	KS
Eastern narrowmouth toad	Amphibian	T	KS
Eastern newt	Amphibian	T	KS
Green frog	Amphibian	T	KS
Green toad	Amphibian	T	KS
Longtail salamander	Amphibian	T	KS
Strecker’s chorus frog	Amphibian	T	KS
Saltwort	Plant	E	NE
American ginseng	Plant	T	NE
Small white lady’s slipper	Plant	T	NE

Land Use

The study area is comprised largely of cultivated cropland interspersed with open grasslands and surface water bodies (Figure 6-30). Lesser amounts of mainly deciduous forests and land used for pasture/hay are also found throughout the area. Larger cities and developed land area also found in the study area; however, developed land mostly found east of the study area around Omaha, Lincoln, Kansas City, and Wichita.

Publicly-Owned Lands, Protected Lands, and Historic Places

The Protected Areas Database of the United States (PAD-US) provides an inventory of public lands and other protected areas in the US (USGS2), Figure 6-31. A map of the publicly-owned lands and lands owned by private non-governmental organizations (NGOs) or other private conservancy organizations is provided in Figure 6-32. Several large tracts of land within the study area are owned by the federal government, including a nearly 35,000-acre agricultural research center that abuts a nearly 4,000-acre Department of Defense (DoD) facility in Clay and Adams Counties, Nebraska, a 31,000-acre recreation area along the Republican River and Harland County Lake that is managed by the Army Corps of Engineers (U.S. ACE) in Harlan County, Nebraska, a 22,000-acre recreational area along the Saline River that is managed by the U.S. ACE in Russell and Lincoln Counties, Kansas, and a nearly 110,000-acre tract of National Forestland in Morton County, Kansas. Multiple large state-owned parcels are also available in the study area, particularly in western Kansas.

The PAD-US database also includes designations under the Gap Analysis Program (GAP), which indicates the management status using a numerical code ranging from 1 to 4 (USGS2):

- 1-The area is managed for biodiversity but that ecological disturbances are allowed.
- 2-The area is managed for biodiversity and that ecological disturbances are not allowed.
- 3-The area is managed for other uses and that extraction of minerals is allowed.
- 4-There are no protection orders or that the data are missing.

In addition, 698 locations in the study area are registered with the National Register of Historic Places (NRHP), including architectural sites, buildings, churches, and bridges (National Park Service, 2017). An additional 1,179 locations are current pending nomination with the NRHP.

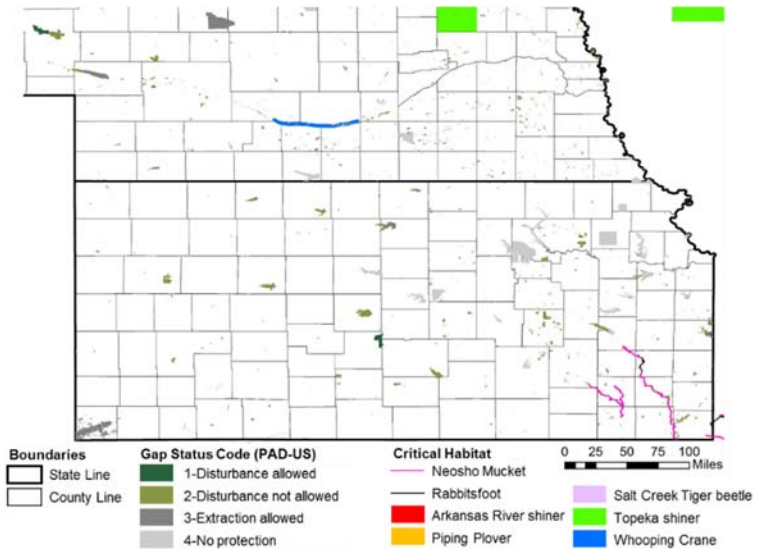

Figure 6-31. Map of GAP Status Code (PAD-US) and critical habitats in the study area.

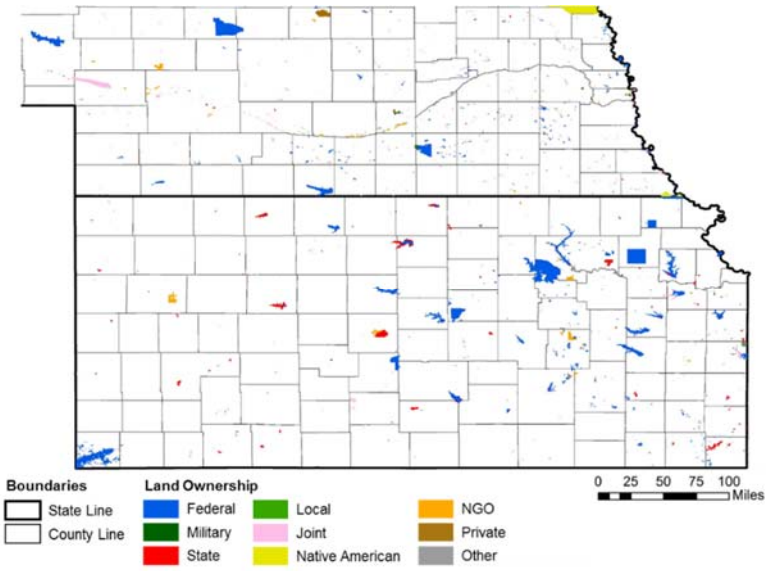

Figure 6-32. Publicly-owned lands in the study area.

Critical Infrastructure and Mining Operations

A map of schools, dams, and airports in the study area is provided in Figure 6-33. These areas will be avoided when selecting a specific pipeline route to avoid complications with existing infrastructure and/or areas that would be sensitive to the surrounding community. Mining operations in the area are mapped in Figure 6-34. Most of these mines are surface mines for unconsolidated materials, that follow major rivers, or solid rock quarries. There are some salt mines and sulfur mines in central and southeast Kansas. Lime or cement mines are also found throughout the study area.

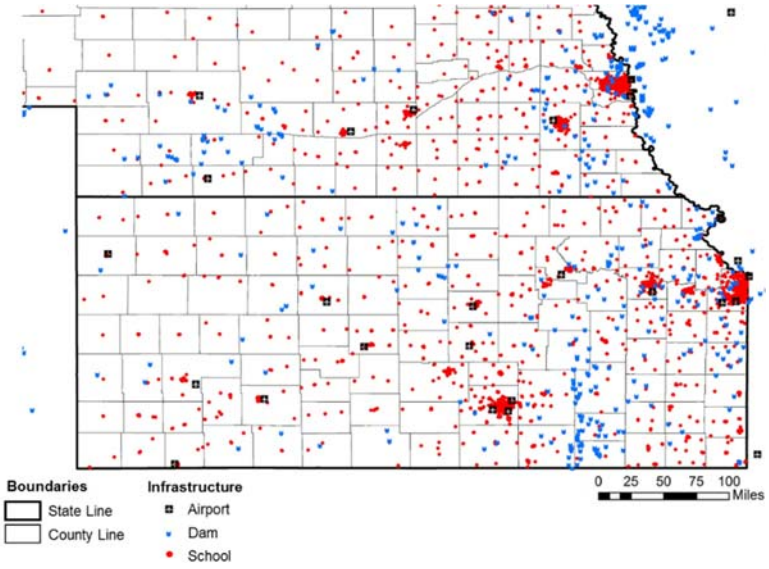

Figure 6-33. Airports, Dams, and Schools in the proposed study area.

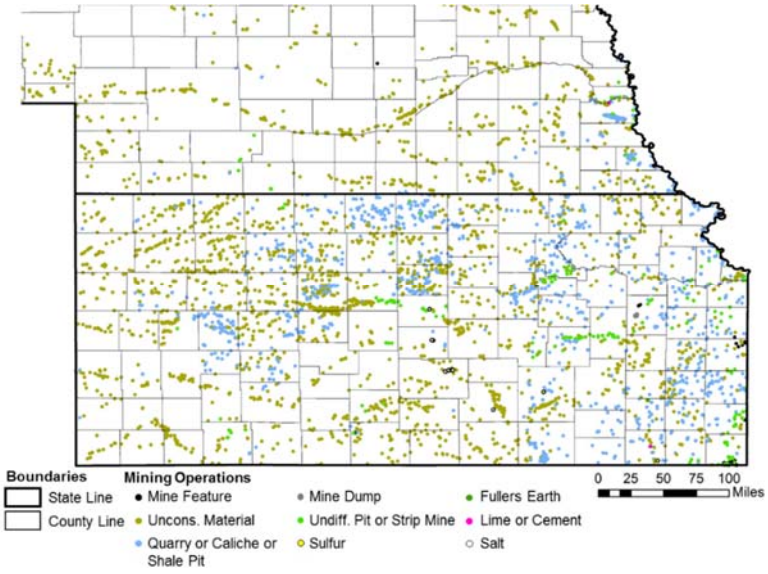

Figure 6-34. Mining operations in the proposed study area.

Parks and Recreation and Visual Resources

The PAD-US provides an inventory of public lands and other protected areas in the US (USGS, 2016a). Several large tracts of land within the study area are owned by the federal government, including a nearly 35,000-acre agricultural research center in Clay and Adams Counties, Nebraska, a 31,000-acre recreation area along the Republican River and Harland County Lake that is managed by the Army Corps of Engineers (U.S. ACE) in Harlan County, Nebraska, a 22,000-acre recreational area along the Saline River that is managed by the U.S. ACE in Russell and Lincoln Counties, Kansas, and a nearly 110,000-acre tract of National Forestland in Morton County, Kansas. Multiple large state-owned parcels are also available in the study area, particularly in western Kansas. A total of 698 locations in the study area are registered with the National Register of Historic Places (NRHP), including architectural sites, buildings, churches, and bridges (National Park Service, 2017). An additional 1,179 locations are current pending

nomination with the NRHP. These areas (shown on the Kansas and Nebraska inset maps only) will be avoided when siting project infrastructure.

Contaminated Sites

All environmentally contaminated sites will be avoided when siting project infrastructure. There are 17 active Superfund National Priority List (NPL) site in Nebraska and 12 in Kansas (U.S. EPA, 2018). Most of the NPL sites are in the eastern half of the states, far from the proposed sinks area, and are near populated areas that would be avoided when siting project infrastructure anyway. In addition, 13 open leaking underground storage tank (LUST) sites can be found in Red Willow County, Nebraska (the sinks area) (NDEQ, nd) and 15 open LUST sites can be found in Finney, Scott, Kearny, and Wichita Counties, Kansas (the sinks area) (KDHE, nd). These sites are often in developed areas and are, thus, not targets for project infrastructure anyway. There are no nuclear contamination sites in the sinks area (Wall Street Journal, nd).

Socioeconomic Resources and Environmental Justice

Socioeconomic resources and environmental justice issues were investigated for the study area using data from the U.S. Census Bureau (U.S. Census Bureau, 2016a, b, c, d). The data were aggregated by Census block group, which were used to generate a series of maps. Much of the study area is either grassland or farmland, meaning population density is less than 50 people per mile for most of the area (Figure 6-35). Population density within the study area increased around cities and towns, often reaching more than 5,000 people per square in larger towns. The sink areas of interest are in rural areas and smaller towns, rarely exceeding 500 people per square mile. The areas with low population density could potentially provide project locations that would not adversely affect residents, particularly in areas that are already industrialized.

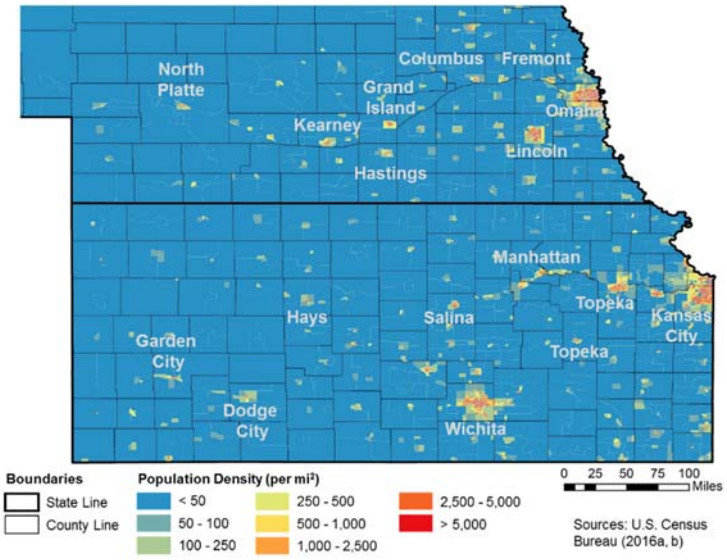

Figure 6-35. Population density in the study area.

The 2015 unemployment rate of residents over the age of 16 that are considered in the labor force is low (i.e., less than 4% or between 4% and 7%) throughout the study area (Figure 6-36). The areas east of the study area have higher unemployment rates, particularly in and around more densely populated incorporated areas. Some less densely populated areas in western Kansas also have higher unemployment rates, specifically in northwest Seward County and northeastern Ellis County.

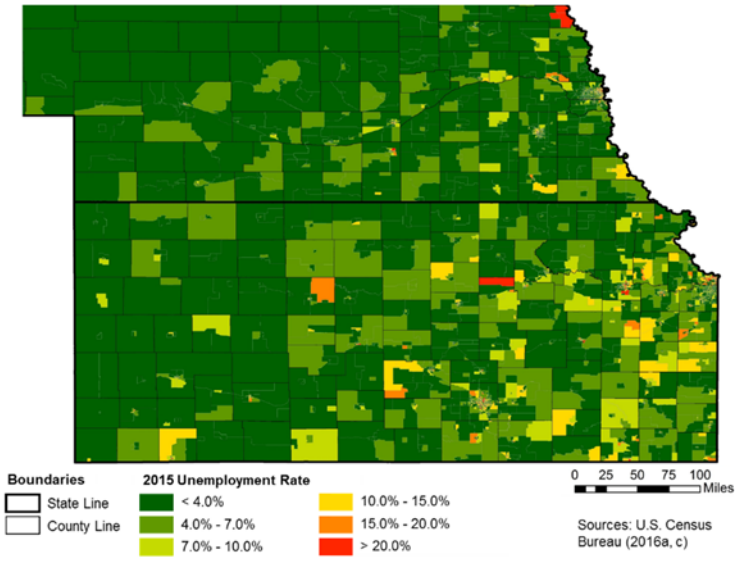

Figure 6-36. 2015 Unemployment rate in the study area.

The median income of the households in each Census Block of Kansas and Nebraska varies from less than $25,000 a year to more than $150,000 a year (Figure 6-37). Most of the Census Block groups in the study area have an average household income between $25,000 and $75,000. The percentage of households making less than $25,000 a year is particularly concentrated in the Census Block Groups in rural areas in south-central Nebraska and western Kansas.

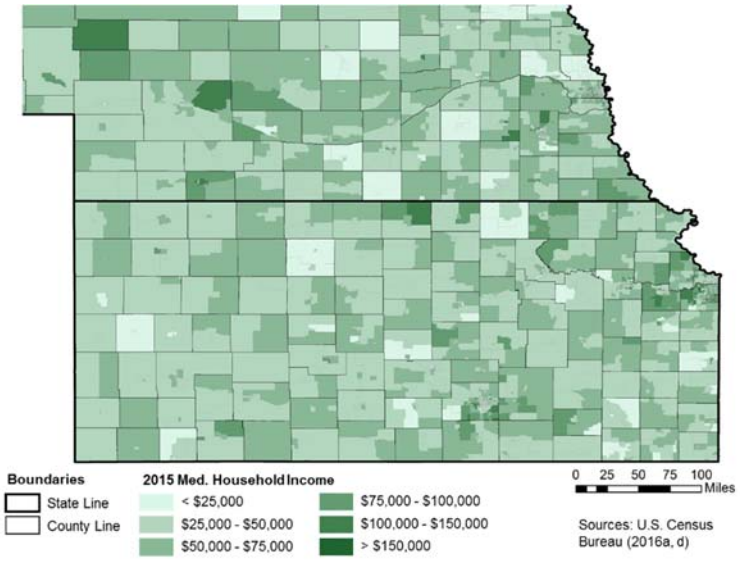

Figure 6-37. Median annual household income in the study area.

6.5.7 Obstacles and barriers to operations

Environmentally sensitive areas were ordered into one of four categories based on land characteristics and associated project requirements:

- *Open areas* include National Land Cover Database (NLCD) (United States Geological Survey [USGS], 2014) designations of grassland, cultivated crops, pasture, or shrubland/scrubland. They are preferred for siting wells, equipment, or pipelines.

- *Wooded areas* include NLCD designations of deciduous evergreen or mixed forests (USGS, 2014). They can be used to stage wells, equipment, or pipelines.
- *Surface Obstacles* include wetlands (United States Fish and Wildlife Service [U.S. FWS], 2017a) and 100-year floodplains (Federal Emergency Management Agency [FEMA], 2017a, b). They can be used to site wells, equipment, or pipelines with a permit or other consideration.
- *Surface Barriers* include areas with a Protected Areas Database of the United States (PAD-US) Gap Analysis Program (GAP) designation of #1 or #2 (protected for wildlife/biodiversity) (USGS, 2016a), critical habitats (U.S. FWS, 2017b), NLCD light, medium, and heavy developed areas (USGS, 2014), scenic rivers (Bureau of Land Management [BLM], NPS, U.S. FWS, and U.S. Forest Service [USFS], 2017), surface water (USGS, 2016b, c), National Historic Places Registry (NHPR) sites (National Parks Service, 2017), wellhead protection areas (NDEQ, 2011), surface water protection buffers (KDHE, 2010), existing surface mineral extraction (USGSa), or contaminated areas (U.S. EPA, 2018; NDEQ, nd; KDHE, nd). These areas should be considered when citing wells, equipment, or pipelines, either by legal requirement and/or potential complications with public acceptance.

A map of these features is shown in Figure 6-38. Ultimately, it was determined that operations in the proposed storage areas will not interfere with environmentally sensitive areas. In addition, pipeline routes that do not interfere with environmentally sensitive areas are also possible between sources and proposed sinks.

The IMSCS-HUB storage complex is targeting saline aquifers located within existing oil and gas field operations, leading to three advantages. First, the residents of targeted sink areas will be accustomed to well drilling operations and the infrastructure, increased traffic, and pipeline operations associated with it. Secondly, while most land in the sinks area is privately owned, residents within the sinks areas will be familiar with negotiating resource leases and could be more amenable to leasing pore space beneath their property. Finally, the area is largely cleared land with a low population density.

There is little risk of resource development conflicts for the project. Most of the mines in Kansas and Nebraska are surface mines for unconsolidated materials, that follow major rivers, or solid rock quarries. There are some salt mines and sulfur mines in central and southeast Kansas. Lime or cement mines are also found throughout the study area. There are some underground limestone mines in eastern Nebraska, far away from the proposed storage area (D. Divine, personal communication).

An evaluation of potential pipeline routes to proposed storage locations was completed based on publicly available information and contractor's industry knowledge. The analysis included identification of all major permit and regulatory requirements and regulatory gaps relevant to the construction, ownership, and operation of the pipeline system. Major environmental considerations were also identified for the potential pipeline routes to potential storage areas within Kansas and Nebraska. A preliminary design basis for the pipeline system configuration was developed, including estimates on capital and operating cost methodology to be used in evaluating each of the pipeline system routes. In association with NRAP research, a preliminary capital and operating cost model was developed to estimate the net present value economics of the potential pipeline system routes based on the CO_2 specification provided. Land owners along the proposed pipeline routes in Nebraska have been identified. A plan to conduct a similar analysis in Kansas can also be implemented using publicly available data once pipeline routes are finalized.

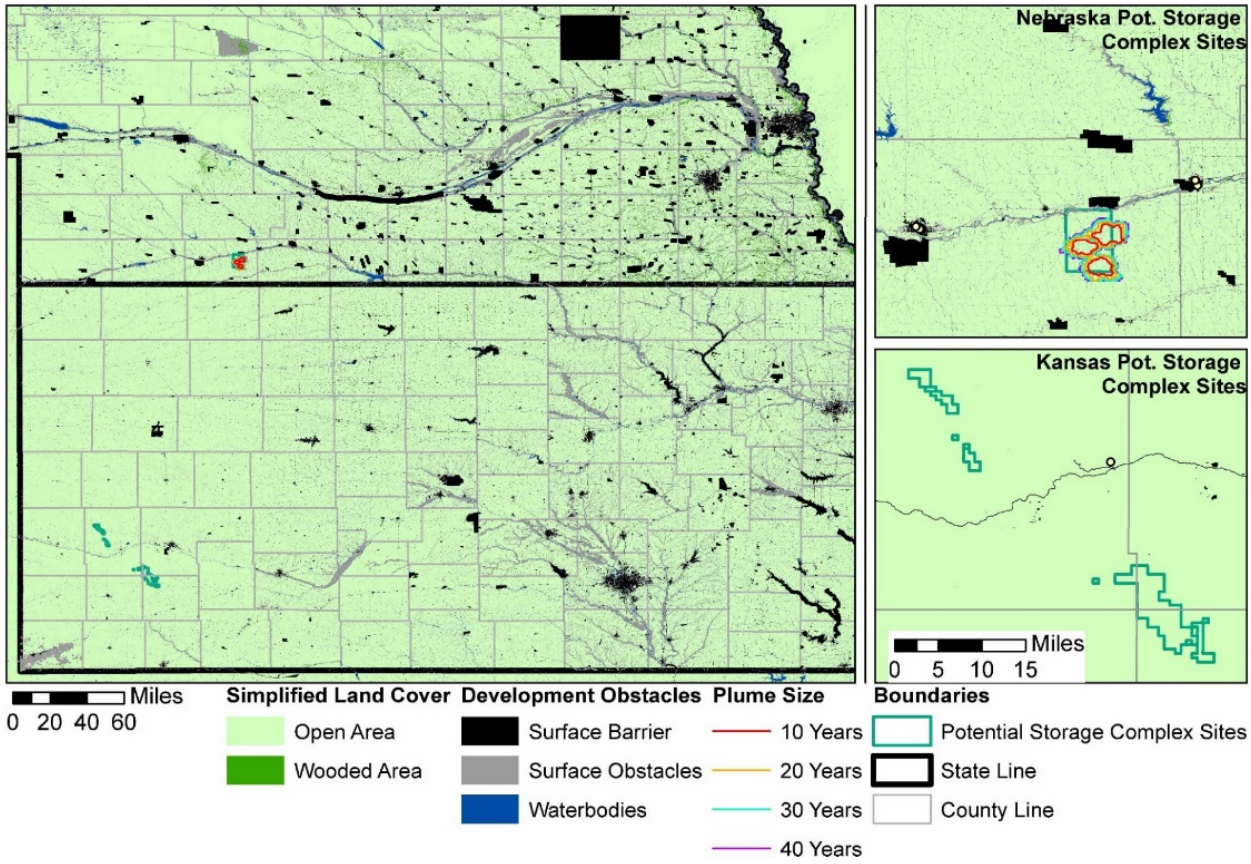

Figure 6-38. Map of simplified land use and project obstacles and barriers.

6.6 Discussion

The main components in the capture of CO_2 at an ethanol plant is dehydration and compression for pipeline transport. As such, capture of CO_2 from ethanol facilities is a relatively inexpensive process compared to other industrial sources. Because capture costs, one of the main costs of CCS, are much lower than for other industrial sources, the viability of a CCS or CO_2-EOR project are much more favorable than for many other sources including electric utilities. With the recent passage of 45Q, the potential of a CCS project with an ethanol facility or facilities as the main source of CO_2 is even greater. Although the cost of capture is considerably higher, two coal fired power plants in the study area, the Gentleman Gerald Station in Lincoln County, Nebraska and the Jeffrey Energy Center in Pottawatomie County, Kansas, have the potential to provide a combined total of nearly 28 Million Tonnes of CO_2 per year. The existence of a significant amount of ethanol sources in addition to electric utility sources in the region could allow for a phased introduction of CO_2 into the project and a phased rollout of storage sites in the storage corridor. The initial focus in this project is collection and storage of CO_2 from ethanol plant to meet DOE's goal of commercial operation by 2025. However, once the infrastructure and storage market are in place electric utilities can tap into the pipeline and market to store their CO_2. This allows more time to commercialize post combustion capture while still storing CO_2 in the near future.

The near-field transport CO_2 for storage near the ADM ethanol plant in Columbus, Nebraska is infeasible because the potential reservoirs are too shallow. Therefore, injected CO_2 would not remain in a super critical state. As a result, the efforts were focused mainly on far-field transport.

Far-field transport was investigated using several methods, including modeling to determine pipeline design, specifications and routing. The pipeline design and specification modeled using PIPESIM suggests that a 12-inch trunk pipeline may be best but other trunk lines including 10-inch and 10-inch/12-inch can work depending on the number and location of booster stations. This diameter of the pipeline and the location of compressor stations balances the cost of construction with the capacity of the pipeline and reduction in pressure loss. While only one compressor station was needed for the modeled route in the prefeasibility phase more detailed modeling including transient modeling will be needed in later phases to ensure pipeline operations including startup and shutdown are safe.

Six viable pipeline routes were modeled across the study area with SimCCS. The combination of routes shows a number of scenarios connecting the ethanol plants and coal fired power plants to the sinks of interest, saline aquifers and oilfields in southwestern Nebraska and eastern Kansas. Trunk pipelines for each simulation connected the largest sources to the sinks. The trunk pipelines can be compared by determining the amount of annual emissions per mile of pipeline delivered to the sink when considering only the sources along the trunk line. This exercise allows for the comparison of trunk lines for each of the scenarios by normalizing pipeline length by the amount of emissions delivered to the source. In addition, it allows for the determination of the efficacy of smaller-scale lines, which were also evaluated based on the amount of CO_2 delivered to the trunk line per year per mile of pipeline. The results for the trunk lines are as follows:

- All 50-50 (two trunk lines): 0.008 Million Tonnes/year/mile pipeline (Nebraska); 0.048 Million Tonnes/year/mile pipeline (Kansas);
- Lettered + Power 50-50 (three trunk lines): 0.006 Million Tonnes/year/mile pipeline (Nebraska); 0.011 Million Tonnes/year/mile pipeline (storage corridor); 0.052 Million Tonnes/year/mile pipeline (Kansas);
- Power 100 (two trunk lines): 0.139 Million Tonnes/year/mile pipeline (Nebraska); 0.066 Million Tonnes/year/mile pipeline (Kansas);
- Power 50-50 (three trunk lines): 0.139 Million Tonnes/year/mile (Nebraska); 0.016 Million Tonnes/year/mile pipeline (storage corridor); 0.052 Million Tonnes/year/mile pipeline (Kansas);
- Lettered SH (one trunk line): 0.006 Million Tonnes/year/mile pipeline; and
- Lettered PP (one trunk line): 0.004 Million Tonnes/year/mile pipeline.

The largest amount of emissions per year per mile of pipeline come from the trunk lines connecting coal the coal fired power plants directly to the sources (i.e., All 50-50 [Kansas], Lettered + Power [Kansas], Power 100 [both trunk lines], and Power 50-50 [Nebraska and Kansas]), with values ranging from 0.048 Million Tonnes/year/mile pipeline to 0.139 Million Tonnes/year/mile pipeline. The values of emissions per year per mile of pipeline were particularly high when the source was close to the sink, as was the case for the Nebraska trunk lines for the Power 100 and Power 50-50 scenarios. The high amounts of emissions per mile of pipeline from the coal fired power plant sources must be weight against the cost of capture (i.e., purity of the source) and long-term viability of the source compared to the ethanol sources in the area.

The ethanol-based-CO_2 trunk lines (i.e., the Nebraska pipelines in the All 50-50 and Lettered + Power 50-50 scenarios and the trunk lines for the Lettered SH and Lettered PP scenarios) had much lower amounts of emissions per year per mile of pipeline, ranging from 0.004 Million Tonnes/year/mile of pipeline to 0.008 Million Tonnes/year/mile pipeline. In most cases, the lower emissions per year per mile of pipeline for the ethanol sources would likely be offset by the lower cost of capture, which are said

account for 70-90% of CCS costs (Global CCS Institute, 2017), and the long-term viability of the ethanol sources.

The yield of the pipeline per mile of pipeline could be increased by the smaller-scale pipelines connecting other ethanol sources to the main trunk line. In instances where a smaller-scale pipeline's emissions per year per mile of pipeline are greater than that of the trunk line for the scenario, the addition of that pipeline would increase the yield of the trunk line. The following smaller-scale pipelines would increase the yield per mile of pipeline under each scenario:

- All 50-50
  - Segments 7 and 8 (connects Jeffrey Energy Center and Flint Resources, Fairmont and Abengoa Bioenergy [York County, NE] to the Nebraska trunk line) - 0.010 Million Tonnes/year/mile pipeline.
  - Segment 10 (connects AGP Corn/Soy Processing and Chief Ethanol Fuels to Nebraska trunk line) - 0.018 Million Tonnes/year/mile pipeline.
  - Segment 17 (connects Gerald Gentleman State directly to the Sleepy Hollow Field) - 0.139 Million Tonnes/year/mile pipeline.
- Lettered + Power 50-50
  - Segment 1 (connects Cargill Corn Milling North America to main trunk line) - 0.006 Million Tonnes/year/mile pipeline.
  - Segment 5 (connects Gerald Gentleman State directly to the Sleepy Hollow Field) - 0.139 Million Tonnes/year/mile pipeline.
- Power 100: No smaller-scale lines.
- Power 50-50: No smaller-scale lines.
- Lettered SH
  - Segment 1 (connects Cargill Corn Milling North America to main trunk line) - 0.006 Million Tonnes/year/mile pipeline.
- Lettered PP
  - Segment 1 (connects Cargill Corn Milling North America to main trunk line) - 0.006 Million Tonnes/year/mile pipeline.
  - Segment 2 (connects Valero Albion Plant to main trunk line) - 0.004 Million Tonnes/year/mile pipeline.

Most of the selected sources have pipelines within the vicinity. The locations shown on the maps included in this report should be considered approximate because they were generated to a shapefile based on estimating the location from the (NPMS) Public Viewer (U.S. DOT, 2018). All but one of the modeled pipeline routes (Power 100) had at least one segment with an overlapping existing pipeline. Generally, these existing pipelines were natural gas transport. These existing routes could serve as rights-of-way for the proposed pipeline routes, potentially circumventing property acquisition through eminent domain and alleviating public opposition.

A recent policy examination by the State CO_2-EOR Deployment Work Group (2017) investigated strategies to increase the scale and availability of CO_2 for the purposes of EOR. The report concluded that one of the main obstacles to large-scale CO_2-EOR is a lack of infrastructure, particularly trunk pipelines, to transport CO_2 to oilfields. The CO_2 pipelines proposed as part of this project could serve as an extension of existing CO_2 pipelines, currently in the Permian Basin, to ethanol and other industrial sources in the mid-continent region (see Figure 6-26). Ultimately, any of the trunk lines presented in the six scenarios outlined in Section 6.5.2 could serve this function.

Property ownership along the pipeline route was not optimized for the number of landowners when the routes were modeled using SimCCS. However, the resulting routes showed that the average pipeline length per landowner was between 0.4 to 0.8 miles, indicating that the pipeline is routed through areas with large parcels with relatively few owners. The number of owners along the pipeline route can be refined in future phases. The landowner analysis in the Red Willow County, Nebraska Plume Area shows that the modeled plume will underlie properties belonging to a reasonable number of landowners (49 owners) that can feasibly be negotiated with and compensated for the pore space filled.

While it is unclear if pipeline incidents involving CO_2 pipelines occur at a lower rate than hazardous liquid or natural gas pipelines, there is evidence to suggest the consequences of these incidents, in terms of property damage, injury, and fatalities, is less likely for CO_2 pipelines than with other types of pipelines (Gale and Davison, 2004). With the proper monitoring, design, and siting of CO_2 pipelines, many potential issues can be avoided.

Finally, while there are environmentally sensitive areas (i.e., wetlands, PAD-US #1 and #2 designated areas, critical habitats, water protection areas, etc.), culturally and historically sensitive areas (Native American Reservations, National Parks, etc.), and other sensitive areas (existing mineral extraction, contaminated sites, etc.) within the study area, there are no “show stoppers” that would prevent a project from moving forward. An analysis of the “obstacles” (areas that can be developed with additional considerations like a permit) and “barriers” (areas that cannot be developed) shows that most obstacles and all barriers can be easily avoided by project infrastructure.

6.7 Conclusions

The IMSCS-HUB project is a significant opportunity to implement a commercial CCS project for many reasons, not the least of which is the potential to link saline storage aquifers and oilfields in southwestern Nebraska and eastern Kansas to ethanol sources in Nebraska and, potentially, the rest of the Great Plains Region. Ethanol-derived-CO_2 provides a relatively pure stream of CO_2 that can be easily captured at commercial volumes with off-the-shelf equipment. The cost of capture at ethanol CO_2 sources is relatively low compared to other industrial sources. Both of these factors allow for early implementation of a commercial carbon storage hub. Furthermore, linking these sources with sinks could provide a feasible path forward for CCS, particularly after the passage of the 45Q rules earlier this year. In addition, linking the trunk pipelines investigated in this project with existing CO_2 pipelines in Texas would allow the delivery of low-cost CO_2 to oilfields in the current study area as well as the Permian Basin.

The results demonstrate that multiple viable pipeline routes capable of delivering 1.7 Million Tonnes per year or more can connect the ethanol and coal fired power plant sources in Nebraska and northeastern Kansas with the storage corridor in southwestern Nebraska and western Kansas. The presence of many existing pipelines in the study area demonstrates the viability of pipeline projects in terms of public perception and government regulations. The pipeline sizing results show that a pipeline can be developed to handle the CO_2 from current ethanol source and still have some extra capacity for growth with a minimal number of booster stations.

An analysis of property owners along the pipeline route shows that the pipeline can be routed through an area with large parcels and relatively few landowners. The routes can be optimized to deal with as few land owners as possible and to take advantage of the most existing rights-of-way as possible in future phases. The assessment of sensitive populations and sensitive area did not find any significant problems that could affect the overall success of the project. Sensitive areas and populations can be avoided by pulling the maps created into SimCCS for further modeling. Safety incidents involving CO_2

pipelines were less severe than those involving hazardous liquid or natural gas pipelines. Finally, while protected and sensitive areas exist throughout the study area, they can be easily avoided and will not significantly impact project infrastructure considerations.

7 Economics and Liability

7.1 Study Area Introduction and Background

7.1.1 Overview

The economic and liability assessment is primarily focused on the potential CO_2 sources and storage sites in a sub-region of the Midcontinent, with the potential storage site located in southwestern Nebraska on the flank of the Cambridge Arch near the western margin of the Denver-Jules Basin (Figure 1-1). Two primary storage sites were analyzed during the Phase II proposal; the Sleepy Hollow Field in Red Willow County, Nebraska, and the Paterson Heinitz Hartland Field in southwestern Kansas. However, for consistency with previous topical reports produced for Phase I of the IMSCS-HUB project, this report is focused on the Sleepy Hollow Field as the primary storage site.

7.1.2 CO_2 Sources: Ethanol Plants

In 2012, Nebraska's CO_2 emission rate from steam electric and natural gas-fired power plants was 2,161 pounds per megawatt-hour. Nebraska's Clean Power Plan sets a 2030 goal of 1,296 pounds per megawatt-hour. This goal represents a 60% reduction and is one of the least stringent when compared to other states. The average overall annual emissions in Nebraska were 19.4 million metric tonnes (Mt) CO_2 equivalent (CO_2e) during the period between 2011 and 2015. Electric power production represents the largest portion of emissions in the region. Five power plants make up approximately 77% of the CO_2 emissions in the study area with emissions of 15 Mt CO_2/year. Ethanol plant emissions make up the next largest portion of study-area-emissions at approximately 3.3 Mt CO_2/year, with an increase in ethanol emissions observed over the past 5 years. Focusing on ethanol as the primary CO_2 source for the project will help meet and potentially exceed DOE's goals to construct a commercial-scale storage facility capable of storing 50 Mt CO_2 from industrial sources by 2025. Based on the average annual emissions for the existing ethanol sources in Nebraska, approximately 98 Mt CO_2e could be emitted over a 30-year period, with only a portion of the ethanol sources in the state needed to achieve a single commercial-scale CO_2 project.

The initial source for the storage complex is Archer Daniels Midland's (ADM) ethanol production facility in Columbus, Nebraska (NE). This facility is comprised of two ethanol plants that have the capacity to produce a total of 1.13 million gallons of ethanol per day, making this facility the largest ethanol producer in the state. The facility processes about 550,000 bushels of corn per day, primarily sourced within 100 miles of the facility, and produces about 3,250 t/day of high purity CO_2 as a byproduct. Capture and conditioning of the CO_2 for the project does not require novel technology development and can be accomplished using the same techniques employed at the Illinois Basin Decatur Project and the Illinois Industrial Carbon Capture and Storage (ICCS) Project. The CO_2 is more than 99% pure after dehydration. Before dehydration, it contains less than 3% water by weight. The CO_2 will be collected from the corn-to-ethanol fermenters at atmospheric pressure and compressed using interstage coolers and knock-out vessels to decrease temperature and remove moisture, and dehydrating (less than 0.005% water by weight) with a triethylene glycol (TEG) contactor to make it ready for pipeline transport. In Illinois, ADM uses a 3250-horsepower, four-stage reciprocating compressor and a dehydration system that uses a TEG absorber-regenerator. It is anticipated that a similar system will be employed in Nebraska. Valero and Cargill ethanol plants are expected to have similarly pure streams of CO_2 after capture and dehydration.

7.1.3 CO_2 Sinks: Deep Saline Storage Zones and EOR Reservoirs

The Sleepy Hollow study area is approximately 28 mi^2 and encompasses the Sleepy Hollow oil field in eastern Red Willow County, Nebraska (Figure 3-3). Sleepy Hollow is the most productive oilfield in Nebraska. The primary area of review is delineated by a high-density cluster of wells (approximately 1 well per 40 acres over 7,360 acres) producing primarily from the Pennsylvanian-age sandstone overlying the Precambrian basement. Basin evolution and regional stratigraphy have played an important role in the development of vertically stacked CO_2-EOR and saline formations conducive to commercial-scale CO_2 injection and storage in the study area (Battelle, 2018b). Due to extensive erosion of Paleozoic strata in the study area, deep saline intervals and oil-bearing zones (e.g., Lansing-Kansas City) occur at depths ranging from approximately 2,700 ft to 3,700 ft. These depths are sufficient for storage of supercritical CO_2 at relatively low costs for well drilling, operation, and maintenance. Basinal areas of the midcontinent were connected to the Illinois and Appalachian basins during highstands of Pennsylvanian sea level, and nearly identical conodont faunas have allowed direct correlation of sequences midcontinent with those of north-central Texas (Boardman and Heckel, 1989), and the Illinois Basin (Heckel, 2008). Deep saline CO_2 injection and storage has been evaluated for the sandstones and porous limestones of the Pleasanton-Marmaton, the Lansing-Kansas City "A" and "D-F" zones, the Shawnee-Douglas, and the Wabaunsee groups. Oil-bearing zones occur between and/or adjacent to the deep saline formations evaluated for CO_2 storage. The stacked saline storage zones and CO_2-EOR reservoirs are separated by thin intervals of mudrock, phosphatic shale, and minor evaporite strata that act as vertical barriers to flow, isolating oil-bearing zones from non-oil-bearing zones. This scenario enhances the potential for synergy between EOR operations in the petroleum industry and geologic storage projects. Late Pennsylvanian and Permian shales, carbonates, and evaporites directly overlie the deep saline storage zones and oil-bearing reservoirs of interest in the study region and represent primary caprocks for the underlying storage complex.

7.2 Economic and Liability Assessment Framework

7.2.1 Liability Assessment Considerations

Liability assessment for IMSCS-HUB includes a review of various non-technical risk factors and project uncertainties that could prevent the project from achieving commercial success. Factors evaluated as part of the liability assessment include:

- potential business models and contractual requirements associated with the project;
- potential impact/role of regulations, state incentives, and policies;
- long-term liability of stored CO_2; and
- surface access and environmental considerations.

Anticipated business contractual requirements were identified/reviewed and used to develop the project plan as part of the proposed work in Phase II and subsequent phases of the IMSCS-HUB project (e.g. Bidgoli and Dubois, 2017). Government regulations, incentives, and policies potentially applicable to CCS projects, such as Underground Injection Control (UIC) program primacy and hydrocarbon and/or ethanol industry-related tax incentives, were evaluated to determine their potential impact on project economics and public acceptance. Legislative approaches and existing precedents associated with CO_2 storage liability were reviewed to assess initial plans for assumption of long-term liability that are aligned with state and federal policies. Analysis of surface access issues included evaluation of liability factors associated with pore-space owners and populations centers, existing land use and resource development, existing pipeline rights-of-way, and environmental issues. The potential impact of these liability factors on project outcomes was evaluated for various IMSCS-HUB scenarios (e.g. Table 7-1;

Figure 7-1)Results of the liability assessment were then incorporated into the economic assessment and used to develop mitigation strategies/contingency plans as part of the proposed work for Phase II.

7.2.2 Economic Assessment Methodology and Project Scenarios

CO_2 Capture and Pipeline Transport Cost Models

The IMSCS-HUB will consist of multiple sources and storage sites. The project will leverage existing, proven technology for CO_2 capture and transport from nearby ethanol sources. Initial analysis of capture, compression, transportation, and storage costs has been conducted for three source-sink and pipeline routing scenarios envisioned for the IMSCS-HUB Project, and one regional-scale scenario (Table 7-1; Figure 7-1) . For the five IMSCS-HUB scenarios, ethanol-derived CO_2 sources analyzed include the ADM plant in Columbus, NE; the Valero plant in Albion, NE; the Cargill plant in Blair, NE; also referred to as the Columbus-Albion-Blair plants (CAB). Power plant-derived CO_2 sources included Nebraska Public Power District's (NPPD) Gerald Gentleman Station (GGS). Scenario 4 represents a regional scenario derived from a white paper released by the State CO_2-EOR Deployment Working Group (2017) wherein CO_2 from 34 ethanol plants in the Midwest is transported through Nebraska, Kansas, and Oklahoma to the northern extent of the Permian Basin pipeline infrastructure. This represents a large-scale regional scenario that could be leveraged by the IMSCS-HUB Project to achieve commercial status.

Table 7-1. CO_2 source-sink pairs and pipeline routing scenarios evaluated for the IMSCS-HUB Project.

Scenario	Source(s)	Sink(s)	Pipeline (mi)	Pipeline Route
1	CAB ethanol plants	Sleepy Hollow	344	From sources to storage sites via oil fields
2	CAB ethanol plants	Sleepy Hollow	295	Direct from sources to storage site
3	GGS power plant	Sleepy Hollow	79	Direct from source to storage site
4	34 ethanol plants	Permian Basin	1,546	Direct from sources to Permian Basin

Estimating the capital and operating costs for CO_2 capture, compression, and dehydration (CCD) from fermenters in an ethanol plant is problematic due to limited publicly available data. There are only three commercial-scale ethanol plant operations that currently process and deliver CO_2 via pipelines for injection into geologic targets, and capital expenditures (CapEx) and operational expenditures (OpEx) are not publicly available for the three privately operated facilities. CapEx estimates were derived from results reported for ADM's Industrial Carbon Capture and Storage (ICCS) Project (McKaskle, 2016) and other DOE-funded projects (IMCCS, 2010; ICCSND, 2017), and then adjusted based on expert opinion (Dubois, 2018). A simple linear equation (Equation 7-1) was developed by fitting CapEx estimates and ethanol plant size in MGY (millions of gallons per year) for the three examples above:

$$CapEx (\$Million) = 0.15 * Plant\ Size\ [million\ gallons\ per\ year\ (MGY)] + 9 \qquad \textbf{Equation 7-1}$$

Capital costs for power plant capture was based on Petra Nova's unofficial capital costs of $1 billion for capturing and compressing 1.4 Mt per year and linearly scaled to the sources in this study. Operating costs for post-combustion capture (PCC) plants are unknown and were not included in this analysis. The cost for compression was the same as that for CO_2 derived from ethanol production. OpEx for CCD from

ethanol plants was estimated to be $8.58/tonne of CO_2. CCD is the largest contributor to OpEx due to energy costs, and it is directly proportional to CO_2 volumes compressed. Savings derived from economies of scale for larger-sized plants were not included. The CO_2 capture equipment and pipelines were modeled as 22-year projects with a 2-year construction phase starting in the year 2022 and ending in 2024, and 20 years of operation with amortization beginning at 2024. A 7% discount factor was assumed for CO_2 capture and transport operations. The price for CO_2 required at the outlet to cover all capital and operating costs and the cost of capital over the 20-year operational life was calculated.

The pipeline routing and cost analysis was conducted using the economic-engineering optimization model for CCS infrastructure SimCCS. The model included identification of all major permit and regulatory requirements and regulatory gaps relevant to the construction, ownership, and operation of the pipeline system. Major environmental considerations were also identified for the potential pipeline routes to selected areas in southwest Kansas and southwest-central Nebraska. For the analysis of the regional-scale scenario, the National Energy Technology Laboratory's (NETL) CO_2 Transport Cost Model (Grant et al., 2013; Grant and Morgan, 2014) was modified by team members at Great Plains Institute (GPI) to calculate costs for multiple pipeline segments (Dubois et al., 2017). Model output includes capital costs accounting for materials, installation labor, right-of-way negotiations, CO_2 surge tanks, pipeline control systems, and pumps. Operational costs include pipeline operation and maintenance, equipment and pumps, and electricity costs for pumps, by segment. Pipeline network scenarios were mapped in ESRI's ArcGIS to determine the route, length, and volume of each segment of the network. Pipeline segment lengths specified were 110% of straight-line distances to account for route departures. Ethanol CO_2 production was set at 90 percent of plant potential based on nameplate ethanol production volumes from the Energy Information Agency (EIA) tables (DOE-EIA, 2017). Resulting cost estimates are in line with a CO_2-EOR industry rule of thumb of $100,000 per inch-mile.

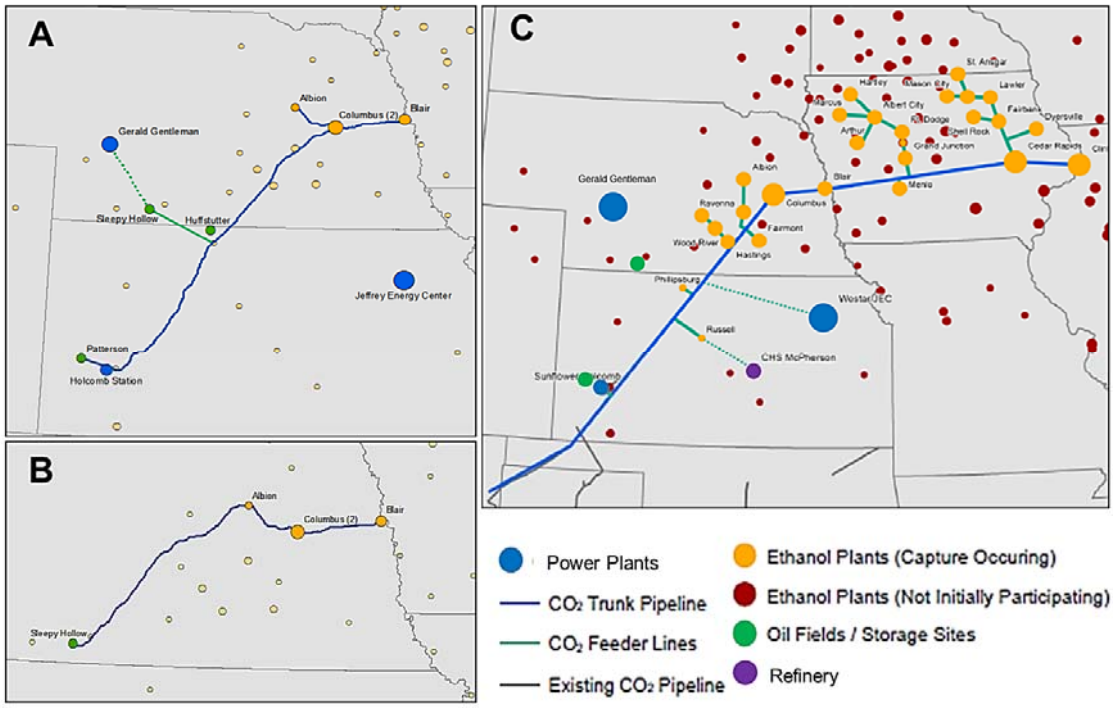

Figure 7-1. Map showing source-sinks pairs and pipeline routes for (A) Scenarios 1 and 3, (B) Scenario 2, and (C) Scenario 4 (Figure Credit: Great Plains Institute (GPI) and Improved Hydrocarbon Recovery,

Inc.). Ethanol plant production capacity is represented by the relative size of each circle from 40 to 250 million gallons per year (DOE-EIA, 2017; State CO_2-EOR Deployment Workgroup, 2017; Dubois, 2018).

CO_2-EOR and Storage Cost Models

Cost Model Scenarios. The potential CO_2 storage costs and revenue associated with the IMSCS-HUB Project were assessed for both deep saline and CO_2-EOR storage scenarios in the Sleepy Hollow study area. Storage costs were estimated for five deep saline storage zones occurring within Pennsylvanian-age strata (see Section 3). The oil-bearing zones included in this assessment were evaluated in the context of their potential to provide a revenue source/economic incentive for CCS via CO_2-EOR and include the Lansing-Kansas City (LKC) "C" zone, and the Pennsylvanian basal sandstone. Another potential source of revenue for the project is a tax credit afforded by the US IRS's Section 45Q tax law, wherein an initial credit of approximately $35 per tonne (t) of CO_2 stored can be earned for EOR operations, and $50/tonne for saline storage operations (US-IRS, 2018). Storage costs were estimated for scenarios with and without the 45Q credit to evaluate the impact of the tax law on IMSCS-HUB project economics. The value of the CO_2 storage credit was calculated based on based on the credit schedule reported by the US-IRS (2018) and inflation adjustment factors derived from the Gross National Product (GNP) Implicit Price Deflator Indices (Table 7-2).

Table 7-2. Value of the 45Q tax credit, in dollars per tonne, for CO_2 storage in saline formations and EOR reservoirs calculated for 12 years of project operation*.

Phase:	Operation												
Year:	2024	2025	2026	2027	2028	2029	2030	2031	2032	2033	2034	2035	2043
EOR	$34	$37	$40	$41	$42	$42	$43	$44	$44	$45	$46	$47	-
Saline	$49	$53	$58	$59	$60	$60	$61	$62	$63	$64	$65	$67	-

* US-IRS (2018); inflation adjusted and reported in constant 2016 USD

Using the Sleepy Hollow study area as the primary storage site (sink) of interest, CO_2 storage quantities and purchase prices for EOR were based on source capture performance and costs reported for the CAB ethanol plants in Scenario 1 and 2, and the GGS power generation facility in Scenario 3 (e.g. Table 7-1). The CO_2-EOR storage cost analysis incorporated reservoir performance and Nebraska-specific cost regressions into a discounted cash flow analysis, with project construction assumed to begin in 2022 and operations to begin in 2024 for all scenarios, consistent with the capture and pipeline models.

CO_2-EOR and Saline Storage Performance Models. Deep saline CO_2 storage costs were calculated based on operational parameters, reservoir properties, and CO_2 injection and storage results derived from static and dynamic simulations (Sections 3 and 4), respectively. CO_2-EOR performance was modeled for the oil-bearing intervals in the LKC "C" zone and the Pennsylvanian basal sandstone using new and existing site-specific reservoir data compiled as part of the geologic assessment. Reservoir simulations were conducted using CO_2-Prophet, a simplified rate model developed by Texaco (Dobitz and Prieditis, 1994) for the U.S. Department of Energy, to predict incremental oil recovery and CO_2-storage performance for one 40-acre 5-spot well pattern in the study area. CO_2-EOR models were run assuming straight CO_2 injection (no water-alternating-gas injection), with CO_2 storage treated as a byproduct of EOR operations and pattern performance modeled to optimize oil production. Key CO_2-EOR reservoir parameters in CO_2-Prophet and associated input for the LKC and basal sandstone are shown in Table 7-3. Per pattern results from the reservoir simulation were used as input in the CO_2-EOR discounted cash flow model to estimate revenue, costs, and net present value of the project with and without 45Q storage credits for the three IMSCS-HUB scenarios.

Table 7-3. Input and definitions of select reservoir parameters used for CO_2-Prophet simulations in the LKC C zone and basal sandstone.

CO_2-Prophet Inputs and Definition		LKC "C" Zone	Basal Sandstone
Field & Operational Parameters	Total Productive Field Area (acres)	5,100	7,243
	Well Pattern	40 acre 5-spot	40 acre 5-spot
	Injection rate of surface CO_2 (t/day)	39	47
	Incremental hydrocarbon pore volumes of CO_2 injected	2	2
	Original Oil in Place (OOIP) (MMSTB)	60	179
Reservoir Properties	Reservoir Depth (ft)	3250	3500
	Reservoir temperature (°F)	97	100
	Reservoir pressure (psia)	1,527	1,645
	Average permeability (mD)	20	2,100
	Net thickness (ft)	19	15
	Porosity (fraction)	0.11	0.21
Fluid Properties	Initial oil saturation (fraction)	0.26	0.46
	Initial water saturation (fraction)	0.7	0.5
	Vertical to horizontal permeability	0.8	0.9
	Viscosity of oil, cp	2	2
	Oil formation volume factor (rb/stb)	1.13	1.21
	Solution gas-oil ratio (scf/stb)	250	280
	Oil gravity (°API)	29	30
	Brine salinity (ppm)	110,000	72,000
	Residual oil saturation to water (fraction)	0.37	0.29
	Connate water saturation (fraction)	0.20	0.14
	Relative permeability of oil to connate water (fraction)	0.40	0.70
	Relative permeability of water to residual oil (fraction)	0.30	0.03

CO_2-EOR and Saline Storage Cost Models. CO_2-EOR costs were estimated using Advanced Resources International's cost regressions reported for the Sleepy Hollow field (2006), including capital and operating expenses associated with new well drilling, completion, and surface equipment, existing well workover, CO_2 recycling, liquid lifting, and general and administrative expenses. The potential financial impact of having a dedicated CO_2 storage component during EOR operations was incorporated into the cost model based on guidelines established by the current 45Q credit requirements (US-IRS, 2018). This includes an assessment of the additional costs associated with site characterization and annual injection-phase expenses (20 years) required to verify CO_2 storage during EOR operations and receive the tax credit, as well as post-injection site care and closure costs (50 years) (Godec et al., 2017a). Storage costs were calculated for a stacked CO_2-EOR-storage operation in one 40-acre 5-spot pattern within the study area, with EOR beginning in the Pennsylvanian basal sandstone and transitioning to the overlying LKC "C" zone after two hydrocarbon pore volumes of injection is achieved. Additional model parameters/ assumptions include an oil price of $55/STB (stock tank barrel), a discount rate of 15%, and inflation adjustments based on the IHS Upstream Capital Cost Index (USCCI), with all costs reported in constant 2016 US dollars (USD). The net present value was calculated for both saline and CO_2-EOR storage operations to determine the value of future cash flows accrued incrementally and cumulatively over the duration of the operation at a discount rate of 20%. The net present value was then used as a metric for potential profitability of the IMSCS-HUB project.

7.3 Liability Assessment Results

7.3.1 Potential Business Models and Contractual Liability

Anticipated business contractual requirements were identified to evaluate their potential impact on the success of the project, and to help develop the project plan as part of the proposed work in Phase II and subsequent phases of the IMSCS-HUB project (e.g. Bidgoli and Dubois, 2017). Two general business models have been considered for the IMSCS-HUB Project based on experience in other states: (1) the public utility model; and (2) the private party model. In the public utility model, the transportation and storage of CO_2 would be accomplished by one or more public utilities. Variations of the model may include a single public utility that is responsible for capture, transportation, and storage of captured CO_2, or separate utilities individually responsible for different facets of the project. Under a private party model, separate private firms would independently conduct capture, transportation, and storage of CO_2. The business contractual requirements are greater under a private party model because custody of the CO_2 would likely change. Under a public utility model, and particularly where a single public utility conducts all operations downstream of the CO_2 source, custody is less likely to change.

Two alternative business arrangements for capture of CO_2 were evaluated. In one scenario, the CO_2 source will install, operate, and maintain the capture technology at the generation facility, or a third-party contractor will do so in the second scenario. If capture is conducted by a third-party, a contractual relationship between the CO_2 source and capture contractor will be established to address the risks of maintenance, repairs, and the liability associated with system failure. System failure liability could include civil penalties for violation of applicable air permits and costs of plant downtime caused by a system failure. Once the CO_2 is captured at the source, it will be transported to qualified storage sites via pipeline. There are many business models for pipeline transportation of CO_2, and it is difficult to precisely anticipate all the contractual considerations at the early stages of exploration and development. Underpinning the business contractual requirements and strategies to secure pore space rights is ownership/title to CO_2. Assuming the CO_2 remains the property of the power generation facility or ethanol plant, the parties will first price the transportation. The price will include charges for maintenance, compression, treatment and processing, and regulatory compliance incurred by the transporter. The price will vary based on the volume delivered to the pipeline, the distance the CO_2 is transported, any potential gas quality issues that may need to be addressed, or a combination of these factors.

The pipeline construction process will begin with right-of-way acquisition entailing consensual easement agreements with landowners, and possibly easements obtained by condemnation. It is assumed that the CO_2 source and transporter will develop an agreement on where and when the transfer of title and responsibility for the CO_2 occurs, with the allocation of risk dependent on which party retains title to the CO_2. These risks may include regulatory fines, damage and/or injury from the pressurized pipeline, response costs, and the technical risks associated with quality of the CO_2 (e.g. impurities and contaminants) and its possible effects on the physical integrity of the pipeline. CO_2 stream quality criteria will be adopted to address these issues in the contract.

The contractual considerations surrounding geologic injection and storage of captured CO_2 begin with obtaining surface/site access, surface landowner permission for seismic surveys and other characterization activities, and subsurface rights for injection in the storage formation. Site operation will be overseen by an operator, which may or may not be the same entity as the CO_2 source, with contractual requirements largely governed by EPA Underground Injection Control (UIC) Class VI well regulations. Post-injection site-closure activities may not be conducted by the same firm overseeing

active storage operations in some scenarios, and a contractual relationship will exist between the two entities to address liability for well plugging and abandonment, leakage into underground sources of drinking water (USDWs), property damage, and migration of CO_2 into adjacent formations (pore-space trespass). Whichever party or parties among the CO_2 source(s), transporter(s), and storage firm(s) bears the risks of casualty loss from leakage or system failure will likely seek to reduce or eliminate these risks through insurance. One of several possible contractual insurance arrangements may involve the penultimate custodian of the CO_2 purchasing a policy of casualty or general liability.

For the IMSCS-HUB Project, the public utility model is advantaged in transportation and storage due to the potential for securing pipeline rights of way and pore space through the condemnation process. Other possible advantages of the utility model are easier and lower cost financing through bonds (capture, transportation and storage), and possibly long-term liability. The ethanol plants (privately owned) considered as sources in the region could take advantage of the recent update to the 45Q tax credit, allowing them to collect up to $35/tonne of CO_2 stored during CO_2-EOR and/or up to $50/tonne for saline storage. Credits can be transferred from capture to the storage site, but not the transportation segment. Both private business and public utilities are eligible for the tax credits.

7.3.2 Potential Impact of State Incentives and Policies

State incentives and government policies were evaluated to determine their potential impact on project economics and public acceptance. Geologic carbon storage has not occurred previously in Nebraska, and there are no pertinent state statutory or common laws. State tax incentives and policies that could positively affect project economics and public response include the Nebraska Advantage Act (Neb. Rev. Stat. § 77-5601), which is a tax amnesty program designed to further the Invest Nebraska Act (Neb. Rev. Stat. § 77-5502), the goals of which are " (1) to aid in the economic and population growth of the state; and (2) assist in the creation of better jobs for the residents of the state." The CO_2 source (and/or storage firm) must invest in qualified property of at least $10 million and the hiring of at least 25 employees. Transportation of personal property (e.g. CO_2 pipeline transport) is also a qualified business. Tax incentives could include a refund of sales taxes paid and investments, and employment credits against income taxes. Depending on tier, a company may pay reduced or no personal property tax for certain timeframes.

Federal and state rules for UIC Class II and VI injection wells were reviewed to evaluate their potential impact on project timelines and determine the ability of potential Sleepy Hollow and nearby sites in Nebraska to meet permit requirements. Class II injection wells in Nebraska are regulated by the Nebraska Oil and Gas Conservation Commission. Approximately 1,598 wells are classified as Class II injection wells in the state, with 138 of those associated with EOR and water disposal in the Sleepy Hollow field (Nebraska Oil and Gas Conservation Commission RBDMS, 2016). Aquifer exemptions permitting injection in all groundwater intervals were approved for Class II EOR wells in all Red Willow County and thirteen other adjacent counties along the southwest border of Nebraska, with a total area of 14,422 mi^2 covered by the exemption (U.S. EPA, 2017). Class II EOR wells that transition to Class VI wells represent the only instance in which aquifer exemptions will be granted for carbon storage projects (U.S. EPA, 2010; 2013a; 2016c). The absence of protected USDWs may decrease the area of review to the extent of the CO_2 saturation plume only. Permitting and oversight authority for the Class VI UIC program in Nebraska is overseen by Federal EPA Region 7. Region 7 is one of few regional offices in the U.S. with Class VI permit experience, with one Class VI permit submitted by Berexco currently being processed. State-level experience with Class II injection well permitting and oversight, as well as existing Class II injection wells at each potential site indicates lawmakers, regulators, and nearby communities are generally familiar with injection operations. Aquifer exemptions in Nebraska and

experience with the UIC Class VI permit process in EPA Region 7 will decrease risks associated with unanticipated regulatory challenges and permit delays.

7.3.3 Long-Term Liability of Stored CO_2

Legislation. Legislative approaches and existing precedents have been evaluated to develop initial plans for assumption of long-term liability for CO_2 that are aligned with current federal EPA rules for Class VI UIC wells (US EPA, 2010). This includes securing liability coverage while the permit is active during injection operations, well plugging, corrective action, post-injection site care, and site-closure phases. Additional requirements for long-term liability of stored CO_2 after site closure are currently uncertain, and clearly defined statutes have not yet been established at the state or federal level. The specific long-term risks associated with a closed CO_2 storage field are similar to those associated with an active/operational site (e.g., pore-space trespass, drinking water contamination, and pressurized injection wells and surface equipment). Several states have codified a procedure by which the state ultimately takes responsibility for monitoring and liability of a closed storage site. Nebraska has not adopted such procedures to-date; consequently, storage firms and CO_2 sources would need to contractually limit their long-term liability for closed storage sites, likely through private insurance. The most likely form of insurance would be a single premium tail or cost cap policy. It is unclear, however, whether there is an insurance market for long-term risks associated with closed CO_2 storage sites. For the project to be feasible, it is likely that a statutory regime shifting responsibility for monitoring and long-term liability to the state would need to be passed. State-level legislative approaches and engagement of policy makers will be considered as part of the plan to establish a potential framework for assuming long-term liability for CO_2 after site closure.

Geologic Structures. The primary structures potentially impacting the confining system at the selected areas include the Cambridge Arch in southern Nebraska and the Central Kansas Uplift in western Kansas. The Cambridge Arch and Central Kansas Uplift have a structural saddle between them (Rothe and Lui, 1983), but are reported as component parts of the same province (e.g., Higley, 1987; 1995). The impact of geologic structures, crustal stresses, and seismicity on the integrity of the confining system in the region warrants further investigation. Recent hazard mapping indicates low seismic hazard in the region, with a 1% probability reported for the likelihood of a seismic event exceeding a Peak Modified Mercalli Intensity rating of IV (light shaking) in any given year (Petersen et al., 2016). However, microseismic events detected in the sub-region and slightly elevated peak ground acceleration near the Central Kansas Uplift have resulted in deployment of microseismic monitoring networks and increased vigilance to reduce the risk of induced seismicity during injection operations. To-date, no studies have been conducted to characterize site-specific stress regimes in the selected areas, and efforts in data collection and modeling have been proposed in Phase II to address this knowledge gap.

Existing Wellbores. Information on wellbores penetrating the primary caprock units at the Sleepy Hollow study area was compiled to assess the potential need for corrective action to prevent CO_2 leakage via surrounding wellbores in accordance with U.S. EPA requirements (U.S. EPA, 2013b). This included compilation of well type, construction, date drilled, location, total depth, and plugging/completion records near the Sleepy Hollow study area. Approximately 300 wells were found to fully penetrate the Lower Nippewalla, Sumner, Council Grove, and Admire caprocks in southwest-central Nebraska. Completion years for these wells range from 1960 to 2006. A majority of the these in each selected area were completed and plugged after 1960, when standards for oil and gas well cements were established by the American Petroleum Institute (Ide et al., 2006; US-EPA, 2013b). The potential increase in CO_2-EOR initiated by the IMSCS-HUB may result in operator-funded wellbore workovers and remediation using modern practices suitable for preventing vertical CO_2 migration.

Crossflow between oil zones has not been noted at either potential site, suggesting good wellbore integrity.

7.3.4 Surface Access and Environmental Considerations

Surface access issues were evaluated to identify features that could impact the suitability of the potential sites to facilitate safe, long-term, commercial-scale storage. This involved evaluation and mapping of pore space owners, populations centers, existing land use, existing resource development, pipeline rights-of-way, and protected and sensitive areas in the region. The analysis considered site characterization and development activities based on typical NEPA environmental assessment factors. These elements were also used to evaluate site infrastructure needs and help develop public outreach strategies.

Much of the sub-region is either grassland or farmland, with largely open areas identified within and near the CO_2 plume extents (Figure 7-2) modeled as part of reservoir simulation, with population density less than 50 people per mi^2. Population density increases around cities and towns, often reaching more than 5,000 people per mi^2 in larger towns. The sub-region encompasses rural areas and smaller towns, rarely exceeding 500 people per mi^2. Potential sites in industrialized areas and locations with low population density help to reduce the risk of adversely affecting residents with project activities. Assuming surface landowners are also pore space owners in a majority of cases, information on surface landowners, such as landowner name, parcel ID, land use, and acreage, was compiled for the Sleepy Hollow study area and along potential pipeline routes (see Figure 7-1). At the potential site in the Sleepy Hollow field, fifty landowners where identified within the modeled plume extents, with agriculture accounting for 90% of the land use, and single-family homes accounting for 10%. This information was used for project planning and estimating potential costs of securing pore space rights, developing outreach strategies, acquiring permission for characterization activities, and Class II EOR and/or Class VI well permits, as required. Due to existing hydrocarbon development and infrastructure in the study area, nearby residents may be accustomed to construction operations, increased traffic, pipeline operations, and negotiating subsurface resource leases. There is little risk of other resource development activities conflicting with the storage project. Surface and underground mines occur almost exclusively in the eastern portions of Nebraska and will not be affected by storage operations. Surface access issues, competing land use, and potential conflicts with existing mineral leases are unlikely to be significant due to industry interest and involvement in project activities.

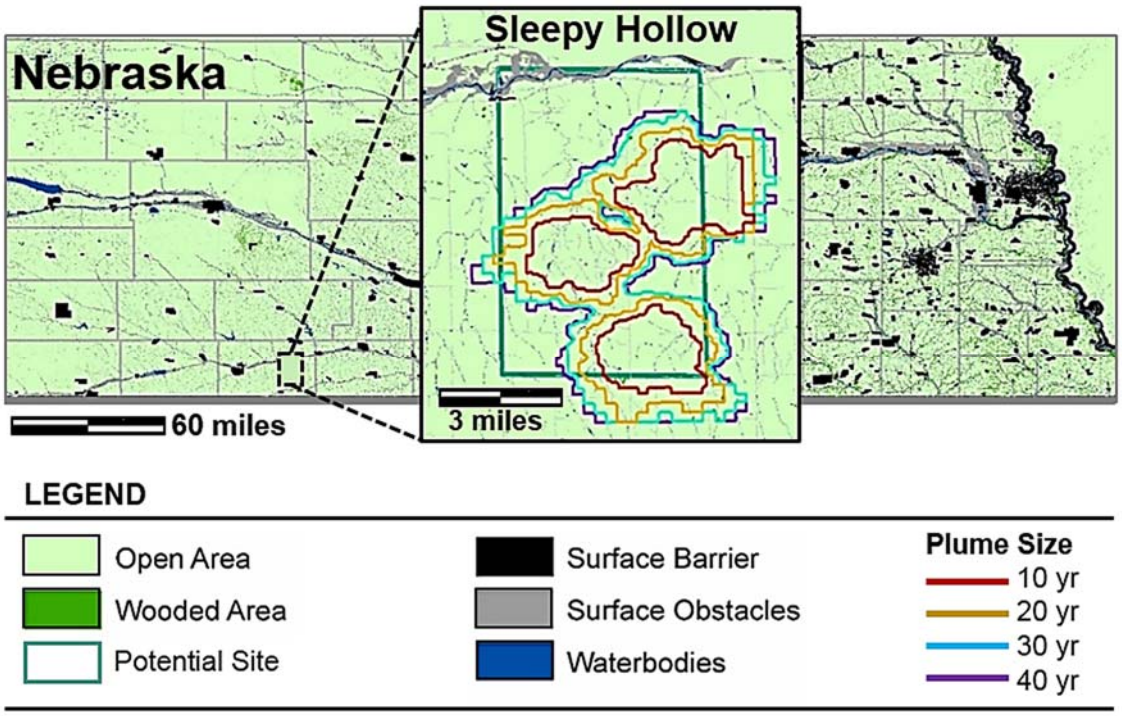

Figure 7-2. Map showing general land use and protected and sensitive areas within and near the modeled plumes at the potential Sleepy Hollow storage site in Nebraska.

Ethanol plants in the region use natural gas as a fuel for processing corn, and natural gas pipelines run to nearly every ethanol plant in Nebraska and Kansas (Figure 7-3a). The existing natural gas pipelines also occur within 3 miles of the potential storage site at the Sleepy hollow Field in Nebraska. The IMSCS-HUB sub-region is also roughly located between existing CO_2 pipeline networks in the U.S (Figure 7-3b). These pipeline rights of way can be leveraged for CO_2 pipeline development for the project. Low population density, and widespread agricultural land use suggests rural areas aren't likely to undergo significant development in the next 20 years, ensuring opportunities will remain for the IMSCS-HUB to expand and access existing CO_2 pipeline networks in the U.S. Wide spread grassland and farmland in the region, along with population densities less than 50 people per mile in the sub-region also reduces the risk of adversely affecting residents with pipeline construction and operation. Analysis of the National Environmental Policy Act (NEPA) environmental assessment factors suggests the potential pipeline routes will likely not interfere with environmentally sensitive areas.

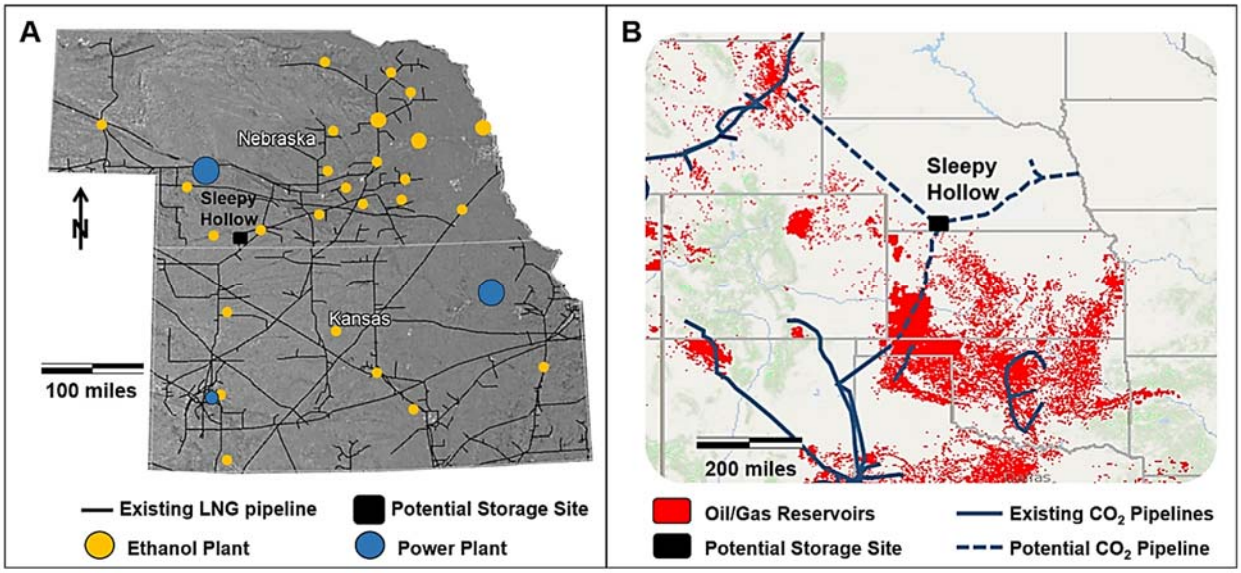

Figure 7-3. (A) Map showing existing natural gas pipelines in Nebraska and Kansas along with locations of ethanol plants, power plants, and the potential Sleepy Hollow storage site;(B) Map showing the Sleepy Hollow site alongside oil/gas fields and existing and potential CO_2 pipelines in the United States (map data from EIA, 2016; NATCARB, 2017).

As part of the liability assessment, environmentally sensitive areas were ordered into one of four categories based on land characteristics and project requirements: (1) *open areas,* including those in the National Land Cover Database (NLCD) (United States Geological Survey [USGS], 2014) designated as grassland, cultivated crops, pasture, or shrubland/scrubland, which are preferred for siting wells, equipment, or pipelines; (2) *wooded areas,* including NLCD designations of deciduous evergreen or mixed forests, which can be used to stage wells, equipment, or pipelines (USGS, 2014); (3) *surface obstacles,* including wetlands (United States Fish and Wildlife Service [U.S. FWS], 2017a) and 100-year floodplains (Federal Emergency Management Agency [FEMA], 2017a, b); and (4) *surface barriers,* which include areas with a Protected Areas Database of the United States (PAD-US) Gap Analysis Program (GAP) designation of #1 or #2 (protected for wildlife/biodiversity) (USGS, 2016a), critical habitats (U.S. FWS, 2017b), NLCD light, medium, and heavy developed areas (USGS, 2014), scenic rivers (Bureau of Land Management [BLM], NPS, U.S. FWS, and U.S. Forest Service [USFS], 2017), surface water (USGS, 2016b, c), National Register of Historic Places (NRHP) sites (National Parks Service, 2017), wellhead protection areas (NDEQ, 2011), surface water protection buffers (Kansas DASC, 2010a, b), existing surface mineral extraction (USGS, 2017), or contaminated areas (U.S. EPA, 2018; NDEQ, nd; KDHE, nd).

The Sleepy Hollow field and nearby sites in southwest-central Nebraska were also evaluated based on their classification and current standing with respect to an array of environmental issues and standards. The National Ambient Air Quality Standards (NAAQS) Green Book Non-Attainment Areas for Criteria Pollutants was consulted (U.S. EPA, 2017). No areas within Nebraska were designated “nonattainment” for any of the criteria pollutants. The Platte River bisects Nebraska through the central part of the state. The Republican River flows from the southwestern corner of Nebraska into Kansas where it empties into the Kansas River.

The principal aquifer in the sub-region is the High Plains Aquifer, also known as the Ogallala Aquifer. The High Plains Aquifer is comprised of Quaternary and Tertiary bedrock deposits, and Quaternary

unconsolidated deposits in southeast Nebraska (Miller and Appel, 1997). The aquifer is also an important source of irrigation water (Miller and Appel, 1997). The depth to aquifer generally ranges from 100–300 ft in the sub-region and is shallower near larger rivers due to hydraulic connectivity of the aquifer with surface water. The chemical composition of water in the High Plains Aquifer generally exhibits less than 250 mg/L of dissolved solids as calcium bicarbonate, with sodium and sulfate becoming more prevalent as the concentration of dissolved solids increases to 500 mg/L (Gutentag et al., 1984). Aquifer exemptions covering the entire geologic column were established for all Class II wells in 1984 for counties in southwestern Nebraska, including Red Willow, Banner, Cheyenne, Deuel, Dundy, Frontier, Furnas, Garden, Harlan, Hitchcock, Kimball, Lincoln, Morrill, and Scotts Bluff. The EPA Class II to Class VI transition guidance document specifies that Class II EOR exemptions will be extended for converted Class VI wells (EPA, 2013a).

7.4 Economic Analysis Results

7.4.1 CO_2 Capture and Pipeline Costs

CO_2 capture and pipeline costs estimated for the four source-sink scenarios (e.g. Table 7-1) are presented in terms of cost per tonne of CO_2 delivered, with no subsidies, 45Q credits for 100% EOR, and for 100% saline storage. Section 45Q credits start at a value of $12.83/tonne CO_2 (EOR) and $22.66/tonne CO_2 (saline) in 2017 and ramp linearly to $35/tonne CO_2 (EOR) and $50/tonne CO_2 (saline storage) in 2026 (Table 7-2). Estimated CO_2 capture and pipeline transport cost for the IMSCS-HUB scenarios are shown in Table 7-4. Saline storage is not an economic proposition even with Section 45Q tax credits. OpEx for CCD from ethanol plants was estimated to be $8.58/tonne of CO_2. CCD is the largest contributor to OpEx is energy costs, and it is directly proportional to CO_2 volumes compressed.

Table 7-4. Summary of estimated capture and transport costs and economics with and without 45Q tax credits for six source-sink scenarios.

Capture and Transport Cost Parameters	Source-Sink Scenarios and Costs* Summary			
	1	2	3	4
Pipeline CapEx ($Million**)	$303	$272	$80	$1,857
Pipeline Annual OpEx ($Million)***	$4.40	$3.70	$1.20	$47
Capture CapEx ($Million)	$132	$132	$1,143	$809
Capture Annual OpEx ($Million)	$16.80	$16.80	$17.20	$84.50
Economics - Capture and Transportation	**CO_2 Price Required for 7% Rate of Return**			
Pipeline Total ($/tonne)	$24.48	$22.13	$4.98	$31.99
Capture Total ($/tonne)	$18.30	$18.44	$71.49	$20.44
Combined Capture and Pipeline Total ($/tonne)	**$42.78**	**$40.57**	**$76.47**	**$52.43**

*2016 USD; **4, 6, 8, 12, 16, and 20-inch pipe size divisions

7.4.2 CO_2-EOR and Saline Storage Costs

The estimated costs of saline storage for the three source-sink scenarios involving the potential Sleepy Hollow storage site are shown in Table 7-5. Based on results from the reservoir simulations, estimated costs assume three saline injection wells will be used to meet the storage requirements for each of the CO_2 sources. OpEx and, to a lesser extent, CapEx costs for saline storage increase with larger capture quantities, as can be seen in the higher OpEx costs ($837 Million) associated with the GGS coal-fired power utility in Scenario 3 relative to the other two scenarios involving the CAB ethanol-derived CO_2

sources. Total storage project costs range from $915 Million ($23/tonne) in Scenarios 1 and 2 to $933 Million ($23/tonne) for Scenario 3. At a discount rate of 15%, the addition of storage credits from the 45Q tax law results in a positive net present value of $358 Million for Scenarios 1 and 2, and $365 Million for Scenario 3. Despite the positive net present values with the 45Q tax credit, the potential net profit (~ $9/tonne CO_2) from saline storage is still less than the combined capture and transport costs estimated for each scenario ($40 - $76/tonne CO_2). Scenario 4 was not included in the saline storage or CO_2-EOR cost assessment because the CO_2 was assumed to be stored in the Permian Basin outside of the IMSCS-HUB project.

Table 7-5. Summary of estimated saline storage parameters, costs, and project economics with and without 45Q storage credits for the three source-sink scenarios of interest.

Deep Saline Storage Cost Parameters	Source-Sink Scenarios and Costs		
	1	2	3
Number of Injection wells	3	3	3
Average Injection Rate Per Well (kt/day)	1.80	1.70	1.64
Average Storage Zone Depth (ft)	3,112	3,112	3,112
Injection Duration (years)	20	20	20
Total Annual Storage Rate (Mt/year)	1.96	1.96	2.00
Cumulative CO_2 Storage at 20 years (Mt)	39	39	40
Total OpEx ($Million)	$821	$821	$837
Total CapEx ($Million)	$94	$94	$96
Total Storage Project Costs ($Million)	**$915**	**$915**	**$933**
– in $/tonne CO_2	**$23**	**$23**	**$23**
Total Storage Project 45Q Credits ($MM)	$1,416	$1,416	$1,445
Net Present Value of Storage Project – w/45Q ($Million)	**$358**	**$358**	**$365**
– in $/tonne CO_2	**$9.13**	**$9.13**	**$9.14**

Results of the CO_2-EOR reservoir performance model are shown in Figure 7-4 for the basal sandstone in the Sleepy Hollow study area. Using an injection rate of approximately 47 tonnes of CO_2 per day, 2 HCPVs of CO_2 injection was achieved after 11 years, representing the per-pattern life of the EOR operation in the basal sandstone. The total estimated incremental oil recovery for the basal sandstone is 170 MSTB, representing 25% of the OOIP (e.g Table 7-3). A total of 189 kilotonnes of gross CO_2 injection and 40 kilotonnes of net CO_2 storage was predicted for the basal sandstone in the 40-acre 5-spot pattern, resulting in gross and net CO_2 utilization factors of 1.1 t/STB and 0.2 t/STB, respectively.

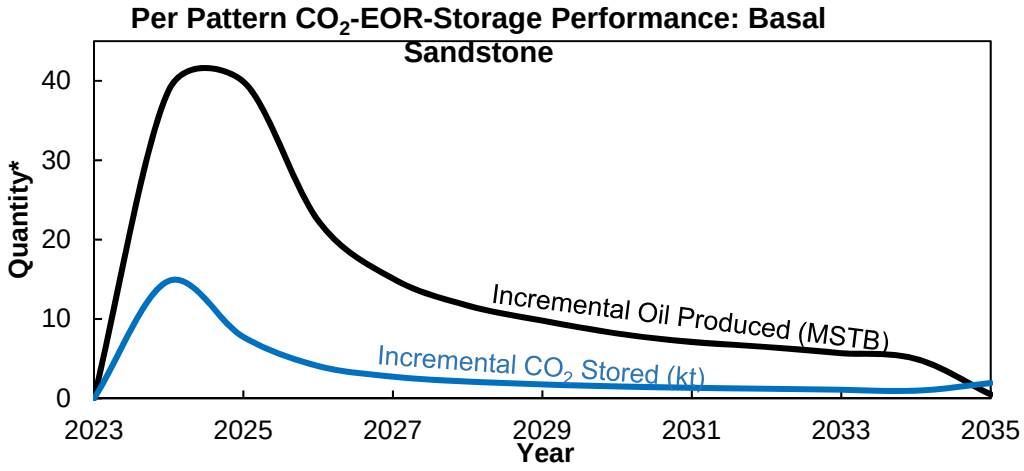

Figure 7-4. Incremental CO_2-EOR and storage performance results for one 40-acre 5-spot well pattern producing from the basal sandstone. *Incremental oil produced is reported in thousand stock tank barrels (MSTB); Incremental CO_2 storage is reported in kilotonnes (kt).

It was assumed that after the EOR operation in the basal sandstone was complete, production and injection would transition into the overlying LKC "C" zone, and operations would continue in the same wells/pattern. Results of the CO_2-EOR reservoir performance model are shown in Figure 7-5 for the Lansing-Kansas City "C" Zone. At an injection rate of approximately 39 tonnes of CO_2 per day, the per-pattern life of the EOR operation in the LKC "C" zone was 9 years before 2 HCPVs of CO_2 injection was achieved. The total estimated incremental oil recovery from EOR in the LKC "C" zone is 65 MSTB, representing 14% of the OOIP (e.g Table 7-3). A total of 117 kilotonnes of gross CO_2 injection and 30 kilotonnes of net CO_2 storage was predicted for the LKC zone in the 40-acre 5-spot pattern, resulting in gross and net CO_2 utilization factors of 1.8 t/STB and 0.5 t/STB, respectively.

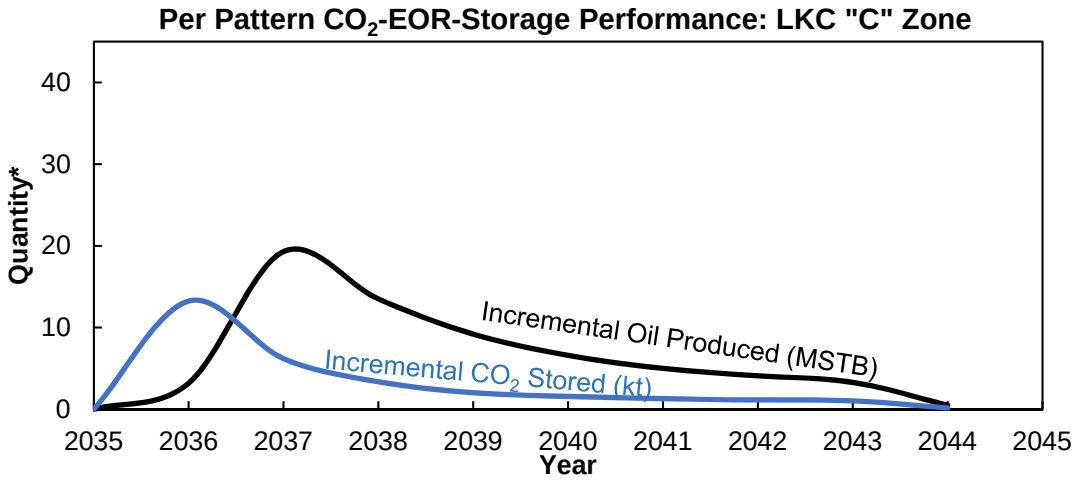

Figure 7-5. Incremental CO_2-EOR and storage performance results for one 40-acre 5-spot well pattern producing from the LKC "C" zone. *Incremental oil produced is reported in thousand stock tank barrels (MSTB); Incremental CO_2 storage is reported in kilotonnes (kt).

The combined, cumulative per pattern results for the basal sandstone and LKC zone EOR performance models are shown in Figure 7-6. Consecutive CO_2-EOR in the two vertically-stacked oil-bearing intervals results in a total pattern life of 20 years, consistent with the operational life of the capture and pipeline transport models developed for the IMSCS-HUB project. The total estimated incremental oil recovery from the combined basal sandstone and LKC zones is 235 MSTB, with a net CO_2 storage quantity of 70 kilotonnes predicted for the 40-acre pattern. Per pattern CO_2-EOR reservoir performance results for the basal sandstone and LKC "C" zone in the Sleepy Hollow study area are summarized in Table 7-6.

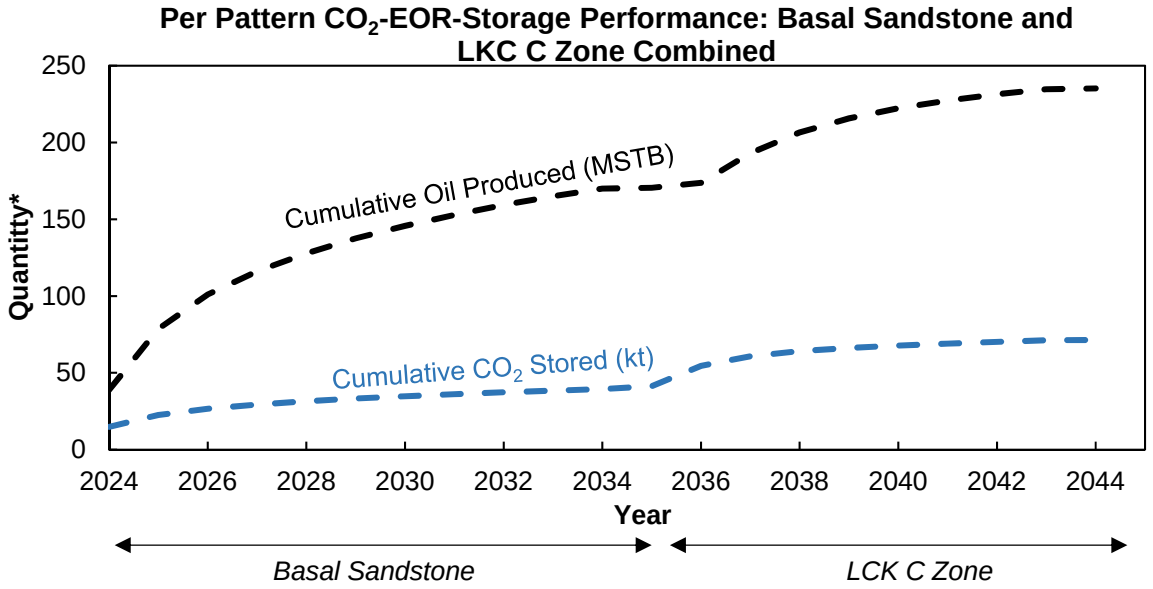

Figure 7-6. Cumulative CO_2-EOR and storage performance results for one 40-acre 5-spot well pattern producing from both the basal sandstone and LKC "C" zone. *Incremental oil produced is reported in thousand stock tank barrels (MSTB); Incremental CO_2 storage is reported in kilotonnes (kt).

Table 7-6 . Per pattern CO_2-EOR reservoir performance results for the basal sandstone and LKC "C" zone in the Sleepy Hollow study area.

Reservoir Performance Result	Basal Sandstone	LKC "C" Zone	Total Pattern
EOR duration (years)	11	9	20
Total Incremental Oil Recovered (MSTB)	170	65	235
Incremental Oil Recovery (% OOIP)	25%	14%	-
Total CO_2 Injection (kt)	189	117	306
Net CO_2 stored (kt)	40	30	70

The estimated per pattern costs of stacked CO_2-EOR in the basal sandstone and overlying LKC "C" zone are shown in Table 7-7 for the three source-sink scenarios involving the potential Sleepy Hollow storage site. Assuming CO_2 costs equal to that of the estimated capture costs for each of the three scenarios, $55/STB oil, and the addition of the 45Q EOR storage tax credit (and the associated costs of verifying

storage during EOR), the net revenue estimated from per pattern recovery of 235 STB of oil in the Sleepy Hollow study is approximately $12.58 Million. Similar to the storage costs estimated for saline storage operations in the field (e.g. Table 7-5), OpEx costs for CO_2-EOR-related storage increase with higher capture costs and quantities, as can be seen in the higher OpEx costs ($10.06 Million) associated with the GGS coal-fired power utility in Scenario 3 relative to the other two scenarios involving the CAB ethanol-derived CO_2 sources ($6.36 Million). Total storage project costs estimated with 45Q storage credits range from approximately $7.5 Million in Scenarios 1 and 2 to $11.2 Million for Scenario 3. Without 45Q tax credits, the profitability of the EOR operation, as indicated by the net present value at a discount rate of 15%, is approximately $3.0 Million for Scenarios 1 and 2 and $1.3 Million for Scenario 3. Without the 45Q EOR storage tax credit, the per pattern net revenue decreases to $11.08 Million, and a decrease of approximately $0.30 Million is observed in the total project costs. The Net Present Value of the EOR operation without 45Q credits decreases by 9% ($2.1 Million) for Scenarios 1 and 2, and by 62% ($0.51 Million) for Scenario 3.

Table 7-7. Summary of estimated per pattern CO_2-EOR costs and project economics with and without 45Q storage credits for the three source-sink scenarios of interest.

Per Pattern CO_2-EOR Cost Model Results		Source-Sink Scenario		
		1	2	3
CO_2 Cost ($/tonne)		$18.30	$18.44	$71.49
Total CO_2 stored (kilotonne)		70	70	70
w/45Q EOR Storage Credits	Net Revenue ($Million)	$12.58	$12.58	$12.58
	Total Capital Costs ($Million)	$1.17	$1.17	$1.17
	Total O&M Costs ($Million)	$6.36	$6.37	$10.06
	Total Project Costs ($Million)	$7.52	$7.53	$11.22
	Net Present Value of EOR - ($Million)	**$2.97**	**$2.96**	**$1.34**
	- in $/tonne CO_2	**$42.43**	**$42.29**	**$19.14**
w/out 45Q EOR Storage Credits	Net Revenue ($Million)	$11.08	$11.08	$11.08
	Total O&M Costs ($Million)	$1.13	$1.13	$1.13
	Total Capital Costs ($Million)	$6.10	$6.11	$9.80
	Total Project Costs ($Million)	$7.22	$7.23	$10.93
	Net Present Value of EOR - ($Million)	**$2.15**	**$2.14**	**$0.51**
	- in $/tonne CO_2	**$30.71**	**$30.57**	**$7.29**

7.5 Discussion and Conclusions

The economic and liability assessment shows Sleepy Hollow Field is in an area with low population density and existing hydrocarbon resource development, helping to reduce the risk of adversely affecting residents with project activities. Analysis of NEPA environmental assessment factors suggests geologic storage operations and proposed pipeline routes will not interfere with environmentally sensitive areas. The lack of major physical or environmental obstacles along with active project participation from oil field operators at each potential site suggests surface access to develop CO_2 storage infrastructure will be easily achieved. The presence of several existing Class II injection wells in

the Sleepy Hollow Field, suggests communities near the potential sites are familiar with injection operations, reducing the likelihood of public backlash toward CO_2 storage activities. Future outreach plans for the project will emphasize economic gains anticipated for residents and stakeholders.

The four ethanol source scenarios (cases 1, 2, 3, and 4) have relatively low delivery costs when 45Q EOR credits are applied (<$27/tonne). The viable market price of CO_2 sold for EOR is largely dependent on the prevailing price of oil (e.g. McCoy and Rubin, 2009), with market rates for CO_2 in the Permian Basin being approximately 20% of the West Texas Intermediate (WTI) oil price. At oil prices of $55-$75/STB, CO_2 captured from the IMSCS-HUB source corridor could be sold at $21/tonne to $29/tonne for EOR, and capture and transportation could be profitable enough to potentially subsidize CO_2 for saline storage in stacked storage operations. A distinct advantage of the IMSCS-HUB Project is that the technology for ethanol-based CO_2 capture and transport for EOR is currently economically feasible and can be commercially deployed today to subsidize ethanol CO_2 saline storage, and provide scalable infrastructure needed to integrate CO_2 capture from power plants in the future.

For saline storage costs and credits, the 45Q tax credit can only be claimed for 12 years after the beginning of capture based on the values in Table 7-2. Assuming inflation continues to be low, about 1.4% per year, the average tax credit per tonne is calculated by dividing the sum of the tax credits received for the first 12 years by the total mass of CO_2 stored in 20 years. Despite the positive net present values with the 45Q tax credit, the discounted net profit from saline storage (~ $9/tonne CO_2) is still less than the combined capture and transport costs estimated for each scenario ($40 - $76/tonne CO_2), suggesting the 45Q tax credit is not enough alone to pay for capture, transport, and saline storage costs associated with an integrated CCS operation in the IMCSCS-HUB. If a project is strictly saline there is no further driving force to cover the deficit, and 45Q credits alone may not provide the economic incentive to pursue commercial-scale industrial CO_2 capture and pipeline development in the region.

The per pattern results of Scenarios 1 through 3 with and without 45Q EOR storage credits show a positive net present value for the Sleepy Hollow Field study area, suggesting that profit could be made to help offset the CO_2 capture costs at the desired rate of return for the EOR operation. Without 45Q credits, the net present value of the EOR operation decreases for each of the three scenarios (e.g. Table 7-7), with more than a 50% decrease observed in the net present value for the project associated with the GGS coal-fired power plant in Scenario 3. Net present values of approximately $42/tonne CO_2 for CO_2-EOR operations with 45Q storage credits suggests the tax credit can be used in conjunction with EOR to close the deficit and pay for the capture, transport, and storage components of the CCS project in the IMSCS-HUB. The economic analysis provides evidence of the need for stacked storage in oil-producing areas where CO_2-EOR and the 45Q tax credit can be used to install the capture and transport infrastructure needed to collect and move CO_2 and then saline projects can take advantage of the infrastructure to store additional CO_2.

An incremental oil recovery of 170 MSTB was predicted for one 40-acre 5-spot well pattern producing from the basal sandstone, representing recovery of 25% of the OOIP (e.g Table 7-6). It was assumed that after the EOR operation in the basal sandstone was complete, production and injection would transition into the overlying LKC “C” zone, and operations would continue in the same wells/pattern. The total estimated incremental oil recovery from EOR in the LKC “C” zone is 65 MSTB, representing 14% recovery of the OOIP. These recovery factors are consistent with those reported in the literature for the Pennsylvanian basal sandstone and LKC “C” zone in the Sleepy Hollow study area (e.g. Kincaid, 1961; ARI, 2006).

Consecutive CO_2-EOR in the two vertically-stacked oil-bearing intervals results in a total pattern life of 20 years, with a combined incremental oil recovery of 235 MSTB and a net CO_2 storage quantity of 70 kilotonnes predicted for the 40-acre pattern. Net CO_2 utilization factors are used as a metric to estimate CO_2 storage and oil recovery potential for depleted oil fields (e.g. Peck et al., 2017). Net CO_2 utilization factors of 0.2 t/STB and 0.5 t/STB calculated on a per pattern basis for the basal sandstone and LKC zone, respectively, can be scaled to the total productive area of each reservoir to estimate the field-wide CO_2-EOR-storage performance of the Sleepy Hollow study area. However, as previously noted, CO_2-EOR reservoir performance was modeled to optimize oil production rather than CO_2 storage. Future work could focus on reservoir performance models and strategies to co-optimize CO_2 storage with oil recovery to derive more accurate estimates of overall storage potential in the field.

7.6 Conclusions

Potential challenges identified as part of the economic and liability assessment for the IMSCS-HUB Project include development of pipeline infrastructure and UIC Class VI corrective actions from existing wellbores in the study area. Collaboration and support from a major pipeline company in the region (MV Purchasing) has been established for Phase II to help address potential contingencies associated with pipeline development and financing. Existing natural gas pipelines routed directly to ethanol plants occur within 3 miles of each potential site, and the IMSCS-HUB study area is roughly located between existing CO_2 pipeline networks in the U.S. These pipeline rights of way can be leveraged for CO_2 pipeline development for the project. The economic incentives for construction of the proposed pipeline will be further evaluated in Phase II, including consideration of CO_2-EOR, 45Q, and the ethanol industry. Low population density, and widespread agricultural land use suggests rural areas aren't likely to undergo significant development in the next 20 years, ensuring opportunities will remain for the IMSCS-HUB to expand and access existing CO_2 pipeline networks. Wellbore information compiled at potential sites will be used to facilitate efforts in Phase II to identify, assess, and plan for corrective action using the EPA's guidance document for Area of Review Evaluation and Corrective Action (EPA, 2013b).

The results show that the liabilities identified for the project are generally similar to those of oil and gas or other subsurface projects and that they can be addressed through regulatory, contractual, and insurance mechanisms. The analysis of the potential for problems with rights of way and environmentally sensitive areas do not look insurmountable because the pipeline and field locations are in sparsely populated areas with few sensitive areas. In addition, problems arising from injection operations are likely to be minimized due to the colocation of the storage site with oil and gas operations, ensuring the public in the area are familiar with drilling and injection equipment and operations.

Existing hydrocarbon resources in the Sleepy Hollow study area and the potential for a hybrid of CO_2-EOR and geologic storage may provide technical advantages, infrastructure, and economic incentives needed to successfully commercialize CCS in the region. Saline storage alone cannot be fully supported by the 45Q tax credit under a saline scenario or a CO_2-EOR scenario. However, the use of EOR as a business case for storage provides an income from oil production that can help subsidize the construction and operation of storage projects allowing future projects to take advantage of the infrastructure, lowering costs.

8 Phase II Planning

8.1 Introduction

The IMSCS-HUB builds on lessons learned from the US Department of Energy (DOE) National Energy Technology Laboratory's (NETL) Regional Carbon Sequestration Partnerships (RCSPs). The team building effort during Phase I the IMSCS-HUB team decided to combine with the two other projects in the region. The other Phase I projects were the Nebraska Integrated Carbon Capture and Storage Pre-Feasibility Study led by EERC, and the Integrated Carbon Capture and Storage for Kansas (ICKan) led by Kansas Geologic Survey.

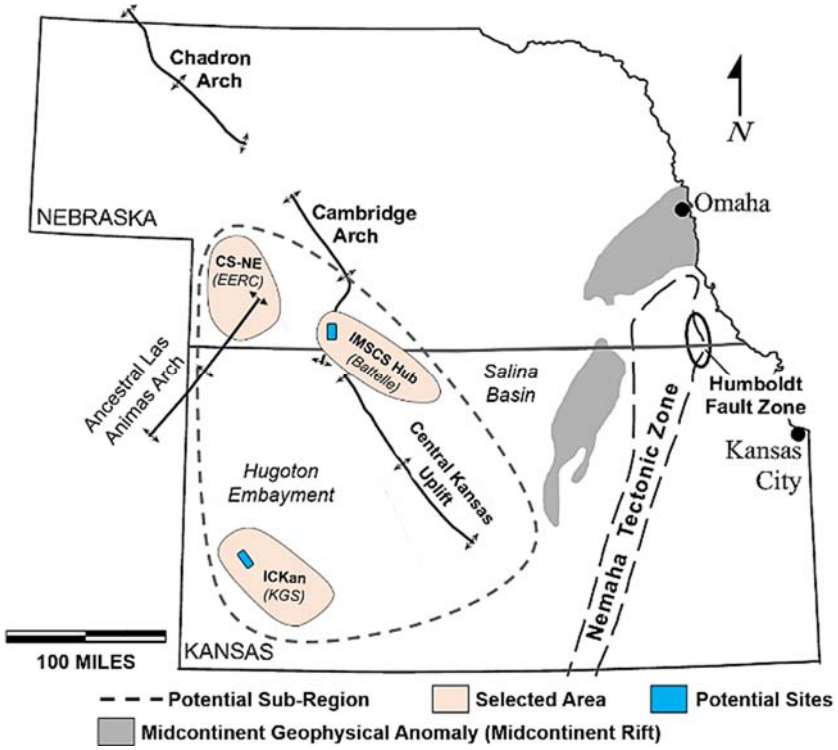

Figure 8-1 Phase I CarbonSAFE projects combining to form the Phase II team.

The team is led by Battelle Memorial Institute and includes: Archer Daniels Midland Company (ADM), the Kansas Geologic Survey (KGS), the Energy and Environmental Research Center (EERC) at the University of North Dakota, Schlumberger, the Conservation and Survey Division (CSD) at the University of Nebraska-Lincoln (UNL) and others. The team has identified a clear strategy that will meet DOE's 2025 objective of commercial implementation by developing a commercial CO_2 market and infrastructure relying on multiple ethanol-based CO_2 sources in the short term and the incorporation of multiple coal-fired power plants when commercial CO_2 capture is implemented. The IMSCS-HUB will benefit from the updated 45Q tax credit, requiring construction to begin by 2024, for CO_2 enhanced oil recovery (EOR) and saline storage to offset the cost of capture and transport. Capture and transport costs for the hub are estimated to be between $43/tonne and $77/tonne depending on the scenario (Section 7). Saline storage is $23/tonne without the 45Q tax credit or $9/tonne with the tax credit (Section 7). This groundwork will eventually provide the infrastructure and economic conditions required to successfully

integrate carbon capture from nearby coal-fired power plants. The proposed storage hub will link numerous CO_2 sources in the Midwest to deep saline storage sites and depleted oil reservoirs in the sub-region.

Work completed independently in Phase I as part of Battelle' IMSCS-HUB Project and KGS's ICKan Project shows that deep saline storage zones in the Sleepy Hollow and Patterson study areas are both able to store 50 Mt of CO_2 or more. The existence of multiple Phase I projects in the area and the wealth of information described in the Project State of Development show that the Paleozoic complex at potential sites southwest NE and KS are well suited for a commercial-scale storage hub.

Phase II will continue to develop the source and stacked storage corridor concept identified during Phase I (Figure 8-2). The source corridor will collect CO_2 from up to 18 ethanol plants running between Blair, NE and Hitchcock County, NE (Table 8-1). The second corridor, the stacked-storage corridor will run between southwest NE to southwest KS. The corridor concept allows commercialization of a robust reliable source of CO_2 and connection to robust reliable storage in the form multiple stacked-storage sites. Stacked-storage in the region will include CO_2-EOR and saline storage in multiple reservoirs at individual sites. The inclusion of CO_2-EOR in the business model provides an additional driver for a commercial CO_2 market that will fund infrastructure development.

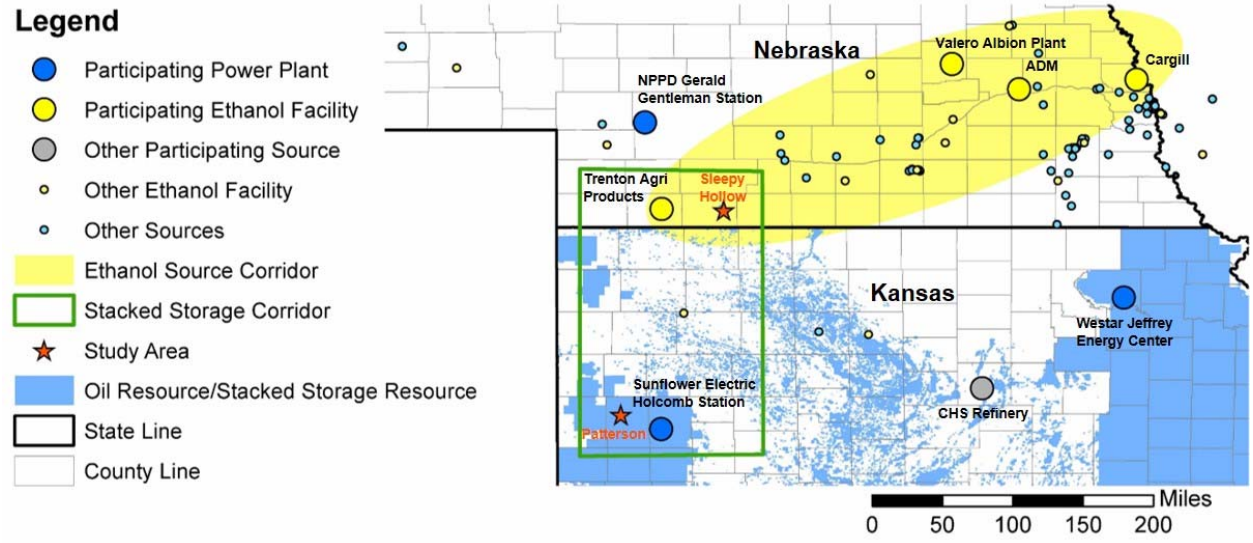

Figure 8-2. The IMSCS-HUB Study area showing the ethanol source and stacked storage corridors.

Table 8-1. List of source providing letters of support (in bold) or considering joining in the IMSCS-HUB along with their average annual emissions (2016 US EPA Reported Data or Personal Communication 2017).

Ethanol Source	Annual CO_2 Emissions (t)	CO_2 Source	Annual CO_2 Emissions (t)
ADM	1,164,813	Holcomb Station	1,726,751
Cargill Corn Milling	592,278	Westar JEC	10,848,198
Valero Renewables	366,648	CHS Refinery	613,756
Trenton Agri Products	112,815	NPPD GGS	7,499,834
AGP Soy/Corn Processing	159,232	Kansas City Board of Public Utilities	1,184,453
Pacific Ethanol (3 plants)	1,130,968		
Green Plains (5 plants)	1,119,687		
Chief Ethanol Fuels (2 plants)	338,444		
Bridgeport Ethanol	47,856		
Total	5,032,741		20,146,241

Two selected areas with high potential for commercial-scale CO_2 storage have been identified as potential sites for further characterization during Phase II. The Patterson Heinitz Hartland Field (Patterson site) in Kearny County, southwestern Kansas, is comprised of three oilfields over an area of 36 mi^2 and is one of five closed geologic structures in the North Hugoton Storage Complex (NHSC). The Sleepy Hollow Field study area, located in Red Willow County, southwestern Nebraska, is delineated by a high-density cluster of wells (one well per 40 acres) over approximately 28 mi^2, and encompasses the most productive oilfield in the state. Existing hydrocarbon resources at the two selected study areas, and the potential for a hybrid of CO_2-EOR and geologic storage may provide technical advantages, infrastructure, and economic incentives needed to successfully commercialize CCS in the region. In addition to the Sleepy Hollow and Patterson sites, the NPPD plans to drill a well at GGS in 2019 and share data from the well to help delineate the northern boundary of the stacked-storage corridor. NPPD will provide access to the wellbore for additional logging and testing as in-kind. The data collected at GGS will be used to update the regional assessment of the IMSCS-HUB area.

8.2 Challenges Being Addressed in Phase II

Technical and nontechnical challenges identified during Phase I that will be addressed during Phase II include mapping caprocks/confining units, minimizing the potential AoR through stacked-storage, and developing monitoring strategies to address stacked CO_2 plumes. Non-technical challenges include outreach; regulatory, contractual, and permitting strategies; pore space ownership; long-term liability; and CO_2 pipeline routing.

8.2.1 Mapping the Extent of the Confining System

Pre-feasibility work in all Phase I projects shows there are regionally extensive caprocks capable of containing CO_2, including Pennsylvanian and Permian shales and evaporites. Log and core data for Nebraska and Kansas indicate there are multiple formations that may act as additional containment units, including the Council Grove Group, Sumner Group, and Carlile Shale in Nebraska and the Meramec, Morrow, and Cherokee-Atokan units in Kansas. In Phase II, the team will collect 3D seismic and drill test wells at a primary study area in Kansas, and if budget allows, drill a test well at a secondary study area called Sleepy Hollow Field in Nebraska. The 3D seismic data will be collected at the Patterson

site to help establish the architecture of the structural closures because there is limited well control in the field. However, 3D seismic data is not needed at Sleepy Hollow because there is better well control. The test wells at both sites plug the data gaps identified above by providing log, core, and test data quantifying the confining system and integrity of multiple caprocks, petrophysical properties of the saline storage reservoir, and geomechanical properties of the caprocks.

8.2.2 Minimize the Areas of Review

The size of the area of review and associated regulatory/permit requirements is a significant challenge facing large-scale CO_2 storage projects. A larger area of review requires more resources to be expended on characterization and monitoring. Stacked-storage will minimize the extent of the area of review by creating several vertically stacked small plumes instead of a single large plume. Data collected during Phase I shows that stacked-storage is feasible all along the stacked-storage corridor. New core and test data along with log data collected in Kansas and Nebraska will validate assumptions made about reservoir properties in Phase I and allow modeling to develop strategies to minimize the potential area of review through well placement, injection volume, and completion strategies (similar to maximizing sweep efficiency for CO_2-EOR).

8.2.3 Public Outreach

The size of the hub presents both a challenge and opportunity. Outreach for the capture, transport, and storage of the CO_2 will require a careful, targeted, outreach program to ensure that stakeholders affected by the hub support its value. In Phase II, Great Plains Institute (GPI) will address outreach with the assistance of the CSD and KGS by targeting industries, NGOs, and trade associations that are supportive of the opportunities that will be afforded by the project, including adding value to corn for the agriculture industry, developing a commodity market for CO_2 in the midcontinent, delivering CO_2 to oilfields for CO_2-EOR, and delivering CO_2 to potential sites for geologic storage. The results of the input from stakeholders during the Phase II outreach will be used to develop an outreach plan that will be implemented during Phases III and IV and commercial operation.

8.2.4 Regulatory, Contractual, and Permitting

A commercial-scale project in the midcontinent will face hurdles regarding regulations governing construction, capture, transportation, and stacked-storage (deep saline and CO_2-EOR). To meet this challenge, the team will conduct a task devoted to studying existing regulations regarding capture, transport, and stacked-storage, identifying contractual needs from the point of view of the CO_2 producer, pipeline operator, and stacked-storage operator to develop model contracts that can be used in future phases of the project. The task will include a subtask for developing a permitting plan for the CO_2 pipeline and stacked-storage sites

8.2.5 Long-term Liability

Long-term liability is perhaps the most important challenge facing CO_2 storage. Neither Kansas nor Nebraska currently have statutes governing long-term liability for saline storage. This risk is mitigated by the focus on stacked-storage. Associated storage through CO_2-EOR does not face challenges with long-term liability. In Phase I, the team identified how long-term liability is being addressed commercially. Currently, ADM has the only active Class VI injection in the United States, and they address long-term liability through characterization and modeling of the site to shorten the default post injection site care period. ADM assumes long-term liability as a corporate entity and covers risks posed by the project through insurance. The regulatory and contractual task will identify additional commercial strategies to address long-term liability and build the strategies into model contracts.

8.2.6 Pipeline Rights of Way

Phase I work on pipeline rights of way indicates sufficient rights of way exist to develop a pipeline that runs between every ethanol plant in the ethanol source corridor and across the entire stacked-storage corridor. Initial modeling using SimCCS provides possible routes. In Phase II, the SimCCS cost surface algorithm will be updated to include additional features, including land use and environmentally sensitive areas, to refine the possible routes. Refined routes and roll-out scenarios will be developed and included in the CO_2 Management and Commercial Development Strategy task.

8.3 Phase II Objectives

The objectives of Phase II build on the lessons learned from the RCSP's and extend the framework for geologic storage site characterization and development to the commercial scale. The IMSCS-HUB Project will systematically address the technical challenges of commercial-scale CO_2 storage and will aid DOE in meeting their Carbon Storage Research and Development Program goals:

(1) Develop and validate technologies to ensure 99 percent storage permanence.
(2) Develop technologies to improve reservoir storage efficiency while ensuring containment effectiveness.
(3) Support industry's ability to predict CO_2 storage capacity in geologic formations to within ±30 percent.
(4) Develop best practice manuals for site characterization, public outreach, risk management and operations for geologic storage.

The Phase II will employ a workflow for integrating site-specific characterization data into stochastic storage efficiency calculations, storage resource estimates, and dynamic simulations of stacked reservoir injection to further industry's ability to predict storage capacity. The proposed tasks for this project are aligned with initial characterization guidelines provided in the DOE-NETL Site Screening, Site Selection, and Site Characterization Best Practice Manual (BPM), as well as other guidelines set forth in DOE's BPMs for public outreach, risk simulation, and storage operations (DOE-NETL, 2017a, b, c, d). Results of the proposed IMSCS-HUB Project will also provide useful input for the development of BPMs related to commercial scale storage.

The overall objective of this program is **to demonstrate the feasibility of having multiple sites within the stacked-storage corridor with a 50-Mt or greater capacity to safely, permanently, and economically store CO_2.** During Phase I, the team identified potential storage areas within the stacked-storage corridor. The Phase I evaluations of the sites indicate that Patterson and Sleepy Hollow study areas meet the 50 Mt saline storage criterion described in DE-FOA-0001584. Midcontinent geology and co-location of both sites with oil production make both sites candidates for stacked-storage. The depth of the potential saline storage units at the Patterson site make saline storage more attractive at that site. Accordingly, it is selected as the primary site for geologic feasibility studies, with a smaller amount of work being conducted at Sleepy Hollow study area to help prove the entire stacked-storage corridor. The specific objectives of the feasibility program coincide with the objectives of the Phase II FOA (DE-FOA-0001450). The program specific objectives are detailed in the following paragraphs.

Objective 1: Demonstrate multiple 50 Mt storage sites for the IMSCS-HUB concept by evaluating a Kansas and Nebraska site, each with the ability to safely, permanently, and economically store anthropogenic CO_2 through stacked-storage. The hub concept is major advancement in CO_2 storage because multiple storage sites within the stacked-storage corridor will share the same capture and transport infrastructure. The size of the stacked-storage corridor will require multiple characterization

wells to provide data that address feasibility. Seismic data will be collected at the Patterson site field because the potential saline units underlie the potential CO_2-EOR units, so there is limited well control to provide the geologic architecture. However, seismic data is not needed at the Sleepy Hollow site because the saline units are between the potential CO_2-EOR units allowing better delineation using existing wells. The Patterson site has two lobes, and a feasibility well will be drilled in each to collect log, core, and test data in caprocks and saline units. The Sleepy Hollow site has better well control and will only require one feasibility well to collect log, core and test data in saline units between and above the oil-bearing units. The data will be used to establish saline storage reservoir properties, reservoir seal integrity, geochemical properties and geochemical compositions for site-specific models and demonstrate commercial feasibility.

Objective 2: Develop 50 Mt+ storage scenarios and provide a basis for UIC permitting. New data will be incorporated into reservoir models to establish updated capacity estimates for the saline storage. Reservoir models in both CMG and ECLIPSE will extend the current state of knowledge for injection strategies by using sensitivity analyses to minimize storage site AoRs by adjusting perforation locations and injection volumes in individual saline reservoirs. Sensitivity analyses will also be used to develop new monitoring strategies specific to identifying CO_2 behavior in multiple stacked reservoirs. The resulting injection and monitoring scenarios will serve as a basis for developing a UIC permit in later program phases.

Objective 3: Demonstrate long-term seal integrity and minimize induced seismicity. The new seismic and well data will be incorporated into existing site reservoir models and new geomechanical models. Reservoir models using ECLIPSE and/or CMG will estimate the areal extent of the caprock, fracture gradients and maximum allowable injection pressures at each site. The same data will be incorporated into geomechanical models using VISAGE to understand existing and potential reservoir and caprock stresses and the likelihood for induced seismic events. Storage strategies will be developed to minimize injection related stress and the likelihood of induced seismicity. Baseline seismic data will be collected using KGS's seismometers.

Objective 4: Develop strategies to manage and store CO_2 from multiple ethanol and coal-fired electric utility CO_2 sources. CO_2 availability is addressed by incorporating multiple sources, ensuring storage in commercial operations is not interrupted. The team will develop pipeline routes, initial schedules for sources joining the hub, and subsequent maintenance schedules for CO_2 management. The team will also identify the timing, location, and number of storage sites needed during commercial operations. LANL will use SimCCS to develop potential pipeline routes and get input from ethanol and electric utility partners to estimate CO_2 capture roll-out and maintenance schedules.

Objective 5: Leverage the data collected to scale the project to develop a regional commercial enterprise (three to ten 50 Mt+ storage sites). Building on the results of Objective 4, the team will identify how ethanol plants to the east of the source corridor can be added to the program. Analyses conducted by GPI shows that the 34 largest ethanol plants in Kansas, Nebraska, Iowa, and Illinois (Figure 2) represent 9.85 Mt per year of CO_2 that could be captured and stored in the stacked-storage corridor. The team will also identify additional candidate sites that can be characterized as commercial operations grow.

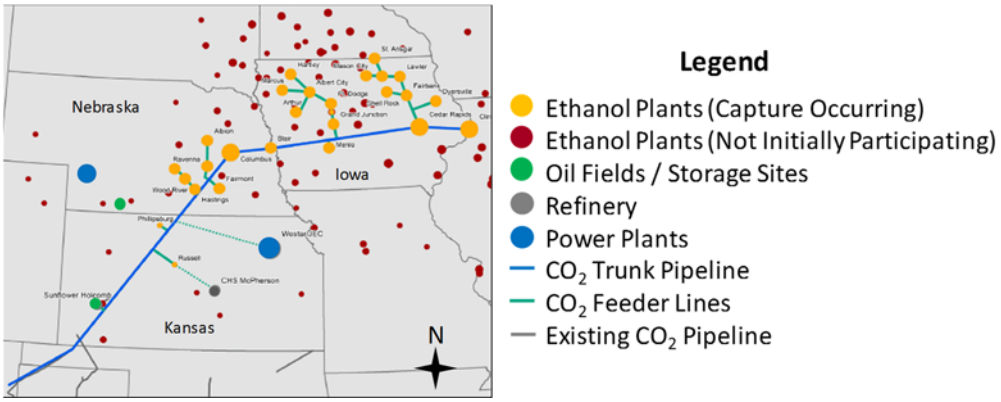

Figure 8-3. Potential pipeline route that could include ethanol plants in Iowa and Illinois (data source: DOE-EIA, 2017; State CO_2-EOR Deployment Workgroup, 2017).

Objective 6: Identify and mitigate public outreach and regulatory barriers to IMSCS-HUB implementation. The team will conduct outreach with local, regional, and federal stakeholders to identify non-technical issues for commercialization. Near the end of Phase II, the team will create an outreach plan for engaging stakeholders during Phase III to highlight the benefits of the hub and mitigate barriers to commercial operations.

Objective 7: Develop a detailed commercial development plan. Battelle and ADM will lead the team creating a commercial development plan that will incorporate the results of Phase II and describe in detail how Phases III and IV and commercial operation will be implemented. The plan will include a business strategy for capture, transport and storage, CO_2 management; CO_2 capture; site characterization; infrastructure construction; permitting; and operation.

8.4 Phase II Project Tasks

The scope of work is divided into nine tasks designed to meet the overall and specific objectives above.

Task 1.0 – Project Management and Planning: This Task includes the necessary activities to ensure coordination and planning of the project with DOE/NETL and other project participants. These activities include, but are not limited to, the monitoring and controlling of project scope, cost, schedule, and risk, and the submission and approval of required National Environmental Policy Act (NEPA) documentation. This Task includes all work elements required to maintain and revise the Project Management Plan, and to manage and report on activities in accordance with the plan. In addition, this Task should also include all work elements required to maintain and revise the Data Management Plan.

Subtask 1.1 Project Management: This subtask includes oversight of schedule, budget, milestones, issues, and interactions with project managers (PMs) and sponsors. The principal investigator (PI) or PM will coordinate team meetings. Specific roles and responsibilities for team members will be defined and tracked. The PM will ensure all technical reports are submitted on a timely basis and will oversee subcontracting procedures and mechanisms required for acquiring the services of all entities involved in the project. This task will include quarterly progress reports, continuation applications, and informal updates to the DOE PM. Project control will involve detailed financial tracking of both labor and

subcontracting in accordance with Battelle and DOE requirements. Efficient and timely project control will enable the project to optimally allocate funds.

Subtask 1.2 Update Project Management Plan. The project management plan (PMP) will be updated with any changes and submitted to the DOE PM within 30 days of project award. In addition, the PMP will be updated as needed throughout the project. Deliverable: updated PMP.

Subtask 1.3 NEPA Reporting. NEPA questionnaire(s) will be finalized upon project award. Updated questionnaires will be submitted as seismic and well locations are identified. Deliverable: updated NEPA questionnaires.

Subtask 1.4 Update Data Management Plan: The Data Management Plan (DMP) explains how data collected during Phase II will be shared and stored. Deliverable: updated DMP.

Task 2.0 – Site Access and Permitting: Battelle will work with Berexco, the Patterson site operator and Central Operating, the Sleepy Hollow site operator to ensure access to all sites and ensure all proper permits are received prior to data collection. This task facilitates data collection to meet Objectives 1 through 3.

Subtask 2.1 Site Access: Access will be negotiated for each site to ensure the team has access to operations and subsequent data required to meet the project objectives. Deliverable: site access agreements.

Subtask 2.2 Permitting: Permits will be obtained as required for seismic acquisition and well drilling. Deliverables: well drilling permits and seismic permit.

Task 3.0 Feasibility Data Collection Planning: Task 3 includes updating existing models to include proprietary data held by the operators (where available) and creating a gap analysis for each study area. The gap assessment will be used to develop the Storage Complex Feasibility Data Collection Plan, which identifies the data to assess feasibility for storage and Class VI UIC permitting. This task also facilitates data collection to meet Objectives 1 through 3.

Subtask 3.1 Geologic and Reservoir Model Update. Proprietary geological, geomechanical, and hydrogeological data held by the study area operators will be compiled and incorporated into the existing site models and simulations. The new data and updated models will help determine current subsurface conditions in the study areas, inform geologic models, refine estimates of storage resource, and aid in characterization and reduction of storage risks. Deliverable: model update technical memo outlining new data incorporated into the site models.

Subtask 3.2 Data Gap Assessment. A data gap assessment will be conducted for each study area considering the updated models from Subtask 3.1 to identify missing data that could provide the team with a better understanding of saline storage units and caprocks. Deliverable: gap assessment technical memo detailing data gaps.

Subtask 3.3 Storage Complex Data Collection Plan. The team will use the gap assessment to select seismic survey locations and logging technologies, core intervals, and test intervals for data collection. The plan will cover the seismic survey, new wells at all sites, and existing wells at Sleepy Hollow Field in detail. The team will consider the UIC Class VI requirements to ensure that any data gaps for permitting

are identified and filled. The plan will guide data collection in Task 4. Deliverable: Storage Complex Data Collection Plan.

Task 4.0 Storage Complex Feasibility Data Collection: This task includes acquisition of formation evaluation data and well tests to evaluate hydrologic conditions and injectivity. These data will be integrated with existing models to prove feasibility and reduce project uncertainties associated with future development and commercial operations. The data collected in this task will be used to meet Objectives 1 through 3.

Subtask 4.1 Seismic Design and Acquisition: The 3D seismic data will be acquired and processed to interpret subsurface structure at the Patterson site to choose the best test well locations for data collection. Deliverable: seismic survey technical memo outlining the acquisition and interpretation.

Subtask 4.2 Well Site Selection: Two appraisal wells are planned for the Patterson site, and one appraisal well is planned for the Sleepy Hollow site. Final site selection will be based on the models from Subtask 3.1, on the Storage Complex Data Collection Plan (Subtask 3.3), and on surface access and topology. Deliverable: wellsite survey.

Subtask 4.3 Well Design. The team design appraisal wells including the operations for construction, logging, coring and testing insuring that required data are collected. Loudon Technical Services will review the plans and a drill well on paper exercise will be conducted for each well to verify the completeness of each well's plan. Additionally, the wells will be constructed to meet all state and local requirements and to ensure there is no conflict with UIC regulations. Deliverable: well designs for each appraisal well.

Subtask 4.4 Well Drilling and Data Collection: Two appraisal wells will be drilled by Berexco at the Patterson site and one well will be drilled at the Sleepy Hollow site. A suite of basic and advanced log data will be acquired in each well, facilitating caprock and deep saline formation evaluation. Basic logs will include triple-combo and pulsed neutron. Advanced logs will include dipole sonic, magnetic resonance and borehole image. Whole core, sidewall cores, drill stem test (DST) data, and reservoir injection test data will be collected. Data collection at Patterson will focus on Mississippian and Ordovician deep saline storage zones within the Osage, Viola, and Arbuckle formations, and confining units such as the Meramec, Morrow and Sumner Group. Data collection at Sleepy Hollow will focus on deep saline intervals in the Pennsylvanian Wabaunsee, Shawnee-Douglas, and Pleasanton-Maramaton groups and caprocks of the Council Grove and Sumner groups. Deliverable: drilling and data collection reports for each well.

Subtask 4.5 Baseline Seismic Monitoring: KGS will install seismometers (3-4 stations) to collect baseline seismic activity data, measuring amplitude and the identifying any temporal or geographical trends at the Patterson site Deliverable: Seismic monitoring report.

Subtask 4.6 Existing Well Selection and Data Collection: Central Operating is providing access to existing wells within the Sleepy Hollow site. The team will work with Central Operating to select wells that meet the needs of the Storage Complex Data Collection Plan (Subtask 3.3). Two to four wells will be selected for logging using cased hole tools such as pulsed neutron and dipole sonic logging to characterize saline and caprock units, enabling better correlation to the appraisal well data from Subtask 4.4. Deliverable: existing well selection and data collection report detailing the location of the well selected and the data collected.

Subtask 4.7 GGS Data Collection: NPPD is drilling a well at GGS in 2019 and will provide access to the well for data collection. The team will work with NPPD to supplement the planed logging and testing program to provide data to help delineate northern boundary of the stacked-storage corridor. Deliverable: GGS data collection report.

Task 5.0 Storage Complex Analysis and Model Update: Task 5 will focus on integration and analysis of new subsurface data. Data analysis will establish baseline hydrogeological and geochemical characteristics of the targeted reservoirs, confining systems, and overlying shallow groundwater aquifer(s). The new subsurface data will be integrated into static and dynamic models to better characterize key reservoir and caprock parameters impacting storage and supply output for Class VI UIC well permits. The results of this task satisfy Objectives 1 through 3.

Subtask 5.1 Data Analysis and Integration: This subtask includes characterization of the feasibility of deep saline storage reservoirs, confining system, and hydrogeologic regime of the storage complex. Petrophysical analysis of log and core data will quantify total and effective porosity, derive permeability transforms and log curves, and determine reservoir and non-reservoir facies. Results of the data analysis will be integrated to construct geologic maps and cross-sections for reservoirs and caprocks, derive site-specific storage efficiency values, and supply input for geologic models and risk assessment. Whole and sidewall cores collected from intervals within the caprock(s) and deep saline storage reservoir(s) will be analyzed to derive formation lithology, heterogeneity, porosity distribution, relative permeability, and geomechanical properties. Core data will be supplemented with reservoir and caprock data from advanced logs such as dipole sonic, nuclear magnetic resonance logs, geochemical logs, and borehole image logs. Core and log data will be compared to establish correlations and calibrations to reduce uncertainty in models and simulations. Fluid samples collected using PVT tools will be analyzed to determine baseline geochemistry of the storage zone(s), caprock(s), and overlying freshwater aquifers. DST and injection tests data will provide information on reservoir permeability and lateral extent, subsurface fluid behavior, pressure boundaries, and feasible conditions for injection operations. Deliverable: data analysis technical memo describing results for all data analyzed.

Subtask 5.2 Storage Complex Model Update: The results of the analyses will be incorporated into geologic models in Petrel and reservoir simulations in CMG and ECLIPSE to refine the models from Task 3. The refined models will be used to assess commercial-scale (50+ Mt) injection into saline stacked-storage units, update storage capacity, develop AoR minimization strategies, and develop stacked-storage monitoring strategies. Deliverable: storage complex geologic and reservoir modeling report detailing both storage sites, including updated storage capacities and associated uncertainties, AoR minimization strategies detailing how injection design can reduce AoRs, and a monitoring plan that includes tools and measurement frequency to monitor stacked-storage at each site.

Subtask 5.3 Geomechanical Modeling of the Storage Complex. Schlumberger and Battelle will model the geomechanical effect of stacked-storage using VISAGE to establish how commercial injection may affect each site. The model will characterize the baseline stresses in the subsurface and provide information on the fracture gradient to estimate the maximum permissible injection pressure, simulate the mechanical integrity of the caprocks, and study the risk of induced seismic events. Deliverable: storage complex geomechanical modeling report.

Task 6.0 Outreach: GPI will lead this task because of their experience working on ethanol and CO_2-EOR topics in the NE-KS region. Work will be conducted to identify stakeholders, evaluate social climate, and assess likely concerns and perceptions related to the proposed project. Work conducted for this task will

be integrated into an effective public outreach program that addresses all anticipated outreach needs for current and future phases of the commercial-scale geologic storage hub. The task develops a timeline of goals and activities to define likely outreach needs for each site. This task satisfies Objective 6.

Subtask 6.1 Government, Industry, and NGO Outreach: The team will build on existing relationships with local, state, and federal agencies to gain insight into their perspective on the project needs and requirements. The team will reach out to oil producers, ethanol plants, electric utilities, and pipeline operators in the region to get perspective on how the project may affect their operations and reach out to environmental NGOs to get their opinion on how hub commercial operations could be consistent with their environmental values. As part of this subtask, GPI will organize a stakeholder meeting where the team will present the project data and plans and facilitate discussions to gain feedback. Deliverable: outreach meeting report detailing the results of the stakeholder meeting.

Subtask 6.2 Outreach Plan: The team will use information gathered in Subtask 6.1 to develop an outreach plan for Phases III and IV and for commercial operation of the IMSCS-HUB. Deliverable: IMSCS-HUB Outreach plan.

Subtask 6.3 Coordination with RCSPs and NATCARB: The team includes of members of four RCSPs, which facilitates RCSP coordination. The team will provide data to NATCARB and the DOE core library as described in the DMP (Subtask 1.4).

Task 7.0 Risk Assessment and Mitigation: To aid in the development of commercial stacked-storage within the proposed storage complex, risk assessments will be conducted to identify potential constraints the storage complex, pipeline network, and non-technical aspects of the IMSCS-HUB. The results of the assessment will be used to develop a risk mitigation plan, incorporating each major risk identified. The team will use the plan to minimize the risk of moving to commercial operation. This task helps facilitate meeting Objectives 1, 3, 6 and 7.

Subtask 7.1 Storage Risk Assessment: The team will conduct a risk assessment for stacked-storage using expert elicitation similar to that of Hnottevange-Telleen et al. [2009] combined with the bowtie method employed at Shell's Quest project [Tucker et al, 2013]. Included in the storage risk assessment will be leakage through natural pathways, leakage through existing wells, and induced seismicity. The risk assessment will incorporate site-specific data to identify high risk scenarios. The team will use the assessment to identify barriers to mitigate risks that will be outlined in a Risk Mitigation Plan (Subtask 7.5). Deliverable: storage risk assessment report for each study area.

Subtask 7.2 Pipeline Risk Assessment: The geology of the region and the large number of CO_2 sources require a robust transportation network. The team will conduct a risk assessment using the same tools used in Subtask 7.3 (expert elicitation and the bowtie method) with a focus on pipeline related risks including construction, operational, and environmental risks. The bowtie method will allow the visualization of risk scenarios to identify barriers that can reduce or eliminate risks. High risks and mitigation barriers will be fed into the Risk Mitigation Plan (Subtask 7.5). Deliverable: Storage Pipeline Assessment Report.

Subtask 7.3 National Risk Assessment Program Tools. PNNL will use tools developed through DOE's National Risk Assessment Partnership (NRAP) to evaluate risks for various aspects of the subsurface storage and containment system as they relate to leakage and induced seismicity. NRAP tools that may be used in the project include: the Integrated Assessment Model – Carbon Storage (NRAP-IAM-CS);

Reservoir Evaluation and Visualization (REV) Tool; Reservoir ROM Generation Tool (RROM-Gen); Wellbore Leakage Analysis Tool (WLAT); Natural Seal ROM (NSealR); Aquifer Impact Model (AIM); Design for Risk Evaluation and Monitoring (DREAM); Term Seismic Forecasting (STSF) Ground Motion Predictions for Induced Seismicity (GMPIS); and the Multiple Source Leakage ROM for atmospheric leakage (MSLR). Deliverable: NRAP Tool Risk Assessment Report.

Subtask 7.4 Non-Technical Risk Assessment: The team will use analogous pipeline and UIC projects in the area along with the results of project outreach to identify significant non-technical risks. Risks will include those related to long-term liability, pore space ownership, public opposition, regulation, contractual obligations, and environmental justice. Risk mitigation will be identified by the team will be fed into the risk mitigation plan (Subtask 7.5). Deliverable: Non-Technical Risk Assessment Report.

Subtask 7.5 Risk Mitigation Plan: The results of Subtasks 7.1 through Subtasks 7.4 will be considered together to develop a risk mitigation plan that will guide the characterization in Phase III, construction in Phase IV, and commercial operations. Deliverable: IMSCS-HUB Risk Mitigation Plan.

Task 8.0 Regulatory and Contractual Requirements Assessment: This task focuses on assessment of federal, state, and local regulations applicable to development of the hub. The task will identify contractual requirements for activities required for commercial development and create model contracts to facilitate a smooth transition from a DOE sponsored project to stand-alone commercial operation by 2025. This task helps meet Objectives 6 and 7.

Subtask 8.1 Regulatory Assessment. The team will build on Phase I work to identify all federal, state, and local regulatory requirements that affect the development of a commercial project. The team will identify regulatory gaps and road blocks and suggest regulatory options to better enable project development. The task will incorporate the greenhouse gas reporting program and the UIC program. This task will also address regulatory and commercial strategies for pore space ownership and long-term liability. Deliverable: Regulatory Assessment Report.

Subtask 8.2 Contractual Assessment. Contractual requirements for evaluated for capture, with input from ADM and other ethanol sources, NPPD, and Westar; for transport, with input from MV Purchasing; and for storage, with input from Berexco, Central Operating, and Great Plains Energy. The results of the evaluations will inform the development of model contracts that cover capture, transport, site access, pore space ownership, and long-term liability and monitoring. Deliverable: Contractual Assessment Report, including model contract clauses.

Subtask 8.3 UIC Permit Planning. The results of Subtask 8.1 and Task 5 will be used to develop a UIC permitting plan for wells at both study areas. This will include how Class II requirements and Class VI requirements are met and how any UIC Class transitions will be implemented. Deliverable: UIC Permitting Plan for each site.

Task 9.0 CO_2 Management and Commercial Development Strategy: The results of this task will include a comprehensive CO_2 management and commercial development strategy for the proposed storage hub. This includes updating site-scale storage resource estimates, pipeline planning, and evaluation of industrial CO_2 source(s) and reliability, and economic analysis based on various injection and operational scenarios at each potential site. Results of subsurface characterization, modeling efforts, outreach assessment, and regulatory analysis from previous tasks will be integrated to develop a detailed commercial development plan.

Subtask 9.1 Regional Storage Resource Characterization. ARI will lead the team to develop a regional stacked-storage resource model that will serve to update their 2006 basin-scale estimate [ARI, 2006]. The team will also incorporate the methodology developed by NETL (DOE-NETL 2010; Goodman et al., 2011) to quantify the prospective CO_2 storage resource of deep saline formations at potential sites and then extrapolate to analogous sites to describe the region. Storage efficiency and storage resource will be estimated stochastically using the CO_2-SCREEN tool (V1) developed by DOE-NETL (Sanguinito et al., 2017) and heterogeneous site-specific characterization data along with dynamic reservoir simulations (Goodman et al., 2016). Deliverable: updated Basin Oriented Strategies for CO_2 Storage document for Nebraska and Kansas.

Subtask 9.2 Pipeline Planning and CO_2 Management: CO_2 stream constituent specifications for capture and transport will be identified along with an estimate of the timing for capture implementation created with the help of the project CO_2 sources. The capture schedule will be incorporated by LANL into SimCCS simulations to update Phase I work on pipeline routing, developing routes and schedules to connect CO_2 sources to stacked-storage sites. The simulations will initially rely on CO_2 from ethanol plants, which will be followed by CO_2 from coal-fired utilities. SimCCS will be modified to include environmental justice variables including environmentally sensitive areas. The CO_2 purity and volumes captured will be used to estimate the pipeline trunk line and spur diameters using PIPESIM. The results of the modeling will provide a basis for the team to develop a transportation and management plan that ensures CO_2 delivery to operators is reliable. Deliverable: Pipeline Planning and CO_2 Management Report.

Subtask 9.3 Economic Analysis: The updated models from Tasks 5, 7, and 8 along with the results of Subtask 9.2 will be used to develop detailed economic analyses of the project as a basis to move from Phase II into future phases. Deliverable: Economic Assessment Report.

Subtask 9.4 Detailed Commercial Development Plan: This task incorporates all project results, including results from subsurface feasibility, modeling efforts, outreach, and regulatory analysis to identify the qualified storage site(s) and develop a detailed commercial development plan for the proposed storage hub. The plan will detail the necessary steps to advance to future development, including filling data and information gaps. It will provide detailed steps to conduct Phase III and general steps for Phase IV and Operations that will be refined during Phase III. Deliverable: Detailed Commercial Development Plan.

9 Conclusions

The combined results from Phase I indicate that a commercial scale project in the study area is likely feasible. The Paleozoic deep saline storage zones in southwest-central Nebraska and southwest Kansas have prospective storage resources ranging from 30 Mt to 50 Mt at the P10 percentile, suggesting a high probability of storing commercial-scale quantities of CO_2 at individual sites in these selected areas. Dynamic simulations at potential sites in the Sleepy Hollow oilfield in Nebraska and the Patterson oilfield in Kansas indicate permanent and safe injection of 50-60 Mt of CO_2 is feasible over 30 years at injection pressures below 90% of the fracture pressure.

The source identification assessment examined a 44-county study area running from eastern to southwestern Nebraska comprising 46 point sources. The results of the CO_2 source assessment (Section 2) indicate that the commercialization of the hub can employ CO_2 derived from ethanol sources. Within the ethanol source corridor, there are 18 ethanol plants with average annual emissions of 5.7 Mt of CO_2 and a standard deviation over the last 5 years of 0.1 Mt per year, indicating dependable ethanol production in the area.

Two large coal-fired electric generation plants that could act as CO_2 emission sources that can deliver CO_2 to the pipeline were also identified. The Westar Energy Company's JEC is a large coal-fired power plant located in St. Mary's KS, and contains three separate 800 MWe (megawatt electricity) units. JEC has 10.8 Mt of annual CO_2 emissions. NPPD's GGS is Nebraska's largest coal-fired electricity-generating station. GGS is located near Sutherland, Nebraska. GGS consists of 665 MWe and 700 MWe generating units with annual emissions of 7.5 Mt of CO_2.

The simpler and cheaper capture process associated with ethanol-derived CO_2 led the Phase I project to focus on ethanol plants as an initial CO_2 Source. This will remain the focus in Phase II. Three hypothetical source corridor routes connecting ethanol plants were discussed, each possible corridor had commercial-scale CO_2 emissions, between 2.1 and 2.4 MMt CO_2e/year. This helps to validate the results of the transportation assessment demonstrating that multiple viable pipeline routes capable of delivering 1.7 MMt per year or more can connect the ethanol and coal fired power plant sources in Nebraska and northeastern Kansas with the storage corridor in southwestern Nebraska and western Kansas. The presence of many existing pipelines in the study area demonstrates the viability of pipeline projects in terms of public perception and government regulations. The pipeline sizing results show that a pipeline can be developed to handle the CO_2 from current ethanol sources and still have some extra capacity for growth with a minimal number of booster stations.

An analysis of property owners along the pipeline route shows that the pipeline can be routed through an area with large parcels and relatively few landowners. The routes can be optimized to deal with as few land owners as possible and to take advantage of the most existing rights-of-way as possible in future phases. The assessment of sensitive populations and sensitive areas did not find any significant problems that could affect the overall success of the project. Sensitive areas and populations can be avoided by pulling the maps created into SimCCS for further modeling to develop routes around them without significant impact on pipeline length. An assessment of safety incidents involving pipelines showed that incidents involving CO_2 pipelines were less severe than those involving hazardous liquid or natural gas pipelines.

Besides ethanol plants, stakeholders for the IMSCS-HUB project include state agencies, businesses, trade associations, non-governmental organizations (NGOs), and the public. During Phase I, the IMSCS-HUB team engaged in outreach with state agencies, businesses, trade associations, and NGOs and secured letters of support from the organizations outlined in Table 9-1. Analysis of stakeholders and communities potentially affected by the proposed project indicates there is a low population density near each potential site, with a majority of the land being used for agricultural and industrial purposes. Nearby residents will be familiar with negotiating oil and gas leases and seeing oil and gas equipment operating; and as such they could be more amenable to leasing pore space beneath their property.

Table 9-1. Stakeholders expressing support for Phase II.

Agency	NGO/Association	Ethanol Producer	Electric Utility	Oil Producer	Other
KS Gov. Colyer	Clean Air Task Force	ADM	NPPD	Berexco	ION Engineering
NE Ethanol Board	Great Plains Institute	Cargill	Westar Energy	Merit Energy	MV Purchasing
NE Dept. of Agriculture	Kansas Independent Oil and Gas Association	Trenton Agri Products	Sunflower Electric Power	Great Plains Energy	The Linde Group
NE Dept. of Environmental Quality	NE Petroleum Producers Association	Valero Renewables	Kansas City Board of Public Utilities	Casillas Petroleum	
NE Corn Board	Renew Kansas	Pacific Eth.		Central Operating	
NE Energy Office					

The pre-feasibility assessment of a commercial-scale geologic CO_2 storage hub in the Midcontinent evaluated the suitability of the Pennsylvanian-Permian interval to serve as a geologic CO_2 storage complex at two selected areas, the Sleepy Hollow Field and the Patterson Heinitz Hartland Field. Porous and permeable Paleozoic deep saline formations have been identified as potential geologic storage complexes in southwest-central Nebraska and western Kansas. Paleozoic sedimentary rocks in the sub-region are characterized by thick stratigraphic successions of alternating marine and non-marine sedimentary rocks comprised of deep saline formations, oil-bearing reservoirs, shales, and evaporites. The proportion of shales and evaporites increases upward through the Paleozoic interval, forming regionally extensive caprock units for the underlying storage zones. Overlying the Paleozoic storage complex are regionally extensive Cretaceous sandstones, limestones, shales, and chalk that have potential to serve as secondary confining units between the Paleozoic storage intervals and the overlying Cenozoic rocks hosting the High Plains Aquifer.

In each selected area, porous and permeable Paleozoic shelf carbonates and sandstones occur within depositional compartments that are vertically isolated from interbedded and overlying oil-bearing zones by laterally extensive shale and impermeable limestones. Ordovician and Mississippian dolomites of the Arbuckle, Viola, and Osage units are potential deep saline storage zones with high potential for commercial-scale storage in southwest Kansas. These zones occur as laterally extensive units that form a northwest-trending, broad structural closure that is ideal for CO_2 storage at the potential site in the Patterson field. In the selected area of southwest-central Nebraska, six vertically stacked intervals of deep saline limestones and sandstones occur in the Wabaunsee, Shawnee-Douglas (Topeka, Deer Creek-

Oread), Lansing Kansas City (A, D-F) and Pleasanton-Marmaton groups. Deep saline storage zones exhibit both structural and stratigraphic trapping mechanisms at the potential site in the Sleepy Hollow field, with reservoir facies pinching out toward the Cambridge Arch in the northeast. The oil reservoirs at each potential site could provide additional zones for CO_2 storage during/after EOR.

Using subsurface pressure and temperature gradients of 0.47 psi/ft and 0.014°F/ft (plus 51°F average surface temperature) calculated for the sub-region, the minimum depth of injection required to store CO_2 in a supercritical state is approximately 2,600 ft. The deep saline formations of interest at both potential sites occur at average depths ranging from approximately 3,000 ft to 6,000 ft below the ground surface where pressures and temperatures are adequate for storage of supercritical CO_2. The shallowest reservoir in the two selected areas is 2,704 ft, occurring along the northern boundary of the Sleepy Hollow field, ensuring the entire anticipated CO_2 plume at each potential site will remain in a supercritical state. The storage depths at each potential site are ideal for achieving adequate protection of USDWs while maximizing storage efficiency and maintaining relatively low costs for well drilling, operation, and maintenance.

Analysis of data from more than 300 digital well logs and more than 200 core analyses in the selected areas indicates the Paleozoic intervals of interest have suitable reservoir properties for storing large quantities of CO_2. Porosities as high as 16–32% and maximum permeabilities ranging from approximately 100 to 1,000 millidarcies (mD) have been measured at each potential site. These values are within range of those reported at large-scale (e.g. 0.4–0.8 Mt CO_2/yr injection) CO_2 storage sites operating onshore in the United States and Canada (e.g., Whittaker and Worth, 2011; Finley et al., 2013; Rocket al., 2017) and imply that both sites will be able to handle commercial scale injection projects.

The structural and stratigraphic framework of Nebraska and Kansas was defined to guide data analysis and inform geologic modeling efforts. Site-specific geologic characterization was conducted via petrophysical analysis, construction of heterogenous site models and geologic maps, and calculation of prospective storage resources for the deep saline interval of the Pennsylvanian system. Results were used to identify potential qualified sites for further characterization and help establish the groundwork for commercial-scale development of geologic CO_2 storage resources in the Midcontinent Region.

The assessment included:

- Construction of 3D SEMs representing the geologic storage framework of the Pennsylvanian-Permian interval at each of the selected study areas
- Development of workflows to establish a consistent, repeatable methodology for site-scale geologic resource characterization that can be easily applied to other potential sites in the region
- Characterization of key confining system components including hydrocarbon trapping mechanisms, and caprock structural and stratigraphic continuity
- Quantification of site-specific storage efficiencies and prospective storage resource of the deep saline Pennsylvanian interval in both study areas

Site-scale analysis and mapping of potential storage zones generally show small variation in formation properties within the Sleepy Hollow Field, with regional structures such as the Cambridge Arch likely responsible for local map variations and the development of reservoir properties. Other key outcomes and takeaways for Sleepy Hollow Field are summarized below:

- Distinct, laterally continuous net reservoir intervals observed in the Wabaunsee and Pleasanton-Marmaton groups at both study areas suggest net reservoir zones may be traceable and continuous over distances of 50 mi or greater.
- Prospective storage resource results calculated at the P_{10} probability value (49.7 - 80.8 Mt) indicate a high level of confidence in the likelihood that the deep saline CO_2 storage resource is 50 Mt or greater at each site; sufficient for commercial-scale CO_2 storage.

Cyclotherms comprised of marine and non-marine sediments are a distinguishing feature of the Pennsylvanian-Permian-age subsurface interval in the Midcontinent. These stratigraphic successions provide alternating sequences of deep saline formations, shale, and oil-bearing zones conducive to vertically-stacked CO_2 injection and storage in oil-bearing and deep saline storage reservoirs. Existing hydrocarbon resources at the two selected study areas, and the potential for a hybrid of CO_2-EOR and geologic storage may provide technical advantages, infrastructure, and economic incentives needed to successfully commercialize CCS in the region. A continued effort is needed to eliminate data gaps and conduct further characterization of potential qualified sites for CO_2 storage in the study region. This initial characterization shows that the Pennsylvanian-Permian interval at the selected study areas has high potential to serve as a long-term, commercial-scale geologic storage complex.

Numerical reservoir modeling of the Sleepy Hollow Field was conducted based on the static earth model of the site. The simulations included different well location configurations, and a sensitivity analysis. The following conclusions are drawn based on the results of these efforts:

- The simulation results with a single injector show very good injectivity performance. One of the studied injectors could inject approximately 34.8 million metric tons after 30 years resulting in an average injection rate of 3,177 metric tons per day.
- No single-well injection case could achieve the storage target (50 million metric tons for 30 years); a multi-injector system is required.
- At least three injection wells are required to satisfy the injection target in the study area.
- In general, the CO_2 plume tends to grow radially centered from each injector. With the injectors of #1, #2, and #5, the entire CO_2 plume extends approximately 9 km in the east-west direction and 11 km in the north-south direction after 30-year injection.
- Major CO_2 storage occurs at Wabaunsee (26%), Kansas City Base (19%), Topeka (18%), Oread (15%), LKC A (8%), and Deer Creek (6%).
- Due to the lack of previous interest in the saline aquifers, there is little data available for the potential saline formations at Sleepy Hollow Field. Non-negligible parameters identified from the sensitivity analysis need to be taken into account in the future work in order to reduce the major uncertainties during Phase II.

Potential challenges identified as part of the economic and liability assessment for the IMSCS-HUB Project include development of pipeline infrastructure and UIC Class VI corrective actions from existing wellbores in the study area. Collaboration and support from a major pipeline company in the region (MV Purchasing) has been established for Phase II to help address potential contingencies associated with pipeline development and financing. Existing natural gas pipelines routed directly to ethanol plants occur within 3 miles of each potential site, and the IMSCS-HUB study area is roughly located between existing CO_2 pipeline networks in the U.S. These pipeline rights of way can be leveraged for CO_2 pipeline development for the project. The economic incentives for construction of the proposed pipeline will be

further evaluated in Phase II, including consideration of CO_2-EOR, 45Q, and the ethanol industry. Low population density, and widespread agricultural land use suggests rural areas aren't likely to undergo significant development in the next 20 years, ensuring opportunities will remain for the IMSCS-HUB to expand and access existing CO_2 pipeline networks.

A distinct advantage of the IMSCS HUB Project is that the technology for ethanol-based CO_2 capture and transport for EOR is currently economically feasible and can be commercially deployed today to subsidize ethanol CO_2 saline storage, and provide the scalable infrastructure needed to integrate CO_2 capture from power plants in the future. For saline storage costs and credits, the 45Q tax credit can only be claimed for 12 years after the beginning of capture but is spread across the total amount of CO_2 stored for the entire project. Despite the positive net present values with the 45Q tax credit, the discounted net profit from saline storage (~ \$9/tonne CO_2) is still less than the combined capture and transport costs estimated for each scenario (\$40 - \$76/tonne CO_2), suggesting the 45Q tax credit is not enough alone to pay for capture, transport, and saline storage costs associated with an integrated CCS operation in the IMCSCS-HUB

The per pattern economic scenario results with and without 45Q EOR storage credits show a positive net present value for the Sleepy Hollow Field study area, suggesting that profit could be made to help offset the CO_2 capture costs at the desired rate of return for the EOR operation. Net present values of approximately \$42/tonne CO_2 for CO_2-EOR operations with 45Q storage credits suggests the tax credit can be used in conjunction with EOR to close the deficit and pay for the capture, transport, and storage components of the CCS project in the IMSCS-HUB. The economic analysis provides evidence of the need for stacked storage in oil-producing areas where CO_2-EOR and the 45Q tax credit can be used subsidize the capture and transport infrastructure needed to collect and move CO_2 and then saline projects can take advantage of the infrastructure to store additional CO_2.

The assessment of the liabilities identified for the project are generally similar to those of oil and gas or other subsurface projects and that they can be addressed through regulatory, contractual, and insurance mechanisms. The analysis of the potential for problems with rights of way and environmentally sensitive areas do not look insurmountable because the pipeline and field sites are likely in sparsely populated locations with few sensitive areas. In addition, problems arising from injection operations are likely to be minimized due to the colocation of the storage site with oil and gas operations, better ensuring the public in the area are familiar with drilling and injection equipment and operations.

Existing hydrocarbon resources in the Sleepy Hollow study area and the potential for a hybrid of CO_2-EOR and geologic storage may provide technical advantages, infrastructure, and economic incentives needed to successfully commercialize CCS in the region. Saline storage alone cannot be fully supported by the 45Q tax credit under a saline scenario or a CO_2-EOR scenario. However, the use of EOR as a business case for storage provides an income from oil production that can help subsidize the construction and operation of storage projects allowing future projects to take advantage of the infrastructure, lowering costs.

The IMSCS-HUB project is a significant opportunity to implement a commercial CCS project for many reasons, not the least of which is the potential to link saline storage aquifers and oilfields in southwestern Nebraska and eastern Kansas to ethanol sources in Nebraska and, potentially, the rest of the Midcontinent region. Ethanol-derived-CO_2 provides a relatively pure stream of CO_2 that can be easily captured at commercial volumes with off-the-shelf equipment. The cost of capture at ethanol CO_2

sources is relatively low compared to other industrial sources. By phasing the stacked storage project to start with CO_2-EOR, oil revenues can be used to offset the cost of capture and transportation infrastructure, reducing the capital burdens for later saline storage phases. These factors will allow for early implementation of a commercial carbon storage hub.

References

Advanced Resources International. 2006. Basin Oriented Strategies for CO_2 Enhanced Oil Recovery: Mid-Continent Region. Prepared for the U.S. Department of Energy Office of Fossil Energy – Office of Oil and Natural Gas.

Battelle. 2017. Integrated Mid-Continent Stacked Carbon Storage Hub: Task 2 CO_2 Source Assessment. Topical Report Submitted July 7, 2017. DOE Award Number DE-FE0029264.

Battelle, 2018a. Integrated Mid-Continent Stacked Carbon Storage Hub (IMSCS-HUB) Task 5 Capture and Transport Assessment Topical Report. May 13, 2018. DOE Agreement DE-FE0029264.

Battelle. 2018b. Integrated Mid-Continent Stacked Carbon Storage Hub. Task 3 Sub-Basinal Geologic Assessment Topical Report. Submitted January 15, 2018. DOE Award Number DE-FE0029264.

Battelle. 2018c. Integrated Mid-Continent Stacked Carbon Storage Hub. Task 4 CO_2 Injection/Storage Assessment Topical Report. Submitted February 2018. DOE Award Number DE-FE0029264.

Bennion, B., Bachu, S., 2005. Relative permeability characteristics for supercritical CO_2 displacing water in a variety of potential sequestration zones, SPE Annual Technical Conference and Exhibition. Society of Petroleum Engineers.

Bidgoli, T., and Dubois, M. 2017. Integrated CCS for Kansas (ICKan). Kansas Geological Survey. DOE Award Number DE-FE0029474. U.S. Department of Energy National Energy Technology Laboratory: Mastering the Subsurface Through Technology Innovation, Partnerships and Collaboration: Carbon Storage and Oil and Natural Gas Technologies Review Meeting. August 1-3, 2017.

Boardman, D.R., and Heckel, P.H., 1989, Glacial-eustatic sea-level curve for early late Pennsylvanian sequence in north-central Texas and biostratigraphic correlation with curve for Mid-continent North America: Geology, v. 17, p. 802-805.

Boyd, D.W., and Lillegraven, J.A., 2011. Persistence of the Western Interior Seaway: historical background and significance of the ichnogenus Rhizocorallium in Paleocene strata, south-central Wyoming: Rocky Mountain Geology, v. 46, p. 43-69.

Brooks, R.H., Corey, A.T., 1966. Properties of porous media affecting fluid flow. Journal of the Irrigation and Drainage Division 92, 61-90.

Bunker, B. J., B. J. Witzke, N. L. Watney, and G. A. Ludvigson. 1988. Phanerozoic history of the central Mid-Continent, United States. In Sedimentary Cover—North American Craton: U.S.: Geological Society of America, Geology of North America D-2, Sloss, L.L. (Ed.), p. 243-60. Boulder, CO: Geological Society of America.

Bureau of Land Management (BLM), National Parks Service (NPS), United States Fish and Wildlife Service (U.S. FWS), and United States Forest Service [USFS], 2017. National Wild and Scenic Rivers System. Retrieved 02 February 2018. <rivers.gov>

Burgess, P. M. 2008. Phanerozoic evolution of the Sedimentary Cover of the North American craton, In Sedimentary Basins of the World, v. 5, ed. A. D. Miall, 31-63. Amsterdam: Elsevier.

Carlson, M.P., Nodine-Zeller, D.E., Thompson, T.L., Witzke, B.J., 1986, Adler, F.J. (Ed.), Correlation of stratigraphic units in North America: Mid-continent Region correlation chart: American Association of Petroleum Geologists.

Carlson, M.P., 1999. Transcontinental Arch—a pattern formed by rejuvenation of local features across central North America: Tectonophysics, v. 305, p. 225-233.

Carmichael, R.S. ed. 1982. Handbook of Physical Properties of Rocks, Vol. 2, 1-228. Boca Raton, Florida: CRC Press Inc.

Cartwright, J., James, D., and Bolton, A., 2003. The genesis of polygonal fault systems: a review. In Van Rensbergen, P., Hillis, R.R., Maltman, A.J., and Morley, C.K. (Eds.), Subsurface Sediment Mobilization: Geological Society of London Special Publications v. 216, p. 223-243.

Calhoun Jr., JC. 1982. Fundamentals of Reservoir Engineering. University of Oklahoma Press, Norman Oklahoma.

Carlson, M.P., 1989, Oil in Nebraska: 50 years of production, 100 years of exploration, 500 million years of history: Conservation and Survey Division, University of Nebraska, Resource Report 11, 86 p.

Cast, L.D., 2000. Gosper County Test-hole Logs: Conservation and Survey Division, University of Nebraska-Lincoln: Nebraska Water Survey Test-Hole Report 37.

Clark, R., 2012. Rangely Weber Sand Unit Case History (RWSU). Presented at the 6th Annual Wyoming CO_2 Conference, 11 July 2012, Casper, Wyoming.

Condra, G.E., and Reed, E.C., 1959, The geological section of Nebraska: Nebraska Geological Survey, Bulletin 14A, 82 p.

Craddock, J.P., and van der Pluijm, B.A., 1999, Sevier-Laramide deformation of the continental interior from calcite twinning analysis, west-central North America: Tectonophysics v. 305, p. 275-286.

Dakota Gasification Company, nd. Souris Valley Pipeline. Retrieved 02 April 2018. <dakotagas.com>

Denbury, 2013. Rocky Mountain Activity Update. Presented at the 7th Annual Wyoming CO_2 Conference, 10-11 July 2013, Casper, Wyoming.

Dennison, J.M., and Ettensohn, F.R. (Eds.), Tectonic and eustatic controls on sedimentary cycles: Concepts in sedimentology and paleontology, SEPM, v.4, p. 65-87.

Dobitz, J.K., Prieditis, J.A., 1994. A stream tube model for the PC. In: SPE/DOE Ninth Symposium on Improved Oil Recovery, 1994, Society of Petroleum Engineers: Tulsa, OK.

Doctor, R., A. Palmer, D. Coleman, J. Davison, C. Hendriks, O. Kaarstad, M. Ozaki, and M. Austell, 2005. Chapter 4 - Transport of CO_2 in Metz, B, O. Davidson, H. de Coninck, M. Loos, and L. Meyer, eds., IPCC Special Report on Carbon Dioxide Capture and Storage: Cambridge University Press, New York, 443 p.

DOE-EIA (US Department of Energy-Energy Information Administration), 2017, Ethanol Plants (EIA-819M Monthly Oxygenate Report, March 27, 2017. https://www.eia.gov/maps/layer_info-m.php Accessed June 1, 2017. DOE-NETL (US Department of Energy-National Energy Technology Laboratory). 2008. The United States 2008 Carbon Utilization and Storage Atlas, Second Edition. Accessed February 19, 2017, at https://edx.netl.doe.gov/no/dataset/2008-carbon-storage-atlas-of-the-united-states-and-canada.

DOE-NETL (US Department of Energy-National Energy Technology Laboratory). 2010. The United States 2010 Carbon Utilization and Storage Atlas, Third Edition. Accessed February 19, 2017, at https://www.netl.doe.gov/KMD/CDs/atlasIII/2010atlasIII.pdf.

DOE-NETL (US Department of Energy-National Energy Technology Laboratory). 2012. The United States 2012 Carbon Utilization and Storage Atlas, Fourth Edition. Accessed February 19, 2017, at https://www.netl.doe.gov/File%20Library/Research/Coal/carbon-storage/atlasiv/Atlas-IV-2012.pdf.

DOE-NETL (US Department of Energy-National Energy Technology Laboratory). 2015. Carbon Storage Atlas, Fifth Edition. U.S. Deparment of Energy - National Energy Technology Laboratory - Office of Fossil Energy. Accessed February 19, 2017, at https://www.netl.doe.gov/research/coal/carbon-storage/natcarb-atlas.

Department of Energy/National Energy Technology Laboratory (DOE/NETL), 2015. A Review of the CO_2 Pipeline Infrastructure in the U.S. DOE/NETL-2014/1681, 52 p.

DOE-NETL (US Department of Energy-National Energy Technology Laboratory). 2017. Best Practices for Site Screening, Selection, and Initial Characterization for Storage of CO_2 in Deep Geologic Formations. DOE/NETL-2017/1844.

DOE-NETL (US Department of Energy-National Energy Technology Laboratory). 2017. Best Practices for Site Screening, Selection, and Initial Characterization for Storage of CO_2 in Deep Geologic Formations. DOE/NETL-2017/1844.

Duan, Z.; Sun, R. 2003. An improved model calculating CO_2 solubility in pure water and aqueous NaCl solutions from 273 to 533 K and from 0 to 2000 bar. Chemical Geology193, 257–271.

Dubois, M.K., 1985, Application of cores in development of an exploration strategy for the Lansing—Kansas City “E” zone, Hitchcock County, Nebraska: Kansas Geological Survey, Subsurface Geology Series 6, pp. 120-132.

Dubois, M. D. McFarlane and T. Bidgoli. 2017. CO_2 Pipeline Cost Analysis Utilizing and Modified FE/NETL Cost Model Tool. U.S. Department of Energy National Energy Technology Laboratory: Mastering the Subsurface Through Technology Innovation, Partnerships and Collaboration: Carbon Storage and Oil and Natural Gas Technologies Review Meeting. August 1-3, 2017.

Eversoll, D.A., 2000a. Frontier County Test-hole Logs: Conservation and Survey Division, University of Nebraska-Lincoln, Nebraska Water Survey Test-Hole Report 32.

Eversoll, D.A., 2000b. Hayes County Test-hole Logs: Conservation and Survey Division, University of Nebraska-Lincoln, Nebraska Water Survey Test-Hole Report 43.

Eversoll, D.A. 2003. Red Willow County Test-hole Logs: Conservation and Survey Division, University of Nebraska-Lincoln, Nebraska Water Survey Test-Hole Report 73.

Eversoll, D.A., 2004. Hitchcock County Test-hole Logs: Conservation and Survey Division, University of Nebraska-Lincoln, Nebraska Water Survey Test-Hole Report 44.

Eves, K.E. and J.J. Nevarez, 2009. Update of Lost Soldier/Wertz Floods - Living in a Constrain CO_2 Environment. Presented at the 15th Annual CO_2 Flood Conference, 10-11 December 2009, Midland, TX.

Federal Emergency Management Agency (FEMA), 2017a. National Flood Hazard Layer, Nebraska. NFHL_26_20170914. Retrieved 02 February 2018. <fema.gov>

Federal Emergency Management Agency (FEMA), 2017b. National Flood Hazard Layer, Kansas. NFHL_26_20170914. Retrieved 02 February 2018. <fema.gov>

Frankforter, M.J., 1982, A subsurface study of the C Zone, Lansing-Kansas City groups, in Red Willow County, Nebraska: Unpublished M.S. thesis, University of Nebraska-Lincoln.

Global CCS Institute, 2014. The Global Status of CCS. Global CCS Institute: Melbourne, Australia. 192 pp.

Global CCS Institute, 2011. Bridging the commercial gap for carbon capture and storage. Retrieved 02 April 2018. <globalccsinstitute.com>

Godec, M. L., Riestenberg, D., & Cyphers, S. 2017. Potential Issues and Costs Associated with Verifying CO_2 Storage During and After CO_2-EOR. Energy Procedia 114, 7399-7414.

Goodman, A., Sanguinito, S., Levine, J., 2016. Prospective CO_2 resource estimation methodology: Refinement of existing US-DOE-NETL methods based on data availability. International Journal of Greenhouse Gas Control 54, 242-249.

Goodman, A., Bromhal, G., Strazisar, B., Rodosta, T., Guthrie, W.F., Allen, D., Guthrie, G., 2013. Comparison of methods for geologic storage of carbon dioxide in saline formations. International Journal of Greenhouse Gas Control 18, 329-342.

Goodman, A., Hakala, A., Bromhal, G., Deel, D., Rodosta, T., Frailey, S., Small, M., Allen, D., Romanov, V., Fazio, J., Huerta, N., McIntyre, D., Kutchko, B., Guthrie, G., 2011. U.S. DOE methodology for the development of geologic storage potential for carbon dioxide at the national and regional scale. International Journal of Greenhouse Gas Control, 5, 952–965.

Great Plains Nature Center (GPNC), nd. Species in Need of Conservation. Retrieved 03 April 2018. <gpnc.org>

Haimson, B.C., 1990, Stress measurement in the Sioux Falls quartzite and the state of stress in the Mid-Continent, In Hustrulid, W.A., and Johnson, G.A. (Eds.), Rock Mechanics Contributions and Challenges: Proceedings of the 31st U.S. Symposium, p. 397-404.

Hattin, D.E., Broeker, M.E., and Winslow, J.D., 1964, Stratigraphy of the Graneros Shale (Upper Cretaceous) in central Kansas: Kansas Geological Survey, v. 173.

Heckel, P.H., 1977, Origin of phosphatic black shale facies in Pennsylvanian cyclothems of Mid-Continent North America: AAPG Bulletin, v. 61, p. 1045-1068.

Heckel, P.H., 1986, Sea-level curve for Pennsylvanian eustatic marine transgressive-regressive depositional cycles along Mid-Continent outcrop belt, North America: Geology, v. 14, p. 330-334.

Heckel, P.H., 1994, Evaluation of evidence for glacial-eustatic control over marine Pennsylvanian cyclothems of North America and consideration of possible tectonic effects, In

Heckel, P.H., 2008, Pennsylvanian cyclothems in Mid-continent North America as far-field effects of waxing and waning of Gondwana ice sheets, In, Fielding, C.F., Frank, T.D., and Isbell, J.L., (Eds.), Resolving the Late Paleozoic Ice Age in Time and Space: Geological Society of America Special Paper 441, p. 275-289.

Heckel, P.H., and Watney, W.L., 2002, Revision of stratigraphic nomenclature and classification of the Pleasanton, Kansas City, Lansing, and lower part of the Douglas Groups (Lower Upper Pennsylvanian, Missourian) in Kansas: Kansas Geological Survey, Bulletin 246, 69 p.

Heckel, P.H., and Weibel, C.P., 1991, Current status of conodont-based biostratigraphic correlation of Upper Pennsylvanian succession between Illinois and Mid-Continent, In Weibel, C.P. (Ed.), Sequence stratigraphy in mixed clastic-carbonate strata, Upper Pennsylvanian, east-central Illinois: Champaign, Great Lakes Section, Society of Economic Paleontologists and Mineralogists, 21st Annual Field Conference, Illinois State Geological Survey, p. 60-69.

Heidbach, O., Rajabi, M., Reiter, K., and Ziegler, M. (Eds.), 2016, World Stress Map 2016, http://escidoc.gfz-potsdam.de/ir/item/escidoc:1680899/components/component/escidoc:1868890/content.

Hillebrand, G.M., Steeples, D.W., Knap, R.W., Miller, R.D., and Bennett, B.C., 1988, Microearthquakes in Kansas and Nebraska 1977-87: Seismological Research Letters v. 59 p. 159-163.

Higley, D.K., 1987, Central Kansas Uplift-Cambridge Arch province oil and gas play summary: U.S. Geological Survey Open-File Report 87-450E.

Higley, D. K., 1995, Cambridge Arch/Central Kansas Uplift Province (053), In Gautier, D. L., Dolton, G.L., Takahashi, K.I., and Varnes, K.L., (Eds.), 1995 National Assessment of United States oil and gas resources--Results, methodology, and supporting data: U.S. Geological Survey Digital Data Series DDS-30, Release 2, one CD-ROM.

Heckel, P.H., 1986, Sea-level curve for Pennsylvanian eustatic marine transgressive-regressive depositional cycles along Midcontinent outcrop belt, North America: Geology, v. 14, p. 330-334.

Heckel, P.H., 2008, Pennsylvanian cyclothems in Mid-continent North America as far-field effects of waxing and waning of Gondwana ice sheets, In, Fielding, C.F., Frank, T.D., and Isbell, J.L., (Eds.), Resolving the Late Paleozoic Ice Age in Time and Space: Geological Society of America Special Paper 441, p. 275-289.

IBDP (Illinois Basin-Decatur Project), 2016, CO_2 Surface Facilities Process Design and Operation, Rev 1.

Ide, T., Friedmann, S.J., & Herzog, H. 2006. Carbon Dioxide Leakage through Existing Wells: Current Technology and Regulations, presented at the 8th International Conference on Greenhouse Gas Control Technologies. June 2006, Trondheim, Norway.

IEA Greenhouse Gas R&D Programme (IEAGHG), 2009. Development of Storage Coefficients for CO_2 Storage in Deep Saline Formations. Technical Study Report No. 2009/13.

IMCCS - Integrated Mid-Continent Carbon Capture, Sequestration & Enhanced Oil Recovery Project, final report for DOE Project # DE-FE-0001942, August 31, 2010.

Joeckel, R.M., 1989, Paleogeomorphology of a Pennsylvanian land surface: the Rock Lake Shale in Nebraska: Journal of Sedimentary Petrology, v. 59, p. 469-481.

Joeckel, R.M., 1994, Virgilian (Upper Pennsylvanian) Paleosols in the Upper Lawrence Formation (Douglas Group) and in the Snyderville Shale Member (Shawnee Group, Oread Formation) of the Northern Mid-Continent, U.S.A.: Pedologic Contrasts in a Cyclothem Sequence: Journal of Sedimentary Research, v. A64, p. 853-866.

Joeckel, R.M., 1995, Tectonic and paleoclimatic significance of a Locally Prominent Upper Pennsylvanian (Virgilian/Stephanian) weathering profile, Iowa and Nebraska, U.S.A.: Palaeogeography, Palaeoclimatology, Palaeoecology, v. 118, p.159-179.

Joeckel, R.M., 1995b, Virgilian (Upper Pennsylvanian) Paleosols in the Upper Lawrence Formation (Douglas Group) and in the Snyderville Shale Member (Shawnee Group, Oread Formation) of the Northern Mid-Continent, U.S.A.: Pedologic Contrasts in a Cyclothem Sequence, Reply to Response by H. Feldman and A. Archer: Journal of Sedimentary Research, v. A65, p. 714-718.

Joeckel, R.M., 1999, Paleosol in Galesburg Formation (Kansas City Group, Upper Pennsylvanian), northern Mid-continent, U.S.A.: Evidence for climate change and mechanisms of marine transgression: Journal of Sedimentary Research, v. 69, p. 720-737.

Johnson, W.C., 1993, Surficial geology and stratigraphy of Phillips County, Kansas, with emphasis on the Quaternary Period: Kansas Geological Survey, Technical Series 1.

Kansas Department of Health and Environment (KDHE), 2010. Kansas Surface Water Register. Retrieved 09 February 2018. <kansasgis.org>

KDHE, nd. Underground/Above Ground Storage Tank Assessment Database. Retrieved 08 February 2018. <kdheks.gov>

Kansas Department of Wildlife, Parks, and Tourism (KDWPT), nd. Kansas Threatened and Endangered Species Statewide. Retrieved January 2018. <kdwpt.state.ks>

Karlstrom, K.E., and Humphreys, E.D., 1998, Persistent influence of Proterozoic accretionary boundaries in the tectonic evolution of southwestern North America: Rocky Mountain Geology, v. 33, p. 161-179.

Kincaid, R.W. 1961. Oil and Gas Field Summary: Sleepy Hollow Field. AAPG Datapages/Archive. R.G.M.A.G. Oil and Gas Field Volume: Colorado-Nebraska. p. 324. archives.datapages.com/data/rmag/OGFieldVol61/sleepyhollow.pdf

Kinder Morgan, 2014. Overview of McElmo Dome Development Plans. Presented to Montezuma County BOCC 27 October 2014. Retrieved 02 April 2018. <montezumacounty.org>

Kluth, C.F., 1986, Plate tectonics of the Ancestral Rocky Mountains, In Peterson, J.A. (Ed.), Paleotectonics and Sedimentation in the Rocky Mountain Region: AAPG Memoir 41, p. 353-369.

Lake, LW. 1989. Enhanced Oil Recovery. Prentice Hall, Englewood Cliffs, New Jersey.

Liu, Shaofeng and Nummedal, Dag and Gurnis, Michael, 2014, Dynamic versus flexural controls of Late Cretaceous Western Interior Basin, USA: Earth and Planetary Science Letters, v. 389, p. 221-229.

Maher, H.D. Jr., 2014, Distributed normal faults in the Niobrara Chalk and Pierre Shale of the central Great Plains of the United States: Lithosphere, v. 6, p. 319-334.

Maher, H., and Shuster, R., 2012, Chalcedony vein horizons and clastic dikes in the White River Group as products of diagenetically driven deformation: Lithosphere, v. 4, p. 167-186.

Massachusetts (MIT), nd. Carbon Dioxide Capture and Storage Projects. Retrieved 02 April 2018. <mit.edu>

McKaskle, R. (2017) Trimeric Corporation, Insights into Costs of CCS gained from the IBDP, 2016 Midwest Carbon Sequestration Science Conference, May 17, 2016.

McCollough, D.E. and R.L. Stiles, 1987. Operation of the Central Basin CO_2 Pipeline System. Society of Petroleum Engineers California Regional Meeting, 8-10 April 1987, Ventura, California.

McCoy, S., and Rubin, E. 2009. The Effect of High Oil Prices on EOR Project Economics. Energy Procedia 1, 4143–4150. doi:10.1016/j.egypro.2009.02.223

Mella, 2002. Kinder Morgan announces new CO_2 pipeline, SACROC expansion. Midland-Reporter Telegram, 27 April 2002.

Melzer, L.S., 2002. The Permian basin CO_2 sequestration model and Ridgeway Petroleum's St. John Project. Presented at the Annual Convention of the Southwest Section of the American Association of Petroleum Geologists, June 2002, Ruidoso, New Mexico.

Miller, J.A. and C.L. Appel, 1997. Ground Water Atlas of the United States - Kansas, Missouri, and Nebraska - High Plains Aquifer. U.S. Geological Survey, Hydrologic atlas 730-D.

Miller, K.G., Kominz, M.A., Browning, J.V., Wright, J.D., Mountain, G.S., Katz, M.E., Sugarman, P.J., Cramer, B.S., Christie-Blick, N., and Pekar, S.F., 2005, The Phanerozoic record of global sea-level change: Science, v. 310, p. 1293-1298.

Moore, V.A., and Nelson, R.B., 1974, Effect of the Cambridge-Chadron structural trend on Paleozoic and Mesozoic thickness, western Nebraska: AAPG Bulletin v. 58, p. 260-268.

Murrell, G. B. Cook, V. Jones, and N. Jones, 2012. Wyoming CO_2 Status and Developments. Presented at the 6th Annual Wyoming CO_2 Conference, 11 July 2012, Casper, Wyoming.

National Carbon Sequestration Database and Geographical Information System (NATCARB). 2016. http://www.natcarbviewer.com/

National Park Service. (2017). National Register of Historic Places. Retrieved 20 November 2017. <nps.gov>

Nebraska Department of Environmental Quality (NDEQ), 2011. Wellhead Protection Area Boundaries statewide, Nebraska.

NDEQ, nd. Leaking Underground Storage Tank and Surface Spill Site Information Search Tool. Retrieved 11 February 2018. <nebraska.gov>

Nebraska Environmental Trust, nd. Nebraska's Threatened and Endangered Species. Retrieved January 2018. <nebraska.gov>

Noothout et al., 2014 – Noothout, P., F. Wiersma, O. Hurtago, D. MacDonald, J. Kemper, and K. van Alphen., 2014, CO_2 Pipeline Infrastructure – Lessons Learnt. Energy Procedia, vol. 63, pp. 2481-2492.

Olszewski, T.D., and Patzkowsky, M.E., 2003, From cyclothems to sequences: The record of eustasy and climate on an icehouse epeiric platform (Pennsylvanian-Permian, North American Mid-Continent): Journal of Sedimentary Research, v. 73, pp. 15-30.

Oxy, (nd). Oxy CO_2 EOR Project - Project Overview. Retrieved 02 April 2018. <energy.ca.gov>

Peppe, D.J., Evans, D.A.D., Smirnov, A.V., 2009, Magnetostratigraphy of the Ludlow Member of the Fort Union Formation (Lower Paleocene) in the Williston Basin, North Dakota: Geological Society of America Bulletin, v. 121, p. 65-79.

Petersen, M.D., Mueller, C.S., Moschetti, M.P., Hoover, S.M., Llenos, A.L., Ellsworth, W.L., Michael, A.J., Rubinstein, J.L., McGarr, A.F., and Rukstales, K.S., 2016, 2016 One-Year Seismic Hazard Forecast for the Central and Eastern United States from Induced and Natural Earthquakes: U.S. Geological Survey Open-File Report 2016–1035.

Peck, W., Azzolina, N., Ge, J., Gorecki, C., Andrew J. Gorz, A., Melzer, S. 2017. Best practices for quantifying the CO_2 storage resource estimates in CO_2 enhanced oil recovery. 13th International Conference on Greenhouse Gas Control Technologies, GHGT-13, 14-18 November 2016, Lausanne, Switzerland. Energy Procedia 114, 4741 – 4749.

Phares, R.A., 1991. Characterization and reservoir performance of the Lansing-Kansas City 'I' and 'J' zones (Upper Pennsylvanian) in the Pen oil field, Graham County, Kansas: Unpublished M.S. Thesis, University of Kansas.

Prather, B.E., 1984, Deposition and diagenesis of an Upper Pennsylvanian cyclothem from the Lansing-Kansas City groups, Hitchcock County, Nebraska, In Hyne, N. J. (Ed.), Limestones of the Mid-Continent: Tulsa Geological Society Special Publication 2, p. 393-419.

Prather, B.E., 1985a. An Upper Pennsylvanian desert Paleosol in the D-zone of the Lansing-Kansas City Groups, Hitchcock County, Nebraska: Journal of Sedimentary Petrology, v. 55, p. 213-221.

Prather, B.E., 1985b. Depositional facies and diagenetic fabrics of the D-Zone cyclothem, Lansing-Kansas City groups, Hitchcock County, Nebraska, In Watney, W.L., Walton, A.W., and Doveton, J.H. (compilers), Core Studies in Kansas: Sedimentology and Diagenesis of Economically Important Rock Strata in Kansas: Kansas Geological Survey Subsurface Geology Series 6, p. 133-144.

Rascoe, B., Jr., 1978, Late Paleozoic Structural Evolution: The Las Animas Arch, In Pruit, J.D. and Coffin, P.E. (Eds.), Energy Resources of the Denver Basin, Rocky Mountain Association of Geologists 1978 Symposium Denver, CO, Rocky Mountain Association of Geologists, p. 113-127.

Rascoe, B., Jr., and Adler, F.J., 1983, Permo-Carboniferous hydrocarbon accumulations, Mid-Continent, USA: AAPG Bulletin, v. 67, pp. 979-1001.

Ritter, S.M., Barrick, J.E., and Skinner, M.R., 2002, Conodont sequence biostratigraphy of the Hermosa Group (Pennsylvanian) at Honaker Trail, Paradox Basin, Utah: Journal of Paleontology, v. 76, p. 495-517.

Rogers, J.P., 1977, Genesis and distribution of Desmoinesian (Pennsylvanian) sandstone reservoir, Sleepy Hollow Field, Red Willow County, Nebraska: AAPG Bulletin, v. 61, pp.1029-1044.

Rothe, G.H., and Lui, C.-Y., 1983, Possible induced seismicity in the vicinity of the Sleepy Hollow oil field, southwestern Nebraska: Bulletin of the Seismological Society of America, v. 73, p. 1357-1367.

Salahuddin, Q., 1993, Depositional environments, diagenesis and stratigraphy of the Upper Pennsylvanian Lansing-Kansas City Group in Nebraska: Unpublished Ph.D. dissertation, University of Nebraska-Lincoln.

Sanguinito, S., Goodman, A., Levine, J.S., 2016, NETL CO_2 Storage prospective Resource Estimation Excel aNalysis (CO_2-SCREEN) User's Manual; NETL-TRS-X-2016; Technical Report Series; U.S. Department of Energy, National Energy Technology Laboratory: Pittsburgh, PA, 2016; p. 31. https://edx.netl.doe.gov/carbonstorage/?page_id=914

Sloss, L. L., 1988, Tectonic evolution of the craton in Phanerozoic time, In Sloss, L.L., (Ed.), Sedimentary Cover—North American Craton: U.S., Geological Society of America, Geology of North America D-2, Boulder, CO: Geological Society of America, p. 25-51.

Smith, F.A., 2003, Furnas County Test-hole Logs: Conservation and Survey Division, University of Nebraska-Lincoln, Nebraska Water Survey Test-Hole Report 33.

Stanley, K.0. and Wayne, W.J., 1972, Epeirogenic and Climatic Controls of Early Pleistocene fluvial sediment dispersal in Nebraska: Geological Society of America Bulletin, v. 83, p. 3675-3690.

Steeples, D.W., Bennett, B.C., Park, C., Miller, R.D., and Knapp, R.W., 1990, Microearthquakes in Kansas and Nebraska 1977-89: Kansas Geological Survey Open-file Report 90-10.

Steeples, D.W., 1982, Structure of the Salina-Forest City interbasin boundary from seismic studies. Kansas Geological Survey Bulletin 226, Geophysics in Kansas, p. 31-52.

Stix, J., 1982, Seasat-satellite investigation of the structure of western Nebraska and its application to the evaluation of geothermal resources: Los Alamos National Laboratory, U.S. Department of Energy Publications 27.

St-Onge, A., 2017, Great Plains polygonal fault system as expressed in Saskatchewan: Late Cretaceous fault initiation and graben formation: Canadian Journal of Earth Sciences, v. 54, p. 477-493.

Swain, R.S., West, R.R., Franseen, E.K., Watney, W.L., and McCauley, J.R., 2006, Carboniferous-Permian boundary in Kansas, Mid-Continent, USA: Kansas Geological Survey, Bulletin 252 Part II, p. 13.

Thomas, S., 2009. LaBarge Field and Shute Creek Facility. Presented at the 3rd Annual Wyoming CO_2 Conference, 24 June 2009.

Tikoff, B., and J. Maxson, 2001, Lithospheric buckling of the Laramide foreland during Late Cretaceous and Paleogene, western United States: Rocky Mountain Geology, v. 36, p. 13-35.

Tracy, K., 2013. A "CO_2 Midstream" Overview. Presented at the EOR Carbon Management Workshop, 10 December 2013, Midland, TX.

Trinity Pipeline, 2018. Trinity Pipeline GP, LLC. Retrieved 02 April 2018. <pdigm.com>

United States Census Bureau. (2016a). TIGER/Line Shapefile, 2016, state, Nebraska, Current Block Group State-based. Retrieved 20 December 2017. <census.gov>

United States Census Bureau. (2016b). TIGER/Line Shapefile, 2016, state, Kansas, Current Block Group State-based. Retrieved 20 December 2017. <census.gov>

United States Census Bureau. (2016b). 2011-2015 American Community Survey 5-Year Estimates - Employment for the Population 16 Years and Older. Retrieved 20 December 2017. <census.gov>

United States Department of Energy, National Energy Technology Laboratory. Carbon Storage Assurance Facility Enterprise (CarbonSAFE): Storage Complex Feasibility, DE-FOA-0001450, June 23, 2016.

U.S. Geological Survey, 2014. Maps: Conterminous US, PGA, 2% in 50 years. https://earthquake.usgs.gov/static/lfs/nshm/conterminous/2014/2014pga2pct.pdf

U.S. Geological Survey, 2014b. Maps: Coterminous US, 5 Hz 2% in 50 yrs. https://earthquake.usgs.gov/static/lfs/nshm/conterminous/2014/2014_5Hz2pct.pdf

US EPA (United States Environmental Protection Agency). 2010. Environmental Protection Agency - 40 CFR Parts 124, 144, 145, et al. Federal Requirements Under the Underground Injection Control (UIC) Program for Carbon Dioxide (CO_2) Geologic Sequestration (GS) Wells; Final Rule. Federal Register.

US EPA (United States Environmental Protection Agency). 2013a. Geologic Sequestration of Carbon Dioxide - Draft Underground Injection Control (UIC) Program Guidance on Transitioning Class II Wells to Class VI Wells. Office of Water.

US EPA (United States Environmental Protection Agency). 2013b. Geologic Sequestration of Carbon Dioxide - Underground Injection Control (UIC) Program Class VI Well Area of Review Evaluation and Corrective Action Guidance. Office of Water.

United States Environmental Protection Agency (US EPA). 2016a. Greenhouse Gas Reporting Program. 13 August 2016. Accessed: 7 June 2017. epa.gov.

United States Environmental Protection Agency (US EPA). 2016b. Greenhouse Gas Reporting Program Frequently Asked Questions, Q721. 22 April 2016. Accessed: 14 June 2017. epa.gov.

US EPA (United States Environmental Protection Agency). 2016c. Geologic Sequestration of Carbon Dioxide - Underground Injection Control (UIC) Program Class VI Well Recordkeeping, Reporting, and Data Management Guidance for Owners and Operators. Office of Water.

US EPA (United States Environmental Protection Agency). 2016d. National Ambient Air Quality Standards Table. Retrieved 19 December 2017. <epa.gov>

US EPA (United States Environmental Protection Agency).). 2017. Aquifer Exemptions in the Underground Injection Control Program. < https://www.epa.gov/uic/aquifer-exemptions-underground-injection-control-program>

US EPA (United States Environmental Protection Agency). 2018. Superfund National Priority List (NPL) Sites Where You Live Mapper. Retrieved 09 February 2017. <epa.gov>

US -FWS (United States Fish and Wildlife Service). 2017a. National Wetlands Inventory - Download Seamless Wetlands Data by State. Retrieved 20 December 2017. <fws.gov>

United States Fish and Wildlife Service (U.S. FWS). 2017b. Threatened & Endangered Species Active Critical Habitat Report. Retrieved 02 February 2017. <fws.gov>

U.S. FWS, 2017c. Environmental Conservation Online System (ECOS). Retrieved December 2017. <fws.gov>

U.S. FWS, 2015a. Listed species believed to or known to occur in Nebraska. Retrieved January 2018. <fws.gov>

U.S. FWS, 2015b. Listed species believed to or known to occur in Kansas Retrieved January 2018. <fws.gov>

USGS (United States Geological Survey). 2017. Mineral Resources Online Spatial Data. Retrieved 12 February 2018. <usgs.gov>

USGS (United States Geological Survey) 2016a. Protected Areas Database of the United States (PAD-US), version 1.4. Retrieved 26 January 2018. <usgs.gov>

USGS (United States Geological Survey). 2016b. National Hydrography Dataset Best Resolution 20170714 for Nebraska State or Territory File GDB 10.1 Model Version 2.2.1. Retrieved 12 September 2017. <usgs.gov>

USGS (United States Geological Survey). 2016c. National Hydrography Dataset Best Resolution 20170714 for Kansas State or Territory File GDB 10.1 Model Version 2.2.1. Retrieved 12 September 2017. <usgs.gov>

USGS (United States Geological Survey). 2014. National Land Cover Dataset (NLCD). Retrieved 12 September 2017. <usgs.gov>

USGS (United States Geological Survey). 2014. Maps: Conterminous US, PGA, 2% in 50 years. https://earthquake.usgs.gov/static/lfs/nshm/conterminous/2014/2014pga2pct.pdf

USGS (United States Geological Survey)., 2014b. Maps: Coterminous US, 5 Hz 2% in 50 yrs. https://earthquake.usgs.gov/static/lfs/nshm/conterminous/2014/2014_5Hz2pct.pdf

USGSa. Mineral Extractions – USGS, 2003. Active Mines and mineral plants in the US. Retrieved 1 June 2017. <usgs.gov>

USGS, 1995. High Plains Aquifer. Retrieved 18 December 2017. <kansasgis.org>

US-IRS (United States Internal Revenue Service). 2018. U.S. Bipartisan Budget Act of 2018: Division D Revenue Measures: Title II Miscellaneous Provisions - Sec. 41119. Enhancement of carbon dioxide sequestration credit. H.R – 1892 -99.

Van der Pluijm, B.A., Craddock, J.P., Graham, B.R., and Harris, J.H., 1997, Paleostress in cratonic North America: Implications for deformation of continental interiors: Science, v. 277, p. 794-796.

Vandewater, B., 1995. Carbon Dioxide Line to Bolster Oil Field. The Oklahoman, 18 July 1995.

Voge, A., 2012. Wyoming, Montana carbon dioxide pipeline opens Jan. 1. Casper Star-Tribune, 19 December, 2012.

Wall Street Journal. nd. Wastelands – America's Forgotten Nuclear Legacy. Available at: <wsj.com.> Accessed: 08 October 2018.

Watney, W.L, 1980, Cyclic sedimentation of the Lansing-Kansas City Groups in northwestern Kansas and southwestern Nebraska: Kansas Geological Survey, Bulletin 220, 73 p.

Watney, W.L., and French, J.A., 1988, Characterization of carbonate reservoirs in the Lansing-Kansas City groups (Upper Pennsylvanian) in Victory Field, Haskell County, Kansas, In Goolsby, S.M., and Longman, M.W. (Eds.), Occurrence and Petrophysical Properties of Carbonate Reservoirs in the Rocky Mountain Region: Rocky Mountain Association of Geologists, pp. 27-46.

Whitmeyer, S.J., and Karlstrom, K.E., 2007, Tectonic model for the Proterozoic growth of North America: Geosphere, v. 3, p. 220-259.

Wiseman, P., 2010. KM expects record year in production and in CO_2. Midland-Reporter Telegram, 20 March 2010.

Wollard, G.P., 1958, Areas of tectonic activity in the United States as indicated by earthquake epicenters: Transactions of the American Geophysical Union, v. 39, p. 1135-1150.

Worthington, PF, and L Cosentino. 2005. The Role of Cutoffs in Integrated Reservoir Studies. SPE Paper 84387-PA, SPE Reservoir Evaluation and Engineering, vol. 8, pp. 276-290.

Ye, H., Royden, L., Burchfiel, C., and Schuepbach, M., 1996, Late Paleozoic deformation of interior North America: The greater Ancestral Rock Mountains: AAPG Bulletin, v. 80, p. 1397-1432.

Young, A.L., 2011, Lithostratigraphy and Diagenesis of the Upper Pennsylvanian (Missourian) Lansing-Kansas City Groups in Rooks County, Kansas, M.S. Thesis, Wichita State University

Young, A.L., 2013, Lithostratigraphy and diagenesis of the Upper Pennsylvanian (Missourian) Lansing-Kansas City Groups in Rooks County, Kansas: Unpublished M.S. Thesis, Wichita State University, Wichita, KS, 30 p.

Zeller, D.E., ed., 1968, The stratigraphic succession in Kansas: Kansas Geological Survey, Bulletin 189, 81 p.

Zoback, M.L., 1992, Stress field constraints on intraplate seismicity in eastern North America: Journal of Geophysical Research, v. 97(B8), p. 11761-11782.

Zoback, M. L., and Zoback, M. D., 1980, State of stress in the conterminous United States: Journal of Geophysical Research, v. 85, p. 6113-6156.

Zoback, M. L., and Zoback, M. D., 1989, Tectonic stress field of the continental United States, In Pakiser, L. C., and Mooney, W. D., (Eds.), Geophysical framework of the continental United States: Boulder, Colorado, Geological Society of America Memoir 172.